INTERNATIONAL COUNCIL FOR BUILDING RESEARCH STUDIES AND DOCUMENTATION

WORKING COMMISSION W18 - TIMBER STRUCTURES

CIB - W18

MEETING TWENTY - FIVE

ÅHUS

SWEDEN

AUGUST 1992

CONTENTS

0 List of Participants

INTERNATIONAL COUNCIL FOR BUILDING RESEARCH STUDIES AND DOCUMENTATION

WORKING COMMISSION W18 - TIMBER STRUCTURES

MEETING TWENTY-FIVE

ÅHUS, SWEDEN, 24-27 AUGUST 1992

LIST OF PARTICIPANTS

CANADA

B Madsen	University of British Columbia, Vancouver
C K A Stieda	Forintek Canada Corp., Vancouver

DENMARK

A Egerup	Euro-Truss
H J Larsen	Danish Building Research Institute, Hørshølm

FINLAND

J Kangas	Technical Research Centre of Finland, Espoo
A Kevarinmaki	Helsinki University of Technology, Espoo
A Ranta-Maunus	Technical Research Centre of Finland, Espoo
T Poutanan	Consultant

FRANCE

F Rouger	C.T.B.A Paris

GERMANY

H Brüninghoff	University of Wuppertal
F Colling	German Society of Wood Research, Munich
J Ehlbeck	University of Karlsruhe
R Görlacher	University of Karlsruhe
M Schlager	University of Karlsruhe
H Werner	University of Karlsruhe

ISRAEL

U Korin	National Building Research Institute, Haifa

ITALY

A Ceccotti	University of Florence

JAPAN

M Yasumura	Building Research Institute, Tsukuba
K Komatsu	Forestry and Forest Products Research Institute

NETHERLANDS

H J Blass	Delft University of Technology
J W G van de Kuilen	TNO-Building & Construction Research, Delft

NORWAY

E Aasheim	Norwegian Institute of Wood Technology, Oslo

POLAND

Z Mielczarek	Politechnika Szczencinska, Plastow

SWEDEN

B L O Edlund	Chalmers University of Technology, Gothenburg
B Källsner	Swedish Institute for Wood Technology Research, Stockholm
J König	Swedish Institute for Wood Technology Research, Stockholm
S Thelandersson	Lund University
H Petersson	Lund University
S Ohlsson	Chalmers University of Technology, Gothenburg
P J Gustsfsson	Lund University
A Mårtensson	Lund University

SWITZERLAND

E Gehri	Eidgenössische Technische Hochschule, Zürich

UK

A R Abbott	TRADA Technology Limited, High Wycombe
B S Choo	Nottingham University
A R Fewell	Building Research Establishment, Watford
C J Mettem	TRADA Technology Limited, High Wycombe
J G Sunley	Private Consultant
T D G Canisius	Building Research Establishment, Watford

USA

M R O'Halloran	American Plywood Association, Tacoma
E G Stern	Virginia Polytechnic Institute and State University, Blacksburg
T E McLain	Virginia Polytechnic Institute and State University, Blacksburg
D W Green	US Forest Products Laboratory, Madison
R Falk	US Forest Products Laboratory, Madison
J Showalter	National Forest Products Association, Washington DC
T Williamson	American Plywood Association, Tacoma

1. Chairman's Introduction

2. Cooperation with other Organisations

3. Reports from Sub-Groups

4. Connections Made Using Punched Metal Plate Fasteners

5. Size Effects

6. EUROCODE 5 Part 1 and CEN Support Standards

7. Fire

8. Open Forum

9. Any other Business

10. Venue and Programme for the Next Meeting

11. Close

INTERNATIONAL COUNCIL FOR BUILDING RESEARCH STUDIES AND DOCUMENTATION

WORKING COMMISSION W18 - TIMBER STRUCTURES

MEETING TWENTY-FIVE

ÅHUS, SWEDEN, 24-27 AUGUST 1992

MINUTES

1. CHAIRMAN'S INTRODUCTION

The Chairman, PROFESSOR BLASS, opened the meeting and gave particular welcomes to representatives of other organizations, namely: DR STIEDA, ISO TC165 and formerly coordinator of CIB W18; DR CECCOTTI, RILEM; MR LARSEN and MR SUNLEY, CEN; PROFESSOR EDLUND, IABSE; PROFESSOR MADSEN, IUFRO S5.02, and DR OHLSSON, CIB-W85.

It was pointed out that this would be the first CIB W18 meeting at which the principle agreed in Oxford of planning an agenda on selected topics would apply. A general forum would also be available for papers not fitting into this pattern.

Finally, the Chairman thanked DR KÖNIG for making all the meeting arrangements in the lovely atmosphere of Åhus.

2. COOPERATION WITH OTHER ORGANIZATIONS

a) CIB W18B

DR LEICESTER had been unable to attend this meeting, but had sent a report. It was stated that a meeting of CIB W18B was shortly to take place in Kuala Lumpur. The technical content included suggestions by CSIRO. Some problems with W18B are the difficulty of representatives from developing countries getting funding to attend, and the diversity of the technical problems and topics involving tropical timbers, which it is trying to address.

It was reported that 'state-of-art' papers as well as research topics have been included in the agenda for the W18B meeting.

Additional recent activities of W18B have included a UNIDO Workshop, which was held in March 1992 for the 'Preferential Trade Area' of Southern Africa. Representatives from this group intend forming a working group of CIB W18B.

W18B has also produced an activity list of six items, including proposals to work on regional grading standards and a design code. In addition, based upon the work of CSIRO and Australia Standards Association, information has been distributed on the strength grouping of tropical timbers, on the basis of small clear properties. Funding is being sought to extend this work to cover further south-east Asian and Central and South American timbers. Further 'workshop' meetings are planned.

b) ISO TC165

DR STIEDA reported on the activities of ISO TC165, and announced that a meeting is planned in Prague in the spring of 1993.

c) RILEM

DR CECCOTTI gave a report on the RILEM activities connected with structural timber and furnished the Secretariat with a report. Activities have flourished in the subjects of fracture mechanics and seismic design.

d) CEN

MR SUNLEY reported on the activities of CEN TC38; 103; 112 and 175. By way of introduction, he said that about 200 standards were being prepared. Many of these were now at an advanced stage. They varied in length from one to twenty pages. It was now the case that the technical contents of the key CEN standards relating to EC5 were established, and most could be described as being at the stage where major changes were unlikely. The emphasis is now on how the standards should be implemented in the member countries. This includes contemplating how national standards are to be withdrawn.

Dealing with TC38 Wood Preservation, it was reported that thirty-eight standards were being drafted. These were divided into two groups. Five of these were considered particularly important for the designer referring to EC5, including, for example, the definition of hazard classes. Some drafts which were rejected for the first time were now more likely to be approved on second submission.

The group known as TC103 Wood Adhesives has been disbanded, and absorbed into TC193, general adhesives, acting as a sub-committee. An important standard for timber engineers was produced on a classification system for structural adhesives. Performance levels are defined in the draft. Four test standards are available for structural timber adhesives. Work has recently been started on casein adhesives, as some European countries still use them extensively.

A large programme of about eighty standards is being dealt with by TC112 Wood-based Panel Products. About sixty of these are at the 'technical content unlikely to change' stage. A test method for creep and for long-term loading has been produced. Taking account of procedures to establish characteristic values produced by TC124, TC112 has developed a similar approach for well-established types of panel products. New types, which have not previously been tested, would have to follow a more basic approach to become established using test standards being drafted by TC112.

A number of the standards being drafted by the group TC175 Round and Sawn Timber for Non-Structural Use are 'non-mandated'. MR SUNLEY thought that the timber industries involved might question the necessity for some of these standards, once the amount of work involved in producing them is realized. Sixty-five standards are now in the process of development. It has been found that in general with standards for non-structural use, there are great differences between the regions of the EC. These exist, for example, between Nordic countries and western Europe. Work is proceeding on user requirements for items such as flooring, joinery and packaging.

MR LARSEN reported on the activities of CEN TC124 and TC250. He described the drafting stages of a EN. These involve a first draft; enquiry stage; second draft; editorial stage and voting. Of the thirty-six standards in the programme of TC124, ten are at first draft stage; seven at enquiry stage; six at second draft stage, and thirteen at editorial stages. Two very new topics are glued-in bolts and panel structures.

A paper was tabled at the meeting and made available to those concerned describing the titles and drafting stage status of each standard being dealt with by the CEN TC124 Secretariat, under four working groups.

With regard to TC250/SC5 - Eurocodes - Timber Structures, MR LARSEN reported that the formal title of EC5 : Part 1 was now prENV 1995-1-1, Eurocode 5 - Design of timber structures - Part 1-1 : General rules and rules for buildings. This was at the stage of final circulation for comment prior to a Voting Meeting scheduled for 19-20 November 1992 in Madrid. If approved by voting, the voluntary code would become available alongside national codes for use in trial design calculations. The Eurocodes are intended to serve as reference documents as a means to prove compliance of building and civil engineering works with the essential requirements of the Construction Products Directive.

Eurocode 5 Part 10 Structural Fire Design, Document CEN TC250/SC5 : 44 was produced as a further working draft in April 1992. It contains sections dealing with basic principles, thermo-mechanical material properties and structural fire design. At present it is expected that this may reach voting stage by April 1993.

Another part to the timber Eurocode, provisionally Part 2, is projected to deal with bridges. However, work on this is not planned until 1993.

e) IABSE

PROFESSOR EDLUND reminded delegates of the role of IABSE, describing the activities of Working Commission No. 2, Steel, timber and composite materials. He announced that an IABSE meeting was shortly to take place in Davos, Switzerland, on structural Eurocodes. MR LARSEN would be attending, to speak on EC5. Other forthcoming events included a Colloquium on Remaining Structural Capacity, in Copenhagen on 17-19 March 1993, and another Colloquium on Structural Serviceability, in Sweden in June 1993. A forthcoming edition of the IABSE Journal would carry a feature on timber structures and PROFESSOR EDLUND was encouraging contributions.

MR LARSEN commented that efforts to apply research and to promote timber structures might be better concentrated in CIB and IUFRO groups, rather than attempting to cover the wide-ranging and costly activities of IABSE. PROFESSOR EDLUND replied that the circles which MR LARSEN described tended to inform one another of details in a field in which all the participants were familiar with the principles. IABSE on the other hand represents an opportunity to communicate structural timber concepts to engineers only familiar with other materials.

f) IUFRO

Reporting on the activities of IUFRO group S5.02, PROFESSOR MADSEN described a recent successful meeting in Bordeaux. The sessions had provided good time for discussion of the topics. A number of RILEM activities, on rheology and fracture mechanics, had led to input to the IUFRO timber engineering group. The research on long-term effects had been incorporating moisture effects. Recently obtained results were indicating a pronounced influence of moisture cycling on the creep and duration of load performance of structural composites such as LVL.

IUFRO groups S5.01 (material properties) and S5.02 had recently formed a new working group concerned with non-destructive testing.

g) CIB-W85

DR OHLSSON reported on the activities of CIB-W85 'Structural serviceability'. He explained that the objective of W85 is to provide information relevant to the structural serviceability of buildings with special attention to structural design. The structural serviceability includes those aspects of building serviceability which are mainly governed by the load-bearing structure and its properties. Deformations and vibrations, and damage to non-structural components are the main phenomena of concern.

Four sub-groups are under formation within W85. These are: Serviceability requirements; Design concepts; Deformations of floors and roofs; Floor vibration. The current work programme includes the preparation of a state-of-the-art document, with chapters corresponding to each of the sub-groups listed above. Three meetings have taken place since 1990. An international colloquium is planned to take place in Göteborg, Sweden, on June 9-11 1993. Themes include performance requirements for structural serviceability; design concepts; service loads, and serviceability aspects on whole structural systems.

h) Joint Committee on Structural Safety (JCSS)

No report was available on JCSS, since currently CIB W18 does not have representation.

i) 1993 CIB-W18 Meeting, Atlanta, Georgia

DR O'HALLORAN announced that CIB-W18 would be welcome to meet in the USA in 1993. He had been investigating the possibility of the University of Georgia, Athens, near Atlanta, as the venue. Convention facilities, accommodation and tourist facilities were described.

Suggestions for further years' meetings included Cairns, Australia, in association with a Pacific Timber Engineering Conference in 1994, and Copenhagen in 1995.

3. REPORTS FROM SUB-GROUPS

a) Derivation of Characteristic Values for Panel Products

No report was available. MR SUNLEY mentioned that the topic related to a subject covered in a paper he was presenting (25-17-2), although he made it clear that he had not been intended to contribute to the Sub-Group.

b) Stability of Structures

PROFESSOR BRÜNINGHOFF reported that this Sub-Group had been unable to meet since the last CIB-W18. However, in the final stages of preparing the EC5 draft it had been noted that several queries regarding clauses concerned with stability had been thrown up. It was proposed, therefore, that the existence of the Sub-Group should be kept on record.

c) Punched Metal Truss Plates

PROFESSOR STERN reported that the Sub-Group had prepared a terminology dealing with the field of punched metal truss plates. A meeting concerning truss plates would shortly be taking place in Kirov, Russia. There was some discussion of the relevance or otherwise of this terminology work, with MR LARSEN suggesting that it would be preferable to direct work towards preparing an international test and evaluation standard.

d) Reliability Based Design (RBD)

There was little to report, although it was noted that a report on RBD had recently been issued as the result of a NATO Workshop on the topic.

4. CONNECTIONS MADE USING PUNCHED METAL PLATE FASTENERS

The following abstracts very briefly the papers which were presented in this subject area, and reports the ensuing discussions:

Paper 25-7-5 "35 years of experience with metal connector plates" was presented by PROFESSOR STERN. It listed 225 publications dealing with such devices. The author described other types of connection device and plates, a number of which have survived in structures more than 35 years old. Improved devices have proliferated in recent years. The industry, as represented for example by the Truss Plate Institute, continues to conduct research.

In answer to a question by DR ROUGER concerning apparent recovery of deflection in one of the author's diagrams, PROFESSOR STERN pointed out that this phenomenon had been observed. It was attributed to changes in humidity causing creep recovery.

Paper 25-14-2 "Design values of anchorage strength of nail plate joints by a two curve method and interpolation" was presented by DR KANGAS. This described a continuation of research covered by a paper presented at CIB-W18 in 1991 (24-7-1). The new paper led to the derivation of design values for anchorage strength, based on a two-curve method of data analysis, and an interpolation procedure for design purposes. Conclusions included the observation that the influence of an angle parameter was not as pronounced as previously thought for the plates in question. This would affect proposals in the EC5 draft. Other angle parameters, however, were more important. A conservative interpolation rule was presented in the paper, together with a revised proposal for EC5.

DR McLAIN asked whether the lack of influence of one of the factors mentioned would be dependent upon the particular plate design. The authors answered that, although three types of plate had been tested, it was possibly as DR McLAIN had suggested. It was not possible to be more definite. It was also questioned whether different angle interactions might be obtained in higher density timbers. Again, this was unknown, as the tests had mainly been concerned with Nordic timbers of a typical density and quality. DR OHLSSON asked whether the interface between the timber members was always especially controlled in the tests and, if so, whether the authors believed that this was a conservative procedure. The answer to both parts of this question was in the affirmative.

Paper 25-14-1 "Moment anchorage capacity and rotational stiffness of nail plates in shear tests" was also presented by DR KANGAS. It described moment anchorage stress calculations which were made essentially by means of elastic theory, with plastic yield taken into account by means of a coefficient. A more comprehensively plastic yield based method devised by DR NOREN had also been assessed. The results of 220 shear tests were used to compare the methods. Eleven different nail plates had been included in the tests. To compare tests with the two theories, tables had been included in the paper, listing a comparison index, with unity representing perfect agreement. Observations and conclusions included the following : only in certain types of plate did contact occur between the timbers, prior to failure; long, narrow plates had the greatest rotation tendency; the presently proposed EC5 method was conservative in all cases, especially for long plates; the proposed simplified plastic theory calculations are easier and simpler to perform than the EC5 proposal, and are therefore recommended.

MR LARSEN questioned whether the investigation had included a critical review of other procedures and research papers, since it was important to know this, if a change to the EC5 draft was to be considered. The author confirmed that this was so and also said that both the anchorage failures and the plate buckling failures had been taken into consideration in developing the formulae. It was felt, therefore, that the proposal covered all the important parameters in plate design. A discussion ensued on the extent of tests that would be necessary to obtain European Technical Approval for a particular design of plate. The participants in the discussion, including MR LARSEN and DR AASHEIM, elucidated the parameters which would have to be evaluated for such a purpose.

5. SIZE EFFECTS

The paper 25-6-5 "Size effects for timber" by DR BARRETT was presented by MR FEWELL. A brittle fracture model was evaluated for predicting the variation in bending, compression and tension parallel to the grain strength of visually graded timber. Relationships between width factor, length factor and a constant ratio size factor were introduced. Predictions from the model were compared with published data. Some north American data gave sufficient information for a separate analysis of the length effect. The research suggested that width or depth effects are masked in many sets of test data, because of difficulties in sample matching, grade variations with size and inadequacy of sample sizes. MR FEWELL pointed out the importance of the final conclusion in relation to CEN standard and EC5 drafting. This was that for international harmonization of procedures for adjusting tension, bending and compression strength properties, the width and length size factors can be taken as equal. For bending and tension, $S_W = S_L = 0.2$. For compression, $S_W = S_L = 0.1$.

DR COLLING asked why it was thought that the European data which were analyzed showed different size effects. Also, he asked whether larger section softwood sizes as used in Germany, for instance, had been analyzed. MR FEWELL said that larger sizes of British-grown softwood had been included in the study, although very thick timbers had not been examined.

MR LARSEN observed that, if length effects were to be introduced specifically into code design procedures, then the implication might also be that there would have to be loading configuration factors in the code, as well. This would lead to considerable complications in design. MR FEWELL felt that there was insufficient agreement amongst researchers as to the nature of the latter to consider their introduction at present.

During these discussions on length and configuration factor effects, PROFESSOR MADSEN made a short presentation on an assessment which he had made of the topic. For bending, he had considered the effect of the moment distribution along the length of the member in relation to studies by A I JOHNSON, Swedish State Committee for Building Research, 1953. PROFESSOR MADSEN showed that it is possible to produce a table of factors for adjusting design strength for load conditions and length to 'standard' conditions.

DR OHLSSON speculated that if ever it became necessary to have so many separately-identified 'adjustment factors' to simple bending theory in design, then it would be very difficult to convince students when teaching structural engineering that, in the simplest model, timber is a straightforward linear elastic material. Perhaps a completely fresh basis for design theory would be necessary.

6. EUROCODE 5 PART 1 AND CEN SUPPORT STANDARDS

MR LARSEN presented paper 25-102-1 "Latest development of Eurocode 5". It was explained that the choice of load factors to be used in conjunction with EC5 had been dictated by writers of other structural materials codes. Furthermore, there was only limited scope for selection of the partial safety factor for materials. A value lower than 1.3 for this would be unlikely to be found acceptable. It was important to study the influence of representative values for variable actions upon load cases, since factors associated with these could have a significant influence upon the economy of the design. Combinations of actions with variable time durations had still not been dealt with to full effect in the EC5 draft.

The method of dealing with depth factors for glulam in both the drafting work on the code and in the associated prEN draft had proved controversial. MR LARSEN felt that a workable solution had now been proposed. However, he still felt that it could not be claimed that design values for glulam were based on any fully accepted and satisfactory theory.

Long discussions had taken place on deflection limits and definitions of deflection, taking into account allowance for creep. In referring to characteristic values, the EC5 draft made use of CEN standards. However, the level of confidence for the fifth-percentile values was now stated in the code itself.

Many final national comments and requests for clarification of draft clauses were expected before the CEN TC250 SC5 meeting in November. However, some pertinent items of the discussion on the EC5 draft which arose from MR LARSEN's presentation were as follows.

MR FEWELL felt that some of the examples given in the table giving modifications related to load duration were misleading. There was a case which inferred that imposed loads could be stipulated as having one particular duration, whereas this was not really so.

DR COLLING commented that he did not agree with the explanation of dissent over glulam design values, which was said to be due to lack of sufficient data. He felt that there were sufficient data, such as a large, recent series of Norwegian beam tests, whose results could be matched well by the Karlsruhe glulam beam model.

The paper 25-102-2 "Control of deflections in timber structures with reference to Eurocode 5" was presented by DR THELANDERSSON. He explained that the studies leading to the paper had arisen as an extension of earlier work at his university on the influences of moisture on creep deflections. The studies had now become more general. New principles and criteria for serviceability aspects of design were now being suggested. Serviceability load combinations could be defined into one of three categories. These were either 'rare combinations', 'frequent combinations' or 'quasi-permanent combinations'. The latter were time-averaged values derived from all permanent and variable loads. Newly recommended deflection limits were included in the paper. Sensitivity studies had been performed on the effect of adopting these as design measures. A less strict criterion was suggested for situations where deflection needed to be limited for reasons of general utility and appearance as opposed to those cases where there was a serious risk of deformation causing damage to other material within the building fabric.

It was also believed that it was now possible to allow for the effects of creep in design more conveniently through adoption of the 'quasi-permanent' load concept. Numerical values for k_{def} were proposed in the paper.

In discussing the paper, MR LARSEN pointed out that EC5 states the principle that serviceability design should include steps to ensure that damage to surrounding material is avoided. He questioned whether it was possible to translate such a principle into firmly stated and fixed deflection limits. The senior author agreed in general with MR LARSEN's views. However, he felt that it was important to give designers examples of suitable values that might be chosen.

DR OHLSSON welcomed the paper, commenting that the topic had been in serious need of attention by timber researchers. Deflections which only occur for short periods may be more acceptable to building owners or users than those which take place more slowly or permanently. Also, it had become well recognised in the concrete industry that local relative differences in levels may be a nuisance. It had been found that it had become necessary to stipulate tolerances on designed pre-cambers. Some performance criteria, such as window-jamming, were fairly material independent, he felt, and limits adopted for other material codes should be considered.

DR CECCOTTI congratulated the authors on a rational paper. He agreed with the suggested approach to k_{def}. He felt, however, that the concept of 'quasi-permanent' load combinations was somewhat strange and difficult to justify.

The paper 25-6-1 "Moment Configuration Factors" was presented by DR CANISIUS. The principles set forth in the paper would need to be considered, if length effects were to be adopted in codes such as EC5.

DR THELANDERSSON commented that there seemed to be a marked sensitivity to the length of the element assumed in the model. He noted that beams with overhang, and continuous beams where strength rather than stiffness governs design, would be strongly influenced in design by the author's suggestions.

MR LARSEN noted that the model uses constant lengths between simulated knots. He felt that it would be difficult to expect good correlation with test results, if adopting such an assumption. DR COLLING also commented on this, and suggested that element lengths more in the order of 150 mm would be preferable. The author noted these comments and said that he wished to attempt to improve the model.

Paper 25-6-4 "On design criteria for tension perpendicular to grain" was presented by DR PETERSSON. The author explained that it dealt with problems where tension perpendicular to grain would be critical in design. The approach was by means of applied fracture mechanics. The background and theory were given in the paper. A difficulty at present appears to be that fracture energy input data for design are not readily available. Present design recommendations for components such as end-notched beams may give the coarsest of guidance. The correlation between fracture energy and density amongst timbers also seems rather poor. The author had found a reasonable basis in GUSTAFSSON's proposals for a test method and for data derivation for EC5. He warned that failure of an end crack in shear is a sudden phenomenon. Hence, one of the fracture parameters needs to assume radically different values, dependent upon whether or not crack propagation occurs.

In discussions on the paper, PROFESSOR EHLBECK observed that the theory and experiments were all restricted to short-term conditions. The author agreed that difficult questions remain unanswered about the influence upon fracture behaviour of longer-term loading and effective reductions in stiffness due to mechano-sorptive creep phenomena. PROFESSOR RANTA-MAUNUS questioned how a decision was made over the value of one of the fracture toughness parameters used in the analysis. It seemed to vary quite radically from 0.5 to 1.0. The author stated that this parameter had been set to values determined in part by judgement, although there was some justification. It is known from other situations, where a suddenly-removed support gives rise to a dynamic force being applied to a member, that this has an influence approximately double the effect of a comparable static load effect. DR COLLING commented on the desirability of analysing glulam ultimate strength behaviour using fracture mechanics. For example, he felt that length effects in glulam beams had to do with the relative volumes over which cracks may propagate in various beams. On the other hand, there were many features of real glulam that would require modelling, such as changes of properties at each finger joint, as well as differences between adjacent laminations. PROFESSOR BRÜNINGHOFF pointed out that researchers should not, however, be deterred. There had been numerous cases in Germany of curved glulam beams failing after periods of ten to fifteen years in service, usually in the spring following a heavy winter snow load.

The paper 25-7-2 "Softwood and hardwood embedding strength for dowel type fasteners" by PROFESSOR EHLBECK and MR WERNER was presented by the latter.

In addition to the quite extensive range of species and hence characteristic densities covered in former test programmes by TRADA and others, further timbers had been added and incorporated in the results analyzed in the paper. Softwood and hardwood embedding strengths now appeared to have been investigated over the full range of timbers likely to be used in structures. Embedding strength relationships had also been established at varying grain angles due to the new work reported here. It was pointed out by the authors that the formulae presented in the paper were only applicable to dowel-type fasteners with round section and a smooth finish. In the discussions, DR KOMATSU mentioned that similar tests in Japan had included tension perpendicular arrangements. PROFESSOR EHLBECK wondered how such tests could avoid the complication of brittle fracture in transverse tension, thus negating a true embedment property. MR METTEM questioned the use of the term 'sensibility' in relation to the splitting propensity of some timbers. Older types of test indicating proneness to splitting, such as cleavage, had shown that dense timbers did not necessarily split more easily, especially if having interlocked grain, such as Ekki. MR LARSEN commented that ideally true material parameters should be aimed for in any such tests. Most of those involved in the discussions agreed, although nobody could suggest a more 'pure' material parameter than that indicated by the embedment test.

DR OHLSSON reminded any researchers planning or conducting embedment tests or similar fastener tests that, due to the need for earthquake design data, upper-bound parameters should be reported, as well as characteristic values. It was often necessary to have such information when calculating the energy dissipation potential of groups of fasteners.

Paper 25-7-6 "Characteristic strength of split-ring and shear-plate connections" was presented by PROFESSOR BLASS. It was explained that a calculation model had been developed, describing the load carrying capacity of split-ring and shear-plate connectors. Old test data had been re-evaluated, to assess how well the model described such results. The model assumes a block shear failure mode for joints loaded in tension. The influence of the bolt on the load-bearing capacity is neglected. Joints loaded at angles to the grain had also been examined, and compression loading had been considered. It was hoped that the results of the evaluation might serve as a basis for determining characteristic values for publication in a European standard under preparation. The work related to discussions which are taking place in Working Group 4 of CEN TC124. It was explained by the presenter that connector spacing rules, member thickness effects and similar variations were not considered in the paper. These would have to be covered by additional rules which would be devised for EC5.

PROFESSOR MADSEN and PROFESSOR STERN both made comments on the latter aspect, during the discussions on the paper. Evidently, in North American codes, quite significant reduction factors are applied when a number of connectors act in line to resist tension forces. DR McLAIN said that under a current draft revision, the US code may be introducing more severe penalties for groups of connectors. Increased connector stiffness seemed to make the situation worse.

Paper 25-7-7 "Characteristic strength of tooth-plate connector joints" was presented by the same author, covering a similar theme, but for tooth-plate connectors. With this type, it had not been possible to develop a 'mechanical calculation model', since it had to be recognised that significant load-sharing occurs, between the connector and the bolt, before full failure develops. Comparisons had been made between a set of proposed empirical formulae for characteristic strengths, and Dutch test results, plus adjusted information taken from existing Dutch and German codes. The model assumes a load-sharing between the bolt and the tooth-plate connector.

In answer to a question from PROFESSOR STERN, it was confirmed that these types of connector were still used quite extensively in various European countries. As with the split-ring and shear-plate characteristic strengths paper, described above, it was intended that this work would be disseminated via WG4 of CEN TC124. Additional information on the performance of these types of connector would be welcomed by those involved in the Working Group.

Paper 25-7-9 "Determination of k_{def} for nailed joints" was presented by the author, MR van de KUILEN. It dealt with a deformation factor, which could be proposed for use in design with codes such as EC5, and which would adjust the calculated instantaneous deformation of nailed joints for conditions of loading such as permanent load, and for designated service classes. The creep equations proposed in the paper were based on tests which were started in Delft University in 1962, and which were extended in 1983. A range of load levels had been incorporated in these tensile creep tests.

The discussions on this paper were concerned mainly with mechano-sorptive influences on the creep of mechanically fastened joints. PROFESSOR EHLBECK asked how the author felt that the laboratory environment in which the creep tests had been taking place compared with other conditions that EC5 designers would normally treat as Service Class 2. The author felt that, although he recognised that deformation factors in codes need not necessarily be quite so severe as research would suggest, due to influences such as the intermittent nature of high loads in real structures, nevertheless the k_{def} values in EC5 draft, for nailed joints, ought to be increased.

The paper 25-7-10 "Characteristic Strength of UK Timber Connectors" was presented by MR METTEM. The paper described work which had been carried out to review the basis for permissible loads for connectored joints in BS 5268, and to re-assess the test data upon which the permissible stress design code had been based, so that characteristic strength equations could be produced. Ring connectors, plate connectors and toothed-plate connectors had all been covered.

Formulae had been developed for calculating characteristic load-carrying capacities parallel to the grain. The formulae allowed for the size and shape of each type of connector, and for the density and thickness of the timber. References were given to the origins of the test data. For ring connectors, some tests on dense Malaysian hardwoods had been reviewed. Results from the proposed formulae were compared with nominal characteristic values derived from the basic loads tabulated in the British timber design code. The comparison indices were nearly all within ten percent of unity.

PROFESSOR EHLBECK commented that it was very encouraging to note that this work, which like that of papers 25-7-6 and 25-7-7 related to the WG4 discussions, was showing good agreement between British, Dutch and German proposals. There was some discussion on the influence of very high density timbers on the performance of connectored joints. It was agreed that modes of failure such as rupture of the connector itself should be provided for. The author stated that a programme of confirmatory tests was being planned, to make a direct assessment of the formulae proposed, in addition to the old data upon which they are presently based.

Papers 25-7-11 and 25-7-12 dealt with a literature and code review, and a series of tests respectively, on multiple-fastener bolted joints. Bolted joints in European whitewood glulam with steel side plates had been tested, and a finite element model had also been used. It was pointed out in the first paper that, although EC5 requires it to be taken into account that the load-carrying capacity of a multiple-fastener joint will be less than the sum of the individual fastener capacities, the modifications for this effect in the application rules given in the draft code are remarkably modest. For example, for one to six bolts in line, no reduction is recommended by EC5, and even for nine bolts, a reduction of only 0.89 is obtained by the relevant code formula. Much larger reductions had been found by the authors, in North American codes, for example. A previous CIB paper (20-7-3) was also cited, which had led to larger reductions than those given in EC5, for bolts with glulam, in the Japanese code.

The tests and analytical investigations in paper 25-7-12 showed that the proportions of load carried by four bolts, compared with a single bolt joint, were very uneven, especially in the perpendicular to grain case. Deductions from the combined results of testing and analysis led the authors to recommend a reduction factor of 0.5 for four bolts loaded perpendicular to the grain, when steel plates were used in conjunction with bolts and glulam.

During the discussions, it was explained that the analysis was purely within the elastic range, and that the matching test arrangements had deliberately been planned to be as near-perfect as possible. For example, precisely aligned holes had been used, and the specimens were of a type in which embedment failures would occur. Previous researchers, including those referenced in the review, had adopted a different approach, and had deliberately tested 'real' bolt assemblies.

The result of this had been that extremely variable load distributions from one bolt to another had been measured. It was agreed that the ratio of member thickness to bolt diameter also affected the load distribution. This had been covered in the research by YASUMURA, and was reflected in formulae in the Canadian code for example. PROFESSOR EHLBECK commented that he would like to see the results of further testing, in which loading was carried to failure, and plastic re-distribution amongst the bolts was considered. This would be more likely to convince the EC5 drafting panel to change the rules.

The paper 25-12-1 "Determination of characteristic bending values of glued laminated timber, EN approach and reality" was presented by PROFESSOR GEHRI. The paper discussed the analytical models used for the bending strength of glulam in developing the clauses given in EN TC124.207 'Glulam strength classes and characteristic properties'. The coefficients used in equations to allow for the influence on bending strength of the finger joints in the laminations were reviewed. Size effects were also reconsidered, the author arguing that both the length and the depth of the beam should be allowed for, when adjusting strengths found from tests, on glulam at other than the reference depth. Tests previously conducted at the Federal Institute of Technology in Zürich had been reviewed in the light of the EN proposals. It was concluded from these studies that the EN draft proposal led to an over-estimate of the wood strength of the unjointed laminations of 25%. Also, there was an over-estimate of the finger joint strength, by 40%. Alternative proposals for the relevant EN equations were suggested.

During the discussions on this paper, MR LARSEN stated that the drafters of the EN had, in general, adopted proposals in previous CIB papers. It was necessary to achieve consistency between the production standard for glulam and the EN listing the strength classes. The drafting committee had agreed not to include depth factors in the EN, in the case of beam depths less than 600 mm. DR COLLING felt that the Swiss tests had shown unusually weak finger joints, in relation to the reported moduli of elasticity of the associated laminations. Reference was made to a succeeding paper on the agenda, by DR AASHEIM and DR FALK, on a large test series on Norwegian glulam. In view of the interest in the topic during the discussions, and the fact that minds were focused on the subject, it was decided to treat this out of agenda order.

Paper 25-10-1 "The strength of Norwegian glued laminated beams" was presented by DR FALK. The paper dealt with the characterization and the performance of glulam beams manufactured from machine stress graded Norwegian spruce. The results were analyzed in relation to the proposal for glulam strength classes and determination of characteristic properties which are being developed as a draft CEN standard. Material testing was carried out on the parent population of laminations. These tests indicated that the laminating timber, which consisted of Norway spruce, could be represented by two of the proposed EN strength classes. There was approximately an even share of the grade yield between each of the two classes. Beams constructed from these grades were laid up into three different beam combinations, two homogeneous layups and one combined layup. Tests on the beams confirmed that in general all of the beams failed as expected, by tension in the outer lamination. The locations of all finger joints were carefully recorded.

At the fifth percentile level, the better grade, homogeneous layup had a similar strength to the combined layup. The ratio of the characteristic strength of the beams to that of the finger joints was similar to the value 0.8, found previously in other tests by COLLING.
There was some discussion, in relation to the Norwegian glulam beam tests, of the precise machine grading techniques used to pre-select the laminations. DR FALK agreed with MR FEWELL's suggestion that higher precision grading machines, possibly used with more enhanced software, could further improve the performance of glulam containing machine graded timber, provided that finger joint performance could also be raised to match. DR AASHEIM explained that the data from the project were still being analyzed, using both the 'Karlsruhe Model' and the US 'PROLAM Model'. A full report would in due course be available from the Norwegian Institute of Wood Technology.

The paper 25-17-2 "A body for confirming the declaration of characteristic values" was presented by MR SUNLEY. It was explained that, although the chief objective of the Single European Act is to produce an open market, most of the current activity in the construction sector is aimed at implementing the Construction Products Directive. As a result, regulatory matters appear to be taking precedence over the aim of free trade.

An outline solution proposed by the paper was to set up an independent organization free from EC or national government control which would be able to approve grading bodies, grading machines and the allocation of characteristic values for timber materials, etc. Possible bases for such organizations were, the author suggested, CIB/W18, CEN committees, Eurowood and EOTC. The latter would depend upon clarifying the aim of the organization.

During the discussions, MR LARSEN spoke strongly in favour of considering EOTC for the role. However, he felt that the approval requirements discussed in the paper could not be satisfied by a body whose membership is voluntary. Also, he considered that it would have to be set up in such a manner that the producers of the goods would pay for the administration of approvals.

The author did not agree that the role could not be fulfilled by a body, membership of which would be voluntary. There were precedents in the UK. Further discussions included the proposition that various producers might claim that materials or products that were inherently similar or identical belonged to different EN material property classes, according to national interpretation of standards or even commercial bias. It was agreed that an informal group would discuss the subject, and that its members would exchange correspondence. The author of the paper took note of the proposed group membership.

7. FIRE

Paper 25-16-1 "The effect of density on charring and loss of bending strength in fire" was presented by its author, DR KÖNIG. The paper described studies on the influence of density on the charring of timber exposed to standard fire conditions. Effective and measured charring rates varied by about 10 per cent in the density range of softwoods from 290 to 420 kg/m^3. There was no influence of density on the loss of bending strength.

During the discussions, DR COLLING described various size effects that might be expected to have an influence on charring rates of a timber at a given density. MR METTEM mentioned that work carried out by TRADA some 18 years ago measured charring rates over a significant range of timbers with varying density. This had led to different charring rates for hardwoods being stated in the British code.

The second paper on fire topics, 25-16-2 "Tests on glued-laminated beams in bending at natural fire exposure" was also presented by DR KÖNIG. A series of fire tests with so-called natural fire exposure (increasing temperature and a cooling period, see paper for details) had been carried out on glulam beams. The time-temperature relationship was determined by an energy balance method. Fire load densities were varied, together with assumed areas of openings. The tests showed that there was a loss of strength and stiffness in the residual cross sections of the beams. These losses continued through the cooling period. They were ascribed to heat flow within the cross-section. In discussing the paper, DR THELANDERSSON remarked that the opening factor design method has considerable complications. 'Natural' fire curves were developed through calibrations against laboratory tests which were performed in small, cubic ovens. The assumed opening factor has a big influence on the resulting calculations, but he believed that evidence from the measured results of real fires in actual buildings did not support this effect.

8. OPEN FORUM

Papers 25-6-3 "Bearing capacity of timber" was presented by DR KORIN. It described work which was being continued on the basis of a paper presented at CIB W18A in 1990. Tests were being conducted using small clear specimens, and also structural-sized test pieces of varying species of softwood. Differing widths of bearing were being assessed. PROFESSOR MADSEN drew attention to remarks on compression perpendicular to grain published in his recent textbook.

Paper 25-7-4 "A guide for application of quality indexes for driven fasteners used in connections in wood structures" was presented by PROFESSOR STERN. Quality indexes for driven fasteners were originally developed for the design of pallets. The paper explained how the principle could be extended to cover the use of factors in a wider range of structural companies. The Chairman thanked the author for the clarity of his paper and exposition; there were no questions.
Paper 25-7-8 "Extending yield theory to screw connections" was presented by DR McLAIN. In this paper, new design criteria for lag screw or coach screw connections to timber members were proposed. The theory was based on the yield theory method for dowel-type fasteners which have been adapted for EC5. A fixed ratio R of the yield moment in the screw thread to that in the shank was assessed in order to produce three simplified evaluations covering a wide range of geometry. Alternative methods of arriving at simplified formulae were considered including an "effective diameter" basis. In discussions on the paper, PROFESSOR EHLBECK commented that this effective diameter procedure had also been considered for some of the Eurocode formulae. In answer to a question of MR METTEM on the proposed procedure in the US Design Code (under revision) for a number of lag screw fasteners in line, fixing steel side plates to glulam or timber, the author commented that a reduction factor would be included similar to that proposed for a number of bolts in line.

Paper 25-8-1 "Analysis of glulam semi-rigid portal frames under long-term load" was presented by DR KOMATSU. Analysis by means of the minimum energy principle and the virtual work method was conducted on portal frames which contained mechanically fastened haunch joints. Testing was also carried out, and good agreement between test and prediction was obtained, particularly in the case of nailed joints. During the discussions, DR THELANDERSSON commented that the long-term behaviour of such frames might be affected by variable climatic conditions. Test conditions were such that a normal laboratory environment was involved.

Paper 25-9-2 "DVM analysis of wood" was presented by DR NIELSEN. It set out theoretical methods based upon a combination of visco-elastic creep theories and fracture mechanics principles, to describe the entire behaviour of wood as an engineering material. Time dependency under load is related to wood quality; short-term strength is related to time under load, and life expectancy of wood under stress is influenced by strength distributions.

PROFESSOR RANTA-MAUNUS asked the author which method he preferred for dealing with the influences of changing moisture content on the DVM model. This was said to have been dealt with in one of the author's recent papers delivered at IUFRO/S5.02 'Timber Engineering Meeting', Bordeaux 1992. Answering a question by MR van de KUILEN on how to deal with non-linear crack propagation effects related to very short duration of failure, the author agreed that these are very difficult to measure due to the masking of such effects by the stiffness of the testing machine itself.

Paper 25-10-2 "Influence of elastic modulus on the simulated bending strength of hyperstatic timber beams" was presented by DR CANISIUS. The importance of considering lengthwise variation of the elastic modulus in calculating the strength of statically intermediate beams was discussed. After the presentation of the paper some remarks were made on the length of the effectively simulated segments in the analysis, in relation to segments of real timber stressed in a grading machine. MR FEWELL said that it was hoped that in future more precise simulations could be achieved by using models containing more elements.

Paper 25-13-1 "Bending strength and stiffness of Izopanel type plates" was presented by DR MIELCZAREK. The purpose of the investigations described was to investigate the strength, stiffness and rheological behaviour of composite panels acting under load perpendicular to their surface. Answering a question from DR CANISIUS, the author agreed that low shear stiffness might be influencing creep behaviour adversely under certain conditions. He said that in future, tests would be included to check on this.

Paper 25-15-1 "Structural assessment of timber framed building systems" was presented by DR KORIN. It described steps that are being taken in Israel to introduce the option to developers of using timber framed housing as an alternative to reinforced concrete structures and block masonry. Steps to draw up performance specifications and a list of items requiring design approval were discussed.

Paper 25-15-2 "A simplified theoretical analytic method for timber beams-columns" was not presented, as the author was unable to attend.

Paper 25-15-3 "Mechanical property of wood-framed shear walls subjected to reversed cyclic lateral loading" was presented by DR YASUMURA. Timber framed shear walls sheathed in various ways were subjected to reversed cyclic lateral loading. The walls were classified into three groups according to their potential seismic resistance capacity. In answer to a question from DR CECCOTTI, the author said that equivalent viscous damping factors were compiled for each type of sheathing investigated. The evd factor ranged from 15 to 20%, depending on the construction. It remained about constant irrespective of sheathing type once a certain number of reversed cycles had been achieved.

Paper 25-17-3 "Moisture content adjustment procedures for engineering standards" was presented by DR GREEN. This paper discussed alternative analytical models which had been developed at the US Forest Products Laboratory for adjusting modulus of elasticity and modulus of rupture values from test results to values suitable for use in design. Five species had been tested, each in two grades and at three levels of conditioned moisture content, to evaluate alternative models. One of the simpler models for MOE adjustment that the tests showed to have been justified was that given in ASTM D1990. In answer to a question by MR SUNLEY on whether the well-known theory of B. Madsen that lower grades were less influenced by moisture content changes was upheld, the author said that this was so. Since there are certain applications for structural timber where it is more efficient to use lower grades, he felt it was important to include them in such research.

9. ANY OTHER BUSINESS

The relative inactivity of the CIB W18 Sub-Groups (see Minutes, item 3) was discussed. The causes related to travelling difficulties under harsh economic circumstances, were understood. It was felt that rather than deciding to abandon the sub-groups immediately, their aims and ability to function should be reviewed again at CIB W18, 1993 meeting. This suggestion by the Chairman was welcomed and generally agreed.

10. VENUE AND PROGRAMME FOR NEXT MEETING

Following preliminary discussions earlier in the meeting (see Item 2i), the invitation was accepted which was offered by DR O'HALLORAN of APA to organize, in collaboration with F.P.L. MADISON, a meeting at the University of Georgia, Athens, near Atlanta. The proposed dates were 21 - 26 August 1993. Outline plans for CIB W18 meetings in subsequent years were also discussed. Suggestions included a meeting related to the Pacific Timber Engineering Conference, Queensland, Australia, which is taking place 11 - 15 July 1994. In 1995, a meeting of CIB W18 may be planned to take place in Copenhagen, in April of that year.

Topics for CIB W18, 1993, were discussed and the following list was agreed:

Reconstituted wood-based products, including panel products and structural members.

Structural Eurocodes, including EC5.

Serviceability considerations in structural timber design.

Seismic design in timber.

Mechanical timber joints.

General topics.

11. CLOSE

PROFESSOR BLASS thanked all participants and authors for their lively contributions and discussions. Appreciation was expressed to the staff of Hotel Åhus Strand for an exceptionally agreeable and well-run venue.

DR KÖNIG and his fellow Swedes were again thanked for all the smoothly run meeting arrangements and the interesting technical and social visits.

The Chairman then closed the 25th Meeting of CIB W18, and said that he looked forward to seeing members in Georgia, USA in 1993.

12. List of CIB-W18 Papers, Åhus, Sweden 1992

12. LIST OF CIB-W18 PAPERS, Åhus, Sweden 1992

25-6-1	Moment Configuration Factors for Simple Beams- T D G Canisius
25-6-3	Bearing Capacity of Timber - U Korin
25-6-4	On Design Criteria for Tension Perpendicular to Grain - H Petersson
25-6-5	Size Effects in Visually Graded Softwood Structural Lumber - J D Barrett, F Lam and W Lau
25-7-2	Softwood and Hardwood Embedding Strength for Dowel type Fasteners - J Ehlbeck and H Werner
25-7-4	A Guide for Application of Quality Indexes for Driven Fasteners Used in Connections in Wood Structures - E G Stern
25-7-5	35 Years of Experience with Certain Types of Connectors and Connector Plates Used for the Assembly of Wood Structures and their Components- E G Stern
25-7-6	Characteristic Strength of Split-ring and Shear-plate Connections - H J Blass, J Ehlbeck and M Schlager
25-7-7	Characteristic Strength of Tooth-plate Connector Joints - H J Blass, J Ehlbeck and M Schlager
25-7-8	Extending Yield Theory to Screw Connections - T E McLain
25-7-9	Determination of k_{def} for Nailed Joints - J W G van de Kuilen
25-7-10	Characteristic Strength of UK Timber Connectors - A V Page and C J Mettem
25-7-11	Multiple-fastener Dowel-type Joints, a Selected Review of Research and Codes - C J Mettem and A V Page
25-7-12	Load Distributions in Multiple-fastener Bolted Joints in European Whitewood Glulam, with Steel Side Plates - C J Mettem and A V Page
25-8-1	Analysis of Glulam Semi-rigid Portal Frames under Long-term Load - K Komatsu and N Kawamoto

25-9-2 DVM Analysis of Wood. Lifetime, Residual Strength and Quality - L F Nielsen

25-10-1 The Strength of Norwegian Glued Laminated Beams - K Solli, E Aasheim and R H Falk

25-10-2 The Influence of the Elastic Modulus on the Simulated Bending Strength of Hyperstatic Timber Beams - T D G Canisius

25-12-1 Determination of Characteristic Bending Values of Glued Laminated Timber. EN-Approach and Reality - E Gehri

25-13-1 Bending Strength and Stiffness of Izopanel Plates - Z Mielczarek

25-14-1 Moment Anchorage Capacity of Nail Plates in Shear Tests - A Kevarinmaki and J. Kangas

25-14-2 Design Values of Anchorage Strength of Nail Plate Joints by 2-curve Method and Interpolation - J Kangas and A Kevarinmaki

25-15-1 Structural Assessment of Timber Framed Building Systems - U Korin

25-15-3 Mechanical Properties of Wood-framed Shear Walls Subjected to Reversed Cyclic Lateral Loading - M Yasumura

25-16-1 The Effect of Density on Charring and Loss of Bending Strength in Fire - J König

25-16-2 Tests on Glued-Laminated Beams in Bending Exposed to Natural Fires - F Bolonius Olesen and J König

25-17-2 A Body for Confirming the Declaration of Characteristic Values - J Sunley

25-17-3 Moisture Content Adjustment Procedures for Engineering Standards - D W Green and J W Evans

25-102-1 Latest Development of Eurocode 5 - H J Larsen

25-102-1A Annex to Paper CIB-W18/25-102-1. Eurocode 5 - Design of Notched Beams - H J Larsen, H Riberholt and P J Gustafsson

25-102-2 Control of Deflections in Timber Structures with Reference to Eurocode 5 - A Martensson and S Thelandersson

13. Current List of CIB-W18(A) Papers

13. CURRENT LIST OF CIB-W18(A) PAPERS

Technical papers presented to CIB-W18(A) are identified by a code CIB-W18(A)/a-b-c, where:

a denotes the meeting at which the paper was presented. Meetings are classified in chronological order:

1 Princes Risborough, England; March 1973
2 Copenhagen, Denmark; October 1973
3 Delft, Netherlands; June 1974
4 Paris, France; February 1975
5 Karlsruhe, Federal Republic of Germany; October 1975
6 Aalborg, Denmark; June 1976
7 Stockholm, Sweden; February/March 1977
8 Brussels, Belgium; October 1977
9 Perth, Scotland; June 1978
10 Vancouver, Canada; August 1978
11 Vienna, Austria; March 1979
12 Bordeaux, France; October 1979
13 Otaniemi, Finland; June 1980
14 Warsaw, Poland; May 1981
15 Karlsruhe, Federal Republic of Germany; June 1982
16 Lillehammer, Norway; May/June 1983
17 Rapperswil, Switzerland; May 1984
18 Beit Oren, Israel; June 1985
19 Florence, Italy; September 1986
20 Dublin, Ireland; September 1987
21 Parksville, Canada; September 1988
22 Berlin, German Democratic Republic; September 1989
23 Lisbon, Portugal; September 1990
24 Oxford, United Kingdom; September 1991
25 Åhus, Sweden; August 1992

b denotes the subject:

1 Limit State Design
2 Timber Columns
3 Symbols
4 Plywood
5 Stress Grading
6 Stresses for Solid Timber
7 Timber Joints and Fasteners
8 Load Sharing
9 Duration of Load
10 Timber Beams
11 Environmental Conditions
12 Laminated Members
13 Particle and Fibre Building Boards
14 Trussed Rafters
15 Structural Stability
16 Fire
17 Statistics and Data Analysis
18 Glued Joints
19 Fracture Mechanics
100 CIB Timber Code
101 Loading Codes
102 Structural Design Codes
103 International Standards Organisation
104 Joint Committee on Structural Safety
105 CIB Programme, Policy and Meetings
106 International Union of Forestry Research Organisations

c is simply a number given to the papers in the order in which they appear:

Example: CIB-W18/4-102-5 refers to paper 5 on subject 102 presented at the fourth meeting of W18.

Listed below, by subjects, are all papers that have to date been presented to W18. When appropriate some papers are listed under more than one subject heading.

LIMIT STATE DESIGN

TIMBER COLUMNS

SYMBOLS

PLYWOOD

9-4-2 The Evaluation of Test Data on the Strength Properties of Plywood - L G Booth

9-4-3 The Sampling of Plywood and the Derivation of Strength Values (Second Draft) - B Norén

9-4-4 On the Use of the CIB/RILEM Plywood Plate Twisting Test: a progress report - L G Booth

10-4-1 Buckling Strength of Plywood - J Dekker, J Kuipers and H Ploos van Amstel

11-4-1 Analysis of Plywood Stressed Skin Panels with Rigid or Semi-Rigid Connections - I Smith

11-4-2 A Comparison of Plywood Modulus of Rigidity Determined by the ASTM and RILEM CIB/3-TT Test Methods - C R Wilson and A V Parasin

11-4-3 Sampling of Plywood for Testing Strength - B Norén

12-4-1 Procedures for Analysis of Plywood Test Data and Determination of Characteristic Values Suitable for Code Presentation - C R Wilson

14-4-1 An Introduction to Performance Standards for Wood-base Panel Products - D H Brown

14-4-2 Proposal for Presenting Data on the Properties of Structural Panels - T Schmidt

16-4-1 Planar Shear Capacity of Plywood in Bending - C K A Stieda

17-4-1 Determination of Panel Shear Strength and Panel Shear Modulus of Beech-Plywood in Structural Sizes - J Ehlbeck and F Colling

17-4-2 Ultimate Strength of Plywood Webs - R H Leicester and L Pham

20-4-1 Considerations of Reliability - Based Design for Structural Composite Products - M R O'Halloran, J A Johnson, E G Elias and T P Cunningham

21-4-1 Modelling for Prediction of Strength of Veneer Having Knots - Y Hirashima

STRESS GRADING

STRESSES FOR SOLID TIMBER

19-6-5 Drying Stresses in Round Timber - A Ranta-Maunus

19-6-6 A Dynamic Method for Determining Elastic Properties of Wood - R Görlacher

20-6-1 A Comparative Investigation of the Engineering Properties of "Whitewoods" Imported to Israel from Various Origins - U Korin

20-6-2 Effects of Yield Class, Tree Section, Forest and Size on Strength of Home Grown Sitka Spruce - V Picardo

20-6-3 Determination of Shear Strength and Strength Perpendicular to Grain - H J Larsen

21-6-1 Draft Australian Standard: Methods for Evaluation of Strength and Stiffness of Graded Timber - R H Leicester

21-6-2 The Determination of Characteristic Strength Values for Stress Grades of Structural Timber. Part 1 - A R Fewell and P Glos

21-6-3 Shear Strength in Bending of Timber -U Korin

22-6-1 Size Effects and Property Relationships for Canadian 2-inch Dimension Lumber - J D Barrett and H Griffin

22-6-2 Moisture Content Adjustements for In-Grade Data - J D Barrett and W Lau

22-6-3 A Discussion of Lumber Property Relationships in Eurocode 5 - D W Green and D E Kretschmann

22-6-4 Effect of Wood Preservatives on the Strength Properties of Wood - F Ronai

23-6-1 Timber in Compression Perpendicular to Grain - U Korin

24-6-1 Discussion of the Failure Criterion for Combined Bending and Compression - T A C M van der Put

24-6-3 Effect of Within Member Variability on Bending Strength of Structural Timber - I Czmoch, S Thelandersson and H J Larsen

24-6-4 Protection of Structural Timber Against Fungal Attack Requirements and Testing - K Jaworska, M Rylko and W Nozynski

24-6-5 Derivation of the Characteristic Bending Strength of Solid Timber According to CEN-Document prEN 384 - A J M Leijten

25-6-1 Moment Configuration Factors for Simple Beams- T D G Canisius

25-6-3 Bearing Capacity of Timber - U Korin

25-6-4 On Design Criteria for Tension Perpendicular to Grain - H Petersson

25-6-5 Size Effects in Visually Graded Softwood Structural Lumber - J D Barrett, F Lam and W Lau

TIMBER JOINTS AND FASTENERS

1-7-1 Mechanical Fasteners and Fastenings in Timber Structures - E G Stern

4-7-1 Proposal for a Basic Test Method for the Evaluation of Structural Timber Joints with Mechanical Fasteners and Connectors - RILEM 3TT Committee

4-7-2 Test Methods for Wood Fasteners - K Möhler

5-7-1 Influence of Loading Procedure on Strength and Slip-Behaviour in Testing Timber Joints - K Möhler

5-7-2 Recommendations for Testing Methods for Joints with Mechanical Fasteners and Connectors in Load-Bearing Timber Structures - RILEM 3 TT Committee

5-7-3 CIB-Recommendations for the Evaluation of Results of Tests on Joints with Mechanical Fasteners and Connectors used in Load-Bearing Timber Structures - J Kuipers

6-7-1 Recommendations for Testing Methods for Joints with Mechanical Fasteners and Connectors in Load-Bearing Timber Structures (seventh draft) - RILEM 3 TT Committee

6-7-2 Proposal for Testing Integral Nail Plates as Timber Joints - K Möhler

6-7-3	Rules for Evaluation of Values of Strength and Deformation from Test Results - Mechanical Timber Joints - M Johansen, J Kuipers, B Norén
6-7-4	Comments to Rules for Testing Timber Joints and Derivation of Characteristic Values for Rigidity and Strength - B Norén
7-7-1	Testing of Integral Nail Plates as Timber Joints - K Möhler
7-7-2	Long Duration Tests on Timber Joints - J Kuipers
7-7-3	Tests with Mechanically Jointed Beams with a Varying Spacing of Fasteners - K Möhler
7-100-1	CIB-Timber Code Chapter 5.3 Mechanical Fasteners;CIB-Timber Standard 06 and 07 - H J Larsen
9-7-1	Design of Truss Plate Joints - F J Keenan
9-7-2	Staples - K Möhler
11-7-1	A Draft Proposal for International Standard: ISO Document ISO/TC 165N 38E
12-7-1	Load-Carrying Capacity and Deformation Characteristics of Nailed Joints - J Ehlbeck
12-7-2	Design of Bolted Joints - H J Larsen
12-7-3	Design of Joints with Nail Plates - B Norén
13-7-1	Polish Standard BN-80/7159-04: Parts 00-01-02-03-04-05. "Structures from Wood and Wood-based Materials. Methods of Test and Strength Criteria for Joints with Mechanical Fasteners"
13-7-2	Investigation of the Effect of Number of Nails in a Joint on its Load Carrying Ability - W Nozynski
13-7-3	International Acceptance of Manufacture, Marking and Control of Finger-jointed Structural Timber - B Norén
13-7-4	Design of Joints with Nail Plates - Calculation of Slip - B Norén
13-7-5	Design of Joints with Nail Plates - The Heel Joint - B Källsner

LOAD SHARING

DURATION OF LOAD

17-9-1	On the Long-Term Carrying Capacity of Wood Structures - Y M Ivanov and Y Y Slavic
18-9-1	Prediction of Creep Deformations of Joints - J Kuipers
19-9-1	Another Look at Three Duration of Load Models - R O Foschi and Z C Yao
19-9-2	Duration of Load Effects for Spruce Timber with Special Reference to Moisture Influence - A Status Report - P Hoffmeyer
19-9-3	A Model of Deformation and Damage Processes Based on the Reaction Kinetics of Bond Exchange - T A C M van der Put
19-9-4	Non-Linear Creep Superposition - U Korin
19-9-5	Determination of Creep Data for the Component Parts of Stressed-Skin Panels - R Kliger
19-9-6	Creep an Lifetime of Timber Loaded in Tension and Compression - P Glos
19-1-1	Duration of Load Effects and Reliability Based Design (Single Member) - R O Foschi and Z C Yao
19-6-1	Effect of Age and/or Load on Timber Strength - J Kuipers
19-7-4	The Prediction of the Long-Term Load Carrying Capacity of Joints in Wood Structures - Y M Ivanov and Y Y Slavic
19-7-5	Slip in Joints under Long-Term Loading - T Feldborg and M Johansen
20-7-2	Slip in Joints under Long-Term Loading - T Feldborg and M Johansen
22-9-1	Long-Term Tests with Glued Laminated Timber Girders - M Badstube, W Rug and W Schöne
22-9-2	Strength of One-Layer solid and Lengthways Glued Elements of Wood Structures and its Alteration from Sustained Load - L M Kovaltchuk, I N Boitemirova and G B Uspenskaya
24-9-1	Long Term Bending Creep of Wood - T Toratti

TIMBER BEAMS

20-10-1 Draft Clause for CIB CodeêforêBeamsêwithêInitial Imperfections
- H J Burgess

20-10-2 Space Joists in Irish Timber - W J Robinson

20-10-3 Composite Structure of Timber Joists and Concrete Slab
- T Poutanen

21-10-1 A Study of Strength of Notched Beams - P J Gustafsson

22-10-1 Design of Endnotched Beams - H J Larsen and P J Gustafsson

22-10-2 Dimensions of Wooden Flexural Members under Constant Loads
- A Pozgai

22-10-3 Thin-Walled Wood-Based Flanges in Composite Beams - J König

22-10-4 The Calculation of Wooden Bars with flexible Joints in Accordance with the Polish Standart Code and Strict Theoretical Methods
- Z Mielczarek

23-10-1 Tension Perpendicular to the Grain at Notches and Joints
- T A C M van der Put

23-10-2 Dimensioning of Beams with Cracks, Notches and Holes. An Application of Fracture Mechanics - K Riipola

23-10-3 Size Factors for the Bending and Tension Strength of Structural Timber
- J D Barret and A R Fewell

23-12-1 Bending Strength of Glulam Beams, a Design Proposal - J Ehlbeck and F Colling

23-12-3 Glulam Beams, Bending Strength in Relation to the Bending Strength of the Finger Joints - H Riberholt

24-10-1 Shear Strength of Continuous Beams - R H Leicester and F G Young

25-10-1 The Strength of Norwegian Glued Laminated Beams - K Solli, E Aasheim and R H Falk

25-10-2 The Influence of the Elastic Modulus on the Simulated Bending Strength of Hyperstatic Timber Beams - T D G Canisius

ENVIRONMENTAL CONDITIONS

LAMINATED MEMBERS

11-6-3	Consideration of Combined Stresses for Lumber and Glued Laminated Timber (addition to Paper CIB-W18/9-6-4) - K Möhler
12-12-1	Glulam Standard Part 2: Glued Timber Structures; Rating (3rd draft)
12-12-2	Glulam Standard Part 3: Glued Timber Structures; Performance (3 rd draft)
13-12-1	Glulam Standard Part 3: Glued Timber Structures; Performance (4th draft)
14-12-1	Proposals for CEI-Bois/CIB-W18 Glulam Standards - H J Larsen
14-12-2	Guidelines for the Manufacturing of Glued Load-Bearing Timber Structures - Stevin Laboratory
14-12-3	Double Tapered Curved Glulam Beams - H Riberholt
14-12-4	Comment on CIB-W18/14-12-3 - E Gehri
18-12-1	Report on European Glulam Control and Production Standard - H Riberholt
18-10-2	Longitudinal Shear Design of Glued Laminated Beams - R O Foschi
19-12-1	Strength of Glued Laminated Timber - J Ehlbeck and F Colling
19-12-2	Strength Model for Glulam Columns - H J Blaß
19-12-3	Influence of Volume and Stress Distribution on the Shear Strength and Tensile Strength Perpendicular to Grain - F Colling
19-12-4	Time-Dependent Behaviour of Glued-Laminated Beams - F Zaupa
21-12-1	Modulus of Rupture of Glulam Beam Composed of Arbitrary Laminae - K Komatsu and N Kawamoto
21-12-2	An Appraisal of the Young's Modulus Values Specified for Glulam in Eurocode 5 - L R J Whale, B O Hilson and P D Rodd
21-12-3	The Strength of Glued Laminated Timber (Glulam): Influence of Lamination Qualities and Strength of Finger Joints - J Ehlbeck and F Colling

PARTICLE AND FIBRE BUILDING BOARDS

7-13-1	Fibre Building Boards for CIB Timber Code (First Draft) - O Brynildsen
9-13-1	Determination of the Bearing Strength and the Load-Deformation Characteristics of Particleboard - K Möhler, T Budianto and J Ehlbeck
9-13-2	The Structural Use of Tempered Hardboard - W W L Chan
11-13-1	Tests on Laminated Beams from Hardboard under Short- and Longterm Load - W Nozynski
11-13-2	Determination of Deformation of Special Densified Hardboard under Long-term Load and Varying Temperature and Humidity Conditions - W Halfar
11-13-3	Determination of Deformation of Hardboard under Long-term Load in Changing Climate - W Halfar
14-4-1	An Introduction to Performance Standards for Wood-Base Panel Products - D H Brown
14-4-2	Proposal for Presenting Data on the Properties of Structural Panels - T Schmidt
16-13-1	Effect of Test Piece Size on Panel Bending Properties - P W Post
20-4-1	Considerations of Reliability - Based Design for Structural Composite Products - M R O'Halloran, J A Johnson, E G Elias and T P Cunningham
20-13-1	Classification Systems for Structural Wood-Based Sheet Materials - V C Kearley and A R Abbott
21-13-1	Design Values for Nailed Chipboard - Timber Joints - A R Abbott
25-13-1	Bending Strength and Stiffness of Izopanel Plates - Z Mielczarek

TRUSSED RAFTERS

24-14-1 Capacity of Support Areas Reinforced with Nail Plates in Trussed Rafters - A Kevarinmäki

25-14-1 Moment Anchorage Capacity of Nail Plates in Shear Tests - A Kevarinmaki and J. Kangas

25-14-2 Design Values of Anchorage Strength of Nail Plate Joints by 2-curve Method and Interpolation - J Kangas and A Kevarinmaki

STRUCTURAL STABILITY

8-15-1 Laterally Loaded Timber Columns: Tests and Theory - H J Larsen

13-15-1 Timber and Wood-Based Products Structures. Panels for Roof Coverings. Methods of Testing and Strength Assessment Criteria. Polish Standard BN-78/7159-03

16-15-1 Determination of Bracing Structures for Compression Members and Beams - H Brüninghoff

17-15-1 Proposal for Chapter 7.4 Bracing - H Brüninghoff

17-15-2 Seismic Design of Small Wood Framed Houses - K F Hansen

18-15-1 Full-Scale Structures in Glued Laminated Timber, Dynamic Tests: Theoretical and Experimental Studies - A Ceccotti and A Vignoli

18-15-2 Stabilizing Bracings - H Brüninghoff

19-15-1 Connections Deformability in Timber Structures: a Theoretical Evaluation of its Influence on Seismic Effects - A Ceccotti and A Vignoli

19-15-2 The Bracing of Trussed Beams - M H Kessel and J Natterer

19-15-3 Racking Resistance of Wooden Frame Walls with Various Openings - M Yasumura

19-15-4 Some Experiences of Restoration of Timber Structures for Country Buildings - G Cardinale and P Spinelli

23-15-3 A Brief Description of Formula of Beam-Columns in China Code - S Y Huang

23-15-4 Seismic Behavior of Braced Frames in Timber Construction - M Yasumara

23-15-5 On a Better Evaluation of the Seismic Behavior Factor of Low-Dissipative Timber Structures - A Ceccotti and A Vignoli

23-15-6 Disproportionate Collapse of Timber Structures - C J Mettem and J P Marcroft

23-15-7 Performance of Timber Frame Structures During the Loma Prieta California Earthquake - M R O'Halloran and E G Elias

24-15-2 Discussion About the Description of Timber Beam-Column Formula - S Y Huang

24-15-3 Seismic Behavior of Wood-Framed Shear Walls - M Yasumura

25-15-1 Structural Assessment of Timber Framed Building Systems - U Korin

25-15-3 Mechanical Properties of Wood-framed Shear Walls Subjected to Reversed Cyclic Lateral Loading - M Yasumura

FIRE

12-16-1 British Standard BS 5268 the Structural Use of Timber: Part 4 Fire Resistance of Timber Structures

13-100-2 CIB Structural Timber Design Code. Chapter 9. Performance in Fire

19-16-1 Simulation of Fire in Tests of Axially Loaded Wood Wall Studs - J König

24-16-1 Modelling the Effective Cross Section of Timber Frame Members Exposed to Fire - J König

25-16-1 The Effect of Density on Charring and Loss of Bending Strength in Fire - J König

STATISTICS AND DATA ANALYSIS

FRACTURE MECHANICS

GLUED JOINTS

20-18-1	Wood Materials under Combined Mechanical and Hygral Loading - A Martensson and S Thelandersson
20-18-2	Analysis of Generalized Volkersen - Joints in Terms of Linear Fracture Mechanics - P J Gustafsson
20-18-3	The Complete Stress-Slip Curve of Wood-Adhesives in Pure Shear - H Wernersson and P J Gustafsson
22-18-1	Perspective Adhesives and Protective Coatings for Wood Structures - A S Freidin

CIB TIMBER CODE

2-100-1	A Framework for the Production of an International Code of Practice for the Structural Use of Timber - W T Curry
5-100-1	Design of Solid Timber Columns (First Draft) - H J Larsen
5-100-2	A Draft Outline of a Code for Timber Structures - L G Booth
6-100-1	Comments on Document 5-100-1; Design of Solid Timber Columns - H J Larsen and E Theilgaard
6-100-2	CIB Timber Code: CIB Timber Standards - H J Larsen and E Theilgaard
7-100-1	CIB Timber Code Chapter 5.3 Mechanical Fasteners; CIB Timber Standard 06 and 07 - H J Larsen
8-100-1	CIB Timber Code - List of Contents (Second Draft) - H J Larsen
9-100-1	The CIB Timber Code (Second Draft)
11-100-1	CIB Structural Timber Design Code (Third Draft)

11-100-2	Comments Received on the CIB Code a U Saarelainen b Y M Ivanov c R H Leicester d W Nozynski e W R A Meyer f P Beckmann; R Marsh g W R A Meyer h W R A Meyer
11-100-3	CIB Structural Timber Design Code; Chapter 3 - H J Larsen
12-100-1	Comment on the CIB Code - Sous-Commission Glulam
12-100-2	Comment on the CIB Code - R H Leicester
12-100-3	CIB Structural Timber Design Code (Fourth Draft)
13-100-1	Agreed Changes to CIB Structural Timber Design Code
13-100-2	CIB Structural Timber Design Code. Chapter 9: Performance in Fire
13-100-3a	Comments on CIB Structural Timber Design Code
13-100-3b	Comments on CIB Structural Timber Design Code - W R A Meyer
13-100-3c	Comments on CIB Structural Timber Design Code - British Standards Institution
13-100-4	CIB Structural Timber Design Code. Proposal for Section 6.1.5 Nail Plates - N I Bovim
14-103-2	Comments on the CIB Structural Timber Design Code - R H Leicester
15-103-1	Resolutions of TC 165-meeting in Athens 1981-10-12/13
21-100-1	CIB Structural Timber Design Code. Proposed Changes of Sections on Lateral Instability, Columns and Nails - H J Larsen
22-100-1	Proposal for Including an Updated Design Method for Bearing Stresses in CIB W18 - Structural Timber Design Code - B Madsen

22-100-2 Proposal for Including Size Effects in CIB W18A Timber Design Code - B Madsen

22-100-3 CIB Structural Timber Design Code - Proposed Changes of Section on Thin-Flanged Beams - J König

22-100-4 Modification Factor for "Aggressive Media" - a Proposal for a Supplement to the CIB Model Code - K Erler and W Rug

22-100-5 Timber Design Code in Czechoslovakia and Comparison with CIB Model Code - P Dutko and B Kozelouh

LOADING CODES

4-101-1 Loading Regulations - Nordic Committee for Building Regulations

4-101-2 Comments on the Loading Regulations - Nordic Committee for Building Regulations

STRUCTURAL DESIGN CODES

1-102-1 Survey of Status of Building Codes, Specifications etc., in USA - E G Stern

1-102-2 Australian Codes for Use of Timber in Structures - R H Leicester

1-102-3 Contemporary Concepts for Structural Timber Codes - R H Leicester

1-102-4 Revision of CP 112 - First Draft, July 1972 - British Standards Institution

4-102-1 Comparsion of Codes and Safety Requirements for Timber Structures in EEC Countries - Timber Research and Development Association

4-102-2 Nordic Proposals for Safety Code for Structures and Loading Code for Design of Structures - O A Brynildsen

4-102-3 Proposal for Safety Codes for Load-Carrying Structures - Nordic Committee for Building Regulations

4-102-4	Comments to Proposal for Safety Codes for Load-Carrying Structures - Nordic Committee for Building Regulations
4-102-5	Extract from Norwegian Standard NS 3470 "Timber Structures"
4-102-6	Draft for Revision of CP 112 "The Structural Use of Timber" - W T Curry
8-102-1	Polish Standard PN-73/B-03150: Timber Structures; Statistical Calculations and Designing
8-102-2	The Russian Timber Code: Summary of Contents
9-102-1	Svensk Byggnorm 1975 (2nd Edition); Chapter 27: Timber Construction
11-102-1	Eurocodes - H J Larsen
13-102-1	Program of Standardisation Work Involving Timber Structures and Wood-Based Products in Poland
17-102-1	Safety Principles - H J Larsen and H Riberholt
17-102-2	Partial Coefficients Limit States Design Codes for Structural Timberwork - I Smith
18-102-1	Antiseismic Rules for Timber Structures: an Italian Proposal - G Augusti and A Ceccotti
18-1-2	Eurocode 5, Timber Structures - H J Larsen
19-102-1	Eurocode 5 - Requirements to Timber - Drafting Panel Eurocode 5
19-102-2	Eurocode 5 and CIB Structural Timber Design Code - H J Larsen
19-102-3	Comments on the Format of Eurocode 5 - A R Fewell
19-102-4	New Developments of Limit States Design for the New GDR Timber Design Code - W Rug and M Badstube
19-7-3	Effectiveness of Multiple Fastener Joints According to National Codes and Eurocode 5 (Draft) - G Steck

19-7-6	The Derivation of Design Clauses for Nailed and Bolted Joints in Eurocode 5 - L R J Whale and I Smith
19-14-1	Annex on Simplified Design of W-Trusses - H J Larsen
20-102-1	Development of a GDR Limit States Design Code for Timber Structures - W Rug and M Badstube
21-102-1	Research Activities Towards a New GDR Timber Design Code Based on Limit States Design - W Rug and M Badstube
22-102-1	New GDR Timber Design Code, State and Development - W Rug, M Badstube and W Kofent
22-102-2	Timber Strength Parameters for the New USSR Design Code and its Comparison with International Code - Y Y Slavik, N D Denesh and E B Ryumina
22-102-3	Norwegian Timber Design Code - Extract from a New Version - E Aasheim and K H Solli
23-7-1	Proposal for a Design Code for Nail Plates - E Aasheim and K H Solli
24-102-2	Timber Footbridges: A Comparison Between Static and Dynamic Design Criteria - A Ceccotti and N de Robertis
25-102-1	Latest Development of Eurocode 5 - H J Larsen
25-102-1A	Annex to Paper CIB-W18/25-102-1. Eurocode 5 - Design of Notched Beams - H J Larsen, H Riberholt and P J Gustafsson
25-102-2	Control of Deflections in Timber Structures with Reference to Eurocode 5 - A Martensson and S Thelandersson

INTERNATIONAL STANDARDS ORGANISATION

3-103-1	Method for the Preparation of Standards Concerning the Safety of Structures (ISO/DIS 3250) - International Standards Organisation ISO/TC98
4-103-1	A Proposal for Undertaking the Preparation of an International Standard on Timber Structures - International Standards Organisation
5-103-1	Comments on the Report of the Consultion with Member Bodies Concerning ISO/TC/P129 - Timber Structures - Dansk Ingeniorforening
7-103-1	ISO Technical Committees and Membership of ISO/TC 165
8-103-1	Draft Resolutions of ISO/TC 165
12-103-1	ISO/TC 165 Ottawa, September 1979
13-103-1	Report from ISO/TC 165 - A Sorensen
14-103-1	Comments on ISO/TC 165 N52 "Timber Structures; Solid Timber in Structural Sizes; Determination of Some Physical and Mechanical Properties"
14-103-2	Comments on the CIB Structural Timber Design Code - R H Leicester
21-103-1	Concept of a Complete Set of Standards - R H Leicester

JOINT COMMITTEE ON STRUCTURAL SAFETY

3-104-1	International System on Unified Standard Codes of Practice for Structures - Comité Européen du Béton (CEB)
7-104-1	Volume 1: Common Unified Rules for Different Types of Construction and Material - CEB

CIB PROGRAMME, POLICY AND MEETINGS

1-105-1	A Note on International Organisations Active in the Field of Utilisation of Timber - P Sonnemans
5-105-1	The Work and Objectives of CIB-W18-Timber Structures - J G Sunley
10-105-1	The Work of CIB-W18 Timber Structures - J G Sunley
15-105-1	Terms of Reference for Timber - Framed Housing Sub-Group of CIB-W18
19-105-1	Tropical and Hardwood Timbers Structures - R H Leicester
21-105-1	First Conference of CIB-W18B, Tropical and Hardwood Timber Structures Singapore, 26 - 28 October 1987 - R H Leicester

INTERNATIONAL UNION OF FORESTRY RESEARCH ORGANISATIONS

7-106-1	Time and Moisture Effects - CIB W18/IUFRO 55.02-03 Working Party

CIB-W18/25-6-1

INTERNATIONAL COUNCIL FOR BUILDING RESEARCH STUDIES AND DOCUMENTATION

WORKING COMMISSION W18 - TIMBER STRUCTURES

MOMENT CONFIGURATION FACTORS FOR SIMPLE BEAMS

by

T D Gerard Canisius

Building Research Establishment

United Kingdom

MEETING TWENTY - FIVE

ÅHUS

SWEDEN

AUGUST 1992

Moment Configuration Factors for Simple Beams[1]

T.D. Gerard Canisius

Building Research Establishment, Bucknal's Lane, Garston, Watford, WD2 7JR, U.K.

Abstract: In the design of a timber beam, its strength is assumed to be constant along the length and to be equal to the (factored) characteristic strength. This can give rise to an unnecessary increase in the safety level of the member and a consequent reduction in economy. This effect may be somewhat reduced by the application of a Moment Configuration Factor to modify the design formula. In order to find these factors, which depend on the bending moment diagram, it is necessary to determine the strengths of beams under different load and support conditions. This paper presents a theoretical investigation of moment configuration factors for some simple beams.

[1]Paper presented at CIB-W18 Meeting 25 at Ahus, Sweden, 24-27 August 1992

1 Introduction

In the standard limit state design of a bending member, its strength is assumed to be uniform and equal to the (modified) characteristic strength, and it is made to resist the maximum applicable bending moment. In other words, the maximum bending moment is implicitly considered to act throughout the whole length of a beam of non-uniform strength, with a minimum strength equal to the (modified) characteristic strength. This design procedure can result in unnecessarily high safety levels and consequent losses of economy for certain beams under certain types of loading. This is so because the maximum moment may act only in a small length of the beam, making the probability of failure much lower. For example, a cantilevered beam with a uniformly distributed load will have a higher safety level than a similar simply supported beam with the same maximum moment given rise to by a similar load.

The above mentioned increase in the safety level has been already studied by several researchers [1,2,3]. Riberholt and Madsen[1,2] developed a method for the conversion of European strength data to the strength of (failure causing) defects which were assumed to be Poisson distributed spatially. This distribution of the strengths of defects (where failure was expected to occur) and the distribution of their occurrences were used in the simulation of beams to study this phenomenon. This method involved, among others, the assumption of independence between strengths of defects and also between their occurrences. Czmoch *et al.* [3] studied this method with correlations assumed to exist. Madsen and Buchanan[4] and Madsen[5] have reported experimental investigations in to this differences in strengths of beams under different load and support conditions.

A research programme is now being carried out to determine the feasibility of applying a 'Moment Configuration Factor' to the design formula to reduce this unnecessary increase in safety and the consequent loss in economy. This factor is defined as the ratio between the strength of a beam under a given load and support conditions and its strength under a constant bending moment acting throughout the length (Fig. 1). The latter simulates the usual design assumption described above. Of course, where the design is based on test results of a component such as a trussed rafter, a moment configuration factor cannot be justified.

This paper presents results from a preliminary investigation carried out as a part of this research programme. It investigates the moment configuration factors for several simple beams, and compares them with available data. The theoretical model uses a finite element analysis with beam properties generated by the multivariate approach of Taylor and Bender[6,7,8]. The results are compared with some results obtained with the Riberholt-Madsen model. The results are discussed also in relation to those presented by Madsen[5].

In using the model of Taylor and Bender, the strength and stiffness properties are considered to follow first order Markov processes spatially. Only a single initial strength distribution is considered here. analysis. obtained from the

2 The Strength Simulation Methods

2.1 The Taylor-Bender Method

In the method of Taylor and Bender [8] the correlated stiffness and strength properties are assumed to be random and stationary. The material properties, which are based on a test element length L_t, are assumed to be available.

2.1.1 The Spatial and Cross-Correlations

Taylor and Bender considered the elasticity moduli to be serially correlated according to a second order Markov process. (A recent paper [9] considers a third order process). However, in the present implementation, the stiffness correlation is considered to be a first order Markov process. Then the higher lag correlation coefficients, for example ρ_k for lag-k, can be obtained from Eq. 1.

$$\rho_k = \rho_1^k \qquad (k > 0) \tag{1}$$

As done by Taylor and Bender, a first order Markov process is used for the strength.

In [8], the determination of cross-correlation coefficients between the strength and the stiffness had been carried out in two ways. First, for beams of length equal to the test beam length, the correlation had been determined from data. Secondly, for longer beams, the coefficients had been determined with Eq. 2.

$$\rho_{k_{e-s}} = \rho_{k_e}\,\rho_{0_{e-s}} \tag{2}$$

where $\rho_{0_{e-s}}$ and $\rho_{k_{e-s}}$ are, respectively, the lag-0 and lag-k cross-correlations between the strength and stiffness and ρ_{k_e} is the lag-k autocorrelation coefficient for stiffness. In the following the first order autocorrelation coefficients for stiffness and strength will be, respectively, denoted by ρ_e and ρ_s. The first order cross-correlation coefficient between them is denoted by c.

2.1.2 The Method of Simulation

The general simulation procedure is given below. In the case of statically determinate beams, the elasticity modulus does not affect the structural analysis. As shown in [10] for a beam with a constant bending moment, the effect of ρ_s and c on the strengths of determinate beams is negligible and are usually within the margin of error allowed by the convergence criterion. Hence, the generation of strengths is carried out with the use only of ρ_s while specifying ρ_e and c to be zero.

The marginal cumulative distribution functions of the strength and stiffness, denoted by F_s and F_e respectively, are assumed to be available from test data. If a beam to be simulated needs n number of property elements of length L_t, then, with the stiffness and strength of each property element being required, the number of unknown properties is $2n$. In the present description it is assumed that the first n variables refer to the stiffness properties and the remainder refers to the strength properties. Let the joint probability distribution function for these $2n$ variables be F_T.

The expected value vector $\{A\}$ and the diagonal of the correlation matrix $[C]$ of F_t are considered to be available from test data. As suggested above, the non-diagonal members of the correlation matrix are found from the Markov behaviour together with the necessary initial values which are assumed available. Also $\rho_{0_{e-s}}$, the lag-0 cross-correlation between the strength and stiffness, is needed. All these coefficients contribute to the correlation matrix $[C]$.

Using the normalised expected value vector $\{\bar{A}\}$ and the normalised correlation matrix $[\bar{C}]$ random values are sampled from a multivariable normal distribution. In the present simulations the multivariate random number generator available with the NAG Fortran Library[11] is used. These standardised normal values are then transformed into equivalent values in the respective marginal distributions F_e and F_s. The conversion is carried out so as to provide the same cumulative distribution function value as in the standardised marginal normal distribution.

2.2 Riberholt-Madsen Model

The Riberholt-Madsen model described in [1,2] is an attempt at modelling the strengths of defects in beams using the data for the least strengths of beams. It assumes that the failure always occurs at a defect (knot). tail of For its use, this model needs the distribution of the occurrences of defects along the member. The distances to the positions of defects are assumed to be uncorrelated, and so are the strengths of adjoining defects. The elastic properties of the members are not considered.

Under the Riberholt-Madsen model, if the distribution of the least strengths of members is given by the cumulative distribution function F_t, then the distribution of the strengths of defects, F_{dRM}, is given by

$$F_{dRM} = -\frac{1}{N}\log(1 - F_t + F_t e^{-N}) \tag{3}$$

where N is the mean number of weak zones along the beam test length of L. The weak zones, which are considered to occur as a Poisson process, are assumed to have a constant intensity of λ. Then

$$N = \lambda L \tag{4}$$

3 Material Properties

3.1 Strength

The strength properties are assumed to be random and stationary. The strength distributions used in the simulations were approximately derived from data available at the Building Research Establishment. A strength distribution (for Canadian Hem-Fir) available in terms of the Weibull parameters of the probability density functions was selected. The strength, which is in terms of the maximum bending stress, has location, scale and shape parameters of $10N/mm^2$, $40N/mm^2$ and 3, respectively.

respectively, distributions. respectively,

For the Taylor-Bender type simulation, using the assumption of independence between the different property elements, the strength distribution was converted to a marginal distribution. This conversion was facilitated by the fact that the available strengths have Weibull distributions. In the case of such a distribution, if the values are independent, then the minima of different independent samples of the same size will also have a Weibull distribution. This new distribution is available in mathematically closed form[12]. If the original distribution has location, scale and shape parameters μ^s, σ^s and λ^s, respectively, then the minima of samples of size n have a Weibull distribution with the same location and shape parameters and a new scale parameter of $\sigma^s/n^{1/\lambda^s}$. Therefore, if the distribution of minima is available, then the original distribution can be obtained from the inverse process.

In carrying out the above inverse process, the number of elements (sampling size) was obtained by assuming property element lengths of 400, 600 and 800mm. Then, assuming a test beam length of 4m, n was determined as 10, 7 and 5, respectively. The above conversion is only an approximate one as it contains many assumptions. The intention was only to obtain a somewhat realistic approximate distribution for the purpose of this study.

It should be noted that although the above process starts with the same strength distribution, the derived mariginal distributions for different property element lengths are different because of the different numbers of elements within a given test beam length. However, although the expected values and the standard deviations in the derived distributions were different, their coefficients of variation (CAV) remained almost the same at approximately 0.31.

For the Riberholt-Madsen simulation the previously given formula (Eq. 3) was used to obtain the strengths of defects. Three values, *viz.* 4, 2 and 1.33, were used as the intensity of defects per metre length. The test beam length was assumed to be 4m.

3.2 Correlation Coefficients

In the case of the Taylor-Bender model, the autocorrelation ρ_s between the property elements were varied between zero and unity. It should be noted that due to the differences in element lengths, the different elements will have different lengthwise correlations even when the correlation coefficients, which are based on the differences between the element numbers, are the same. The longer ones, while having constant properties for longer lengths, will also have correlations which extend to larger distances. Hence, the obtained results for different element lengths under a given ρ_s do not refer to the same real lengthwise correlations, but to higher correlations as the element length increases.

4 The Finite Element Model and the Simulation of Beams

A beam finite element programme was written for the purpose of structural analysis. It consisted of a simple cubic beam element. Each of the finite elements was assumed to have constant material and strength properties. Only linear elastic analyses were carried out. The use of a finite element programme makes the analysis of statically determinate beams easier, while it is necessary for the efficient simulation of indeterminate beams with lengthwise variation of elasticity modulus.

For Taylor-Bender type of simulation, the properties were generated from the multivariate distribution. The finite element properties corresponded to those of the property element that contained it (Fig. 2). The lengths of the finite elements and the property elements were, generally, different. If a finite element had parts of it in two adjoining property elements, a weighted mean value of the properties was used. This was determined according to the amounts of the finite element corresponding to each property element.

In the case of analysis using the Riberholt-Madsen model, the generated positions and strengths of defects can be allocated to the finite elements that correspond to their positions. Finite elements which do not contain any defects can be provided with very high strengths so as to prevent failure at such locations. The results presented here were not obtained with such a procedure, but by including the analytically determined bending moment diagrams in the computer code.

5 The Definition of the Strength of a Beam

In this paper, the definition presented in Czmoch *et.al.*[3] is used in determining the strength of a beam. It is defned as the maximum bending moment (stress) that can be applied at the position of maximum moment (stress) without inducing failure at any position along the beam. Its determination is briefly described below.

Consider the load effect function $S(x)$, which in the present case is the applied bending moment or stress. Here x is the length coordinate of the beam. $S(x)$ is expressed in terms of a non-dimensional function $\sigma(x)$ and a parameter Z, which is the maximum load effect for the given load, as

$$S(x) = Z\sigma(x) \tag{5}$$

Z and S are in the units of the bending strength $R(x)$ of the beam cross-section. Then the load carrying capacity of the beam is defined as

$$Z = \min\left[\frac{R(x)}{\sigma(x)}\right] \qquad \textit{(for all } x\textit{)} \tag{6}$$

In the analysis of Czmoch *et. al.* this took the discreet form

$$Z = min\left[\frac{R_1}{\sigma(x_1)}, \dots \frac{R_i}{\sigma(x_i)}, \dots \frac{R_N}{\sigma(x_N)}\right] \tag{7}$$

where N is the random number of weak zones (defects) in the given beam length, and x_i and R_i are , respectively, the position of the ith weak zone and its strength. For the finite element analysis, N refers to the number of finite elements and i to the finite element number. (The forces within each finite element are constant due to the displacement shape functions used). Expressed differently, Z is the maximum bending moment(stress) at the position of maximum moment(stress), providing a minimum strength/moment(stress) ratio of unity within the whole beam length.

6 Results for Statically Determinate Beams

The structures and loads considered in the present study are shown in Fig. 3. Among them, the beam with a constant bending moment acts as the basic case for the calculation of the Moment Configuration Factors (MCFs). All cases were analysed with a beam length of 3.6m. Additionally, the uniform moment and central concentrated load cases were analysed with a beam length of 7.2m. Unless mentioned otherwise, the presented results refer to those obtained with the Taylor-Bender method of property simulation.

The results were obtained with a convergence of at least 1% in both the fifth percentile and the mean. This was generally achieved with 4000 simulations.

6.1 MCFs for Different Moment Configurations (3.6m Beam)

Figs. 4 and 5 present the moment configuration factors, on both the mean (expected value) and the fifth percentile for the above structures, as a function of the strength autocorrelation ρ_s. Figs. ?? Here it should be noted that the property element length is larger than the finite element length.

In Fig. 4, which is for MCFs on the expected values with the 400mm element, the different levels of the curves for different cases indicate the effect of each bending moment diagram. Factors for all of them are nearly constant within low ρ_s values, while they tend to unity as ρ_s reaches 1. This implies a larger gradient in the drop of MCFs for cases with higher factors, for example the cantilever beam. Also, the lowering of values for the higher factor cases begins earlier (*i.e.* under lower ρ_s) than for low MCF cases. This indicates the possibility of using constant factors on the mean for low ρ_s values, while being mindful that its effect needs to be considered earlier for higher factor cases than for the lower factor cases.

Fig. 5 shows the similar details as for Fig. 4, but now with respect to the fifth percentiles. While the earlier comments are still valid, the faster drops in the MCF values now generally occur much later, *i.e.* at much higher ρ_s levels.

6.1.1 Factors Derived with Different Property Elements

The variations of the Moment Configuration Factors with respect to ρ_s for different structure/load cases are shown in Fig. 6 to 13. In each of the figures, the results from all property elements, with respect to both the expected value and the fifth percentile, are shown. 7.2m beam results are provided only with respect to the central concentrated load case.

Central Concentrated Load: Fig. 6, which is for the central concentrated load on the 3.6m beam, shows that for lower ρ_s values the MCFs on the mean are higher than those on the fifth percentile using the same element. This is reversed as ρ_s approaches unity. The use of a 400mm property element implies a lesser correlation distance-wise and also a lesser length with constant properties. Therefore it is much closer to a case of total randomness than the use of 600mm and 800mm elements. Hence its factors can be expected to be higher than those for the longer elements with larger effective correlations.

Also provided in the figure is the result obtained as the factor on the fifth percentile using the Riberholt-Madsen (R-M) model with an analytically determined bending moment diagram and 2000 simulations. (A summary of these results is provided in Table 1). This R-M model value is large compared to the present results and is very close to the MCF on the mean for 400mm elements. This is to be expected as the Riberholt-Madsen model results have been obtained with no correlation assumed to exist between the properties, whereas the consideration of correlations reduces the factors as suggested by the results presented in Table 2 of [3]. The MCFs calculated on the basis of those results on a 3.0m beam are presented in Table 2. In the table NZSTR and NZDLT, respectively, refer to the correlation parameters of the strengths of defects and of the distances to their occurrences. Higher

Defect Intensity per metre	1.33		2		4	
Beam Length L (m)	3.6	7.2	3.6	7.2	3.6	7.2
Central Conc. Ld.	1.41	1.46	1.39	1.39	1.39	1.35
UDL	1.21	1.22	1.21	1.25	1.21	1.20
0.25L Overhang	-	-	1.39	1.39	-	-
0.33L Overhang	-	-	1.82	1.74	-	-
Cantilever	-	-	1.68	1.65	-	-

Table 1: MCF with Riberholt-Madsen Model. 2000 Simulations.

Corr. Parameters		Prop. Set 1		Prop. Set 2		Prop. Set 3	
NZSTR	NZDLT	R_u/R_t	R_{uR}/R_{tR}	R_u/R_t	R_{uR}/R_{tR}	R_u/R_t	R_{uR}/R_{tR}
0	0	1.31	1.34	1.34	1.37	1.32	1.40
0	2	1.33	1.35	1.34	1.35	1.31	1.37
2	0	1.31	1.40	1.28	1.40	1.34	1.46
2	2	1.31	1.38	1.30	1.37	1.31	1.43
8	8	1.18	1.40	1.19	1.38	1.20	1.41

Table 2: MCF from results of Czmoch *et.al.* 2000 simulations

parameter values indicate higher correlations. R_u/R_t is the MCF using the 'correct' properties, while R_{uR}/R_{tR} is the MCF obtained from the Riberholt-Madsen model. There, the 'correct' results are smaller than the R-M model results for all property sets, even when no correlations are present.

It is also interesting to note that a value of 1.40, very close to the R-M value of 1.39 on the fifth percentile, had been reported by Johnson[13], for a material with a lower limit on strength of zero when the CAV of both beam strengths is approximately 0.2. This had been derived on the basis of the brittle fracture theory with the assumption of total statistical independence between properties. This is the value reported also by Madsen [5] in his Table 12.33. The values on the mean provided by Johnson range from zero for CAV of zero to approximately 1.7 for CAV of 0.5, and are applicable to all percentiles in the absence of a location parameter.

The MCFs calculated on the mean are seen to be higher than those on the fifth percentile for lower ρ_s values. In the graph the factors for the 800mm element are slightly higher than those for the 600mm element. This may be so because an element length of 800mm can be too large when compared to a beam length of 3.6m. This is somewhat confirmed by the fact that this did not occur with the 7.2m beam results shown in Fig. 7. In this case the results for 600mm and 800mm on the fifth percentile show different relative sizes depending on the value of ρ_s, and so still casts doubts on the appropriateness of the latter size.

In the case of the results presented in Fig 7 for 7.2m beam, it can be seen that the MCFs have now increased due to the lesser effects of the correlation coefficients, and the drift towards independence, as the length increases. The MCF on mean value has now increased above 1.45 and is approaching the value of 1.52 for CAV of approximately 0.30 of Johnson, although it may not be reached in reality.

A comparison of MCFs for 3.6 and 7.2m beams under different property element lengths can be made with Figs. 8 and 9 which are for 400mm and 600mm elements, respectively. All these indicate that the MCFs increase with the beam lengths because of the decrease in the importance of the spatial correlations.

Other Moment Configurations: Some results with respect to other moment configurations on the 3.6m beam are presented in Figs. 10 to 13. All these show trends similar to those discussed earlier with respect to the central concentrated load case.

The results on the fifth percentile obtained with the R-M model are also shown in the above figures. In the case of the uniformly distributed load on the simply supported beam (Fig. 10), the value of 1.21 is approximately half-way between the MCFs on the mean and fifth percentile with 400mm elements. As shown also by other structures, the relative positions of the R-M values are dependent upon the moment configuration. For the simply supported beam with a 0.9m overhang (Fig. 11), the R-M value is again half-way between the factors on the fifth percentile and the mean of the 400mm element simulations. In contrast to this is the factor presented for the beam with the 1.17m overhang (Fig. 12) where there is a high hogging moment peak and a small mid-span moment. The R-M factor of 1.82 was obtained with an overhang of 1.19m and this cannot be the reason for its very high value compared to those obtained with the present simulation. In the case of the cantilever beam (Fig. 13), the R-M value is just above the MCF on the mean value based on the 400mm element. It is interesting to note that the value quoted by Madsen[5] for the beam with UDL is 1.20, although it may not have any relation to the values presented here.

6.2 Length Effect on the MCF

The present model shows a very slight length effect on the Moment Configuration Factors due to the correlations that exist between the strengths of property elements. The length effect from the R-M model is negligible. None is evident for simply supported beams from the results of Madsen[5] as the length effects on the strengths of different simply supported beams are said to be the same. The assumption of uncorrelated properties used in the brittle fracture theory does not give rise to a length effect on the MCF.

The length effect on the MCFs, shown by the present model, is shown in Fig. 14. The effect of doubling the length is negligible with the 400mm element, except under high ρ_s values (except near unity). There is an increase of approximately 10% in the MCF for 7.2m beam, when compared to that for the 3.6m beam, under the 600mm element. These indicate that the length effect can be neglected under low correlations. In the case of higher correlations their effect may be neglected without adverse effects on safety, provided that the basic MCFs are determined for shorter lengths where the effect of correlation is more and the MCFs higher than for a longer beam. Then the use of the lower values also for the longer beams will not result in a decrease of safety.

6.3 Statically Indeterminate Beams

No results with regard to statically indeterminate beams are presented in this paper. However, in the light of the results quoted by Madsen[5], it is felt to be relevant to speculate on the following matter.

As a result of his tests, Madsen cited the observation that the length effect factor for clamped beams is approximately one-third of that of a simply supported beam. This is with reference to the strength and not the Moment Configuration Factor. In the apparent absence of a conversion factor for support conditions, as the brittle fracture theory does not consider the redundancy, this implies that the ratio between the strength of a clamped beam and a simply supported beam will increase with the increase in length, and also will decrease with the decrease in length. Hence it is interesting to know how a single ratio of 1.4 between the uniform moment and the concentrated load cases in Table 12.33 of [5] can be used.

Let the above value of one-third be with respect to the reduction and not the factor itself. If the apparent length effect factor of 0.86 in Table 12.34 of [5] is used for simply supported beams, then the length effect factor for clamped conditions should be approximately 0.96. Then the ratio of 1.4 between the clamped concentrated load case and the uniform moment case will have an increased value of 1.56 on doubling the length and a decreased value of 1.25 on halving the length from a reference value. That is, an additional factor of 1.12, which increases or decreases the overall moment configuration factor, exists. Therefore, if a value such as 1.4 is given, it seems reasonable to base it on a reference length, so the factors for other lengths can be worked out.

7 Conclusion

A study of moment configuration factors (MCFs) for simple beams were presented in this paper. Several statically determinate beams were computer simulated while considering the spatial correlation of the strength properties. The method of Taylor and Bender, based on different property element lengths, was used in generating the beam properties. Also some results obtained with the Riberholt-Madsen model was presented.

The results obtained by the use of the present model showed that for a given beam length, the MCF values are almost constant under small correlations. The MCFs on the fifth percentiles were smaller than those on the expected values when the correlation coefficient ρ_s was smaller. The presence of correlation, expressed in terms of the property element length, provided lower MCFs than those obtained by methods based on the assumption of statistical independence. occur, than

The length effect on the MCFs for a simply supported beam with a central concentrated load was seen to be negligible under small correlations. Increased correlations in terms of the property element length, only increased the MCF values when the beam length was doubled. Hence if no length effect is to be considered, and correlations are to be present, then it is advisable to base the factors on a small beam length where the latter can be important. Otherwise, lower levels of safety may result.

As the length effects on the strengths of clamped beams are said to be different from that of a simply supported beam, also the MCFs for them should vary with the beam length. Therefore, it is advisable to base these also on a reference beam length. Otherwise, there will be a loss of economy in the case of longer beams and a higher risk of failure in the case of beams shorter than the reference length.

It is expected to carry out further theoretical studies with respect to these, but at least some of them should be verified experimentally for further confidence in results.

8 Acknowledgment

The author wishes to acknowledge the support and encouragement provided by Mr. A.R. Fewell towards this research.

References

[1] Riberholt, H. and Madsen, P. H.; *Strength Distribution of Timber Structures. Measured Variation of Cross Sectional Strength of Structural Lumber*, Struct. Res. Lab., Tech. Univ. of Denmark, Rept. R114, 1979.

[2] Riberholt, H.; *Safety of Timber Structures*, Struct. Res. Lab., Tech. Univ. of Denmark, June 1979.

[3] Czmoch, I., Thelanderson, S. and Larsen, H. J.; *Effect of Within Member Variability on Bending Strength of Structural Timber*, Proc., Int'l Council for Building Research Studies and Documentation, Working Commission W18A, Meeting 24, Oxford, U.K., Sept. 1991.

[4] Madsen, Borg, and Buchanan, A.H.; *Size Effects in Timber Explained by a Modified Weakest Link Theory*, Can. J. of Civ. Eng., **13**, pp. 218-232, 1986.

[5] Madsen, Borg; *Structural Behaviour of Timber*, Timber Eng. Ltd., North Vancouver, Canada, 1992.

[6] Taylor, S. E. and Bender, D. A.; *Simulating Correlated Lumber Properties Using a Modified Multivariate Normal Approach*, Trans. ASAE, **31**(1), pp.182-186, 1988.

[7] Taylor, S. E. and Bender, D. A.; *A Method for Simulating Multiple Correlated Lumber Properties*, For. Prod. J., **39**(7/8), pp. 71-74, 1989.

[8] Taylor, S. E. and Bender, D. A.; *Stochastic Model for Localized Tensile Strength and Modulus of Elasticity in Lumber*, Wood and Fibre Sc., **23**(4), pp. 501-519, 1991.

[9] Richburg, B. A. and Bender, D. A.; *Localized Tensile Strength and Modulus of E-Related Laminating Grades of Lumber*, Wood and Fibre Sc., **24**(2), pp. 225-232, April 1992.

[10] Canisius, T.D.G.; *The Influence of Elasticity Modulus on the Simulated Bending Strength of Hyperstatic Timber Beams*, Proceedings, CIB-W18 Meeting 25, Ahus, Sweden, Aug. 1992.

[11] NAG Fortran Library Mk14, NAG Ltd., Oxford, England, 1990.

[12] Bury, K. V.; *Statistical Models in Applied Science*, Wiley, N.Y. 1975.

[13] Johnson, A.I.; *Strength, Safety and Economical Dimensions of Structures*, Swedish State Committee for Building Research Bulletin No.22, 1953.

Figure Captions

Fig. 9: 3.6m and 7.2m Simply Supported Beams with Central Concentrated Load: MCFs under 600mm Property Element.

Fig. 10: Simply Supported 3.6m Beam with Uniformly Distributed Load: MCFs under Different Property Element Lengths.

Fig. 11: Simply Supported 3.6m Beam with 0.9m Overhang and Uniformly Distributed Load: MCFs under Different Property Element Lengths.

Fig. 12: Simply Supported 3.6m Beam with 1.17m Overhang and Uniformly Distributed Load: MCFs under Different Property Element Lengths.

Fig. 13: 3.6m Cantilever with Uniformly Distributed Load: MCFs under Different Property Element Lengths.

Fig. 14: 3.6m and 7.2m Simply Supported Beams with Central Concentrated Load: Length Effect on MCF.

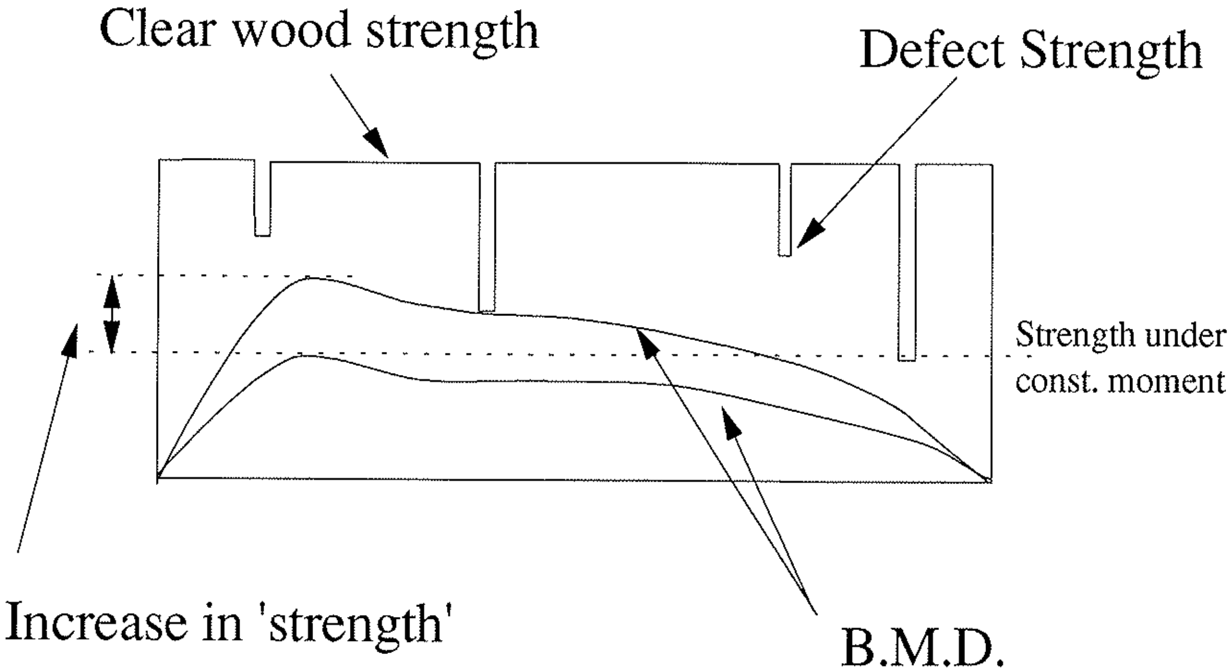
Clear wood strength
Defect Strength
Strength under
const. moment
Increase in 'strength'
B.M.D.

Fig. 1

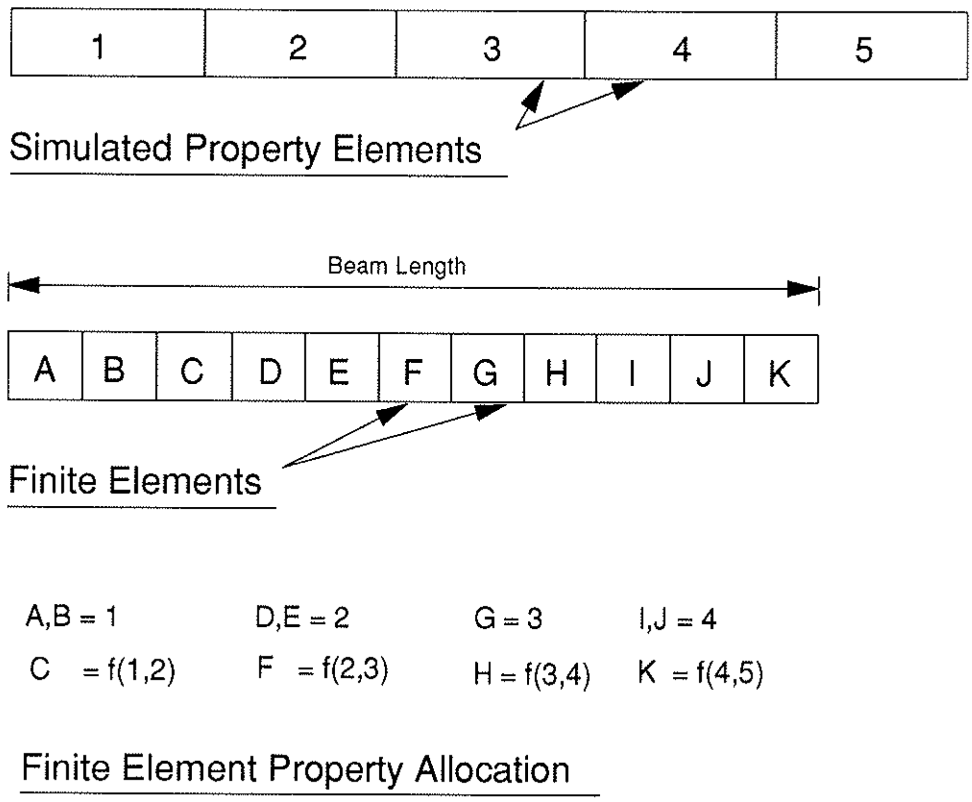
1
2
3
4
5
Simulated Property Elements
Beam Length
A
B
C
D
E
F
G
H
I
J
K
Finite Elements
A,B = 1
C = f(1,2)
D,E = 2
F = f(2,3)
G = 3
H = f(3,4)
I,J = 4
K = f(4,5)
Finite Element Property Allocation

Fig. 2

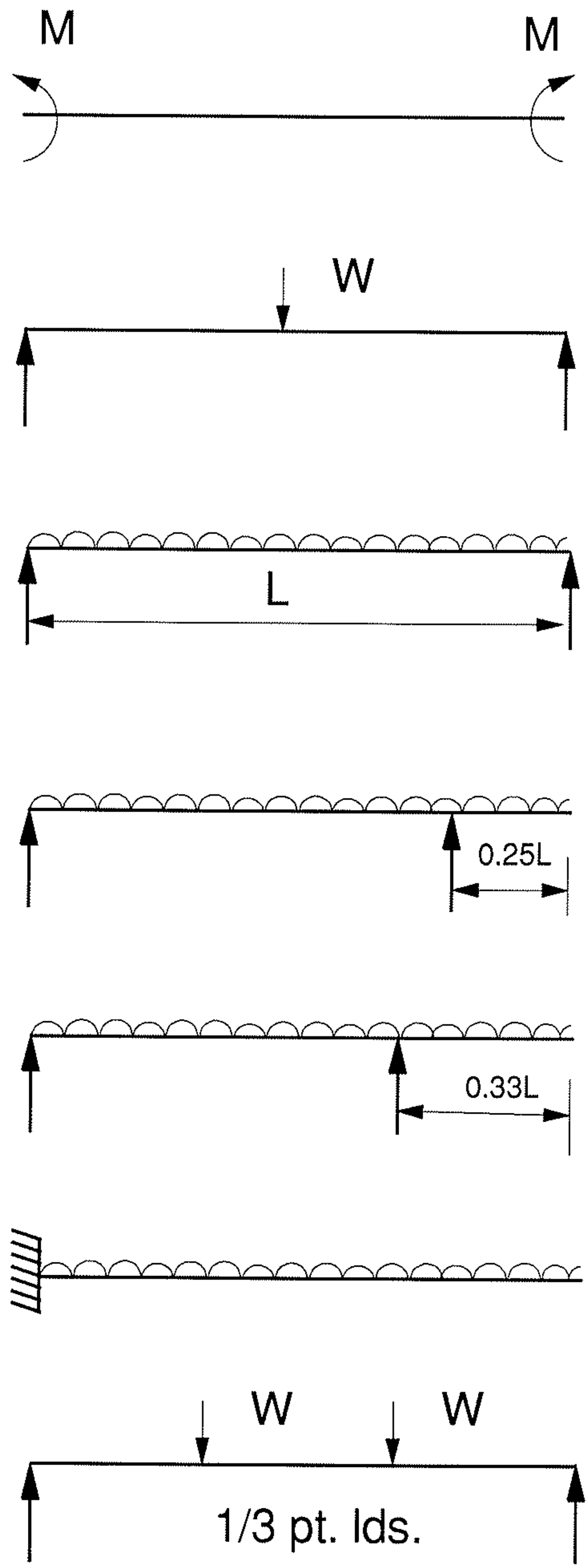

Fig. 3

MCFs on the Mean: 3.6m Beam

400mm Property Elements

Fig. 4

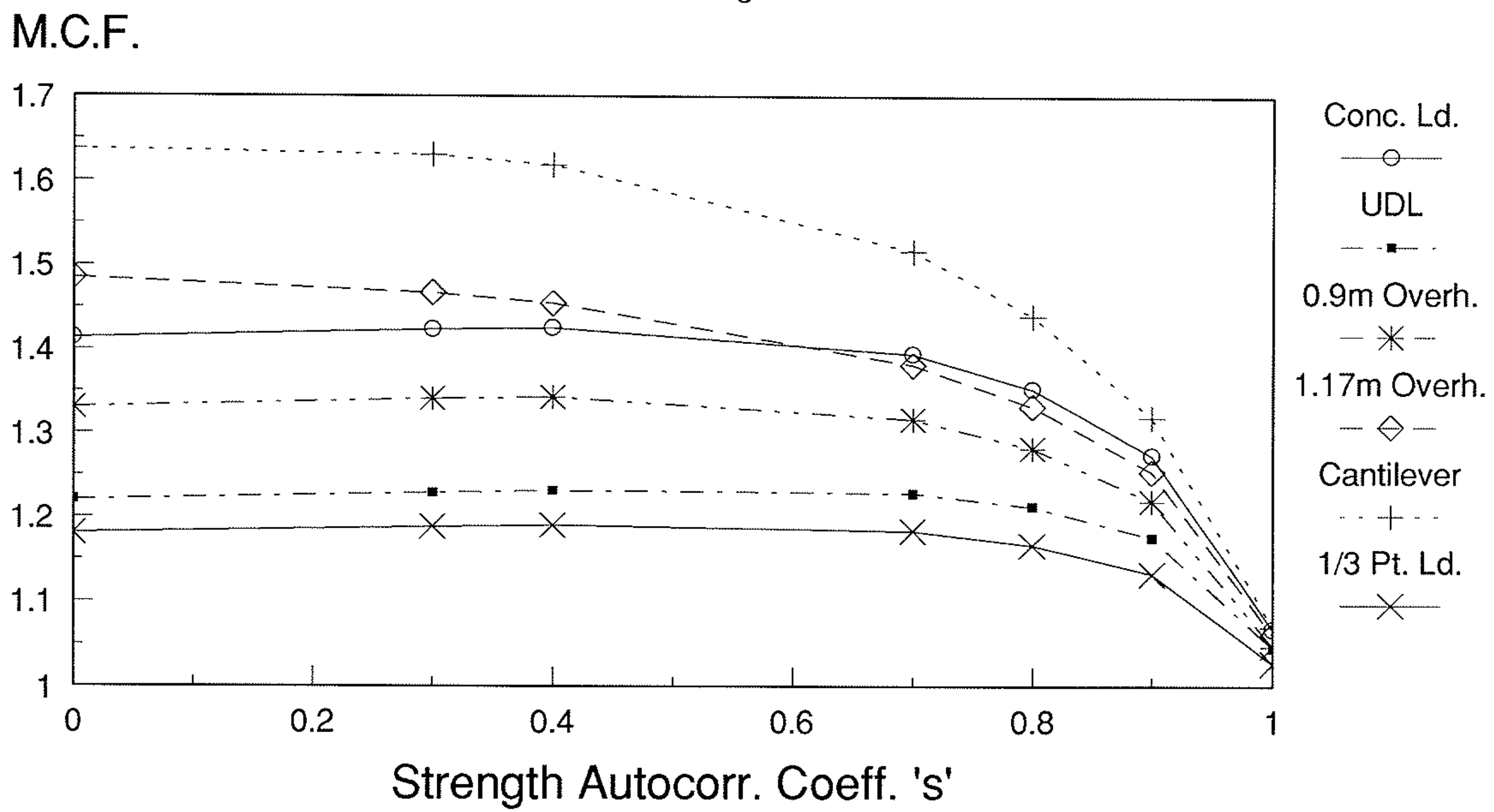

MCFs on the 5th Perc.: 3.6m Beam

400mm Property Elements

Fig. 5

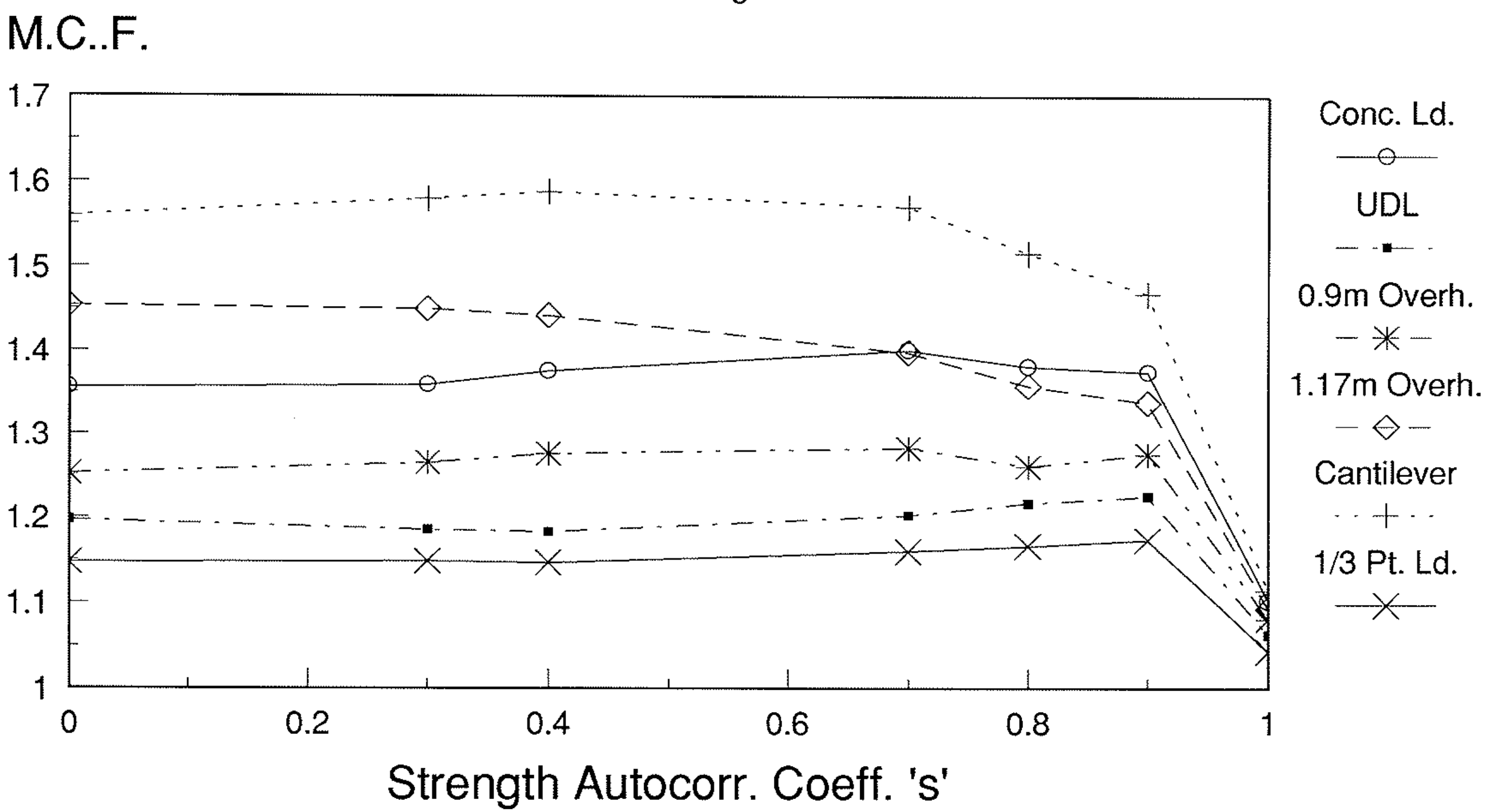

MCFs for 3.6m Beam: Effect of Property Element

Central Concentrated Load

Fig. 6

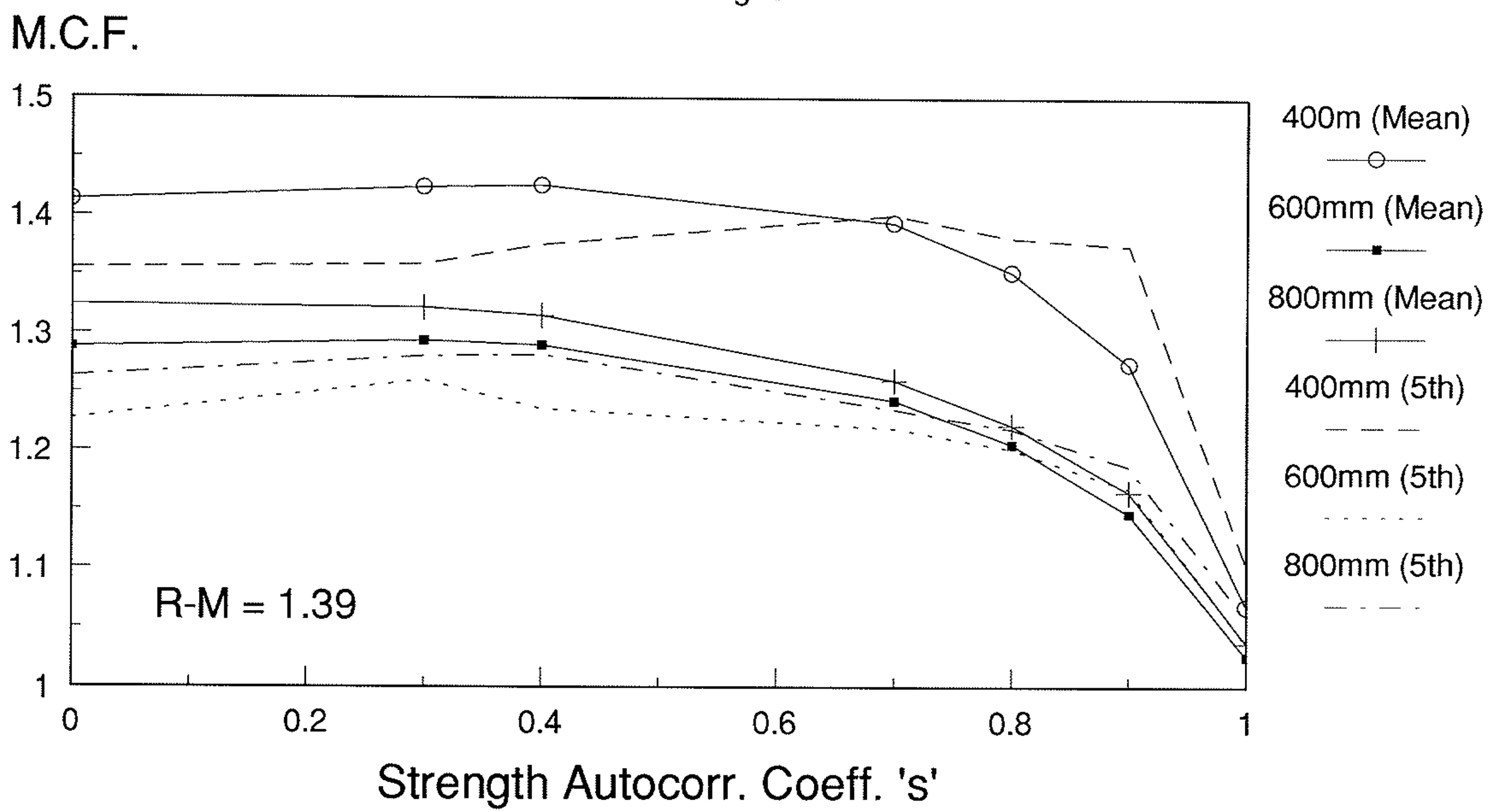

MCFs for 7.2m Beam: Effect of Property Element

Central Conc. Load on SS Beam

Fig. 7

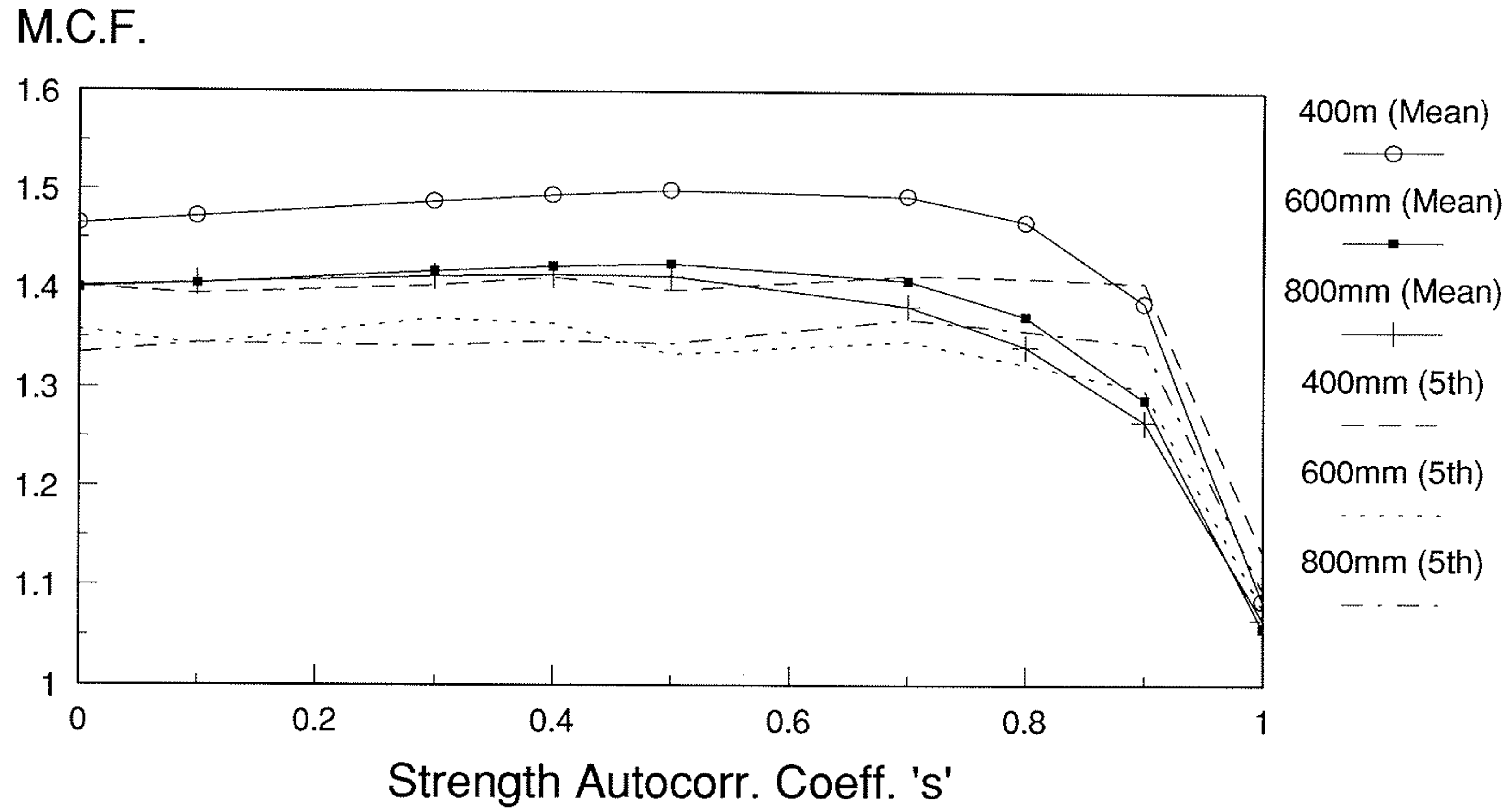

MCFs for 3.6m and 7.2m Beams

Central Conc. Load. 400mm Elements

Fig. 8

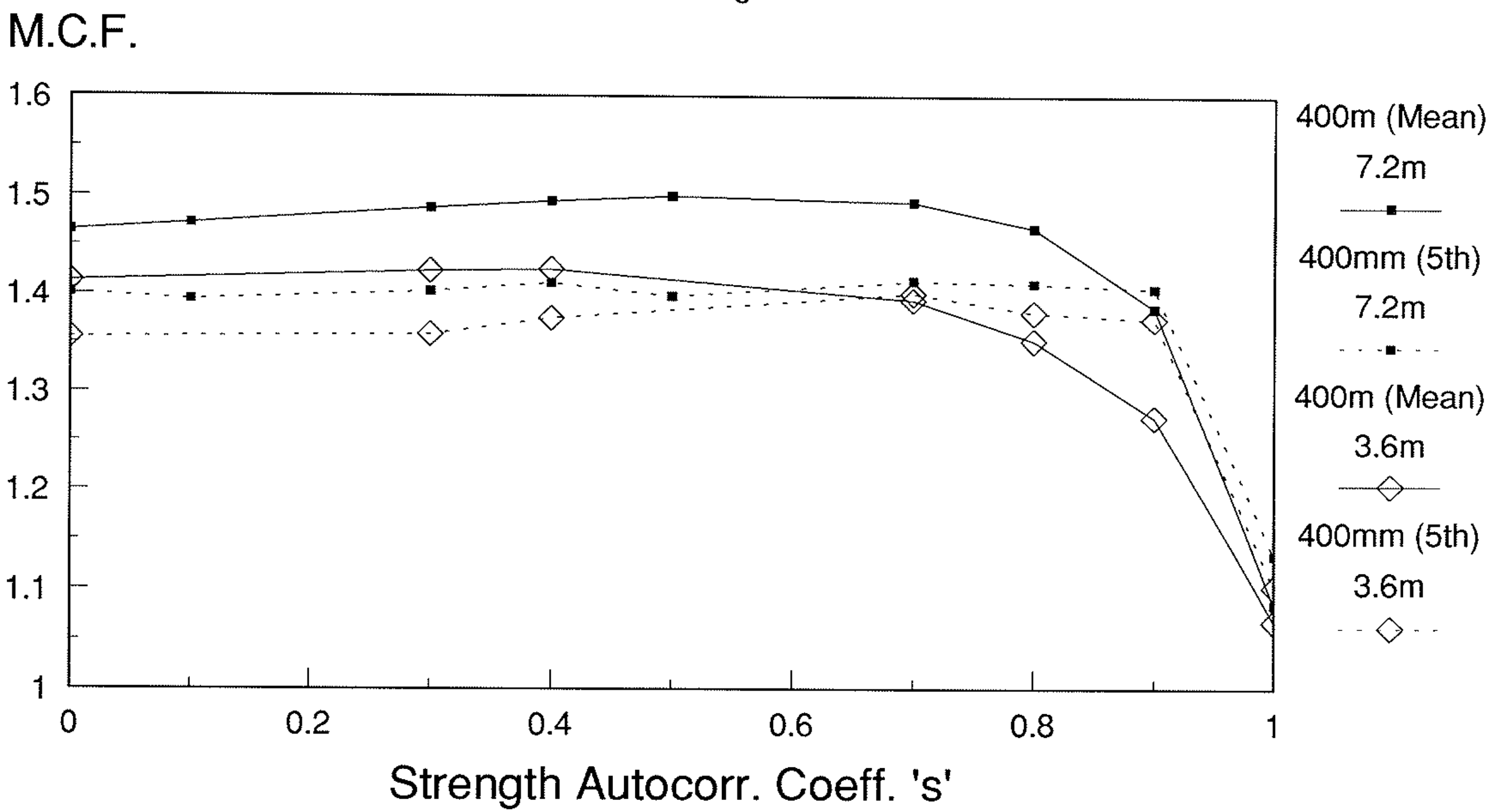

MCFs for 3.6 & 7.2m SS Beams

Central Conc. Load. 600mm Elements

Fig. 9

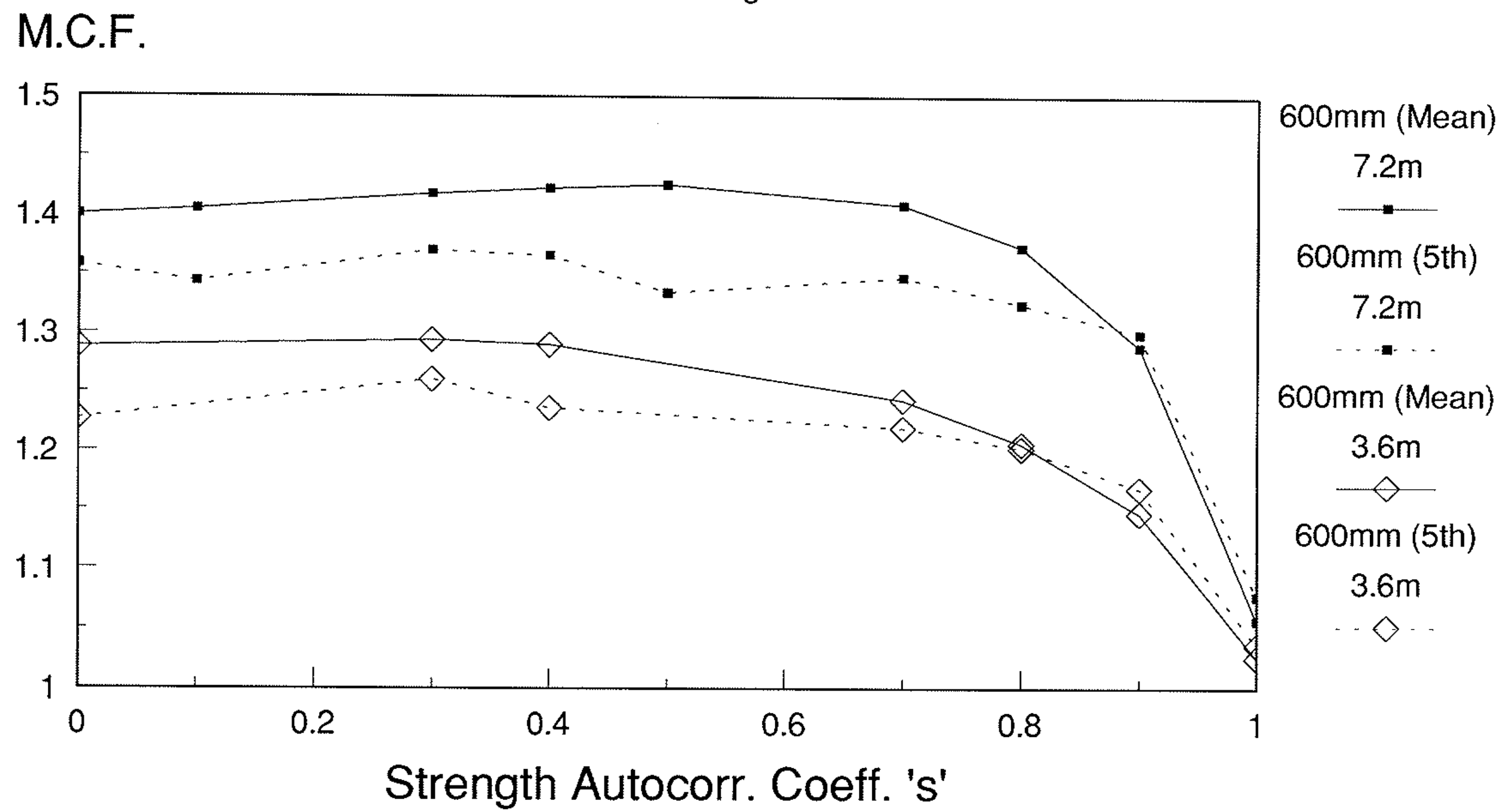

MCFs for 3.6m Beam: Effect of Property Element

UDL on SS Beam

Fig. 10

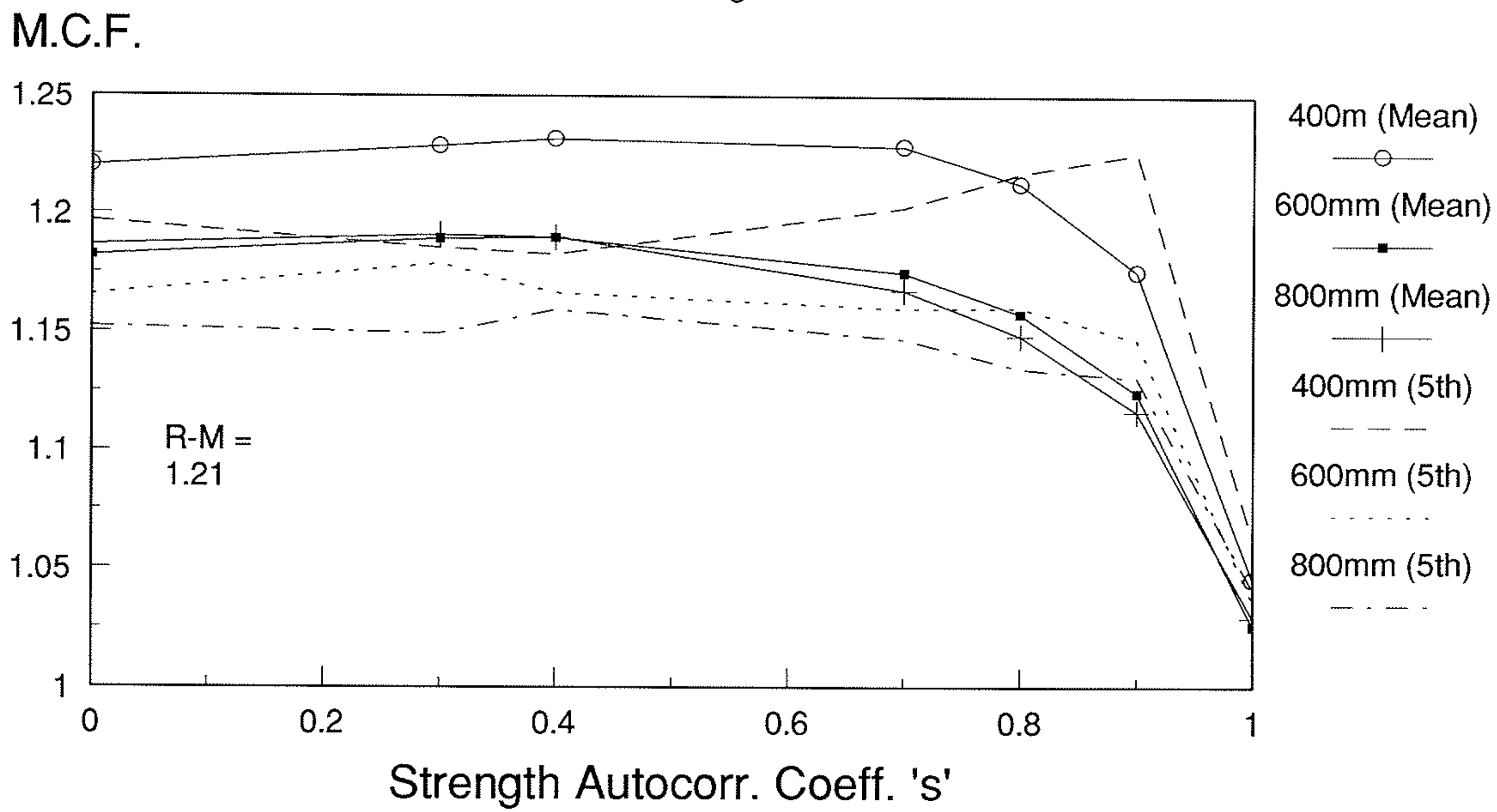

MCFs for 3.6m Beam: Effect of Property Element

S.S. Beam with UDL and 0.9m Overhang

Fig. 11

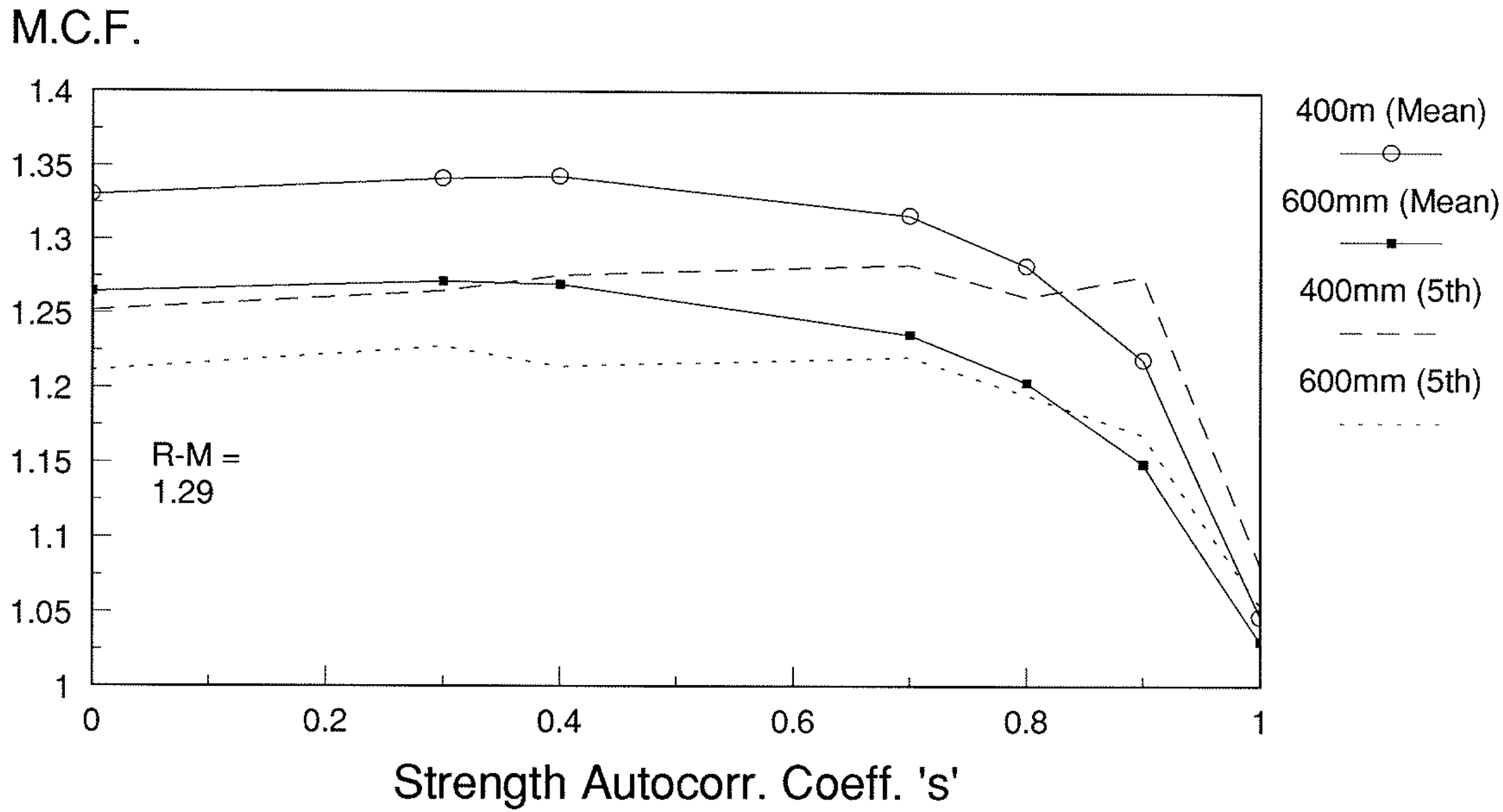

MCFs for 3.6m Beam: Effect of Property Element

S.S. Beam with UDL and 1.17m Overhang

Fig. 12

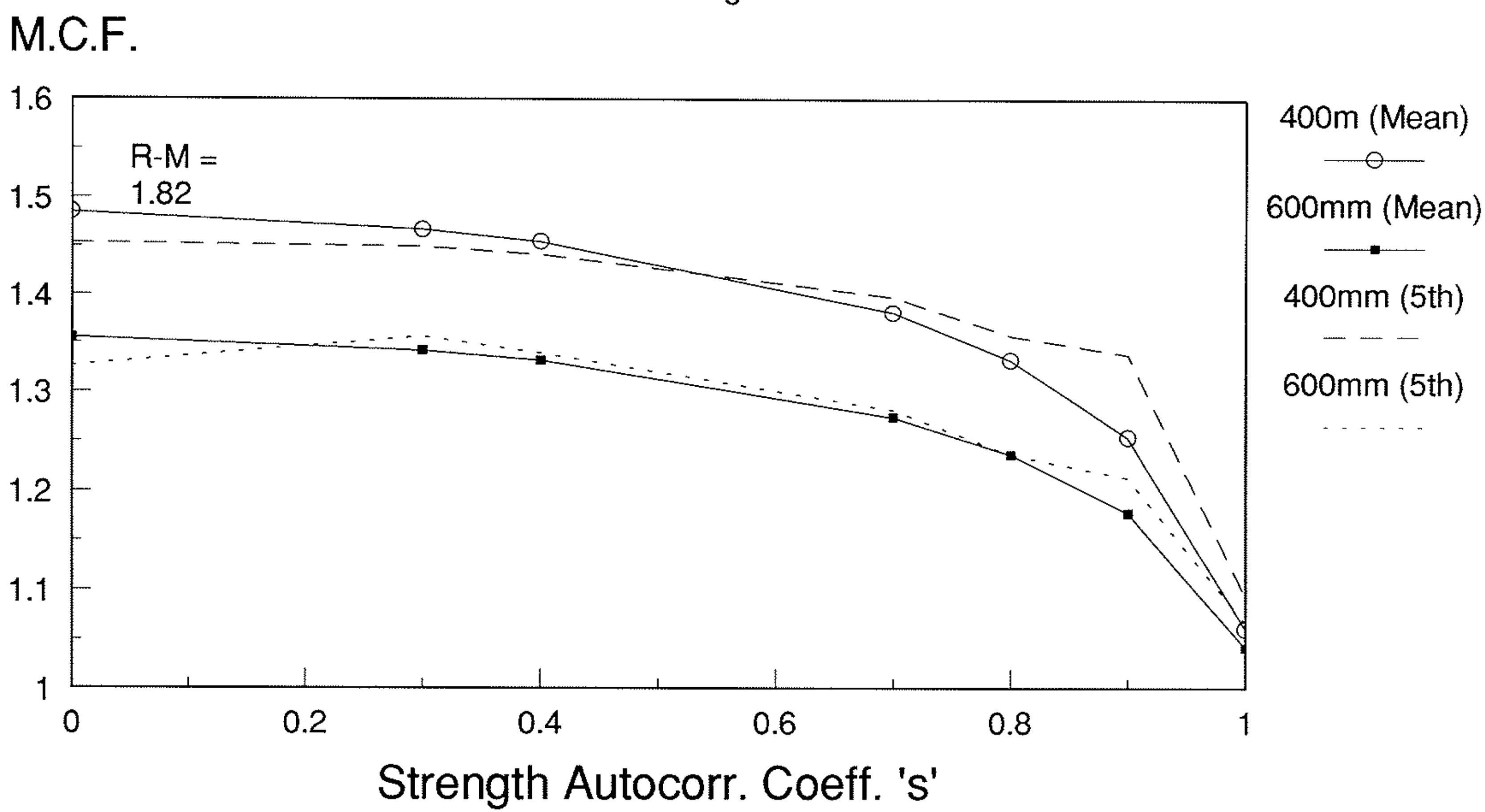

MCFs for 3.6m Beam: Effect of Property Element

Cantilever with UDL

Fig. 13

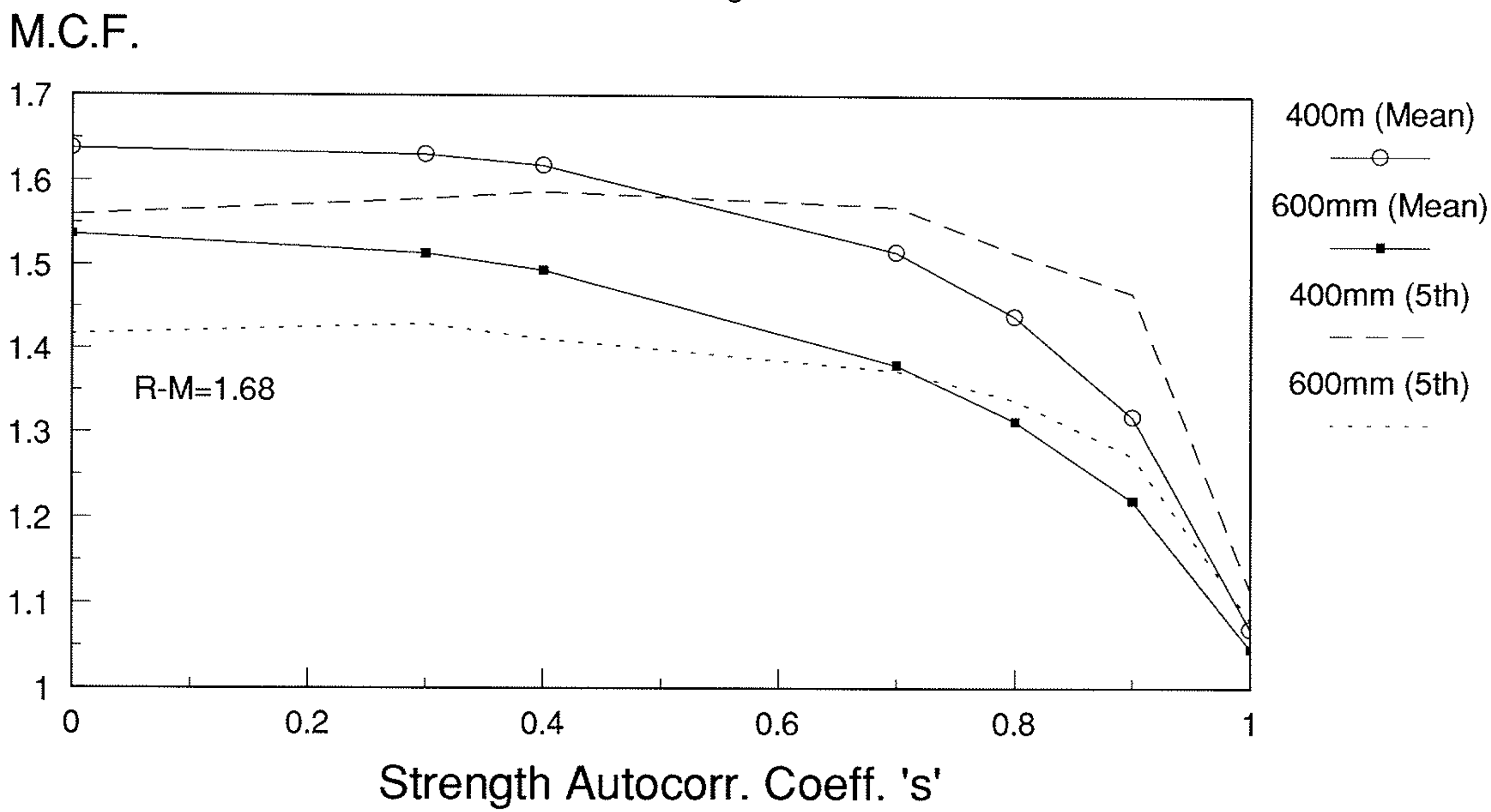

Length Effect on MCF

Concentrated Load on SS Beam

Fig. 14

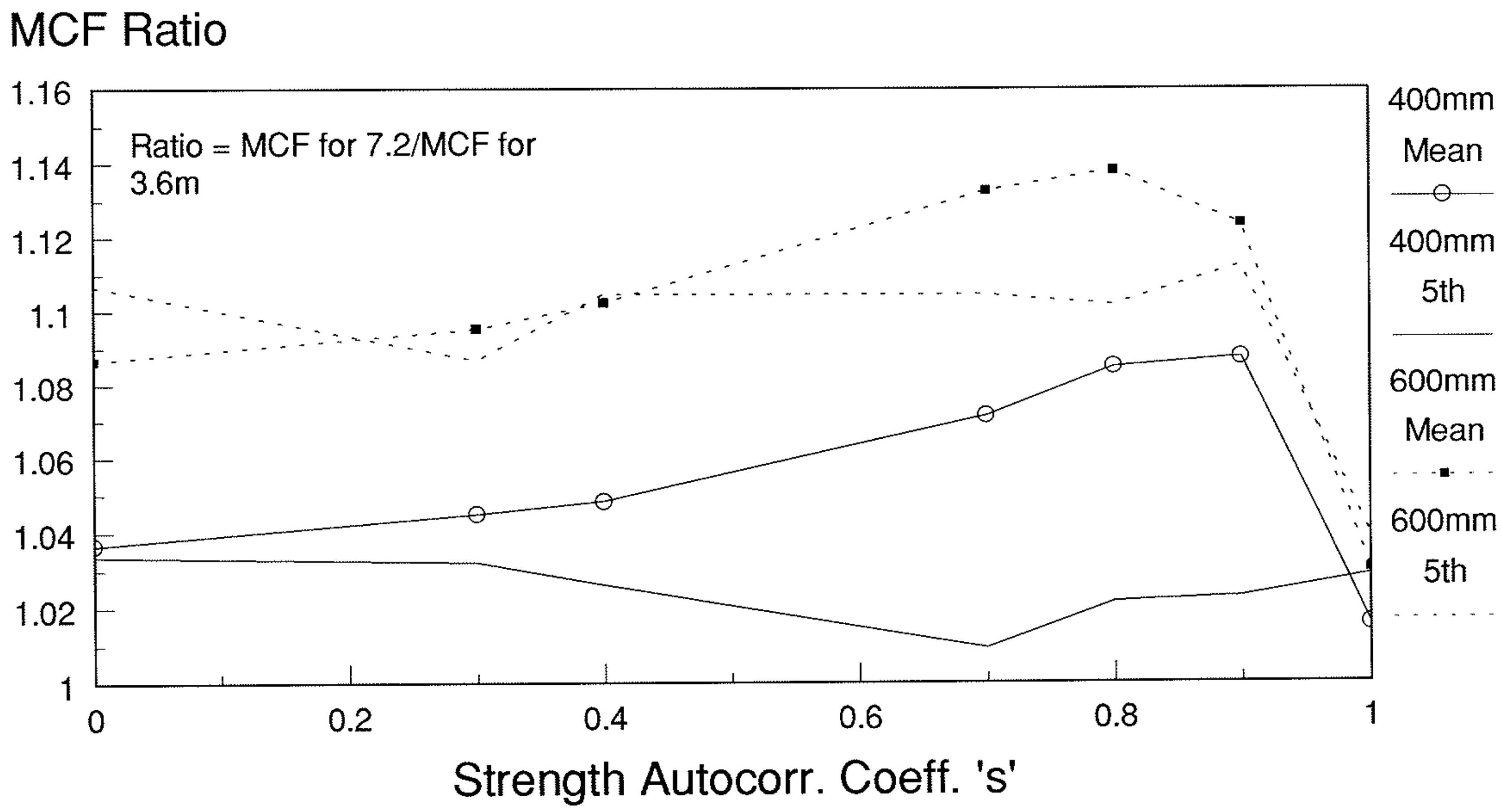

CIB-W18/25-6-3

INTERNATIONAL COUNCIL FOR BUILDING RESEARCH STUDIES AND DOCUMENTATION

WORKING COMMISSION W18 - TIMBER STRUCTURES

BEARING CAPACITY OF TIMBER

by

U Korin
National Building Research Institute
Israel

MEETING TWENTY - FIVE

ÅHUS

SWEDEN

AUGUST 1992

BEARING CAPACITY OF TIMBER

U. Korin*

1. Scope

Some preliminary research work, concerning the behaviour of timber in compression perpendicular to grain (bearing capacity of timber) was presented by the author at the Lisbon 1990 meeting (1).

The investigation of the behaviour of timber in compression perpendicular to grain has since been continued.

This paper reports the data obtained from the extended investigation.

2. The investigation parameters

Types of timber

Whitewood, North-East U.S.A.; Redwood, Finland.

Cross-section of lumber after planning

Whitewood	(2"x4")	- 41x90 mm
	(2"x6")	- 41x138 mm
	(2"x8")	- 41x190 mm
Redwood	(2"x5")	- 46x117 mm
	(2"x6")	- 45x142 mm
	(2"x8")	- 45x185 mm

3. Tests performed

a. Mechanical and physical tests.

b. ASTM D143 "Compression perpendicular to grain of small clear specimens".

c. Bearing capacity tests using loading strips of different widths. The loading was performed at end sector and central sector of the loaded specimens.

The study has not yet been completed, and the final conclusions will be submitted at a later stage.

1. U. Korin, "Timber in Compression Perpendicular to Grain", CIB W18A, Lisbon, Sept. 1990.

---

* Head, Testing Division, National Building Research Institute, Technion, Haifa, Israel.

CIB-W18/25-6-4

INTERNATIONAL COUNCIL FOR BUILDING RESEARCH STUDIES AND DOCUMENTATION

WORKING COMMISSION W18 - TIMBER STRUCTURES

ON DESIGN CRITERIA FOR TENSION PERPENDICULAR TO GRAIN

by

H Petersson
Lund Institute of Technology
Sweden

MEETING TWENTY - FIVE

ÅHUS

SWEDEN

AUGUST 1992

ON DESIGN CRITERIA FOR TENSION PERPENDICULAR TO GRAIN

Hans Petersson
Division of Structural Mechanics
Lund Institute of Technology
Sweden

1. INTRODUCTION

For notched beams, curved beams and beams with openings, cracking and tension perpendicular to the grain is an important matter in design. A standard procedure is to calculate the tensile stresses caused by the loads by using linear elastic assumptions. Normally some formula is used in a hand calculation for the determination of the load effects or, alternatively, a finite element analysis is performed. The stress obtained is compared with some allowable stress value, i.e. some form of stress criterion is used. We may write that

$$\text{calculated stress value} \leq f_{\text{material}} \tag{1}$$

This is a practical approach as long as the material parameter f_{material} can be considered as independent of the size of the structure. However, in a large number of experiments on different types of wooden structures the results clearly indicate a strong influence of size effects.

From the proposal for Eurocode No. 5 [1] the basic rule for ultimate limit state and tension perpendicular to the grain is of special interest for this paper. For solid timber

$$\sigma_{t,90,d} \leq f_{t,90,d} \tag{2}$$

and for glued laminated timber

$$\sigma_{t,90,d} \leq f_{t,90,d} \left[\frac{V_0}{V}\right]^{0.2} \tag{3}$$

where V in m^3 is assumed to be an equivalent stressed volume and V_0 a reference volume of 0.01 m^3.

A background for formula (3) and size effects may be found in [2]. If the size of V can be defined by the length ℓ, the depth h and the width b, then the size effect is

$$\left[\frac{V_0}{V}\right]^{0.2} = \left[\frac{\ell_0}{\ell}\right]^{0.2} \left[\frac{h_0}{h}\right]^{0.2} \left[\frac{b_0}{b}\right]^{0.2} \tag{4}$$

and relates to a Weibull model. This model results in failure when the "weakest link" is broken, and does not distinguish between cases where the maximum load is reached, and cases where the load–bearing capacity is substantially larger than (3) indicates due to stress redistributions. Further, formula (3) does not work well in case of stress concentrations [3].

It may be questioned whether the stress criterion discussed above should not be replaced by a fracture mechanics criterion in combination with a proper selection of a crack surface. The benefit of such an approach would be a better prediction of the load–bearing capacity of the structure; compare [4] for notched beams. Another advantage of a fracture mechanics criterion combined with a fracture analysis is that it may offer a tool to predict what happens when the predicted load is obtained. The question is whether there will be a sudden collapse with a running crack, or if the loading can be increased further due to stable crack propagation. A design method that can give an answer to this would be valuable for the design engineer if it is not too complex to use.

The consequences of changing from the present proposal according to formula (2) or (3) to a fracture mechanics approach could for a typical example of crack opening perpendicular to the grain, say for a curved beam, result in

$$\sigma_{t,90,d} \le f_{material} \cdot k_\ell \cdot k_h \cdot k_b \tag{5}$$

where

$$k_\ell = \begin{cases} 1.0 & \text{stable crack growth} \\ 0.5 & \text{risk of a running crack with sudden loss of load–bearing capacity} \end{cases} \tag{6a}$$

$$k_h = \sqrt{\frac{h_0}{h}} \tag{6b}$$

$$k_b = \begin{cases} 1.0 & \text{no risk of side cracks} \\ \sqrt{\frac{b_c}{b}} & \text{risk of side cracks (remaining uncracked width is } b_c) \end{cases} \tag{6c}$$

and

$$f_{material} = \text{constant} \cdot f_{t,90,d} \tag{7}$$

Some theoretical and experimental support for the validity of the design rule indicated by (5)–(7) will be presented in this paper, but further research is needed in order to determine proper values of k_ℓ, k_h and k_b.

2. THEORY

Study the two–dimensional structure in Figure 1 with a set of reference loads $\{P\}$

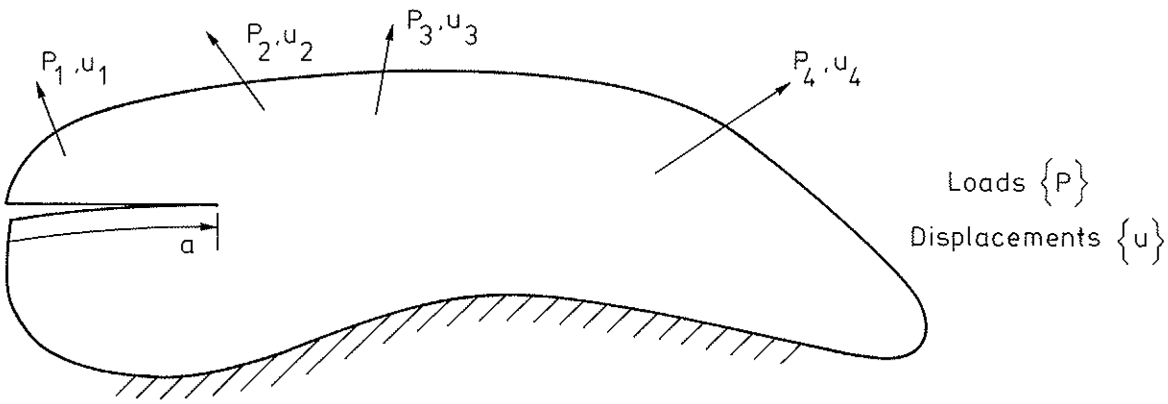

Figure 1 Two–dimensional body with a crack

Assume that the material is linear elastic and denote the associated displacements with $\{u\}$, where

$$\{P\} = \begin{bmatrix} P_1 \\ P_2 \\ \vdots \\ P_n \end{bmatrix} \qquad \{u\} = \begin{bmatrix} u_1 \\ u_2 \\ \vdots \\ u_n \end{bmatrix} \tag{8}$$

Denote the crack length with a and the fracture energy per unit length with $b_c G_c$ where G_c is a material parameter. Then assume that the loads are increased proportionally, i.e. the actual loads are $\alpha\{P\}$ where α is gradually increased up to the value α_c, corresponding to stable or unstable crack growth.

The displacements $\{u\}$ can be expressed by the flexibility relation

$$\{u\} = [f]\{P\} \tag{9}$$

where the flexibility matrix $[f]$ is square and symmetric. The internal energy for linear elastic materials is

$$W = \frac{1}{2}\alpha^2\{P\}^T[f]\{P\} \tag{10}$$

Let us now assume that the reference load $\{P\}$ and the load multiplication factor α are kept constant with respect to a variation of the crack length a. This gives us

$$\frac{\partial W}{\partial a} = \frac{1}{2}\alpha^2\{P\}^T \left[\frac{\partial f}{\partial a}\right]\{P\} \tag{11}$$

For the critical value of $\alpha=\alpha_c$ we obtain

$$\frac{1}{2}\alpha_c^2\{P\}^T \left[\frac{\partial f}{\partial a}\right]\{P\} = b_c G_c \tag{12}$$

or

$$\alpha_c = \sqrt{\frac{2b_c G_c}{\{P\}^T\left[\frac{\partial f}{\partial a}\right]\{P\}}} \tag{13}$$

From a hand calculation point of view it is of special interest to study cases where the matrix [f] is diagonal and where each component of [f] can be expressed simply as a function of the crack length a.

Let us assume that [f] is diagonal with the diagonal elements, f_1, $f_2 \ldots f_n$, which yields

$$\alpha_c = \sqrt{\frac{2b_c G_c}{\sum_{i=1}^{n} \frac{\partial f_i}{\partial a}(P_i)^2}} \tag{14}$$

Let us next study some simple beam structures with an <u>opening</u> crack, say a simply supported beam or the cantilever beam shown in Figure 2.

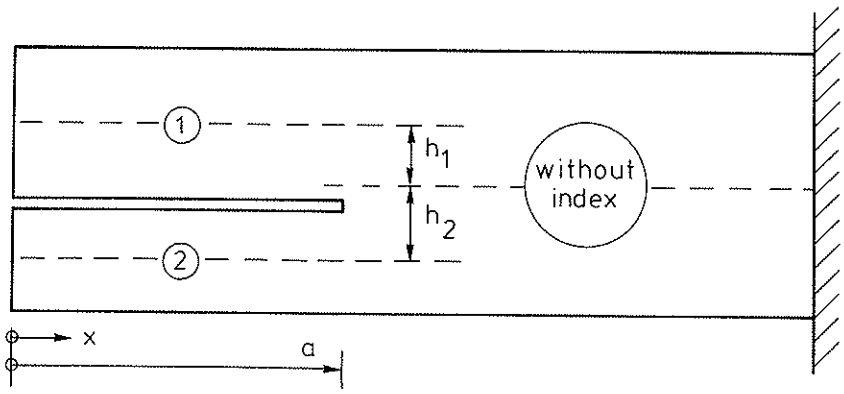

Figure 2 Cantilever beam with a crack

It is assumed that we have some reference loading and a load multiplication factor α that is common to all loads. The sectional forces will be functions of the current crack length a and the notations used are shown in Figure 3.

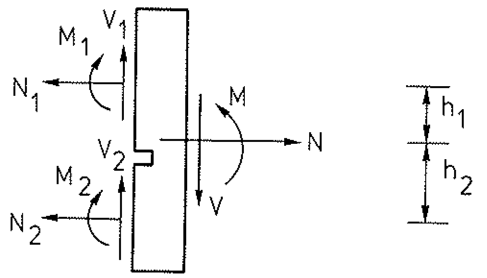

Figure 3 Sectional forces close to the crack tip for α=1 (h_1 and h_2 denote distances between gravity axes).

In order to simplify the following derivations it is assumed that the cross sections remain undeformed. Including energy contributions according to ordinary beam theory only, we may approximately write

$$\alpha_c = \sqrt{\frac{2b_cG_c}{\frac{\beta V_1^2}{GA_1} + \frac{\beta V_2^2}{GA_2} - \frac{\beta V^2}{GA} + \frac{M_1^2}{EI_1} + \frac{M_2^2}{EI_2} - \frac{M^2}{EI} + \frac{N_1^2}{EA_1} + \frac{N_2^2}{EA_2} - \frac{N^2}{EA}}} \tag{15}$$

Since both b_cG_c and the sectional forces in a general case are functions of the crack length a, also the critical load factor α_c is a function of a.

If all the sectional parameters (GA_1/β, EI_1, EA_1, etc.) are constant and there are no external loads close to the crack tip (for x=a) we may write

$$\frac{d\alpha_c}{da} = -\frac{(\alpha_c)^3}{2b_cG_c}\left[\frac{M_1}{EI_1}V_1 + \frac{M_2}{EI_2}V_2 - \frac{M}{EI}V\right] + \frac{\alpha_c}{2bG_c}\frac{d}{da}(b_cG_c) \tag{16a}$$

For $\alpha=\alpha_c$ the risk of a running crack is avoided if

$$\frac{d}{da}(b_cG_c) \geq (\alpha_c)^2\left[\frac{M_1V_1}{EI_1} + \frac{M_2V_2}{EI_2} - \frac{MV}{EI}\right] \tag{16b}$$

This means that not only the value of b_cG_c is of importance but also the variation of this quantity along the crack path expressed by derivative $\frac{d}{da}(b_cG_c)$.

3. APPLICATION EXAMPLES

As an application of Eqs. (15) and (16) we may choose the end–notched beam shown in Figure 4.

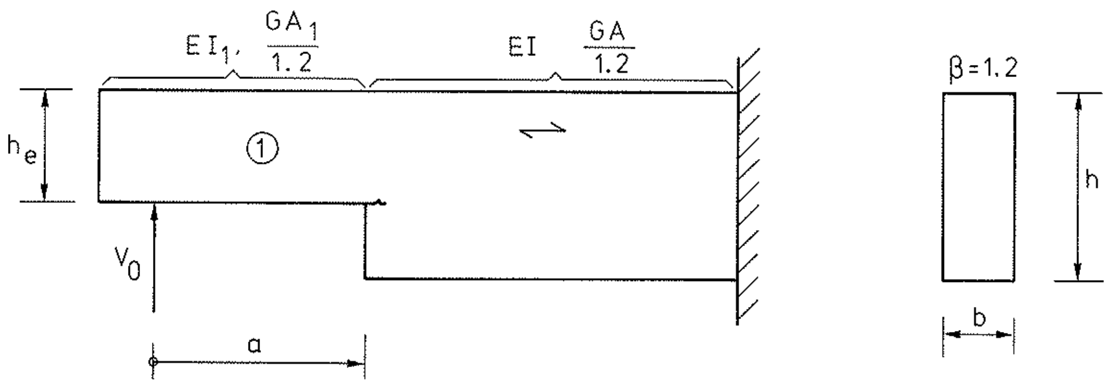

Figure 4 Notched beam with shear force

With the notation $V_c=\alpha_c V_0$ and observing that $V_2=N_1=N_2=N=0$, $M_2=0$, $V_1=V=V_0$ and $M_1=M=aV_0$ we get from (15)

$$V_c = \sqrt{\frac{2b_c G_c}{\frac{\beta}{G}(\frac{1}{A_1} - \frac{1}{A}) + \frac{a^2}{E}(\frac{1}{I_1} - \frac{1}{I})}} \tag{17}$$

This formula is not in full agreement with the results presented in references (3)–(5) as it is based on somewhat different assumptions.

Use of Eq. (16a) with $\alpha_c = V_c/V_0$ yields

$$\frac{d\alpha_c}{da} = \frac{\alpha_c}{2b_c G_c}\left[\frac{d}{da}(b_c G_c) - V_c^2 \frac{a}{EI_1}(1 - \frac{I_1}{I})\right] \tag{18}$$

This means that the fracture energy parameter must be increasing, i.e.

$$\frac{d}{da}(b_c G_c) > V_c^2 \frac{a}{EI_1}(1 - \frac{I_1}{I}) \tag{19}$$

if a running crack is to be avoided. An end–notched beam with a shear force is thus from a structural safety point of view a dangerous case.

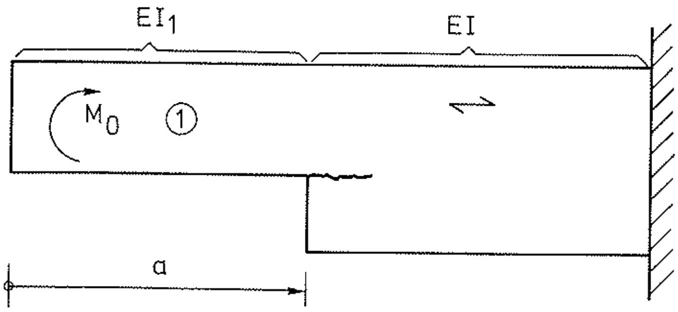

Figure 5 Notched beam with moment load

For the beam in Figure 5 with an end–moment M_0 the critical load $M_c=\alpha_c M_0$ is

$$M_c = \sqrt{\frac{2b_cG_c}{\frac{1}{E}(\frac{1}{I_1}-\frac{1}{I})}} \tag{20}$$

and in this case it is sufficient that

$$\frac{d}{da}(b_cG_c) > 0 \tag{21}$$

for stable crack growth. This is a much more favourable situation than the case of the shear loading in Figure 4.

Due to non–structural reasons, notches are sometimes poorly located as in Figure 6. The critical load $V_c=\alpha_c V_0$ can be calculated by Eq. (15) with $V=V_0$ and $M=(\ell-a)V_0$ resulting in a larger critical value than for the problem in Figure 4 if $\ell > a$. However, the most interesting observation is that the requirement for stable crack growth is much more advantageous for the central notch,

$$\frac{d}{da}(b_cG_c) + V_c^2\,\frac{a}{EI_1}(1-\frac{I_1}{I}) > 0 \tag{22}$$

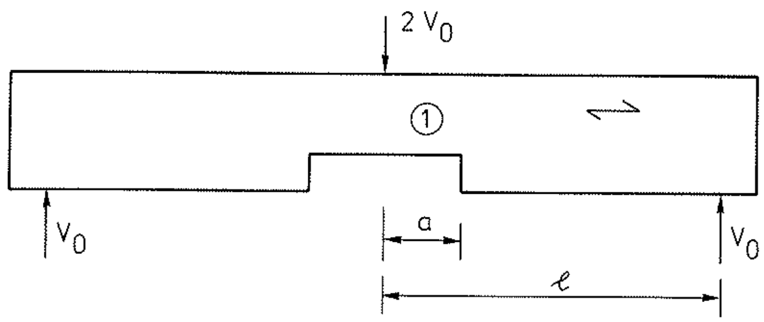

Figure 6 Beam with central notch

This means that a central notch normally gives a more stable crack growth than an end–notch.

Tension test

In the application examples treated up to now, deformations perpendicular to the grain due to tension have been neglected. These deformations must obviously be included for the test specimen for glued laminated timber shown in Figure 7.

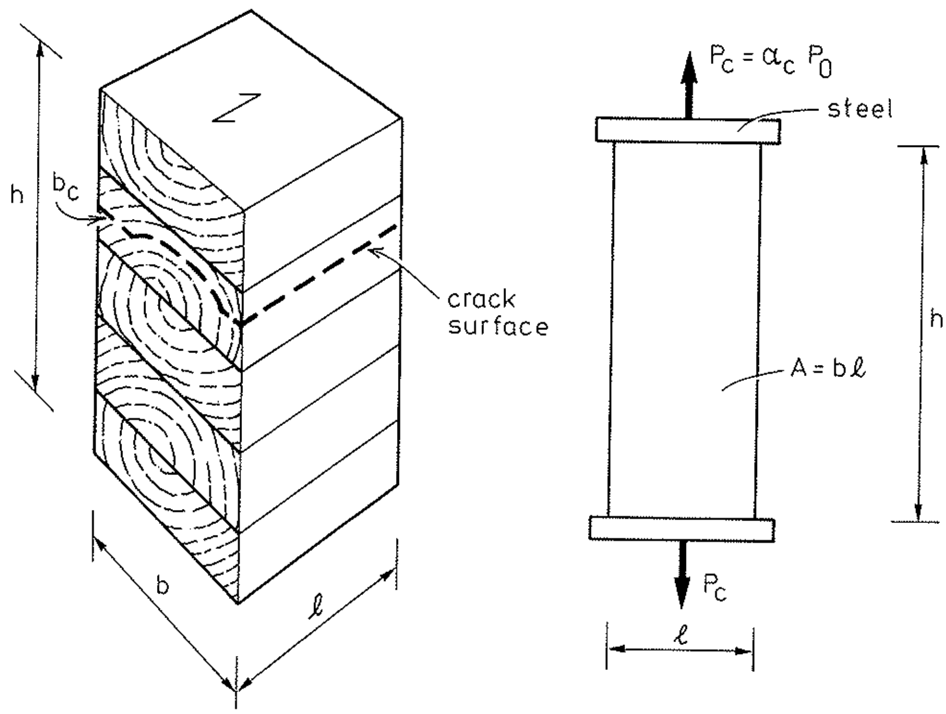

Figure 7 Test specimen for tension perpendicular to grain

The basic assumption is that the failure will occur due to one or several defects initiating a major cracking process. The problem is that we do not know the size of the initial cracks. It is, however, from a fracture mechanics point of view reasonable to start from an elementary case referring to a small value of $h=h_0$ (say, for conifer, about 5 mm). We assume for this elementary case that the stress is applied first, then the two opposite loaded sides are clamped and finally a crack is introduced. For this case we can find the critical stress value

$$\sigma_c = \sqrt{\frac{2G_c E_I}{h_0}} \tag{23}$$

where E_I takes the orthotropic behaviour of wood into account. A theoretical value of E_I for conifer is about double the value for the elasticity modulus E_{90} perpendicular to the grain. In order to be conservative (risk of load crack instability) E_I will be replaced in the following by E_{90}

and G_c by $\frac{b_c}{b}G_c$. The last change is a simple engineering modification to facilitate accounting for a major initial crack or a curved crack path. For $h=h_0$ we then arrive at

$$\sigma_c \geq \sqrt{2\frac{b_c}{b}\ \frac{G_c E_{90}}{h_0}} = f_{t0} \tag{24}$$

Now, by assuming that the specimen in Figure 7 consists of h/h_0 "links" in a Weibull model, we may write, see (3) and reference [8],

$$f_t = f_{t0}\left[\frac{V_0}{V}\right]^{\frac{1}{\eta}} \tag{25}$$

where a value of η=6.0 is not unrealistic [8], although (3) indicates that η should be set at 5.0. We choose here the value η=6.0 considering the additional assumption that for the volume

$$V = \frac{b}{h}\frac{\ell}{h}h^3 \tag{26}$$

the ratios b/h and ℓ/h should have no influence on the size effect. This yields with η=6 that

$$f_t = f_{t0}\left[\frac{h_0}{h}\right]^{\frac{3}{\eta}} = f_{t0}\sqrt{\frac{h_0}{h}} \tag{27}$$

Substitution of f_{t0} according to (24) into (27) and conservatively dropping the unequal sign yields

$$\sigma_c = \sqrt{2\ \frac{b_c}{b}\ \frac{G_c E_{90}}{h}} = f_t \tag{28}$$

Curved beam

The final example refers to a curved beam with constant depth, where the curved part is loaded by a constant moment $M=P\ell$, see Figure 8. The mid–curvature is denoted by R and the cross section has the area bh. Denoting the maximum stress perpendicular to the grain by σ_c we get approximately

$$\sigma_c \approx 1.5\,\frac{h}{R}\,\frac{M_c}{b\,h^2} \tag{29}$$

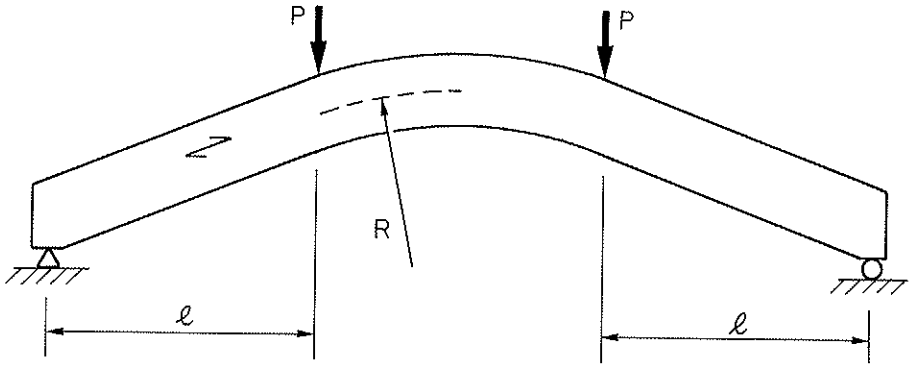

Figure 8 Curved beam with constant depth

from a simple equilibrium study. It is then assumed that the stress perpendicular to the grain has a parabolic variation over the depth h, which corresponds to an equivalent length of 8h/15 from an energy point of view. Assuming that the crack occurs where the stress in the fibre direction is zero we obtain according to Eq. (28) that

$$\sigma_c = \sqrt{2 \frac{b_c}{b} \frac{G_c E_{90}}{\frac{8}{15}h}} \tag{30}$$

Eqs. (29) and (30) then yield

$$M_c = bhR \sqrt{\frac{5}{3} \frac{b_c}{b} \frac{G_c E_{90}}{h}} \tag{31}$$

We again return to Eq. (30), which can be written as

$$\sigma_c = \sqrt{3.75 \frac{b_c}{b} \frac{G_c E_{90}}{h}} \tag{32}$$

If we denote the average stress for the uniaxial tension test according to Eq. (28) with f_t we obtain for the curved beam

$$\sigma_c = \sqrt{1.875}\, f_t = 1.37\, f_t \tag{33}$$

5. EXPERIMENTAL VERIFICATION

The theory and examples treated in the previous two sections need to be correlated with experimental results. For end–notched beams references are made to the investigation reported in [3] to [5], and the relevance of a fracture mechanics approach for analysis of this type of notched structures is confirmed.

In comparison of theoretical and experimental results we need basic material parameters such as the elasticity modulus and the fracture energy for tension perpendicular to grain. Based on results shown in Figure 9 the relation

$$G_c = 1.04\rho - 146 \tag{34}$$

has been suggested for the mean value of the fracture energy per unit area [Nm/m^2 or J/m^2] where ρ is the density in kg/m^3, see [6]. Dealing with conifer, a reasonable mean value of ρ would be 450 kg/m^3, if a single value has to be chosen. This density corresponds to

$$G_c \approx 320 \text{ J/m}^2 \tag{35}$$

The value chosen for the elasticity modulus is partly based on the values reported in [7] for glued laminated timber of Swedish spruce (class L40 and b=0.115 m)

$$E_{90} = 330 \text{ MPa} \tag{36}$$

According to the European standard draft for characteristic values of mechanical properties this value should be increased to 400 MPa. Nevertheless, the values according to (35) and (36) will be the basis for the following comparison between theoretical and experimental results.

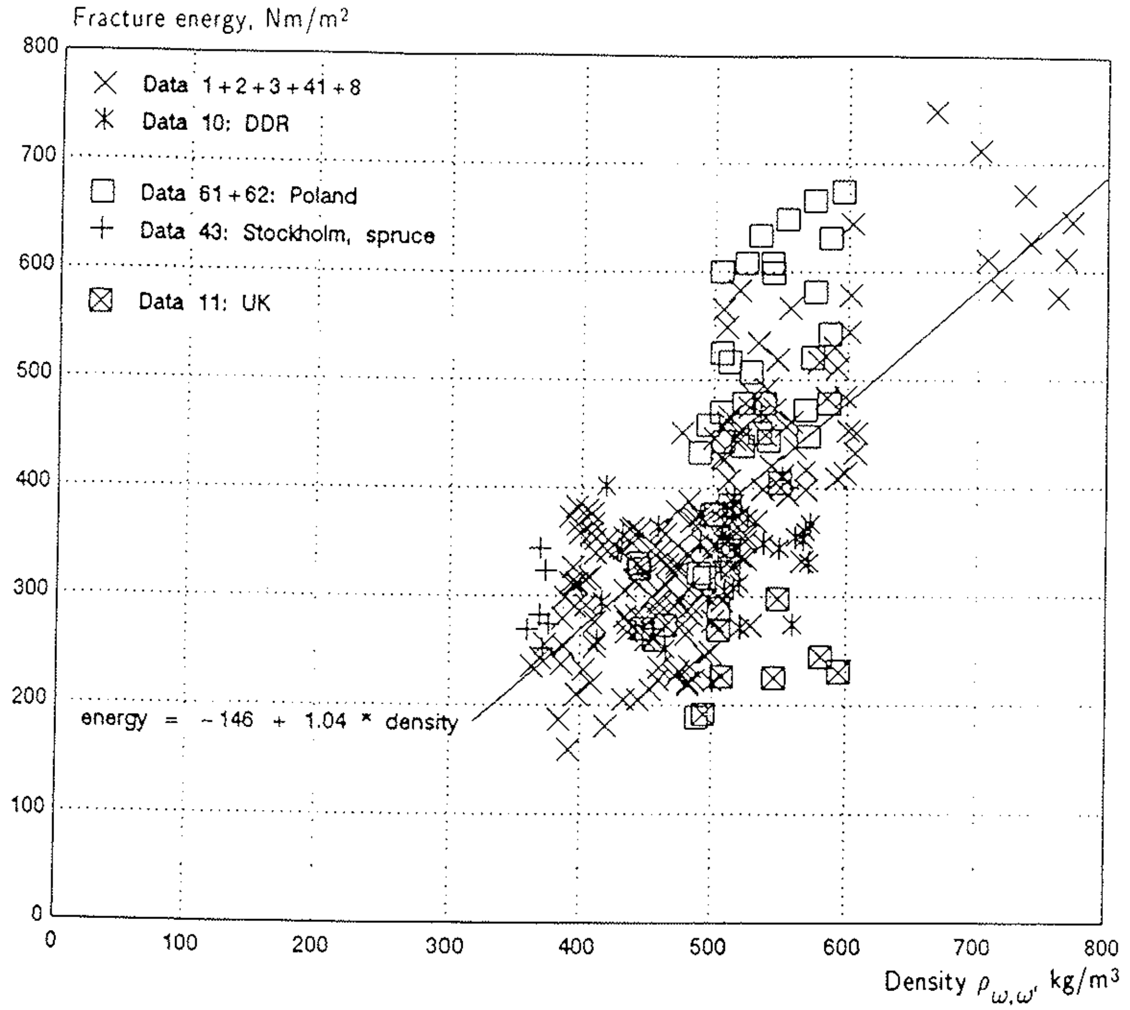

Figure 9 Fracture energy versus density for European softwoods (regarded as one population) [6]

Uniaxial tension test

Eq. (28) requires determining the ratio between b_c and b. The experimental results reported in [7] indicate that in some tests b_c/b could be as high as 1.15, but in the following this ratio is set at

$$\frac{b_c}{b} = 1.0 \tag{37}$$

This may be a conservative assumption for the mean values of specimens without any visible side cracks. Substitution of (35), (36) and (37) into (28) yields

$$\sigma_c = f_t = \sqrt{2\frac{0.32 \cdot 0.33}{h}} \text{ MPa}$$

or

$$f_t = \sqrt{\frac{h_0}{h}}\ \text{MPa} \qquad (38)$$

with $h_0 = 0.211$ m.

The simple relation according to (38) is for h_0=0.21 and 0.3 m compared to the two Danish investigations reported in [7] and [8], see Table 1 and Figure 10.

Table 1 Tensile strength perpendicular to the grain for spruce (mean values)

Reference	Size (mm) b	ℓ	h	Number of specimens	Experiment f_t (MPa)	$\sqrt{\frac{0.21\ \text{m}}{h}}$	$\sqrt{\frac{0.3\ \text{m}}{h}}$
[7]	115	175	330	50	1.11	0.80	0.95
[8]	90	97	300	87	1.09	0.84	1.00
[8]	139	141	1336	18	0.63	0.40	0.47
[8]	139	141	128	18	1.00(?)	1.28	1.50
[8]	90	97	294	18	1.04	0.85	0.98
[8]	45	46	133	36	1.87	1.26	1.50
[8]	20	20	67	36	2.38	1.77	2.12

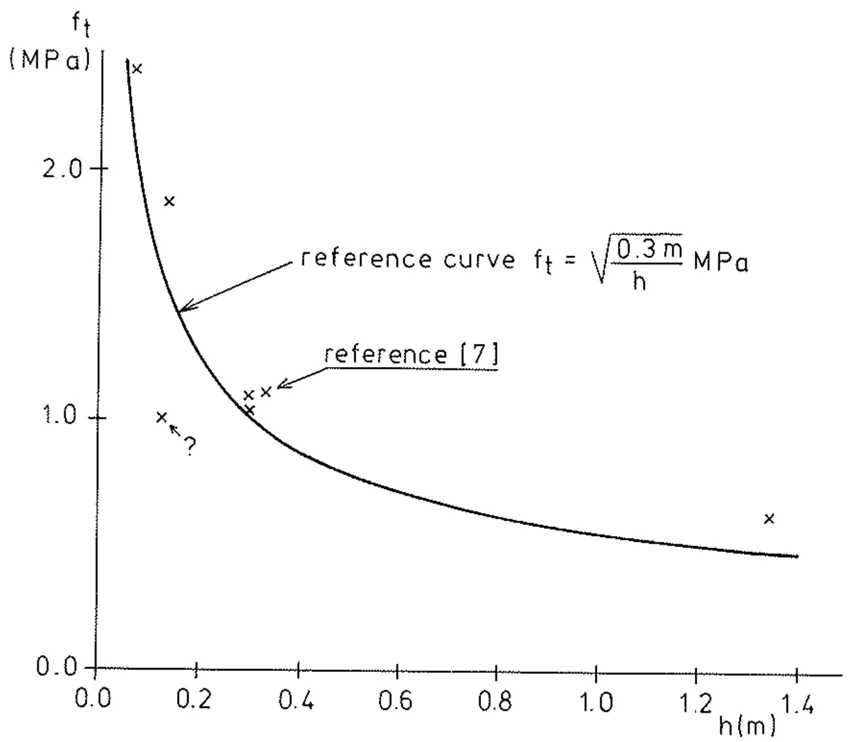

Figure 10 Tensile strength perpendicular to the grain (from [7] and [8]) compared with a reference curve

From the results we can observe a strong influence of the height h of the specimen. The formula (38) seems to give a reasonable agreement with experimental results. It is also interesting to use (38) for prediction of the strength for small–scale experiments. For $h=0.1\ h_0$ we get according to (38) a tensile strength of 3.2 MPa, which is in agreement with experimentally obtained results.

Curved beam with constant depth

In order to compare Eq. (31) with experimental results the moment $M_c=P_c\ell$ is replaced by the load P_c,

$$P_c = \frac{bhR}{\ell}\sqrt{\frac{5}{3}\,\frac{b_c}{b}\,\frac{G_cE_{90}}{h}} \tag{39}$$

The experimental results are taken from references [9] and [10], where some tests were carried out with a groove located in the most critical curved portion of the beam according to Figure 11. The results are shown in Table 2. In the calculations the material parameters have been chosen according to (35) and (36).

The calculated values partly based on fracture mechanics agree reasonably well with experimental results. The values to be used for the material parameters in the German tests are somewhat uncertain as little information about the wood quality was reported in [10].

It is of special interest to note that the ratio between the failure loads for beams with and without a groove is in close agreement with the suggested formula (39), i.e. equal to $\sqrt{b_c/b}$.

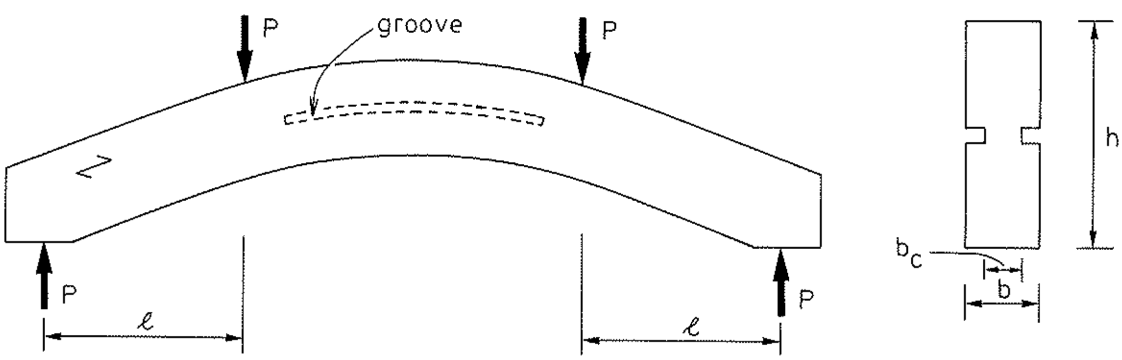

Figure 11   Curved beam with constant depth and width with a groove [9].

Table 2 Load at failure for curved beams (mean values)

Reference	Number of tests	b	Geometry [m] h	R	ℓ	$\frac{b_c}{b}$	Experiment P_{c1} [kN]	According to Eq. (39) P_{c2} [kN]	$\frac{P_{c1}}{P_{c2}}$
[9]	5	0.06	0.24	1.36	0.50	1.0	31.5	33.4	0.94
[9]	3	0.06	0.24	1.36	0.50	0.5	23.5	23.6	1.00
[10]	2	0.12	1.00	5.00	2.75	1.0	96.8	91.5	1.06
[10]	2	0.12	0.77	3.85	2.31	1.0	68.2	73.6	0.93
[10]	2	0.12	0.53	2.65	1.59	1.0	53.5	61.1	0.88
[10]	2	0.12	0.30	1.50	0.90	1.0	39.8	46.0	0.87

6. CONCLUDING REMARKS

Cracks that run in the fibre direction and open perpendicular to the grains are of major concern in the design of wooden structures. The use of fracture mechanics seems quite natural. In this paper a number of applications have been treated to provide a background for the discussion of size effects. As a summary we may, for the sake of simplicity, conclude that the stress σ calculated by elementary theory should be compared with the fracture material parameter $\sqrt{G_c E}$. We may symbolically write

$$\sigma \leq \sqrt{\frac{b_c}{b}} \sqrt{\frac{2G_c E}{h}} \; k_\ell \tag{42}$$

where the influence of the length effect expressed by k_ℓ should differ substantially depending on the risk of a running crack. Such a large difference as

$$k_\ell = \begin{cases} 1.0 & \text{for stable crack growth} \\ 0.5 & \text{unstable crack growth probable} \end{cases} \tag{43}$$

may by further research be found to be reasonable for use in design. It should again be pointed out that stable or unstable crack growth depends not only on the loading conditions but also on the variation of $b_c G_c$ along the crack path.

REFERENCES

[1] Eurocode No. 5, Design of Timber Structures, Part 1, Prepared for CEN, April 1992.

[2] R.O. Foschi, B.R. Folz and F.Z. Yao; Reliability–Based Design of Wood Structures, Structural Research Series, Report No. 34, Department of Civil Engineering, University of British Columbia, Vancouver 1989.

[3] P.J. Gustafsson and B. Enquist: Strength of wooden beam at right angle notch (in Swedish), Report TVSM–7042, Lund Institute of Technology, Division of Structural Mechanics, Lund 1988.

[4] P.J. Gustafsson: Eurocode 5 Draft Design Criterion for Notched Beams, International Timber Engineering Conference, Volume 1, London 1991.

[5] P.J. Gustafsson: A study of strength of notched beams, CIB–W18A, Paper No. 21–10–1, Vancouver 1988.

[6] H.J. Larsen and P.J. Gustafsson: The fracture energy of wood in tension perpendicular to the grain – results from a joint testing project, CIB–W18A, Paper No. 23–10–2, Lisbon 1990.

[7] T. Feldborg: Timber in structural sizes. Stiffness and strength perpendicular to grain. Documentation for project R13–83, Danish Building Research Institute, Structural Division, 1992.

[8] H.J. Larsen and H. Riberholt: Tensile strength perpendicular to the grain, Institute of Building Technology and Structural Engineering, Report No. 8110, Aalborg, Denmark 1981.

[9] H.J. Larsen, P.J. Gustafsson and B. Enquist: Tests with glass–fibre reinforcement of wood perpendicular to the grain, Lund Institute of Technology, Division of Structural Mechanics, Report TVSM–7067, 1992.

[10] J. Ehlbeck and J. Kürth: Influence of perpendicular–grain stressed volume on the loadcarrying capacity of curved and tapered glulam beams, CIB–W18A, Paper No. 24–12–2, Oxford 1991.

CIB-W18/25-6-5

INTERNATIONAL COUNCIL FOR BUILDING RESEARCH STUDIES AND DOCUMENTATION

WORKING COMMISSION W18 - TIMBER STRUCTURES

SIZE EFFECTS IN VISUALLY GRADED SOFTWOOD STRUCTURAL LUMBER

by

J D Barrett
F Lam
W Lau
The University of British Columbia
Canada

MEETING TWENTY - FIVE

ÅHUS

SWEDEN

AUGUST 1992

Size Effects in Visually Graded Softwood Structural Lumber

by

J. D. Barrett[1] F. Lam[2], Associate Member ASCE and W. Lau[2]

Abstract

A brittle fracture model has been evaluated for predicting the variation in bending, compression and tension parallel to grain strength of visually graded dimension lumber. Size effect factors for visually graded lumber bending, tension and compression strength are established. Size effect parameters for visually graded lumber are anisotropic. Size effects for changes in member width are typically greater than the size effects for changes in length. Relationships between width (S_W), length (S_L) and constant ratio (S_R) size factors have been introduced. Size factors derived from length effect tests are used to estimate ratios of tension strength to bending strength. Results agree closely with tension/bending property ratios published in the literature. Size factors for bending and tension are recommended for international harmonization of procedures for derivation of characteristic properties of visually graded lumber at standard sizes.

Introduction

Modern design codes, based on reliability concepts, have adopted full size member testing as the basis for establishing structural properties of wood products. Full-size test properties of many wood products including visually graded lumber show structural properties vary with member size, loading conditions and failure mode - bending tension or compression. Standards for derivation of characteristic properties for design now recognize the need to adjust materials properties to standard conditions

---

[1]Professor, Department of Harvesting and Wood Science, University of British Columbia, Vancouver, B.C., Canada V6T 1Z4.

[2]Research Engineer, Department of Harvesting and Wood Science, University of British Columbia, Vancouver, B.C., Canada V6T 1Z4.

(moisture content, temperature, duration of loading) and a standard member size and load configuration (cf. ASTM 1991a, CEN 1991).

Characteristic properties of bending members are presented at a standard depth, member span to depth ratio, and loading condition. European standards (CEN 1991) reference bending strength to a 150 mm depth, 18 to 1 span to depth ratio and 1/3 point load condition. ASTM standards (ASTM 1991a) adopted a characteristic bending member with a 17 to 1 span to depth ratio, 184 mm depth and 1/3 point load distribution. The characteristic properties are derived from test data adjusted to the characteristic size using size adjustment models.

Size adjustment procedures adopted in CEN and ASTM standards are conceptually similar but the property adjustment relationships are significantly different. Consider a simple case where bending strength data collected on 75 mm deep bending members is to be adjusted to a 150 mm depth while retaining the standard span to depth ratio. CEN procedures (CEN 1991a) would require a strength reduction of approximately 0.87 $= (75/150)^{0.2}$, whereas the ASTM adjustment would be $0.74 = (75/150)^{0.43}$. ASTM requires tension member strength adjustments for member length and width. CEN standards provide only width adjustments for tension members. Size adjustment models for visually graded lumber must be rationalized in order to encourage the safe and efficient use of structural timber.

Brittle fracture (weakest link) theory has been used widely to study statistical size effects in structural materials including concrete, ceramics, glass and structural wood products. Variation in ultimate capacity of timber structural members, timber connections and small clear test specimens have been rationalized using brittle fracture concepts. Applications of the classical brittle fracture analysis for the tension perpendicular to grain failure mode (Barrett 1974, Barrett *et al.* 1975, Colling 1986), and the shear parallel to grain failure mode (Foschi and Barrett 1976, Colling 1986) related strength to the stressed material volume. Bohannan (1966) showed the bending strength of clear wood members varied with the beam aspect area (i.e., the width times the length).

The classical weakest link model must be modified to incorporate different size effect factors for length effects and width effects in structural wood products (Buchanan 1984, Madsen and Buchanan 1986, Johnson *et al.* 1989, Barrett and Fewell 1990, Sharp and Suddarth 1991, Madsen 1992). With this exception, the literature suggests that the weakest link size effects analysis provides a useful framework for assessing effects of load configuration and member size on strength of visually graded lumber. Experimental studies (Madsen and Nielson 1976, Buchanan 1984, Madsen 1990, Madsen 1992) show that length effects for tension and bending members, failing in tension parallel to grain, are similar (Barrett and Fewell 1990, Madsen 1992). Width effect factors deduced from constant length members tested at different widths are somewhat greater than would be anticipated from size parameters based on length effect studies (cf., Madsen and Nielsen 1976, Johnson *et al.* 1989, Madsen 1990, Barrett and Fewell 1990).

Visually graded 38 mm dimension lumber is produced in standard grades (NLGA 1991). The grading rules define maximum permissible appearance and strength limiting characteristics for each grade. In NLGA dimension lumber grades, maximum permitted knot sizes increase as the member width increases. In this context, each member width may be considered to be a different material since the defect size distributions vary by width. If defect size increases with width then the apparent width effect will be greater than predicted from length effect studies.

Size effects for visually graded lumber may also vary with material quality. Size effects appear to be much greater for visually grade lumber than for clear wood (Bohannan

1966, Barrett and Fewell 1990, Madsen and Tomoi 1991, Madsen 1992). The high quality material within a visual grade may exhibit a smaller width and length size effect than weak material in the same grade. Thus, size effects could be dependent on strength level.

Size effects in bending members are related to tension and compression behavior. Buchanan (1984) provides a theoretical model for predicting bending strength given knowledge of tension and compression strength behavior. The model relates tension strength to bending strength using a weakest link failure concept. Size effects in bending strength for low quality material, are determined almost exclusively by tension behavior since compression strength exceeds tension strength. In high quality material tension strength exceeds compression strength in the failure region and compression yielding occurs prior to ultimate load. Bending capacity is affected by the redistribution of tension stress occuring as a result of compression yielding. Bending size effects may be influenced by clear wood compression strength behavior.

Bending strength varies with changes in member length and width (Madsen and Nielsen 1976, Madsen and Nielsen 1978a, Johnson *et al.* 1989, Barrett and Fewell 1990, Madsen and Tomoi 1991). The most extensive studies of size effects in bending evaluated beams having a constant ratio of length to depth (width). These studies do not permit direct calculation of separate size factors for width or length effects. Published research provides conflicting evidence on the relative importance of width and lengths effects in bending members. Madsen and Buchanan (1986) found no consistent width effect in an analysis of their own and other published research. Madsen (1990) provides preliminary estimates of width effects for bending members which are of the same order of magnitude as the tension length effect. Madsen (1992) finds no consistent width effect in several studies of bending strength.

Barrett and Fewell (1990) provided a preliminary analysis of bending and tension tests from several North American and European sources. The analysis focussed on size effects at the 5th percentile strength level. Length effects and width effects were species independent. Length effects (S_L = 0.17) and width effects (S_W = 0.23) for tension and bending were similar across a number of species and grades.

The purpose of this paper is to evaluate and rationalize apparent differences in size effect parameters obtained for visually graded structural lumber produced in Canada and the United States. Published research will be combined with unpublished experimental results to evaluate size effect factors for length and width for the bending, tension and compression parallel to grain failure modes.

Brittle Fracture Theory

A large body of published and unpublished research shows that strength properties - tension, compression and bending strength - of visually graded structural dimension lumber vary with member size. A modification of the classical weakest link size effect model has been proposed for analysis of size effects in lumber (Madsen and Buchanan 1986, Johnson *et al.* 1989, Barrett and Fewell 1990, Sharp and Suddarth 1991) which incorporates the anisotropy in size effects observed in lumber products. Elements of the classical weakest link theory needed for the analysis to be presented herein are presented and extended for analysis of size effects in lumber.

Classical Weakest Link Model

The classical weakest link Weibull theory will be developed assuming, without loss in generality, that the stress distribution in a member can be normalized and expressed as

$$\tau\,(x,y,z) = \hat{\tau}\,G(x,y,z) \qquad 1$$

where $\hat{\tau}$ is a characteristic stress for the member. According to the classical 2 parameter Weibull theory the probability of failure F, for a volume V subjected to the stresses of Eqn. 1 is given by

$$F=1-\exp(-\int_{v}(\hat{\tau}G/m)^{k}dV) \qquad 2$$

where m and k are the scale and shape parameters for the distribution

Consider two volumes V_1 and V_2, then at a specified probability level F,

$$\hat{\tau}_{1}^{k}\int_{V_1}G_{1}^{k}\,dV=\hat{\tau}_{2}^{k}\int_{V_2}G_{2}^{k}\,dV \qquad 3$$

where $\hat{\tau}_1$ and $\hat{\tau}_2$ can be the maximum stress in the members the integral of Eqn. 3 can also be expressed as

$$\hat{\tau}_{1}^{k}\int_{V_1}G_{1}^{k}\,dV=\hat{\tau}_{1}^{k}K_{1}V_{1} \qquad 4$$

therefore $$\hat{\tau}_1/\hat{\tau}_2=(K_2V_2/K_1V_1)^{1/k} \qquad 5$$

where $$K_i=\frac{1}{V_i}\int_{v}G_i^{\,k}\,dV$$

For similar members subjected to the same loading condition $K_1 = K_2$ and then Eqn. 5 yields

$$\hat{\tau}_1/\hat{\tau}_2=(V_2/V_1)^{1/k} \qquad 6$$

From Eqn. 6, strengths of members with similar loading conditions can be related according

$$\ell n\,\hat{\tau}=a-\frac{1}{k}\,\ell n\,V \qquad 7$$

The shape parameter k, required for analysis of size effects can be derived either by fitting the Weibull distribution to test data at fixed member sizes (Eqn. 2), or by comparing strengths of members subjected to different loading conditions (Eqn. 5) or by regressing logarithm of strength against logarithm of volume (Eqn. 7). For a perfectly brittle material the shape parameter k, should be a material constant.

Weibull (1939) recognized that the size effect may not be volume dependent. If strength was influenced by surface defects strength may depend on member surface area. In more complex cases, competing failure mechanisms - perhaps surface and volume based - affect the failure process. The statistical size effect model must be modified appropriately for each type of material and application.

Size Effects in Visually Graded Lumber

By the late 1970's a large body of experimental data was accumulated that showed size effects in 38 mm thick, visually graded structural lumber strength properties were substantially greater than anticipated from tests of small clear specimens (cf., Schniewind and Lyon 1971, Kunesh and Johnson 1974, Madsen and Nielsen 1976, McGowan *et al.* 1977, Madsen 1978a, 1978b, Littleford 1978).

Size factors for visually graded lumber have been derived using five principle tests.

1. Width effect test (WET) - member length and loading conditions were fixed and members of different width evaluated.

2. Length effect test (LET) - member width and loading conditions were fixed and members of different length evaluated.

3. Constant ratio test (CRT) - member loading conditions were fixed and member length and width changed while maintaining a constant length to width ratio.

4. Load configuration test (LCT) - member width and length fixed and load configuration varied.

5. Random ratio test (RRT) - member loading is fixed but member length, width and thickness are varied independently from one test specimen size to another.

The Weibull weakest link theory provides a basis for analyzing WET, LET, CRT, LCT and RRT results for length and width size factors. In this study, thickness effects are not considered.

Consider the RRT involving members of two different widths W_1 and W_2 and lengths L_1 and L_2, subjected to the same load configuration. The relationship between member areas ($A_1 = W_1 L_1$ and $A_2 = W_2 L_2$), and member ultimate strengths (τ_1 and τ_2) derived from Eqn. 3 is:

$$\tau_1 / \tau_2 = (A_2 / A_1)^{S_A} \qquad 8$$

where S_A is the size parameter derived when member area (A), is used as the scale factor.

For lumber applications, Eqn. 8 can be specialized to accommodate different size factors for width (S_W) and length (S_L) as follows:

$$\tau_1 / \tau_2 = (W_2 / W_1)^{S_W} \quad (L_2 / L_1)^{S_L} \qquad 9$$

For members with a constant length to width ratios, Eqn. 9 becomes

$$\tau_1 / \tau_2 = (W_2 / W_1)^{S_R} = (L_1 / L_2)^{S_R} \qquad 10$$

where S_R is the size parameter for members with constant length to width ratios. For consistency the parameter S_R must satisfy the following identities (Barrett and Fewell 1990):

$$S_R = S_W + S_L \qquad 11a$$

and

$$S_R = 2S_A \qquad 11b$$

The size parameters S_A, S_L, S_W and S_R are commonly determined from the slope of a linear regression relating logarithm of strength to logarithm of a scale factor (Eqn. 7). The size factors are double subscripted to indicate the scale factor (L, W, A or R) and the test mode (bending (b), tension (t) or compression (c)). Thus S_{Lt} is a length effect factor for tension strength; that is, the size factor associated with changes in member length for a tension member.

If tension and bending strength of visually graded lumber follows a weakest link failure mechanism, then the following hypotheses would be true:

Hypothesis I:

Length size factors for bending (S_{Lb}) and tension (S_{Lt}) are identical.

Hypothesis II:

Width size factors for bending (S_{Wb}) and tension (S_{Wt}) are identical.

Hypothesis III:

The ratio of tension to bending strength for a fixed width is related to the length size factor.

Hypothesis IV:

Load configuration factors in bending members at a fixed width (depth) are related to the length size factor.

The weakest link concept, specialized for the case of visually graded lumber can be used to derive the relationship between tension strength and bending strength and the effect of load configuration on bending strength. If the bending strength is measured using 2 concentrated loads spaced at a distance a, then the relationship between tension (τ_t) and bending strength (τ_b) for a member of a fixed width is given by:

$$\frac{\tau_t}{\tau_b}=\left[\frac{L_b}{L_t}\ \frac{1+ak/L}{2(k+1)^2}\right]^{1/k} \qquad 12$$

where $k = 1/S_L$ and S_L is the length effect size factor

L_b and L_t are the lengths of the bending and tension members

The bending strength of lumber depends on the beam size and load configuration. Let τ_1 be the bending strength of a standard size beam subjected to a standard load configuration (eg. 1/3 point loading). The standard beam is assumed to have depth $d = d_1$, and a standard span to depth ratio. The strength τ_2, for a member with a length L_2 an arbitrary load configuration and is related to τ_1 according to

$$\tau_2=\tau_1\left(\frac{K_1\,L_1}{K_2\,L_2}\right)^{S_L} \qquad 13$$

where $K_1 = \frac{1}{V_1} \int_{V_1} G_1 \, dV$

$$K_2 = \frac{1}{V_2} \int_{V_2} G_2 \, dV$$

and S_L = length effect size factor

For beams with a standard span to depth ratio and load condition the strength τ_1 at a depth d_1 is related to the strength τ_0 at a standard depth d_0, according to

$$\tau_1 = \left(\frac{d_0}{d_1}\right)^{S_R} \tau_0 \qquad 14$$

Then Eqn. 13 yields

$$\tau_2 = \tau_0 \left(\frac{d_0}{d_1}\right)^{S_R} \left(\frac{K_1 L_1}{K_2 L_2}\right)^{S_L} \qquad 15$$

Integrations required to evaluate the coefficients K_1 and K_2 are performed over the regions of positive bending stresses (ie. G = 0 for regions where bending stresses are less than or equal to zero).

Size Factor Variability

Size factors for visually graded lumber can be highly variable. Madsen and Buchanan (1986) evaluated length effects in bending for 2 grades and 4 sizes of visually graded lumber. The size parameter S_L, at the 5th percentile property level varied from 0.095 to 0.323 (mean = 0.20, standard deviation = 0.066). Size parameter variability can be affected by grade, sample sizes, the number of different widths (or lengths) evaluated, the inherent variability of the material, test group matching efficiency and the probability level chosen for size factor analysis.

Lam and Varoglu (1990) showed that size factor variability can be reduced using group matching techniques. A method for calculating the expected variance of size factors at the mean strength level was provided. Group matching techniques are most applicable to LET or LCT studies, where matched groups of specimens of the same width are selected from the same population. Conventional group matching techniques are difficult to implement for width effect studies.

Variability in size factors can be studied by considering a generic size effect test. Without loss of generality, consider a test to estimate the parameter S_L, involving members of m different lengths $L_1, L_2, \ldots, L_m$. Samples of size n are chosen for each test length.

Assume that the distribution of property values at the length L_1 is 2-parameter Weibull (Eqn. 2), with shape parameter k and scale parameter m_1. For a true weakest link fracture mode then the shape parameter $k = 1/S_L$ (Eqn. 7). Studies of structural lumber show that S_L, is not generally equal to $1/k$. Therefore, we adopt a 2-parameter Weibull representation of the property distribution for any length L_i ($i = 1, \ldots, m$) with the following form:

$$\tau_i = m_1 (L_i / L_1)^{S_L} (-\ell n(1-p))^{1/k} \qquad 16$$

where τ_i is the strength of a member of length L_i. S_L is the size parameter characterizing length effects and p is the probability of failure. This representation will yield individual property distributions for members of any length L_i, having the same constant shape parameter k. The scale parameter for the distribution varies with length. The size effect analysis is based on evaluations of matched groups of members tested at different gauge lengths. Specimens can be allocated to test groups using matching techniques or a random procedure.

Let τ_i (p) denote the strength of a member of length L_i, at the p-th probability level. Linear regression (Eqn.7) yields a slope parameter $1/k = S_L$, independent of probability level. For this example, only test length is varied between groups of specimens. Here, the slope of the linear regression (Eqn. 7) can be expressed as:

$$S_L = \frac{1}{\zeta} \sum_{i=1}^{m} \alpha_i \ Y_i \qquad 17$$

where $X_i = \ell n \, L_i$ and $Y_i = \ell n \, \tau_i \, (p)$

ζ and α_i are constants given by

$$\zeta = m \sum_{i=1}^{m} X_i^2 - (\sum_{i=1}^{m} X_i)^2$$

$$\alpha_i = m X_i - \sum_{j=1}^{m} X_j$$

Expanding Eqn. 17 in a Taylor series about the mean values of the random variables Y_i $(i = 1,.. m)$ and truncating the series at the linear terms, the expected value of S_L is given as:

$$E\,[S_L] = \frac{1}{\zeta} \sum_{i=1}^{m} \alpha_i \ Y_i \qquad 18$$

Similarly it can be shown that $\sigma^2[S_L]$, the variance of S_L, can be expressed as:

$$\sigma^2 \ [S_L] = \frac{1}{\zeta^2} \left\{ \sum_{i=1}^{m} \left(\alpha_i \, Y_i\right)^2 + \sum_{i=1}^{m} \sum_{j=1}^{m} \alpha_i \, \alpha_j \rho_{ij} \sigma_{Y_i} \ \sigma_{Y_j} \right\} \qquad 19$$

where σ_{Y_i} is the standard deviation of Y_i and ρ_{ij} is the correlation coefficient between Y_i and Y_j

The sampling distribution of $\tau_i\,(p)$ for each member length L_i, will be asymptotically normal (Bury 1986) and the variance of $\tau_i\,(p)$ is given by:

$$\sigma^2\left[\tau_i(p)\right]=(p\,(1-p))/\left(n\left(f_W\left[P_i\,(p)\right]\right)\right) \qquad 20$$

where p = the probability level for the size analysis, n = the sample size for each length L_i, and $f_W[\tau_i(p)]$ is the 2-parameter Weibull frequency at property level τ_i, corresponding to probability level p.

It can be shown that the coefficient of variation of τ_i(p) at each length L_i, is:

$$CV\left[\tau_i(p)\right]=(p(1-p))/\left(k^2 n(-\ell n(1-p))^2\right)=\mathrm{B}_i \qquad 21$$

and $\sigma^2\,[\ell n\ \tau_i(\rho)]$ can be approximated by:

$$\sigma^2\left[\ell n\,\tau_i(p)\right]=CV\left[\tau_i(p)\right] \qquad 22$$

Therefore the variance of the size parameter S_L is given by the approximation:

$$\sigma^2[S_L]=\frac{1}{\zeta^2}\left\{\sum_{i=1}^{m}\mathrm{B}_i\,\alpha_i^2+\sum_{\substack{i=1\\ i\neq j}}^{m}\sum_{j=1}^{m}\alpha_i\alpha_j\rho_{ij}\left(\mathrm{B}_i\mathrm{B}_j\right)^{1/2}\right\} \qquad 23$$

The variance of the size parameter S_L, depends on the particular experimental design; i.e., the sizes of members (L_i), the number of test groups (m), the correlation coefficient ρ_{ij}, the sample size for each group (n), probability level (p) chosen for the evaluation.

Let the standard deviation $\sigma[S_L]$ be a reference standard deviation calculated for a particular choice of L_i, m, ρ_{ij}, n and p. Then the standard deviation $\sigma^*[S_L]$ for other probability levels p^* and sample sizes n^* is given by:

$$\sigma^*[S_L]=\sigma[S_L]\left(\frac{p^*}{1-p^*}\right)\left(\frac{1-p}{p}\right)\left[\frac{\ell n(1-p)}{\ell n(1-p^*)}\right]^2 \frac{n}{n^*} \qquad 24$$

where k and n are identical for property levels τ_i and τ_i.

The expression for the standard deviation of the size parameter can be used to evaluate trial experimental designs. To illustrate the process, consider a length effect experiment as a case study. Assume $m = 3$, $n = 100$ and test lengths of 2.5, 3.75 and 5.0 m respectively. The standard deviation of size parameter, S_L, at the 5th percentile strength level was evaluated for a range of shape parameters k, and a range of ρ_{ij} (the correlation coefficient between test groups i and j).

Figure 1 shows the relationship between $\sigma[S_L]$ and k at the 5th percentile strength level. With this experimental design, variability in the size effect parameter can be large for randomly sampled groups ($\rho = 0$). It is clear that when k and ρ increase, $\sigma[S_L]$ decreases. For this experiment the standard deviation at the 50th percentile is 32 percent of the standard deviation at the 5th percentile (Eqn. 24). If the sample size is increased from 100 to 400 specimens per group the standard deviation will be decreased by a factor of 2 (Eqn. 24). Size factor variability can also be reduced by group matching techniques which increase the correlation coefficient ρ_{ij}. With this knowledge, the experimenter can optimize experimental designs by increasing ρ_{ij} or n.

Next, consider a width effect experiment where four widths (89, 140, 184, 235 mm) are evaluated. Since group matching strategies are not generally applicable in width effect experiments, $\rho_{ij} = 0$ is assumed. The variance in size parameter S_W, at the 5th percentile strength level was evaluated for a range of shape parameters k for two sample sizes n = 100 and 400 (Figure 2). The results are similar to those obtained in the length effect case study. It is evident that unless sample size is rather large, large variability in size parameter can be expected.

Experimental Database

Bending, tension and compression parallel to grain properties for 38 mm, Canadian softwood dimension lumber were developed as part of large research program known as the Canadian Wood Council (CWC) Lumber Properties Program. Results from the CWC study will be evaluated to determine size effects in bending, tension parallel to grain and compression parallel to grain.

Sampling

Bending, tension and compression parallel to grain properties of Canadian commercial species groups - Douglas fir-Larch (D Fir-L), spruce-pine-fir (S-P-F) and Hem-Fir softwood lumber have been evaluated by the in-grade testing method. Sampling for the CWC database was conducted on a stratified basis. The target sample size for each size/grade cell for each commercial species group was 360 pieces.

Specimens were sequentially sampled in "on-grade" lots of 10 pieces from randomly sampled packages of lumber. Each lot (10 pieces) of bending, tension and compression specimens was selected sequentially from each package whenever possible. For each mill, a maximum of 20 pieces was sampled for each size/grade/property combination. Additional randomly sampled packages were selected to complete the sampling required in each mill. Actual sample sizes attained for the property evaluations conducted on select structural (SS), No. 2 grade and No. 3 grade material are given in Table 1.

Test Methods

Structural property evaluations were conducted in accordance with requirements of ASTM D 4761 (ASTM 1991b). All specimens were conditioned to approximately 15 percent moisture content using a combination of mild kiln drying and or air-drying. Flatwise bending modulus of elasticity (MOE) profiles and edge bending MOE were obtained for all specimens prior to destructive testing. A comprehensive set of information including defect sizes, grade controlling characteristic size and location, maximum strength reducing defect (MSRD) size and location and moisture content was recorded for each specimen.

Edge bending MOE and modulus of rupture (MOR) were evaluated using 1/3 point loading and a span of 17 times the member width (depth). For bending evaluations the MSRD was located at random within the 17 times width bending test span whenever feasible. The tension edge of bending specimens was chosen at random.

Tension and compression specimens were evaluated at the gauge lengths given in Table 2. Compression specimens were evaluated full-length with lateral restraints to prevent buckling. Tension specimens were evaluated full length except that approximately 24 inches at each end of the member would be gripped. Whenever possible the MSRD was located in the tested length.

Size Effects Analysis

Bending Properties

Constant Ratio Size Factor S_{Rb}

Bending size effects were evaluated for individual grades using the CWC database. The size parameter S_{Rb} was determined directly from test data.

The S_{Rb} was calculated at selected probability levels; using Eqn. 17 with width (depth) as the scale factor. The database was examined to determine if S_{Rb} was strength level dependent. For each species and grade, test results for the three sizes were examined at 19 probability levels (0.02, 0.05, 0.10,..., 0.95, 0.98). The regression relationship was used to generate a strength at a 184 mm width for each probability level. The size factors S_{Rb}, obtained for three species and grades are shown in Figure 3 as a function of the predicted strength at 184 mm width. Linear regression shows a slight tendency for the size factor to decrease with increasing strength.

The influence of grade on S_{Rb} was studied in detail at two probability levels (p= 0.05 and 0.50) for the three commercial species groups. Size factors are provided for individual property level/grade/species cells and combined grades, combined property levels and combined species data sets in Table 3. Analysis of covariance was used to test the hypothesis that the size parameters S_{Rb} were equal. Rejections of the hypothesis are indicated by an asterisk. All evaluations are made at a 5 percent significance level. For all data combined S_{Rb} = 0.45. There were no significant differences in S_{Rb} across the probability levels, grades and species considered with the exception of the probability level effect detected in the S-P-F select structural grade.

Since member width and length both vary with the same scale factor it was not possible to isolate a pure length effect (S_{Lb}) or the pure width effect (S_{Wb}) from the CWC bending properties data set directly.

Length Effect Size Factor S_{Lb}

Bending length effects data for Hem-Fir and S-P-F published by Madsen and Nielsen (1978) and Madsen (1990) were analyzed with length as the scale factor. The best fitting common length effect parameters (S_{Lb}) for the Hem-Fir and S-P-F data sets were 0.18 and 0.16 respectively. The analysis of covariance showed that the hypothesis of common slopes could not be rejected. Pooled results yielded an overall S_{Lb} = 0.17 with no significant differences between the slope parameters for the individual tests. Madsen (1992) reports S_{Lb} = 0.19 and 0.31 at the 10th and 50th percentiles for a second study of No. 2 and better Hem-Fir.

Width Effect Size Factor

The bending width size factor (S_{Wb}) can be calculated using Eqn. 11, when S_{Rb} and S_{Wb} are known. Adopting the values S_{Rb} = 0.45 (CWC database) and S_{Wb} = 0.17, yields S_{Wb} = 0.28 as the estimated width effect for bending strength of visually graded lumber.

Tension Properties

Tension specimens were evaluated at different gauge lengths (Table 2) precluding direct evaluation of width, length or constant ratio size parameters. The size parameters S_{At}, were calculated using the as-tested tension strength data and area (A = width x test gauge length) as the scale factor. Results for combined data sets are given in Table 4. No significant differences is S_{At} were found across the grade, percentiles or species combinations evaluated.

Tension Length Size Factor S_{Lt}

Length effect factors can be established based on test data from the literature (Showalter *et al.* 1987; Lam and Varoglu 1990; Madsen 1990). Analysis of covariance showed the tension size factors for S-P-F obtained by Lam and Varoglu (1990) was 0.12, independent of grade and percentile level. A length effect S_{Lt} = 0.15 was obtained for southern pine (Showalter *et al.* 1987). Madsen (1990) provides results for S-P-F which yield and overall common size parameter S_{Lt} = 0.18 with no significant differences between percentiles (p = 0.05 and 0.50) or section widths (89 mm and 184 mm). Analysis of covariance yielded the common size parameter S_{Lt} = 0.17 for the three data sets combined. Madsen (1992) reports S_{Lt} = 0.26 and 0.20 at the 10th and 25th percentile levels for a second study of Hem-Fir No. 2 and better grade.

Tension Width Size Factor S_{Wt}

Tension strengths for 89 mm wide specimens evaluated in the CWC project, were adjusted to the 3.68 m length using S_{Lt} = 0.17. The width effect parameter S_{Wt} was derived from the length adjusted CWC database. Analysis of covariance yielded a common size parameter S_{Lt} = 0.21 for the CWC database (Table 5). Eqn. 11a, provides a constraint on the relationship between the area, length and width parameters. S_{Wt} + S_{Lt} = 0.38 which is in close agreement with the requirement that $S_{Wt} + S_{Lt} = 2\ S_A$ since 2 S_A = 0.42 for the CWC database.

Madsen and Nielsen (1978) reported tension strength results for individual grades tested at a constant gauge length. Analysis of the 5th percentile data for select structural and No.2 grades yields S_{Wt} = 0.212 as the common size parameter for the three major commercial species groups. The hypothesis of a common size parameter could not be rejected.

Compression Properties

Compression strength test specimens in the CWC project were evaluated at different lengths precluding analysis of length, width or constant ratio size factors. The size factor S_{Ac} = 0.11 was established as the common size factor using the member area as the scale factor (Table 6). The hypothesis that all data sets had a common size factor was not rejected. Madsen(1990) provided compression length effect results for S-P-F structural lumber. Analysis of covariance yielded a common size parameter S_{Lc} = 0.10 with no significant differences in the parameter across the width (89 and 184 mm) and property levels (0.05 and 0.50) studied. Madsen (1992) reports a S_{Lc} = 0.09 in a second study of a No. 2 and better Hem-Fir grade mix.

Compression property data from the CWC study was adjusted to a common gauge length of 3.66 metres using a size factor $S_{Lc} = 0.10$. The adjusted compression data set was then analyzed to establish the width parameter S_{Wc} (Table 7). The overall common size factor $S_{Wc} = 0.11$ was obtained. Then $S_{Wc} + S_{Lc} = 0.11 + 0.10 = 0.21$ and is therefore approximately equal to 2 $S_A = 0.22$ satisfying requirements of Eqn. 11. There were no significant differences in the size parameters across species, grades and property levels.

Discussion

The Canadian Wood Council project was conducted as part of a coordinated Canadian and U.S. lumber properties research program to evaluate structural properties of individual grades of commercial species groups of 38 mm thick softwood dimension lumber. The two programs followed very similar sampling, testing and analysis philosophies. Douglas-fir, Hem-Fir and southern pine results collected in the United States are summarized in two reports (Anon 1989; Green and Evans 1989). Selected results from the major Canadian and US studies are summarized in Table 9 and compared with selected results from the earlier in-grade study conducted in Canada (Madsen and Nielsen 1978a, 1978b).

Foschi *et al.* (1990) used the CWC database to evaluate the structural reliability of lumber members in single member applications. Size adjustment factors were developed to modify design strength properties to maintain uniform reliability. Size adjustment factors derived using the reliability approach were $S_{Rb} = 0.48$, $S_{At} = 0.18$ and $S_{Ac} = 0.13$.

Bending Size Factors

The bending size factor S_{Rb}, shows a slight decreasing trend with increasing strength. For very high quality lumber, the size factor would be expected to approach the size factor for a value clear wood behavior. Bohannan (1966) reports $S_{Rb} = 0.11$ for clear Douglas-fir members. Other Douglas-fir and Hem-Fir clear lumber data (Kunesh and Johnson 1974), yields a tension size factor $S_{Wt} = 0.16$ for width effects. If the length length effect is approximately equal to the width effect then S_{Rb} for this material would be approximatley 0.3, somewhat smaller than observed for visually grade lumber. Analysis of spruce-pine-fir data (Madsen and Tomoi 1991) yields a common size parameter $S_{Rb} = 0.15$ for clear material. Figure 1 shows S_{Rb} for visually graded lumber is much higher than these clear wood values throughout the entire bending strength range.

The size factor $S_{Rb} = 0.45$ obtained for Canadian softwood lumber agrees closely with US studies ($S_{Rb} = 0.40$) and results derived from earlier Canadian studies ($S_{Rb} = 0.43$) shown in Table 8. Thus, there is consensus that the bending size factor (S_{Rb}) is approximately 0.4 for the 38 mm dimension lumber produced in Canada and the United States.

There is conflicting evidence as to which effect - length or width - dominates bending behavior. The length effect parameter available from the studies evaluated in this paper is $S_{Lb} = 0.17$ independent of species grade and size. This result is in general agreement with results published in the literature including the most recent studies (Madsen 1992) which suggested $S_{Lb} \cong 0.2$.

The major Canadian and US in-grade studies of bending strength of individual grades suggest $S_{Rb} \cong 0.4$ (Table 8). If $S_{Rb} \cong 0.4$ and $S_{Lb} \cong 0.2$, then $S_{Wb} = S_{Rb} - S_{Lb} \cong 0.2$ in order to satisfy Eqn. 11. Madsen (1992) reports no width effect for bending members even though earlier studies of individual grades (Madsen and Nielsen 1978a, Green and Evans 1989, Barrett and Fewell 1990) report $S_{Rb} \cong 0.4$.

Studies summarized by Madsen (1992) which yielded no width effect in bending, mainly involved evaluation of samples of a No. 2 and better grade mix rather than pure grades. Variation in grade mix from size to size will increase the variance of the estimate of the size parameter and could completely mask the true size effect. For instance, Madsen and Nielsen (1976) report results of tests at four widths (89, 140, 184 and 235 mm) which do not yield a consistent size effect (Madsen and Buchanan 1986). The study was conducted with a No. 3 and better grade mix. The select structural grade percent included in the four widths was 44, 54, 56 and 44 percent respectively. these grade shifts could explain why pure grades yield a consistent width effect in bending across several species while the studies based on samples of mixed grades yield no consistent size effect for bending.

Madsen (1992) found inconsistent evidence of width effects in studies using randomly sampled test groups with a sample size $n \cong 100$ per group. Fits of 2-parameter Weibull distributions to bending strength data yield shape parameters k, in the range 4 to 6 for visually graded lumber. Fig. 2 results (k = 5 and S_{Wb} = 0.2) show that an S_{Wb} test result (5th percentile strength level) $0.08 \leq S_{Wb} \leq 0.32$ would be within one standard deviation of the expected value. Thus, the expected range of S_{Wb} is very large. For the CWC database ($n \cong 400$) the comparable range of S_{Wb} is S_{Wb} $0.14 \leq S_{Wb} \leq 0.26$. The precision of the estimate of S_{Wb} obtained from the CWC database is significantly improved over results based on a sample size n = 100. Thus, the low sample size and the random sampling process used for studies of width effects reported by Madsen (1992) would explain the inconsistences reported.

Tension Size Factors

Analysis of tension length effect studies from the literature yielded S_{Lt} = 0.17 for the length effect in tension. If member capacity is controlled by a weakest link mechanism in tension then a weakest link model would predict size effects for length to be the same for bending and tension member. Thus, the experimental result ($S_{Lt} = S_{Lb} = 0.17$) supports Hypothesis I. If these results are accepted then there is a strong argument for adopting the weakest link model for adjusting tension and bending strength data for member size or loading conditions.

As with bending, it was not possible to derive S_{Wt} directly from the CWC data base. Rather S_{Wt} was calculated to yield S_{Wt} = 0.21. This value is consistent with the width effect in bending (S_{Wb}= 0.28) considering the limitation discussed previously.

In the earlier Canadian tension testing program (Madsen and Nielsen, 1978b), all tension tests were conducted at the same gauge length. These results (Bury, 1979) were reanalyzed using analysis of convariance methods to yield a common width effect S_{Wt} = 0.22 for tension. Madsen (1992) reports S_{Wt} = 0.19 for the same data set. The US studies (Green and Evans 1989) yield S_{Wt} = 0.28 for the three US species. The estimates of the width effect for visually graded lumber in tension range from 0.21 to 0.28 (Table 9). Width effects in tension for the pure grades also differ from the tension width size factors for mixed grades reported by Madsen (1992).

Bending and tension width effect results reported herein are quite similar considering the limitations of the bending width effect data base. The differences in width effect factors are sufficiently small that it could be claimed that the width effects are similar for tension and bending thereby supporting Hypothesis II. If this were true the analysis of size effects in structural lumber would be greatly simplified.

Compression Size Factors

Length size factors in compression were derived from a study of S-P-F lumber (Madsen 1990). The length effect factor $S_{Lc} = 0.1$ was used to convert the CWC database to a common length for width effect analysis. The compression width effect was $S_{Wc} = 0.11$ and $S_{Rc} = 0.11 + 0.10 = 0.21$ for the three Canadian species (Table 8). Recently published results for a second Hem-Fir study (Madsen 1992), confirm $S_{Lc} \cong 0.1$.

Compression parallel to grain studies were conducted in the US used short column compression specimens with a length 2.5 times the member width. Each short column specimen was selected to contain the maximum strength reducing defect located within the full length member. These CRT results were analyzed to yield $S_{Rc} = 0.12$. The size effect S_{Rc}, agrees closely with the width effect obtained from the Canadian compression data (Table 8). This result reflects the differences in test methods adopted for compression tests in Canada and the US. In the US tests the worst defect has been selected for testing. Since only one strength controlling defect exists in each specimen, the size effect can only be associated with a width effect. Thus the results of the two programs are in substantial agreement.

Related Issues

Tension to Bending Relationships

The Canadian and US lumber databases include test results for bending and tension strength which have been used to derive factors to relate strength to member size. The data can also be used to study the ratio of bending strength to tension strength. When a weakest link mechanism controls strength in tension and bending members then the ratio of tension strength to bending strength is related to the length effect size factor according to Eqn. 12 where $S_L = 1/k$.

Green and Kretschmann (1991) analyzed the US lumber property data on an "as tested" basis. Gauge lengths for tension specimens differed from size to size. Bending members were subjected to 1/3 point loads. At bending strengths less than 50 MPa, tension strength was found to be approximately 56 percent of bending strength. This property ratio would be consistent with the size parameter $S_{Lt} = S_{Lb} \cong 0.166$.

Barrett *et al.*, (1992) have completed a detailed investigation of property relationships for Canadian species. The tension to bending property ratios are species dependent. Results for three species adjusted to a 38 x 184 x 3130 mm basis are shown in Figure 4. The non-linear trend in the tension/bending property ratio suggests that the size effect may change with strength level. In the lower 50 percent of the bending strength range the tension strength is approximately 55 percent of bending strength. For a ratio of 0.55, the computed size parameter is $S_L = 0.174$ (Eqn. 16). This size factor is remarkably consistent with the size factor $S_L = 0.17$ obtained from tension and bending length effect tests. The tension to bending strength ratio can be calculated based on the weakest link theory and the tension (or bending) length effect size parameters (S_{Lb} or S_{Lt}) thereby support Hypothesis III.

Tension and bending size factors for Canadian dimension lumber agree closely with those derived by Barrett and Fewell (1990) based on an analysis of European and Canadian species. The ratio of tension strength to bending strength is also very similiar for European, Canadian and US species.

Load Configuration Factors

Madsen (1992) reports two limited studies where bending strength has been evaluated for different load conditions including center point, 1/3 point, and 1/4 point loads for simply supported and built-in beam conditions. The general agreement between the expected (Eqn. 17, $S_L = 0.17$) and the observed results, supports Hypothesis IV.

Further experimental studies based on pure grades is required to evaluate Hypothesis IV in detail.

Harmonized Size Factors for Codes

The consistency observed in tension to bending property ratios and the length and width size factors for Canadian, US and European species suggests the adoption of a common set of size adjustment factors for visually graded softwood lumber. For harmonization of international standards the size factors should be based on as many species, sizes and grades as possible. Barrett and Fewell (1990) suggested size factors for length ($S_L = S_{Lb} = S_{Lt} = 0.17$) and width ($S_W = S_{Wb} = S_{Wt} = 0.23$) for bending and tension which agree closely with the results herein. Compression size factors for length ($S_{Lc} = 0.10$) and width ($S_{Wc} = 0.11$) are consistent across several Canadian and US species groups.

Considering all available results and the variability associated with the size analysis, the rounded size factors given in Table 10 are recommended for use in conjunction with a weakest link fracture model to adjust test data to the characteristic sizes.

Conclusions

Brittle fracture theory provides a rational framework for evaluating the influence of member size and loading conditions on tension and bending strength properties of structural lumber. Weakest link brittle fracture theory was used to establish size factors for bending, tension and compression strength for visually graded softwood structural lumber. The results of the analysis support the following conclusions:

1. Size effects in visually graded structural lumber are remarkably consistent. Hypothesis tests that specific size factors are equal across grades, species and property percentile level were not rejected at the 5 percent significance level.

2. Length effect factors for tension (S_{Lt} = 0.17) and bending (S_{Lb} = 0.17) are similar.

3. Width effect factors calculated for bending (S_{Wb} = 0.28) are slightly higher than the tension factor (S_{Wt} = 0.21) for Canadian commercial species groups.

4. The length and width size factors for compression are S_{Lc} = 0.10 and S_{Wc} = 0.11.

5. The relationship between tension and bending strength for member of the same width can be determined using a weakest link failure model and a size factor S_{Lt} = S_{Lb}= 0.17.

6. The effect of load condition on bending strength at a fixed width (depth) can be calculated using weakest link analysis and a length effect size factor S_L = 0.17.

7. The size factors S_{Rb}, S_{At} and S_{Ac} derived in this study agree closely with those required to achieve constant reliability and therefore the same size factors may be used for both allowable stress design and load and resistance factor design code applications.

8. For international harmonization of procedures for adjusting tension, bending and compression strength properties, the width and length size factors can be taken to be equal. For bending and tension S_W = S_L = 0.2 and for compression S_W= S_L = 0.1 for softwood visually graded lumber.

References

Anon. (1989) "In-grade testing of structural lumber." Forest Products Research Society, Madison, WI.

ASTM (1991b) "ASTM D 4761 - 88: Standard methods for mechanical properties of lumber and wood-base structural material." American Society for Testing and Materials. Annual Book of ASTM Standards. Philadelphia.

ASTM (1991a) "ASTM D 1990 - 91: Standard practise for establishing allowable properties for visually graded dimension lumber from in-grade tests of full-size specimens." Annual Book of ASTM Standards. American Society for Testing and Materials. Philadelphia.

Barrett, J. D. (1974) "Effect of size on tension perpendicular to grain strength of Douglas-fir". Wood and Fiber, 6(2), 126-143.

Barrett, J. D., and Fewell, A. R. (1990) "Size factors for the bending and tension strength of structural lumber." Proceedings CIB Working Commission W18A - Timber Structures. Meeting 23 Lisbon, Portugal.

Barrett, J. D., Liliefna, D., and Lau, W. (1992) "Structural property relationships for visually graded lumber - A unified model." In preparation.

Barrett, J. D., Foschi, R. O., Fox, S. P. (1975) "Perpendicular-to-grain strength of Douglas-fir" Can. J. Civil Eng., 2(1), 50-57.

Bohannan, B. (1966) "Effect of size on bending strength of wood members." USDA Forest Service, Research Paper FPL 56, Forest Products Laboratory, Madison, WI.

Buchanan A. H. (1984) "Strength model and design methods for bending and axial load interaction in timber members." Thesis presented to the University of British Columbia (Dept. Civ. Eng.), in partial fulfillment of the of the reguirments of the degree of Doctor of Philosophy.

Bury K. V. (1975) "*Statistical Models in Applied Science*" John Wiley and Sons. New York.

Bury, K. V. (1979) "Statistical analysis of NLGA tension tests." Dept. Mech. Eng., Univ. Brit. Col. Vancouver.

Bury, K. V. (1981) "Statistical analysis of NLGA bending tests." Dept. Mech. Eng., Univ. Brit. Col. Vancouver.

CEN (1991) "prEN 384: Structural Timber - Determination of characteristic values of mechanical properties and density." European Committee for Standardization. Brussels.

Colling, F. (1986) "Influence of volume and stress distribution on the shear strength and tensile strength perpendicular to grain." Proc. IUFRO Wood Eng. Florence, Italy September 1986.

Foschi, R. O., Folz, B. R. and Yao, F. Z. (1989) "Reliability-based Design of Wood Structures." Struct. Res. Ser., Rept. No. 34., Dept. Civil Eng., Univ. Brit. Col., Vancouver, Canada.

Foschi, R. O., and Barrett, J. D. (1976) "Longitudinal shear strength of Douglas-fir." Can. J. Civil Eng., 3(2), 198-208.

Green, D. W., and Evans, J. W. (1989) "Mechanical properties of visually graded lumber: Vol. I, A Summary." Nat. Tech. Inform. Serv. Publ. No. PB-88-159-389. Springfield, VA.

Green, D. W., and Kretschmann, David E. (1991) "Lumber property relationships for engineering design standards." Wood and Fiber Science, 2(3), 423-456.

Johnson, L. A., Evans, J. W., and Green, D. W. (1989) " Volume effect adjustments for the in-grade data." In Ingrade Testing of Structural Lumber. Forest Products Research Society, Madison, WI.

Kunesh, R. H. and Johnson, J. W. 1974. "Effect of size on tension strength of clear Douglas-fir and Hem-fir dimension lumber." For. Prod. J., 24(8), 32-36.

Lam, F. and Varoglu, E. (1990) "Effect of length on the tensile strength of lumber." For. Prod. J., 40(5), 37-42.

Littleford, T. W. (1978) "Flexural properties of dimension lumber from western Canada." Inform. Rept. VP-X-179. Western Forest Products Laboratory, Vancouver.

Madsen, B. (1992). *Structural Behavior of Timber.* Timber Engineering Ltd., North Vancouver, B.C., Canada.

Madsen, B., and Buchanan, A. H. (1986) "Size effects in timber explained by a modified weakest link theory." Can. J. Civil Eng., 13(2), 218-232.

Madsen, B., and Nielsen, P. (1976) "In-grade testing - size investigation on lumber subjected to bending." Struct. Res. Ser. Rept. No. 15., Dept. Civil Eng., Univ. Brit. Col., Vancouver.

Madsen, B., and Nielsen, P. (1978a) "In-grade testing: Bending tests in Canada. June 1977-May 1978." Struct. Res. Ser. Rept. No. 25. Dept. Civil Eng., Univ. Brit. Col., Vancouver.

Madsen, B., and Nielsen, P. (1978b) "In-grade Testing: Tension tests in Canada." Prepared for the National Lumber Grades Authority. Dept. Civil Eng., Univ. Brit. Col., Vancouver.

Madsen, B., and Tomoi. M. (1991) "Size effects occurring in defect-free spruce-pine-fir bending specimens." Can. J. Civil Eng., 18(4), 637-643.

Madsen, B. (1990) "Length effects in 38 mm spruce-pine-fir dimension lumber." Can. J. Civil Eng., 17(2), 226-237.

McGowan, W. M., Rovner, B. and Littleford, T. W. (1977) "Parallel-to-grain tensile properties of dimension lumber from several western Canadian species." Inform. Rept. VP-X-172. Western Forest Products Laboratory, Vancouver.

NLGA. 1991. Standard grading rules for Canadian lumber. National Lumber Grades Authority. Vancouver.

Schniewind, A. P., and Lyon, D. E. (1971) "Tensile strength of rdwood dimension lumber - I: Relation to grade and working stress." For. Prod. J., 21(7). 18-27.

Sharp, D. J., and Suddarth, S. K. (1991) "Volumetric effects in structural composite lumber." Proc. Intl. Timber Eng. Conf., London, 3, 427-433.

Showalter, K. L., Woeste, F. E., and Bendsten, B. A. (1987) "Effect of length on the tensile strength of lumber." Research Paper FPL-RP-482, USDA Forest Service, Forest Products Laboratory, Madison. WI.

Weibull, W. (1939) "A statistical theory of the strength of materials." Proc. Roy. Swed. Inst., No. 151, Stockholm.

Table 1. **Species, Properties, Grades and Sample Sizes for CWC Lumber Properties Project**

Species Group	Width (mm)	Bending Grade SS	Bending Grade 2	Bending Grade 3	Compression Grade SS	Compression Grade 2	Tension Grade SS	Tension Grade 2
D Fir-L	89	370	370	150	372	374	372	373
	184	373	370	149	374	371	373	371
	235	372	374	150	375	373	373	370
Hem-Fir	89	381	380	170	382	381	360	362
	184	382	402	158	383	382	381	381
	235	379	385	159	381	380	383	378
S-P-F	89	441	440	180	440	441	440	444
	184	444	986	200	440	443	441	440
	235	440	441	210	420	418	446	463

Note: No. 3 grade was sampled for bending only.

Table 2. Test Spans and Gauge Lengths for Bending, Tension and Compression Property Tests.

Member Width (mm)	Test Span	Gauge Length	
	Bending (mm)	Tension (mm)	Compression (mm)
89	1510	2640	2440
184	3130	3680	3660
235	3990	3680	4270

Table 3: **Bending Strength Size Parameters, S_{Rb}.**

Property Level		SPECIES D. Fir-Larch	Hem-Fir	S-P-F	All Species
5th	SS	0.516	0.579	0.452	0.516
	No. 2	0.368	0.466	0.386	0.407
	No. 3	0.397	0.555	0.513	0.487
	All Grades	0.426	0.533	0.450	0.470
50th	SS	0.306	0.439	0.395	0.380
	No. 2	0.447	0.521	0.372	0.446
	No. 3	0.425	0.455	0.504	0.461
	All Grades	0.393	0.471	0.424	0.429
All	SS	0.411	0.509	0.424*	0.448
	No. 2	0.407	0.493	0.379	0.427
	No. 3	0.409	0.505	0.508	0.474
	All Grades	0.409	0.502	0.437	0.449

*Reject H_0: All size parameters are equal (significance level 5%)

Table 4: **Tension Strength Size Parameters for Area, S_{At}, Obtained Using Member Width Times Length as the Scale Factor.**

Property Level	GRADE	D. Fir-Larch	Hem-Fir	S-P-F	All Species
5th	All	0.215	0.251	0.197	0.220
50th	All	0.153	0.224	0.194	0.190
ALL	All	0.184	0.238	0.193	0.205

All grades: No. 2 and SS

Table 5: Tension Strength Size Parameters for Width, S_{Wt} obtained using Tension Strength Properties Adjusted to a Length L = 3.68 m.

Property Level	Grade	D Fir-Larch	Hem-Fir	S-P-F	All Species
5TH	SS	0.222	0.253	0.287	0.254
	No. 2	0.263	0.306	0.107	0.225
	All Grades	0.242	0.280	0.197	0.240
50th	SS	0.122	0.257	0.230	0.203
	No. 2	0.139	0.232	0.130	0.167
	All Grades	0.131	0.245	0.180	0.185
All	SS	0.172	0.255	0.258	0.229
	No. 2	0.201	0.269	0.119	0.196
	All Grades	0.186	0.262	0.188	0.212

Table 6: Compression Strength Size Parameters for Area, S_{Ac}

Property Level	Grade	D Fir-Larch	Hem-Fir	S-P-F	All Species
5th	All	0.103	0.121	0.122	0.115
50th	All	0.073	0.091	0.125	0.096
All	All	0.088	0.106	0.123	0.106

All Grades: No. 2 and Select Structural

Table 7: Compression Strength Size Parameters for Width, S_{Wc}.

Property Level	Grade	D Fir-Larch	Hem-Fir	S-P-F	All Species
		Species			
5th	All	0.105	0.133	0.133	0.124
50th	All	0.058	0.086	0.139	0.094
All	All	0.082	0.110	0.136	0.109

Table 8: **Summary of Bending, Compression and Tension Size Parameters.**

Property	**Size Parameters**					
	S_R (1)	S_W (2)	S_L (3)	S_A (4)	$S_R = 2S_A$ (5)	$S_R = S_L + S_W$ (6)
Bending	0.45	0.28	0.17[1]	------	------	------
Tension	0.40[5]	0.21	0.17[2]	0.21	0.42[4]	0.38[4]
Compression	0.21[5]	0.11	0.10[3]	0.11	0.22[4]	0.21[4]

[1]Based on Madsen and Buchanan (1986), Madsen and Nielson (1976), Madsen (1990).
[2]Based on Lam and Varoglu (1990) and Showalter *et al.*, (1987), Madsen (1990).
[3]Madsen (1990).
[4]Calculated value.
[5]Average of calculated values from Col. 5 and 6.

Table 9: Comparisons of Size Parameters Derived from Evaluations of Canadian and U.S. Commercial Species Groups.

Property	Size Parameter	Project		
		Canadian[1]	Canadian[2]	U.S.[3]
Bending	S_{Rb}	0.45	0.43	0.40
Tension	S_{Wt}	0.21	0.22	0.28
Compression	S_{Rc}	0.21		0.12

[1]CWC Database - 5th and 50th percentile data.

[2]Madsen and Nielson (1978a, 1978b) - 5th percentile data.

[3] Green and Evans (1989) - 5th and 50th percentile data for Hem-Fir, Douglas-fir and Southern Pine commercial species groups.

Table 10: Size Factors Recommended for Code Harmonization.

Property	Size Factor S_L	S_W
Bending	0.2	0.2
Tension	0.2	0.2
Compression	0.1	0.1

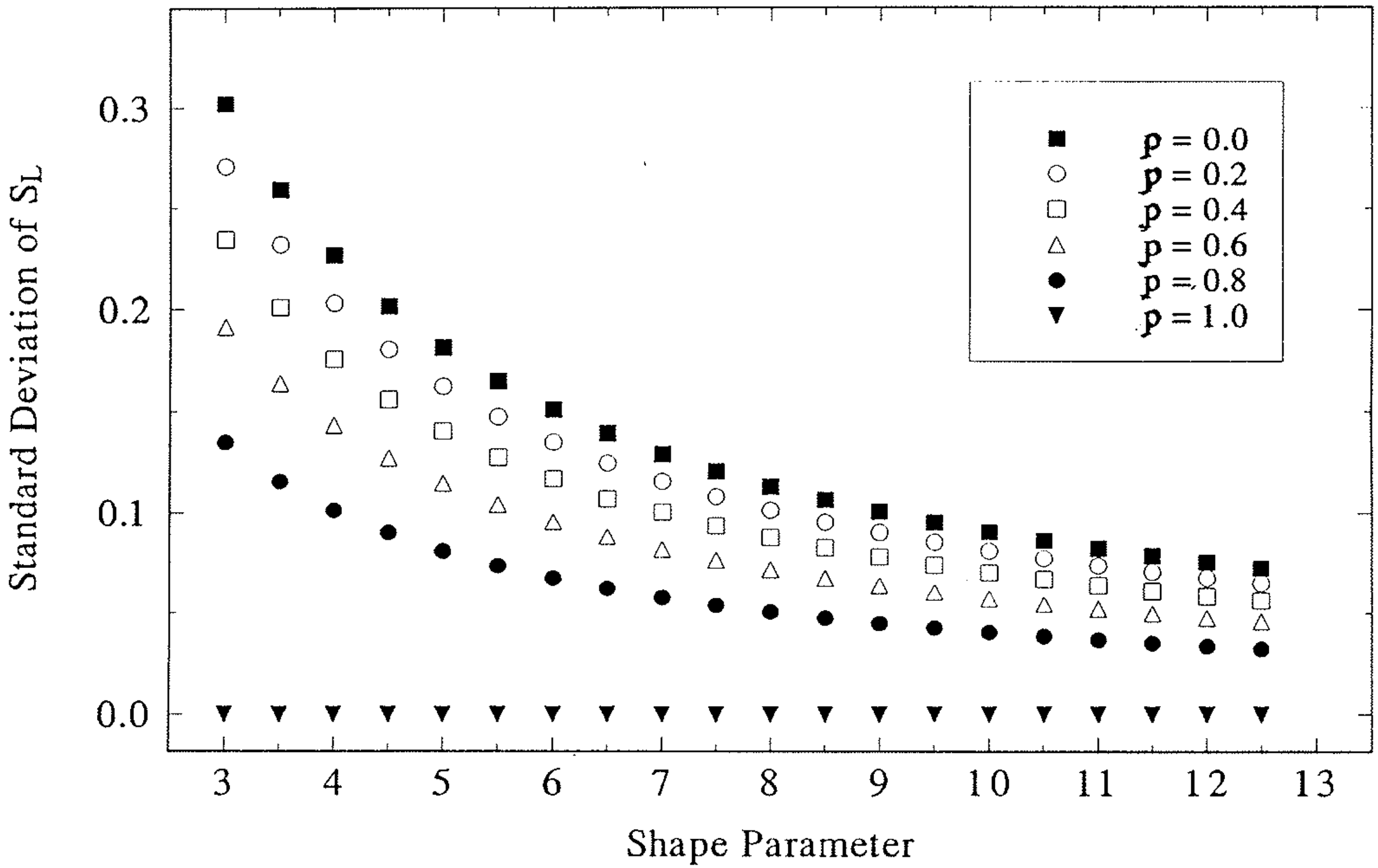

Figure 1. Influence of Weibull shape parameter (k) and between group correlation coefficient (ρ) on standard deviation of the size parameter S_L for a typical length effect test.

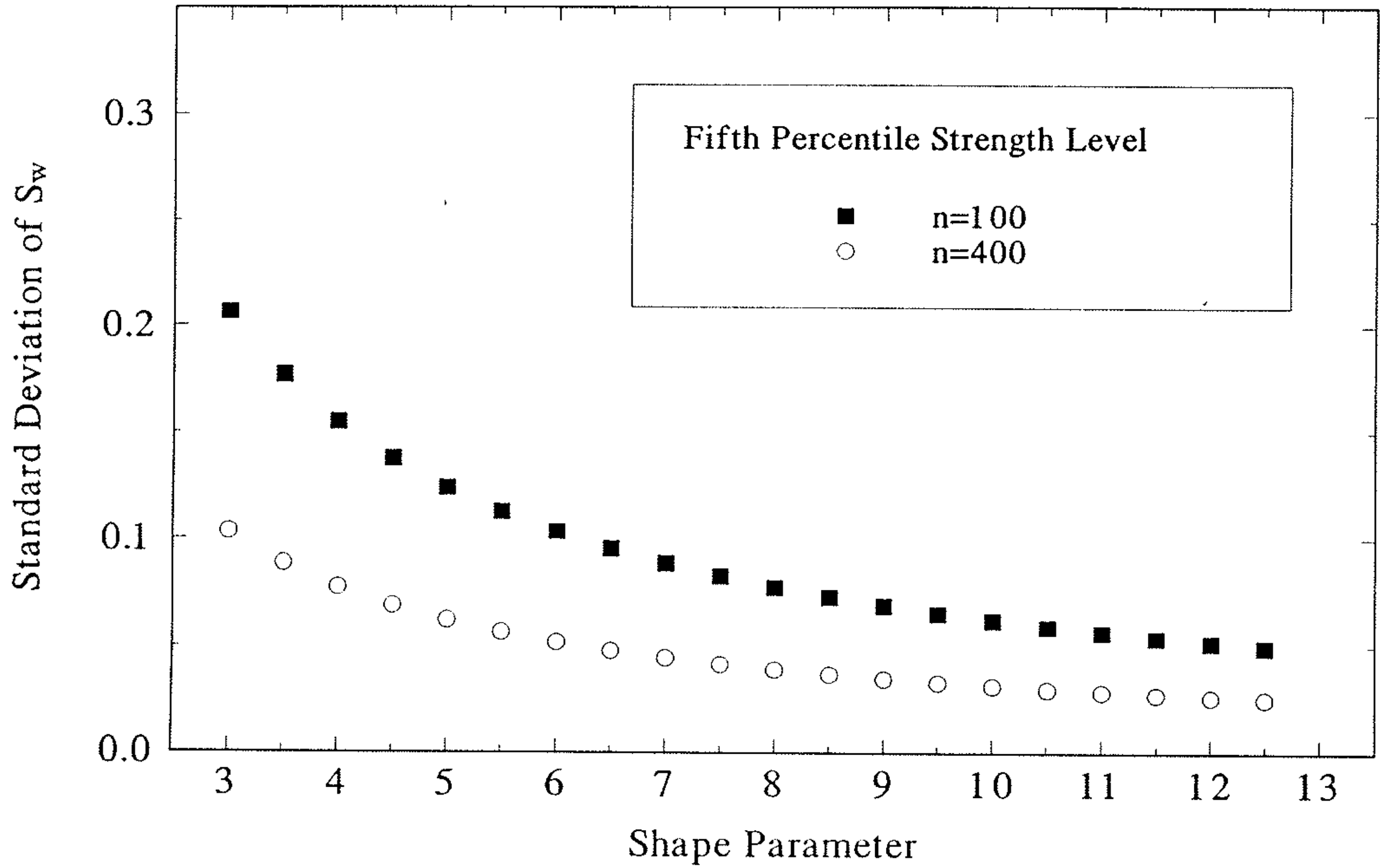

Figure 2. Influence of Weibull shape parameter and sample size on the standard deviation of the size parameter S_L.

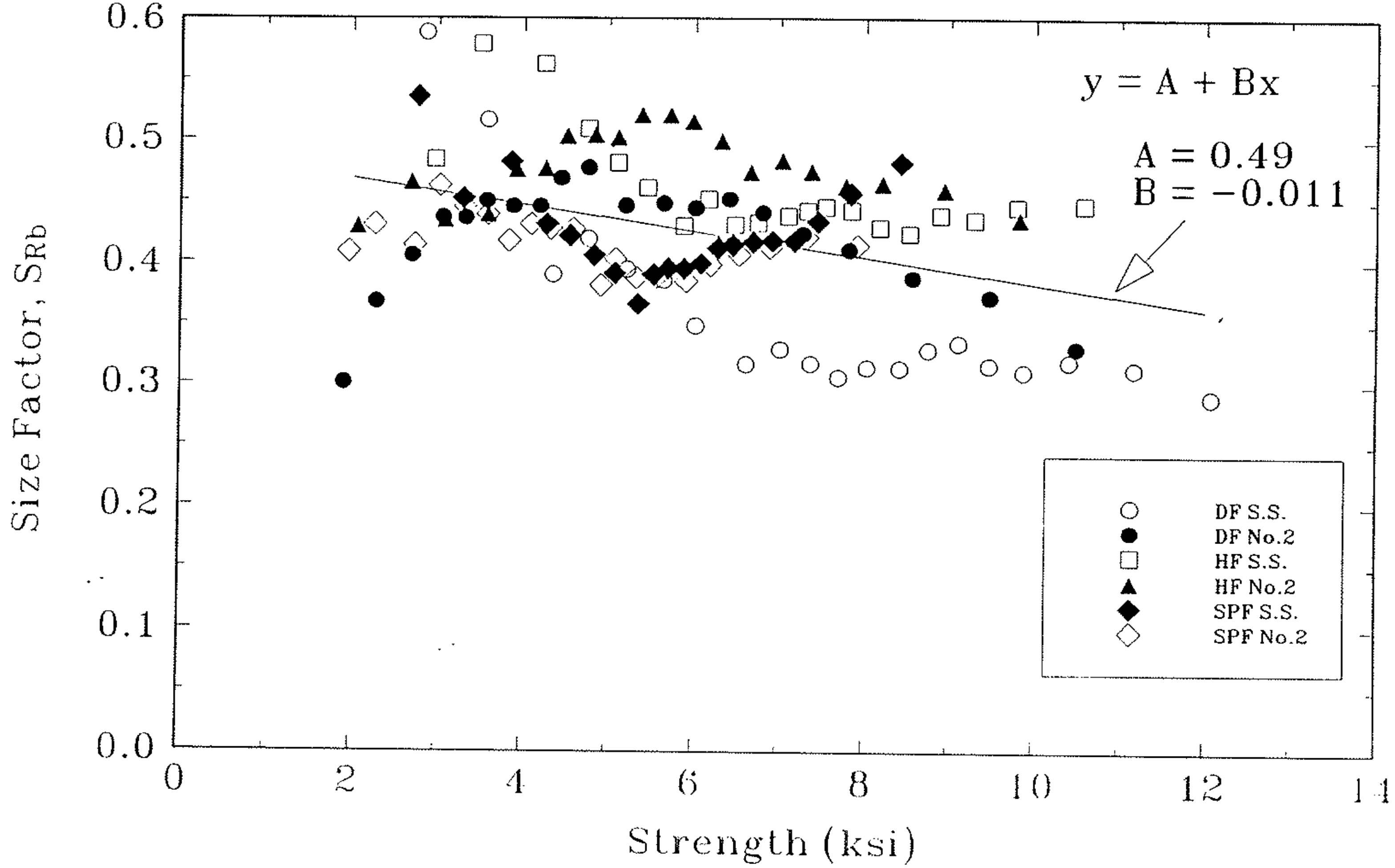

Figure 3. Variation of the bending size parameter S_{Rb} with strength level.

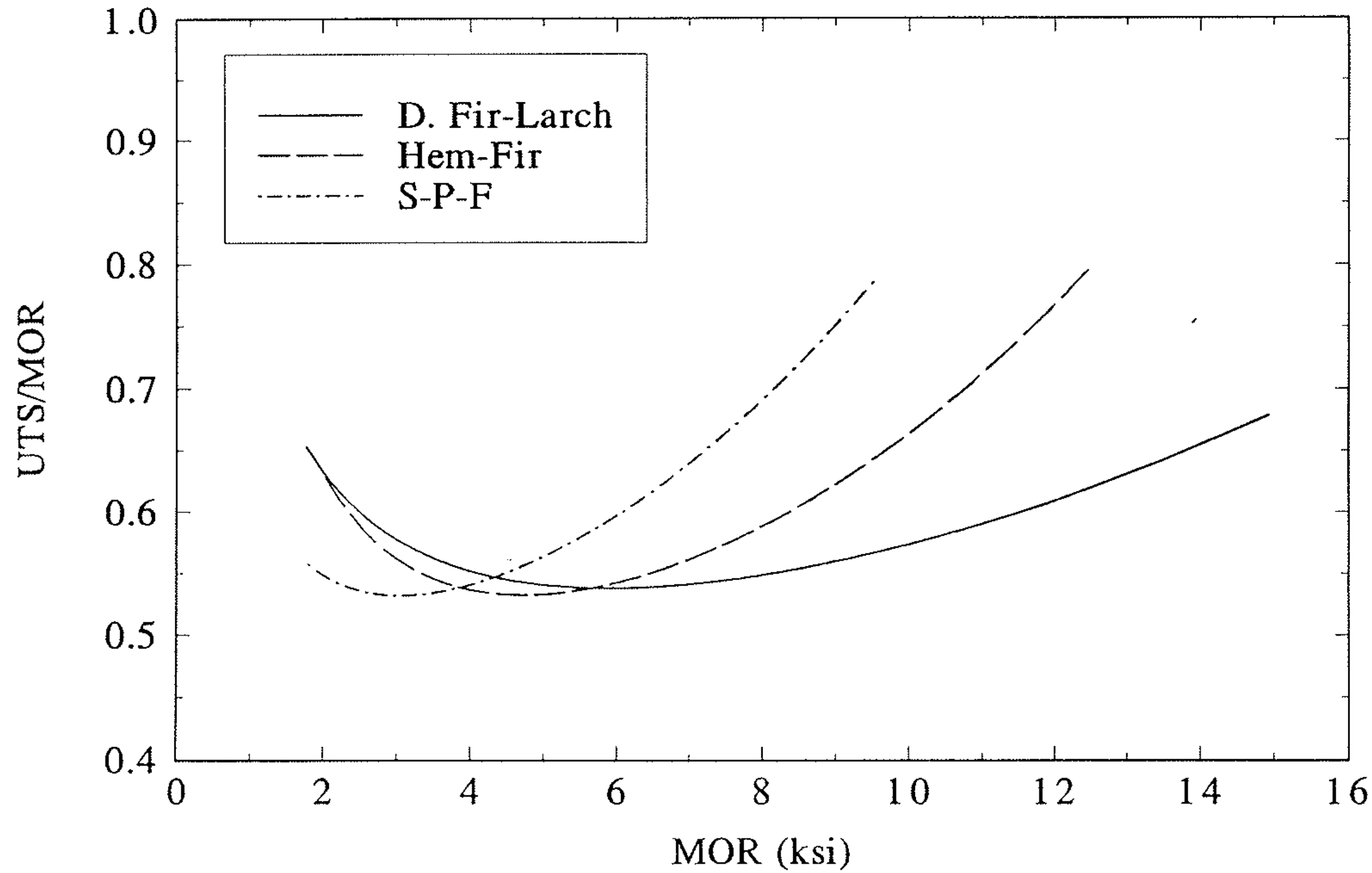

Figure 4. Variation of the ratio of tension strength to bending strength with bending strength load.

CIB-W18/25-7-4

INTERNATIONAL COUNCIL FOR BUILDING RESEARCH STUDIES AND DOCUMENTATION

WORKING COMMISSION W18 - TIMBER STRUCTURES

A GUIDE FOR APPLICATION OF QUALITY INDEXES FOR DRIVEN FASTENERS USED IN CONNECTIONS IN WOOD STRUCTURES

by

E G Stern
Virginia Polytechnic Institute and State University
U S A

MEETING TWENTY - FIVE

ÅHUS

SWEDEN

AUGUST 1992

91111501
92022001
92051801

A GUIDE FOR APPLICATION OF QUALITY INDEXES FOR DRIVEN FASTENERS USED IN CONNECTIONS IN WOOD STRUCTURES

by

E. George Stern
Earle B. Norris Research Professor Emeritus of Wood Construction
Virginia Polytechnic Institute and State University
Blacksburg, VA 24063-0361 USA

ABSTRACT

Quality indexes for driven fasteners, designed to resist axial and lateral forces, were originally developed to facilitate the computerized design of wood pallets and related structures. This guide makes it feasible to apply these indexes to a broader range of structural components and structures. The use of the information presented in this guide can result in accurate prediction of the structural performance of nailed and stapled connections in wood structures and in optimum benefits which can be provided by these fasteners.

Prepared for Presentation at Meeting of
International Council for Building Research Studies and Documentation (CIB)
Working Commission on Timber Structures (W18A)
in Åhus, Sweden, August 24-27, 1992

APPLICATION OF QUALITY INDEXES FOR DRIVEN FASTENERS USED IN CONNECTIONS IN WOOD STRUCTURES

By
E. George Stern
Earle B. Norris Research Professor Emeritus of Wood Construction
Virginia Polytechnic Institute and State University, Blacksburg, VA 24063-0361 USA

This guide suggests an expanded application of a design system which was originally developed for wood pallets and related structures. It is based on the use of certain quality indexes for driven fasteners, empirical formulae, and extensive test data on, and structural models derived for, wood pallets, to be applied to the broader range of wood-framed components and structures. It is applicable to such engineered structural components and structures that are exposed to high vibrational and impact forces, waves, and wind gusts. They include wood trestles, bridges, grandstands, marine structures, and pole-type structures framed with non-treated, treated, and pressure-impregnated wood and wood-base products. This guide does not apply to such non-engineered wood-frame construction as standard residential construction where fastener quality has little influence on the performance of the finished product.

In such engineered structural components and structures, the connections and, especially, rigid connections of members and components can be of influence on the performance of the structures. The use of improved fasteners and engineered design of the connections can result in improved and longer lasting as well as vibration and impact, earthquake, wave, and storm-resistant structures.

This guide provides practical, effective, and efficient means of determining design values for driven fasteners of many kinds, styles, sizes, and quantities for designing connections of wooden structural components and structures assembled with these fasteners. The use of the information presented in this practice results in the optimum benefits that can be provided by these fasteners. They include nails, spikes, and staples made of regular-stock and stiff-stock steel, aluminum, stainless steel, copper, brass, bronze, Monel, and certain plastics; bright and coated, with plain and helically threaded shanks, and, if of steel, non-hardened and hardened.

The quality indexes, covering the Fastener Withdrawal Index (FWI) and the Fastener Shear Index (FSI), are based on the geometry and the material properties of the fasteners and are applicable to the fastener per se and independent of the connection assembled with these fasteners. The application of FWI and FSI to driven fasteners of shank diameters smaller and larger than those listed in Tables 11 and 12 is based on extrapolation of the data presented in these tables. Such extrapolated data have not been verified by tests.

Significance and Use

The withdrawal and shear quality indexes (FWI and FSI) are used in determining the fastener withdrawal resistance (FWR) and the fastener shear resistance (FSR), respectively. Using these indexes, the structural performance of nailed connections in wood structures can be predicted.

For connections containing multiple driven fasteners for load transfer from member to member, a conservative strength estimate is made if the design load of a single driven fastener is multiplied by the number of fasteners in the connection. This is the case, in the light of the load sharing by the closely spaced fasteners and in the light of the fact that the mean strength of a group of driven fasteners is considerably above that of the lower fifth-percentile exclusion limit of the sum of single driven fasteners. If the multiple fasteners are load sharing and act in the connection as a group, a more realistic, higher-percentile, lower exclusion limit value, closer to the mean value, can be justified because of the anticipated load redistribution and the resulting low probability of system failure, provided appropriate engineering data are available to justify such a step.

Rationale

The deterministic design of connections of structural members assembled with driven fasteners is, in the USA, normally based on the tabulated normal allowable withdrawal and shear resistance values for driven fasteners which are adjusted by the appropriate modification factors for given design parameters as published in the National Design Specification for Wood Construction (NDS). These design values were derived from empirical formulae developed by the U.S.D.A. Forest Products Laboratory and published in the Wood Handbook. These design values are applicable to plain-shank steel nails and spikes as well as "threaded" hardened-steel nails and spikes; although the shear values for the threaded fasteners need to be limited to helically threaded, hardened-steel nails and spikes in the light of the decreased thread-root diameter of annularly threaded fasteners, which would govern their shear resistance.

The 1986 and 1991 editions of NDS do not cover staples and do not give any consideration to the effects of (a) variations in the specific materials of which the fasteners are made, (b) variations in the fastener treatment and the resulting variations in the toughness of the fasteners, (c) the thread geometry of the threaded fasteners, that is the thread type, the thread-crest diameter, the thread angle, and the number of thread grooves, (d) the type and size of the fastener point and head and their influence on the fastener performance, (e) permissible tolerances and other factors, such as fastener coatings and finishes. All of these variables should be given consideration in the determination of fastener quality. In the light of their importance, the significance of these variables is covered in the following sections.

Materials

Nails, spikes, and staples are made of regular-stock steel, that is low-carbon steel with less than 0.15 pct carbon content, and medium low-carbon steel with 0.15 to 0.23 pct carbon content; while nails and spikes are also made of harder and tougher stiff-stock steel, that is low or medium high-carbon steel with 0.23 to 0.44 pct carbon content which makes feasible effective hardening of these fasteners. Other fastener materials are 2024, 5056, 6061, and 6110-alloy aluminum, austenitic (304) and ferritic (400) stainless steel, copper, copper-clad steel, brass, bronze, Monel, and certain plastics.

Stiff-stock steel nails and spikes resist higher buckling forces during driving and transfer shear forces deeper into the connected members than similar regular-stock steel fasteners. Properly hardened stiff-stock steel nails and spikes are even more effective.

Regular-stock steel fasteners shall have a minimum average ultimate tensile stress, depending on the fastener-shank diameter, as is indicated in Table 1.

Table 1. - Minimum Average Ultimate Tensile Stress of Regular-Stock Steel Fasteners

Fastener-Diameter Ranges In. (Mm)	Minimum Average Ultimate Tensile Stresses Psi (MPa)
< 0.063 (1.6)	100,000 (690)
$> 0.063 \leq 0.110$ ($> 1.6 \leq 2.8$)	85,000 (585)
$0.110 \leq 0.193$ ($> 2.8 \leq 4.9$)	72,000 (500)
> 0.193 (> 4.9)	65,000 (450)

Stiff-stock steel fasteners and those made of other metals shall have a minimum average ultimate tensile stress, as shown in Table 2.

Table 2. - Minimum Average Tensile Stresses of Fasteners Other Than Regular-Stock Steel Fasteners

Fastener Materials	Minimum Average Ultimate Tensile Stresses Psi (MPa)
Stiff-stock steel	120,000 (825)
Hardened stiff-stock steel	166,000 (1140)
Stainless steel	99,000 (620)
Aluminum	55,000 (380)
Copper	32,000 (220)
Brass	50,000 (340)

Minimum average flexural yield stress values for driven fasteners have not been established.

Occasionally, the hardness of the rod or wire, from which nails and spikes are made, is specified in an attempt to provide quality criteria for these fasteners. However, their hardness and toughness are influenced by work hardening of the steel resulting from the wire-drawing procedure as well as the deformation of the wire during fastener manufacture. Thus, the hardness of the rod or wire can be different from the hardness of the finished fastener. Therefore, the specified hardness of the rod or wire is useful as a guide for the fastener manufacturer in selecting the appropriate rod or wire; but not for the fastener user to predict fastener quality.

Stiff-stock steel nails and spikes are non-hardened or hardened to increase their toughness; hence, to increase their buckling resistance during driving and their bending resistance during lateral load transfer between connected members. Because of this improved performance, properly hardened nails and spikes, especially if provided with highly effective threads along their shanks, can be relatively slender, offering decreased driving resistance and reduced wood-splitting characteristics during driving. Therefore, slender fasteners allow the location of an increased number of nails and spikes in a given connection area and nearer the member end.

If made of inappropriate steel or improperly hardened, such hardened-steel nails and spikes are often brittle. Such brittle fasteners shall not be used, as they can break during driving and/or transfer of shear loads and, especially, impacted shear loads. The driving of brittle nails and spikes is dangerous because of the possibility of breakage and flying particles during driving. Hardened-steel nails and spikes shall not be driven without appropriate protection of workers and others in the work area.

All fasteners shall be sufficiently ductile to withstand static cold bending through a given number of degrees over a mandrel not greater than the shank diameter, unless specified otherwise. The minimum average static cold bend angles to be attained without fracture of the fastener for some of the common materials of which driven fasteners are made are listed in Table 3.

Table 3. - Minimum Average Static Cold Bend Angle of Driven Fasteners

Fastener Materials	Minimum Average Static Bend Angles Deg
Regular-stock steel	180
Stiff-stock steel	90
Hardened steel	20
Stainless steel	180
Aluminum alloys	90
Copper and brass	180

The macroscopic observation of a partial or complete break is considered failure.

The Morgan Impact Bend Angle Nail Tester (MIBANT device) provides information on the resistance of driven fasteners to given impact forces. The mass of the impacting weights can be changed for testing of fasteners of largely different slenderness. Thus, the standard 2.50-lb (15.6-N) drop weight is exchanged for one of lesser mass when warranted. The MIBANT angle is influenced by the diameter of the fastener shank and the material from which the fastener is made as well as by the way the fastener wire is drawn, formed, or deformed. Acceptable ranges of average MIBANT angles for the classification of fasteners of 0.106 to 0.135-in (2.9 to 3.4-mm) shank diameter and their quality ranking, based on 25 random samples from a single lot of fasteners, are given in Tables 4a and 4b.

Table 4a. - Fastener Classification According to MIBANT Angles

Average Bend Angles Deg.	Fastener Classification
8 to 28	Hardened steel
29 to 46	Stiff-stock steel
47 and more	Soft steel

Table 4b. - Fastener Quality Ranking According to MIBANT Angles

Average Bend Angles Deg.	Relative Fastener Quality
8 to 24	Excellent
25 to 35	Good
36 to 46	Accepatable
47 and more	Acceptable only for clinch nailing

These bend-angle ranges are valid if a given mass is dropped from a given height to impact on the head of the cantilevered fastener. A certain percentage of partial and complete head and shank failures are acceptable without causing fastener rejection. When using the standard 3.50-lb (15.6-N) drop weight, free-falling from a height of 12 in. (300 mm), not more than 8 pct of the nail heads and shanks shall fail during impact.

Whenever cold-bend or MIBANT data cannot be provided, stiff-stock steel nails and spikes shall have a minimum hardness of HRC 24, as determined by conversion of tensile strength to hardness in accordance with SAE J 417b; while hardened-steel nails and spikes shall have a minimum hardness of HRC 37, unless specified otherwise.

Nail (Spike) Shank

The purpose of the nail shank is to hold two or more connection members together and to transfer withdrawal and shear forces from the nailed member to the nailing member and vice versa.

The shank length and wire diameter of driven fasteners are basic parameters of influence on the performance of connections assembled with these fasteners. The connection geometry influences the selection of both variables. Where feasible, the minimum fastener penetration into the nailing member of plain-shank fasteners should be 1-1/2 in. (38 mm) and that of high-quality threaded nails should be 1-1/4 in. (32 mm) where high-quality connections are, or should be, specified. Where the end distance of the fastener and the spacing between fasteners has to be short, the fastener should be slender to reduce, if not to eliminate, fastener splitting of the wood member. This is particularly important in the fastening of dense woods and is a major reason for giving preference to the use of tool-driven slender staples over nails where these staples can economically fulfil the performance requirements.

Stout nails and spikes, having a low length/diameter ratio and 1/4-in (6.4-mm) or larger shank diameters, act like pins and dowels inserted into undersize holes when transferring shear loads, especially in connections with such multiple fasteners. Their effectiveness shall be determined accordingly.

Helically threaded nails are roll-threaded, with a non-threaded section, called clearance, between head and threads. If no more than two-thirds of the nail shank nearest the point is threaded, the thread is fully effective in the nailing member under most conditions normally encountered. A clearance of one-third of the nail length usually allows the nail to turn during final driving and, thus, the nailed member to be drawn tightly to the nailing member.

If a plain-shank section exists between helical thread sections along the nail shank, the nail cannot form as effective a helical thread as a threaded nail without such a section in the wood into which the nail is driven. This interrupted thread results in a lower nail-withdrawal resistance compared to that of a nail with a continuous helical thread along its shank. Performance factors for such nails have not been established.

Helically threaded nails can be provided with a variety of threads. Flat-bottom threads are more effective than round-bottom threads. Non-symmetrical, one-directional, one-way threads with a fish-hook-like performance are more effective than symmetrical threads. The effectiveness of one-directional threads is readily determined by placing the threaded portion of the nail shank between thumb and finger, applying pressure, and trying to pull the nail in both directions along the nail axis. An effective thread allows the nail to be pulled in the direction of the nail point and resists pull in the direction of the nail head.

Thread crests are either single or double, with the latter type of crest being more effective. Threads can be designed in such a way that the wood fibers slide over the thread crests into the thread grooves during nail driving. The thread configuration shall prevent the wood fibers from sliding back during application of withdrawal forces. To accomplish this, the leading flank on the point side of the thread shall be noticeably inclined; while the following flak on the head side of the thread shall be nearly perpendicular to the axis of the nail shank. These "improved" threads result in the superior performance expected of well-threaded nails, particularly if their thread-crest diameter is large relative to the shank diameter and the thread angle is not excessive, that is within the range of 60 to 67 deg from the vertical to the nail shank. These "improved" nails justify the high design values attributed to these fasteners.

If provided with a steep thread angle, larger than 60 deg to the nail-shank axis, a helically threaded nail turns like a wood screw during driving through the fastened member into the fastening member and forms a thread in the wood, that mates with the thread of the nail. As a result, the driven nail acts much like a wood screw. During forced nail withdrawal, the wood fibers which cantilever into the space between the thread flanks are basically stressed in compression perpendicular to the grain of the wood. The wood fibers have to be sheared off before connection failure can occur, provided the nail does not back out due to an excessively large thread angle.

Because of the fact that the withdrawal resistance of properly threaded nails is only overcome when the wood fibers cantilevering into the space between the thread flanks are sheared off, and because the shear resistance of wood fibers increases when wood seasons to a lower moisture content after nail driving, the withdrawal resistance of properly threaded nails increases slightly during such seasoning of the connection. On the other hand, the withdrawal resistance of plain-shank nails, relying solely on friction between the nail shank and the surrounding wood, decreases considerably, as much as four-fifths, because of the relaxation of the wood fibers which were compressed during nail insertion and because of shrinkage of the wood surrounding the nail shank during wood seasoning after its assembly. This is the reason why the NDS requires that the permissible withdrawal and shear-load values be reduced by 75 and 25 pct, respectively, if plain-shank nails are driven into green or partially seasoned wood which dries out after nailing or into dry wood which repetitively absorbs and loses moisture during service; while threaded nails do not require the application of these design-load reduction factors.

The thread-crest diameters shall be at least 12 pct, preferably 18 pct and more, larger than the shank diameters. For example, a nail with a 0.110-in. (2.8-mm) shank diameter should have a 0.138-in. (3.5-mm) thread-crest diameter and a nail with a 0.120-in. (3.05-mm) shank diameter should have a 0.145-in. (3.7-mm) thread-crest diameter. The relative assessment of nail quality of helically threaded nails according to the difference between thread-crest diameter and wire diameter is given in Table 5.

Table 5. - Quality Ranking of Helically Threaded Nails According to Difference Between Thread-Crest Diameter and Wire Diameter of Fastener

Difference Between Thread-Crest Diameter and Wire Diameter, in In.	Relative Fastener Quality
More than 0.020	Excellent
0.016 to 0.020	Good
0.012 to 0.015	Marginal
Less than 0.012	Poor

The thread-root diameter is slightly larger than twice the shank diameter minus the thread-crest diameter; e.g., $2 \times 0.110 - 0.138 \geq 0.082$ in. (2.1 mm) in the case of the nail with a 0.110-in. (2.8-mm) shank diameter.

Optimum thread angles, measured perpendicular to the nail-shank axis, for helically threaded nails range from 60 to 67 deg. Nails with larger thread angles, often called "lazy" helically threaded nails, can provide decreased withdrawal resistance, as they tend to turn backward during application of withdrawal forces after friction between nail shank and surrounding wood has been overcome. Thread angles smaller than 60 deg reduce the possibility of the helically threaded nail turning during driving and forming a clean thread in the wood similar to the thread along the nail shank.

The number of continuous helical grooves along the threaded portion of the nail shank with a thread angle of 60 to 67 deg should be four and not more than six.

Staple Legs

The purpose of staple legs is the same as that of the nail shank.

The usually slender staple legs are plain or coated to reduce driving resistance and possibly increase withdrawal resistance. The pair of staple legs provide some torsional resistance for the connection; while a single nail shank does not.

Nail (Spike, Staple) Point

The principal purpose of the nail point is to facilitate nail driving.

The nail point is usually a pyramidically shaped diamond point, unless specified otherwise or another type of point is considered to be the standard point for a given fastener. Nails are manufactured with blunt points, that is, points less than 0.150 in. (4 mm) in length, or even pointless where excessive splitting during driving of a pointed nail would result in unsatisfactory and unacceptable connections. Some points, such as wedge points, act to some extent like wedges during driving, tending to split the wood; while pointless nails act like broaches. Such pointless nails are likely to penetrate the wood in a straight manner, thereby reducing, if not eliminating, points protruding from the sides of narrow wood members, that is, "shiners".

Nail (Spike) Head

The purpose of the nail head is to provide a strike surface for the hammer and tool and machine driver, and a bearing area to resist head pull-through forces. Standard head diameters for nails of given shank diameter are listed in Table 11. Slightly larger head diameters of high-quality nails can improve nail performance under certain use conditions, especially in the fastening of low-density wood to higher-density wood and of plywood.

The nail head is usually round with a flat top surface and requires a fillet between head and shank. The striking surface of the flat head may be plain, lettered, numbered, checkered, striated, or knurled. Countersunk heads, used where countersinking is required, are conically shaped on their underside, having a medium included angle of 75 to 99 deg or a large included angle of 100 to 160 deg.

Some nails have an incomplete head, that is, with a segment of the head deleted to make it feasible to collate nails tightly next to each other in strips or coils to be fed into the magazine of driving tools. Nails with incomplete heads shall have the same bearing areas under the heads as similar nails with complete heads of the same shank diameter, if the same head pull-through resistance is required.

Staple Crown

The purpose of the staple crown, located opposite the staple-point ends, is to connect the two staple legs effectively, and to serve the same purpose as the nail head.

The staple crown is flattened to provide a larger bearing area than would be provided by round or rounded wire. The staple-crown length, that is, the distance between the staple legs is critical in evaluating effectiveness of the staple crown in resisting crown pull-through forces.

Nail (Spike, Staple) Surface

The purpose of modifying the nail surface is to decrease the driving resistance and possibly increase the withdrawal resistance as well as the corrosion resistance of the fastener, in addition to providing a clean surface.

The nail surface is bright or blued; chemically treated, eg., parkerized or phosphatized (bonderized); chemically etched, resulting in a microscopically roughened surface; barbed, serrated, or knurled; lacquered, painted (japanned), enameled, aluminized and/or anodized; electro-plated; cement, resin, or conversion-coated with thermo-plastic or thermo-setting polymers; galvanized, that is tumbled in zinc powder (sheradized), hot-dip galvanized, that is dipped into molten zinc once or, if necessary, twice, or mechanically galvanized (peen galvanized), that is provided with an impacted zinc coating, without or with a supplementary chromate or dichromate treatment.

Hot-dip and mechanical galvanizing are, practically speaking, equally effective for many use conditions, if an equal amount of zinc is deposited onto the fastener surface, and are equally acceptable in many instances. However, hardened-steel nails shall be mechanically galvanized, not hot-dip galvanized, since the required hardness is affected detrimentally by the heat applied during hot-dip galvanizing. The galvanized coating shall meet the specified requirements of weight and adherence.

Staples are often fabricated from galvanized-steel wire which shall meet the specified requirements.

Nail (Spike) Identification and Codification

Nails are identified by grip marks along the shank near the head and at times by letters, numbers, or embossed or indented designs on the nail head. Identification of the size of nails used in diaphragm connections is not required if the nail heads are larger than those required for standard, plain-shank, common wire nails; and, if stouter, helically threaded, diaphragm nails with large heads are used. A centered nail-head depression of 0.01-in. (0.25 mm) depth and 0.106 to 0.126-in. (2.7 to 3.2-mm) diameter is required for pallet nails of less than 3-1/2-in. (90 mm) length, if the nails are to meet the requirements of Specification UCFI 435-2 for European pool pallets.

Helically threaded nails are codified and referenced by descriptive code, as shown on Table 11, that is by numbers indicative of the nail length and shank diameter, followed by two letters referring to the thread-crest diameter and the thread angle. Thus, a 250x112AA nail is 2-1/2 in. (64 mm) long and has a 0.112-in. (2.8-mm) shank diameter, a 0.132-in. (3.4-mm) thread-crest diameter, and a 60-deg thread angle.

Staple Identification and Codification

Staple are identified by the dimensions of the leg length and cross-section as well as the color of the coating(s).

Staples are codified and referenced by descriptive code, as is shown in Table 12, that is by numbers indicating the staple length and nominal wire diameter, followed by one letter referring to a bright or coated finish, in line with Standard MH1.7. Thus, a 250 x 072A staple is 2-1/2 in. (64 mm) long, has a 0.072-in. (1.8-mm) nominal wire diameter, and is bright, that is without a coating; while a 250 x 0.72B staple is identical to the above staple, yet provided with a coating.

Nail (Spike) Tolerances

Nail and spike tolerances are applicable to the fastener length, shank diameter, thread-crest diameter, thread angle, and head diameter. The tolerances are not applicable where minimum or maximum values are specified.

With the nail length measured from the maximum diameter in the head-bearing surface to the extreme point end, the nail- and spike-length tolerances listed in Table 6 are applicable.

Table 6. - Length Tolerances for Nails and Spikes

Nail Lengths In. (Mm)	Tolerances In. (Mm)	or	Tolerances In. (Mm)
≤ 1.0 (25)	± 0.047 (1.2)		± 0.031 (0.8)
>1.0 to 2.5 (25 to 64)	± 0.079 (2.0)		± 0.062 (1.6)
> 2.5 (64)	± 0.118 (3.0)		± 0.094 (2.4)
>7.0 (178) and more	----------		± 0.125 (4.8)

NOTE: 1 - For evaluation of nail performance, use one-third of the length of the nail point.

With the shank diameter measured away from the grip marks and prior to the application, or after removal, of any finishes or coatings, the nail-shank diameter tolerances shown in Table 7 are applicable.

Table 7. - Shank-Diameter Tolerances for Nails

Shank Diameters In. (Mm)	Tolerances In. (Mm)
≤ 0.079 (2.0)	± 0.002 (0.05)
>0.079 to 0.117 (2.0 to 3.0)	± 0.004 (0.10)
>0.117 (3.0)	± 0.008 (0.20)

With the thread-crest diameter being the maximum diametric dimension along the deformed portion of the nail shank, the crest-diameter tolerances shown in Table 8 are applicable.

Table 8. - Thread-Crest Diameter Tolerances for Nails

Crest Diameters In. (Mm)	Tolerances In. (Mm)
≤ 0.177 (3.0)	± 0.004 (0.10)
> 0.177 (3.0)	± 0.008 (0.20)

With the thread angle, in deg, measured from the perpendicular to the nail-shank axis, the thread-angle tolerance is ± 2 deg.

With the major and minor nail-head diameters not to exceed 15 pct of the nominal head diameter, its tolerance is ± 15 pct.

Staple Tolerances

With the length of the tool-driven staples measured from the top of the staple crown to the tip of the staple points, the length tolerances of these staples are the same as those for nails. With the length of hammer-driven staples measured from the underside of the staple crown to the tip of the staple points, the length tolerance of these staples is ± 0.10 in. (2.5 mm).

The nominal wire diameter of staples is measured prior to staple forming. The staple width and thickness are measured prior to the application, or after removal, of finishes or coatings, or along that staple-leg portion which is not coated. The diameter tolerances for flattened wire staples are shown in Table 9.

Table 9. - Leg-Width Tolerances for Staples

Leg Widths In. (Mm)	Tolerances In. (Mm)
0.020 to 0.028 (0.51 to 0.71)	± 0.001 (0.025)
>0.028 to 0.035 (0.71 to 0.89)	± 0.0015 (0.038)
>0.035 to 0.112 (0.89 to 2.80)	± 0.002 (0.050)

Dimensional Nail (Spike, Staple) Variables

Actual variations in the physical properties of driven fasteners are influenced by the permissible fastener tolerances. Length, shank diameter, thread angle, and number of thread grooves vary relatively little within and between fastener lots from the same source. However, thread-crest diameter and thread depth vary considerably more, since they are influenced by the die and the amount of its wear with which the fastener shanks are threaded. This wear influences the fastener quality properties, that is the Fastener Withdrawal Index (FWI) and the Fastener Shear Index (FSI). The quality is governed by the permissible tolerances of the thread-crest diameters which, for this reason, are important dimensions to be controlled rigorously during the manufacture of threaded nails and spikes.

For a number of lots of helically threaded, non-hardened or hardened steel nails of 0.113 to 0.121-in. (2.9 to 3.1-mm) shank diameters, the standard deviations shown in Table 10 were observed.

Table 10. - Standard Deviations for Nails of Given Shank Diameters

Nail Properties	Mean Shank Diameters In. (Mm) or Deg	Standard Deviations In. (Mm) or Deg
Shank Diameter:	0.113 (2.9)	0.0012 (0.03)
	0.121 (3.1)	0.0009 (0.02)
Thread-Crest Diameter:	0.126 (3.2)	0.069 (1.8)
	0.136 (3.5)	0.069 (1.8)
Thread Angle:	67 for 0.113 (2.9)	2.10
	67 for 0.121 (3.1)	1.90
MIBANT Angle:	39 for 0.113 (2.9)	12.13
	33 for 0.121 (3.1)	16.47
Head Diameter:	0.274 (7.0)	0.127 (3.2)
	0.280 (7.1)	0.089 (2.3)

Performance of Driven Fasteners

The flexural yield stress of plain-shank, regular-stock steel nails is influenced slightly by the shank diameter, with nails of smaller diameter having higher yield stresses, most likely because of the work-hardening during wire drawing. This observation is not applicable to hardened-steel nails, because the effects of work-hardening is overshadowed by the effects of heat-treatment and subsequent tempering during the hardening process. Similarly, for plain-shank, regular-stock steel nails and for non-hardened and hardened steel nails of 0.106 to 0.135-in. (2.7 to 3.4-mm) shank diameters, changes in yield stresses have not been observed. This is explained by the small range of the shank diameters investigated. Fig. 1 provides regression lines for the data observed for regular-stock steel nails and spikes of various shank diameters.

The quality and performance of nails, spikes, and staples are measured by the Fastener Withdrawal Index (FWI) and the Fastener Shear Index (FSI), based on the geometry and the material properties of the fasteners. Both indexes are representative of the quality and performance of the fastener per se and independent of the connection assembled with the fastener.

When the head pull-through resistance is smaller than the shank withdrawal resistance of nails and spikes and when the crown pull-through resistance is smaller than the leg withdrawal resistance of staples, the former property is the governing criterion and shall be determined.

FWI is independent of the material properties of the fasteners; while FSI is influenced by these material properties, that is the fastener toughness as is indicated by the MIBANT angle of the finished fasteners.

Both FWI and FSI are relative measures of fastener quality and performance. Both represent the performance of a particular fastener relative to the performance of the "base" nail with FWI = 100 and FSI = 99. With respect to FWI, the helically threaded, steel, "base" nail has a 0.112-in. (2.8 mm) shank diameter, a 0.132-in. (3.4-mm) thread-crest diameter, four helical grooves, a 60-deg thread angle, and 5.57 helixes per in. (per 25.4 mm) of thread length. With respect to FSI, this "base" nail is classified as a hardened-steel nail with a 20-deg MIBANT angle.

The relative quality indexes for standardized, helically threaded, non-hardened and hardened-steel nails of 1-1/2 to 3-1/2-in. (38 to 90-mm) lengths are given in Table 11, with the nail length, shank diameter, thread-crest diameter, thread angle, and nail toughness as variables. The relative quality indexes for standardized, bright and coated, regular-stock steel, tool-driven staples of 2 to 3-3/4-in. (50 to 95-mm) lengths are given in Table 12, with the staple length, nominal wire diameter, finish, and staple toughness as variables. The quality indexes of driven fasteners of sizes different from those given in Tables 11 and 12 are determined, as required, from available test data or by extrapolation (see Fig. 2).

Fastener Withdrawal Index (FWI)

FWI is determined by using the following formulae:

For plain-shank, round-wire fasteners, where the number of helixes and the difference between shank diameter and thread-crest diameter is zero, insert factors 1.00 in formulae 2a and 2b:

for Imperial units: $FWI = 221\ (WD)$ (1a)

for SI units: $FWI = 8.7\ (WD)$ (1b)

For helically threaded nails and spikes,

for Imperial units: $FWI = 221\ (WD)\ [1 + 27.15\ (TD - WD)\ (H/TL)]$ (2a)

for SI units: $FWI = 8.7\ (WD)\ [1 + 27.15\ (TD - WD)\ (H/TL)]$ (2b)

For flattened-wire staples with two same-length legs,

for Imperial units: $FWI = 221\ (1.273)\ (WW + WT)$, for each staple leg (3a)

for SI units: $FWI = 8.7\ (1.273)\ (WW + WT)$, for each staple leg (3b)

NOTE 2 - For coated plain-shank fasteners, whose delayed withdrawal resistance is at least 33 pct higher than that of an identical non-coated fastener, a factor not exceeding 1.33 shall be applied. For coated fasteners, whose immediate or delayed withdrawal resistance is lower than that of an identical non-coated fastener, the lower withdrawal resistance value shall be governing.

Fastener Shear Index (FSI)

FSI per shear plane is determined by using the following formulae:

For plain-shank and helically threaded, round-wire fasteners of given MIBANT angle (M):

for Imperial units: $FSI = 263{,}260\ (WD)^{1.5}/(3M + 40)$ (in the case of staples, for each staple leg) (4a)

for SI units: $FSI = 2056\ (WD)^{1.5}/(3M + 40)$ (in the case of staples, for each staple leg) (4b)

For flattened-wire staples with two same-length legs,

for Imperial units: $FSI = 263{,}260\ [(0.848\ (WW + WT)]^{1.5}/(3M + 40)$ (5a)

for SI units: $FSI = 2056\ [(0.848\ (WW + WT)]^{1.5}/(3M + 40)$ (5b)

NOTE 3 - For annularly threaded nails and spikes and helically threaded screwnails and spikes with a thread angle of less than 20 deg, WD shall be the thread-root diameter.

Performance of Connections Assembled with Driven Fasteners

The performance of connections assembled with nails, spikes, and staples is measured by the Fastener Withdrawal Resistance (FWR) and the Fastener Head/Crown Pull-Through Resistance (HPR), whichever is smaller, and the Fastener Shear Resistance (FSR). Based on the lower fifth-percentile exclusion limits for FWR and HPR and based on the ultimate connection load, requiring the application of a reduction factor of six to seven to arrive at the design load at the allowable connection slip of 0.015 in. (0.38 mm) for FSR, the allowable design values, in lbf (N), are determined by using the following formulae:

Fastener Withdrawal Resistance,

for Imperial units: $$FWR = 222.2\,(FWI)\,(GS)^{2.25}(P)/(MC - 3) \quad (6a)$$

for SI units: $$FWR = 38.9\,(FWI)\,(GS)^{2.25}(P)/(MC - 3) \quad (6b)$$

NOTE 4 - The following improved, alternate, Imperial-unit formula was introduced for use in the computerized Pallet Design System (PDS):

$$FWR = (1\text{-}A)\,[11.2\,(FWI)\,(GS)^{2.25}\,(P)] + 148\,(A) \quad (6c)$$

Fastener Head/Crown Pull-Through Resistance,

For nails and spikes,

for Imperial units: $$HPR = 1{,}250{,}000\,(T)(GD)^{2.25}[(HD)^2 - (WD)^2]/(MC - 3) \quad (7a)$$

for SI units: $$HPR = 339\,(T)\,(GD)^{2.25}[(HD)^2 - (WD)^2]/(MC - 3) \quad (7b)$$

For flattened-wire staples,

for Imperial units: $$HPR = 1{,}592{,}000\,(T)(GD)^{2.25}[(HD)^2 - (WD)^2]/(MC - 3) \quad (8a)$$

for SI units: $$HPR = 432\,(T)\,(GD)^{2.25}[(HD)^2 - (WD)^2]/(MC - 3) \quad (8b)$$

Fastener Shear Resistance,

for Imperial units: $$FSR = 61.93\,(FSI)\,(G)\,(T)/(MC - 3) \quad (9a)$$

for SI units: $$FSR = 10.84\,(FSI)\,(G)\,(T)/(MC - 3) \quad (9b)$$

NOTE 5 - In the case of torsional shear resistance, FSR applies to connections assembled with two nails within the range $0.20 \leq T/P \leq 1.90$, and to each nail in connections assembled with more than two nails, within the above range, with the thickness of the fastened member being at least 3/8 in. (9.5 mm) and that of the fastening member meeting the requirements for fastener penetration stated in Note 6.

NOTE 6 - For the computation of the FSR values, the depth of penetration in the fastening member is 10, 11, 13, and 14 shank diameters for species Groups I, II, III, and IV, respectively, with the species Groups identified in Table 8.1A of 1986 edition of NDS. The corresponding, actual minimum depths of penetration for effectively helically and annularly threaded, non-hardened stiff-stock steel fasteners are 7.5, 8.2, 9.8, and 10.5 shank diameters; and for such hardened steel fasteners are 5.0, 5.5, 6.5, and 7.0 shank diameters. The FSR values cannot be increased when the depth of penetration is larger than that specified. When the depth of penetration is less than that specified for plain-shank, regular-stock steel fasteners and the specified FSR values for the specified depth of penetration are to be applied, these fasteners shall be clinched for a length of at least three shank diameters at an angle ranging from 45 to 90 deg to the fiber direction of the fastening member. When the depth of penetration is less than that specified, the FSR values are determined by straight-line interpolation between zero and the applicable FSR value, except that the depth of penetration shall not be less than one-third of the applicable value.

Design Parameters

The described design procedure, based on the computed fastener - evaluation procedures, leads to the establishment of normal design values comparable to those published in Tables 8.8B and C of the 1986 edition and Tables 12A to D of the 1991 edition of NDS. Such parameters as grain direction, depth of fastener penetration, moisture content and changes in moisture content in the wood members, member treatment, duration of load, single and multiple shear, as published in NDS, shall be given consideration and the appropriate factors applied when the performance is determined of connections assembled with driven fasteners.

The 1991 edition of NDS, in establishing design procedures, refers to the following design parameters covering driven fasteners:

Specific Gravity of Wood

Average oven-dry specific gravity, $G^{1.75}$, based on weight and volume of representative clear oven-dry sample specimen of fastening member, of wood species used, ranging from 0.31 to 0.73 for common commercial North-American wood species; applicable to fastener withdrawal resistance in pounds per inch of penetration into the side grain of fastening member.

Embedding Resistance of Wood

Dowel bearing resistance of wood members of connection, in psi (Pa).

Fastener Bending Yield Stress

Average flexural yield stress of fastener, in psi (Pa), determined by the 5 pct diameter offset method of analyzing the load-displacement curves generated from fastener bending tests. (This represents a major change in design approach which was based on the ultimate stress in previous NDS editions. Minimum average flexural yield stress values for driven fasteners have not been established.)

The yield stress, as used in the 1991 edition of NDS, is found by drawing a line parallel to the initial linear region of the load-deformation curve with an offset equal to a deformation of 5 pct of the fastener-shank diameter. This yield stress lies between the proportional-limit and the ultimate stresses and is generally below the stress level at which micro-cracking occurs during the bending test. This yield stress is approximately equal to the numeric average of fasteners tensile yield stress and tensile ultimate stress. In contrast, the fastener flexural yield stress, as used in the CIB Code and in the Eurocode, is defined as the ultimate stress at fastener failure or that at the 45-deg bend angle of the fastener during the bending test, whichever is the smaller value.

Fastener Diameter

Fastener shank diameter in the case of plain-shank and helically threaded nails along clearance between head and threads (thread-root diameter in the case of annularly threaded nails), in in. (mm).

Fastener Penetration Depth

Depth of penetration of fastener in fastening or main member of connection, in in. (mm), for determination of withdrawal resistance; and to be twelve shank diameters for determination of lateral (shear) resistance of connection, with minimum penetration to be six shank diameters for proportionally reduced design value.

Member Thickness

Thickness of fastened or side member of connection, in in. (mm).

Wood Grain

For fasteners not driven into the side grain of the connection members, a reduction in strength values is prescribed. For fastener driven into the end grain of the connection member, with the fastener axis parallel to the wood fibers, the wood grain factor for laterally loaded fasteners is 0.67. This wood grain factor is not applicable to driven fasteners axially loaded in withdrawal and driven into the end grain of the connection member, since driven fasteners are not to be loaded in withdrawal from end grain. (The latter provision should not be applicable to properly helically threaded nails, where the wood grain factor of 0.67 should be applicable.)

Fastener Bending Yield Mode

The yield mode design procedure is applicable to laterally loaded driven fasteners in wood-to-wood and metal-to-wood or wood-to-metal connections, with the fastener in single shear (two-member connection) or double shear (three-member connection), where (a) the fastener is driven into the side grain of the wood members perpendicular to the wood fibers, and (b) the fastener penetration depth in the fastening or main member is greater than or equal to the minimum penetration required for proportionally reduced design values. The lateral design values are determined as influenced by the applicable yield mode,

(a) with Modes I_s, III_m, III_s, and IV applicable to wood-to-wood connections in single shear;

(b) with Modes III_m, III_s, and IV applicable to wood-to-metal or metal-to-wood connections in single shear, and with the metal plates to resist forces in tension, shear, and compression (bearing of metal on metal); and

(c) with Modes I_s, III_m, III_s, and IV applicable to wood-to-wood connections in double shear, with lateral design values for the connection to be twice the smallest design value based on the applicable yield mode, and with the side members thicker than six fastener shank diameters, and with the penetration- depth parameter applicable to the fastener penetration into the third connection member.

Load Duration

Based on 10-year occupancy live loads, the design values are multiplied by

0.90 for permanent loads, such as dead loads
1.15 for 2-month loads, such as snow loads
1.25 for 7-day loads, such as construction loads
1.60 for 10-min loads, such as wind and earthquake loads

except when the connection capacity is controlled by the strength of the metal of the fastener and connection member.

Diaphragm Design

In diaphragm construction, a factor of 1.1 is applicable for driven fasteners transmitting lateral (shear) loads.

Wet Service

For wood connections of unseasoned (wet) or partially seasoned (with moisture content above 19 pct) members or exposed to wet service conditions (subject to wetting and drying), a factor of 0.25 is applicable to driven fasteners transmitting axial withdrawal loads; and a factor of 0.75 is applicable to driven fasteners transmitting lateral (shear) loads. These reduction factors are not applicable to toe nails transmitting axial withdrawal loads and to threaded hardened-steel nails and should not be applied to threaded stainless-steel nails.

Temperature

For wood connections assembled with driven fasteners with sustained exposure to elevated temperatures up to 150° F, the following temperature factors are applicable:

In-Service		Temperature Factor	
Moisture Condition	$T < 100°F$	$100°F < T < 125°F$	$125°F < T < 150°F$
Dry	1.0	0.8	0.7
Wet	1.0	0.7	0.5

Toe Nails

For wood connections assembled with driven toe-nailed fasteners transmitting axial withdrawal loads, a toe-nail factor of 0.67 is applicable and, in the case of lateral (shear) load transmission, a toe-nail factor of 0.83 is applicable.

Wood Treatment

An appropriate factor is to be applied as required by the company providing the treatment and redrying the wood members of the connection.

Application of Quality Indexes for Driven Fasteners

Quality indexes for nails, spikes, and staples are tools for the designer of connections in wood structures. These indexes give the fastener manufacturer and user the opportunity to select the most effective and efficient fastener which is readily available for given end-use conditions and requirements.

The fastener manufacturer can indicate, in addition to the customary description of the fastener, the fastener quality indexes of his products in his catalogues, order forms, invoices, and package labels. Thereby, he provides a meaningful statement of the quality of his products, which he guarantees.

The fastener specification writer can call for the use of the optimum fastener under given conditions and can expect it to perform as anticipated, if his specification refers to the applicable fastener indexes.

The fastener user orders, warehouses, and controls the quality of the specified fastener on the basis of the guaranteed quality indexes. He gives the fastener manufacturer the opportunity to recommend substitution of a readily available fastener for another specified fastener on the basis of fastener quality and performance.

Thus, the introduction of fastener quality indexes opens up new opportunities which are beneficial to all involved.

The described design procedure for connections in wood structures assembled with driven fasteners, based on their quality indexes, is a more comprehensive approach than that based on the empirical formulae developed by the USDA Forest Products Laboratory years ago and that based on the conservative design values tabulated in the NDS. This procedure is more comprehensive because full consideration is given in the design of connections to the pertinent, actual physical and mechanical properties of the fasteners; while the previously advanced design procedures had to be based on conservative performance values in the light of the variability of the fasteners on the market.

FWI and FSI have been used successfully in the computerized design of such wood assemblies as pallets, where the use of highly effective fasteners is of considerable benefit to the performance of the assemblies. Thus, by selecting the most appropriate nail of 32 standardized nails, listed in Table 10, the anticipated life of a pallet can be increased as much as 3-1/2 times in comparison with the life of an identical pallet assembled with the least performing of the standardized pallet nails meeting the appropriate specifications for that pallet. This large increase in pallet performance is based on the computerized Pallet Design System (PDS) estimate.

Similar benefits can result from the use of improved fasteners in other wood-framed structures, especially if built of pressure-impregnated wood and wood-based products exposed to adverse environmental conditions.

APPENDIX A

DOCUMENTATION

ASTM Standards, ASTM, Philadelphia, PA, USA

A 153-82	Specification for Zinc Coating (Hot Dip) on Iron and Steel Hardware
A 641-80	Specification for Zinc-Coated (Galvanized) Carbon Steel Wire
B 695-85	Specification for Coating of Zinc Mechanically Deposited on Iron and Steel
D 1761-88	Methods of Testing Mechanical Fasteners in Wood
F 547-77(90)	Terminology of Nails for Use with Wood and Wood-Base Materials
F 592-84	Terminology of Collated and Cohered Fasteners and Their Application Tools
F 680-80(87)	Test Methods for Nails

ASME Standards, ASME, New York, NY, USA

MH1.6-87	Procedures for Determination of Durability of Wooden Pallets and Related Structures
MH1.7-88	Driven Fasteners for Assembly of Pallets and Related Structures

SAE Standard, Society of Automotive Engineers, SAE, Warrendale, VA, USA

SAE J 417b	Hardness Tests and Hardness Number Conversion

UCFI Standard, Union Chermain de Fer International, UCFI, Paris, France

UCFI 435-2	Quality for European Flat Pallets Made of Wood, with Floor Openings and Measuring 800 by 1200 Mm

Other Publications

National Forest Products Association. National Design Specification for Wood Construction. National Forest Products Association, Washington, DC, 1986. Also, 1991 Edition.

U.S.D.A. Forest Products Laboratory. Wood Handbook - Wood as an Engineering Material. Agricultural Handbook No. 72. U.S. Government Printing Office, Washington, DC, 1987.

Loferski, Joseph R., and Thomas E. McLain. Development of a Reliability-Based Design Procedure for Wooden Pallets. Forest Products Journal 37(7/8):7-14, 1987. Also, Loferski, Joseph R., Thomas E. McLain, and Stephen T. Collie. Analysis of Racked Wood Pallets. Wood and Fiber Science 20(3):304-319, 1988.

Loferski, Joseph R., and E. George Stern. Understanding Impact Testing of Pallet Nails and Staples. ASTM Journal of Testing and Evaluation 19(5):379-384, 1991.

McLain, Thomas E., L.A. Soltis, D.G. Pollock, Jr., and Patrick J. Pellicane. Timber Connection Design in the U.S. Converting to LRFD Format. Proceedings of 1991 International Timber Engineering Conference in London, England: pp 2.277-2.285, 1991.

Stern, E. George. Variables of Pallet Nails Influence PDS-Predicted Pallet Performance, A Review of the State of the Art. Presented at ISO TC51 WG 2-3 Meeting in Berlin, FRG, February, 1988. Condensation, Pallet Enterprise 8(2):47-50, 1988.

Werner, H., and W. Siebert. New Investigations with Nails for Wood Structures. Holz als Roh-und Werkstoff 48:191-198, 1991.

White, Marshall S. Quality Fasteners in Wood Pallets Makes All the Difference. NWPCA Newsletter 92(04):9-10, 1992, and Pallet Enterprise 12(4):10-11, 1992. Also, Quality Nails Make the Difference in Wood Pallets. NAWGA Review 8(4):24-25, 1992.

APPENDIX B

Terminology Specific to This Guide

Driven fasteners - nails, 6 in. (150 mm) or less in length; spikes, nail-like fasteners, with few exceptions longer than 6 in. (150 mm); staples with two same-size legs connected by crown; designed to be driven by hammer, machine, or special tool

Connections - structural junctions of wood and wood-base members, components, and assemblies of wood structures, assembled with driven fasteners

Fastener withdrawal index (FWI) - factor representing the measure of anticipated quality of a driven fastener with respect to its resistance to withdrawal forces, based on fastener geometry; applicable to fastener per se and independent of connection assembled with fastener; based on lower fifth-percentile exclusion limit of maximum withdrawal-resistance values

Fastener shear index (FSI) - factor representing the measure of anticipated quality of a driven fastener with respect to its resistance to shear forces, based on fastener geometry and material properties; applicable to fastener per se and independent of connection assembled with fastener; based on lower fifth-percentile exclusion limit of maximum shear-resistance values

APPENDIX C

Symbols

A = 0.016 (28 - MC)

CL = staple-crown length, in in. (mm), the distance between the staple legs

F = number of thread grooves along fastener shank

FSI = fastener shear index

FSR = fastener shear resistance, in lbf (N), per shear plane; based on mean load at connection deformation of 0.015 in. (0.38 mm); applicable to connections within the range $0.20 \leq T/P \leq 1.90$

FWI = fastener withdrawal index

FWR = fastener withdrawal resistance, in lbf (N); based on mean maximum test value

G = oven-dry specific gravity of wood members; published mean value for member with lowest specific gravity (see Table 8.1A of NDS)

GD = oven-dry specific gravity of fastened wood member; published mean value (see Table 8.1A of NDS)

GS = oven-dry specific gravity of fastening wood member; published mean value (see Table 8.1A of NDS)

H = number of helixes along thread length; that is, number of points, along thread length, at intersections of thread crests and parallel to nail-shank axis; arrived at by (a) measuring the thread length, in in. (mm), (b) observing the number of helixes per inch (25.4 mm) (by dividing the number of helixes with their observed overall distance, in in. (mm), along the parallel to the nail-shank axis), and (c) multiplying the number of helixes per inch (25.4 mm) with the thread length, in in. (mm). Also, thread length (TL) divided by thread lead (TE), with TE = 3.14 WD times tangent of thread angle (TA); or H = TL/(3.14 x WD x tan TA)

NOTE - The calculation of the number of helixes is a convenient step in determining the area of the helical thread in contact with the wood penetrated by the nail. The formula is based on the assumption that the mean of the thread-crest and thread-root diameters approximates the shank diameter of the nail. The formula is valid for the numbers of helixes penetrating the fastening member. If the depth of shank penetration into the fastening member is shorter than the thread length, multiply the number of helixes by the ratio of the depth of penetration of the helical portion of the nail shank and the thread length. This is necessary in order to obtain the number of helixes applicable for the calculation of the contact area of the helical portion of the nail shank with the wood surrounding it.

HD = nail-head diameter, in in. (mm)

HPR = head/crown pull-through resistance factor, in lbf (N); limited by $T \leq 3/4$ in. (19 mm)

M = MIBANT angle of fastener, in deg; average value of 25 random samples

MC = moisture content of wood members during connection assembly; maximum for green wood: 28 pct; minimum for dry wood: 12 pct

P = penetration of plain-shank fastener or threaded portion of fastener shank in fastening member, in in. (mm). A depth of penetration of 10, 11, 13, and 14 shank diameters is required in the fastening member of species Groups I, II, III, and IV, respectively (as identified in Table 8.1A of NDS) for the computation of FSR of all driven fasteners.

T = thickness of fastened member, in in. (mm); limited to maximum of 3/4 in. (19 mm) for the computation of HPR

TA = thread angle, in deg, of fastener with four thread grooves, with TA = ARCTAN [F/(TD x Pi x (H/TL))] and with ARCTAN = 1/TAN

T/P = ratio of thickness of fastened member to penetration of fastener shank or legs in fastening member, limited to range $0.20 \leq T/P \leq 1.90$ when computing FSR

TD = thread-crest diameter of fastener, in in. (mm)

TL = thread length along fastener shank, in in. (mm)

WD = diameter of plain shank or plain-shank section of fastener, in in. (mm)

WT = thickness of staple leg, in in. (mm); measured parallel to crown axis

WW = width of staple leg, in in. (mm); measured perpendicular to crown axis

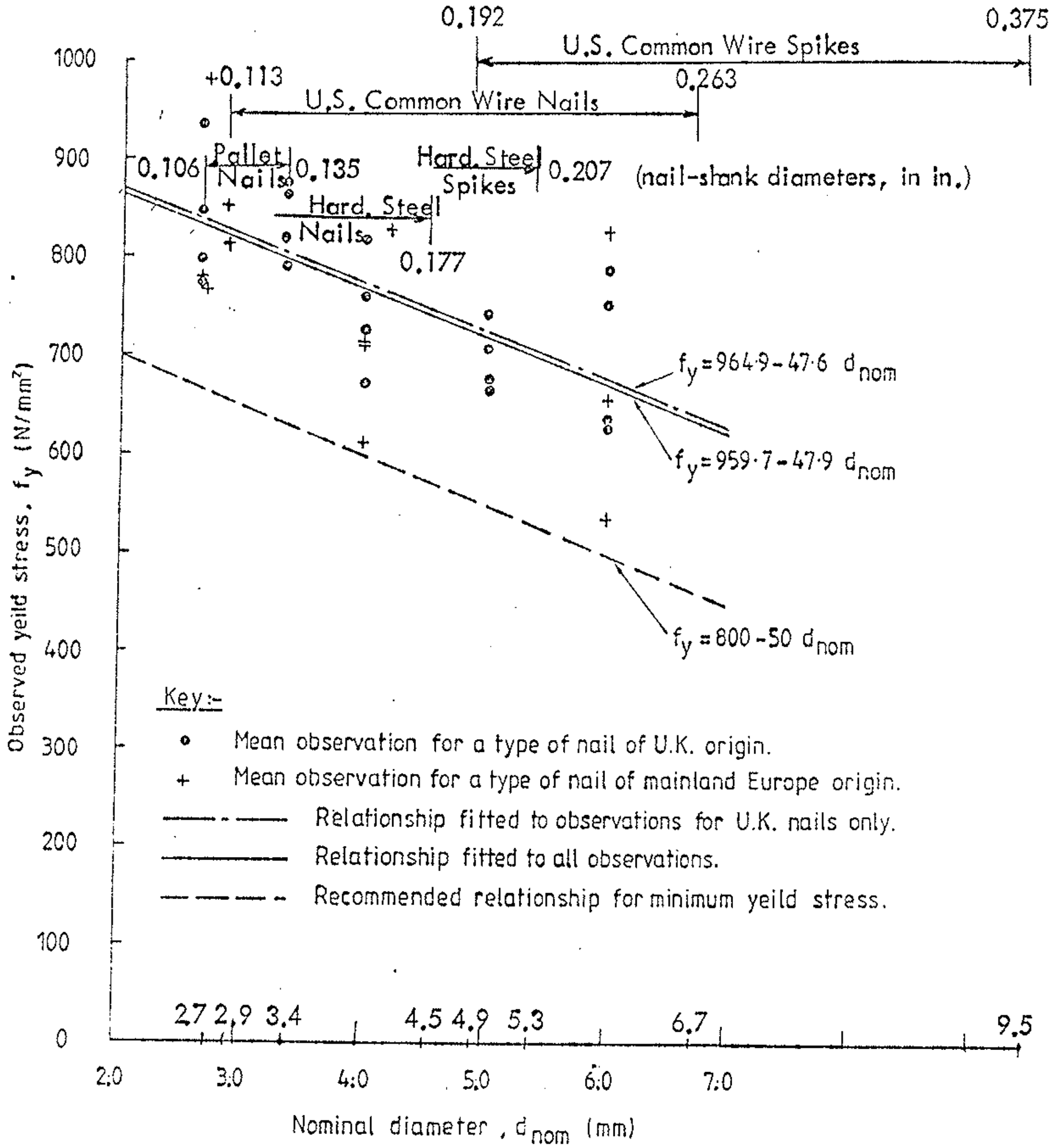

Fig. 1.- Influence of shank diameter on yield stress of regular-stock steel nails and spikes (based on Smith, Ian, and L. J. Whale. 1985. Mechanical Properties of Nails and Their Influence on Mechanical Properties of Timber Joints Subjected to Lateral Load. Part 2: Tests on Nails of Mainland Europe Origin, Comparison of Results with Those for Nails of U.K. Origin and Conclusions. Research Report 9/85. Timber Research and Development Association, Hughenden Valley, High Wycombe, Buckinghamshire, England. Confirmed by White, M.S., T. E. McLain, D. Padla, and B. Kasal. 1989. Hardness Gradient Within Roll-Threaded Steel Nails. Unpublished Report. Department of Wood Science and Forest Products, Virginia Polytechnic Institute and State University, Blacksburg, VA.)

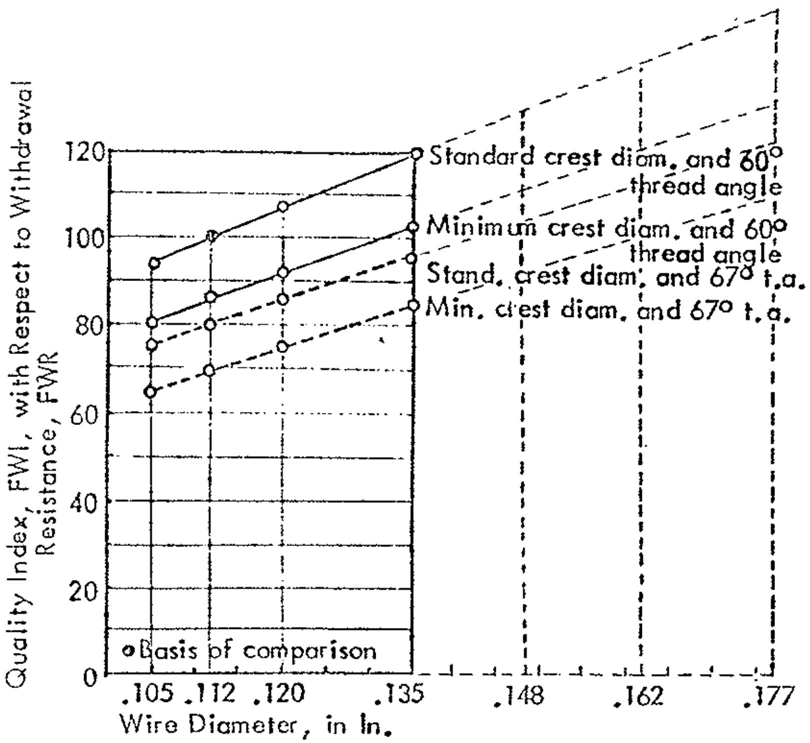

Fig. 2a.- Relationship between quality index with respect to withdrawal resistance and wire diameter, thread-crest diameter, and thread angle of standard pallet nails.

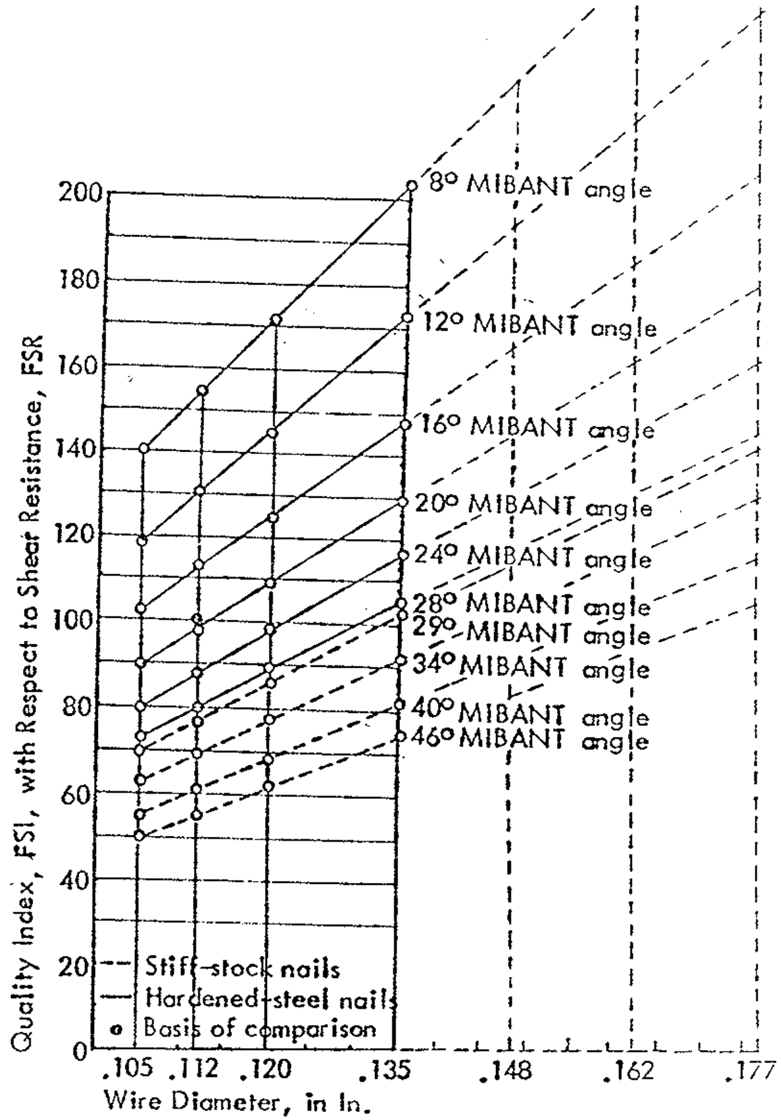

Fig. 2b.- Relationship between quality index with respect to shear resistance and wire diameter and MIBANT angle of standard pallet nails.

Fig. 2.- Relationship between fastener quality index values, FWI and FSI, and physical and mechanical properties of common steel nails (based on Stern, E. G. 1988. Variables of Pallet Nails Influence PDS-Predicted Pallet Performance, A Review of the Status of the Art. Paper presented at ISO/TC51/WG 2-3 Meeting in Berlin, Federal Republic of Germany, February 24-26, 1988. Department of Wood

Table 11

Standard, Helically Threaded, Non-Hardened and Hardened, Stiff-Stock Steel, Pallet Nails with Flat Head, Pointless or Short (Blunt) or Medium (< 5/32-In.) Diamond or Chisel Point (not wider than wire diameter), Four Thread Flutes, and 60 to 67-Deg Thread Angle, in Imperial Units (ASME MH1.7)

Code	Length In.	Shank Diam. In.	Crest Diam. Stand. In. A	Crest Diam. Min. In. B	Thread Angle Stand. Deg A	Thread Angle Max. Deg B	Head Diam. In.	Quality Index FWI with Respect to Withdrawal Resistance	Quality Index, FSI, with Respect to Shear Resistance for Given MIBANT Angle: Non-Hardened Steel Nails 29	34	40	46	Hardened Steel Nails 8	12	16	20	24	28 Deg
150x105AA	1½	0.105	0.124	--	60	--	0.25	94	70*	63*	56	50	140*	118*	102*	90*	80*	72*
AB			0.124	--	--	67	0.25	76	70*	63*	56	50	140*	118*	102*	90*	80*	72*
BA			--	0.120	60	--	0.25	81	70*	63*	56	50	140*	118*	102*	90*	80*	72*
BB			--	0.120	--	67	0.25	66	70*	63*	56	50	140*	118*	102*	90*	80*	72*
175x105AA	1¾	0.105	0.124	--	60	--	0.25	94	70	63	56	50	140*	118*	102*	90	80	72
AB			0.124	--	--	67	0.25	76	70	63	56	50	140*	118*	102*	90	80	72
BA			--	0.120	60	--	0.25	81	70	63	56	50	140*	118*	102*	90	80	72
BB			--	0.120	--	67	0.25	66	70	63	56	50	140*	118*	102*	90	80	72
175x112AA	1¾	0.112	0.132	--	60	--	0.28	100	78	70	62	55	154*	130	112	99	88	80
AB			0.132	--	--	67	0.28	80	78	70	62	55	154*	130	112	99	88	80
BA			--	0.128	60	--	0.28	87	78	70	62	55	154*	130	112	99	88	80
BB				0.128	--	67	0.28	70	78	70	62	55	154*	130	112	99	88	80
200x105AA	2	0.105	0.124	--	60	--	0.25	94	70	63	56	50	140	118	102	90	80	72
AB			0.124	--	--	67	0.25	76	70	63	56	50	140	118	102	90	80	72
BA			--	0.120	60	--	0.25	81	70	63	56	50	140	118	102	90	80	72
BB			--	0.120	--	67	0.25	66	70	63	56	50	140	118	102	90	80	72
200x112AA	2	0.112	0.132	--	60	--	0.28	100	78	70	62	55	154	130	112	99	88	80
AB			0.132	--	--	67	0.28	80	78	70	62	55	154	130	112	99	88	80
BA			--	0.128	60	--	0.28	87	78	70	62	55	154	130	112	99	88	80
BB			--	0.128	--	67	0.28	70	78	70	62	55	154	130	112	99	88	80
200x120AA	2	0.120	0.142	--	60	--	0.28	108	86	77	68	62	171	144	124	109	98	88
AB			0.142	--	--	67	0.28	87	86	77	68	62	171	144	124	109	98	88
BA			--	0.137	60	--	0.28	92	86	77	68	62	171	144	124	109	98	88
BB			--	0.137	--	67	0.28	75	86	77	68	62	171	144	124	109	98	88
225x112AA	2¼	0.112	0.132	--	60	--	0.28	100	78	70	62	55	154	130	112	99	88	80
AB			0.132	--	--	67	0.28	80	78	70	62	55	154	130	112	99	88	80
BA			--	0.128	60	--	0.28	87	78	70	62	55	154	130	112	99	88	80
BB			--	0.128	--	67	0.28	70	78	70	62	55	154	130	112	99	88	80
225x120AA	2¼	0.120	0.142	--	60	--	0.28	108	86	77	68	62	171	144	124	109	98	88
AB			0.142	--	--	67	0.28	87	86	77	68	62	171	144	124	109	98	88
BA			--	0.137	60	--	0.28	92	86	77	68	62	171	144	124	109	98	88
BB			--	0.137	--	67	0.28	75	86	77	68	62	171	144	124	109	98	88
** 250x112AA	2½	0.112	0.132	--	60	--	0.28	100**	78	70	62	55	154	130	112	99	88	80
AB			0.132	--	--	67	0.28	80	78	70	62	55	154	130	112	99	88	80
BA			--	0.128	60	--	0.28	87	78	70	62	55	154	130	112	99	88	80
BB			--	0.128	--	67	0.28	70	78	70	62	55	154	130	112	99	88	80
250x120AA	2½	0.120	0.142	--	60	--	0.28	108	86	77	68	62	171	144	124	109	98	88
AB			0.142	--	--	67	0.28	87	86	77	68	62	171	144	124	109	98	88
BA			--	0.137	60	--	0.28	92	86	77	68	62	171	144	124	109	98	88
BB			--	0.137	--	67	0.28	75	86	77	68	62	171	144	124	109	98	88
250x135AA	2½	0.135	0.159	--	60	--	0.30	120	103	92	82	73	204	172	148	130	117	105
AB			0.159	--	--	67	0.30	96	103	92	82	73	204	172	148	130	117	105
BA			--	0.154	60	--	0.30	103	103	92	82	73	204	172	148	130	117	105
BB			--	0.154	--	67	0.30	84	103	92	82	73	204	172	148	130	117	105
275x120AA	2¾	0.120	0.142	--	60	--	0.28	108	86	77	68	62	171	144	124	109	98	88
AB			0.142	--	--	67	0.28	87	86	77	68	62	171	144	124	109	98	88
BA			--	0.137	60	--	0.28	92	86	77	68	62	171	144	124	109	98	88
BB			--	0.137	--	67	0.28	75	86	77	68	62	171	144	124	109	98	88
275x135AA	2¾	0.135	0.159	--	60	--	0.30	120	103	92	82	73	204	172	148	130	117	105
AB			0.159	--	--	67	0.30	96	103	92	82	73	204	172	148	130	117	105
BA			--	0.154	60	--	0.30	103	103	92	82	73	204	172	148	130	117	105
BB			--	0.154	--	67	0.30	84	103	92	82	73	204	172	148	130	117	105
300x120AA	3	0.120	0.142	--	60	--	0.28	108	86	77	68	62	171	144	124	109	98	88
AB			0.142	--	--	67	0.28	87	86	77	68	62	171	144	124	109	98	88
BA			--	0.137	60	--	0.28	92	86	77	68	62	171	144	124	109	98	88
BB			--	0.137	--	67	0.28	75	86	77	68	62	171	144	124	109	98	88
300x135AA	3	0.135	0.159	--	60	--	0.30	120	103	92	82	73	204	172	148	130	117	105
AB			0.159	--	--	67	0.30	96	103	92	82	73	204	172	148	130	117	105
BA			--	0.154	60	--	0.30	103	103	92	82	73	204	172	148	130	117	105
BB			--	0.154	--	67	0.30	84	103	92	82	73	204	172	148	130	117	105
350x135AA	3½	0.135	0.159	--	60	--	0.30	120	103	92	82	73	204	172	148	130	117	105
AB			0.159	--	--	67	0.30	96	103	92	82	73	204	172	148	130	117	105
BA			--	0.154	60	--	0.30	103	103	92	82	73	204	172	148	130	117	105
BB			--	0.154	--	67	0.30	84	103	92	82	73	204	172	148	130	117	105

** Basis of comparison. * Values for nails not available commercially. 1 in. = 25.4 mm

Table 12

Standard, Bright and Coated, Plain-Leg, Regular-Stock Steel Staples with Two Equal-Length Flattened Legs, Short (Blunt) Chisel Points, and ½-In. Crown Width, in Imperial Units (ASME MH1.7)

Code	Length In.	Nominal Wire Diameter In.	Cross-Section Thickn. In. (Used for Determination of FWI and FSI Only)	Cross-Section Width In. (Used for Determination of FWI and FSI Only)	Finish Bright A	Finish Coated B	Quality Index (FWI) with Respect to Withdrawal Resistance Bright	Quality Index (FWI) with Respect to Withdrawal Resistance Coated	Quality Index (FSI) with Resp to Shear Resistance for Give Computed MIBANT Angle, D for Bright or Coated Fastene 85 Deg	115 Deg	150 Deg
200x062A	2	0.062	0.055	0.061	x	--	33	--	--	--	17
B					--	x	--	50	--	--	17
200x072A		0.072	0.067	0.073	x	--	39	--	--	28	--
B					--	x	--	59	--	28	--
200x080A		0.080	0.075	0.080	x	--	44	--	42	--	--
B					--	x	--	65	42	--	--
225x062A	2¼	0.062	0.055	0.061	x	--	33	--	--	--	17
B					--	x	--	50	--	--	17
225x072A		0.072	0.067	0.073	x	--	39	--	--	28	--
B					--	x	--	59	--	28	--
225x080A		0.080	0.075	0.080	x	--	44	--	42	--	--
B					--	x	--	65	42	--	--
250x072A	2½	0.072	0.067	0.073	x	--	39	--	--	28	--
B					--	x	--	59	--	28	--
250x080A		0.080	0.075	0.080	x	--	44	--	42	--	--
B					--	x	--	65	42	--	--
300x072A	3	0.072	0.067	0.073	x	--	39	--	--	28	--
B					--	x	--	59	--	28	--
300x080A		0.080	0.075	0.080	x	--	44	--	42	--	--
B					--	x	--	65	42	--	--
375x072A	3¾	0.072	0.067	0.073	x	--	39	--	--	28	--
B					--	x	--	59	--	28	--
375x080A		0.080	0.075	0.080	x	--	44	--	42	--	--
B					--	x	--	65	42	--	--

1 in. = 25.4 mm

CIB-W18/25-7-5

INTERNATIONAL COUNCIL FOR BUILDING RESEARCH STUDIES AND DOCUMENTATION

WORKING COMMISSION W18 - TIMBER STRUCTURES

35 YEARS OF EXPERIENCE WITH CERTAIN TYPES OF CONNECTORS AND CONNECTOR PLATES USED FOR THE ASSEMBLY OF WOOD STRUCTURES AND THEIR COMPONENTS

by

E G Stern
Virginia Polytechnic Institute and State University
U S A

MEETING TWENTY - FIVE

ÅHUS

SWEDEN

AUGUST 1992

35 YEARS OF EXPERIENCE WITH CERTAIN TYPES OF CONNECTORS AND CONNECTOR PLATES USED FOR THE ASSEMBLY OF WOOD STRUCTURES AND THEIR COMPONENTS

by

E. George Stern
Earle B. Norris Research Professor Emeritus of Wood Construction
Virginia Polytechnic Institute and State University
Blacksburg, VA 24063-0361

ABSTRACT

This paper describes some personal experiences of the author in the field of connectors and connector plates used for the assembly of wood structures and their components and lists as many as 225 publications covering this subject matter and published in the USA and abroad.

Certain connectors and connector plates among those described have been successfully used, or are proposed for use, for connecting members and components of lumber trusses and, particularly trussed rafters, frames, and other building components made of wood. Some of these connecting devices have also served to reinforce components of wood pallets, such as notched stringers; and connections of deckboards to stringers, stringerboards, and blocks of wood pallets; as well as anti-splitting devices for railway ties, scaffolding planks, and pallet stringer ends.

The performance has been observed over the years of five types of connections used for the assembly of trussed rafters of W-design and 9.1-m (30-ft) free span of an architectural laboratory building of the Building Construction Department of Virginia Polytechnic Institute and State University at Blacksburg, Virginia, erected 35 years ago. These trussed rafters did, and hopefully will, continue to serve their purpose for many years to come. The connectors used include lumber and plywood gusset plates nailed or nail-glued to the structural members, split-ring connectors, and solid and prepunched metal connector plates. None of the trussed rafters described were assembled with the metal connector plates with integral teeth in common use today.

Prepared for Presentation at Meeting of
International Council for Building Research Studies and Documentation (CIB)
Working Commission on Timber Structures (W18A)
in Âhus, Sweden, August 24-27, 1992

35 YEARS OF EXPERIENCE WITH CERTAIN TYPES OF CONNECTORS AND CONNECTOR PLATES USED FOR THE ASSEMBLY OF WOOD STRUCTURES AND THEIR COMPONENTS

By
E. George Stern
Earle B. Norris Research Professor Emeritus of Wood Construction
Virginia Polytechnic Institute and State University, Blacksburg, VA 24063-0361 USA

Metal Connector Plates, a Subject of Worldwide Standardization

Metal connector plates, commonly called "truss plates", are, solid or prepunched plates, with or without nail holes and/or integral teeth (barbs, plugs, and prongs) projecting perpendicular from one or both plate surfaces. They are fabricated from 0.9 to 2.0-mm (0.035 to 0.080-in.; 20 to 14-gage) coiled strips of structural quality steel sheet and, for certain end uses, stainless steel. They are a product originally introduced in the USA after World War II, with their use having subsequently been spread worldwide. The many types of plates, commercially introduced by more than a dozen American plate manufacturers (see Fig. 1) and the design of trussed rafters based on the use of these plates have been subject to standardization for many years. Originally, this was the task of the Joint Industry Advisory Committee on Roof Truss Design, activated during 1961 under the chairmanship of Hugh Angleton of the National Association of Home Builders' Research Laboratory. During the same year, the Truss Plate Institute (TPI), a trade association, was established to coordinate the efforts and correlate the vast amount of research of the major fabricators of connector plates. Considerable technical assistance was provided to this industry for many years by the University of Illinois' Small Homes Council - Building Research Council under the leadership of Don. H. Percival and Stan K. Suddarth.

In addition to industry standards, as promulgated by TPI, American voluntary consensus standards covering metal connector plates were developed by the American Society for Testing and Materials (ASTM) and its Committee E06 on Performance of Building Constructions. These standards are under the jurisdiction of Subcommittee E06.13 on Performance of Connections in Building Constructions, with the author as its chairman since its inception some 25 years ago. ASTM standard test methods for tensile and shear strength properties of metal connector plates are covered in E489 and E767, respectively. A test method on the performance of metal connector plates in connections of wood members is covered in ASTM Standard D1761 on Testing Mechanical Fasteners in Wood. This standard is under the jurisdiction of ASTM Committee D07 on Wood and its Subcommittee D07.05.02 on Wood Connections.

The Rule of Assessment of Punched Metal Plate Timber Fasteners was published by the European Union of Agrement (EUA) in M.O.A.T. No. 16, during 1979. The International Standards Organization (ISO) published, during 1990, ISO 8969 on Timber Structures -- Testing of Unilateral Punched Metal Plate Fasteners and Joints. A Working Group of the Technical Committee of the European Standards Organization, CEN/TC124/WG1, is preparing at this time a European test standard for connectors with integral nail plates. In addition, the International Council for Building Research Studies and Documentation (CIB) established CIB/W18A/TC6 on Assessment of Punched Metal Plate Timber Fasteners. Its partial scope reads as follows:

> "to identify significant problems and establish requirements, including the need for specific information, to serve as a basis for the establishment and promulgation of an appropriate up-to-date ISO test standard which leads to reliable test data, making it feasible to evaluate them properly and to design appropriately connections of timber (lumber) components and assemblies fabricated with metal connector plates (truss plates) with or without integral teeth."

Major voluntary consensus standards covering metal connector plates are listed in Appendix A. Additional American Standards promulgated by TPI are listed in Appendix B.

Metal connector plates are, according to ASTM E489, manufactured from coiled strips of structural quality sheet metal with or without integral plate projections or nail holes, or a combination of both. The projections are sheared from the solid plate. They project from the plate in a single direction or both directions perpendicular to the plate-surface area. Common plate thicknesses (gages), are given in Table 1.

Table 1. - Common thicknesses of metal connector plates.

Mm	In.	Washburn & Moen Steel Gage	ASTM Standard A 525 (Table 17) for Galvanized Sheet Steel, In.
0.9	0.035	20	0.0396
1.0	0.041	19	0.0456
1.2	0.047	18	0.0516
1.4	0.054	17	0.0575
1.6	0.063	16	0.0635
1.8	0.072	15	0.0710
2.0	0.080	14	0.0785

Metal connector plates are produced in various sizes, that is lengths and widths, and designed to connect wood members and to transmit forces from one wood member (or section) to another member (or section).

Types of Metal Connector Plates

The various types of metal connector plates promulgated for use during the past 3-1/2 decades (Fig. 1) include solid plates; prepunched plates with nail holes located at specified locations in given patterns (Fig. 2) and with nail holes reinforced with concentric dimples with or without pointed, moon-shaped, or ring-shaped projections (Fig. 3); prepunched with a single triangular barb per plate hole (Fig. 4), multiple (four) barbs per plate hole (Fig. 5), and two barbs per plate hole and additional nail holes as well as reinforcing plate corrugations (Fig. 6); prepunched with four barbs per plate hole projecting in both directions perpendicular to the plate area (Fig. 7); prepunched with a single tooth per plate hole (Fig. 8), with two teeth per plate hole (Fig. 9), and three teeth per plate hole (Fig. 10).

A combination prepunched metal connector plate is the proposed Finnish plate with two projecting teeth per nail hole and a row of peripheral teeth (Fig. 11). A so-called hybrid metal connector plate has one section with projecting teeth to be machine-pressed into the wood member and another section with nail holes for field-nailing a pre-assembled building component to another one, as in the case of field-assembled multi-section trusses (Fig. 12). A special plate with integral teeth, consisting of two parts which can be rotated around a connecting grommet (Fig. 13), allows angular adjustment of connected members of folded or fully assembled trussed rafters. It can be used with or without a load-transferring bolt penetrating the grommet in a pinned connection.

Some of these metal connector plates are no longer commercially produced; while some others are in the development stage.

Typical uses of metal connector plates are for the connections of members of trussed rafters, such as in heel connections (Fig. 14) and ridge connections (Fig. 15). Metal connector plates with barbs projecting into both directions from the plate area (Fig. 7) are used when the plates are placed between the wood members and the barbs pressed into the faces of adjacent members (Fig. 16).

Long-Time Performance of Metal Connector Plates

The performance of trussed rafters made of lumber members and assembled with five types of connecting means, commercially used during the middle of this century, was observed and recorded at Virginia Polytechnic Institute and State University (VPI&SU) for a period of almost 35 years. These trussed rafters were used for the roof structure of a student-built, wind and weather-exposed laboratory of the University's Building Construction Department. This laboratory was built under the guidance of the late Professor William L. Favrao. The observations were made by the staff of the University's Wood Research and Wood Construction Laboratory (WR&WCL) in cooperation with the industries involved. The 21 trussed rafters of W-design (Fig. 17) of 9.1-m

(30-ft) free span and 3 in 12 roof slope were spaced 0.61-m (2-ft) on centers. They were designed to carry a roof load of 1675 Pa (35 psf).

The five means of connecting the lumber members are listed below:

(1) All-nailed connections designed and assembled by the staff of the University's WR&WCL, with the lumber gusset and splice plates fastened to the members with 82-mm (3-1/4-in.), helically threaded, hardened-steel nails, a product of the Independent Nail and Packing Company of Bridgewater, MA. All nails were driven from one side of the trussed rafter and loaded in double shear.

(2) Split-ring connections designed by the Timber Engineering Company of Washington, DC, and student-assembled with TECO's Wedge-Fit split rings of 64-mm (2-1/2-in.) diameter.

(3) H-BRACE connections designed by the H-Brace Company of West Palm Beach, FL, and assembled by the James River Lumber Company of Richmond, VA. The connectors were one-piece, 1.0-mm (19-gage), prepunched, steel plates bent to form an H between the members and fastened with 38-mm (1-1/2-in.), helically threaded, hardened-steel nails driven through both prepunched side plates of the connector.

(4) TIM-PLATE connections designed and assembled by Timber Fabrications of Perry, FL, using 0.9-mm (20-gage), solid, galvanized-steel plates inserted into two symmetrically spaced saw kerfs at each member end. The shear loads were transmitted by 38-mm (1-1/2-in.), helically threaded, hardened-steel nails driven through the lumber members and inserted solid steel plates. All nails were driven from one side of the trussed rafter and transmitted load in double shear.

(5) Nail-glued connections designed by the Small Homes Council of the University of Illinois and assembled by Lester Brothers of Martinsville, VA. The connections were made with exterior-type Douglas-fir plywood nail-glued to the members.

Trussed rafters assembled with the five types of connections are no longer commercially produced mainly for economic reasons, since metal connector plates with integral teeth projecting from the plates took the place of the formerly popular means of connecting the lumber members of commercially produced trussed rafters. Nonetheless, the observed performance of the installed trussed rafters provides valuable comparative information.

The performance of the trussed rafters was observed by measuring their deflection at midspan before, during, and after their installation, at appropriate times up to almost 35 years after their assembly. The individual test data for the quadruple trussed rafters were averaged and the average test values were plotted (Fig. 18).

The following observations were made:

(1) The moisture content of the southern pine 2x6s of the trussed rafters, almost 35 years after their installation, was approximately 8%, when the temperature was 46° F, with a low of 36° F and a high of 54° F during the day when the deflection readings were taken.

(2) The average midspan deflections, in in., of the lower chord of the five types of trussed rafters were observed and are presented in Table 2.

Table 2. - Average mid-span deflections, in in., of the lower chord of five types of trussed rafters of 9.1-m (30-ft) free span.

Connections	After Installation	After 1/2 yr	After 3/4 yr	After 1 yr	After 2 yr	After 3-½ yr	After 4-¾ yr	After 6 yr	After 34 yr
All-nailed	0.53	0.76	0.84	0.88	0.86	0.97	0.95	0.98	1.00
Split-ring	0.58	0.77	0.83	0.78	0.74	0.83	0.78	0.76	0.76
H-BRACE	0.75	0.86	0.80	0.83	0.80	0.89	0.85	0.86	1.00
TIM-PLATE	0.78	0.80	0.76	0.82	0.86	0.88	0.93	1.07	0.80
Nail-glued	0.90	0.95	0.95	0.93	1.10	1.16	1.15	1.18	1.38*

* Two of the four trussed rafters deflected as much as 1.65 and 1.68 in., while the other two deflected only 1.05 and 1.14 in.

(3) While most of the trussed rafters performed satisfactorily, with their average mid-span deflections not exceeding 25 mm (1 in.) 34 years after their installation, two of the four nail-glued trussed rafters, located next to the building gable, had deflected more than 38 mm (1-1/2 in.) at that time. The relatively large deflection may be attributable to the deterioration of the bond between glue line and lumber surface and mold formation along the glue line, as observed 3-1/2 years after trussed rafter installation (Fig. 19).

In the light of the observations made, four of the five, if not all five, types of trussed rafters can be expected to fulfill their anticipated purpose. The nail-glued trussed rafters call for continued observation especially after any exposure to full, and possibly excessive, design loading, if such loading should occur.

Metal Connector Plate Improvements

Recent research in the field of metal connector plates covers the use of improved plates with integral teeth projecting in both directions (Fig. 7), with triple teeth per plate hole (Fig. 10), and with peripheral teeth (Fig. 11). Additionally, the performance is studied, at the U.S. Forest Products Laboratory, of metal connector plates in lumber connections under a variety of field conditions by using not only standard test procedures to derive connection model parameters for a variety of plate configurations, wood species, and treatments; but also nonstandard tests to evaluate connections subject to combined bending and tension forces, high temperature exposure, various load durations, and moisture cycling. Tests are also under way, at VPI&SU, on the potential improvement in performance of pallet stringers as a result of their reinforcement with metal connector plates.

Literature Survey

Research papers and publications covering metal connector plates and their use are listed in Appendix B.

Summary

This limited survey of the status of the art and the published literature provides an overview of the some of the activities undertaken during the past 3-1/2 decades. It does not cover the vast amount of research and development work undertaken by the industries involved, as represented by the Truss Plate Institute.

APPENDIX A: RELATED STANDARDS

International Standards Organization, Geneva, Switzerland (ISO):

ISO 6891 (1983) Timber Structures - Joints made with mechanical fasteners - General principles for the determination of strength and deformation characteristics.

ISO 8969 (1990) Timber Structures - Testing of unilateral punched metal plate fasteners and joints.

ISO/TC165 N118 (1987) Timber Structures - Testing of punched metal plate fasteners.

ISO R86 (Tensile testing of steel sheet and strip.

ISO R87 (Adhesion of coating)

European Standards Organization,

prEN 26-891 (1990) Timber Structures - Joints made with mechanical fasteners - General principles for the determination of strength and deformation characteristics.

European Union of Agrement, Paris, France (UEAtc):

M.O.A.T. No. 16 (1979) Rule for the assessment of punched metal plate timber fasteners.

International Union for Testing and Research Laboratories for Materials and Structures, Paris, France (RILEM):

RILEM/CIB 3TT (1981) Testing methods for joints with mechanical fasteners in load-bearing timber structures, Annex A: Punched metal plate fasteners, pp. 307-317.

American Society for Testing and Materials, Philadelphia, PA, USA (ASTM):

ASTM A446 Specification for steel sheet, zinc-coated (galvanized) by the hot-dip process, structural (physical) quality.

ASTM E 489 Test method for tensile strength properties of steel truss plates (metal connector plates).

ASTM E 767 Test method for shear resistance of steel truss plates (metal connector plates).

APPENDIX B: RELATED LITERATURE

Aasheim, E. 1989. NTI og spikerplater - en sammensatt historie, NTI's 40-ars-jubileum, Sundevolden. Norwegian Institute of Wood Technology, Blindern, Norway.

Aasheim, E. 1991. Design of trusses. Proceedings of 1991 International Timber Engineering Conference in London, England, pp. 1.89-1.96.

Aasheim, E., and Solli, K.H. 1980. Proposal for design code for nail plates. Proceedings of Meeting of International Council for Building Research Studies and Documentation Working Commission W18A on Timber Structures in Lisbon, Portugal, 23-7-1.

American Society for Testing and Materials. 1985. Standard methods of testing mechanical fasteners in wood. ASTM D1761. ASTM, Philadelphia, PA.

Aplin, E.N. 1973. Factors affecting the stiffness and strength of metal plate connector joints. Eastern Forest Products Laboratory, Ottawa, Canada, Information Report OP-X-57.

Arbek, T. 1979. The effect of time on the strength of truss plate joints. Department of Civil Engineering, Carleton University.

Aune, P. 1970. Investigations on strength and stiffness of joints made with hydro-nail truss plates. Acta Polytechnica Scandinavica Ci 67, Technical University of Norway, Trondheim, Norway.

Batchelar, M.L., and A.D. Hunt. 1991. Composite plywood and steel gussett plates for moment resisting joints in timber frames. Proceedings of 1991 International Timber Engineering Conference in London, England, pp. 3.104-3.110.

Beineke, L.A., and S.K. Suddarth. 1979. Modeling joints made with light-gage connector plates. Forest Products Journal 29(8):39-45.

Blumer, H., and M. Masney. 1991. New production technology - a challenge for structural and aesthetic timber construction. Proceedings of International Timber Engineering Conference in London, England, 4.437-4.444.

Bohnhoff, D.R., and R.W. Wolfe. 1991. Shear transfer plates: Evaluation and uses. Presented at 1991 International Winter Meeting of American Society of Agricultural Engineers in Chicago, Illinois, Paper 194540.

Bohnhoff, D.R., R. C. Moody, S.P. Verrill, and L.F. Shirek. 1991. Bending properties of reinforced and unreinforced spliced nail-laminaed posts. USDA Forest Service, Forest Products Laboratory, Madison, Wisconsin, Research Paper FPL-RP-503

Bohnhoff, D.R., R.C. Moody, and G.D. Williams. 1991. Tensile strength and stiffness of spliced mechanically laminated posts. Presented at 1991 International Winter Meeting of American Society of Agricultural Engineers in Chicago, Illinois, Paper 914527.

Bohnhoff, D.R., R.W. Wolfe, and R.A. Gardner. 1991. Stiffness and strength properties of shear transfer plate connections. Unpublished Report.

Borgin, K.B., G.F. Loedolff, and G.R. Saunders. 1968. Laminated wood beams, reinforced with steel strips. Journal of the Structural Division of the American Society of Civil Engineers, 94(St 7), 1681-1705.

Boult, B.F. 1988. Multi-nailed moment resisting joints. Proceedings of International Timber Engineering Conference in Seattle, Washington, 2:329-335.

Bovim, N.I., and E. Aasheim. 1985. The strength of nail plates. Proceedings of Meeting of International Council for Building Research Studies and Documentation Working Commission W18A on Timber Structures in Beit Oren, Israel, 18-7-6.

Brynildsen, O.A. 1976. Structural models for trussed rafters. Proceedings of Meeting of International Union of Forestry Research Organizations in Munich, Germany.

Brynildsen, O.A., and A. Aas. 1974. Trussed rafters. Norwegian Institute of Wood Technology, Blindern, Norway, Report 50.

Brynildsen, O.A., and N.I. Bovim. 1976. Mechanical timber connectors. Norwegian Institute of Wood Technology, Blindern, Norway, Report 24.

Buchanan, A.H. 1984. Strength model and design method for bending and axial load interaction in timber members. University of British Columbia, Vancouver, British Columbia, Canada.

Buchanan, A.H. 1991. Multi-story timber buildings in New Zealand (Fig. 7, Anchorage detail). Proceedings of International Timber Engineering Conference in London, England, 2.68-2.76.

Buchanan, A.H., R. Chinniah, and P.J. Moss. 1989. Behaviour of nailed gusset connections under simulated fire exposure. Proceedings of Second Pacific Timber Engineering Conference in Auckland, New Zealand, 2:125-129.

Bulleit, W.M., and L.J. Yates. 1988. Stochastic finite element analysis of metal plate connected wood trusses. Proceedings of International Timber Engineering Conference in Seattle, Washington, 1:125-131

Bulleit, W.M., and L.J. Yates. 1989. Stochastic behavior of metal plate connected wood trusses. Proceedings of Second Pacific Timber Engineering Conference in Auckland, New Zealand, 2:89-94.

Byerly, M.S., F.E. Woeste, and A.L. DeBonis. 1982. Nail laminated posts with metal plated joints. Transactions of American Society of Agricultural Engineers.

Canfield, L.R., S.H. Niu and H. Liu. 1991. Uplift resistance of various rafter-wall connections. Forest Products Journal 41(7/8):27-34.

Canadian Standards Association. 1980. Methods of test for evaluation of truss plate used in lumber joints. CSA Standard S347-M1980. Canadian Standards Association, Rexdale, Ontario, Canada.

Carling, O. 1990. Strain rate in nailed connection between steel sheeting and timber when it is loaded in shear and subjected to temperatures above 300°C. Department of Building Materials, Royal Institute of Technology. Stockholm, Sweden, Report TRITA-BYMA 1990-2.

Carling, O. 1991. Fire behaviour of metal connectors in wood structures. Proceedings of International Timber Engineering Conference in London, England, 4.106-4.113.

Carlson, D.O. 1981. Automation in housing and systems building news illustrated/commercial dictionary of industrialized/manufactured housing. Automation in Housing & Systems Building.

Cidras, J.M., V.K. Kumar, and E.G. Stern. 1971. Mass-produced foundations for mass-produced houses. Virginia Polytechnic Institute and State University, Wood Research and Wood Construction Laboratory, Bulletin 103.

Cramer, M.S., R.W. Wolfe, and A. Peyrot. 1988. Modelling roof systems for reliability analysis. Proceedings of International Timber Engineering Conference in Seattle, Washington, 1:143-150.

Crovella, P.L., and K.G. Gebremedhin. 1990. Analysis of light frame wood truss tension joint stiffness. Forest Products Journal 40(4):41-47.

Davis, J., and F. Woeste. 1989. Five laminated post designs compared. Rural Builders 1989(5):58, 60.

Dudley, H.T. 1966. Determination of net section properties of metal truss plates. Forest Products Journal 16(5).

Edlund, G. 1971. Splicing of timber joints with nail plates. Swedish Institute for Building Research, Stockholm, Sweden, Report R40.

Edlund, G. 1973. Nail plates as connectors in trusses. Swedish Institute for Building Research, Stockholm, Sweden, Report R52.

Edlund, G. 1974. Example of dimensioning structures assembled with nail plates. Swedish Institute for Building Research, Stockholm, Sweden, Report B, 296 TT B:54.

Egerup, A. 1975. Theoretical and experimental determination of stiffness and the ultimate load of timber trusses. Technical University of Denmark, Hellerup, Denmark.

Egerup, A.R. 1979. European practice and future development in the design of metal plate connected wood trusses. Proceedings of FPRS Conference on Metal Plate Wood Truss in St. Louis, Missouri. Forest Products Research Society, Madison, Wisconsin, pp 117-122.

Egerup, A.R. 1979. Design of metal plate connected wood trusses. Proceedings of Meeting of International Council for Building Research Studies and Documentation Working Committee W18A on Timber Structures in Vienna, Austria, 11-14-1.

Egerup, A.R. 1979. Truss design method for CIB Timber Code. Proceedings of Meeting of International Council for Building Research Studies and Documentation Working Committee W18A on Timber Structures in Otaniemi, Finland, 13-14-1.

Egerup, A. 1987. Practical design methods for trussed rafters. Proceedings of Meeting of International Council for Building Research Studies and Documentation Working Committee W18A on Timber Structures in Dublin, Ireland, 20-14-3.

Ehlbeck, J., and R. Gorlacher. 1984. Shear connections with nail plates. Bauen mit Holz 9:587-591.

Emanuel, J.H., D.B. Brakeman, and C.M. Newhouse. 1988. Investigation of metal-plate connected, double 4X2 beams. Proceedings of International Timber Engineering Conference in Seattle, Washington, 2:163-169.

Feldborg, T., and M. Johansen. 1981. Wood trussed rafters design, strength and stiffness tests on joints under short-term loading. Deflection of W-trussed rafters under long-term loading. Danish Building Research Institute, Hoersholm, Denmark.

Feldborg, T., and M. Johansen. 1981. Wood trussed rafter design. Proceedings of Meeting of International Council for Building Research Studies and Documentation Working Committee W18A on Timber Structures in Warsaw, Poland, 14-14-1.

Forest Products Research Society. 1979. Metal plate wood truss conference, Proceedings of Conference in St. Louis, Missouri. Forest Products Research Society, Madison, Wisconsin.

Foschi, R.O. 1977. Analysis of wood diaphragms and trusses, Part II: Truss plate connections. Canadian Journal of Civil Engineering 4(3):353-362.

Foschi, R.O. 1979. Truss plate modeling in the analysis of trusses. Proceedings of FPRS Conference on Metal Plate Wood Truss in St. Louis, Missouri. Forest Products Research Society, Madison, Wisconsin, pp 88-97. Also, 1981. Proceedings of Meeting of International Council for Building Research Studies and Documentation Working Commission W18A on Timber Structures in Warsaw, Poland, 14-14-2.

Gang-Nail Systems. 1990. The Trussed Rafter Manual. Aldershot, Hants, England.

Gebremedhin, K.G., and P.L. Crovella. 1991. Load distribution in metal plate connectors of tension joints in wood trusses. Transactions of American Society of Agricultural Engineers 34(1):281-287.

Granholm, H. 1949. On composite beams and columns with particular regard of nailed timber structures. Transactions of Chalmers Institute of Technology 88, 16-17.

Groom, L.H. 1990. Effect of adhesive applied to the tooth-wood interface on metal-plate connections located in tension. Forest Products Journal 41(4):33-35.

Gupta, R. 1990. Reliability analysis of semirigidly connected metal plate residential wood trusses. Ph.D. Dissertation, Cornell University, Ithaca, New York.

Gupta, R., and K.G. Gebremedhin. 1988. Strength and stiffness of metal plate connected tension splice wood truss joints. American Society of Agricultural Engineers 88-4008.

Gupta, R., and K.G. Gebremedhin. 1988. Experimental investigation to determine the strength of tension splice joints. Proceedings of International Conference on Timber Engineering in Seattle, Washington, 1:257-265.

Gupta, R., and K.G. Gebremedhin. 1990. Destructive testing of metal-plate connected wood truss joints. ASCE Journal of the Structural Division 116(7):1971-1982.

Gupta, R., K.G. Gebremedhin, and M.D. Grigoriu. 1991. Probabilistic characterization of strength of metal plate connected wood truss joints. (Transactions of American Society of Agricultural Engineers).

Hansen, F.T., and N.L. Mortensen. 1991. Full-scale testing of pre-fabricated timber frames subjected to dynamic load. Proceedings of International Timber Engineering Conference in London, England, 3.97-3.103.

Hartl, H., D.S. Hoppe, V. Sedlak, and G. Kattinger. 1991. Timber structures with stressed membranes. Proceeding of International Timber Engineering Conference in London, England, 2.46-2.49.

Hayashi, T., H. Sasaki, and M. Masuda. 1980. Fatigue properties of wood butt joints with metal plate connectors. Forest Products Journal 30(2):49-54.

Heard, L.R., S.G. Winistorfer, and O.A. Grossthanner. 1988. Analysis of metal plate connected high capacity tension splices for wood trusses. Proceedings of International Conference on Timber Engineering, Seattle, Washington, 2:149-162.

Hirashima, Y., and F. Kamiya. 1991. Testing method and determination of basic working loads for timber joints with mechanical fasteners. Proceedings of Meeting of International Council of Building Research Studies and Documentation Working Commission W18A on Timber Structures in Oxford, England, 24-7-2.

Hoyle, R.J., Jr. 1975. Steel-reinforced wood beam design, Forest Products Journal 25(4):17-23.

Hunt, R.D., and A.H. Bryant. 1988. Moment resisting nail plate joints, Recent developments at Auckland University. Proceedings of International Timber Engineering Conference in Seattle, Washington, 1:251-256.

International Council for Building Research Studies and Documentation Working Commission W18A on Timber Structures. 1990. Proceedings of 23rd Meeting in Lisbon, Portugal.

International Truss Plate Association. 1990. ITPA Technical Handbook. Rowlands Castle, Hampshire, England.

Kaellsner, B. 1980. Design of joints with nail plates -- the heel joint. Proceedings of Meeting of International Council for Building Research Studies and Documentation Working Commission W18A on Timber Structures in Otaniemi, Finland, 13-7-5.

Kaellsner, B. 1981. The effect of support eccentricity on the design of W and WW trusses with nail plate connectors. Proceedings of Meeting of International Council for Building Research Studies and Documentation Working Commission W18A on Timber Structures in Warsaw, Poland. 14-7-5.

Kaellsner, B., and Y. Kangas. 1991. Theoretical and experimental tension and shear capacity of nail plate connections. Proceedings of Meeting of International Council for Building Research Studies and Documentation Working Commission W18A on Timber Structures in Oxford, England, 24-7-1.

Kangas, J. 1985. Principles for design values of nailplates in Finland. Proceedings of Meetings of International Council for Building Research Studies and Documentation Working Commission W18A on Timber Structures in Beit Oren, Israel, 18-7-5.

Kangas, J. 1985. A detailed testing method for nail plate joints. Proceedings of Meeting of International Council for Building Research Studies and Documentation Working Commission W18A on Timber Structures in Beit Oren, Israel, 18-7-6.

Kangas, J. 1991. Anchorage capacity of nail plate. Proceeding of Meeting of International Council for Building Research Studies and Documentation Working Commission W18A on Timber Structures in Oxford, England, 24-7-3.

Karlsson, P. 1980. Effect of moisture variation on strength and stiffness of nail-plate joint. Tampere University of Technology, Tampere, Finland.

Kauranen, P. 1979. Study of stiffness of nail-plate joint. Tampere University of Technology. Diplomityo. Tampere, Finland.

Keenan, F.J. 1978. Design of truss plate joints. Proceedings of Meeting of International Council for Building Research Studies and Documentation Working Commission W18A on Timber Structures in Perth, Scotland, 9-7-1.

Keenan, F.J., et al. 1983. Strength interactions of finger joints and truss plate joints in light wood trusses. Canadian Journal of Civil Engineering 10:466-480.

Keenan, F.J., et al. 1985. Behavior of truss plate and metal web joints in machine-stress-rated lumber trusses. Canadian Journal of Civil Engineering 12:700-716.

Kevarinmaki, A. 1991. Mechanical behaviour of nail plate joint - Part I: Mechanical behaviour of tooth. Helsinki University of Technology, Espoo, Finland.

Kevarinmaki, A. 1991. Capacity of support areas reinforced with nail plates in trussed rafters. Proceedings of Meeting of International Council for Building Research Studies and Documentation Working Commission W18A on Timber Structures in Oxford, England, 24-14-1.

King, C.G., and D.L. Wheat. 1988. Deflection and member behavior of metal-plate-connected parallel-chord wood trusses. Proceedings of International Timber Engineering Conference in Seattle, Washington, 1:482-487.

Kirk, L.S., T.E. McLain, and F.E. Woeste. 1989. Effect of gap size on performance of metal-plated joints in compression. Wood and Fiber Science 21(3):274-288.

Klein, Gary. 19--. Effect of partial embedment on the strength of plate-connected joints. Presentation to Truss Plate Institute Technical Advisory Committee.

Kocher, L. 1986. An experimental investigation of buckling in the unsupported regions of metal connector plates as used in parallel-chord wood truss joints. M.S. Thesis, Marquette University.

Kohei, K. 1989. Behaviour of nailed timber joints and steel side plates. Proceedings of Second Pacific Timber Engineering Conference in Auckland, New Zealand, 2:38-88.

Komatsu, K. 1989. Behavior of nailed timber joints and steel side plates. Proceedings of Second Pacific Timber Engineering Conference in Auckland, New Zealand, 2:89-94.

Komatsu, K., N. Kawamoto, K. Harle, and M. Narada. 1991. Modified glulam moment-resisting joints. Proceedings of International Timber Engineering Conference in London, England, 3.111-3.118.

Kumar, V.K. 1972. Industrialized foundations for low-rise light-weight buildings. Virginia Polytechnic Institute and State University, Wood Research and Wood Construction Laboratory, Bulletin 109.

Kumar, V.K., E.G. Stern, and T. Szabo. 1972. Build-up and composite beams. Virginia Polytechnic Institute and State University, Wood Research and Wood Construction Laboratory, Bulletin 110.

Laasonen, M. 1986. Moments and deflections of trussed rafters. Tampere University of Technology. Diplomityo. Tampere, Finland.

Laasonen, M., and M. Leivo. 1988. Trussed rafters. Valtion teknillinen tutkimuskeskus. Technical Research Centre of Finland, Espoo, Finland, Report 842.

Laidlaw, R.A., and R.N. Cox. 1983. The effect of preservatives on the corrosion of galvanized metal plate fasteners in timber. Part I: Effect on joint strength and the significance for trussed rafter roofs. The International Journal of Wood Preservation 3(2):51-60.

Lam, F., and E. Varoglu. 1988. Effect of truss plate placement and sizing on the short-term reliability of trusses. Proceedings of International Timber Engineering Conference in Seattle, Washington, 1:340-344.

Lau, P.W.C. 1977. The effect of specific gravity of wood on the strength of truss plate joints. B.S. Thesis, University of Toronto.

Lau, P.W.C. 1987. Factors affecting the behavior and modeling of toothed metal-plate joints. Canadian Journal of Civil Engineering 14(2):183-195.

Leivo, M. 1983. Test loading of nail plate trusses. Tampere University of Technology. Diplomityo. Tampere, Finland

Leivo, M. 1986. Effect of duration of load and environment on deflection of trussed rafters. Tampere University of Technology. Lisensiaatintyo. Tampere, Finland.

Leivo, M. 1991. On the stiffness changes in nail plate trusses. Technical Research Centre of Finland, Espoo, Finland, Publication No. 80.

Lhuede, E.P. 1990. A reappraisal of nailed timber joints. Proceedings of Second National Structural Engineering Conference of Institution of Australian Engineers in Adelaide, Australia, 361-365.

Lhuede, E.P., and H.O. Breitinger. 1989. Load capacities of punched nail plates in wood with defects. Proceedings of Second Pacific Timber Engineering Conference in Auckland, New Zealand, 2:83-88.

Lindal, S.W. 1971. Prestressed vertically laminated beam of wood. U.S. Patent No. 3,605,360.

Lowe, P.G., and M.R. Edwards. 1984. Aspects of ductility in nailed timber connections. Proceedings of First Pacific Timber Engineering Conference in Auckland, New Zealand, 2:622-626 Paper 227.

Maraghechi, K., and R.Y Itani. 1984. Influence of truss plate connectors on the analysis of light frame structures. Wood and Fiber Science 16(3):306-322.

Masse, D.I., and J. Salinas. 1988. Analysis of timber trusses using semi-rigid joints. Canadian Journal of Agricultural Engineering 30(1):111-124.

McAlister, R.H. 1986. Performance of truss plate joints in structural flakeboard and southern pine dimension lumber. Forest Products Journal 36(3):41-43.

McAlister, R.H. 1989. Interaction between truss plate design and type of truss framing. Forest Products Journal 39(7/8):17-24.

McAlister, R.H. 1990. Tensile loading characteristics of truss plate joints after weathering and accelerated aging. Forest Products Journal 40(2):9-15.

McAlister, W.R. 19--. Experiences with truss plates. Proceedings of Building Research Institute Conference in Washington, DC.

McAlister, W.R. and T.D. Foust. 1989. Load/deflection parameters for metal-plate connectors in yellow-poplar and sweetgum structural lumber. Forest Products Journal 42(3):60-64.

McAlpine, W.R., and O.A. Grossthanner. 1979. Proposed design methods for three typical truss details. Proceedings of FPRS Conference on Metal Plate Wood Truss in St. Louis, Missouri. Forest Products Research Society, Madison, Wisconsin. , 227-231.

McCarthy, M., and R.W. Wolfe. 1987. Assessment of truss plate performance model applied to southern pine truss joints. USDA Forest Service, Forest Products Laboratory, Madison, Wisconsin, Res. Pap. FPL-RP-483.

McKenna, J.P., and L.A. Smith. 19--. Evaluation of laminated veneer lumber joined with metal plate connectors.

McLain, T.E. 1983. Mechanical fastening of structural wood members - design and research status. Proceedings of Workshop on Structural Wood Research in Milwaukee, Wisconsin, 33-70.

McLain, T.E. 1986. Resistance distribution of connections. Symposium on Reliability Based Wood Design. Purdue University.

McMartin, K.C., A.T. Quaile, and F.J. Keenan. 1984. Strength and structural safety of long-span light wood roof trusses. Canadian Journal of Civil Engineering 11:978-992.

Meeks, J.E. 1979. Industrial profile of the metal-plate connected wood truss industry. Proceedings of FPRS Conference on Metal Plate Wood Truss in St. Louis, Missouri. Forest Products Research Society, Madison, Wisconsin, 3-5.

Meeks, J.E. 1979. U.S. and Canadian Design Methodology. Proceedings of FPRS Conference on Metal Plate Wood Truss in St. Louis, Missouri. Forest Products Research Society, Madison, Wisconsin, 114-116.

Misra, R.D. 19--. An analytical and experimental investigation of stress distribution in the punched metal plate of a timber joint. Ph.D. Thesis, Michigan State University.

Misra, R.D., and M.L. Esmay. 1966. Stress distribution in the punched metal plate of a timber joint. Transactions of the American Society of Agricultural Engineers 9(6):839-842, 845.

Mjos, N. and O. Ellingsrud. 1982. Upward lifting of trussed rafters. Norwegian Institute of Wood Technology, Blindern, Norway, Report 62.

Moehler, K. 1962. Research covering nailed sheet-steel/wood joints. Tests on nailed wood constructions (Holznagelbau Versuche). Berichte aus der Holzforschung 24, 38-51.

Moehler, K. 1977. Testing of integral nail plates as timber joints. Proceedings of International Council for Building Research Studies and Documentation Working Committee W18A on Timber Structures in Stockholm, Sweden, 7-7-1.

Moehler, K. 1981. Derivation of the allowable load in case of nail-plate joints perpendicular to grain. Proceedings of Meeting of International Council for Building Research Studies and Documentation Working Committee W18A on Timber Structures in Warsaw, Poland, 14-7-6.

Moss, P.J. 1991. Seismic performance of moment-resisting joints in timber frames. Proceedings of International Timber Engineering Conference in London, England.

National Forest Products Association. 1991. National Design Specification for Wood Construction. National Forest Products Association, Washington, DC.

Njoto, I., and I. Salim. 19--. Tensile strength of eccentric roof truss tension splices. Department of Civil Engineering and Applied Mechanics, McGill University.

Noguchi, M. 1980. Ultimate resisting moment of butt joints with plate connectors stressed in pure bending. Wood Science 12(3):168-175.

Noren, B. 1979. Design of joints with nail plates. Proceedings of Meeting of International Council for Building Research Studies and Documentation Working Commission W18A on Timber Structures in Bordeaux, France. 12-7-3. Also, 1980. Ibidem, in Potaniemi, Finland, 13-7-8. Also, 1981. Ibidem, in Warsaw, Poland, 14-7-1.

Noren, B. 1980. Design of joints with nail plates - Calculation of slip. Proceedings of Meeting of International Council for Building Research Studies and Documentation Working Commission W18A on Timber Structures in Otaniemi, Finland, 13-7-4.

Noren, B. 1981. Design of joints with nail plates. Proceedings of Meeting of International Council for Building Research Studies and Documentation Working Committee W18A on Timber Structures in Warsaw, Poland, 14-7-1.

Noren, B. 1981. Wood failure in joints with nail plates. Proceedings of Meeting of International Council for Building Research Studies and Documentation Working Committee W18A on Timber Structures in Warsaw, Poland, 14-7-4.

Noren, B. 1986. Design of joints with nail plates - Principles. Proceedings of Meeting of International Council for Building Research Studies and Documentation Working Committee W18A on Timber Structures in Florence, Italy, 19-7-7.

Noren, B. 1986. Shear tests for nail plates. Proceedings of Meeting of International Council for Building Research Studies and Documentation Working Committee W18A on Timber Structures in Florence, Italy, 19-7-8.

Palka, L.C. 1983. Effect of load duration upon timber fasteners: Load-slip characteristics of toothed truss-plate joints in static tension. Prediction of load-slip characteristics of timber joints made with metal plate connectors. Development of an economical test system for automatic measurements and recording of long-term slip in timber joints. Forintek Canada Corporation, Vancouver, BC, Canada.

Palka, L.C. 1984. Effect of wood density of truss plate joint strength. Forintek Canada Corporation FR26.

Palka, L.C. 1985 and 1987. Effect of load duration upon timber fasteners: Short- and long-term models. Forintek Canada Corporation.

Palka, L.C. 1986. Effect of load duration upon timber fasteners: Second data report. Forintek Canada Corporation, Project No. FCC-54-10-009.

Palka, L.C. 1986. Creep and load duration of truss-plate joints in tension. Proceedings of Meeting of International Union of Forestry Research Organizations in Ljubljiana, Yugoslavia.

Palka, L.C. 1987. Effect of load duration upon timber fasteners: Third data report. Forintek Canada Corporation.

Palka, L.C. 1988. Exploratory study of short-term and long-term behaviour of truss-plate joints in tension under ambient laboratory conditions. Forintek Canada Corporation.

Palka, L.C. 1989. Review of an exploratory study of truss-plate joints in tension under ambient laboratory conditions. Forintek Canada Corporation.

Palka, L.C., and B. Rovner. 1985. Effect of load duration upon timber fasteners: First data report. Forintek Canada Corporation, Project No. FCC-02-50-10-009.

Parameswar, H.C., and M.G. Mansell. 1989. Limit state design of nail plate joints in timber trusses. Proceedings of Second Pacific Timber Engineering Conference in Auckland, New Zealand. 1:151-154.

Percival, D.H., and S.K. Suddarth. 1971. An investigation of the mechanical characteristics of truss plates on fire-retardant treated wood. Forest Products Journal 21(1).

Percival, D.H. and S.K. Suddarth. 1989. Long-term tests of 4x2 parallel-chord metal-plate-connected wood trusses. Small Homes Council - Building Research Council, Res. Rep. 89-2.

Percival, D.H., et al. 19--. Test results from an investigation of parallel-chord, top-cord bearing wood trusses. Small Homes Council - Building Research Council, Res. Rep. 85-1.

Percival, D.H., and J.M. Denny. 19--. Performance of four raised-heel or cantilevered wood roof truss designs. Small Homes Council - Building Research Council, Res. Rep. 82-1.

Pienaar, F.R.P. 1984. Design of nailed plated joints in timber structures for strength and stiffness. National Timber Research Institute, Pretoria, South Africa, Report No. CSIR/SR/HOUT - 360.

Piskunov, Y.V. 1989. The development of design codes for timber structures made of composite bars with plate joints based in cylindrical nails. Proceedings of Meeting of International Council for Building Research Studies and

Documentation Working Commission W18A on Timber Structures in Berlin, Germany, 22-7-12.

Ploos van Amstel, H. 1990. Comparison of five models in creep prediction of joints with Menig plates: 13 years' creep data available. Stevin Laboratories Delft, The Netherlands, Report 4-84-7.

Poutanen, T.T. 1982. Model for trussed rafter design. Proceedings of Meeting of International Council for Building Research Studies and Documentation Working Commission W18A on Timber Structures in Beit Oren, Israel, 18-14-2.

Poutanen, T.T. 1984. Model for timber strength under axial load and moment. Proceedings of Meeting of International Council for Building Research Studies and Documentation Working Commission W18A on Timber Structures in Rapperswill, Switzerland, 17-2-1.

Poutanen, T.T. 1986. Joint eccentricity in trussed rafters. Proceedings of Meeting of International Council for Building Research Studies and Documentation Working Commission W18A on Timber Structures in Florence, Italy, 19-14-3.

Poutanen, T.T. 1987. Some notes about testing nail plates subjected to moment load. Proceedings of Meeting of International Council for Building Research Studies and Documentation Working Commission W18A on Timber Structures in Dublin, Ireland, 20-14-1.

Poutanen, T.T. 1987. Moment distribution in trussed rafters. Proceedings of Meeting of International Council for Building Research Studies and Documentation Working Commission W18A on Timber Structures in Dublin, Ireland, 20-14-2.

Poutanen, T.T. 1988. Eccentricity in a nail plate joint. Proceedings of International Timber Engineering Conference in Seattle, Washington, 1:266-273.

Poutanen, T.T. 1988. Method for moment measurement in timber cross-section. Proceedings of Meeting of International Union of Forestry Research Organizations in Turku, Finland.

Poutanen, T.T. 1988. Nail plate joint under shear loading. Proceedings of International Union of Forestry Research Organizations in Parksville, Vancouver Island, Canada, 21-7-3.

Poutanen, T.T. 1989. Analysis of trusses with metal connector plate joints. Proceedings of Second Pacific Timber Engineering Conference in Auckland, New Zealand, 1:155-159.

Poutanen, T.T. 1990. Tests on moment measurement in timber cross-section. Tampere University of Technology, Tampere, Finland.

Poutanen, T.T. 1990. Notes on truss analysis. Proceedings of Meeting of International Council for Building Research Studies and Documentation Working Commission W18A on Timber Structures, Truss Group, in Copenhagen, Denmark.

Poutanen, T.T. 1990. Trussed rafters with nail-plate joints. Tampere University of Technology, Tampere, Finland.

Quaile, A.T., and F.J. Keenan. 1979. Truss plate testing in Canada: Test procedures and factors affecting strength properties. Proceedings of Conference on Metal Plate Wood Truss in St. Louis, Missouri. Forest Products Research Society, Madison, Wisconsin, pp 105-112.

Reece, P.O. 1982. The design of continuous members in timber trussed rafters with punched metal connector plates. Proceedings of Meeting of International Council for Building Research Studies and Documentation Working Commission W18A on Timber Structures in Karlsruhe, Germany, 15-14-9.

Riberholt, H. 1990. Analysis of timber trussed rafters of the W-type. Proceedings of Meeting of International Council for Building Research Studies and Documentation Working Commission W18A on Timber Structures in Lisbon, Portugal, 23-14-1.

Riberholt, H. 1990. Proposal for Eurocode 5 text on timber trussed rafters. Proceedings of Meeting of International Council for Building Research Studies and Documentation Working Commission W18A on Timber Structures in Lisbon, Portugal, 23-14-2.

Roald, B., and E. Aasheim. 1991. Fire testing of nail plate connected wood trusses. Proceedings of International Timber Engineering Conference in London, England, 4.114-4.121.

Samuelsson, S. 19--. Approximate analysis methods for mechanically joined trussed rafters. Report for the Swedish State Research Institute for Farm Buildings, Sweden.

Sasaki, Y., and T. Takemura. 1990. Non-linear analysis of metal-plate wood trusses. Proceedings of International Timber Engineering Conference in Tokyo, Japan, 3:701-708.

Schjoot, R. 1961. Calculation of stresses in rigid joints. Proceedings of the First International Conference on Timber Engineering.

Sheppard, I. 1969. An analytical and experimental investigation of contact area stress distribution and buckling strength of light gauge punched metal heel plates for timber trusses. Ph.D. Thesis, Michigan State University.

Sletteland, N.T., G.L. Pratt, and R.T. Schuler. 1977. Fatigue life of metal connector plates. American Society of Agricultural Engineers 77-4037.

Sliker, A., and B. Radcliffe. 1965. Deflection and creep characteristics of trussed rafters with metal plate fasteners. Forest Products Journal 15(11):473-479.

Smith, G.W. 1988. Production of long length beams by nail-plate butt jointing. Proceedings of International Timber Engineering Conference in Seattle, Washington, 1:100-107.

Smith, G.W. 1989. Acceptance criteria for mechanically jointed beams. Proceedings of Second Pacific Timber Engineering Conference in Auckland, New Zealand, 1:119-124

Smith, G.W., R. Thomson, and C.J. Rogers. 1991. Innovative use of metal plate connectors for timber products. Proceedings of Innovation and Economics in Building Conference in Brisbane, Australia, 171-176.

Soltis, L.A. 1985. Partially continuous floor joints. USDA Forest Service, Forest Products Laboratory, Report 461.

Soltis, L.A., and S. Hansen 1991. Strength of light-gauge steel nailed connections. Forest Products Journal 91(5):57-60.

Stern, E.G. 1957. Wood, plywood, or steel gusset plates for nailed trussed rafters. Virginia Polytechnic Institute and State University, Wood Research Laboratory, Research Report.

Stern, E.G. 1961. Fastening of truss plates with "Screwtite Hi-Load" nails. Virginia Polytechnic Institute and State University, Wood Research Laboratory, Bulletin 43.

Stern, E.G. 1964. Fastening of steel truss plates with threaded nails. Virginia Polytechnic Institute and State University, Wood Research Laboratory, Bulletin 54.

Stern, E.G. 1971. The heel joint of trussed rafters - A progress report. Virginia Polytechnic Institute and State University, Wood Research Laboratory, Bulletin 101.

Stern, E.G. 1971. Plate-assembled trussed rafters with improved heel joints - A pilot study. Virginia Polytechnic Institute and State University, Wood Research Laboratory, Bulletin 104.

Stern, E.G. 1980. Up-grading of wood structures by use of improved mechanical fasteners. American Society of Civil Engineers, Reprint 80-525.

Stern, E.G. 1982. Nailed flitch beams and girders providing new opportunities in wood construction. American Society of Civil Engineers, Preprint 82-002.

Stern, E.G. 1988. Truss plate with plurality of teeth stamped from same plate hole. Proceedings of International Timber Engineering Conference in Seattle, Washington, 1:274-280.

Stern, E.G. 1992. Definitions of terms pertaining to metal connector plates. Presented at Meeting of International Council for Building Research Studies and Documentation Working Commission W18A on Timber Structures in Ahus, Sweden,-----------------.

Stern, E.G., and V.K. Kumar. 1973. Flitch beams, Forest Products Journal 23(5), May, 40-47.

Stern, E.G., J.R. Reeves, and W.C. Griggs. 1979. Mechanical fastening of wood - A review of the state of the art. Committee on Fastening of Forest Products Research Society, Madison, Wisconsin.

Suddarth, S.K. 19--. Determination of member stresses in wood trusses with rigid joints. Purdue University Wood Research Laboratory. Report No. 714.

Suddarth, S.K., F.E. Goodrick, and S.L. Samuelsson. 1964. Report to the Design Subcommittee of the Joint Industry Advisory Committee on Roof Trusses.

Suddarth, S.K. 1972. A computerized wood engineering system - The Purdue plane structures analyzer. USDA Forest Service, Forest Products Research Laboratory, Madison, Wisconsin, Research Report FPL 168.

Suddarth, S.K., D.H. Percival, and Q.B. Comus. 1979. Variability in tension performance of metal plate connections. Proceedings of Conference on Metal Plate Wood Truss in St. Louis, Missouri. Forest Products Research Society, Madison, Wisconsin, 98-104.

Suddarth, S.K., and D.H. Percival. 1988. Testing and analysis of 4x2 parallel-chord metal-plate-connected trusses. Small Homes Council-Building Research Council. Research Report 81-1. Also, Proceedings of International Timber Engineering Conference in Seattle, Washington, 1:475-481.

Tan, R. 1989. Case histories of Gang-Nail structures, designed and built in New Zealand. Proceedings of Second Pacific Timber Engineering Conference in Auckland, New Zealand, 1:223-228.

Temple, M.C., D. Racic, and S. Pavlica. 1984. Floor trusses subjected to a concentrated load. Canadian Journal of Civil Engineering 11:355-362.

Thurston, S.J., and P.F. Flack. 1979. Cyclic loading of large T joints incorporating nailed steel sideplates. Central Laboratories, Ministry of Works and Development, Wellington, New Zealand, Report 5-79/6.

TRADA. 1991. Domestic trussed rafters. Advisory Sheet 10. Timber Research and Development Association, Hughenden Valley, High Wycombe, Buckinghamshire, England.

Triche, M.S. 1984. Analysis and design of metal plate connections. M.S. Thesis, Purdue University.

Triche, M.S., and S.K. Suddarth. 1988. Advanced design of metal plate connector joints. Forest Products Journal 38(9):7-12.

Truss Plate Institute. 1966. Design specification for light metal plate connected wood trusses. TPI-66, TPI-68. Also, 1970. Design specification for light metal plate connected wood roof trusses. TPI-70 and TPI-74. Also, Design specification for metal plate connected wood trusses. TPI-78 and TPI-85. Also, Recommended design practice of Truss Plate Institute. TPI-85, Addendum, Appendix C: Standard method of test for determining lateral resistance strength of metal connector plate teeth. Appendix E: Standard method of test for strength properties of metal connector plates under pure tension forces. Appendix F: standard method of test for strength properties of metal connector plates under pure shear force. Truss Plate Institute, Madison, Wisconsin.

Truss Plate Institute. 1977. Quality control manual for light metal-plate connected wood trusses. Truss Plate Institute, Madison, Wisconsin. QCM-77.

Truss Plate Institute. 1978 and 1985. Design specifications of metal plate connected wood trusses. Truss Plate Institute, Madison, Wisconsin, TPI-85.

Truss Plate Institute. 1980. Design specifications for metal plate connected parallel chord wood trusses. Truss Plate Institute, Madison, Wisconsin, PCT-80.

Truss Plate Institute. 1985. Design specification for metal plate connected wood trusses. Truss Plate Institute, Madison, Wisconsin.

Truss Plate Institute. 1985. Interim design methodology for PCT-CII 2x4/2x6 wood trusses. Truss Plate Institute, Madison, Wisconsin, TPI-85 Supplement.

Truss Plate Institute. 1985. Interim design methodology for PCT-CII 4x2 wood trusses. Truss Plate Institute, Madison, Wisconsin, PCT-80 Supplement.

Truss Plate Institute. 1986 and 1988. Quality standard for metal plate connected wood trusses. Truss Plate Institute, Madison, Wisconsin, QST-86 and 88.

USDA Forest Service, Forest Products Laboratory. 1987. Wood Handbook. USDA Agricultural Handbook 72 (rev.). USDA Forest Service, Forest Products Laboratory, Madison, Wisconsin.

Van der Put, T.A.C. 1984. Discussion on the design of nail plate connections. Proceedings of First Pacific Timber Engineering Conference in Auckland, New Zealand, I:22-28.

Varoglu, E. 1984. Structural analysis of trusses and roof truss systems. Forintek Canada Corporation. Project FCC 02-50-65-590.

Walford, G.B. 1988. Analysis of timber portal frame gusset joints. Proceeding of International Timber Engineering Conference in Seattle, Washington, 1:428-435.

Whale, R.J. 1991. Some non-domestic examples of trussed rafter usage in the UK. Proceedings of Timber Engineering Conference in London, England, 2.91-2.98.

Whale, R.J. 1991. Eurocode 5 -- Joint design. Proceedings of 1991 International Timber Engineering Conference in London, England, pp. 1.97-1.106.

Wight, M. 1977. Moisture content effects on the strength of truss plate connector joints. B.S. Thesis, University of Toronto.

Wilkinson, T.L. 1971. Theoretical lateral resistance of nailed joints. ASCE Journal of the Structural Division. 97(ST5):1381-1397.

Wilkinson, T.L. 1978. Longtime performance of trussed rafters with different connection systems: 10-year evaluation. USDA Forest Service, Forest Products Laboratory. Madison, Wisconsin, Report 204.

Wilkinson, T.L. 1984. Long-term performance of trussed rafters with different connection systems. USDA Forest Service, Forest Products Laboratory. Madison, Wisconsin, Research Paper 444.

Wilkinson, T.L. 19--. Moisture cycling of trussed rafter joints. USDA Forest Service, Forest Products Laboratory. Madison, Wisconsin, Research Paper FPL-67.

Wilson, F. 1978. The effect of time between assembly and testing on the strength of truss plate joints. B.S. Thesis, University of Toronto.

Woeste, F.E., A.L. DeBonis, T.E. McLain, and L.D. George. 1984. Strength of nail laminated columns with metal plated joints. Transactions of American Society of Agricultural Engineers 24(1).

Wolfe, R.W. 1990. Metal-plate connectors loaded in combined bending and tension. Forest Products Journal 40(9):17-23.

Wolfe, R.W., T. LaBissoniere, and S.M. Cramer. 1988. Performance tests of light-frame roof assemblies. Proceedings of International Timber Engineering Conference in Seattle, Washington, 2:3-11.

Wolfe, R.W., D.H. Percival, and R.C. Moody. 1986. Strength and stiffness of light-frame sloped trusses. USDA Forest Service, Forest Products Laboratory, Madison, Wisconsin. Research Paper FPL 471.

Wolfe, R.W., and D. McDonald. 1991. Performance of metal plate connectors. Presented at Conference on Environmental Impacts of Wood-Based Products and Processes: A Mandate for Change, USDA Forest Service, Forest Products Laboratory, Madison, Wisconsin (Poster Session, Abstract).

APPENDIX C: TERMINOLOGIES IN RELATED FIELDS

American Society for Testing and Materials. 1977 (84). Standard definitions of terms relating to nails for use with wood and wood-base materials. ASTM F547. ASTM, Philadelphia, PA.

American Society for Testing and Materials. 1978 (84). Standard definitions of terms relating to collated and cohered fasteners and their application tools. ASTM F592. ASTM, Philadelphia, PA.

Stern, E.G. 1967. Nails - Definitions and sizes, a handbook for nail users. Virginia Polytechnic Institute and State University, Wood Research Laboratory, Bulletin 61.

Stern, E.G. 1985. Glossary of terms in pallet field, an 18-language glossary of 226 terms and their definitions in English. Virginia Polytechnic Institute and State University, William H. Sardo Pallet and Container Research Laboratory, Blacksburg, VA.

Stern, E.G. 1992. Definitions of terms pertaining to metal connector plates. (Prepared for presentation at meeting of International Council for Building Research Studies and Documentation (CIB) Working Commission on Timber Structures (W18A) Task Group on Assessment of Punched Metal Plate Timber Fasteners (TG6) in Åhus, Sweden, August 25-27, 1992.)

Fig. 1 - Various types of prepunched metal connector plates in use or proposed for use.

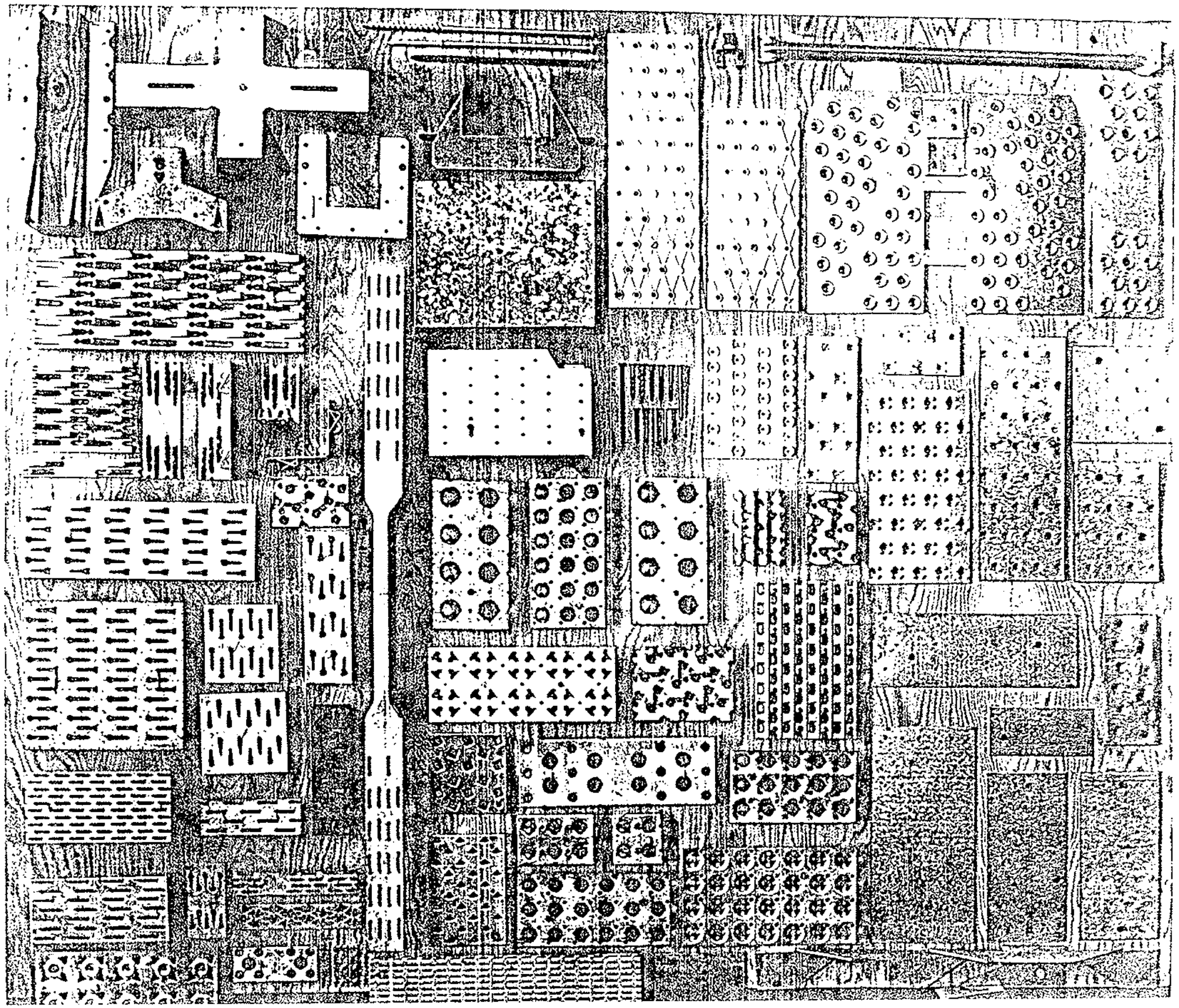

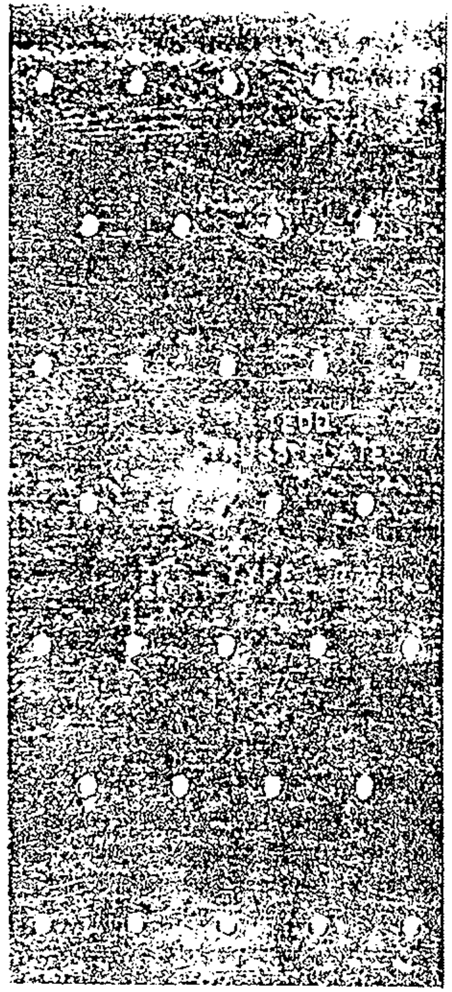

Fig. 2a.- Flat, prepunched, 0.9-mm (20-gage), galvanized-steel, TECO metal connector plate nailed to each side of the connection with 38 x 3.43-mm ($1\frac{1}{2}$ x 0.135-in.), galvanized-steel nails driven from both sides of member and loaded in single shear.

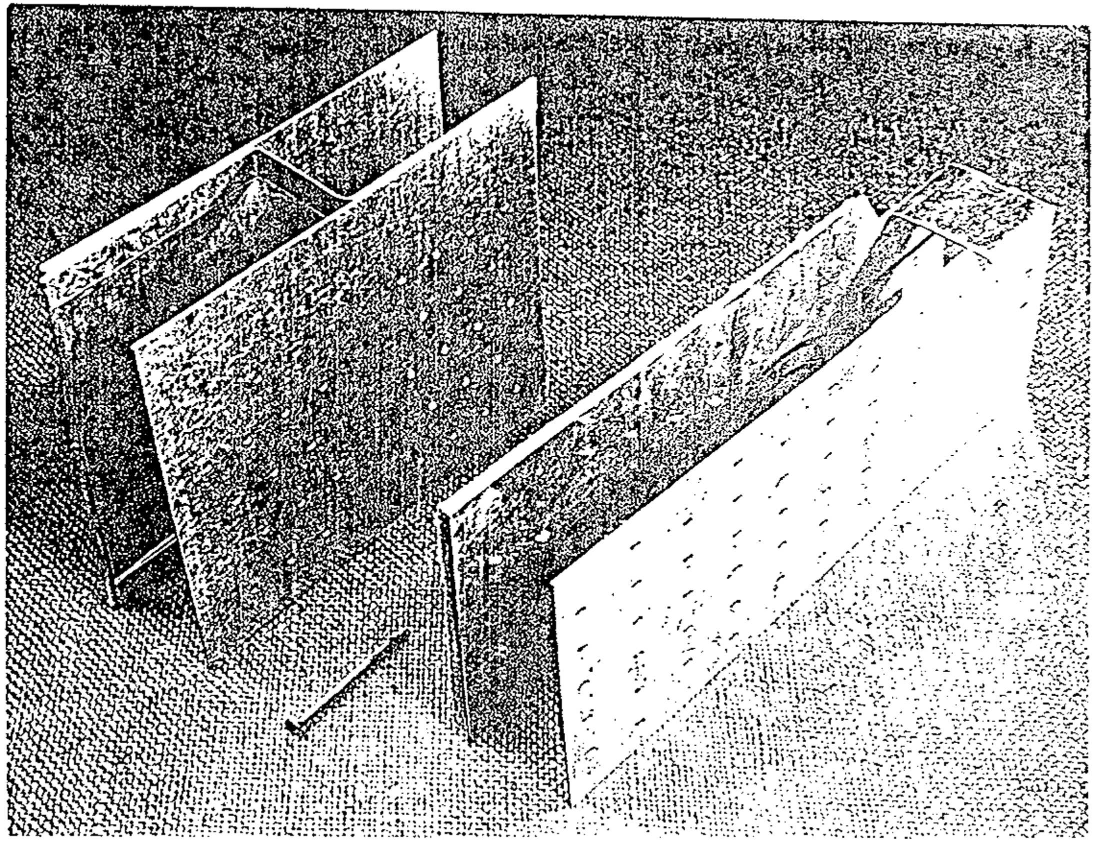

Fig. 2b.- Single piece H-BRACE plate fabricated from 0.9-mm (20-gage), galvanized steel, with one plate side prepunched with patterned nail holes and other plate side backed by fiberboard to allow automatic clinching of a special, cement-coated, 57 x 3.33-mm ($2\frac{1}{4}$ x 0.131-in.) nail with clinching notch near nail point. Nailing is accomplished from one side, with nails loaded in double shear. An alternate H-BRACE plate is a single-piece plate with both sides pieces provided with prepunched nail holes and fastened to the members with 38-mm ($1\frac{1}{2}$-in.), helically threaded, hardened-steel nails driven from both member sides and loaded in single shear.

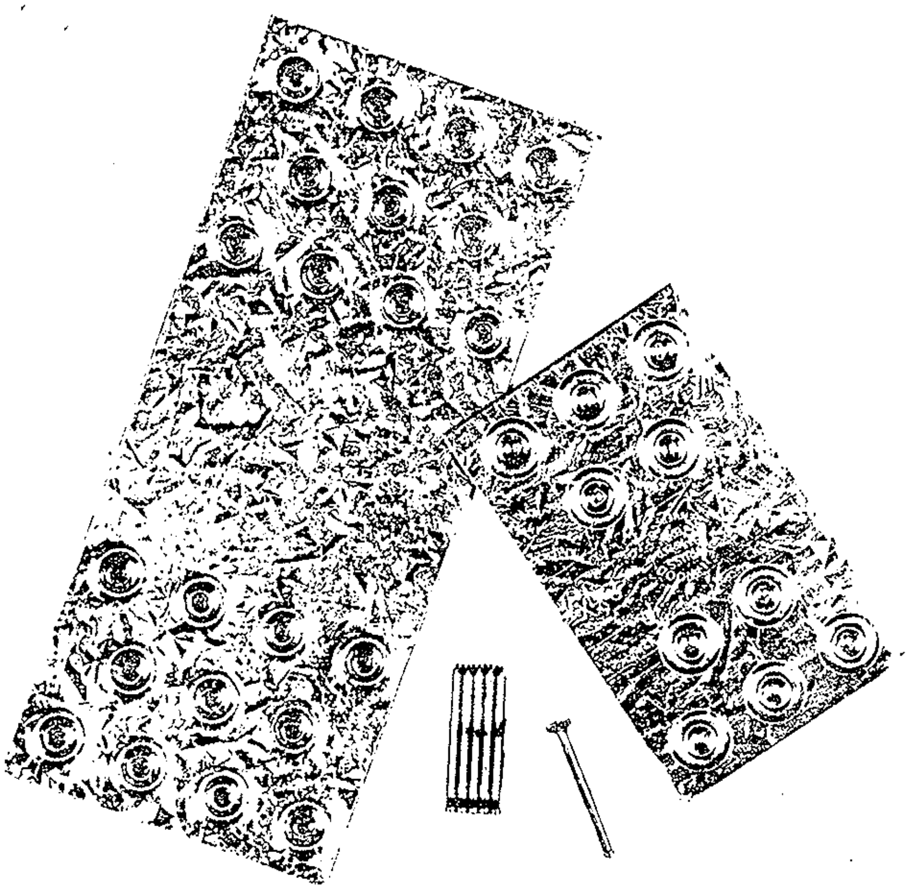

Fig. 3.- Galvanized, 0.9-mm (20-gage), DENWOOD plates with ring-shaped projections and concentric dimples around punched nail holes to facilitate tool-driving of 38 x 2.87-mm (1½ x 0.113-in.), T-head nails with large head fillet.

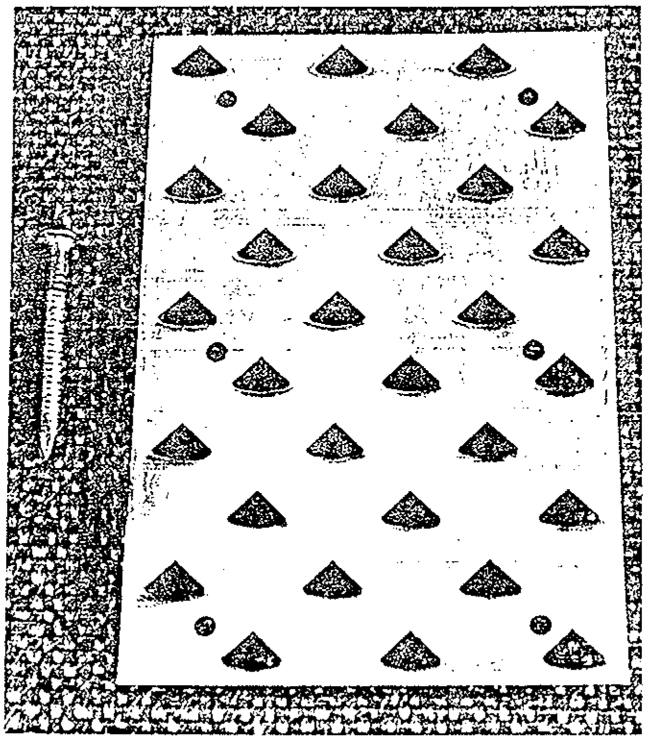

Fig. 4.- SANFORD GRI-P-LATE with single triangular barb per plate hole, to be supplementary fastened to wood member with annularly threaded nail.

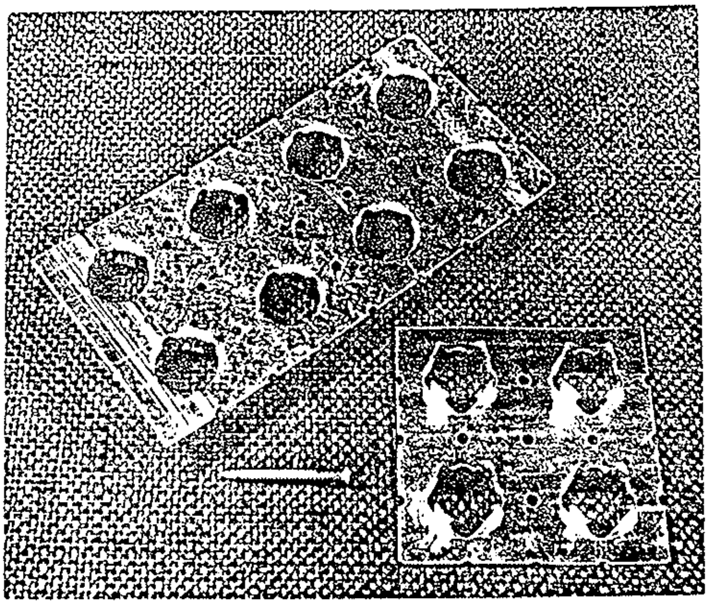

Fig, 5a.- Galvanized BARBGRIP plates with four barbs per plate hole, to be supplementary fastened to wood member with annularly threaded nail.

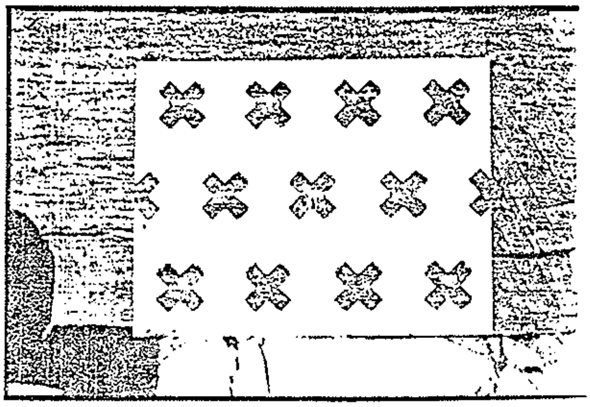

Fig. 5b.- Galvanized MITEK X-CELLENT plate with four barbs per plate hole.

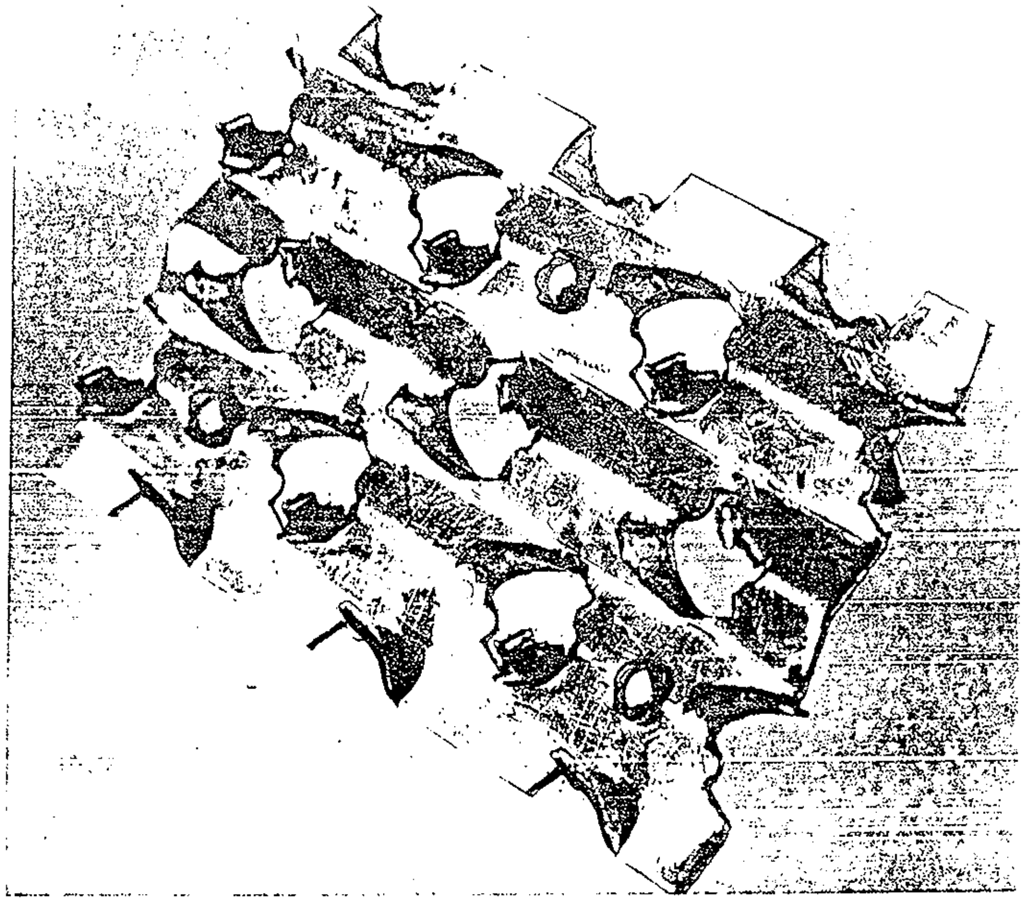

Fig. 6.- Galvanized, corrugated SANFORD GRIP-MASTER plate with two barbs per plate hole, to be supplementary fastened to wood member with hammer-driven nails.

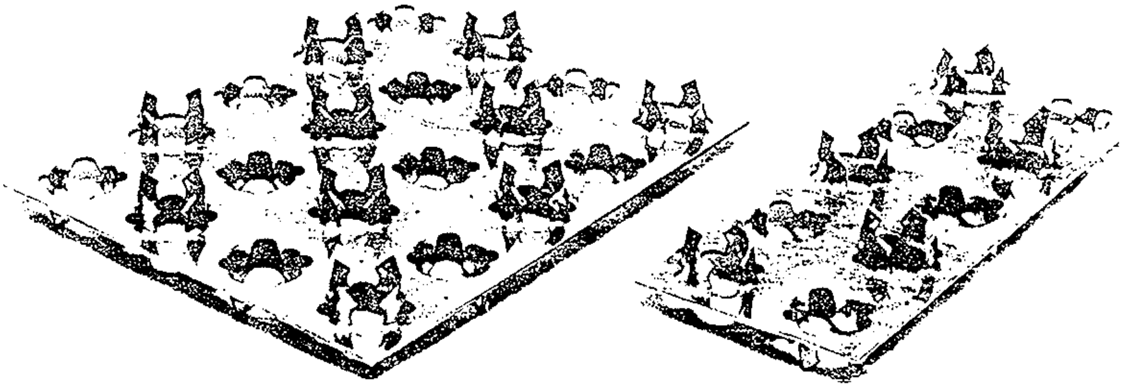

Fig. 7.- Galvanized WALTERS 102 by 127-mm (4.0 by 5.0-in.) and 51 by 127-mm (2.0 by 5.0-in.) shear transfer plates of 0.9-mm (20-gage) steel with four 8-mm (5/16-in.) long teeth per plate hole punched in both directions perpendicular to plate area.

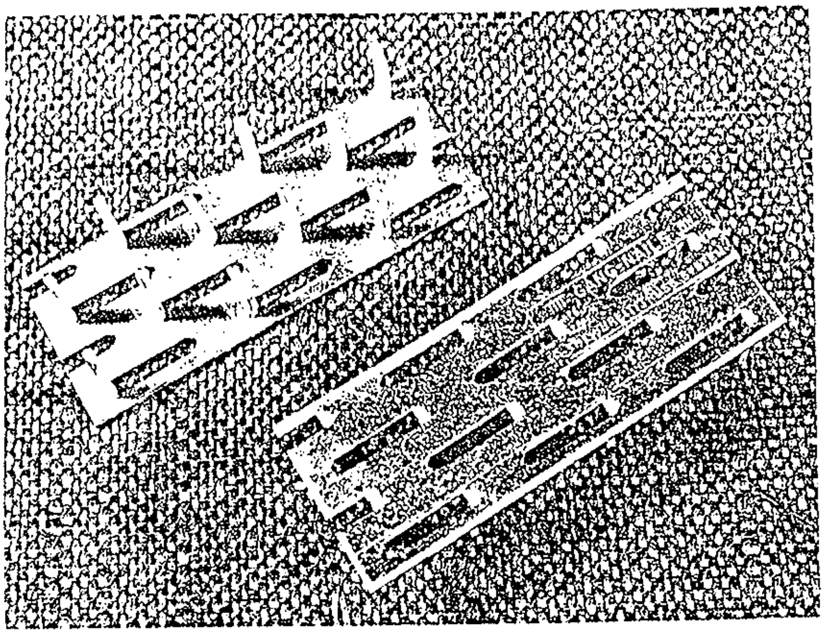

Fig. 8a.- Galvanized GANG-NAIL plate with single tooth per nail plate, front and back view.

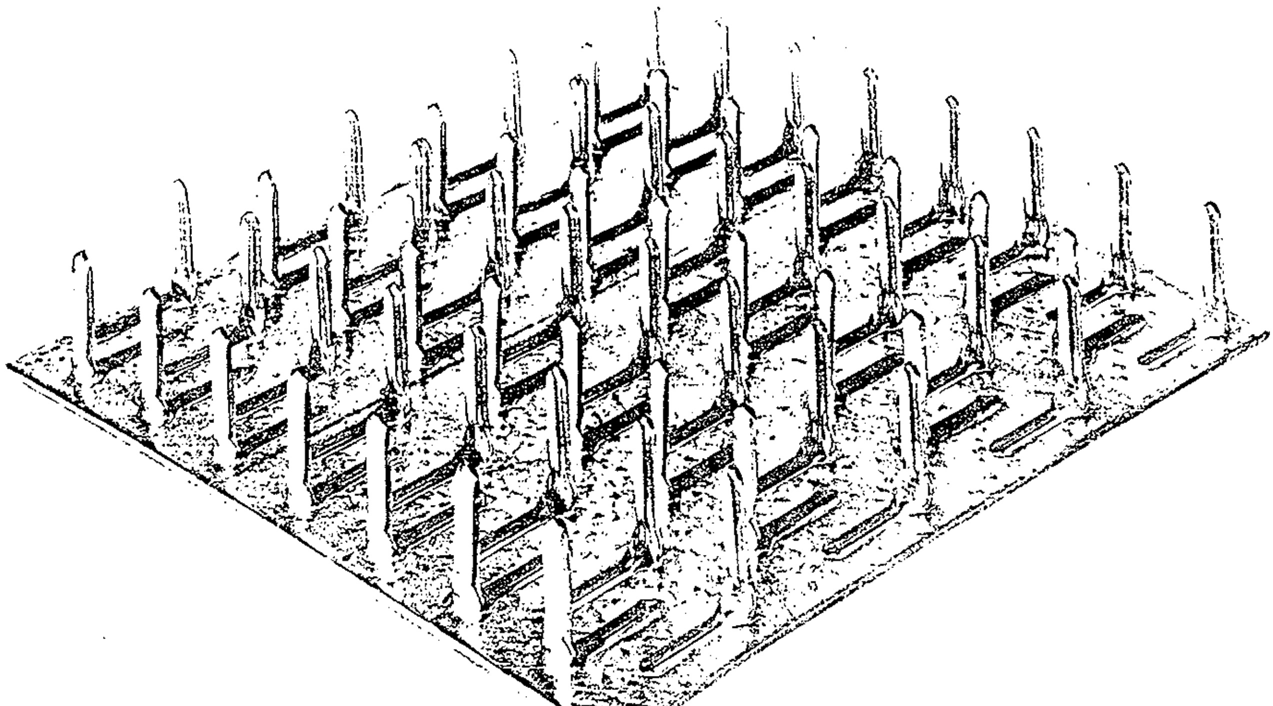

Fig. 8b.- Galvanized TRUSS-O-MATIC plate of 2-mm (14-gage) steel with curved, 20-mm (3/4-in.) long teeth spaced 10 mm 3/8 in.) on centers.

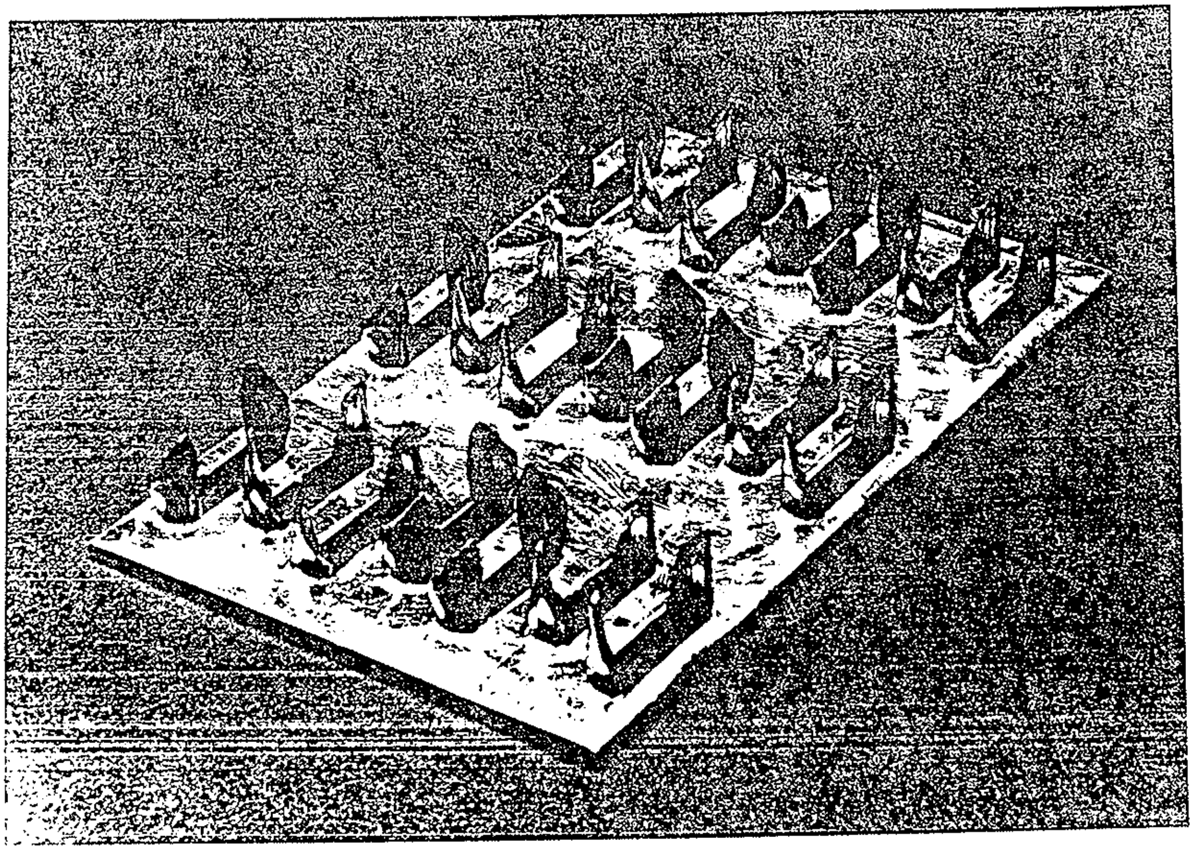

Fig. 9.- Galvanized connector plate of 0.9-mm (20-gage) steel with two integral 7-mm (9/32-in.) long teeth per plate hole.

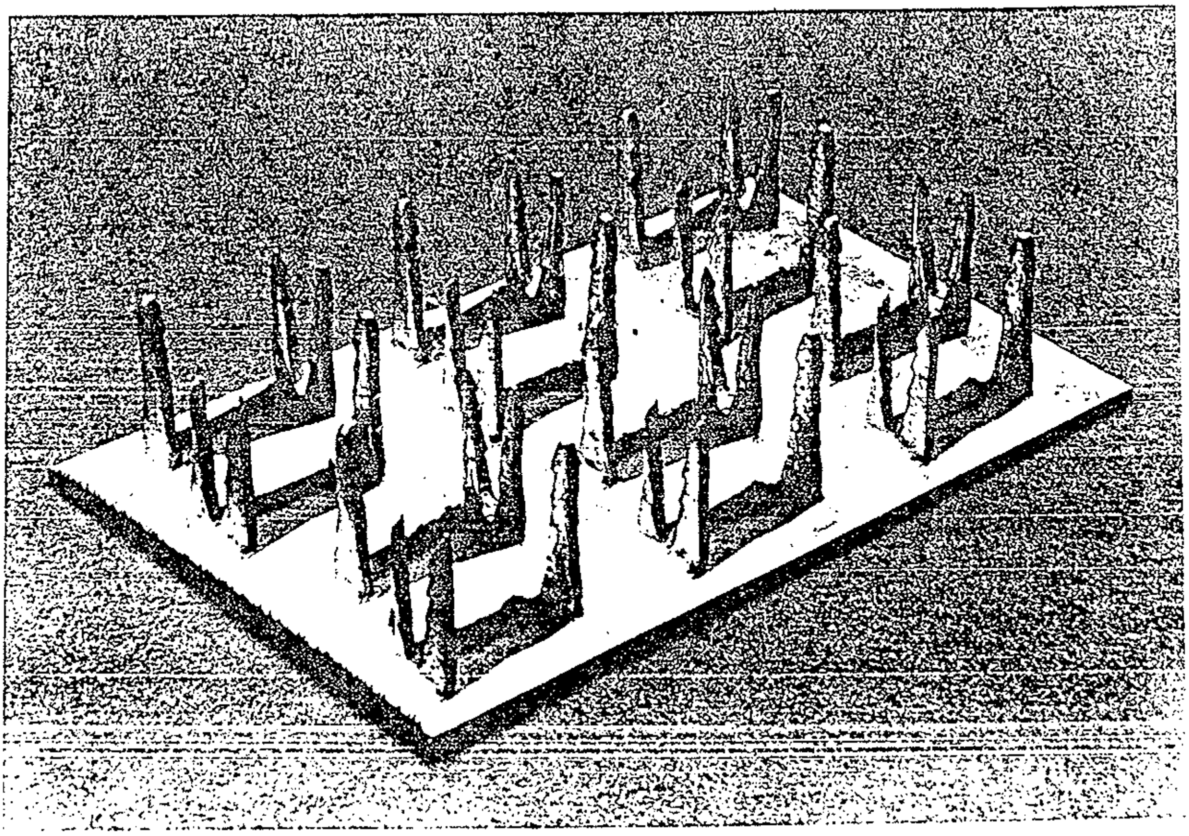

Fig. 10.- Galvanized Finnish connector plate of 1.2-mm (18-gage) steel with three integral 12.7-mm (½-in.) long teeth per plate hole.

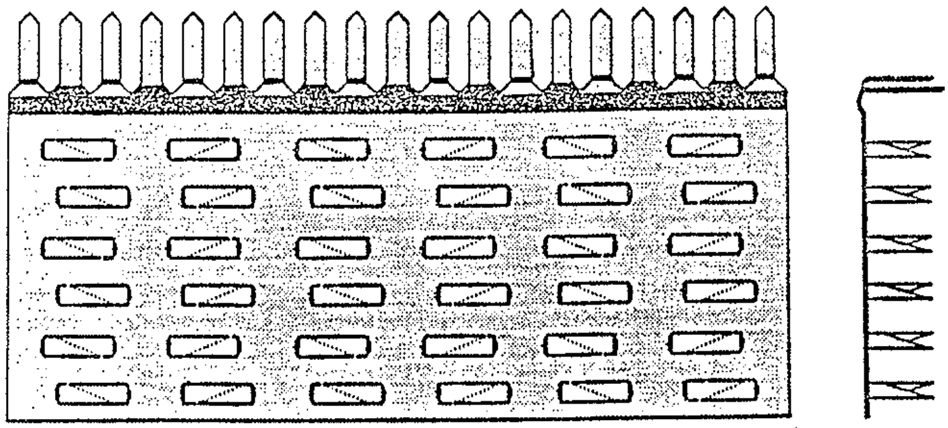

Fig. 11.- Proposed Finnish metal connector plate with two projecting teeth per nail hole and a row of peripheral teeth, left, prior to bending and, right, after bending perpendicular to plate area, patented by Tuomo Poutanen, Tampere, Finland.

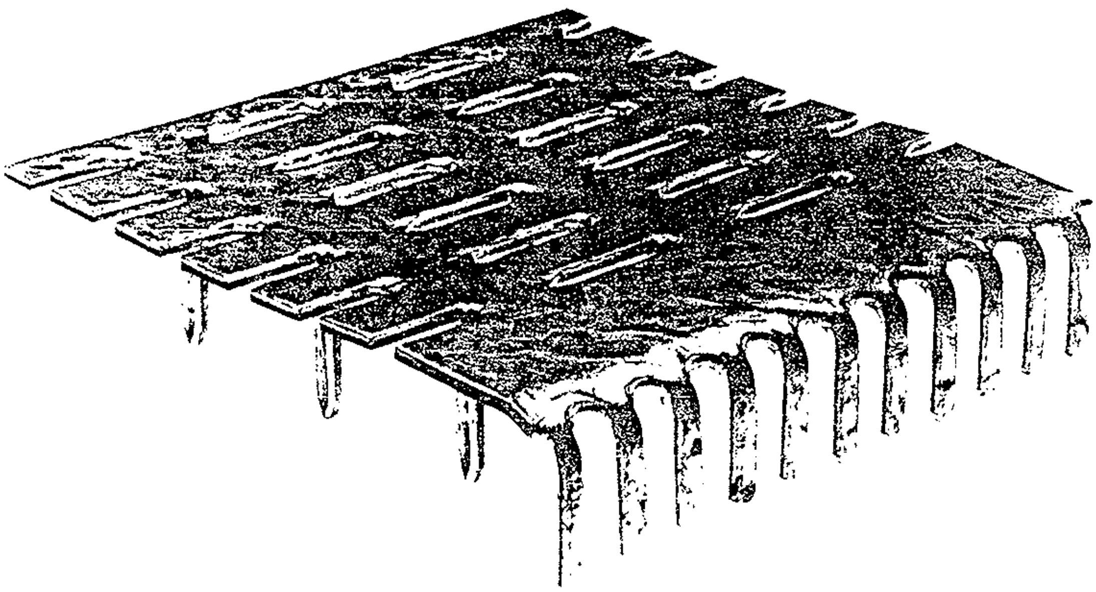

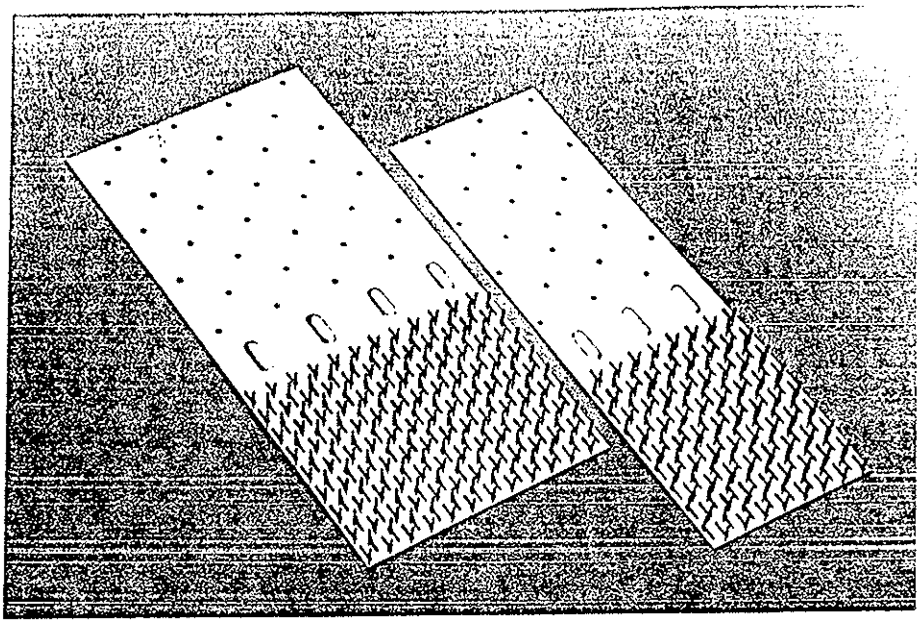

Fig. 12.- Metal connector plates with one section with projecting teeth to be machine-pressed into the wood member and another section with nail holes for field-nailing the preassembled component to another one.

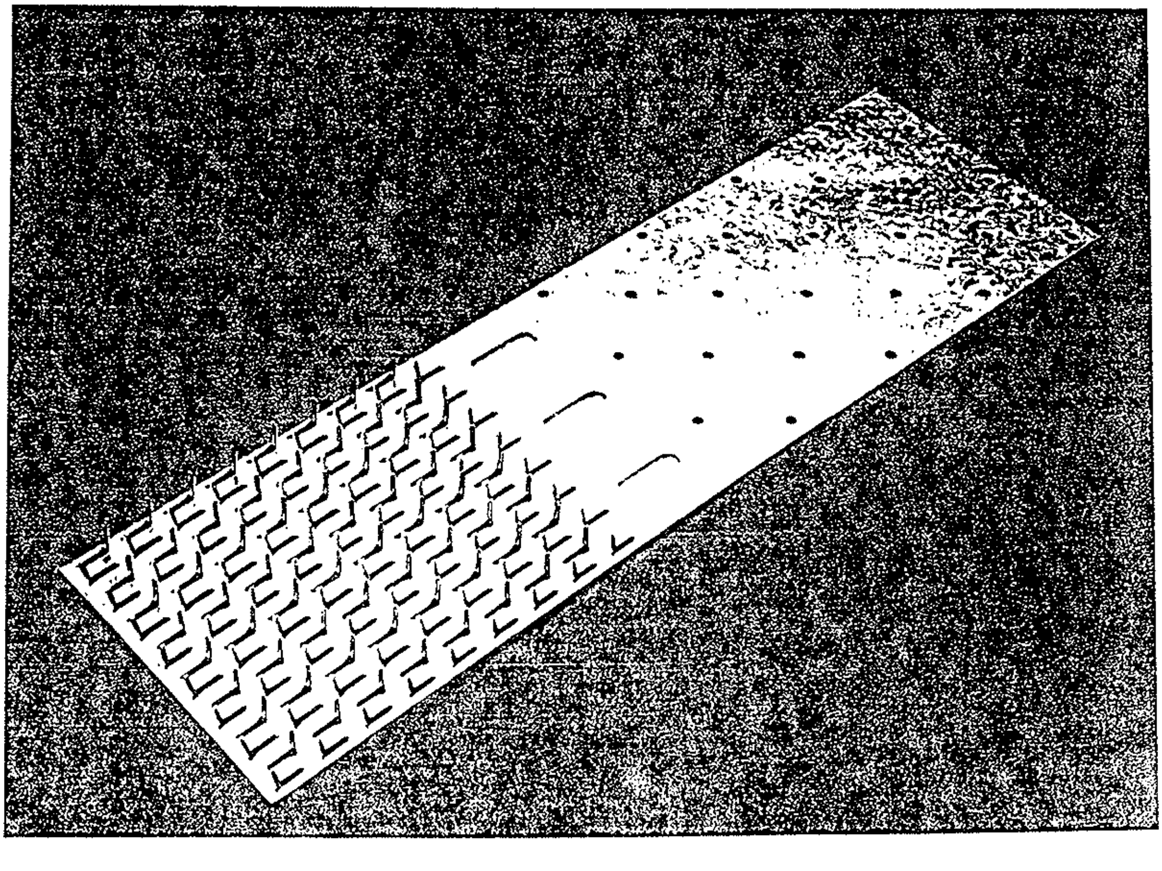

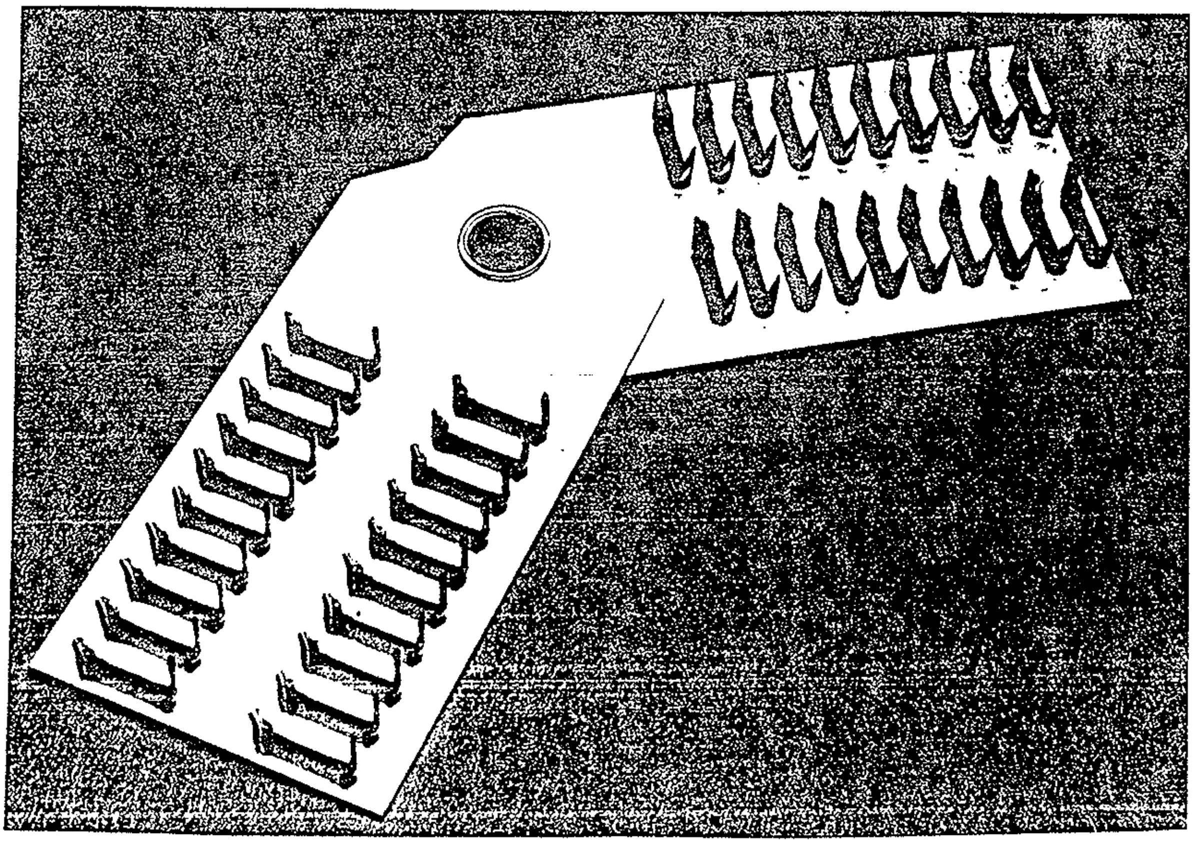

Fig. 13.- Two-part galvanized ALPINE connector plate of 0.96-mm (19½-gage) steel with two integral 8.7-mm (11/32-in.) long teeth per plate hole, with the two plate parts rotatable around a 10.3-mm (13/32-in.) inside-diameter connecting grommet.

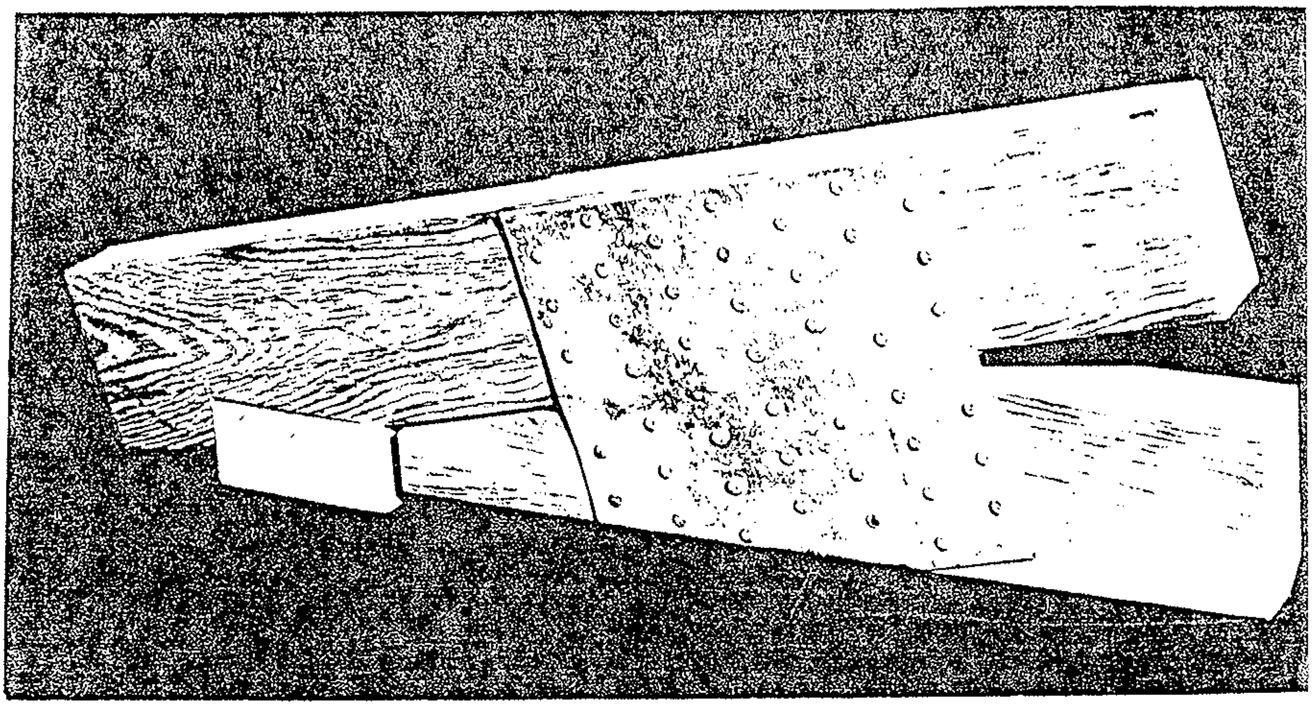

Fig. 14a.- Heel connection of trussed rafter assembled with H-BRACE metal connector plate, with nails driven from both member sides and loaded in single shear.

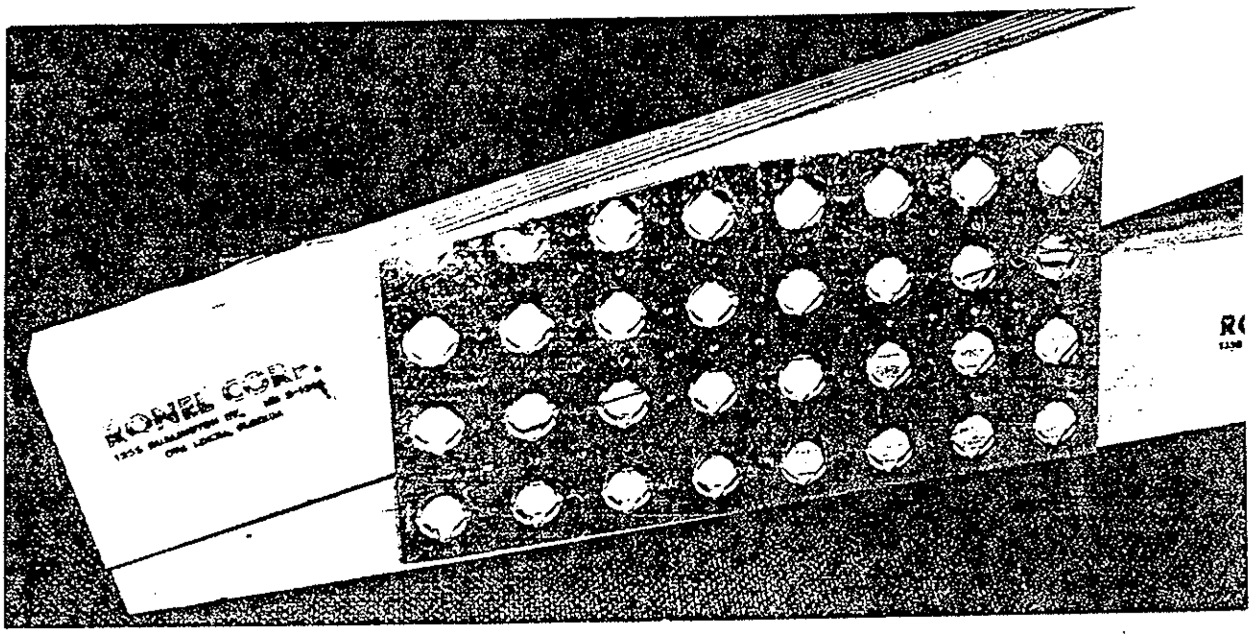

Fig. 14b.- Heel connection of trussed rafter assembled with BARBGRIP metal connector plates with barbs machine-pressed into both member sides.

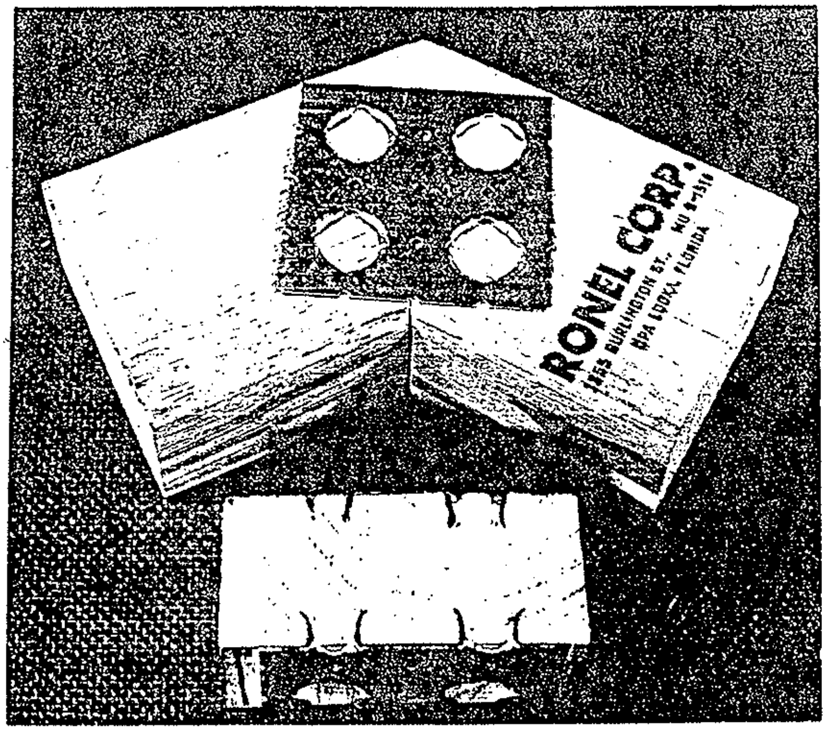

Fig. 15.- Ridge connection of trussed rafter assembled with BARBGRIP metal connector plates with barbs machine-pressed into both member sides, front view and cross-section through barbs.

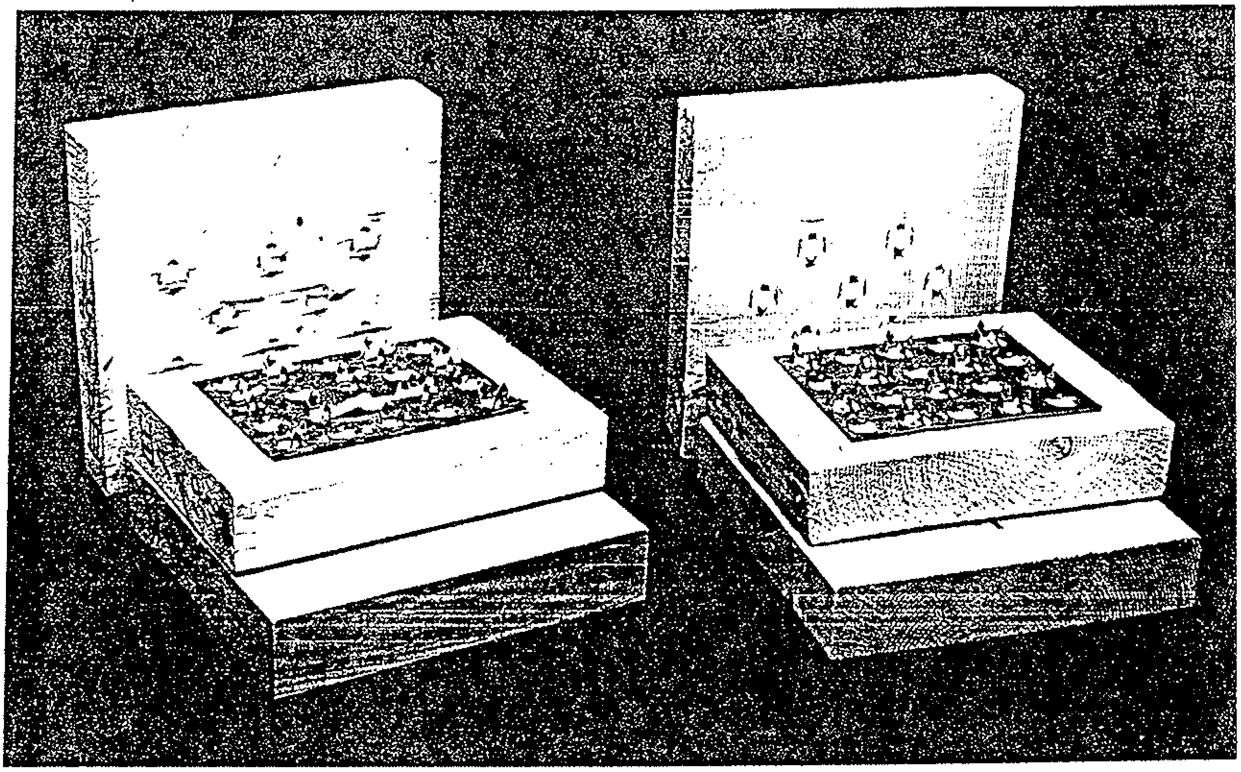

Fig. 16.- Three-member connection of parallel-arranged wood members assembled with metal connector plates with barbs projecting into both directions from plate area and plates placed between wood members, with one side member removed for inspection.

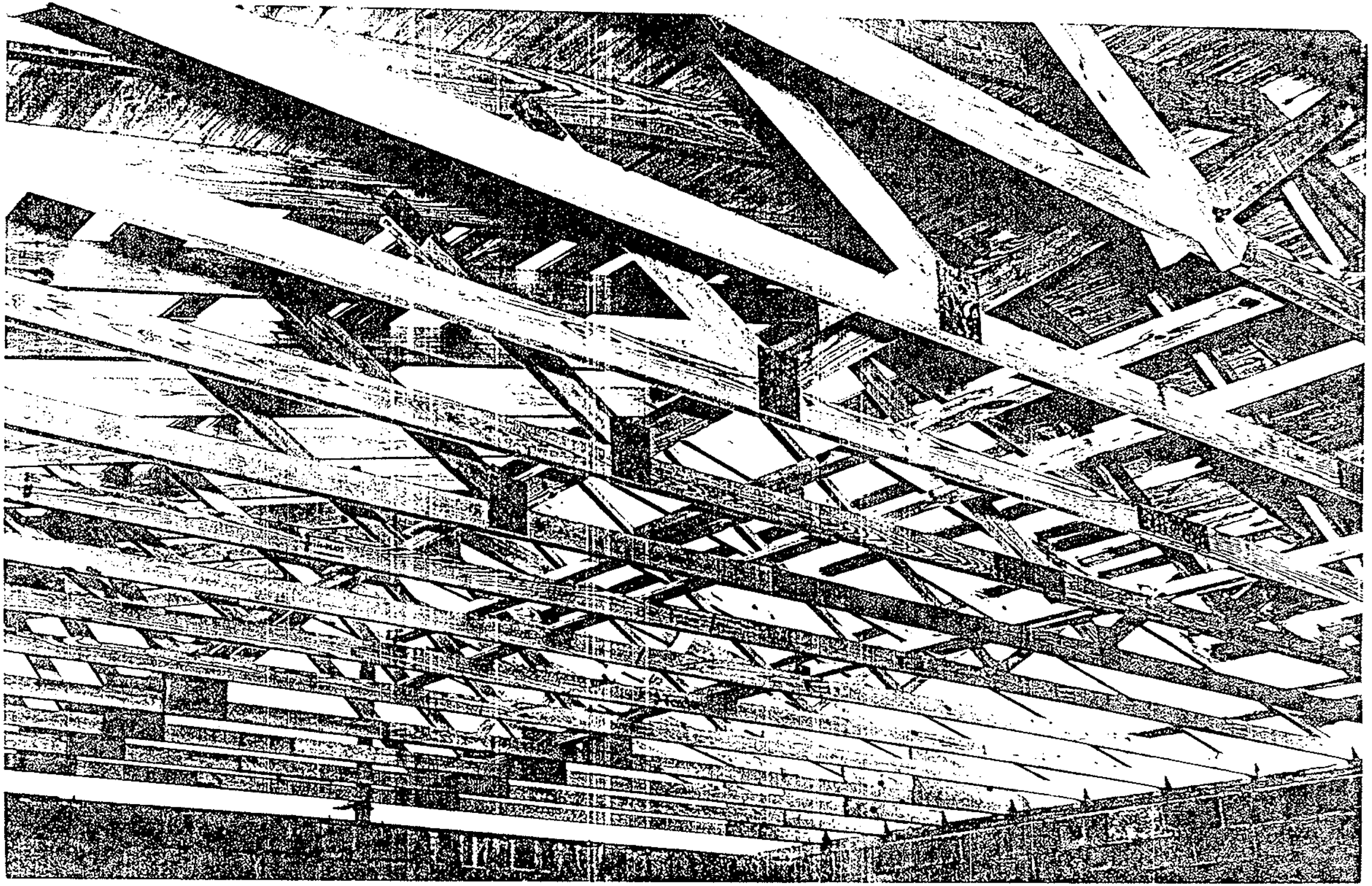

Fig. 17.- Some of the 21 trussed rafters used for roof construction of Architectural Laboratory Building at Virginia Polytechnic Institute and State University. From back to front, nail-glued, TIM-plate connected, H-BRACE connected, and split-ring connected trussed rafters.

91112201

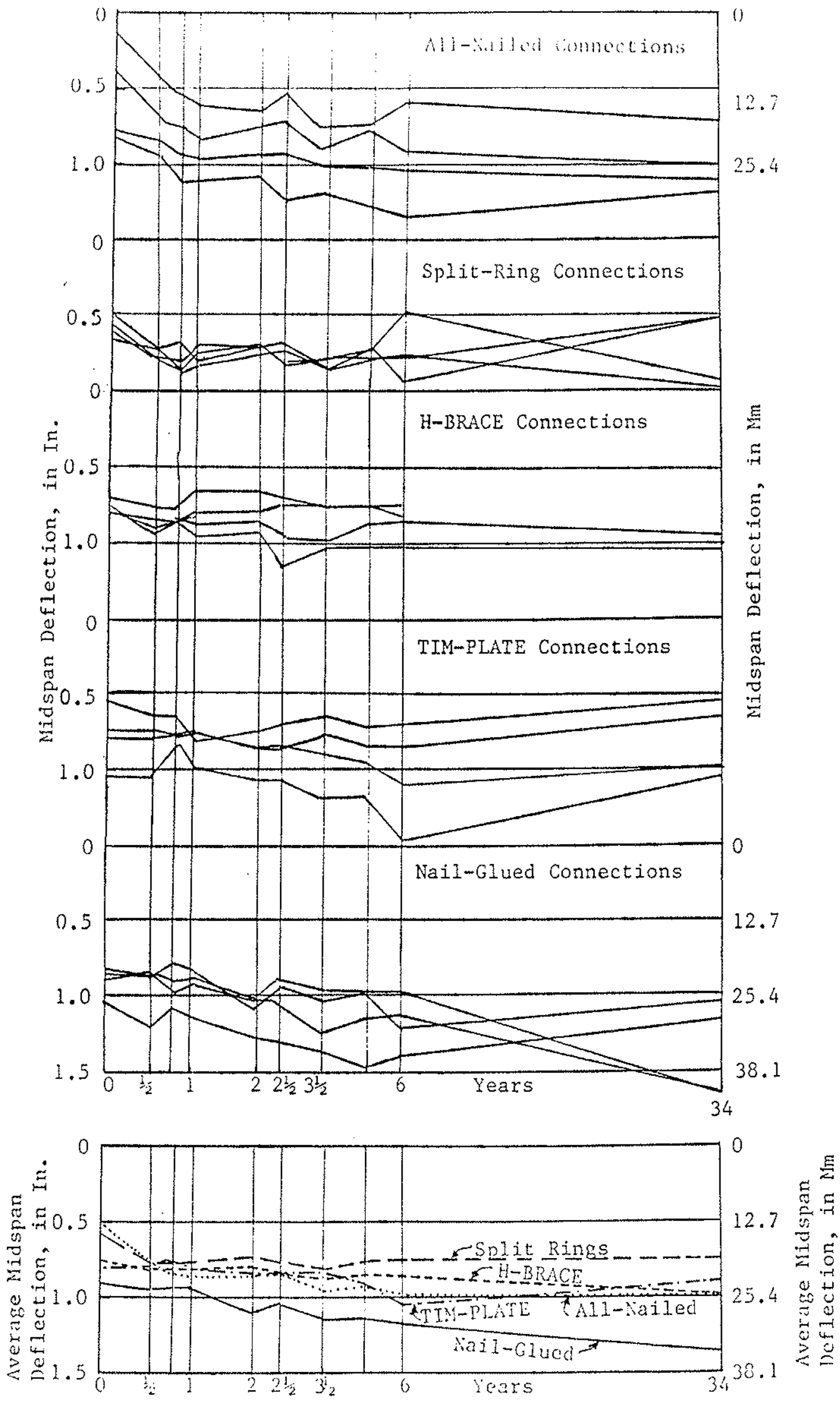

Fig. 18.- Midspan deflection of five types of trussed rafters at VPI&SU Architectural Laboratory Buildings during 34 years of service.

Fig. 19.- Contact side of plywood gusset plate of nail-glued trussed rafter, located next to the gable end of the VPI&SU Architectural Laboratory Building, after removal 3½ years after trussed-rafter installation from connection by pulling the nails, samples of which are shown. Note complete glue coverage, minimal wood failure, almost 100% glue failure, and mold formation.

CIB-W18/25-7-6

INTERNATIONAL COUNCIL FOR BUILDING RESEARCH STUDIES AND DOCUMENTATION

WORKING COMMISSION W18 - TIMBER STRUCTURES

CHARACTERISTIC STRENGTH OF SPLIT-RING AND SHEAR-PLATE CONNECTIONS

by

H J Blass
Technical University of Delft
The Netherlands
J Ehlbeck
M Schlager
University of Karlsruhe
Germany

MEETING TWENTY - FIVE

ÅHUS

SWEDEN

AUGUST 1992

Characteristic strength of split-ring and shear-plate connections

H.J. Blass, J. Ehlbeck and M. Schlager

Introduction

During the last CEN TC 124 WG4 meeting in Trento, Italy, the convenor of WG4 presented a calculation model describing the load-bearing behaviour of split-ring and shear plate connections subjected to tensile forces parallel to the grain. Using this model existing test data are evaluated to determine characteristic strength values of split-ring and shear-plate connections. The result of the evaluation is compared to today's allowable loads of this type of mechanical timber connections.

Calculation model

The model used to describe the failure of split-ring and shear-plate connections assumes a shear block failure of the wood in front of the connector [1]. The embedment stresses which in reality are unevenly distributed over the half circle of the split-ring are assumed to be uniformly distributed and acting parallel to the load direction. The embedment stresses are then transferred through shear stresses into the tension member (see Fig. 1). For tension members the capacity of the bolt is neglected, since the bolt usually is placed in oversized holes and only just starts bearing when the split-ring connection fails. Figure 2 shows a failed tension test specimen with shear failure both in the middle and one side member.

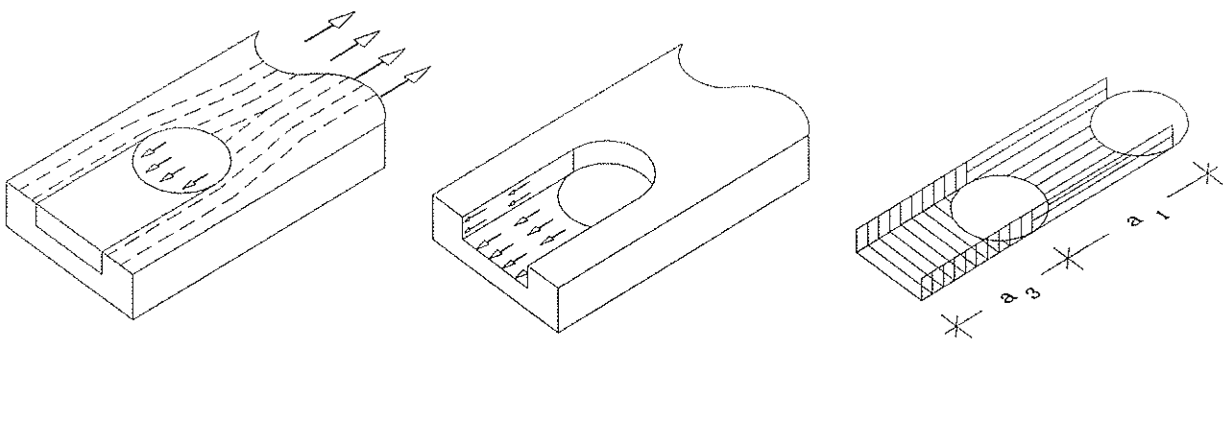

Fig. 1: Stresses in a split-ring joint and corresponding shear areas

The capacity of the connection consequently depends on the shear area in front of the connector and on the shear strength of the wood. The shear area within the connector is not taken into account since in most tests the wood core within the connector sheared off before the ultimate load of the connection was reached.

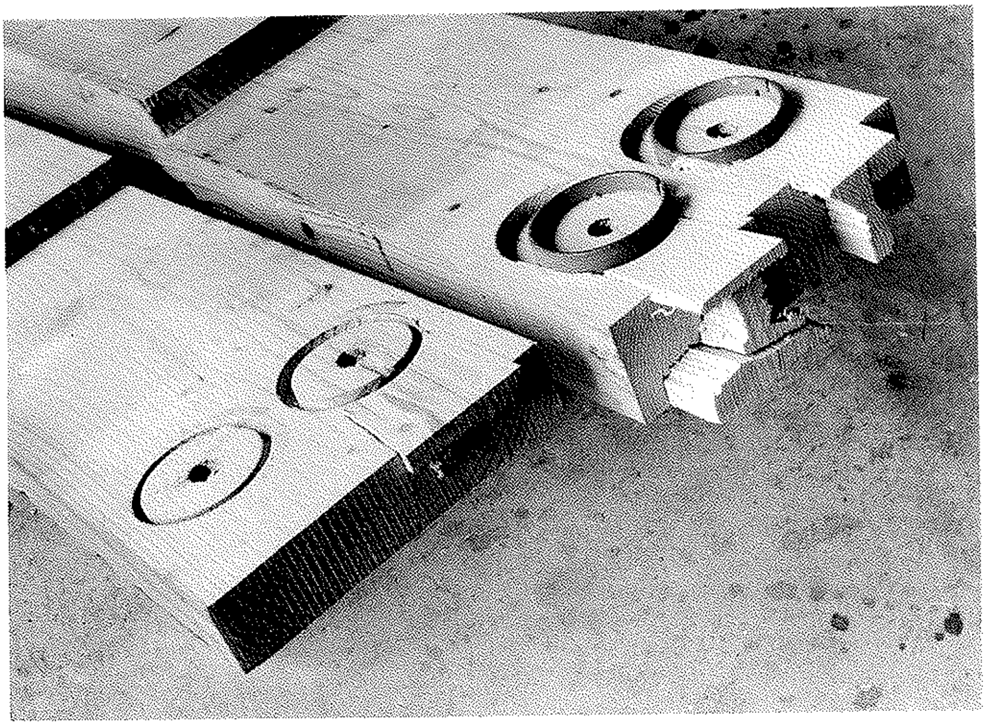

Fig. 2: Shear failure of middle and side member in a split-ring connection loaded in tension

The load bearing capacity of a split-ring or shear-plate connector loaded in tension parallel to the grain can therefore be written as:

$$\mathbf{R_c = f_v \cdot A_s} \qquad (1)$$

where

R_c = load bearing capacity of one connector,
f_v = apparent or average shear strength and
A_s = shear area per connector.

The apparent shear strength decreases with increasing shear area. In [1] the following relation between the apparent shear strength and the shear area is proposed:

$$\mathbf{f_v = K \cdot A_s^{-0,25}} \qquad (2)$$

Hence, the load bearing capacity of a split-ring or shear-plate connector results as:

$$R_c = K \cdot A_s^{0,75} \quad (3)$$

For a joint with one connector per shear plane the shear area is (see Fig. 1):

$$A_s = (d_c + h_c) \cdot a_{3,t} - \pi \cdot d_c^2 / 8 \quad (4)$$

where

d_c = connector diameter
h_c = connector height for split-ring connectors and twice the connector height for shear-plate connectors
$a_{3,t}$ = loaded end distance.

For joints with several connectors arranged in a line, the shear area for the second and each further connector is:

$$A_s = (d_c + h_c) \cdot a_1 - \pi \cdot d_c^2 / 4 \quad (5)$$

where

a_1 = connector spacing parallel to the grain.

For connectors arranged in a staggered pattern, the shear area per connector can be calculated by determining the corresponding average shear area from the joint geometry.

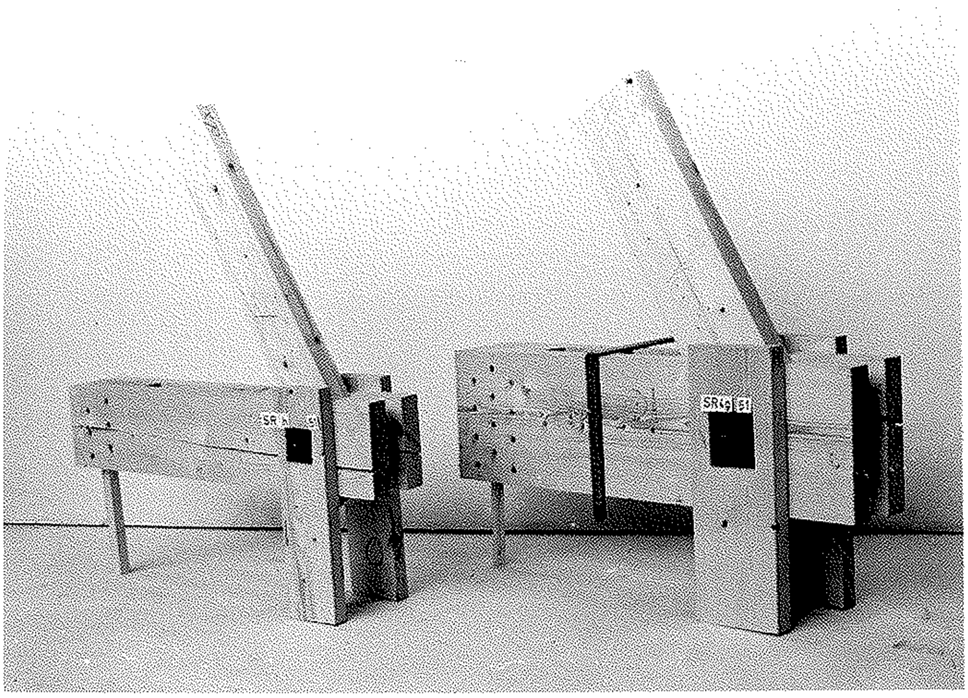

Fig. 3: Splitting failure of split ring connections loaded under an angle to the grain

Connector joints loaded in tension under an angle of more than 30° to the grain or in compression, respectively, show different failure modes. Connections with load-grain angles between about 30° and 150° show a splitting failure mode, whereas compression joints fail in a combined embedding-splitting failure mode (see Figs. 3 and 4). The sometimes considerable deformation of bolts in failed compression joints indicates a load sharing between bolt and connector for this type of loading.

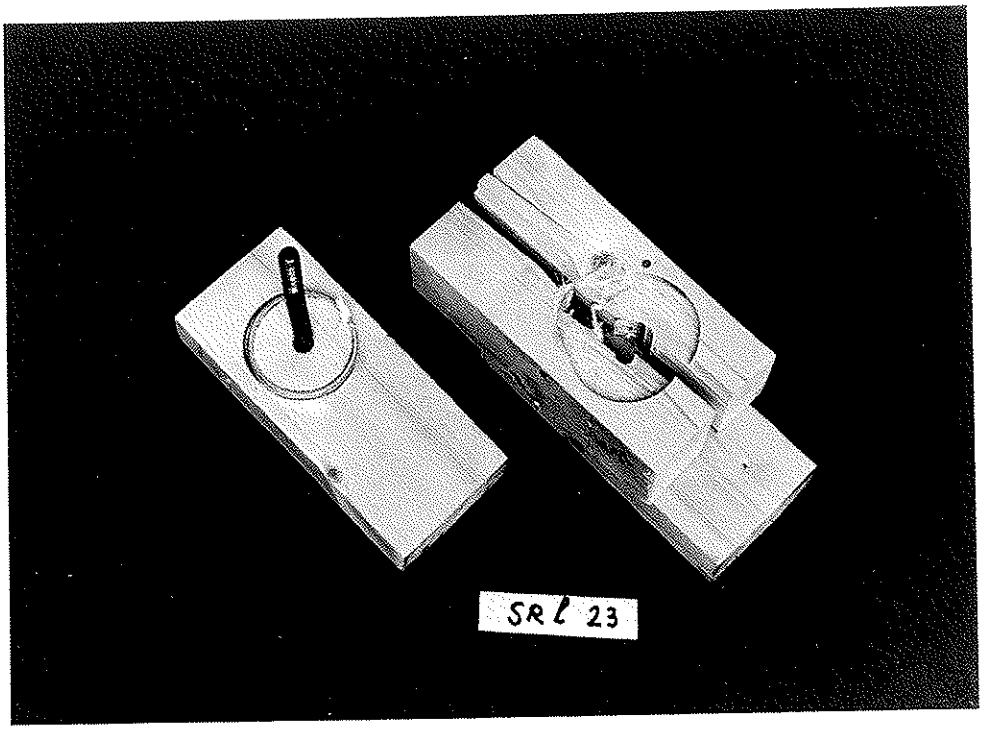

Fig. 4: Embedding-splitting failure of a split ring connection loaded in compression

Tests with split-ring and shear-plate connections

The tests reported here [2 - 24] were performed in the Stevin-Laboratory of Delft University of Technology between 1957 and 1991. One shear-plate diameter, 67 mm, and two split-ring diameters, 73 mm and 112 mm, were used. A total amount of 908 tests were evaluated. Table 1 gives the number of tests with the different configurations of species, connector diameter, angle between force and grain direction and number of connector units of the test specimens. Tests with an angle of 0° are tension tests parallel to the grain, whereas an angle of 180° denotes a compression test. Since all tests have been carried out as double-shear tests, one connector unit stands for two connectors and one bolt.

The test procedure of those tests carried out before 1962 includes two deloading steps from 50% and 70%, respectively, of the estimated maximum load F_{est} down to 10% of F_{est} and a third deloading from 90% down to 30% of F_{est}. The time necessary to reach the ultimate load was about 20 minutes. From 1962 on the tests followed the procedure described in EN 26891 with one deloading step from 40% to 10% of the estimated maximum load. In the evaluation of the test results, the influence of the different test procedures on the results has been neglected.

Table 1: Species, connector diameter, load-grain angle and number of connector units of the tested connections

Load-grain angle and number of connectors per shear plane	Timber species and connector diameter [mm]						
	Spruce 73	Spruce 112	Spruce Steel 67	Yang 73	Yang 112	Afzelia 73	Sum
0°/1	227	28	30	20	10	5	320
0°/2	48	56	10	5	-	-	119
0°/3	25	-	-	-	-	-	25
30°/1	35	49	-	-	-	-	84
45°/2	3	-	-	-	-	-	3
60°/1	30	40	-	4	10	5	89
60°/2	-	-	-	4	-	-	4
70°/1	21	-	-	-	-	-	21
180°/1	79	34	10	5	10	5	143
180°/2	40	15	-	-	-	-	55
180°/3	45	-	-	-	-	-	45
Sum	553	222	50	38	30	15	908

The purpose of the tests originally was to establish allowable loads for timber connections with split-rings and shear-plates for the Dutch timber code. A large number of tests was necessary to estimate the influence of parameters like moisture content, end and edge distance or timber dimensions on the ultimate load of connector joints. Table 2 shows the range of those parameters covered by the reported tests. The spacing a as given in Table 2 is the actual distance between two connectors, independent of the connector arrangement ($a = (a_1^2 + a_2^2)^{0,5}$).

Table 2: Range of related specimen dimensions and of moisture content

	a_3/d_c	a/d_c	t_m/h_c	t_s/h_c	b_m/d_c	moisture content
Tension						
Average	1,57	1,66	2,56	2,06	1,55	14,6
Maximum	3,42	2,55	3,09	3,54	2,64	27,1
Minimum	0,89	1,18	1,63	1,13	1,27	9,0
Number	665	151	645	645	665	417
Compression						
Average	1,25	1,67	2,73	1,89	1,77	14,2
Maximum	1,61	2,55	3,09	2,92	3,12	18,0
Minimum	0,89	1,18	1,63	1,17	1,27	10,0
Number	243	100	243	233	243	143

Evaluation of the tests

From the ultimate load and the timber dimensions the parameter K according to equation (3) was determined for each test specimen. To take into account the influence of the moisture content, the value of the parameter K was then multiplied by 1.24 if the average moisture content of the timber members exceeded 20%. The factor 1.24 was derived from the average ratio of the k_{mod}-values for service class 1/2 and 3, respectively, according to draft Eurocode 5 Part 1, 3.2.4 (Working draft Christmas 1991).

The influence of the member thickness was taken into account as follows: If the middle and side member thicknesses exceeded minimum values of 2.5 and 1.67 times the connector height h_c, respectively, the thickness factor applied was 1.0. If those minimum thickness values were not reached, the factor applied was the ratio between the minimum and the actual thickness.

The different characteristic density of the timber used for the joint specimens required a third modification factor for the parameter K. Apart from spruce with an assumed characteristic density of 380 kg/m^3, the tropical hardwood species Yang and Afzelia were used for split-ring connections. Based on data in [25], the characteristic density of those two species was estimated to 560 kg/m^3 for Yang and 680 kg/m^3 for Afzelia. The modification factor applied was the square root of the ratio of the characteristic values of the density.

For each test, the parameter K consequently was determined as:

$$K = (R_c \ / \ A_s^{0.75}) \cdot k_1 \cdot k_2 \cdot k_3 \qquad (6)$$

where

k_1 = modification factor moisture content

k_1 = 1.24 for moisture content exceeding 20%

k_1 = 1 for moisture content below 20%

k_2 = modification factor member thickness

k_2 = 1
if $t_m \geq 2.5\ h_c$ and $t_s \geq 1.67\ h_c$

k_2 = max $(2.5\ h_c/t_m;\ 1.67\ h_c/t_s)$
if $t_m < 2.5\ h_c$ and/or $t_s < 1.67\ h_c$

k_3 = modification factor characteristic density of timber

k_3 = $(380/\rho_k)^{0.5}$

t_m = middle member thickness

t_s = side member thickness

Table 3 shows the average, standard deviation, maximum and minimum values as well as the non-parametric 5-percentile value of the parameter K in $N/mm^{1.5}$ according to equation (6) for the tension specimens.

Although the calculation model only describes the behaviour of tension specimens loaded under an angle up to about 30°, equation (6) has been applied to all tested connector joints. Apart from the specimens with one connector unit loaded under an angle of 70° with a very large end distance of 250 mm, the model gives rather uniform results with respect to the 5-percentile value of the parameter K.

This can be explained by the fact that the end distance and the connector spacing also influence the ultimate load for other failure modes than block shearing. If splitting is the governing failure mode, an increased end distance obviously increases the area loaded in tension perpendicular to the grain up to a certain extent. The same applies for embedding failure, which is nearly always combined with the splitting of the wood through the bolt hole (see Fig. 4).

Only if the end distance becomes very large and the failure mode does not include splitting, a further increase of connection strength with increasing end distance cannot be expected. In this case, the value of the parameter K becomes unrealistically low.

Table 3: Average, standard deviation, maximum and minimum values and non-parametric 5-percentile value of the parameter K for different tension test configurations

test configuration	average	standard deviation	maximum	minimum	5-percentile	number
one connector 0°	30.2	8.28	72.8	14.7	19.6	320
two connectors 0°	26.1	4.34	38.4	15.6	20.3	119
three connectors 0°	27.8	3.54	32.9	21.2	21.7	25
all 0°	29.0	7.48	72.8	14.7	20.0	464
one connector 30°	36.6	9.00	54.9	14.0	20.4	84
one connector 60°	32.1	6.89	55.2	20.0	22.6	89
one connector 70°	37.2	3.86	44.6	30.2	31.5	11
all	30.5	8.03	72.7	14.0	20.1	655

For the compression tests, Table 4 contains the corresponding values of the parameter K according to equation (6). Since the bolt takes over part of the load in connector joints loaded in compression, the load carrying capacity of the bolt was deducted from the ultimate load per connector before calculating the parameter K. Here, the ultimate load per connector denotes the ultimate test load of the connection divided by the number of connectors. The characteristic value of the bolt capacity was determined according to draft Eurocode 5 Part 1, 6.2 (Working draft Christmas 1991). A value of 320 N/mm^2 was assumed for the mean value of tensile and yield strength of the bolt steel.

The results of the tension test evaluation show no indication of an influence of number of connectors for up to three connector units per joint. The same applies for the compression joints where a clear relation between the 5-percentile value of the parameter K and the number of connector units per joint cannot be established.

Table 4: Average, standard deviation, maximum and minimum values and non-parametric 5-percentile value of the parameter K for different compression test configurations

test configuration	average	standard deviation	maximum	minimum	5-percentile	number
one connector 180°	44.3	14.0	85.4	21.1	25.6	143
two connectors 180°	27.9	6.89	41.7	13.8	18.6	55
three connectors 180°	34.4	11.3	63.8	20.9	22.4	45
all 180°	38.7	14.0	85.4	13.8	21.7	243

Although the number of tests with load-grain angles between 30° and 70° is not very large, the 5-percentile value of the parameter K also seems to be independent of the load-grain angle in this area.

Design proposal

Based on the results of tests with split-ring and shear-plate connections, the following equation to determine the characteristic strength per connector of joints with up three split-ring or shear-plate connector units, respectively, is proposed:

$$\mathbf{R_{c,k} = K \cdot A_s^{0,75} \; / \; (k_1 \cdot k_2 \cdot k_3) \; + \; \eta \cdot R_{b,k}} \qquad \mathbf{(7)}$$

where

K = 20 $N/mm^{1.5}$

A_s = shear area per connector according to Fig. 1 in mm^2

k_1, k_2, k_3 = modifying factors taking into account the influence of moisture content, member thickness and characteristic density (see equation (6))

η = 0 for load-grain angles between 0° and less than 150°

η = 1 for load-grain angles between 150° and

180°

$R_{b,k}$ = characteristic load-carrying capacity of the bolt in N according to Eurocode 5 Part 1

Comparison with allowable loads

In order to compare today's allowable loads of split-ring and shear-plate connections with the characteristic load-carrying capacities according to equation (7), the ratios between the characteristic strength and the corresponding allowable loads according to the Dutch NEN 3852 "TGB Hout" and the German DIN 1052 "Holzbauwerke - Berechnung und Ausführung" have been calculated. The calculation is based on double-shear tensile joints in service class 1/2, a load-grain angle of 0° and one connector unit per joint. The timber dimensions and the end distances have been chosen to fulfil the respective minimum code requirements.

Table 5: Ratio between characteristic connection strength and allowable loads according to Dutch and German standards

Standard	d_c [mm]	h_c [mm]	t_m [mm]	t_s [mm]	a_3 [mm]	$R_{c,k}$ [kN]	$R_{c,all}$ [kN]	$R_{c,k}/R_{c,all}$
NEN 3852	73	19.1	39	27	140	17.3	8.0	2.16
	73	19.1	45	33	140	20.0	8.5	2.35
	73	19.1	58	39	140	21.2	9.5	2.23
	112	24	45	33	180	24.8	13.0	1.91
	112	24	58	39	180	32.0	14.5	2.21
	112	24	70	45	180	33.1	16.0	2.07
DIN 1052	65	30	60	40	140	17.9	11.5	1.56
	80	30	60	50	180	24.1	14.0	1.72
	95	30	60	60	220	30.8	17.0	1.81
	126	30	60	60	250	39.0	20.0	1.95
	128	45	60	60	300	33.2	28.0	1.19
	160	45	100	100	340	67.9	34.0	2.00
	190	45	100	100	430	90.0	48.0	1.87

Table 5 contains the connector and timber dimensions, the allowable loads and the characteristic strength values of all split-ring and shear-plate connectors listed in the two standards. The ratio between the characteristic joint strength and the allowable load corresponds to the product of the partial safety coefficients for actions and resistance, respectively, divided by the modifying factor k_{mod}.

The comparatively low values of the ratio between characteristic strength and allowable loads according to DIN 1052 are mainly caused by the low minimum member thicknesses related to the connector height.

Conclusions

In order to establish characteristic strength values of split-ring and shear-plate connections old test data have been evaluated. The results of the evaluation show the suitability of a calculation model presented and discussed in Working Group 4 of CEN TC 124. This model assumes a block shear failure mode for joints loaded in tension. The influence of the bolt on the load-bearing capacity is neglected. Besides, the model provides consistent results also for joints loaded under an angle to the grain. For joints loaded in compression, the capacity of the bolt may additionally be taken into account.

An influence of number of connector units per joint could not be found within the range covered by the test data. The same applies to the influence of the angle between load and grain direction. For angles up to 70° the 5-percentile value of the strength per connector was independent of the load-grain angle.

The results of this evaluation may serve as a basis for determining characteristic values for split ring and shear plate connections in EN.TC 124.402. The authors ask for further available test data from other institutions to include them into the evaluation.

References

[1] Steurer, A. 1981. Einführung in die Norm SIA 164 (1981) Holzbau. Publikation Nr. 81-1, Kapitel 8 Einlass- und Einpressdübel, Baustatik und Stahlbau, ETH Zürich, Switzerland.

[2] Kuipers, J. 1956.
Onderzoek naar de invloed van de houtdikte op het draagvermogen van ringdeuvelverbindingen.
Rapport 4-56-2-HV-2, Stevin-Laboratorium, Delft University of Technology, Netherlands.

[3] Kuipers, J. 1956.

Onderzoek naar het draagvermogen van houtverbindingsmiddelen.
Rapport 4-56-1-HV-1, Stevin-Laboratorium, Delft University of Technology, Netherlands.

[4] Kuipers, J. 1956.
Onderzoek naar het draagvermogen van houtverbindingsmiddelen. De rechte eenassige tweevoudige trekverbinding.
Rapport 4-56-3-HV-3, Stevin-Laboratorium, Delft University of Technology, Netherlands.

[5] Kuipers, J. 1957.
Aanvullend onderzoek naar het draagvermogen van meer--assige ringdeuvel-drukverbindingen.
Rapport 4-57-4-HV-8, Stevin-Laboratorium, Delft University of Technology, Netherlands.

[6] Kuipers, J. 1957.
Onderzoek naar het draagvermogen van houtverbindingsmiddelen. De twee- en drie-assige, op druk belaste ringdeuvelverbindingen.
Rapport 4-57-1-HV-5, Stevin-Laboratorium, Delft Univerity of Technology, Netherlands.

[7] Kuipers, J. 1957
Onderzoek naar het draagvermogen van houtverbindingsmiddelen. De twee- en drieassige, op trek belaste ringdeuvelverbindingen.
Rapport 4-57-2-HV-6, Stevin-Laboratorium, Delft University of Technology, Netherlands.

[8] Kuipers, J. 1959.
Proeven op rechte ringdeuvelverbindingen met verschillend vochtgehalte in het hout, en met een afwijkende eindafstand.
Rapport 4-59-3-HV-17, Stevin-Laboratorium, Delft University of Technology, Netherlands.

[9] Kuipers, J. 1961.
Druk- en trekproeven op rechte, een-assige verbindingen met TECO-ringdeuvels 112 mm (4").
Rapport 4-61-13-R-1, Stevin-Laboratorium, Delft University of Technology, Netherlands

[10] Kuipers, J. 1973.
De sterkte van verbindingen met plaatdeuvels 67 mm bij toepassing van volgplaten met verschillende afmetingen.
Rapport 4-73-5-V-17, Stevin-Laboratorium, Delft University of Technology, Netherlands

[11] Kuipers, J. and P.B.J. Kurstjens. 1986.
Creep and damage research on timber joints. Part one.
Rapport 4-86-15-HD-23, Stevin-Laboratorium, Delft University of Technology, Netherlands.

[12] Kurstjens, P.B.J. 1984.

Duurproeven ter bestudering van het verband tussen belastingduur en sterkte bij houtverbindingen. Sterkteverminderingsproeven.
Rapport 4-84-4-HD-21, Stevin-Laboratorium, Delft University of Technology, Netherlands.

[13] Kurstjens, P.B.J. 1989.
Creep and damage research on timber joints. Part two.
Rapport 25.4-89-15/C/HD-24, Stevin-Laboratorium, Delft University of Technology, Netherlands.

[14] Kurstjens, P.B.J. 1990.
Creep and damage research on timber joints. Part three.
Rapport 25.4-90-12/C/HD-26, Stevin-Laboratorium, Delft University of Technology, Netherlands.

[15] Kurstjens, P.B.J. and P. Stolle. 1991.
Creep and damage research on timber joints. Part four.
Rapport 25.4-91-06/C/HD-28, Stevin-Laboratorium, Delft University of Technology, Netherlands.

[16] Schippers, J. 1962.
Proeven op scheve, een-assige verbindingen met TECO-ringdeuvels 73 mm.
Rapport 4-62-1-HV26, Stevin-Laboratorium, Delft University of Technology, Netherlands.

[17] Schippers, J. 1962.
Proeven op 2-assige rechte verbindingen met TECO-ringdeuvels 112 mm.
Rapport 4-62-10-R-3, Stevin-Laboratorium, Delft University of Technology, Netherlands.

[18] Schippers, J. 1962.
Proeven op scheve, 2-assige verbindingen met TECO-ringdeuvels 73 mm.
Rapport 4-62-13-HV27, Stevin-Laboratorium, Delft University of Technology, Netherlands.

[19] Schippers, J. 1964.
Proeven op rechte en scheve 1-assige verbindingen met TECO-ringdeuvels 112 mm en 73mm.
Rapport 4-64-3-R-4, Stevin-Laboratorium, Delft University of Technology, Netherlands.

[20] Vermeyden, P. 1962.
Duurproeven ter bestudering van het verband tussen belastingduur en sterkte bij houtverbindingen: bepaling van de breukbelastingen.
Rapport 4-62-11-HD-10, Stevin-Laboratorium, Delft University of Technology, Netherlands.

[21] Vermeyden, P. 1963.
Proeven op ringdeuvel- en draadnagelverbindingen vervaardigd uit hout met lage druksterkte.
Rapport 4-63-17-V-5, Stevin-Laboratorium, Delft Univer-

sity of Technology, Netherlands.

[22] Vermeyden, P. 1967.
Proeven op ring- en plaatdeuvelverbindingen in vurehout; onderzoek naar de invloed van bout, resp. draadeind.
Rapport 4-67-13-R-11, Stevin-Laboratorium, Delft University of Technology, Netherlands.

[23] Vermeyden, P. 1967.
Proeven op ringdeuvelverbindingen in yang.
Rapport 4-67-1-R-8, Stevin-Laboratorium, Delft University of Technology, Netherlands.

[24] Vermeyden, P. and N.H. van Leeuwen. 1967.
Ringdeuvelverbindingen in loofhout. Enkele houteigenschappen, proefresultaten van verbindingen in afzelia en voorstel toelaatbare belastingen.
Rapport 4-67-10-R-10, Stevin-Laboratorium, Delft University of Technology, Netherlands.

[25] Laming, P.B, J.F. Rijsdijk and J.C. Verwijs. 1978.
Houtsoorten. Informatie voor de praktijk.
Houtinstituut TNO, Delft, Netherlands.

CIB-W18/25-7-7

INTERNATIONAL COUNCIL FOR BUILDING RESEARCH STUDIES AND DOCUMENTATION

WORKING COMMISSION W18 - TIMBER STRUCTURES

CHARACTERISTIC STRENGTH OF TOOTH-PLATE CONNECTOR JOINTS

by

H J Blass

Technical University of Delft

The Netherlands

J Ehlbeck

M Schlager

University of Karlsruhe

Germany

MEETING TWENTY - FIVE

ÅHUS

SWEDEN

AUGUST 1992

Characteristic strength of tooth-plate connector joints

H.J. Blass, J. Ehlbeck and M. Schlager

Introduction

The change of code formats in European timber codes from an allowable load format towards a partial safety coefficient format requires characteristic strength values of the material and of connections. For joints with pin-type fasteners, the characteristic connection strength can be calculated using a solution based on the work of Johansen [1]. Eurocode 5 provides those equations to calculate single and double-shear joints with nails, screws, dowels or bolts based on the joint geometry and the strength of the timber and the fastener. For other types of mechanical timber joints, characteristic strength values have still to be determined. The members of CEN TC 124 WG4 have the task to establish characteristic strength values for connector joints. During the last CEN TC 124 WG4 meeting in Trento, Italy, a calculation model describing the load-bearing capacity of tooth-plate connections was presented. Using this model existing test data are evaluated to determine characteristic strength values of tooth-plate connections. The result of the evaluation is compared to today's allowable loads of this type of mechanical timber connections.

Calculation model

The model used to describe the load-carrying capacity of tooth-plate connections is based on the assumption of a load-sharing between tooth plate connector and bolt. The connection strength can therefore be described by:

$$\mathbf{R_{j,k} = R_{c,k} + \eta \cdot R_{b,k}} \tag{1}$$

where

$R_{j,k}$ = characteristic load-carrying capacity of the tooth plate connection containing both tooth plates and bolts

$R_{c,k}$ = characteristic load-carrying capacity of the tooth plate connector

$R_{b,k}$ = characteristic load-carrying capacity of the bolt according to Eurocode 5 Part 1

η = factor between 0 and 1 to account for the effect of load distribution between tooth-plate connector and bolt

An evaluation of the allowable loads of tooth-plate connectors according to DIN 1052 "Holzbauwerke - Berechnung und Ausführung" resulted in the following relation between the load-carrying capacity of a circular tooth-plate connector and its diameter:

$$R_{c,k} = A \cdot d_c^{1.5} \tag{2}$$

where

A = factor depending on the connector type to determine through tests

d_c = connector diameter

Tests with tooth-plate connections

The tests reported here [2 - 11] were performed in the Stevin-Laboratory of Delft University of Technology between 1957 and 1991. Only one type of tooth-plate connector, the Bulldog connector, was used. Circular connectors with diameters between 50 mm and 117 mm, two square shaped connectors with 100 mm and 130 mm side length and an oval connector 70 mm by 130 mm were tested in spruce specimens. A total amount of 426 tests has been evaluated. Table 1 gives the number of tests in the different configurations of connector dimension, angle between force and grain direction and number of connectors per shear plane of the test specimens. Tests with an angle of 0° are tension tests parallel to the grain, whereas an angle of 180° denotes a compression test. Since all tests have been carried out as double-shear tests, one connector unit stands for two connectors. Apart from 17 tests with one Bulldog ⌀ 75 mm per shear plane where two bolts were used, all tests have been carried out with one bolt per connector unit.

The failure mode of the tested specimens was in many cases embedding failure of the wood under both the connector teeth and the bolt. With increasing deformations, splitting and shear failure of the wood could be observed (see Fig. 1).

The test procedure of those tests carried out before 1962 includes two deloading steps from 50% and 70%, respectively, of the estimated maximum load F_{est} down to 10% of F_{est} and a third deloading from 90% down to 30% of F_{est}. The time necessary to reach the ultimate load was about 20 minutes. From 1962 on the tests followed the procedure described in EN 26891 with one deloading step from 40% to 10% of the estimated maximum load. In the evaluation of the test results, the influence of the different test procedures on the results has been neglected.

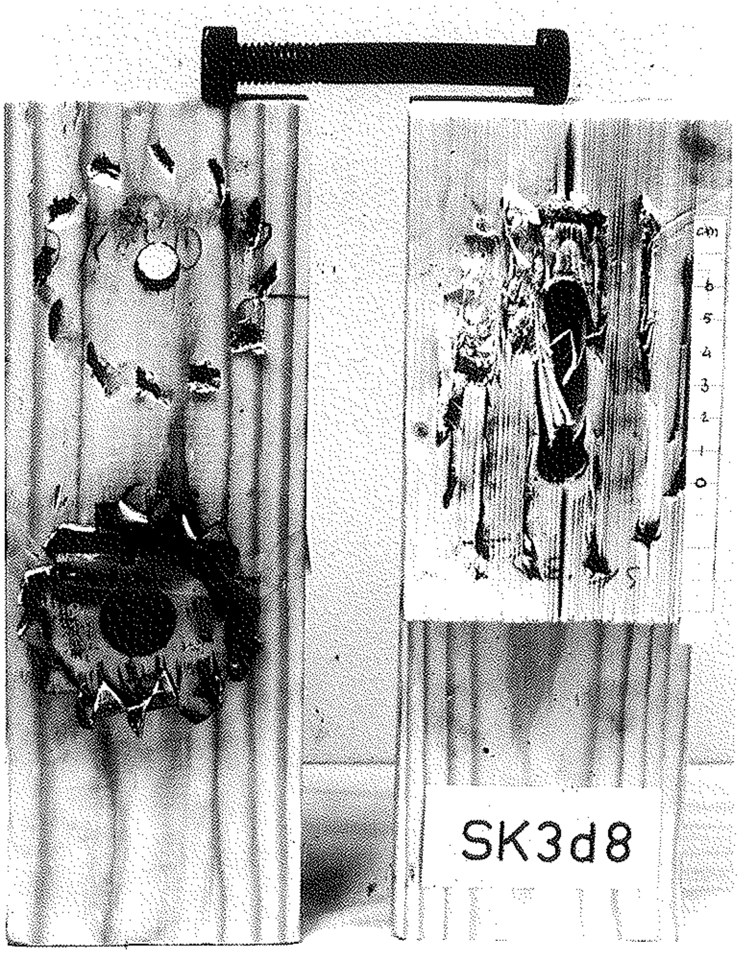

Fig. 1: Typical failure of a Bulldog tooth-plate connection

Table 1: Connector dimension, load-grain angle and number of connector units of the tested tooth-plate connections

Load-grain angle and number of connectors per shear plane	Tooth-plate connector dimensions [mm]								
	⊕ 50	⊕ 62	⊕ 75	⊕ 95	⊕ 117	square 100	square 130	70 x 130	Sum
0°/1	20	15	115	52	5	40	25	10	282
0°/2	-	-	25	39	-	5	-	5	74
0°/3	-	-	5	-	-	5	-	5	15
30°/1	-	-	10	-	-	10	-	-	20
60°/1	-	-	10	-	-	10	-	-	20
90°/1	-	-	5	-	-	5	-	-	10
180°/1	-	-	5	-	-	-	-	-	5
Sum	20	15	175	91	5	75	25	20	426

As for similar tests with split-ring and shear-plate connections, the purpose of the tests originally was to establish allowable loads for timber connections with Bulldog connectors for the Dutch timber code. Table 2 shows the range of the related parameters end distance, spacing, timber, bolt and connector dimensions covered by the reported tests. For the square and oval tooth plate connectors, a connector diameter d_c has been calculated which corresponds to a circle with the same area as the actual connector area. The spacing a as given in Table 2 is the actual distance between two connectors, independent of the connector arrangement ($a = (a_1^2 + a_2^2)^{0,5}$).

Table 2: Range of related dimensions and of moisture content

	a_3/d_c	a/d_c	t_m/h_c	t_s/h_c	b_m/d_c	a_3/d_b	a/d_b	moisture content
Average	1,14	1,53	2,48	1,37	1,27	6,48	8,70	13,6
Maximum	1,81	1,80	4,38	2,19	1,93	7,48	9,80	17,0
Minimum	0,68	1,28	1,53	0,88	1,12	4,02	6,41	9,0
Number	426	89	426	426	426	426	89	406

a_3 = end distance
a = connector spacing
d_c = connector diameter
h_c = connector height
t_m = middle member thickness
t_s = side member thickness
b_m = middle member width
d_b = bolt diameter

Evaluation of the tests

From the timber dimensions the characteristic load-carrying capacity of the bolt was determined for each specimen according to draft Eurocode 5 Part 1, 6.2 (Working draft Christmas 1991). A value of 320 N/mm^2 was assumed for the mean value of tensile and yield strength of the bolt steel. The characteristic density of the spruce was assumed to 380 kg/m^3. For those specimens, where the required loaded end distance of 7d for bolted connections was not reached, the corresponding characteristic embedding strength value of the timber was decreased by the factor k_a according to draft Eurocode 5 Part 1, Table 6.6a (Working draft Christmas 1991). The resulting load-carrying capacity of the bolt multiplied with the load-distribution factor η was then deducted from the ultimate load per connector before calculating the parameter A. Here, the ultimate load per connector denotes the ultimate test load of the connection divided by the number of connectors.

The parameter A according to equation (2) was determined for each test specimen. A modification to take into account the different moisture content of the test specimens has not been carried out since all specimens had an average moisture content within the range of service class 1/2 according to draft Eurocode 5 Part 1, 3.2.4 (Working draft Christmas 1991).

The influence of the member thickness was automatically taken into account through the calculation of the characteristic load-carrying capacity of the bolt. A further influence of member thickness on the connection capacity was not considered.

For each test, the parameter A consequently was determined as:

$$\mathbf{A} = (\mathbf{R}_{j,k} - \eta \cdot \mathbf{R}_{b,k}) / \mathbf{d}_c^{1.5} \tag{3}$$

Table 3 shows the average, standard deviation, maximum and minimum values as well as the non-parametric 5-percentile value of the parameter A in $N/mm^{1.5}$ according to equation (3) for the tested specimens and η = 1.0. The corresponding values for η = 0.9 and η = 0.8 are shown in Table 4 and 5, respectively.

Table 3: Average, standard deviation, maximum, minimum and non-parametric 5-percentile value of the parameter A for different test configurations and η = 1.0

test configur-ation	average	standard deviation	maximum	minimum	5-percen-tile	number
one connector 0°	20.1	4.28	37.3	11.0	14.8	282
two connectors 0°	23.6	5.36	33.0	8.3	15.3	74
three connectors 0°	19.1	4.10	25.2	12.8	13.4	15
all 0°	20.8	4.73	37.3	8.3	14.8	371
one connector 30°-180°	25.8	4.98	34.3	14.1	16.1	55
all	21.4	5.05	37.3	8.3	14.8	426

Table 4: Average, standard deviation, maximum, minimum and non-parametric 5-percentile value of the parameter A for different test configurations and η = 0.9

test configuration	average	standard deviation	maximum	minimum	5-percentile	number
one connector 0°	21.1	4.43	39.3	12.7	15.6	282
two connectors 0°	24.7	5.27	33.9	9.7	16.6	74
three connectors 0°	20.2	4.01	26.2	13.9	14.7	15
all 0°	21.8	4.82	39.3	9.7	15.5	371
one connector 30°-180°	26.6	5.00	35.1	14.8	16.8	55
all	22.4	5.13	39.3	9.7	15.5	426

Table 5: Average, standard deviation, maximum, minimum and non-parametric 5-percentile value of the parameter A for different test configurations and η = 0.8

test configuration	average	standard deviation	maximum	minimum	5-percentile	number
one connector 0°	22.0	4.60	41.2	13.5	16.3	282
two connectors 0°	25.8	5.19	34.8	11.2	17.7	74
three connectors 0°	21.4	3.92	27.2	15.0	15.9	15
all 0°	22.8	4.93	41.2	11.2	16.3	371
one connector 30°-180°	27.3	5.00	35.9	15.6	17.6	55
all	23.4	5.16	41.2	11.2	16.3	426

The results of the test evaluation show no indication of an influence of number of connectors on the strength per connector for up to three connector units per joint. Although the number of tests with load-grain angles between 30° and 180° is quite small, the 5-percentile value of the parameter A also seems to be independent of the load-grain angle.

Design proposal

Based on the results of tests with tooth-plate connections, the following equation to determine the characteristic connection strength per Bulldog connector and shear plane for joints with up to three connector units is proposed:

$$\mathbf{R_{j,k} = R_{c,k} + R_{b,k}} \tag{4}$$

where

$R_{j,k}$ = characteristic load-carrying capacity in N of the tooth plate connection containing both tooth plates and bolts

$R_{c,k}$ = characteristic load-carrying capacity in N of the tooth plate connector

$R_{b,k}$ = characteristic load-carrying capacity in N of the bolt according to Eurocode 5 Part 1

$$\mathbf{R_{c,k} = 15 \cdot d_c^{1.5}} \tag{5}$$

where

d_c = connector diameter for circular connectors and

d_c = $(4 \cdot A_c / \pi)^{0.5}$ for non-circular connectors

A_c = connector area

Comparison with allowable loads

In order to compare today's allowable loads of tooth-plate connections with the characteristic load-carrying capacities according to equation (4), the ratios between the characteristic strength and the corresponding allowable loads according to the Dutch NEN 3852 "TGB Hout" and the German DIN 1052 "Holzbauwerke - Berechnung und Ausführung" have been calculated. The calculation is based on double-shear tensile joints in service class 1/2, a load-grain angle of 0° and one connector unit per joint. The timber dimensions and the end distances have been chosen to fulfil the respective minimum code requirements.

Table 6 contains the connector and timber dimensions, the allowable loads and the characteristic strength values of all Bulldog-connectors listed in the two standards. The ratio between the characteristic joint strength and the allowable load corresponds to the product of the partial safety coefficients for actions and resistance, respectively, divided by the modifying factor k_{mod}.

Table 6: Ratio between characteristic connection strength and allowable loads according to NEN 3852 and DIN 1052

Stan-dard	d_c [mm]	d_b [mm]	t_m [mm]	t_s [mm]	$R_{c,k}$ [kN]	$R_{b,k}$ [kN]	$R_{c,all}$ [kN]	$R_{b,all}$ [kN]	ratio
NEN 3852	50	10	20	19	5.3	2.8	2.0	0.9	2.8
	62	12	26	19	7.3	4.3	3.0	1.4	2.63
	75	12	29	19	9.7	4.8	4.0	1.6	2.61
	95	16	38	25	13.9	8.0	5.5	2.7	2.65
	117	20	58	39	19.0	14.5	8.0	5.2	2.53
	100x100	16	32	21	18.0	6.7	7.0	2.3	2.66
	130x130	20	40	27	26.7	10.0	11.0	3.6	2.51
	70x130	16	58	39	15.2	10.1	6.0	4.2	2.49
DIN 1052	48	12	60	40	5.0	6.4	5.0	0	2.29
	62	12	60	40	7.3	6.4	7.0	0	1.97
	75	16	60	50	9.7	10.8	9.0	0	2.28
	95	16	60	50	13.9	10.8	12.0	0	2.06
	117	20	80	80	19.0	18.2	16.0	0	2.32
	140	24	80	80	24.8	22.7	22.0	0	2.16
	165	24	80	80	31.8	22.7	30.0	0	1.82
	100x100	20	60	60	18.0	15.0	17.0	0	1.94
	130x130	24	60	60	26.7	17.1	23.0	0	1.90

The allowable loads for bolts according to DIN 1052 are given as zero, since DIN 1052 only provides allowable loads for connector/bolt combinations. The ratios between the characteristic connection strength and the allowable loads according to DIN 1052 for those connectors with a diameter or a side length of 130 mm and more are in reality larger, because DIN 1052 requires one or two additional bolts per splice for these connectors at the splice ends.

Conclusions

In order to establish characteristic strength values of Bulldog tooth-plate connections old test data have been evaluated. The results of the evaluation show the suitability of a calculation model presented and discussed in Working Group 4 of CEN TC 124. This model assumes a load-sharing between bolt and connector. The characteristic load-bearing capacity of the connector has been determined on the basis of the assumption of a complete load-sharing.

An influence of number of connector units per joint could not be found within the range covered by the test data. The same applies to the influence of the angle between load and grain direction. Hence, the design proposal is based on independency between characteristic load-bearing capacity of a Bulldog tooth-plate connection and load-grain angle or number of fasteners, respectively. This applies to connections with up to three connector units.

The results of this evaluation may serve as a basis for determining characteristic values for tooth-plate connections in EN.TC 124.402. The authors ask for further available test data from other institutions to be able to extend the evaluation.

References

[1] Johansen, K.W. 1949.
Theory of timber connections.
IABSE publication 9:249-262.

[2] Kuipers, J. 1957.
Inleidend onderzoek naar het draagvermogen van kramplaatverbindingen.
Rapport 4-57-6-HV-10, Stevin-Laboratorium, Delft University of Technology, Netherlands.

[3] Kuipers, J. and P. Vermeyden. 1961.
Onderzoek van kramplaatverbindingen - Beproevingsresultaten trekverbindingen met Bulldog-kramplaten 75 mm en 95 mm.
Rapport 4-61-16-K-1, Stevin-Laboratorium, Delft University of Technology, Netherlands.

[4] Kuipers, J. and P.B.J. Kurstjens. 1986.
Creep and damage research on timber joints. Part one.
Rapport 4-86-15-HD-23, Stevin-Laboratorium, Delft Univer-

sity of Technology, Netherlands.

[5] Kurstjens, P.B.J. 1984.
Duurproeven ter bestudering van het verband tussen belastingduur en sterkte bij houtverbindingen. Sterkteverminderingsproeven.
Rapport 4-84-4-HD-21, Stevin-Laboratorium, Delft University of Technology, Netherlands.

[6] Kurstjens, P.B.J. 1989.
Creep and damage research on timber joints. Part two.
Rapport 25.4-89-15/C/HD-24, Stevin-Laboratorium, Delft University of Technology, Netherlands.

[7] Kurstjens, P.B.J. 1990.
Creep and damage research on timber joints. Part three.
Rapport 25.4-90-12/C/HD-26, Stevin-Laboratorium, Delft University of Technology, Netherlands.

[8] Kurstjens, P.B.J. and P. Stolle. 1991.
Creep and damage research on timber joints. Part four.
Rapport 25.4-91-06/C/HD-28, Stevin-Laboratorium, Delft University of Technology, Netherlands.

[9] Vermeyden, P. 1962.
Duurproeven ter bestudering van het verband tussen belastingduur en sterkte bij houtverbindingen: bepaling van de breukbelastingen.
Rapport 4-62-11-HD-10, Stevin-Laboratorium, Delft University of Technology, Netherlands.

[10] Vermeyden, P. 1962.
Literatuuronderzoek kramplaatverbindingen en voorstel onderzoekprogramma.
Rapport 4-62-3-K-2, Stevin-Laboratorium, Delft University of Technology, Netherlands.

[11] Vermeyden, P. 1963.
Proeven op kramplaatverbindingen.
Rapport 4-63-13-K-3, Stevin-Laboratorium, Delft University of Technology, Netherlands.

CIB-W18/25-7-8

INTERNATIONAL COUNCIL FOR BUILDING RESEARCH STUDIES AND DOCUMENTATION

WORKING COMMISSION W18 - TIMBER STRUCTURES

EXTENDING YIELD THEORY TO SCREW CONNECTIONS

by

T E McLain
Virginia Polytechnic Institute and State University
U S A

MEETING TWENTY - FIVE

ÅHUS

SWEDEN

AUGUST 1992

EXTENDING YIELD THEORY TO SCREW CONNECTIONS

T. E. McLain

SUMMARY

New design criteria for lag or coach screw connections to wood members are proposed. These equations are based on full consideration of all possible yield modes. The development of the equations is reviewed and a potential simplification is proposed which utilizes a fixed ratio of the yield moment in the screw thread to that in the shank. The result is three equations which may be applied to a wide range of steel and wood side plate geometries.

INTRODUCTION

Design provisions for connections with dowel-type fasteners in Eurocode 5 and codes of many countries are based on "yield theory." Johansen (1949) and later, Möller (1950), derived a set of predictive equations for the load-carrying capacity of joints with varying geometry. The accuracy of these equations for predicting a yield load in connections with bolts, nails or dowels have been confirmed by several research groups in recent years (eg. Whale and Smith 1986, Soltis et al 1986).

For laterally-loaded screw connections, however, applying yield theory may be problematic. This is because the geometry of the screw, primarily the length and characteristics of the threaded portion, may alter some of the yield patterns predicted using equations derived for prismatic fasteners. The purpose of this paper is to describe the results of a recent study made to extend the yield theory to laterally-loaded screw connections. This study was part of a major effort in the United States to incorporate European yield theory into working stress and limit states design codes.

For single shear bolt, nail or dowel connections, up to six possible yield modes may occur (Whale 1991). Loads for each possible mode are calculated and the minimum load is the characteristic load-carrying capacity. Besides component dimensions, the yield strength of the fasteners, sometimes expressed as yield bending moment, and a characteristic embedding stress or bearing strength are input to the yield equations. The yield properties of the fasteners are established by test or a minimum manufacturing specification. The embedding stress may be established as a function of fastener type and diameter, species density and the angle of the transferred shear force vector to the grain of the timber. Whale (1991) summarizes the levels of, and interrelationships between, these properties prescribed in Eurocode 5. Similar relationships have recently been established for North American species (Wilkinson 1991).

With single shear lag screw connections, some dowel yield modes are not possible; also, the fastener may yield in either the shank or the thread. Larsen and Reestrup (1969) identified three potential yield modes shown in Figure 1. Mode I (U.S. code nomenclature) represents bearing yield in the cleat or side member. Modes III and IV result from the formation of one or two yield points in the screw as shown. Mode II yielding, where the fastener rotates, causing bearing failure in both members, is found in bolted joints and is not possible in lag screw connections meeting minimum geometry specifications. Larsen and Reestrup (1969) derived predictive equations for these yield modes. This derivation is reviewed next.

YIELD EQUATIONS

The location of the yield point in the block or main member is important to the magnitude of the yield load for Modes III and IV. With SP as shown in Figure 2, define two values of SP, X_1, and X_2, that describe boundaries on the location of maximum moment and yield stress in the screw. If SP $\geq X_1$ then yield occurs in the shank at the point of maximum moment. If SP $\leq X_2$ then yielding occurs at the point of maximum moment which is in the threaded region. For $X_2 <$ SP $< X_1$ the maximum moment will be in the shank but the yield point is in the transition between shank and thread. Consequently, for each of Modes III and IV there are three yield equations corresponding to three possible yield locations. The resulting seven behavioral equations are shown below:

<u>MODE I</u>

$$P_y = \frac{d\, t_1\, f_2}{\beta} = d\, t_1\, f_1 \qquad (1)$$

<u>MODE III</u>

For $\frac{SP}{d} \geq \frac{X_1}{d}$:

$$P_y = \frac{t_1\, d\, f_2}{(2+\beta)} \left[\sqrt{\frac{2(1+\beta)}{\beta} + \frac{2\, f_y\, (2+\beta)}{3\, f_2\, (t_1/d)^2}} - 1 \right] \qquad (2)$$

For $\frac{SP}{d} \leq \frac{X_2}{d}$:

$$P_y = \frac{t_1\, d\, f_2}{(2+\beta)} \left[\sqrt{\frac{2(1+\beta)}{\beta} + \frac{2\, R_m\, f_y\, (2+\beta)}{3\, f_2\, (t_1/d)^2}} - 1 \right] \qquad (3)$$

For $\frac{X_2}{d} < \frac{SP}{d} < \frac{X_1}{d}$:

$$P_y = \frac{2\, t_1\, d\, f_2}{\beta} \left[\sqrt{\frac{(2+\beta)\, (SP/d)^2}{(t_1/d)^2} + \frac{(SP/d)^2}{(t_1/d)} + \frac{\beta R_m\, f_y}{6\, f_2\, (t_1/d)^2}} - \frac{SP}{t_1} - \frac{1}{2} \right] \qquad (4)$$

where:

$$\frac{X_1}{d} = \frac{(t_1/d)}{(2+\beta)} \left[\sqrt{\frac{2(1+\beta)}{\beta} \frac{2\, f_y\, (2+\beta)}{3\, f_2\, (t_1/d)^2}} - 1 \right] + \frac{1}{f_2} \sqrt{\frac{f_2\, f_y\, (1-R_m)}{3}} \tag{5}$$

$$\frac{X_2}{d} = \frac{(t_1/d)}{(2+\beta)} \left[\sqrt{\frac{2(1+\beta)}{\beta} + \frac{2\, R_m\, f_y\, (2+\beta)}{3\, f_2\, (t_1/d)^2}} - 1 \right] \tag{6}$$

<u>**MODE IV**</u>

For $\frac{SP}{d} \geq \frac{X_1}{d}$:

$$P_y = d^2 \sqrt{\frac{2\, f_y\, f_2}{3\, (1+\beta)}} \tag{7}$$

For $\frac{SP}{d} \leq \frac{X_2}{d}$:

$$P_y = d^2 \sqrt{\frac{f_y\, f_2\, (1+R_m)}{3\, (1+\beta)}} \tag{8}$$

For $\frac{X_2}{d} < \frac{SP}{d} < \frac{X_1}{d}$:

$$P_y = (SP/d)\, \frac{f_2\, d^2}{\beta} \left[\sqrt{\frac{f_y\, (1+R_m)\beta}{3\, (SP/d)^2\, f_2} + (1+\beta)} - 1 \right] \tag{9}$$

where:

$$\frac{X_1}{d} = \frac{1}{f_2} \sqrt{\frac{f_y\, f_2}{3}} \left[\sqrt{\frac{2}{(1+\beta)}} + \sqrt{1-R_m} \right] \tag{10}$$

$$\frac{X_2}{d} = \frac{1}{f_2} \sqrt{\frac{f_y\, f_2}{3} \frac{(1+R_m)}{(1+\beta)}} \tag{11}$$

VALIDATION OF EQUATIONS

Larsen and Reestrup (1969) provide strong supporting evidence for the viability of the seven equations to predict yield load. However, there is a need to validate these equations for a broader range of joint geometries and species density used by Larsen/Reestrup.

Additionally, Larsen/Reestrup defined connection yield load on the basis of a fixed value of angular rotation of the screw. This is a practical definition of yield resulting from the observation that, over the range of load-deformation curves obtained for various joint geometries, there is no single, consistently identifiable yield or maximum load point. This problem was addressed by Harding and Fowkes (1984) and Patton-Mallory (1989) with bolted connections who defined yield on a 5%d offset basis as shown in Figure 3. This definition was adopted for U. S. codes. The offset yield point is, experimentally reasonably unambiguous and generally occurs at a load level below the development of microcracking common to perpendicular-to-grain connections. Use of a predicted yield load requires a minimum fastener spacing geometry to avoid brittle failures such as splitting or a failure mode not predicted by the theory.

Validation test data, in the form of individual load-deformation traces and density of all members, were obtained from studies made by Newlin and Gahagan (1938) and McLain and Carroll (1990).

Useable data were obtained from a total of 213 tests with wood side plates and 36 tests with steel plates from the Newlin and Gahagan (1938) study (Note: data were collected in discrete increments and $P_{5\%}$ could not be identified for all samples from available records). These tests were of parallel-to-grain connections of three softwood species (white pine, southern pine, Douglas-fir) and white oak. Test screw diameters ranged from 6.4 mm to 25 mm (¼ to 1 in.) but most joints contained 16 mm (⅝ in.) screws of varied length. All steel side plates were 12.5 mm (½ in.) thick. Results of the Newlin and Gahagan tests have been the basis for lag screw connection lateral strength design values in North America for the past 50 years.

Data from 50 tests of steel side plate connections using two screw sizes, 9.5 mm and 16 mm (⅜ in. and ⅝ in.) and blocks of southern yellow pine and spruce-pine-fir were also available. These parallel-to-grain tests are described in McLain and Carroll (1990).

For each test, the actual dimensions and density of each cleat and block were obtained as well as connection proportional limit, maximum load (P_{max}), and the 5% diameter offset yield load ($P_{5\%}$).

Additional verification data were taken from Tokuda, et al. (1989 a,b) who reported tests of parallel-to and perpendicular-to-grain connections using steel side plates. Three lengths (65mm, 100mm and 150mm) each, of 9mm and 20mm screws, were used to fasten

6mm and 12mm thick steel plates to Douglas-fir and Hem-fir blocks. An average $P_{5\%}$ was estimated by fitting a reasonable curve to tabulated load-deformation points. Additional data for some sets were collected directly from published load-deformation curves. Included in the analysis are 12 species-geometry combinations, six each for parallel-to and perpendicular-to-grain metal side plate connections.

Calculating Yield Loads

The dowel bearing strength or embedding stress and the fastener yield strength are input to the yield equations. These values were not available for the specific test data at hand and were estimated as described below.

Dowel bearing strength: Wilkinson (1991) conducted extensive embedding tests of various fasteners in North American species and developed the following relationships for dowel-type fasteners greater than 6.4mm (0.25 in) in prebored holes:

(parallel-to-grain)

$$f_h = 77.2G \tag{12}$$

(perpendicular-to-grain)

$$f_h = 230\ G^{1.45}\ d^{-0.5} \tag{13}$$

where: f_h = dowel bearing strength, MPa
G = relative density of wood at 12% moisture content
d = shank diameter, mm.

These equations differ from those of Whale, Smith, and Larsen (1987) in that they predict mean embedding stress on a 5%D offset basis and encompass a greater number of species. The offset stress varied little from maximum stress in most cases. For steel plates, f_h = 400 MPa for plates with $t_1 \geq$ 6.4mm (0.25 in.) and f_h = 310 MPa for thinner plates was assumed.

Fastener yield strength: Yield strength may be found from bending or tension tests. For relatively short fasteners with large diameter, bending tests are impractical. In the U. S. a yield strength of 310 MPa (45 ksi) is traditionally assigned to screws meeting the requirements of ASTM A307 (1984). This value is approximately the average of the ultimate tensile strength of the screw and the minimum tensile yield strength.

Carroll (1988) sampled 9.5 mm (⅜ in.) and 16 mm (⅝ in.) lag screws from seven different manufacturers. Ten replicates were taken at random from shipments of 100+

screws of each size from each manufacturer. Bending yield strength, f_y, on a 5% of diameter offset basis, was found by testing cantilevered lag screws are a manner similar to that of Larsen and Reestrup (1969). f_y was found to range from 372 to 551 MPa (54 to 80 ksi) with relatively little variation between manufacturers. A minimum f_y of 310 MPa (45 ksi) is not contraindicated. Additional screws with 9.5mm (⅜ in.), 12mm (½ in.), 16 mm, (⅝ in.) and 19mm (¾ in.) diameter, five replicates each, were tested such that the point of maximum moment was in the thread. The ratios of yield moment in thread of that of the shank, R_m, were 0.36, 0.45, 0.50 and 0.61, respectively. These compare favorably with Larsen/Reestrup (1969) values of 0.37 and 0.53 for 9.5mm (⅜ in.) and 16 mm (⅝ in.) screws, respectively. A regression of these data showed:

$$M_t/M_s = R_m = 0.14 + 0.024d \quad \text{..........} \quad (14)$$

where R_m = ratio of yield moment in thread, M_t, to that of the shank, M_s,
d = nominal shank diameter, mm

Dimensions: Actual dimensions of screws and members were used to calculate the yield load, P_y, if they were available. Stated mean or nominal dimensions were used if actual dimensions were not available.

THEORETICAL AND EXPERIMENTAL COMPARISONS

The ratio of the experimental yield load to the calculated yield load, $P_{5\%}/P_y$, was computed for each of the 212 different wood-wood connections. The results, shown in Table 1 and graphically in Figure 4, indicate a slightly conservative prediction of the experimental yield loads. This is judged acceptable given the wide range of input geometries and the assumptions necessary to make the comparisons.

However, the yield equations generally over predicted $P_{5\%}$ for steel side plate connections. This was also found by Soltis and Wilkinson (1987) for steel-wood bolted connections. The reason for this discrepancy is probably the actual fixity conditions at the steel plate. Yield theory assumes that the screws fit snugly into holes drilled in all members. For thin steel plates, any oversize hole leads to connection deformation not considered by the theory. This deformation, however, will be manifested in the measured offset yield strength.

The Newlin and Gahagan data come from tests where the holes in the steel plates were oversize by less than 0.8mm on average. In contrast, are the results from McLain and Carroll where the holes were 1.6mm oversize and the screws were not snug. The lack of fixity in the latter group resulted in a Mode III action early in the loading process. At higher loads, near failure, the double bend Mode IV was readily apparent. The effect of oversized holes may be simulated by artificially reducing f_h of the metal side plates. For example, if f_h is reduced by a factor of 2 then the $P_{5\%}/P_y$ ratio for the McLain and Carroll data becomes 1.02 and the average expected mode changes from IV to III. This shows the sensitivity of the verification to a definition of yield that is partially deformation-based.

The actual dimensions used by Tokuda, et al (1989) are unknown. Given the potential error of estimating P_y and $P_{5\%}$, as well as the breadth of joint geometries, the demonstrated accuracy is acceptable. That the $P_{5\%}/P_y$ ratio for perpendicular-to-grain connections is similar to that for the parallel-to-grain joints supports a broad application of the theory.

PENETRATION DEPTH FACTOR

Ultimate lag screw connection strength may be influenced by the amount of the screw that penetrates the main member. Based on Newlin and Gahagan's (1938) recommendations, screw penetration requirements in the U. S. have been a function of density with an optimum value ranging between 7d to 11d depending on density. A penetration factor (PF) adjusts design strength between a lower limit and optimum penetration. The stated purpose of PF is to keep the ratio of design strength to ultimate strength approximately equal over a range of penetration depths.

Newlin and Gahagan's (1938) data do not directly support the historic U. S. penetration requirements. With the recent adoption of yield theory the penetration limits in the U. S. have been changed to an optimum penetration of 8d and minimum of 4d. This is illustrated in Figure 4 where the ratio of ultimate strength to $P_{5\%}$ strength is plotted against penetration of the screw into the block. The data are from Newlin and Gahagan (1938) and represent a wide variety of species and geometries. Superimposed is the new penetration factor. Different levels of penetration factor by species are not warranted based on these data. No evidence was found to suggest that the experimental yield load ($P_{5\%}$) was affected by penetration depth, provided that a minimum of 4d is maintained.

SIMPLIFICATION OF EQUATIONS

The full seven yield equations are unwieldy and are not practical for a design specification. Further, it is useful to simplify the equations so that the user sees design with screws as a special case of the design of single-shear bolted joints.

One approach to simplification is to assume a prismatic effective shank diameter, less than nominal d, and use only the three full-shank equations (1), (2) and (7). This was explored but the use of a single effective diameter resulted in too great of variation between the predictions of a reduced set of equations and that of the full set of seven equations. This is because, over a practical range of geometries (described below), a large percentage of the expected failures were in Mode I, where the effective diameter equals the actual diameter. Choosing a reduced effective d will cause under prediction of Mode I actions.

A more efficient alternative was chosen for codification. The Modes III and IV equations for yielding in the threaded region (Eq. 3 and 8) degenerate to those for yielding in the shank (Eq. 2 and 7) as R_m approaches unity. R_m is the ratio of the yield moment of the screw in the thread region to that in the shank region. A mathematically clean simplification fixes R_m at a level below 1.0 and uses only the Mode III and IV equations for $SP \leq X_2$ (Eq. 3 and 8) and Mode I (Eq. 1). Note that this is equivalent to using a fictitious diameter with Modes III and IV and the actual diameter in Mode I.

To find R_m, the yield load for a specific joint geometry is first determined using the full set of seven equations. Then, the R_m necessary to achieve the same load with the reduced set of three equations is found by substitution or iterative solution. R_m values were calculated for a total of 381 wood side plate geometries and 147 steel side plate geometries that were simulated using the following conditions:

- $G = 0.42$, 0.51, 0.55 and 0.60 (This is the principal range of commercial structural species.)
- Cleat thickness, t_1, ranged from 25mm to 140mm in 12mm increments for wood side plates; $t_1 = 6.4$, 9.5 and 12.5mm for metal side plates.
- Screw length, L, ranged from 102mm to 279mm in 25mm increments except that length, diameter and cleat thickness were limited to those cases where $0 \leq SP/D \leq 7$.
- Screw dimensions followed ANSI/ASME B18.6.1-1981. These are similar to many metric standards. The critical factor is that thread length is equal one half the nominal length plus 12mm, or 127mm, whichever is shorter.

Table 2 shows the results of these calculations. The grand average effective R_m was 0.804. However, setting $R_m = 0.75$ results in a 1% change in predicted loads and a better balance between the results for steel and wood side plate geometries with respect to any penalty for simplification. Using the reduced equations with $R_m = 0.75$ actually improved the mean prediction of experimental results at the cost of some increased variability. For example, with $R_m = 0.75$, the ratio of $P_{5\%}/P_y$ for wood and metal side plate geometries in Table 1 changed to 1.07 and 0.82, respectively. These should be compared with the values for the full set of equations in Table 1.

One could argue that different R_m should be set for Modes III and IV and for wood and metal side plate connections. However, on a weighted average basis, the ratios for the modes are similar and the resulting loads are insensitive to relatively small changes in R_m. The additional level of complexity does not seem warranted.

In summary, the full set of behavioral equations for lag screw connections can be reduced to the following for use into a design specification

Mode I (12)

$$P_y = \frac{d\, t_1\, f_2}{\beta}$$

Mode III (13)

$$P_y = \frac{t_1\, d\, f_2}{(2+\beta)} \left(-1 + \sqrt{\frac{2(1+\beta)}{\beta} + \frac{f_y\,(2+\beta)\, d^2}{2\, f_2\, t_1^2}} \right)$$

Mode IV (14)

$$P_y = d^2 \sqrt{\frac{7\, f_y\, f_2}{12\ (1+\beta)}}$$

Alternate formulations are, of course, possible. An effective $R_m = 0.75$ implies an effective diameter of $\sqrt[3]{0.75} = 0.9d$ for use only in equations (2) and (7) or for computing the yield moment of a fastener.

Use of these reduced equations must be limited to screws with a geometry similar to "standard" lag screws. Connections with fully threaded screws or screws with deep threads, for example, should not be designed with these equations without additional consideration of the effective R_m or diameter.

NOTATION

The following symbols are used in this paper:

d	= dominal shank diameter;
f_1,f_2	= dowel bearing strength of cleat and block material, respectively;
f_y	= bending yield stress of lag screw;
G	= relative density of wood at 12% moisture content;
P_{max}	= maximum connection load;
P_y	= calculated yield load;
$P_{5\%}$	= experimental 5%d offset yield load;
R_m	= ratio of the yield moment in screw thread region to that in shank region;
SP	= depth of shank penetration into block;
X_1,X_2	= critical values of shank penetration;
β	= f_2/f_1
t_1	= cleat thickness;

REFERENCES

ANSI/ASME B18.2.1-1981. "Square and Hex Bolts and Screws--Inch Series." American Society of Mechanical Engineers, New York, NY.

ASTM A307-84. (1984). "Specification for Carbon Steel Externally Threaded Standard Fasteners." American Society for Testing and Materials, Philadelphia, PA.

Carroll, J. D. (1988). "Withdrawal and combined load capacity of threaded-fastener wood joints." M.S. thesis. Dept. of Wood Science and Forest Products. Virginia Tech. Blacksburg, VA.

Harding, N. and Fowkes, A. H. R. (1984). "Bolted timber joints." Proceedings, Pacific Timber Engineering Conferences, Auckland, New Zealand, Vol. III: pp. 872-883.

Johansen, K. W. (1949). "Theory of timber connections." International Association for Bridge and Structural Engineering Publication 9:249-262.

Larsen, H. J. and Reestrup, V. (1969). "Tests on screws on wood," Bygningsstatiske Meddelelser Vol. 40, No. 1, pp. 3-36.

McLain, T. E. and Carroll, J. D. (1990). "Combined load capacity of threaded fastener wood connections." J. Struct. Engr. 116(9):2419-2432.

Möller, T. (1950). En ny metod for berakning av spikforbrand: New method for estimating the bearing strength of nailed wood connectors. Chalmers Tekniska Hogskolas Handlingar, Goteborg, Sweden, Report No. 117, p. 77. (In Swedish with English translation.)

Newlin, J. A. and Gahagan, J. M. (1938). "Lag-screw joints: their behavior and design" U. S. Dept. of Agric. Tech. Bull. No. 597, 27 p.

Patton-Mallory, M. (1989). "Yield theory of bolted connections compared with current U. S. design criteria." Proceedings, Pacific Timber Engineering Conference, Auckland, NZ, pp. 323-329.

Smith, I., Whale, R. J., Anderson, C.: Hilson, B. O. and Rodd, P. D. (1988). "Design properties of laterally loaded nailed or bolted wood joints. Can. J. Civil Engr. 15(4):633-643.

Soltis, L. A., Hubbard, F. K. and Wilkinson, T. L. (1986). "Bearing strength of bolted timber joints" J. of Struct. Engr., Vol. 112, No. 9, pp. 2141-2153.

Tokuda, M., Hirashima, Y. and Matsubara, H. (1989a). "The strength of lag-screw joints I. Lateral strength parallel-to-grain." J. Jap. Wood Res. Soc., Vol. 35, No. 6. pp. 473-481.

Tokuda, M., Hirashima, Y. and Miyakoshi, M. (1989b). "The strength of lag-screw joints II. Lateral strength perpendicular-to-grain." J. Jap. Wood Res. Soc., Vol. 35, No. 6., pp. 482-488.

Whale, L. R. J. (1991). "Eurocode 5-joint design," Proced. 1991 Intl. Timber Engr. Conf., Vol. 1, London, UK. Timber Res. and Dev. Assn. Buckinghamshire U.K. pp. 1.97-1.106.

Whale, L. R. J. and I. Smith. (1986). "The derivation of design clauses for nailed and bolted joints in Eurocode 5." CIB-W18A Paper 19-7-6. Florence, Italy.

Whale, L. R. J., I. Smith and H. J. Larsen (1987) "Design of nailed and bolted joints. Proposals for revision of existing formulae in draft Eurocode 5 and CIB code." CIB-W18A paper 20-7-1, Dublin, Eire.

Wilkinson, T. L. (1991). "Dowel bearing strength." Research Paper FPL-RP-505. USDA Forest Service Forest Products Lab., Madison, Wisconsin, USA.

Table 1. Ratios of experimental to calculated yield load. All seven yield equations were used to calculate P_y.

Reference	Number of test geometries	Number of Useable Tests	Ratio, $P_{5\%}/P_y$ Mean	Std. dev.	Max.	Min.
WOOD-WOOD CONNECTIONS						
Newlin & Gahagan (1938)	36	212[1]	1.08	0.14	1.67	0.70
STEEL-WOOD CONNECTIONS						
Newlin & Gahagan (1938)	4	15[1]	0.95	0.12	1.13	0.72
McLain & Carroll (1990)	2	50	0.66	0.11	0.94	0.47
Tokuda (1989a) Para.-to-grain	6	12[2]	0.79	0.14	1.03	0.60
Tokuda (1989b) Perp.-to-grain	6	12[2]	0.82	0.14	1.02	0.56

[1]Samples for which a $P_{5\%}$ could be obtained.
[2]Only the average of six tests could be retrieved.

Table 2. Effective R_m values for 381 wood side plate or 147 (steel side plate) joint geometries.

Side Plates (1)	Cleat/Block grain direction[1] (2)	G = 0.42 Mode III (3)	G = 0.42 Mode IV (4)	G = 0.42 Mode ALL (5)	G = 0.51 Mode III (6)	G = 0.51 Mode IV (7)	G = 0.51 Mode ALL (8)	G = 0.55 Mode III (9)	G = 0.55 Mode IV (10)	G = 0.55 Mode ALL (11)	G = .60 Mode III (12)	G = .60 Mode IV (13)	G = .60 Mode All (14)	Average III (15)	Average IV (16)	Average ALL (17)
Wood Side Plates	P/P	0.80	0.68	0.75	0.82	0.72	0.77	0.83	0.73	0.78	0.87	0.72	0.79	0.83	0.71	0.77
	P/Q	0.78	0.65	0.71	0.76	0.64	0.69	0.78	0.65	0.71	0.78	0.68	0.72	0.78	0.66	0.71
	Q/P	0.79	0.64	0.77	0.83	0.69	0.79	0.83	0.72	0.80	0.84	0.74	0.81	0.82	0.70	0.79
Metal Side Plates	-/P	0.90	0.88	0.90	0.92	0.91	0.92	0.93	0.93	0.93	0.94	0.94	0.94	0.92	0.91	0.92
	-/Q	0.78	0.72	0.77	0.83	0.84	0.83	0.85	0.85	0.85	0.86	0.88	0.87	0.83	0.82	0.83

[1] P = parallel to grain, Q = perpendicular to grain

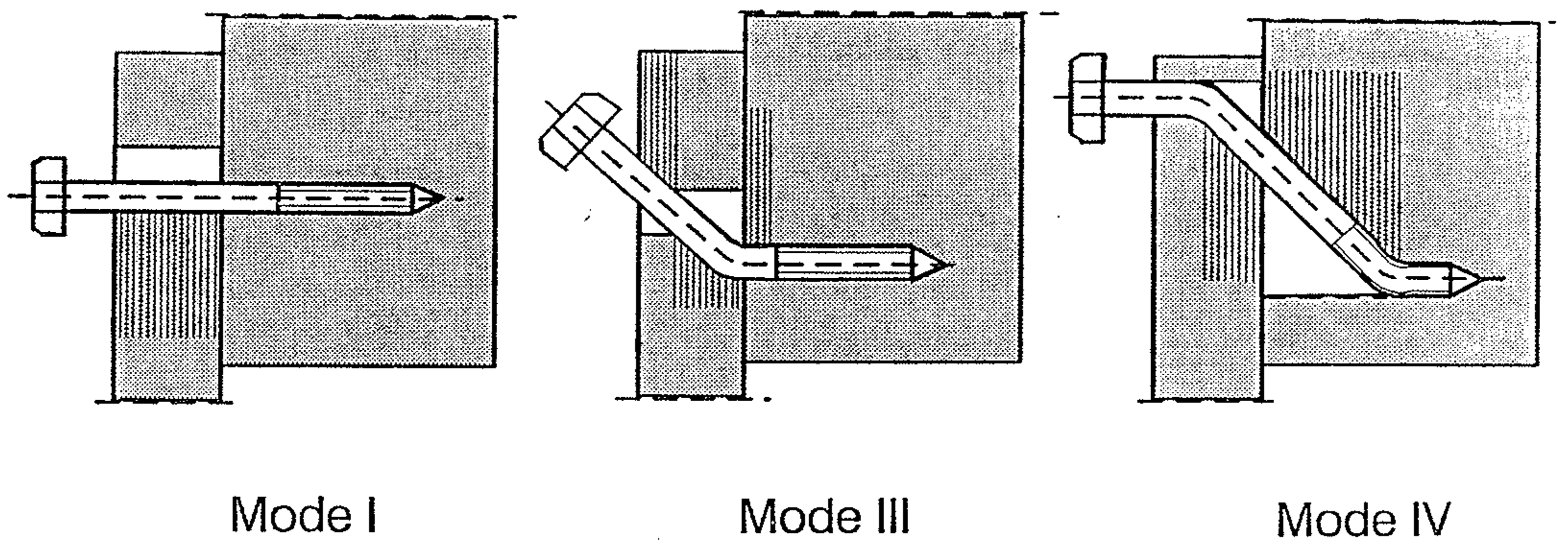

Figure 1. Potential yield modes.

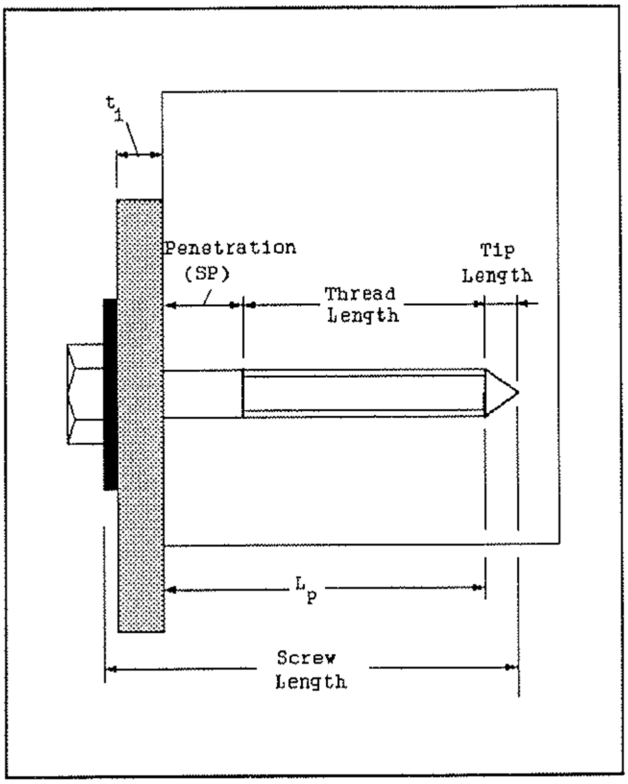

Figure 2. Two member lag screw connections.

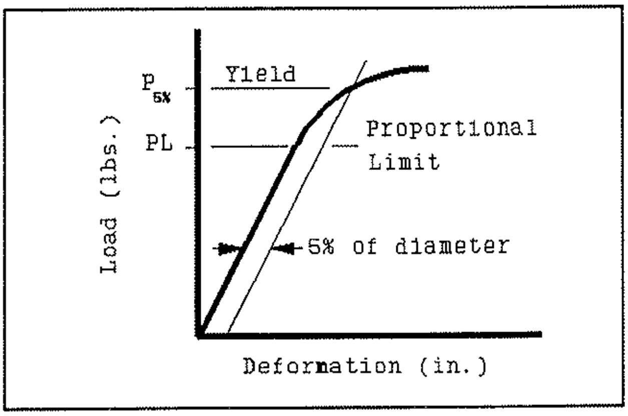

Figure 3. Five percent of diameter offset yield strength defined.

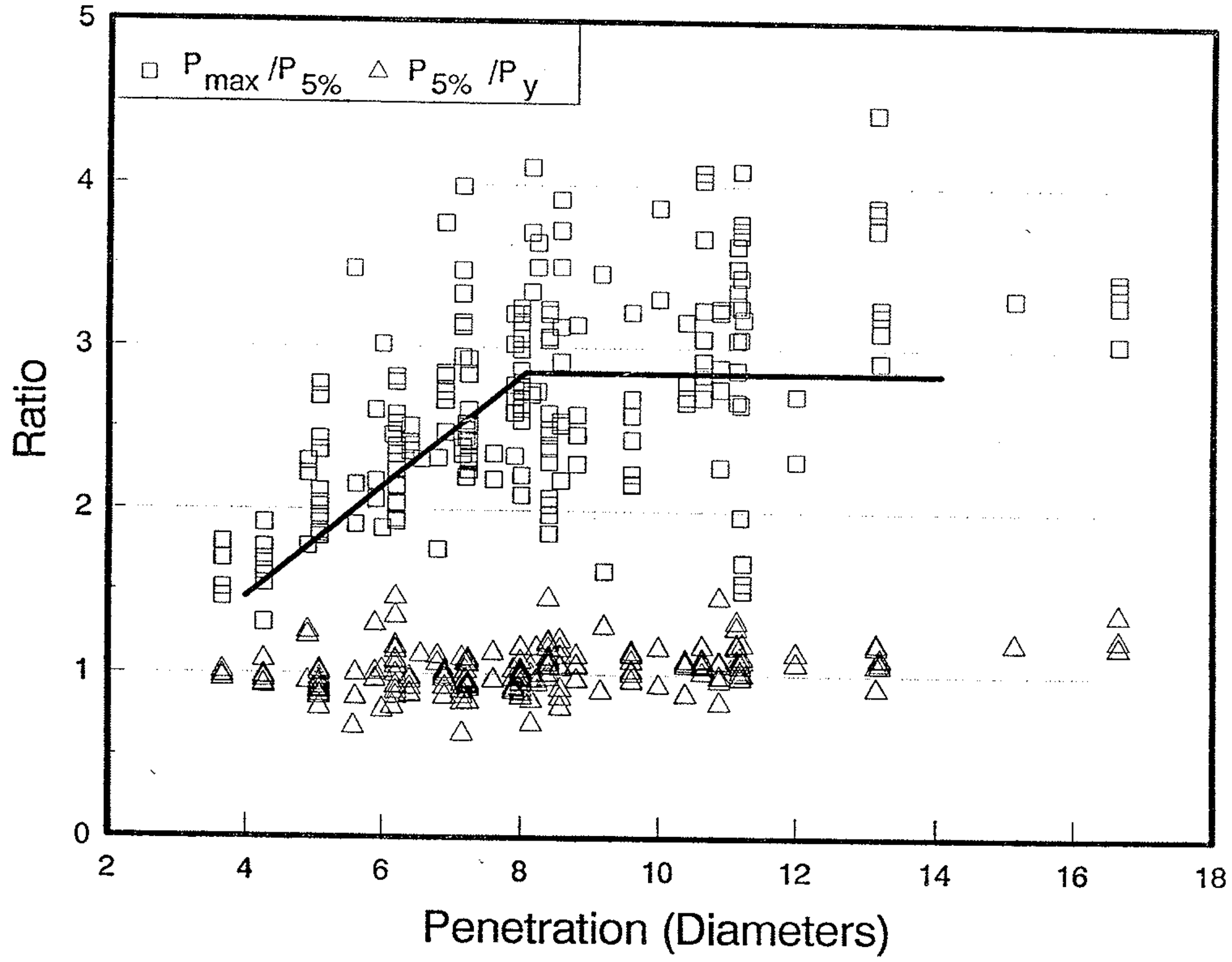

Figure 4. Ratio of maximum load to $P_{5\%}$ and $P_{5\%}$ to calculated P_y for Newlin and Gahagan wood side plate connections.

CIB-W18/25-7-9

INTERNATIONAL COUNCIL FOR BUILDING RESEARCH STUDIES AND DOCUMENTATION

WORKING COMMISSION W18 - TIMBER STRUCTURES

DETERMINATION OF k_{def} FOR NAILED JOINTS

by

J W G van de Kuilen
TNO Building and Construction Research
The Netherlands

MEETING TWENTY - FIVE

ÅHUS

SWEDEN

AUGUST 1992

DETERMINATION OF k_{def} FOR NAILED JOINTS

Ir. J-W.G. van de Kuilen
TNO Building and Construction Research / Delft University of Technology

Summary

On the basis of creep tests, first started in 1962 and extended in 1983, a $\underline{k}_{def}$ factor has been derived for nailed joints. Nailed joints were loaded in tension at load levels of 30, 40, 50, 60 and 65% of short duration strength. Tests with 60 and 65% load level were started in 1962, 30,40 and 50% in 1983. The climate in the laboratory hall corresponds to service class 2 of Eurocode 5. The starting date in the season had significant effect on the creep effects and the measured values of $\underline{k}_{def}$. Based on the theory of deformation kinetics a creep equation is proposed.

1. Introduction

In 1962 a comprehensive test program was started at the Stevin laboratory at Delft University of Technology to study load duration effects in timber joints. Nailed joints, tooth-plate and split-ring joints were incorporated in the program [1]. The load levels chosen were 60, 65, 70, 75, 80 ,85 and 90% of the short duration strength. Meanwhile all specimens failed except the nailed joints at the 60 and 65% load levels.
In 1983 the original test program was extended in an EC-sponsored project with specimens of the same type but at lower load levels. The load levels were chosen at 30, 40 and 50%. The 30% load level is considered as the level of a service load [2].
In the meantime a general creep and damage model has been developed based on reaction equations of plastic deformation in the molecular structure and on the transformation of stresses to surrounding elastic material [3]. This model used to determine parameters and deformation factors.

2. The creep and damage model

The model is based on the reaction rate theory. The reaction rate theory describes the process of bond breaking and reformation in a molecular structure. The rate is dependent on temperature, moisture and stresses. The reaction rate equation, where the number of bonds is the main parameter can be rewritten in the form of a strain rate equation:

$$\frac{d\epsilon}{dt}=\frac{d\sigma_i}{K_i dt}+(A_i+B_i\epsilon_i)\sinh(\sigma_i\phi_i(1-C_i\epsilon_i)) \qquad (1)$$

The strain rate equation can be considered as a parallel system of Maxwell elements with a non-linear dashpot.

For structural applications the parameter C may be neglected. The equation can be solved for either neglecting the term A or $B\epsilon$. The solution of equation 1 then represents two branches of the creep line on a logaritmic time scale. Neglecting $B\epsilon$ describes a recoverable creep process while neglecting A describes a non-recoverable creep process.

For loading levels below about 50% the lines of the non-recoverable creep process are straight. For higher loading levels the creep lines are curved and an additional process is acting. The branched creep curve is shown in Figure 1 together with the approximations for the two branches.

3. Solution of the strain rate equation for creep

Equation 1 can be solved for governing A and governing $B\epsilon$ respectively, as is done in [3]. In most cases the parallel Maxwell elements may be reduced to a three element model with one Maxwell element and a parallel spring. For constant load $d\sigma/dt$ equals 0. In most cases $C\epsilon$ may be neglected. This term accounts for a hardening process which is neglectable for structural timber in service conditions.

Approximations of the solutions are straight lines on a logaritmic time scale giving the following equation for the creep factor Cf:

$$Cf = \frac{\epsilon - \epsilon_0}{\epsilon_0} = C_1 \ln(1 + C_2 t) \qquad (2)$$

This equation is used to analyse the test results of nailed joints.

4. Creep tests

4.1 Introduction

Creep test results were gathered over a 29 year period since the first creep tests started at the Stevin Laboratory of Delft University of Technology. In 1962 creep tests in tension were started at several load levels to study the Duration Of Load (DOL) effect. At this moment the tests on 60 and 65% load level are still running, giving unique information on creep of joints. Deformation, temperature and relative humidity have been recorded over almost 30 years.
In 1983 an additional EC-sponsored DOL project started and nailed joints were loaded at 30, 40 and 50% load levels. Within this project control specimen were used to analyse the effect of climatical changes in the laboratory hall.
The results of the creep tests are analyzed using the logarithmic approximations of the creep and damage model.

4.2 Test specimens

The test specimens were made of spruce with a joint length of 180 mm and a width of 95 mm containing 60 nails with a diameter of 2.8 mm. The shape and dimensions of the test specimens are given in Figure 2. Before loading the average moisture content of the specimens was approximately 9%. The average ultimate load in a standard short duration test (SSD) of 20 specimens was 45.0 kN, giving a load of 27.0 kN for the 60% and a load of 29.2 kN for the 65% specimens. In 1983 some additional short term tests were carried out with material from 1962 resulting in an average value of 48.9 kN. SSD-tests with new material performed in 1983 resulted in an average strength value of 44.6 kN. The average strength of all test results was 45.7 kN and the coefficient of variation of 6%. The characteristic load carrying capacity of the joints based on the calculation method given in Eurocode 5 [4] results in a characteristic strength of 33.7 kN based on a density of 387 kg/m^3.

4.3 Creep test results

In Figure 3 the average creep results of all load levels are shown in a deformation - time plot. It can be seen from the old tests that the deformation can become very large without failure. In the very beginning of the creep curves it can be seen that a sudden increase in deformation occurs during a very short period. This happens at all load levels and is caused by atmospheric changes in the laboratory hall. It can also be seen that there are differences in the mechano-sorptive effects for the different load levels. At high load levels it seems that the sudden increase occurs only once and that the climatic changes of the following years do not show a similar effect. For the lower load levels (30, 40% and 50%) the climatic changes do show increases in deformation after more than one season but so far never more than three seasons except if the changes in climate are very extreme.
The effect of cyclic moisture changes is clearly seen when the creep factor Cf is plotted versus log(t) as is done in Figure 4. The first major climatic change causes the creep process to change from the first to the second process. The mechano-sorptive effect induces the creep process to change from the first process to the second process. Apparently the change in moisture content increases the number of flow units in the microstructure above

the necessary level for the second process to start.
According to the theory the creep line of the highly loaded specimens should bend off first. The fact that this does not occur here, is caused by the starting dates of the tests.
The high-load tests (60 and 65%) were started on 5/6 September 1962 while the lower loaded tests (30, 40 and 50%) were started on 14 March 1984, 2 Februari 1984 and 19 January 1984 respectively.
The changes in relative humidity in the laboratory hall are shown in Figure 5 for the first four years for the new tests. It is clear that the increases in creep rate are caused by the increase in relative humidity in the spring. The relative humidity increases from winter to summer generally from about 40% to about 80% resulting in an increase in moisture content of the spruce from 10 to 16% [5]. The differences in relative humidity were 15% in 1963 compared to 30% in 1984. Sometimes the increase in relative humidity takes several weeks, but it still leads to a deformation increase.
To compare the creep lines from the old and the new tests, the lines should consequently be shifted over a period of approximately 6 months.

It seems that the internal stresses and strains are released by the mechano-sorptive effect in one step at high load levels and in several consecutive steps at low load levels.
This indicates a maximum plastic flow to be released by cyclic moisture changes in the first stages of the second branch of the creep curve. Apart from this they depend on the change in relative humidity. On a linear time scale the mechano-sorptive change in 1963 is smeared over a long period compared to the first change in 1984.

At the end of the lifetime of the specimen in the accelerating creep stage or at very high load levels it can be shown that cyclic moisture changes cause crack initiation and propagation.
This is shown in Figure 6 for a tooth-plate connector.
The mechano-sorptive changes in the last years lead to higher

deformations as can also be seen in the results of the 65% nails. They occur during the same time period in the nailed joints, but do not yet lead to failure.

The first part of the creep curve on log(t) scale is for all load levels a straight line, showing that structural changes can be neglected as was to be expected from the creep equations. Then at time t′ (the delay time) the second process starts. For the lower load levels these are straight lines as well, for the higher load levels (60 and 65%) these lines are curved, strongly indicating a third acting process. At the lower load levels this process is not noticeable. It is not certain, however, that the curvature means that there is damage increase.

5. Parameter estimation

5.1 General parameter estimation for the three element model

From Figure 4 the starting date of the second branch of the creep curve can be determined for the 40, 50, 60 and 65% load level. For the 30% load level there is a continuous curved intermediate stage between the first and the second branch, caused by the starting date of the test. The test was started on 14 March, so it will be difficult to distinguish the increase in creep at the start of the summer in such a short period. It seems that in this case the actual first large moisture change occurs only in the following year.

The 65% delay time is difficult to compare, because this delay time is highly influenced by the time interval chosen to fit the second process. This means that the intersect between the two fitted curves is highly affected by the time scale used for a curve fit in the second branch.
It was found that the constants of equation (3) only change slightly when a fit is made for the second branch only or for the total creep curve. This can be explained by the fact that the

second branch contains much more data than the first. However, to determine the parameters for the two processes a fit has been made for each of the process, but only the results of second process are given here. The mechano-sorptive changes in the second branch are averaged as being changes in deformation measurements. Although the strain rate is increased during a mechano-sorptive change, the average steepness is hardly affected.
As an approximation to determine k_{def} this is acceptable since the largest mechano-sorptive changes occur in the first years of the creep process and data is already available for 8 years (30%, 40% and 50%) and 29 years (60% and 65%).

In Table 1 the values of C_1 and C_2 for the second process are assembled. For the old 60% and 65% load levels the constants have also been determined for the first 8 years of the process so they can be compared with the new tests.

Table 1. Constants for 3-element model, equation 2
second process estimation

load level		C_1	C_2	ϵ (mm)
30 %		0.4708	4.135E-2	0.336
40 %		0.5809	2.674E-2	0.551
50 %		0.5408	3.759E-2	0.994
60 %	(8 years)	0.4184	1.223E-2	2.120
	(29 years)	0.4729	8.333E-3	
65 %	(8 years)	0.5709	8.158E-3	2.709
	(29 years)	0.7884	3.638E-3	

It can be seen that C_1 is more or less constant for these load levels as is to be expected from the log(t) plot, where the creep curves run parallel in the second process. Complications arise because of the curvature in the second branch of the 60 and 65% load levels, being the result of a damage process. In this case the straight line approximation seems no longer justified, although still reasonably good predictions of the deformation can be made, as will be shown in paragraph 4.2. A threshold value seems to exist at a load level between 50 and 60%.

The average value for C_1 = 0,53 is determined on the basis of the 30, 40 and 50% tests because these load levels show linearity on a logaritmic time scale.
The determination of the delay time of the second process is more difficult, because this delay time highly depends on the starting date of the creep tests over the season. This is the reason why the delay times for the low load levels are equal as well as for the high load level. In general this delay time may be taken as 180 days, so the average bending off point is taken.

5.2 Extrapolation of measurements

Using the constants given in Table 1 it is possible to make predictions of deformations over longer periods.
With equation (3) the prediction of the deformation after a period of 29 years can be made, based on the constants determined with 8 year measurements. The results are shown in table 2.

Table 2. Prediction of deformation in mm after 29 years

	measured	predicted with 8 year fit	predicted with 29 year fit
60 %	6.79	6.34 (- 6.6%)	6.60 (-2.8%)
65 %	10.77	9.42 (-12.6%)	10.52 (-2.4%)

Both predictions are lower than the actual value. It is obvious that this is caused by the straight line approximation of the log-time plot. The 29 year predictions, however, are very close to the actual value, showing the accuracy of the model even with the assumption of only one dominating process at high loading levels.

5.3 Failure mode

The calculation of the strength of the joints is done according to Eurocode 5. The failure modes observed in the long duration tests however show a different type of failure.
The transition between the failure modes may be caused by splitting directly under the nails (the highest loaded area) or the change in joint geometry caused by the long-term deformations. The splitting may be facilitated by the fact that the holes were not predrilled.

6. Conclusions

6.1 Conclusions from the study

Creep measurements of nailed joints have been analyzed using the creep and damage model of Van der Put [3].
The creep results are analyzed as two processes. Both may be described by a simple ln (t) formula with two parameters. The first parameter represents the steepness of the creep line on a logaritmic time scale. The second parameter represents the bending point in the creep line approximation.
In the evaluation the sudden increases in deformation which occur in the first years of the tests are not considered. After longer periods this effect seems no longer noticeable. It seems clear, however, that the second process is induced by climatical changes. The changes occur during a distinct change in relative humidity. This change introduces a change in the microstructure i.e. the number of flow units or the number of load-bearing molecular bonds.
The start of the second process depends on the season in which the creep test was started. Hence, to predict the deformation of a joint over a number of years may be done with an average delay time. Based on the above mentioned creep tests, this average delay time may be taken as half a year or 180 days. The accuracy of the prediction highly depends on the time of loading. From

Figure 4 it can be seen that the relative creep of the 60% load level is 1.75 after 5000 days while for the 30% load level this is already the case after 2100 days, totally due to the moisture effect.
For engineering purposes the second branch of the creep line and the fits with the ln(t)-equation can be used. There is hardly any difference in the constants when the second equation (2) is used with the overall data, starting from t=1.
The following equation can be used for the creep factor of nailed joints in climate class II:

$$Cf = 0.53\ln(\frac{t}{180}) = 1.20\log(\frac{t}{180}) \tag{3}$$

with:

Cf is the creep factor = $(\epsilon - \epsilon_0) / \epsilon_0$ with:
ϵ_0 is the deformation at t = 1 day
t is time in days.

6.2 Comparison with EC5

The deformation ϵ at t = 0 can be calculated with Eurocode 5 as:

$$U_{inst}=\frac{3F(\frac{40d^{0.8}}{\rho_k})}{F_k} \tag{4}$$

in which:

d	is nail diameter	= 2.8 mm
F	is characteristic strength	= 41.2 kN
ρ	is characteristic density	= 387 kg/m^3
F	is load level	= $0.3F_k$ to $0.5F_k$

giving:
$u_{inst} = 0.7\ F/F_k$

In Table 3 the results are compared with the measured values after 3 minutes and 1 day loading:

	u_{inst} (mm) (EC 5)	u (mm) (measured) 3 min	1 day
30%	0.21	0.280	0.336
40%	0.28	0.437	0.551
50%	0.35	0.656	0.994

In reality the instantaneous deformation is larger than the predicted value of equation (4). The value of 0.21 mm was also found as the average elastic slip in the joints tested according to the RILEM Recommendation 3TT-1 (SSD-test). Equation (3) can be modified for deformation at t = 0 (ϵ = 0.21 mm) instead of at t = 1 day (ϵ = 0.336 mm). Equation (3) then becomes:

$$Cf = 0.848\ln\left(\frac{t}{180}\right) + 0.6 = 1.95\log\left(\frac{t}{180}\right) + 0.6 \qquad (5)$$

Applying equation (4) together with the deformation factor k_{def} = 0.8 for permanent loading and service class II total deformation at t=∞ is 0.38 mm for a 30% load level. Comparing this with the test results and using equation (5) for the creep factor Cf after 8 years (= 2.96), a total deformation of 0.83 mm results, which is more than twice the Eurocode 5 value.
The actual measured deformation after 8 years is 1.086 mm. With a deformation at t = 0 of 0.21 mm this results in a creep factor Cf = 4.15. However, this high value was caused by the starting date of the test.

With a load duration of 50 years for permanent loads, or 18,250 days, interpolation of equation (5) leads to a k_{def} factor of:

$$k_{def} = Cf = 0.848\ln\left(\frac{18250}{180}\right) + 0.6 \approx 4.5 \qquad (6)$$

It is recognized that in a structure the loads will almost always be below the design loads and therefore have less affect than the loads in this creep test. Based on the measurements and the application of the deformation kinetics model it is suggested to increase the k_{def} values in Eurocode 5 for nailed joints without predrilled holes.

Literature

[1] Long duration tests on timber joints
ir. P. Vermeyden
Report 4-74-11 (in Dutch)
Delft University of Technology

[2] Creep and Damage Research on Timber Joints
Part One
Prof. ir. J Kuipers, Ing. P.B.J. Kurstjens
Report 4-86-15/HD-23
Delft University of Technology

[3] Deformation and Damage Processes in Wood
Ph.D. Thesis
Dr.Ir. T.A.C.M. van der Put
Delft University of Technology

[4] Eurocode 5
Christmas version 1991

[5] Timber species
P. Laming, J.F. Rijsdijk c.s.
Houtinstituut TNO (in Dutch)

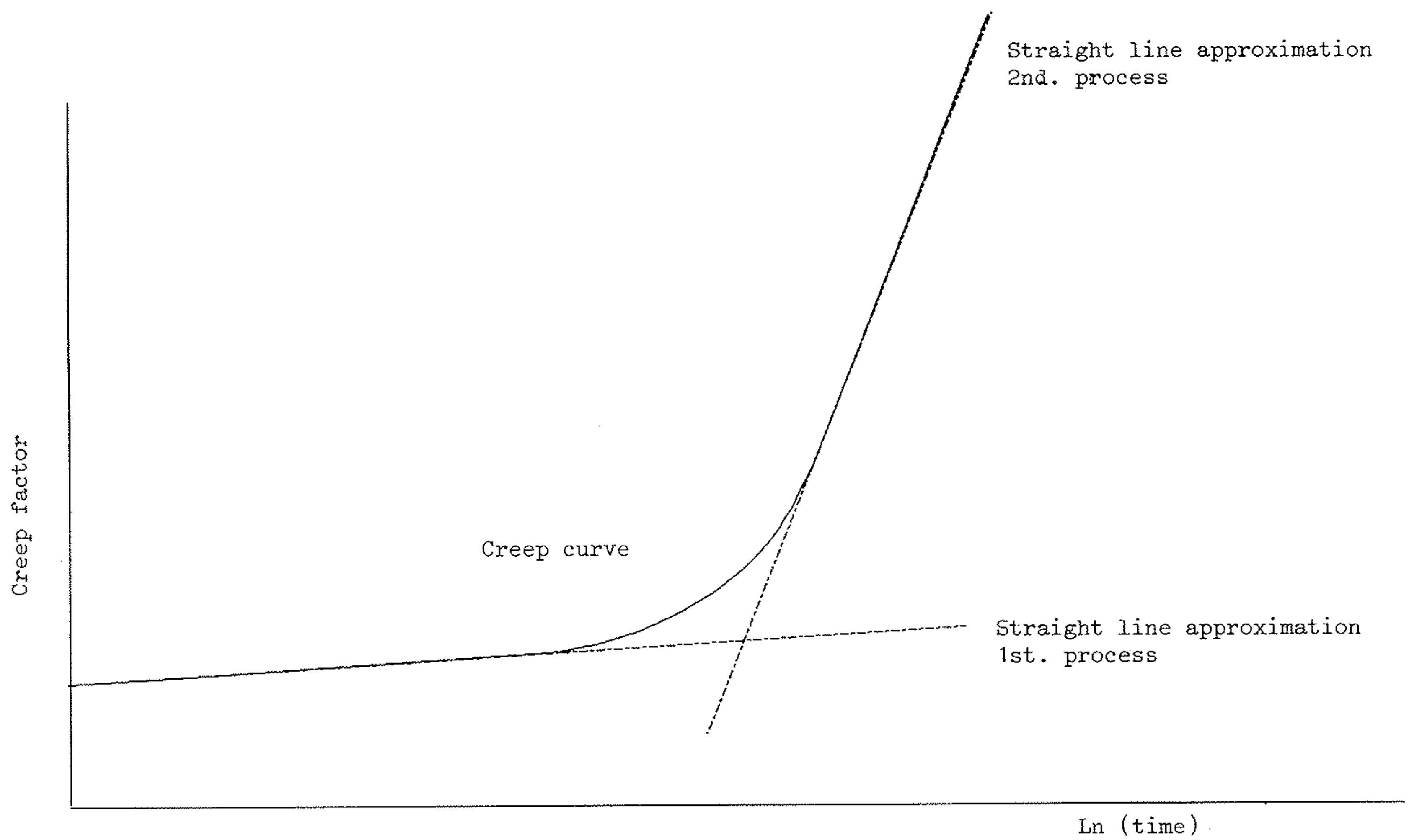

Figure 1. Master creep curve
Two processes with straight line approximations

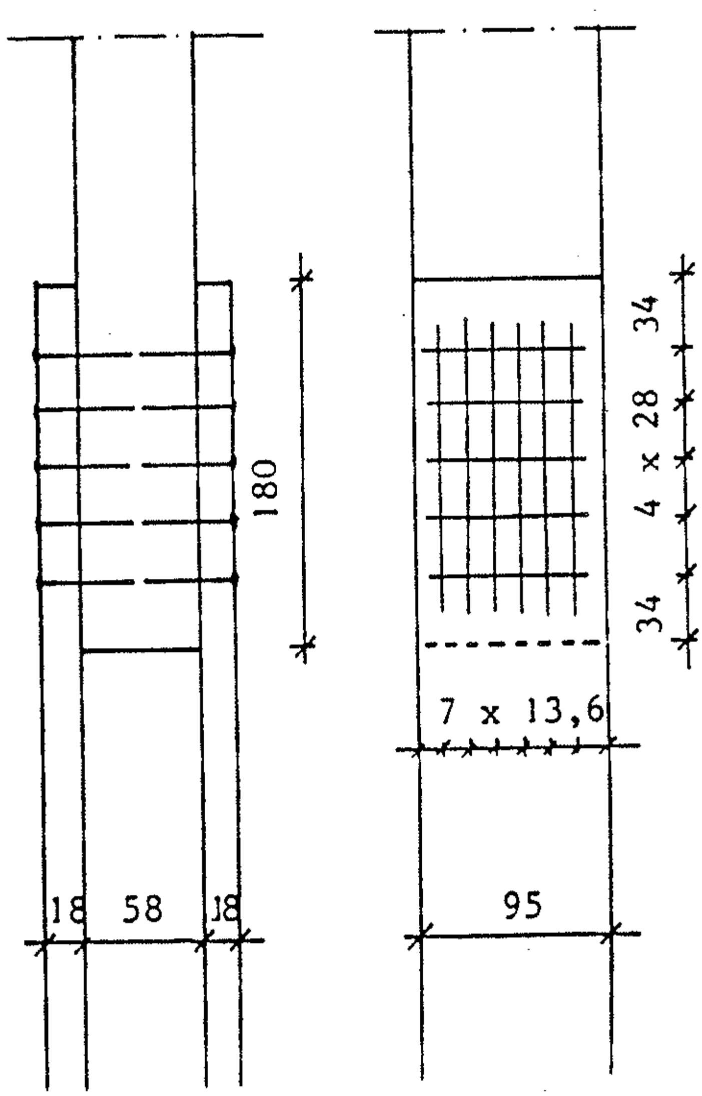

Figure 2. Test specimen

Nails: l = 45 mm, d = 2.8 mm

2 x 5 x 6 nails

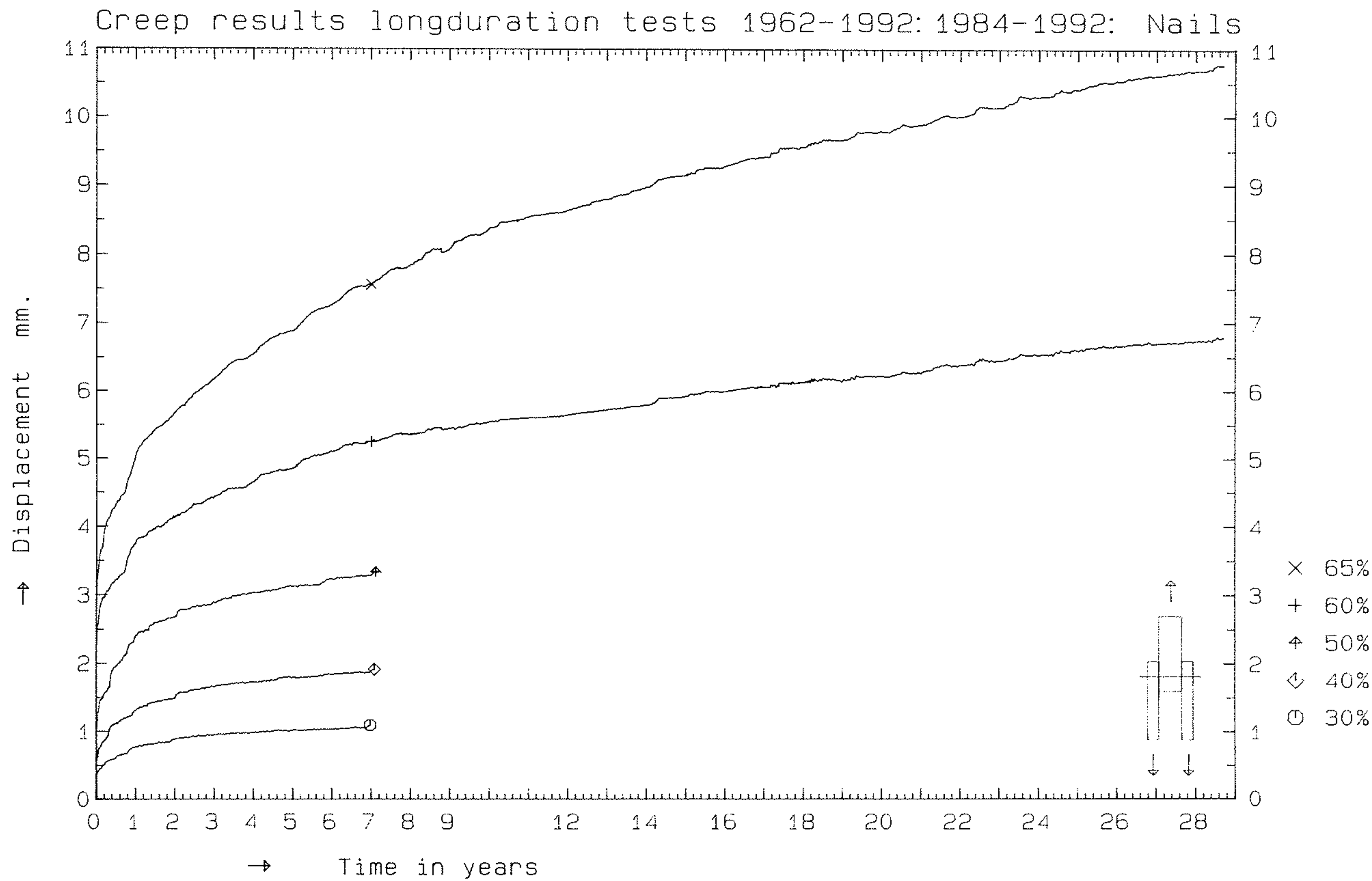

Figure 3. Average creep results of all load levels

TUDelft

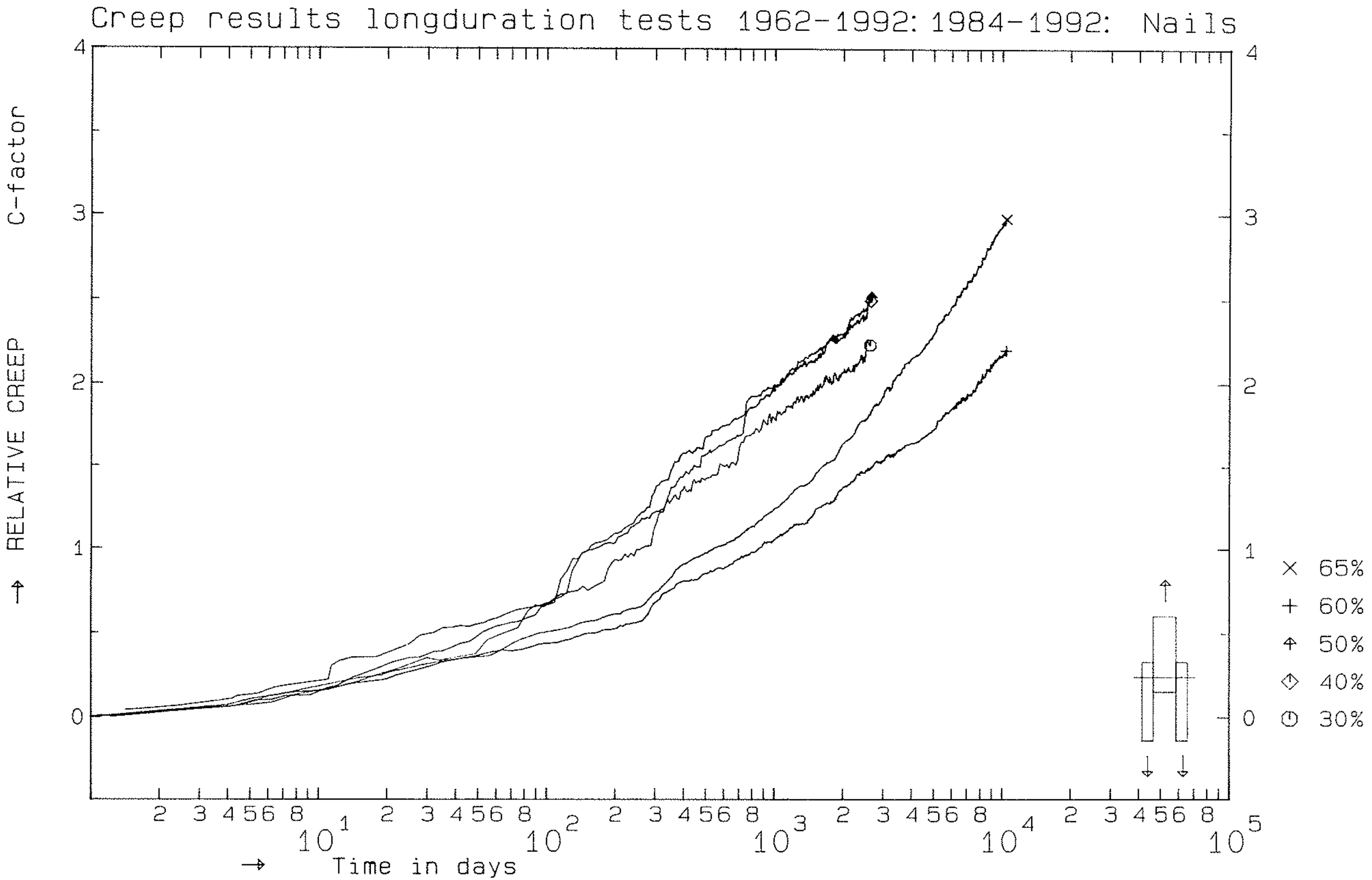

Figure 4. Relative creep versus log(t)

TUDelft

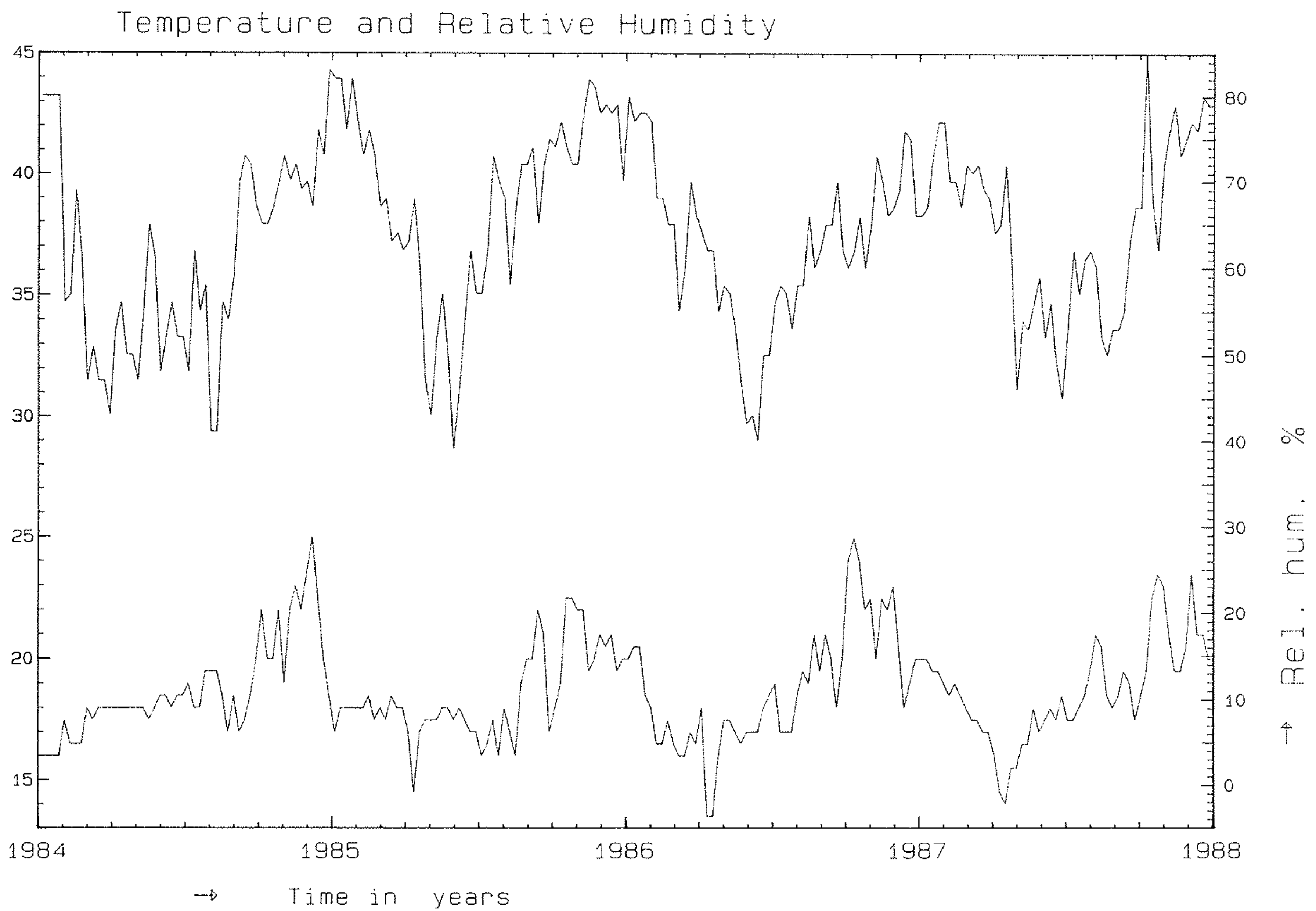

Figure 5. Temperature and relative humidity

TUDelft

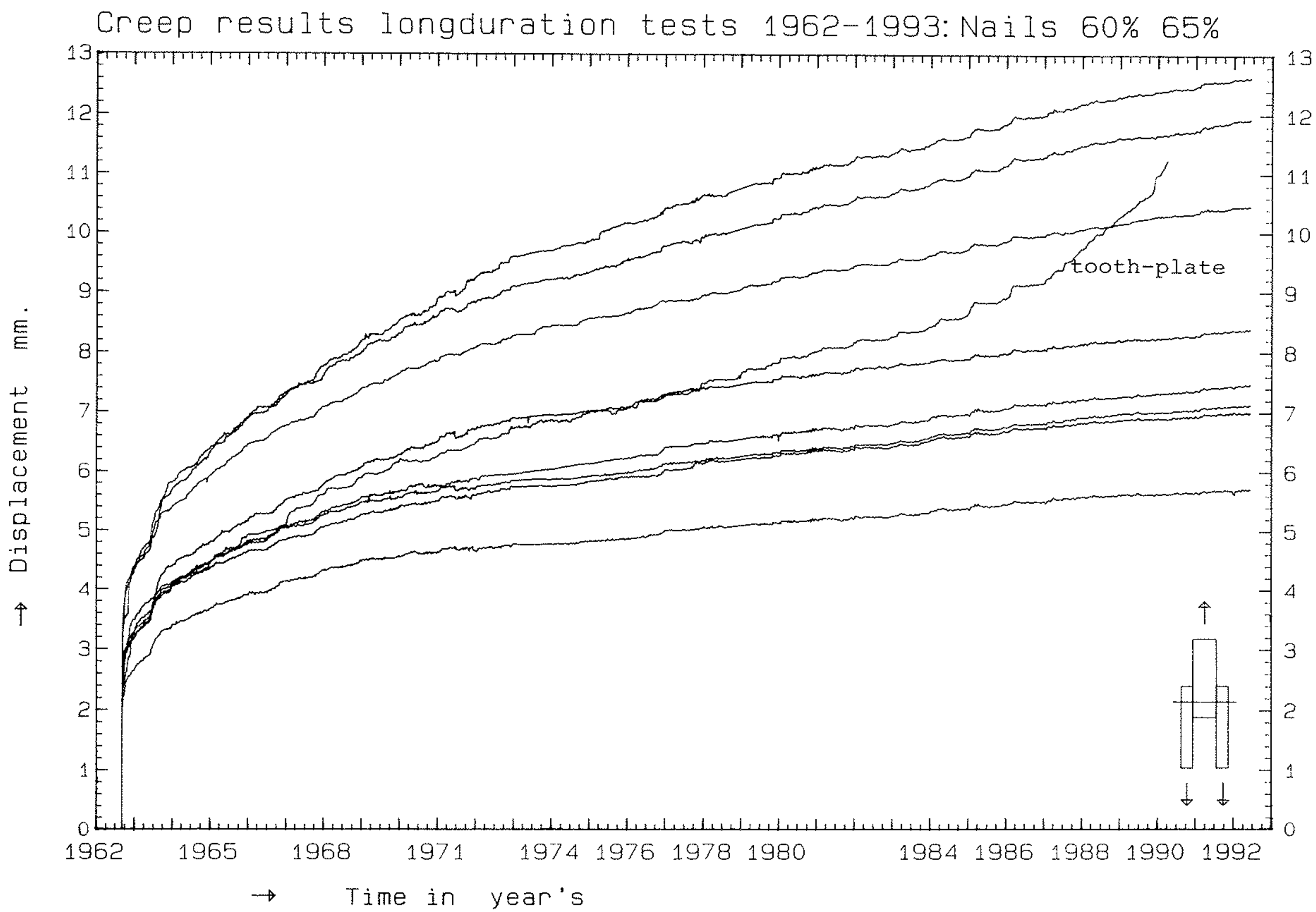

TUDelft

Figure 6. 60% and 65% nails, 65% tooth-plate

CIB-W18/25-7-10

INTERNATIONAL COUNCIL FOR BUILDING RESEARCH STUDIES AND DOCUMENTATION

WORKING COMMISSION W18 - TIMBER STRUCTURES

CHARACTERISTIC STRENGTH OF UK TIMBER CONNECTORS

by

A V Page

C J Mettem

TRADA Technology Limited

United Kingdom

MEETING TWENTY - FIVE

ÅHUS

SWEDEN

AUGUST 1992

CHARACTERISTIC STRENGTH OF UK TIMBER CONNECTORS

A.V. Page and C.J. Mettem

1. SUMMARY

Formulae are developed for calculating the characteristic load-carrying capacities parallel to the grain of the three principal types of timber connector used in the UK. The formulae allow for the size and shape of each connector and the density and thickness of the timber members. Minimum member thicknesses are also specified.

Results from the proposed formulae were compared with nominal characteristic values derived from the basic loads tabulated in the British timber design code, BS 5268: Part 2. The two sets of results were generally well within 10% of each other.

2. CONTENTS

Diameter of connector mm	Diameter of bolt mm
38	10/14
50	12/14
63	12/14
75	12/14

Types C8 and C9 are similar, but square, with side lengths equal to the diameters of the round connectors. The same diameters of bolt are used.

5. PERMISSIBLE LOADS

Permissible loads on connectored joints are obtained from data given in BS 5268 : Part 2 [3].

Connector units

In BS 5268 : Part 2, a "connector unit" is defined. The definition depends upon the type, and is given as:-

(i) one ring connector with its bolt in single shear in a timber-to-timber joint.

(ii) two plate connectors used back-to-back with the bolt in single shear in a timber-to-timber joint; or one shear plate with its bolt in single shear in a steel plate-to-timber joint.

(iii) one double-sided toothed-plate connector or two single-sided toothed-plate connectors back-to-back, with the bolt in single shear in a timber-to-timber joint; or one single-sided toothed plate connector with its bolt in single shear in a steel plate-to-timber joint.

Basic loads

BS 5268 : Part 2 tabulates "basic loads" for one connector unit. These relate to:

* long-term load duration (e.g. dead + permanent imposed loading)
* specified standard spacings, end- and edge- distances
* dry timber in "dry exposure" conditions (in which the moisture content of timber does not exceed 18% for any significant period)

The values given depend on the following parameters:

* the kind of connector unit
* the nominal size of the connector
* the strength group of the timber
* the thickness of the timber members in the connection
* the direction of the load relative to the grain

These parameters will now be considered in turn.

Table 1 Characteristic densities for BS 5268 : Part 2 joint strength class groups

1 Joint strength class group	SC1/SC2	SC3/SC4	SC5	SC6 to SC9
RING AND PLATE CONNECTORS				
2 $G_{mean,12\%}$	0.34	0.39	0.48	0.58
3 ρ_k (kg/m^3)	314	360	443	535
TOOTHED PLATE CONNECTORS				
4 $G_{0.01,18\%}$	0.24	0.29	0.34	
5 ρ_k (kg/m^3)	314	375	443	

For toothed-plate connectors, reference [4] states that the basic loads were based on $G_{0.01,18\%}$, the one per cent exclusion values of the specific gravity based on oven-dry weight and volume at 18% moisture content, as shown in line 4 of the table. Although these too can be converted to characteristic densities, the results do not entirely match the basic values for these connectors given in BS 5268 : Part 2, and it is believed that the values of ρ_k given in line 5 correspond to the densities which were finally used to calculate the basic loads for toothed plate connectors.

The minimum permissible thicknesses of the timber members are shown in Table 2.

Table 2 Minimum timber thicknesses for connectors, from BS 5268 : Part 2

Connector description	Connector on one side of the timber only mm	Connectors on both sides of the timber mm
64mm ring connector	22	32
102mm ring connector	29	41
67mm plate connector	41	41
102mm plate connector	41	44
Toothed-plate connector (all sizes)	16	32

Basic loads are tabulated for a number of different member thicknesses in each table. In the case of toothed plate connectors, test data were obtained from only one thickness each of the middle and outer members, as shown in Table 3. The values for the other thicknesses were obtained from separate data on the strength of bolted joints. In the case of the ring and plate connectors, however, tests were conducted on a range of timber thicknesses, and the values tabulated are therefore based directly on test data. It will be observed that in Tables 4 to 7 the strength of these joints, as for toothed-plate joints, is related to the thickness of the timber members.

For ring connectors and plate connectors, it was proposed in [1] that

$$R_{c,k} \quad = \quad 30\ d_c^{\ 1.5}\left(\frac{\rho_k}{380}\right)^{0.5} \qquad N \qquad (3)$$

This is the same as (1), except that no allowance is made for the contribution of the bolt because of the relatively large tolerances on the bolt hole dimensions.

Note that formulae (1) and (3) relate to parallel-to-the-grain loading only, to EC5 service class 1, and to one connector unit.

Two comments on these proposals may be made.

<u>Calculation of $R_{c,d}$</u>

In the case of formula (1), there is a problem in converting $R_{c,k}$ to $R_{c,d}$, the design value of the load-carrying capacity, as mentioned in reference [1],. Normally the design value of a material property is calculated as

$$X_d \quad = \quad \frac{k_{mod}X_k}{{}_m}$$

where γ_m = 1.3 for timber materials or 1.1 for steel used in joints, and for steel k_{mod} = 1.0 in all circumstances.

Since joints contain both steel and timber, there is no direct way to convert $R_{b,k}$ to $R_{b,d}$, so the bolt design formulae give $R_{b,d}$ directly. For the toothed-plate component in formula (1) it is not obvious which values of γ_m and k_{mod} should be used, since failure can occur either in the wood or in the metal teeth. Without further information, it may be necessary to use the values for timber, but in some combinations of load duration and service class this could give errors of 100% or more in the toothed-plate component of formula (1) if failure actually occurs in the teeth.

<u>Relationship between $R_{c,k}$ and $_k$</u>

In both formulae the calculated load-carrying capacity is proportional to the square root of the timber density, i.e. $R_k = k_1 \rho_k^{\ 0.5}$ where k_1 is a constant. However, in extensive tests conducted by the Building Research Establishment on toothed-plate connectors [7], it was found [8] that the load-carrying capacity and density were related in the form

$$R_{ult} \quad = \quad k_2 \rho^{1.325} \qquad (4)$$

This is illustrated in Figure 2. Since the basic loads for toothed plate connectors given in BS 5268 : Part 2 are derived from this relationship, it is unlikely that they can be brought into agreement with formula (1) for more than one value of density, unless the formula is adjusted accordingly.

Similarly, it was reported by Scholten [9] that, in split-ring connections, the load-carrying capacity and the timber density were related in the form

$$R_{ult} \quad = \quad k_3 \rho^{1.0} \qquad (4A)$$

This is illustrated in Figure 3. The basic loads for ring connectors given in BS 5268 : Part 2 are based on the above relationship. Chu [13] also reported tests made on joints with ring connectors in fourteen different species of timber.

8. COMPARISON OF CHARACTERISTIC LOAD-CARRYING CAPACITIES

Using a factor of 2.9, the basic loads given in BS 5268 : Part 2 for connector units loaded parallel to the grain may therefore be converted to nominal characteristic values and compared with the values calculated from formulae (1) and (3).[1]

For the comparison exercise the characteristic timber densities given in Table 2 were used. For formula (1) a value of 320 N/mm^2 was assumed for the mean value of the tensile and yield strength of the bolt.[2] For the square toothed-plate connectors, formula (2) was used to calculate d_c in formula (1).

The results of the comparison exercise are shown in Tables 3 to 7. They apply to one connector unit in a joint consisting of three solid timber members joined together by two connectors and a bolt. In these tables:-

(i) the values in the column headed "BS 5268" are basic values multiplied by a factor of 2.9.

(ii) the values in the column headed "E Gehri" are derived from formula (1) for toothed-plates and from formula (3) for the other connectors.

(iii) CI(G) is a comparison index relating the two sets of values.

(iv) the values in the final columns are calculated from formulae which are presented in Section 9 of this paper.

(v) with reference to Table 4 on toothed-plate connectors, BS 5268: Part 2: Table 74 tabulates basic loads corresponding to various member thicknesses. The member thicknesses chosen for inclusion in Table 4 are the nearest ones to the original thicknesses tested.

Table 74 in the Code gives the same values for round and square plates in the 38mm and 64mm sizes. (In the case of the 64mm plates, this is because only round plates were tested, and the same may be true for the 38mm plates also). Consequently, the values given in the Code for square plates in these sizes are probably too low, and to use them in this comparison exercise would be misleading. They have therefore been omitted from Table 4.

---

1 *In practice this involves making the following assumptions and approximations:*

(a) The nominal diameters of the round UK connectors may be entered as d_c in formulae (1) and (3); and the values of d_c for square connectors may be calculated from formula (2);

(b) The values of $R_{c,k}$ calculated from formulae (1) and (3) relate to the load-carrying capacities for the standard (not minimum) spacing, end- and edge-distances given in BS 5268 : Part 2, since these are the distances for which basic loads are tabulated;

(c) When characteristic values thus derived are converted by EC5 procedures to design values for other load durations, the solutions thus derived will only match the solutions which would be produced by BS 5268 design if the conversion factor used is $\frac{k_{mod}}{1.3}$.
This may not be correct for the bolt element in formula (1), for which k_{mod} = 1.0 and γ_m = 1.1 if there is failure in the bolt.

2 *This value, which was also used by Blass et al. [6], is consistent with the material specifications for black bolts; however, tests by TRADA [12] showed that, after manufacture, the mechanical properties of bolts improve considerably, and for small cold-formed bolts can be nearly double the quoted values.*

Table 4 Comparison of characteristic plate connector loads parallel to the grain for 67mm diameter shear-plate connector units with 20mm diameter bolts

Timber				Characteristic load-carrying capacity						
BS 5268	Density	Thickness of members					connector on one side		connector on two sides	
strength class	ρ_k kg/m	side mm	middle mm	BS 5268 kN	Gehri kN	CI(G)*	Formula 6 kN	CI(6)*	Formula 6 kN	CI(6)*
SC1/SC2	314		41	18.70	14.96	0.80	-	-	19.09	1.02
			50	22.39	14.96	0.67	-	-	21.08	0.94
			63	23.81	14.96	0.63	-	-	23.66	0.99
		41	67	24.13	14.96	0.62	24.40	1.01	24.40	1.01
SC3/SC4	360		41	21.43	16.01	0.75	-	-	21.89	1.02
			50	25.66	16.01	0.62	-	-	24.17	0.94
			63	27.32	16.01	0.59	-	-	27.13	0.99
		41	67	27.67	16.01	0.58	27.98	1.01	27.98	1.01
SC5	443		41	26.39	17.76	0.67	-	-	26.93	1.02
			50	31.61	17.76	0.56	-	-	29.74	0.94
			63	33.64	17.76	0.53	-	-	33.39	0.99
		41	67	33.93	17.76	0.52	34.43	1.01	34.43	1.01
SC6-SC9	535		41	31.90	19.52	0.61	-	-	32.53	1.02
			50	34.51	19.52	0.57	-	-	35.92	1.04
			63	34.51	19.52	0.57	-	-	40.32	1.17
		41	67	34.51	19.52	0.57	41.58	1.20	41.58	1.20

* CI(G) comparison index = $\dfrac{\text{Characteristic load-carrying capacity according to E. Gehri}}{\text{Nominal characteristic load-carrying capacity according to BS 5268 : Part 2}}$

CI(6) comparison index = $\dfrac{\text{Characteristic load-carrying capacity according to formula (6)}}{\text{Nominal characteristic load-carrying capacity according to BS 5268 : Part 2}}$

Table 6 Comparison of characteristic ring connector loads parallel to the grain for 64mm diameter split-ring connector units with 12mm diameter bolts

Timber				Characteristic load-carrying capacity						
BS 5268 strength class	Density ρ_k kg/m	Thickness of members side mm	Thickness of members middle mm	BS 5268 kN	Gehri kN	CI(G)*	connector on one side Formula 7 kN	connector on one side CI(7)*	connector on two sides Formula 7 kN	connector on two sides CI(7)*
SC1/SC2	314	22	32	15.17	13.96	0.92	15.34	1.01	15.24	1.00
		25	40	18.33	13.96	0.76	18.23	0.99	18.43	1.01
		29	50	22.27	13.96	0.63	22.27	1.00	22.27	1.00
SC3/SC4	360	22	32	17.40	14.95	0.86	17.59	1.01	17.48	1.00
		25	40	21.02	14.95	0.71	20.90	0.99	21.13	1.01
		29	50	25.55	14.95	0.59	25.54	1.00	25.54	1.00
SC5	443	22	32	21.43	16.58	0.77	21.64	1.01	21.50	1.00
		25	40	25.87	16.58	0.64	25.72	0.99	26.00	1.00
		29	50	31.32	16.58	0.53	31.42	1.00	31.42	1.00
SC6-SC9	535	22	32	25.87	18.23	0.70	26.14	1.01	25.97	1.00
		25	40	31.32	18.23	0.58	31.06	0.99	31.39	1.00
		29	50	37.99	18.23	0.48	37.95	1.00	37.95	1.00

$$\text{* CI(G) comparison index} = \frac{\text{Characteristic load-carrying capacity according to E. Gehri}}{\text{Nominal characteristic load-carrying capacity according to BS 5268 : Part 2}}$$

$$\text{CI(7) comparison index} = \frac{\text{Characteristic load-carrying capacity according to formula (7)}}{\text{Nominal characteristic load-carrying capacity according to BS 5268 : Part 2}}$$

9. DISCUSSION OF RESULTS

In Tables 3 to 7 a comparison index, CI(G), gives the ratio between the characteristic load-carrying capacities calculated from E. Gehri's formulae, and the nominal characteristic values obtained from BS 5268 : Part 2. The following comments may be made.

9.1 Table 3. Toothed-plate connectors

The comparison index, CI(G), shows that formula (1) produces values of $R_{k,c}$ which on average are very close to the nominal characteristic values derived from BS 5268. Also the formula accurately allows for the size of the connector. The similarity of the values of CI for the round and square connectors in the 51mm and 76mm sizes shows that formula (2) gives an accurate assessment of the effective diameter of a square toothed-plate.

Nevertheless, the values of CI(G) demonstrate that formula (1) is incorrect in its assessment of the effect of density on strength. A formula which produces results closer to those derived from BS 5268, and which therefore reflects more accurately the experimental data[3] would be:-

$$R_{c,k} = 15\, d_c^{1.5}\left(\frac{\rho_k}{380}\right)^{1.5} + R_{b,k} \quad N$$

9.2 Tables 4 and 5. 67mm and 102mm plate connectors

The comparison indices CI(G) in these and the two subsequent tables are based on values of $R_{c,k}$ calculated from formula (3). This means that there is no allowance for the contribution of a bolt and therefore there is no allowance for the influence of member thickness. This means that the values of $R_{c,k}$ fall increasingly short of the nominal characteristic values as the thickness of the timber members increased, particularly in the case of the 102mm diameter connector. In general the values of $R_{c,k}$ calculated from the formula are too low, and again there is an inadequate allowance for the influence of density, which the test work showed was directly proportional to the strength. The fact that the values of CI are relatively higher in Table 5 means that the formula assumes that the diameters of the connectors influence the strength more than they really do.

Formulae which produce results closer to those derived from BS 5268 and which therefore reflect more accurately the experimental data would be as follows.

For 67mm connectors on one side of a member only

$$R_{c,k} = 441\, d_c\left(\frac{\rho_k}{380}\right) \quad N$$

or, for connectors on both sides and on the same bolt

$$R_{c,k} = 441\, d_c\left(\frac{\rho_k}{380}\right)\left(\frac{t_2}{67}\right)^{0.5} \quad N$$

---

3 Note that in formula (4) the contributions of the toothed plate and the bolt are combined into one expression.

For non-circular connectors $d_c = \left(\frac{4A_c}{\pi}\right)^{0.5}$

where A_c = the connector area in mm^2

The minimum permissible thickness of timber is 16mm for connectors on one side of a member only, and 32mm for connectors on two sides and on the same bolt."

"For plate connectors, the characteristic looad-carrying capacity of one connector unit is:

$$R_{c,k} = 1.16\ d_c\ \rho_k\ k_p \quad N \qquad (6)$$

where d_c = the nominal diameter of the connector in mm

ρ_k = the characteristic density of the timber in kg/m^3

k_p = 1.0 for connectors on one side of a member only

$k_p = \left(\frac{t}{t_{standard}}\right)^{0.5}$ for connectors on two sides of a member and on the same bolt

where t = thickness of the member in mm

$t_{standard}$ = the standard thickness of the member taken from Table 8

In no case may k_p exceed 1.0.

The minimum permissible thicknesses of the timber members are given in Table 8."

Table 8. Member thicknesses for plate connectors

	Diameter of connector	Thickness mm	
	mm	t_{min}	$t_{standard}$
Connector on one side only	67 102	41 44	
Connector on both sides and on the same bolt	67 102	41 44	67 90

"For ring connectors, the characteristic load-carrying capacity of one connector unit is

$$R_{c,k} = 0.21\ d_c^{1.4}\ \rho_k\ k_r \quad N \qquad (7)$$

REFERENCES

[1] CEN/TC 124/WG4 Document N16, 24 February 1992

[2] Draft of EN TC 124.401 Timber fasteners - Specifications for connectors for timber. CEN/TC 124/WG4. February 1992

[3] BS 5268 : Part 2 : 1991. Structural use of timber : Code of practice for permissible stress design, materials and workmanship. BSI, 1991

[4] "Derivation of permissible loads for mechanical fasteners", prepared by Princes Risborough Laboratory. CSB 32/7-80/2, May 1980

[5] Page, A.V. Characteristic and mean densities for use with BS 5268 strength classes. Unpublished. TRADA, 1992

[6] Blass, H.J., Ehlbeck, J. and Schlager, M. Characteristic strength of tooth-plate connector joints. CIB-W18/25-7-7, Sweden, 1992

[7] Brock, G.R. The strength of toothed-plate timber connector joints. Unpublished. Princes Risborough Laboratory, 1952

[8] Brock, G.R. Permissible loads for toothed-plate timber connector joints. Unpublished. Princes Risborough Laboratory, 1958

[9] Scholten, J.A. Timber-connector joints : their strength and design. USDA FPL, 1944

[10] Booth, L.G. and Reece, P.O. The structural use of timber, p. 166. Spon, London, 1967

[11] Page, A.V. and Mettem, C.J. Final report for efficient detailing of mechanical joints in engineered timber structures. PIF 73/6, TRADA, 1992

[12] Whale, L.R.J. and Smith, I. Mechanical joints in structural timber - information for probabilistic design. Research Report 17/86, TRADA, 1986

[13] Chu, Y.P. Strength of split-ring connectored joints . Malaysian Forester, Vol 42, No.2, 1979

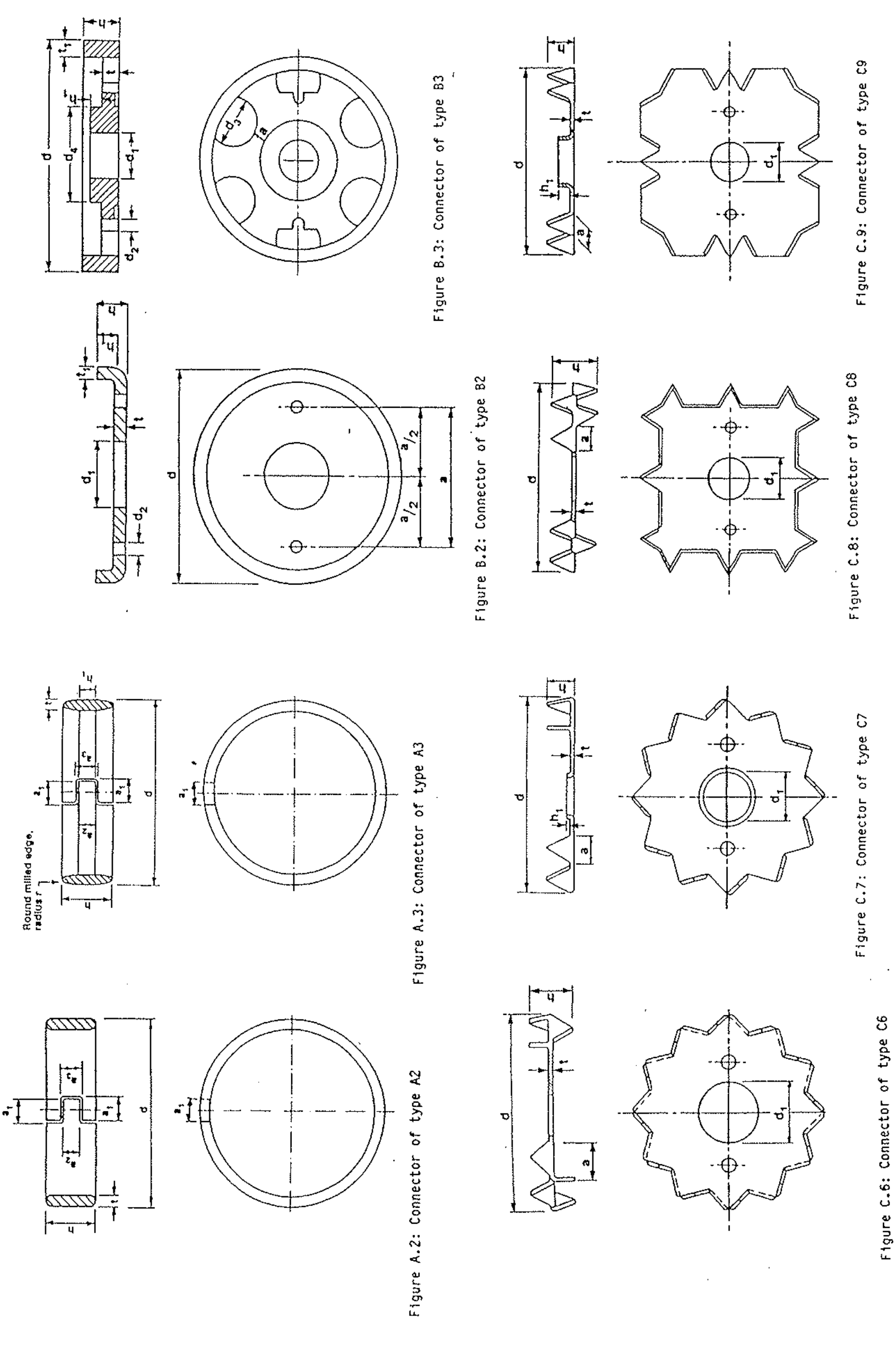

Figure 1 - Timber connectors used in the United Kingdom

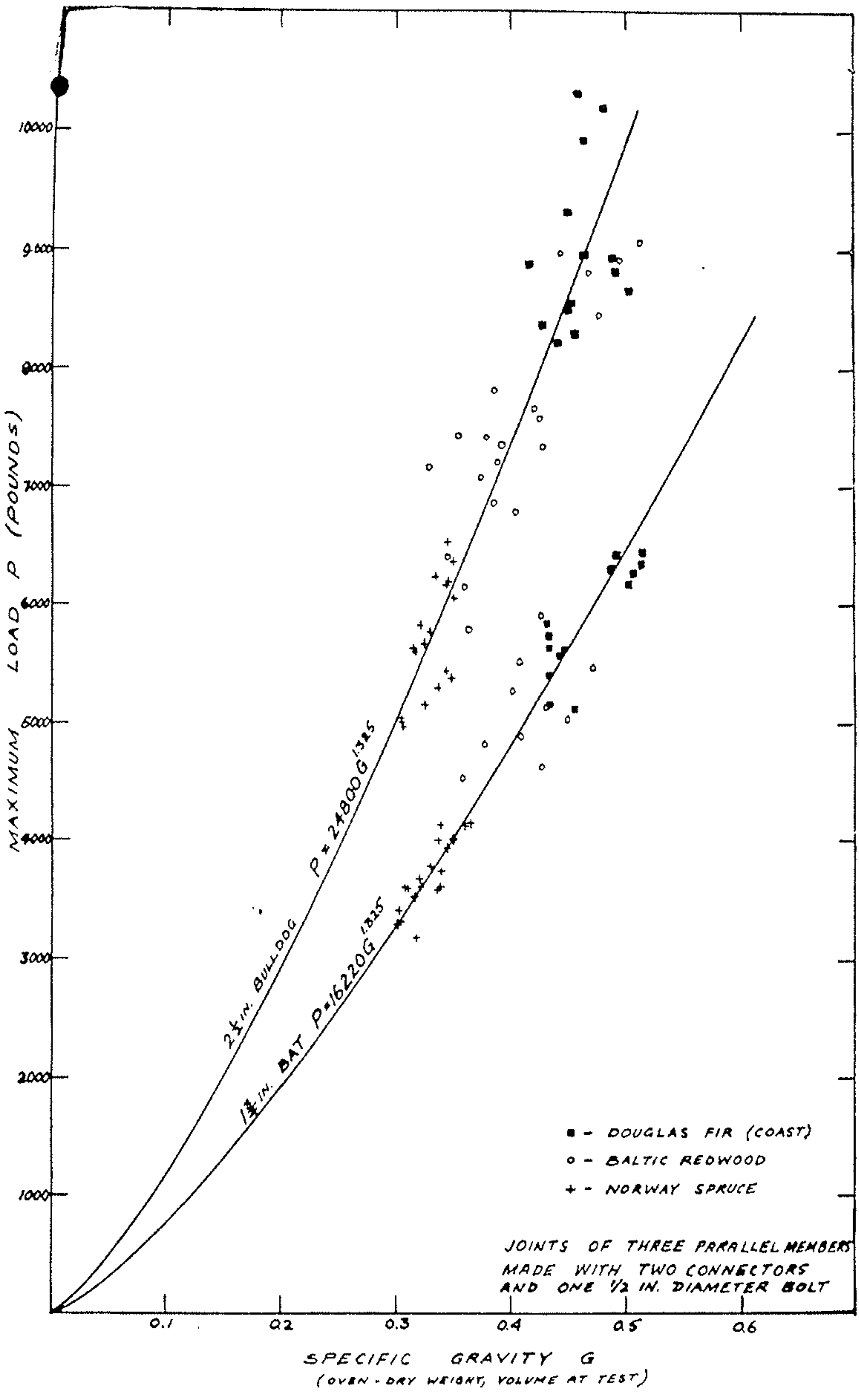

FIG. 2 THE RELATIONSHIP BETWEEN STRENGTH IN COMPRESSION AND SPECIFIC GRAVITY FOR TOOTHED-PLATE CONNECTOR JOINTS OF WOOD AT 18 PER CENT MOISTURE CONTENT

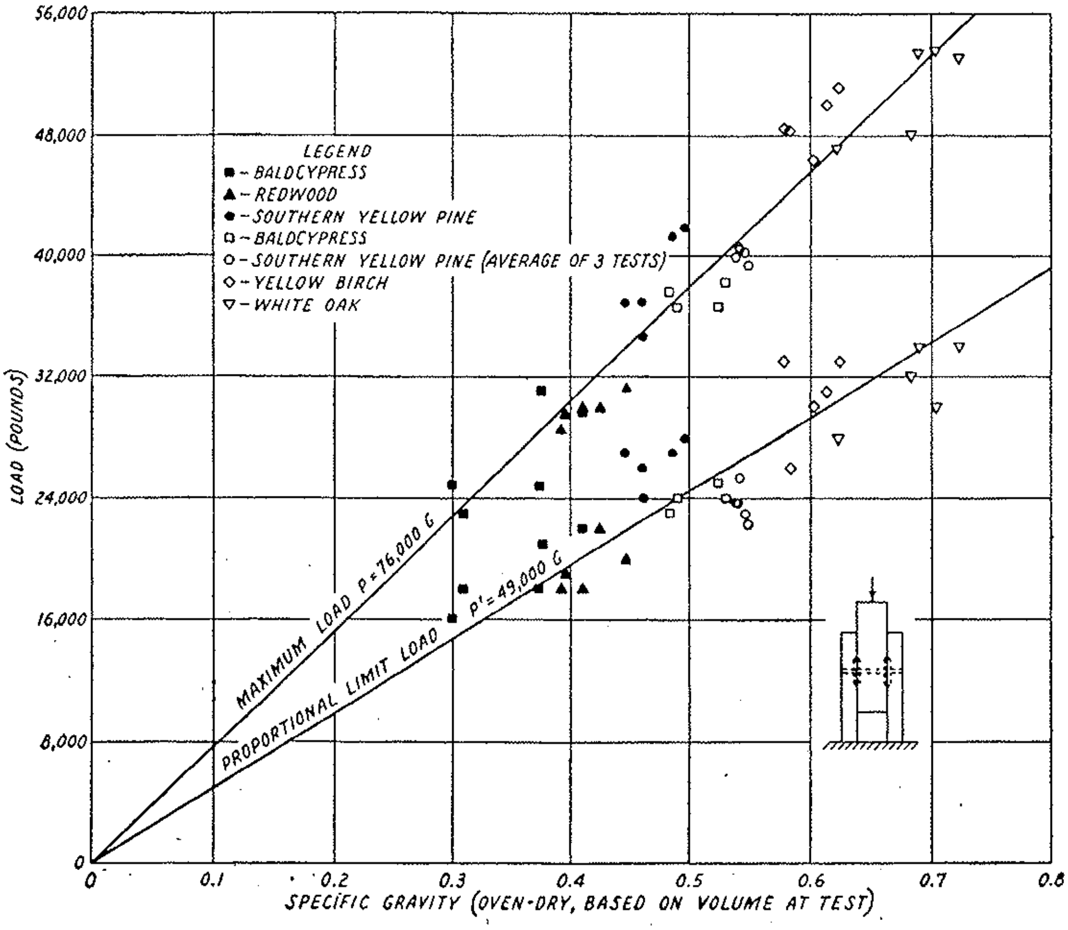

FIGURE 3.—Relation between load bearing parallel to the grain and specific gravity of air-dry wood for a split-ring connector joint consisting of two 4-inch connectors and a ¾-inch bolt. The solid and open symbols for the same species indicate marked differences in specific gravity.

CIB-W18/25-8-1

INTERNATIONAL COUNCIL FOR BUILDING RESEARCH STUDIES AND DOCUMENTATION

WORKING COMMISSION W18 - TIMBER STRUCTURES

ANALYSIS OF GLULAM SEMI-RIGID PORTAL FRAMES UNDER LONG-TERM LOAD

by

K Komatsu

N Kawamoto

Forestry and Forest Products Research Institute

Japan

MEETING TWENTY - FIVE

ÅHUS

SWEDEN

AUGUST 1992

Paper presented to the 25th Meeting of CIB-W18A, Sweden, 1992.

Analysis of Glulam Semi-Rigid Portal Frames under Long-Term Load

by

Kohei Komatsu* and Norio Kawamoto*

ABSTRACT

Deformation of glulam portal frame whose beam-column joints were connected using such mechanical fasteners as nails or drift-pins were analysed in this study. A closed form solution for the mid-span deflection δ of the beam member was derived by applying the minimum energy principle and the virtual work method. Axial, shear and rotational rigidity were considered for taking the effect of semi-rigid behaviour of joints into the analysis. Experiments were done by using two kinds of glulam portal frames of 5.4m span length and 1.8m height, one of which was composed of nail-on-steel plate joint and the other was composed of drift-pin joints. Two points dead loads were applied for about 200 days. Coincident between theoretical prediction and experimental measurement were much better in the nailed jointed specimen than the drift-pin jointed one, because the former had less clearance between nails and pre-drilled nail holes.

1.Introduction

Deformation of glulam portal frame built using the mechanical fasteners is strongly affected by the fasteners's mechanical properties. Usually, deformation of this kind of semi-rigid frame can be easily analysed by employing a nonlinear finite element method program. FEM solution is, however, not feasible to understand the basic characteristics of semi-rigid portal frame because it is a kind of particular solution for a particular material and geometrical combination. In order to analyze more fundamental aspect of the semi-rigid glulam portal frame, it might be necessary to derive a closed form solution in which basic parameters such as joint rigidity, material parameters, geometrical parameters involved.

For this end, we derived a closed-form solution of the deformation of a single-story glulam portal frame whose column-beam joints were composed of nails or/and drift-pins with steel gusset plates, by applying the principle of minimum energy and virtual work theory which was first proposed by Hirai[1] in the field of the analysis of the semi-rigid glulam portal frames.

* Laboratory of Engineered Timber Joints
Forestry and Forest Products Research Institute
P.O. Box 16, Tsukuba Norin Kenkyu Danchi, Ibaraki 305, Japan

2. THEORY

2.1 Definition of portal frame and symbols used

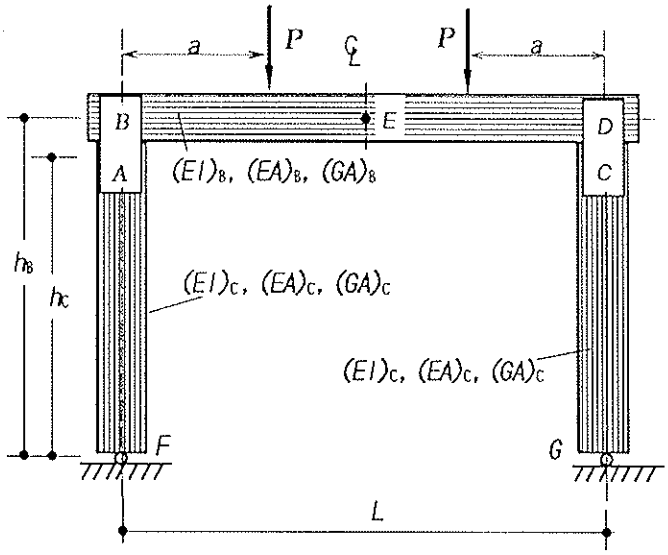

Fig.1 Glulam portal frame to be analyzed.

Figure 1 shows a glulam portal frame as the objective of our analysis. Joints A,B,C, and D are assumed as the linear semi-rigid joint. In Fig.1, definition of the symbols used are as follows;

L = Span of portal frame (m)

h_B = Distance between support of column and center-line of beam member (m)

h_C = Distance between support and upper rotation center of column member (m)

$(EI)_B$ = Flexural rigidity of beam member (kNm^2)

$(EA)_B$ = Axial rigidity of beam member (kN)

$(GA)_B$ = Shear rigidity of beam member (kN)

$(EI)_C$ = Flexural rigidity of beam member (kNm^2)

$(EA)_C$ = Axial rigidity of beam member (kN)

2.2 Joints rigidity

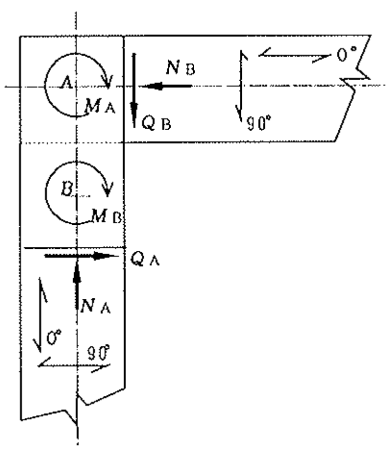

$$M_J = R_J \cdot \theta_J \qquad \text{......1)}$$

$$N_J = D_J \cdot \Delta_{0J} \qquad \text{......2)}$$

$$Q_J = S_J \cdot \Delta_{90J} \qquad \text{......3)}$$

Fig.2 Definition of forces acting in the joints.

Within the joint-J of the portal frame, we assume that a linear relationship between forces $\{M_J, N_J, Q_J\}$ and displacement $\{\theta_J, \Delta_{0J}, \Delta_{90J}\}$ can be held as shown in equations1) ,2) and 3).

where,

$R_J = n_{SJ}\{\Sigma K_{0i}y_i^2 + \Sigma K_{90i}x_i^2\}$:(Rotational rigidity of joint-J) ......4)

$D_J = n_{SJ}\Sigma K_{0i}$:(Axial rigidity of joint-J) ......5)

$S_J = n_{SJ}\Sigma K_{90i}$:(Shear rigidity of joint-J) ......6)

n_{SJ} : number of shear plane where K_{0i}, and K_{90i} are considered.
K_{0i} : the slip modulus of i-th fastener parallel to the grain (kN/m)
K_{90i} : the slip modulus of i-th fastener perpendicular to the grain (kN/m)
x_i, y_i : x-y coordinates of i-th fastener
i=1 ~ n: number of single-shear fastener per joint-J

2.3 Horizontal reaction force

2.3.1 *Stress distribution*

Figures 3, 4 and 5 show moment, shear and axial force diagram expressed involving with the unknown horizontal reaction force *H*.

Moment distribution

From point F to B;

$M_y = -Hy$ ....7)

From point B to loading point P;

$M_x = Px = -Hh_B$ ....8)

Between two loading points;

$M_x = Pa - Hh_B$ ....9)

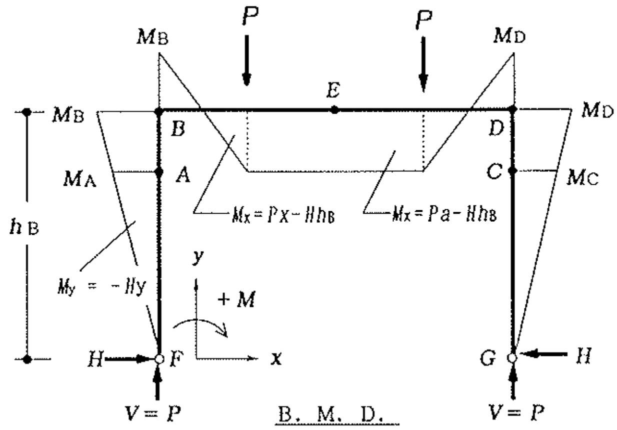

Fig.3 Moment diagram

Shear force distribution

From point F to B;

$Q_y = dM_y/dy = -H$ ....10)

From point B to loading point;

$Q_x = dM_x/dx = P$ ....11)

Between two loading points;

$M_x = dM_x/dx = 0$ ....12)

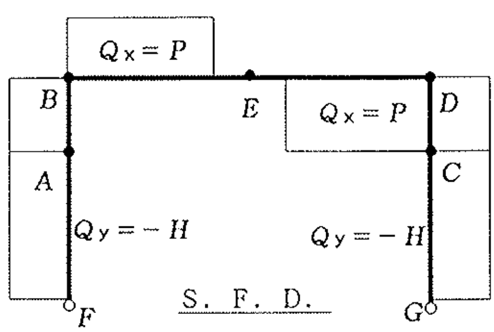

Fig.4 Shear force diagram

Axial force distribution

For column members;

$$N_y = V = P \qquad \text{....13)}$$

For beam member;

$$N_x = Qy = -H \qquad \text{....14)}$$

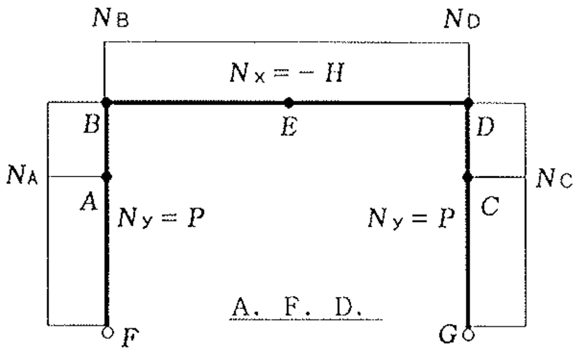

Fig.5 Axial force diagram

2.3.2 *Complementary energy*

Energy due to member moment U_M

$$U_M = 2\int_0^{h_C} \frac{M_y{}^2}{2(EI)_C} y + 2\left\{\int_0^{a} \frac{M_x{}^2}{2(EI)_B} dy + \int_0^{L/2} \frac{M_x{}^2}{2(EI)_B} dx\right\}$$

$$= \frac{H^2 h_C{}^3}{3(EI)_C} + \frac{1}{(EI)_B}\left\{\frac{h_B{}^2 LH^2}{2} - (Pah_B L - Pa^2 h_B)H + \left(\frac{P^2 a^2 L}{2} - \frac{2P^2 a^3}{3}\right)\right\} \qquad \text{....15)}$$

Energy due to member shear force U_S

$$U_S = 2\int_0^{h_C} \frac{Q_y{}^2}{2(GA)_C} \kappa\, dy + 2\int_0^{a} \frac{Q_x{}^2}{2(GA)_B} \kappa\, dx = \frac{H^2 h_C \kappa}{(GA)_C} + \frac{P^2 a \kappa}{(GA)_B} \qquad \text{.....16)}$$

Energy due to member axial force U_N

$$U_N = 2\int_0^{h_C} \frac{N_y{}^2}{2(EA)_C} dy + \int_0^{a} \frac{N_x{}^2}{2(EA)_B} dx = \frac{P^2 h_C}{(EA)_C} + \frac{H^2 L}{2(EA)_B} \qquad \text{.....17)}$$

Energy due to joint moment U_{JM}

$$U_{JM} = 1/2(M_A\theta_A + M_B\theta_B + M_C\theta_C + M_D\theta_D)$$

$$= \frac{H^2}{2}\left\{h_C{}^2\left(\frac{1}{R_A} + \frac{1}{R_C}\right) + h_B{}^2\left(\frac{1}{R_B} + \frac{1}{R_D}\right)\right\} \qquad \text{......18)}$$

Energy due to joint shear force U_{JQ}

$$U_{JQ} = 1/2(Q_A \Delta_{90A} + Q_B \Delta_{90B} + Q_C \Delta_{90C} + Q_D \Delta_{90D})$$

$$= \frac{1}{2} \{ H^2 (\frac{1}{S_A} + \frac{1}{S_C}) + P^2 (\frac{1}{S_B} + \frac{1}{S_D})\} \qquad \ldots\ldots 19)$$

Energy due to joint axial force U_{JN}

$$U_{JN} = 1/2(N_A \Delta_{OA} + N_B \Delta_{OB} + N_C \Delta_{OC} + N_D \Delta_{OD})$$

$$= \frac{1}{2} \{ P^2 (\frac{1}{D_A} + \frac{1}{D_C}) + H^2 (\frac{1}{D_B} + \frac{1}{D_D}) \} \qquad \ldots\ldots 2$$

The unknown vertical reaction force H can be determined so as to minimize the total complementary energy stored in the portal frame. Namely;

$$\frac{\partial \Sigma U}{\partial H} = 0 \qquad \ldots\ldots 21)$$

where,

$$\Sigma U = U_M + U_S + U_N + U_{JM} + U_{JQ} + U_{JN} \qquad \ldots\ldots 22)$$

Substituting equations 15) to 20) into equation 22) then executing equation 21), we obtained equation 23) for the determination of H.

$$H = \frac{Pah_B(L-a)}{2h_C{}^3 k/3 + h_B{}^2 L + 2h_C \omega \kappa + q_B L + \lambda} \qquad \ldots\ldots 23)$$

where,

$$k = (EI)_B/(EI)_C, \quad \omega = (EI)_B/(GA)_C$$
$$\lambda = (EI)_B \cdot \phi, \quad q_B = (EI)_B/(EA)_B \qquad \ldots\ldots 24)$$

and

$$\phi = h_C{}^2 (\frac{1}{R_A} + \frac{1}{R_C}) + h_B{}^2 (\frac{1}{R_B} + \frac{1}{R_D}) + (\frac{1}{S_A} + \frac{1}{S_C}) + (\frac{1}{D_B} + \frac{1}{D_D}) \qquad \ldots\ldots 25)$$

2.4 MID-SPAN DEFLECTION

The deflection of mid-span point E, i.e. δ_E, can be derived by applying so-called virtual work method as shown in equation 26).

$$\delta_E = \Sigma \int \frac{M\bar{M}}{EI} ds + \Sigma \frac{M_J \bar{M}_J}{R_J} \quad \text{(moment)}$$

$$+ \Sigma \int \frac{Q\bar{Q}}{GA} \kappa \, ds + \Sigma \frac{Q_J \bar{Q}_J}{S_J} \quad \text{(shear force)}$$

$$+ \Sigma \int \frac{N\bar{N}}{EA} ds + \Sigma \frac{N_J \bar{N}_J}{D_J} \quad \text{(axial force)} \qquad \text{......26)}$$

In the equation 26), $\bar{M}$, $\bar{Q}$, $\bar{N}$ and $\bar{M}_J$, $\bar{Q}_J$, $\bar{N}_J$ are the moment, shear force and axial force when a unit load is applied on the mid-span point E. Figures 6-a, 6-b, and 6-c show moment, shear force and axial force diagram when the unit

load is applied on the point E. Corresponding reaction force $\bar{H}$ is easily obtained by substituting $a=L/2$ and $P=1/2$ into equation 23) as follows;

$$\bar{H} = \frac{(h_B L^2/8)}{(2h_C{}^3 k/3 + h_B{}^2 L + 2h_C \omega \kappa + q_B L + \lambda)} \qquad \text{......27)}$$

2.4.1 *Calculation of* δ_E

<u>Deflection due to moment</u>

$$\delta_{EM} = 2\int_0^{h_C} \frac{M_y \bar{M}_y}{(EI)_C} dy + 2\left\{\int_0^a \frac{M_x \bar{M}_x}{(EI)_B} dx + \int_a^{L/2} \frac{M_x \bar{M}_x}{(EI)_B} dx\right\}$$

$$+ \frac{Hh_C \bar{H} h_C}{R_A} + \frac{Hh_B \bar{H} h_B}{R_B} + \frac{Hh_C \bar{H} h_C}{R_C} + \frac{Hh_B \bar{H} h_B}{R_D}$$

$$= \frac{2H\bar{H}h_C{}^3}{3(EI)_C} + \frac{2}{(EI)_B}\left\{\frac{PaL^2}{16} - \frac{Pa^3}{12} - \frac{Pa\bar{H}h_B}{2}(L-a) - \frac{Hh_B L^2}{16} + \frac{H\bar{H}h_B{}^2 L}{2}\right\} + H\bar{H}f(R) \qquad \text{......28)}$$

$$f(R) = h_C{}^2\left(\frac{1}{R_A} + \frac{1}{R_C}\right) + h_B{}^2\left(\frac{1}{R_B} + \frac{1}{R_D}\right) \qquad \text{......29)}$$

For simplicity, next expression is used.

$$\delta_{EM}(EI)_B = 2H\bar{H}h_C{}^3 k/3 + H\bar{H}(EI)_B f(R) + Pa(L^2/8 - a^2/6) - Pa\bar{H}h_B(L-a)$$
$$- Hh_B L^2/8 + H\bar{H}h_B{}^2 L \qquad \text{......30)}$$

Deflection due to shear force

$$\delta_{EQ} = 2\int_0^{hc} \frac{Q_y \bar{Q}_y}{(GA)_C}\kappa\, dy + 2\int_0^{a} \frac{Q_x \bar{Q}_x}{(GA)_B}\kappa\, dx + \frac{Q_A \bar{Q}_A}{S_A} + \frac{Q_B \bar{Q}_B}{S_B} + \frac{Q_C \bar{Q}_C}{S_C} + \frac{Q_D \bar{Q}_D}{S_D}$$

$$= \frac{2\kappa\, H\bar{H}h_C}{(GA)_C} + \frac{Pa\kappa}{(GA)_B} + H\bar{H}\left(\frac{1}{S_A} + \frac{1}{S_C}\right) + \frac{P}{2}\left(\frac{1}{S_B} + \frac{1}{S_D}\right) \qquad \text{......31)}$$

For simplicity, next expression is used.

$$\delta_{EQ}(EI)_B = 2\bar{H}Hh_C\,\omega_C\,\kappa + Pa\kappa\,\omega_B + \bar{H}H(EI)_B f(S) + (P/2)(EI)_B(1/S_B + 1/S_D) \qquad \text{.....32)}$$

where,

$$f(S) = 1/S_A + 1/S_C, \quad \omega_C = (EI)_B/(GA)_C, \quad \omega_B = (EI)_B/(GA)_B \qquad \text{.....33)}$$

Deflection due to axial force

$$\delta_{EN} = 2\int_0^{hc} \frac{N_y \bar{N}_y}{(EA)_C}\, dy + 2\int_0^{L} \frac{N_x \bar{N}_x}{(EA)_B}\, x + \frac{N_A \bar{N}_A}{D_A} + \frac{N_B \bar{N}_B}{D_B} + \frac{N_C \bar{N}_C}{D_C} + \frac{N_D \bar{N}_D}{D_D}$$

$$= \frac{Ph_C}{(EA)_C} + H\bar{H}\frac{L}{(EA)_B} + H\bar{H}\left(\frac{1}{D_B} + \frac{1}{D_D}\right) + \frac{P}{2}\left(\frac{1}{D_A} + \frac{1}{D_C}\right) \qquad \text{......34)}$$

For simplicity, next expression is used.

$$\delta_{EN}(EI)_B = H\bar{H}q_B L + Ph_C q_C + H\bar{H}(EI)_B f(D) + (P/2)(EI)_B(1/D_A + 1/D_C) \qquad \text{......35)}$$

where,

$$f(D) = 1/D_A + 1/D_C, \quad q_C = (EI)_B/(EA)_C, \quad q_B = (EI)_B/(EA)_B \qquad \text{......36)}$$

Total deflection δ_{Etotal}

Total deflection is the summation of each deflection component, i.e.;

$$\delta_{Etotal} = \delta_{EM} + \delta_{EQ} + \delta_{EN} \qquad \text{.....37)}$$

Substituting equations 30, 32), and 35) into 37) and considering equations 23) and 27) for H and $\bar{H}$, we obtained the final equation for δ_{Etotal} as follows;

$$\delta_{Etotal} = \frac{P(aL^2/8 - a^3/6)}{(EI)_B} + \frac{Pa\kappa}{(GA)_B} + \frac{Ph_C}{(EA)_B} + \frac{P}{2}\left(\frac{1}{S_B} + \frac{1}{S_D} + \frac{1}{D_A} + \frac{1}{D_C}\right)$$

$$- \frac{Ph_B{}^2(aL^3 - a^2L^2)}{8(EI)_B\{2h_C{}^3k/3 + h_B{}^2L + 2h_C\,\omega_C\,\kappa + q_B L + \lambda\}} \qquad \text{.....38)}$$

3. EXPERIMENT

3.1 Test specimen

Full-scale glulam portal frame of 5.4m in span (L) and 1.8m in height (h_B) were made using Ezo-Todo glulam (Abies and Spruce mixed-species glulam) as shown in Figures 6 or/and 7. Cross section of the glulam members were 150mm in width and 500mm in height and its average modulus of elasticity was 9.2 GPa.

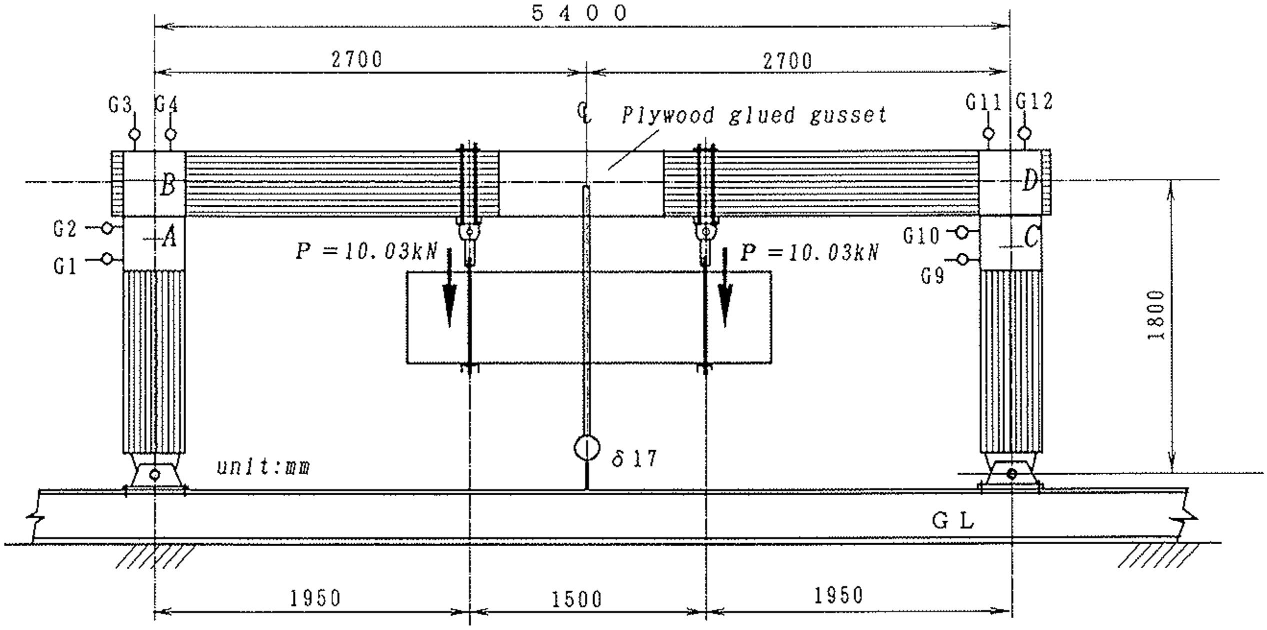

Fig. 6-a Glulam portal frame composed of nail-on-plate joints.

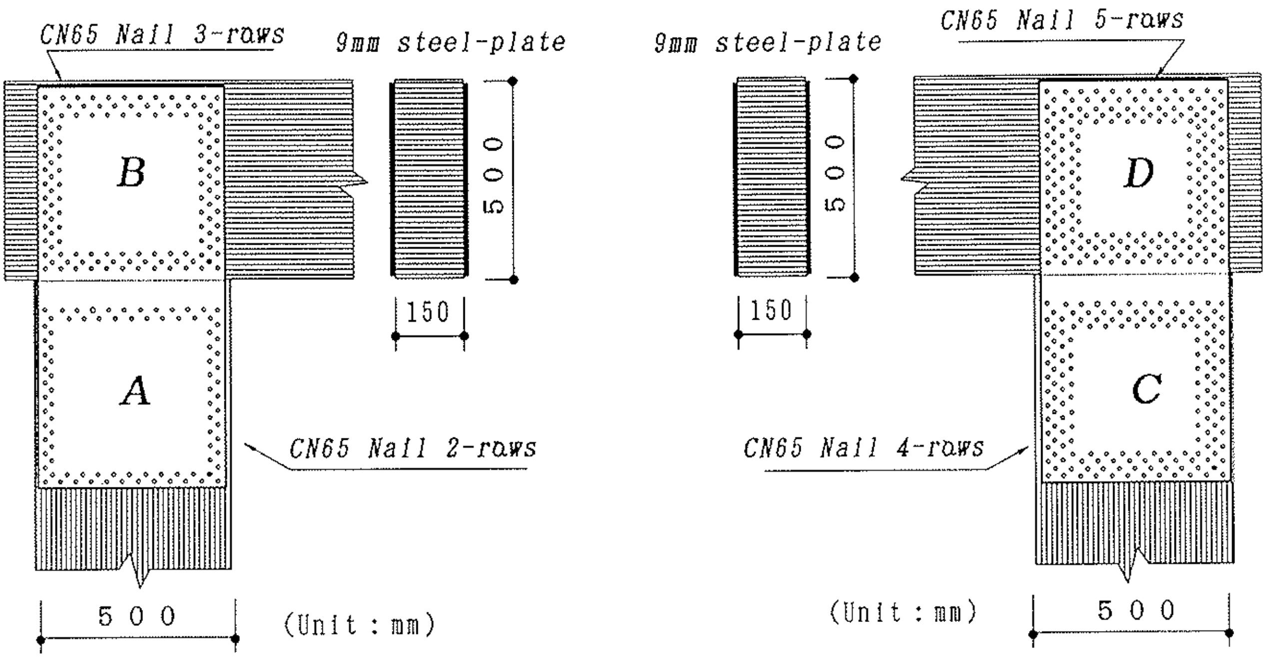

Fig. 6-b Details of the joints in the specimen-1

Figure 6-a shows the specimen-1 built using nailed joint with steel side plates. Nails of 3.3mm in diameter were used and steel plates of 9mm in thickness were used. Diameter of pre-drilled nail hole was about 3.4mm. Figure 6-b) shows the details of the joints A, B, C and D in the specimen-1.

Figure 7-a shows the specimen-2 built using drift pinned joint with steel insert plate. Drift-pins of 18mm in diameter were used. Same steel plates as specimen-1 were used. Figure 7-b shows the details of the joints A, B, C and D in the specimen-2.

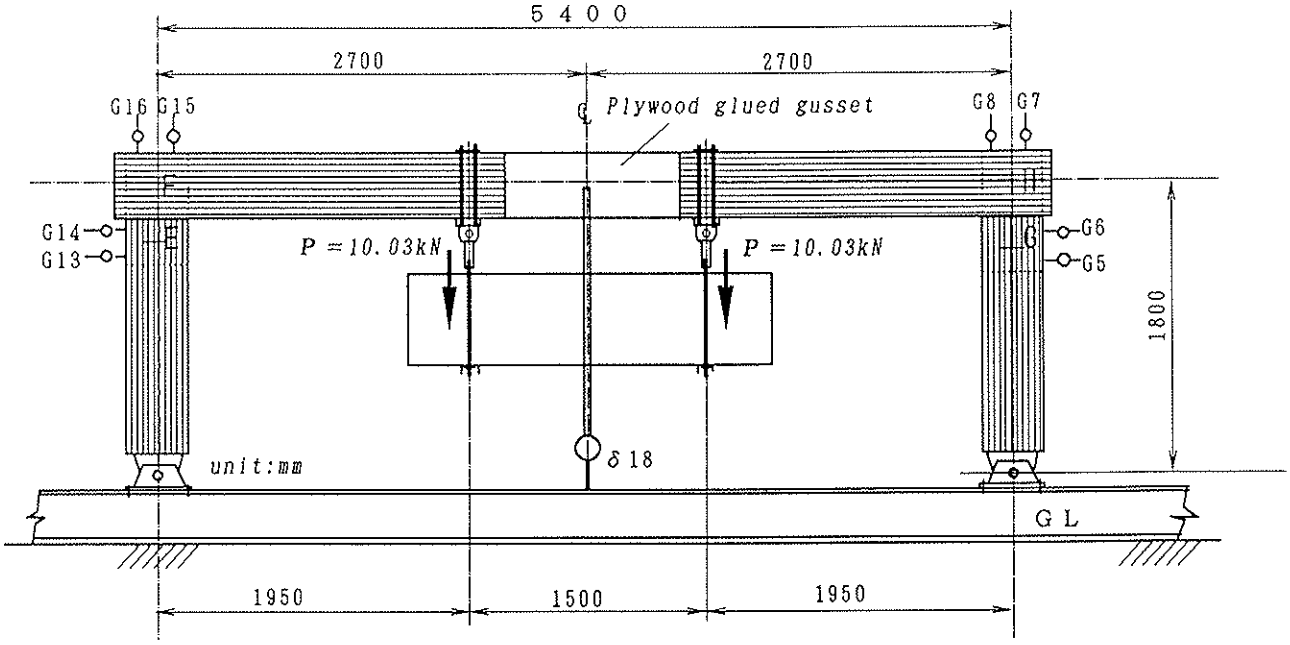

Fig. 7-a Glulam portal frame composed of drift-pins with steel insert plate(s).

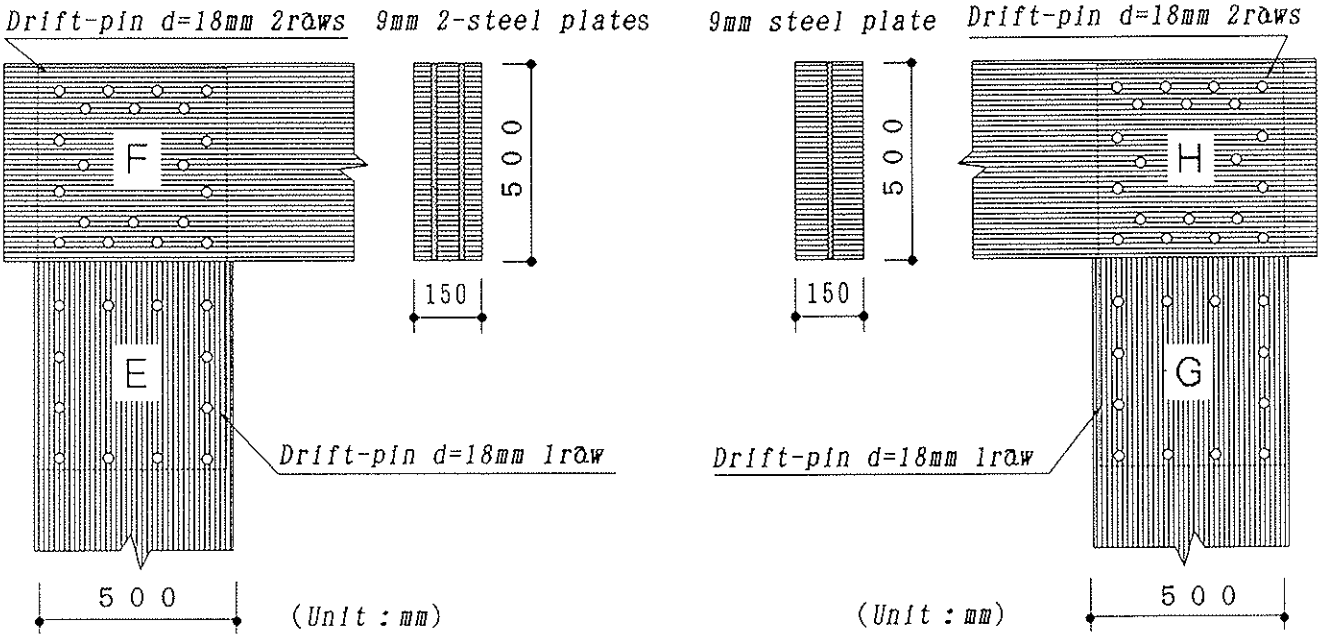

Fig. 7-b Details of the joints in the specimen-2

3.2 Joint Details

Configuration of each joint were all different intentionally as shown in figures 6-b and 7-b for knowing the contribution of semi-rigidity from each joint on the total deflection of the glulam portal frame.

Two points vertical loads were applied using I-section steel members. At first P1=3.04kN was applied per loading point. Next, P2= 4.02kN was added. Finally P3=2.97kN was added. Consequently, a total load P=P1+P2+P3=10.03kN (1022.5kgf) was applied per loading point. This load level was roughly equivalent to the force by which most critical fastener reached its long-term allowable force.

3.3 Estimation of Joint Rigidity

For the calculation of creep deflection of timber, wood based materials or/and built-up timber components, such empirical formula as shown in the equation 39) has been often used up to date.

$$\delta_t = \delta_o + At^N$$

$$\text{or} \quad \delta_t / \delta_o = 1 + (A/\delta_o)t^N \qquad \text{......39)}$$

where, δ_o is the instantaneous deflection at t=0, and t is time.
A and N are constant to be determined experimentally.

According to Arima[2)], who summarized previous data for the creep deflection of sixteen kinds of nailed built-up truss or nail-plated timber truss, it is recognized that A/δ_o and N take almost constant value for 16 kinds of timber trusses as shown in figure 8. The mean value of 0.19 for A/δ_o and 0.25 for N were obtained. If it can be assumed that the same creep relationship as equation 39) is held good also for the nailed steel or the drift-pinned steel timber joints, the following creep equations for the joint rigidity might be assumed.

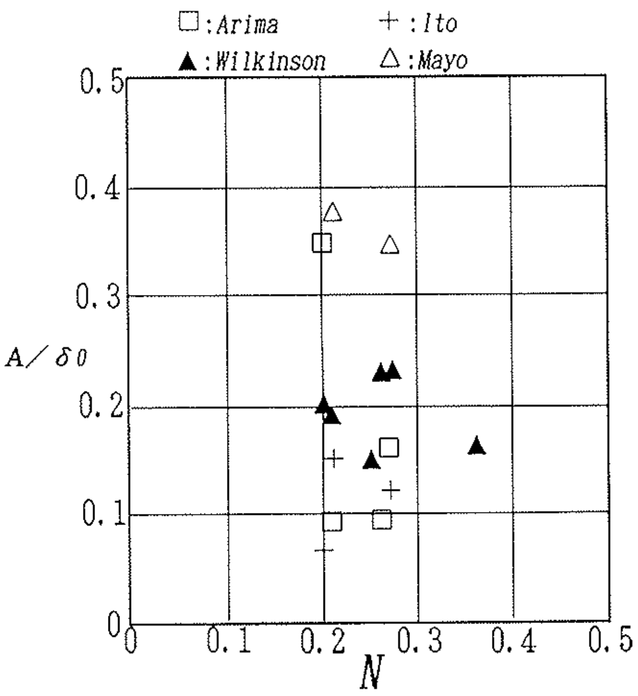

Fig.8 A/δ_o vs. N

$$R_J(t)=R_{Jo}/(1 + 0.19\cdot t^{0.25}) \quad \text{......40)}$$

$$S_J(t)=S_{Jo}/(1 + 0.19\cdot t^{0.25}) \quad \text{......41)}$$

$$D_J(t)=D_{Jo}/(1 + 0.19\cdot t^{0.25}) \quad \text{......42)}$$

(unit of t is "day")

In equations 40),41), and 42), $R_J(t)$, $S_J(t)$, and $D_J(t)$ are the time dependent rotational rigidity, shear rigidity and axial rigidity of the semi-rigid joints, respectively. While, R_{J0}, S_{J0}, and D_{J0} are the instantaneous rigidity at t=0. The instantaneous joint rigidity can be calculated using the slip modulus K_{s0} or K_{s90} as well as the x,y coordinates of each fasteners as shown in equations 4), 5) and 6).

4. RESULTS AND DISCUSSION

4.1 Load-Slip Curves of Fasteners

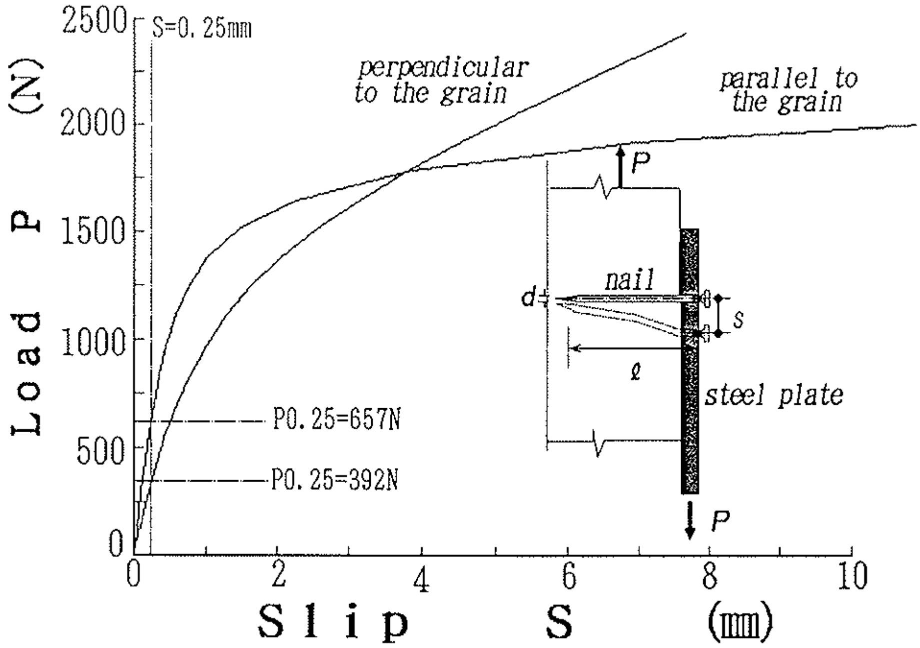

Figure 9 Load(P) - Slip(S) curve of nail-on-plate timber joint

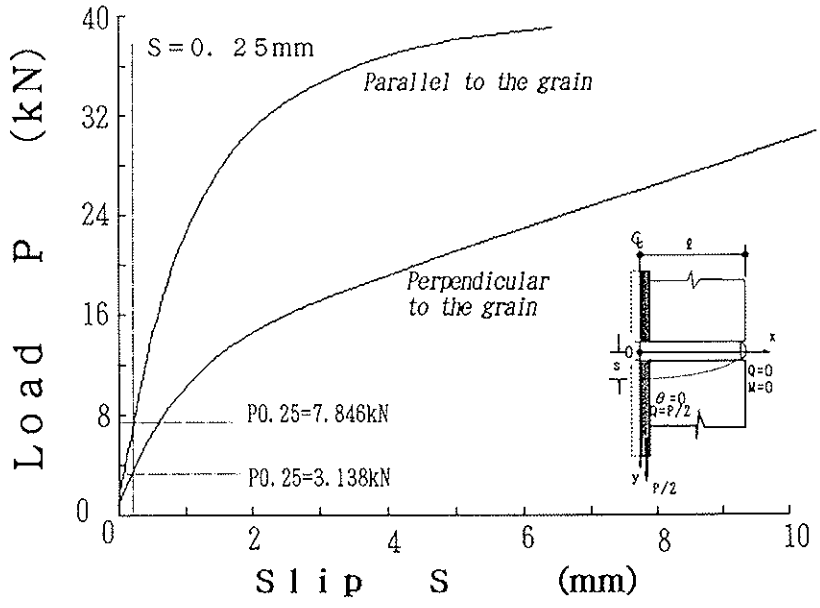

Fig.10 Load(P) - Slip(S) curve of drift-pin joint with insert steel-plate.

Figures 9, and 10 show load(P)- slip(S) curves of nail-on-plate timber joint, drift-pin timber joint with single insert steel-plate, respectively. These P-S curves were obtained theoretically by employing the non-linear FEM[3].

Table 1 shows some parameters used in the non-linear FEM analysis and also the slip modulus defined as K_0 or K_{90} = $P_{0.25}$/0.25mm, where $P_{0.25}$ is estimated load at joint slip of 0.25mm.

Table 1 Parameters used in the FEM analysis[4] and slip modulus estimated.

- Modulus of elasticity of timber : E_w =9.2x10^6 kN/m^2
- Embedment parameters : k_{s-0}=98.07E_w/(0.0316+0.109d), d:diameter in"m"
- Correlation among parameters : k_{s-90}=k_{s-0}/3, k_{u-0}=0, k_{u-90}=k_{s-0}/8.8
  σ_{0-0}=3.3x10^{-3}E_w (in kN/m^2), σ_{0-90}= σ_{0-0}/3

- Assumption for embedment stress σ and embedment e of timber:

$\sigma = (\sigma_{0-0} + k_{u-0} \cdot e)\{1 - \exp(-k_{s-0} \cdot e/\sigma_{0-0})\}$ for parallel to the grain.

$\sigma = (\sigma_{0-90} + k_{u-90} \cdot e)\{1 - \exp(-k_{s-90} \cdot e/\sigma_{0-90})\}$ for perpendicular to the grain.

- Assumption for steel rod bending : perfect elasto-plastic
- Conversion factor from the gravity system unit to the SI unit : 1kgf=9.807N

--------- Computed results ----------

- Slip modulus of drift-pin (d=18mm): K_0=31382kN/m, K_{90}=12553kN/m.
- Slip modulus of nail (d=3.3mm) : K_0= 2628kN/m, K_{90}= 1569kN/m.

4.2 Joint Rigidity

Tables 2 and 3 show the instantaneous joint rigidity R_{J0}, S_{J0}, and D_{J0} estimated using the slip modulus in table 1 and fastener's coordinate values through equations 4),5) and 6).

Table 2 Estimation of the instantaneous joint rigidity for the specimen-1 (nail-on-plate joint: refer to figure 6-b)

Joint	Nail raw	Nail per plane	R_{J0} eq.4) (kNm/rad)	S_{J0} eq.5) (kN/m)	D_{J0} eq.6) (kN/m)
A	2	104	25472	313800	525600
B	3	150	39088	470700	788400
C	4	192	40619	577392	967104
D	5	230	52434	721740	1208880

Table 3 Estimation of the instantaneous joint rigidity for the specimen-2 (drift-pin joint : Refer to figure 7-b)

Joint	Insert plate	Number of pins	R_{J0} eq.4) (kNm/rad)	S_{J0} eq.5) (kN/m)	D_{J0} eq.6) (kN/m)
A	double	12	26506	301272	753168
B	double	20	34876	502120	1255280
C	single	12	13253	150636	376584
D	single	20	17438	251060	627640

4.3 Contribution from each rigidity to the total deflection

Table 4 shows how each rigidity contributes to the total deflection δ_E shown in the equation 38).

Table 4 Contribution from each rigidity to the total deflection δ_E

i	Condition assumed $(EI) \neq \infty$	Specimen-1 (Nailed joint) (mm)	(i/7.)	Specimen-2 (Drift-pined joint) (mm)	(i/7.)
1.	Rigid frame, only $(GA)=\infty$	1.44	(0.52)	1.44	(0.47)
2.	Rigid frame, only $(EA)=\infty$	2.28	(0.82)	2.28	(0.74)
3.	Rigid frame, both $(GA),(EA) \neq \infty$	2.32	(0.83)	2.32	(0.75)
4.	Semi-rigid, only $R_J \neq \infty$	2.74	(0.99)	3.03	(0.98)
5.	Semi-rigid, only $S_J \neq \infty$	2.35	(0.85)	2.37	(0.77)
6.	Semi-rigid, only $D_J \neq \infty$	2.34	(0.84)	2.3	(0.76)
7.	Semi-rigid, all $R_J, S_J, D_J \neq \infty$	2.78	(1.00)	3.09	(1.00)
8.	Observed deflection (t=0)	2.91	(1.05)	3.68	(1.19)

(EI) = Flexural rigidity of member, (EA) = Axial rigidity of member
(GA) = Shear rigidity of member, R_J = Rotational rigidity of joint
D_J = Axial rigidity of joint, S_J = Shear rigidity of joint

It is obvious from table 4 that the effect of shear rigidity (GA) of glulam member on the total deflection δ_E is quite large (see column 1. in table 4). This might be caused because the span (L)-depth(h) ratio L/h of glulam member was relatively small, thus the percentage of member shear deformation was not negligible. Moreover, the effect of the rotational rigidity of joint R_J on the total deflection is dominant, while the joint's shear rigidity and axial rigidity have a little contribution to the total deflection. Thus, it is a reasonable simplifying for practical design purpose to neglect the joint's shear rigidity and axial rigidity in the deflection calculation of semi-rigid glulam portal frame. Contrary to this, it might not be a reasonable simplifying, however, to neglect the member's shear rigidity for the calculation of semi-rigid glulam portal frame in some cases.

4.4 Comparisons between observed creep deflections and computed ones

Figure 11 shows comparisons between the creep deflection observed at the point-E and those computed using equation 38). In the calculation of the deflection, following creep equation for glulam members were also assumed according to the result of Arima[2].

$$E(t)=E_0/(1+0.19\cdot t^{0.25}) \quad ......43)$$

where, $E(t)$ is the time-dependent modulus of elasticity of glulam member, and E_0 is the instantaneous modulus of elasticity of glulam.

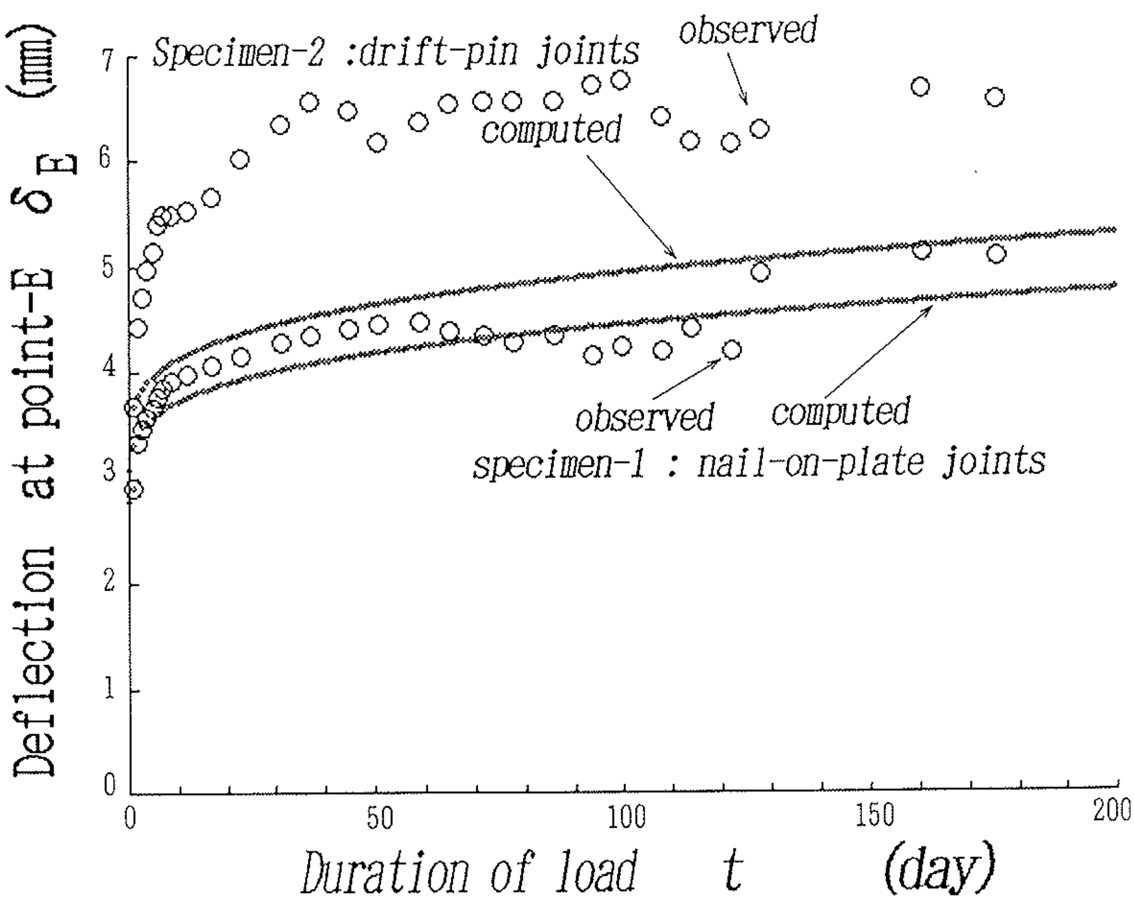

Fig.11 Comparisons between observed and computed creep deflections.

Relatively good coincidence between observed deflections and those computed was observed in the case of specimen-1, nail-on-plate joints. While, in the case of the specimen-2, drift-pin joints with insert steel-plate, the creep deflections observed were far larger than those of computed using equation 38). This might be partly because there were about 1mm initial clearance between pre-drilled holes and diameter of drift-pins, so deflection quickly increased when dead loads were applied.

Anyway, in order to predict the creep deflection of the semi-rigid glulam portal frame more precisely, further basic investigations on the time-dependent embedment characteristics of timber will be necessary.

5. CONCLUSION

The deflection of the semi-rigid single story glulam portal frame could be obtained in a closed form with considering every joint rigidity as well as every member rigidity. Effect of member shear rigidity and joint rotational rigidity were dominant. Creep deflection at mid-span of beam member could be reasonably predicted by assuming power low creep equation for both joint rigidity and member rigidity. In order to predict the creep deflection of the semi-rigid glulam portal frame more precisely, further basic investigations on the time-dependent embedment characteristics of timber will be necessary.

Acknowledgement

The authors wish to thank Mr. Shigeto Fukutome of Kagoshima Technical Research Center, Kagoshima for his contribution to the experimental jobs.

REFERENCES

1) Hirai, T. : Deformation of semi-rigid wooden-frames (1) Beams and frames assembled with nailed gusset-plates, Research Bulletins of the College Experimental Forests, Faculty of Agriculture, Hokkaido University, Vol.44,No.1 pp.297-326, 1987. (in Japanese)
2) Arima, T. et al. :Creep of wood, wood-based materials and wood composite building elements in changes of loading conditions and its application, Bulletins of the Faculty of Agriculture, Shizuoka University, No.36, pp.43-50, 1986.
3) Komatsu, K., Kamiya, F., and Hirashima, Y. :Full-size test and analysis on glulam two-storied portal frames, Proceedings of the 1988 ICTE, vol.2, pp.205-220, Seattle, 1988.
4) Komatsu, K. :Behaviour of nailed timber joints with steel side plates, Proceedings of the 2nd PTEC, vol.2, pp.89-94, Auckland, 1989.

CIB-W18/25-9-2

INTERNATIONAL COUNCIL FOR BUILDING RESEARCH STUDIES AND DOCUMENTATION

WORKING COMMISSION W18 - TIMBER STRUCTURES

DVM ANALYSIS OF WOOD
LIFETIME, RESIDUAL STRENGTH AND QUALITY

by

L F Nielsen
Technical University of Denmark
Denmark

MEETING TWENTY - FIVE

ÅHUS

SWEDEN

AUGUST 1992

Lecture to be held wednesday 26 august at the CIB-W18 Meeting in Åhus, Sweden

DVM-analysis of wood

Lifetime, residual strength, and quality

Lauge Fuglsang Nielsen
Building Materials Laboratory
Technical University of Denmark
DK-2800 Lyngby, Denmark

ABSTRACT

Wood is a material with significant viscoelastic mechanical properties. One manifestation of this is that wood loaded by a constant load can exhibit time dependent deformation which is of the same order of magnitude as the initial elastic deformation in a relatively short time (months). Wood is also a material which contains cracks and other defects (e.g. knots) which may cause a considerable strength reduction. This reduction is time dependent just like the deformation. One speaks about short-time strength which is the load wood can maintain for about 1 minute - and long-time strength which is the load which can be maintained for 10 years before failure takes place. The 10-year strength is about 60% of the short-time strength.

To consider wood as a viscoelastic material is an old idea. There is also nothing new in considering wood as a cracked material to which elastic fracture mechanics can be applied to determine strength. However, the mentioned models cannot individually explain a number of phenomenons which are very important features characterizing the mechanical behavior of wood. For instance, that lifetime is influenced by wood quality (clear, structural), that short-time strength is influenced by time under load, and that lifetime is influenced by strength distribution.

A penetrating explanation of such significant materials properties was first made possible when an integrated materials concept for the behavior of wood was presented by the author: Wood is a damaged viscoelastic material (DVM) whose mechanical behavior can only be described in sufficient details by coupling the theories of viscoelasticity and fracture mechanics. One cannot (as it was done previously) consider wood either as a cracked elastic material or as a homogeneous viscoelastic material without losing the possibility of describing important features of mechanical behavior. One important advantage of the DVM theory relative to other theories dealing with damage (or crack) propagation in viscoelastic media is that it is valid also at high loads. This feature is needed to explain the influence on lifetime of material quality. Formally the DVM-theory appears as a so-called theory of damage accumulation where damages range from large cracks to very small defects not visible to the naked eye.

Essential parts of the DVM-theory are summarized in the lecture. Experimental justifications are presented together with some results obtained by the theory in areas of great importance in wood design. Examples are, Lifetime and residual strength of wood versus wood quality, Lifetime distribution versus strength distribution, and Lifetime of wood versus ambient humidity.

CIB-W18/25-10-1

INTERNATIONAL COUNCIL FOR BUILDING RESEARCH STUDIES AND DOCUMENTATION

WORKING COMMISSION W18 - TIMBER STRUCTURES

THE STRENGTH OF NORWEGIAN GLUED LAMINATED BEAMS

by

K Solli
E Aasheim
The Norwegian Institute of Wood Technology
Norway
R H Falk
Forest Products Laboratory, Madison
U S A

MEETING TWENTY - FIVE

ÅHUS

SWEDEN

AUGUST 1992

THE STRENGTH OF NORWEGIAN GLUED LAMINATED BEAMS

Kjell Solli, Erik Aasheim, Robert H. Falk

This paper focuses on the characterization and the performance of glued laminated (glulam) timber beams manufactured from machine stress graded Norwegian spruce in comparison to developing CEN standards. Material property testing indicated that the supplied laminating timber can be represented by two CEN strength classes, C37-14E and C30-12E, with about 50% yield in each class. Beams constructed from these grades exhibited strength and stiffness meeting the requirements of CEN combinations LH35, LH40 and LC38.

INTRODUCTION

This paper reports on research performed in Norway by Robert H. Falk in close cooperation with The Norwegian Institute of Wood Technology.

The study was performed during the period from September 1990 until September 1991, and was linked to the draft CEN standards applicable in 1990, as shown in the appendix of this paper.

The research was sponsored by Royal Norwegian Council for Scientific and Industrial Research, Norwegian Glulam Producers Association and The Norwegian Instutute of Wood Technology.

OBJECTIVES

The basic objective of this research is to characterize the performance of glulam beams manufactured from machine stress graded Norwegian spuce relative to the developing CEN standards. This study involves the strength and stiffness testing of Norwegian spruce timber for the establishment of lamination grades meeting CEN standards, testing of finger joints and testing of full size beams in bending.

Specific objectives are to:

1. Characterize the mechanical properties of lamination timber and determine the yield of laminating grades meeting CEN standards.

2. Evaluate the performance of full size glulam beams constructed from the established lamination grades.

3. Quantify the relationship between the bending and tensile stength of the finger joints and lamination material and the required performance of these elements on the tension side of the beam.

This paper will focus on objective 2. A complete report from the research are beeing finalized and will be published this year.

MATERIAL DESCRIPTION

The Norway spruce (*Picea abies*) lamination timber utilized in this study was visually graded by the manufacturer to meet the requirements of the Norwegian glulam industry visual grades LT20 and LT30. 5602 laminations, nominally 40 mm x 95 mm in cross section, were provided in random lengths. The lengths varied from 2.20 m to 5.65 m, with an average length of about 4.30 m.

Each lamination was run through a Computermatic MK-IV machine stress grader. Specialized data acquisition equipment developed for this study was used to record deflection (bit) values at 150 mm intervals along each lamination.

MATERIAL TESTING

Using the machine stress grader data, the parent population of laminations was ranked according to MOE_{mac} and specimens were selected from throughout this ranking for material property testing. These material property tests provided the information necessary to establish lamination grades meeting CEN requirements.

The lamination property tests performed were ; (1) bending stiffness (including flatwise and edgewise bending), (2) bending strength (edgewise), (3) tension strength and (4) average density. Laminations to be tested were selected in such a way that the stiffness distribution of each material property test group matched as closely as possible the stiffness distribution (MOE_{mac}) of the parent population of laminations. All tests were performed on specimens 38 mm x 90 mm in cross section. Specimen length varied depending on the specific test performed and the requirements of the test standard ISO 8375. All MOE test data were corrected to 12 % moisture content in accordance with CEN standards.

LAMINATING GRADES

To determine the laminating grades representative of the parent population of supplied laminations, the results of the machine stress grading, bending stiffness and strength testing, and tension tests were statistically analyzed. Laminating grades meeting the requirements of EN TC 124.203 including C37-14E, C30-12E, C24-11E and C21-10E, were targeted.

The results of this procedure indicated that 48% fall into the C37-14E grade and 50% into the C30-12E grade. The balance of the laminations fall into the C24-11E grade.

Table 1 summerizes the distribution estimates of the lamination bending strength. Note that the bending strength data have been adjusted to the reference depth of 200 mm.

Table 1
Summary of distribution estimates of lamination bending strength.

GRADE		PERCENTILE ESTIMATES *) MPa		
		50th	5th	COV (%)
C30-12E	Nonparametric	44,2	30,4	-
	Distributional	44,5	29,7	20
C37-14E	Nonparametric	55,9	38,4	-
	Distributional	56,3	36,9	20,9
*) Adjusted to reference depth of 200 mm				

Table 2 summerizes the distribution estimates of the bending stiffness.

Table 2
Summary of distribution estimates of lamination bending stiffness.

GRADE		PERCENTILE ESTIMATES MPa		
		50th	5th	COV (%)
C30-12E	Nonparametric	12802	8522	-
	Distributional	12505	8965	15,9
C37-14E	Nonparametric	15102	11550	-
	Distributional	15180	11865	14,7

BEAM PRODUCTION

The balance of the laminations not utilized in the material property and finger joint tests were sorted into the established C30-12E and C37-14E grades and three different beam combinations were produced, two homogeneous (LH35 and LH40) and one combined (LC38*). Since the combined combination utilized C37-14E/C30-12E and not C37-14E/C24-11E as specified in the CEN standard, this layup is referred to as LC38*.

All beams were constructed of nine laminations 33 mm in thickness and resulted in test beams 300 mm in depth and 90 mm in width. Figure 1 indicates the beam combinations. A total of 312 beams were manufactured; 104 LH35, 112 LH40, and 96 LC38*. The beams were manufactured by a commercial laminator in 24 m length using phenol-resorcinol resin. Four 6 m test beams were cut from each full length beam.

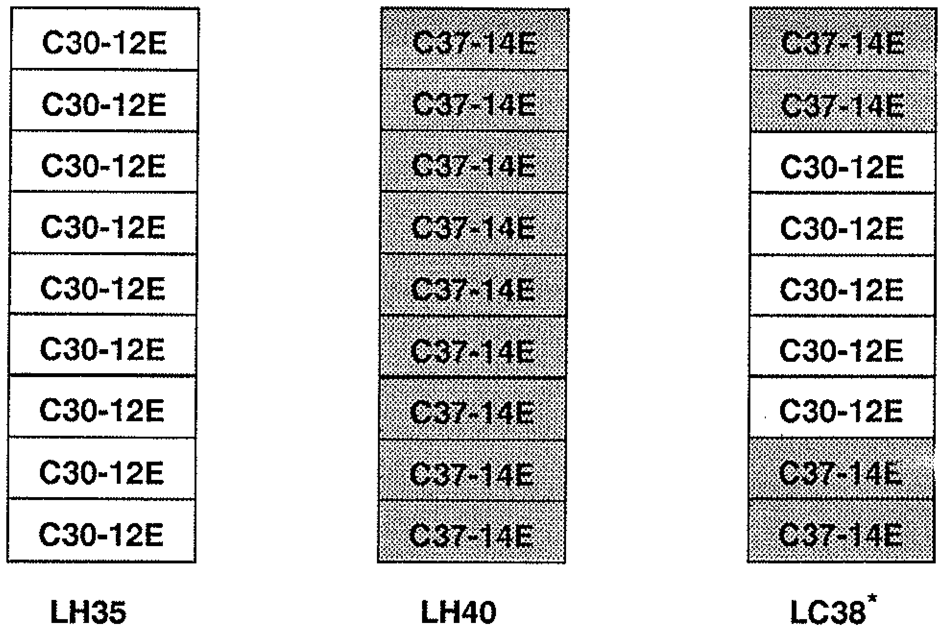

Figure 1
Beam combinations manufactured and tested

BEAM TESTING

The beams were tested according to ISO 8375 over a 5.40 m span with 1.80 m between the load heads. The MOE was measured in the shear free zone between the load heads over a 1.50 m span using an electronic trancducer. Moisture content readings were taken on each glulam beam and the MOE was adjusted to standard conditions (12% MC).

The location of all finger joints in each beam were noted before testing as well as the identifying number of each lamination.

BEAM TEST RESULTS

In general, the 312 glulam beams tested in this study failed as expected, that is, in tension in the outer lamination.

Table 3 summarizes the distribution estimates of the beam bending strength. Note that there was no depth effect adjustment applied to the data. The distribution estimates for bending stiffness is shown in Table 4.

Table 3
Summary of distribution estimates of beam bending strength.

BEAM GROUP		PERCENTILE ESTIMATES MPa		
		50th	5th	COV (%)
LH35	Nonparametric	44,3	32,8	-
	Distributional	44,1	34,3	12,6
LH40	Nonparametric	52,5	39,4	-
	Distributional	52,3	39,4	14,6
LC38*	Nonparametric	47,7	37,9	-
	Distributional	48,6	39,2	13,4

Table 4
Summary of distribution estimates of beam MOE

BEAM GROUP		PERCENTILE ESTIMATES MPa		
		50th	5th	COV (%)
LH35	Nonparametric	13073	11305	-
	Distributional	13000	11242	7,5
LH40	Nonparametric	15395	13421	-
	Distributional	15362	13409	7,2
LC38*	Nonparametric	14618	12928	-
	Distributional	14596	13049	6

It is seen that all the beam combinations meet or exceed the CEN stiffness requirements. The LH40 beam combination has a slightly higher stiffness than the LC38* combination due to the uniform use of the higher stiffness C37-14E lamination grade.

For the LC38* combination the CEN standards are exceeded also in bending. The 5th percentile estimates of beam strength are seen to be within two percent of the CEN requirements for the LH35 and LH40 beam combinations.

Note that the LC38* combination had a characteristic bending strength equal to the LH40 combination though the LC38* combination uses 55% less high grade laminations. This indicates the material efficiencies realized through the use of the combined glulam layup.

CONCLUSION

In general, the results of this study show that high yields of two machine stress rated Norwegian spruce laminating grades meeting the requirements of the draft CEN standards, C37-14E and C30-12E, can be generated from the supplied laminating timber. Futhermore, glulam beams manufactured from these grades can meet or exceed the strength and stiffness requirements of CEN beam combinations LH35, LH40 and LC38.

CONCLUDING REMARKS

The data from this project are still beeing analyzed. The data are used as input to the "Karlsruhe Model" and to the American "PROLAM-model", and the results from these simulations will be reported at a later stage.

REFERENCES

1. Draft Standard EN TC 124.203 "Structural Timber - Strength Classes", August 1990

2. Draft Standard EN TC 124.207 "Glued Laminated Timber - Strength Classes and Determination of Characteristic Properties", January 1990

3. International Organization for Standardization, ISO 8375 "Solid Timber in Structural Sizes - Determination of Some Physical and Mechanical Properties", 1985

Appendix: Extract from EN TC 124.203 (1990) and EN TC 124.207 (1990)

APPENDIX

Extract from EN TC 124.203 and EN TC 124.207

Table A.1
Strength classes.

Strength classes			C13-7E	C15-8E	C15-11E	C18-9E	C21-10E	C21-13E	C24-11E	C30-12E	C30-15E	C37-14E	C48-20E	C60-22E
Strength properties in MPa														
BENDING	$f_{m,k}$		13	15	15	18	21	21	24	30	30	37	48	60
TENSION PARALLEL	$f_{t,o,k}$		8	9	9	11	13	13	14	18	18	22	29	36
TENSION PERPENDICULAR	$f_{t,90,k}$		0,3	0,3	0,3	0,3	0,4	0,4	0,4	0,4	0,4	0,4	0,6	0,7
COMPRESSION PARALLEL	$f_{c,o,k}$		16	17	17	19	20	20	21	24	24	28	35	40
COMPRESSION PERPENDICULAR	$f_{c,90,k}$		4,8	4,8	5,2	5,2	5,4	5,7	5,7	6,3	6,7	6,7	9,0	10,5
SHEAR	$f_{v,k}$		1,6	1,7	1,7	1,8	2,1	2,1	2,4	3,0	3,0	3,7	4,8	6,0
Stiffness properties in MPa														
MOE MEAN PARALLEL	$E_{o,mean}$		7000	8000	11000	9000	10000	13000	11000	12000	15000	14000	20000	22000
MOE MINIMUM PARALLEL	$E_{o,min}$		4900	5500	7400	6500	7000	8700	7400	8500	10300	10000	14000	15000
MOE MEAN PERPENDICULAR	$E_{90,mean}$	S'Woods	230	270	370	300	330	430	370	400	500	450	–	–
		H'Woods	470	530	730	600	670	860	730	800	1000	900	1300	1500
SHEAR MODULUS MEAN	G_{mean}		440	500	690	560	630	800	690	750	900	800	1250	1400
Density in kg/m³														
DENSITY	ρ_k		290	300	450	320	350	480	380	410	520	450	600	700

Table A.2
Classification of glulam.

Strength classes for homogeneous glulam	LH25	LH28	LH30	LH35	LH40
Required lamination strength class	C18-9E	C21-10E	C24-11E	C30-12E	C37-14E
Strength classes for combined glulam	LC24	LC26	LC28	LC33	LC38
Required strength class of:					
Outer laminations	C18-9E	C21-10E	C24-11E	C30-12E	C37-14E
Inner laminations	C13-7E	C15-8E	C18-9E	C21-10E	C24-11E

Table A.3
Characteristic strength of homogeneous glulam.

Strength class		LH25	LH28	LH30	LH35	LH40
Bending	$f_{m,k,g}$	25	28	30	35	40
Tension						
- par.	$f_{t,0,k,g}$	20	23	25	28	32
- perp.	$f_{t,90,k,g}$	0.3	0.4	0.4	0.4	0.4
Compression						
- par.	$f_{c,0,k,g}$	25	26	27	29	33
- perp.	$f_{c,90,k,g}$	5.7	5.9	6.3	6.9	7.4
Shear	$f_{v,k,g}$	2.7	2.9	3.1	3.5	4.0
Modulus of Elasticity par.						
+ bending	$E_{mean,m,g}$	10000	11000	11500	12500	13000
+ axial	$E_{mean,a,g}$	10000	11000	11500	12500	13000
Density	kg/m³	320	350	380	410	450

Table A.4
Characteristic strength of combined glulam.

Strength class		LC24	LC26	LC28	LC33	LC38
Bending	$f_{m,k,g}$	24	26	28	33	38
Tension						
- par.	$f_{t,0,k,g}$	17	19	21	24	26
- perp.	$f_{t,90,k,g}$	0.3	0.3	0.3	0.4	0.4
Compression						
- par.	$f_{c,0,k,g}$	22	23	25	27	30
- perp.	$f_{c,90,k,g}$	5.7	5.9	6.3	6.9	7.4
Shear	$f_{v,k,g}$	2.5	2.6	2.7	2.9	3.1
Modulus of Elasticity par.						
+ bending	$E_{mean,m,g}$	9500	10500	11000	12000	13000
+ axial	$E_{mean,a,g}$	8500	9500	10500	11500	12000
Density	kg/m³	250	300	320	350	380

CIB-W18/25-10-2

INTERNATIONAL COUNCIL FOR BUILDING RESEARCH STUDIES AND DOCUMENTATION

WORKING COMMISSION W18 - TIMBER STRUCTURES

THE INFLUENCE OF THE ELASTICITY MODULUS ON THE SIMULATED BENDING STRENGTH OF HYPERSTATIC TIMBER BEAMS

by

T D Gerad Canisius
Building Research Establishment
United Kingdom

MEETING TWENTY - FIVE

ÅHUS

SWEDEN

AUGUST 1992

The Influence of the Elasticity Modulus on the Simulated Bending Strength of Hyperstatic Timber Beams[1]

T.D. Gerard Canisius

Building Research Establishment,

Bucknal's Lane, Garston, Watford, WD2 7JR, U.K.

Abstract: In the design of a timber beam, its strength is assumed to be constant along the length and to be equal to the characteristic strength. This gives rise to an increase in the safety level of the member. In order to find this increase in safety, it is necessary to find the strengths of beams under different loading conditions. In the case of statically determinate beams, the structural analysis is not affected by the variations in the elasticity modulus. The importance of considering the lengthwise variation of the elasticity modulus in calculating the strengths of hyperstatic beams is investigated in this paper. The multivariate approach of Taylor and Bender is used in generating beam properties. Finite elements are used for stress analysis. Subject to the assumptions made, it is shown that in simulating the beam strengths, the correlated elasticity modulus needs to be considered in both the generation of properties and the analysis of problems if the desired accuracy is high.

[1]Paper presented at the CIB-W18 Meeting 24 at Ahus, Sweden, 24-27 August, 1992

1 Introduction

In the standard limit state design of a bending member, its strength is assumed to be uniform and equal to the characteristic strength. Therefore it is designed for the maximum applicable bending moment. In other words, the maximum bending moment is implicitly considered to act throughout the whole length of a beam of non-uniform strength with a minimum strength equal to the characteristic strength. This design procedure can result in higher safety levels for certain beams under certain types of loading. This is so because the maximum moment may act only in a small length of the beam, making the probabilty of failure much lower. For example, a cantilevered beam with a uniformly distributed load will have a higher safety level than a similar simply supported beam with the same maximum moment given rise to by a similar load.

A research programme is now being carried out to determine the feasibility of applying a 'Moment Configuration Factor' to the design formula to reduce this unnecessary increase in safety and the consequent loss of economy. This factor is defined as the ratio between the strength of a beam under a given load and support conditions and its strength under a constant bending moment acting throughout the length. The latter simulates the usual design assumption described above. Of course, where the design is based on test results of a component such as a trussed rafter, a moment configuration factor cannot be justified. This paper presents results from a preliminary investigation carried out as a part of this research programme.

The above mentioned increase in the safety level has already been analytically studied by several researchers [1,2,3]. Riberholt and Madsen[1,2] developed a method for the conversion of European strength data to the strength of (failure causing) defects which were assumed to be Poisson distributed spatially. This distribution of the strengths of defects and the distribution of the occurrencess of defects were used in the simulation of beams. This method involved, among others, the assumption of independence between strengths of defects and also between their occurrences. Czmoch *et al.* [3] showed that this method provides more conservative results than when correlations were assumed to exist. Some experimental results with respect to this difference in strengths due to different load and support configurations have been reported by Madsen and Buchanan[4].

Although it does not consider the lengthwise variability in the elasticity modulus of timber, the above simulation method has been applied also to the analysis of continuous beams. This neglected the accompanying possible changes in the bending moment diagrams of hyperstatic beams. Therefore, based on a different strength simulation model, the importance of considering the variability of the elasticity modulus and its correlation to the bending strength is investigated in this paper.

In this investigation, the spatial correlations and cross-correlation of strength and stiffness properties are considered approximately using the method proposed by Taylor and Bender [5,6,7]. This involves the simultaneous sampling of variables from a multivariate normal distribution and their transformation to the distributions of interest. The strength and stiffness are assumed to follow first order Markov processes spatially.

A beam finite element model is used in the structural analysis. The strengths and stiffnesses of the property elements, as determined by the random number generator, are allocated to the finite elements.

2 The Simulation of Beam Properties

In the method of Taylor and Bender [7] the correlated stiffness and strength properties are assumed to be random and stationary. The material and statistical properties, which are based on a test element length L_t, are assumed to be available.

2.1 The Spatial and Cross-Correlations

Taylor and Bender considered the elasticity moduli to be serially correlated according to a second order Markov process. (A recent paper [8] considers a third order process). This follows on the work of Kline *et al.* [9]. However, in this preliminary study, the stiffness correlation is considered to be a first order Markov process. This allows the determination of all the spatial autocorrelation coefficients with only the lag-1 coefficient, ρ_1, which is assumed to be known. This is felt to be reasonable for the present study as, according to

Czmoch [10], the correlation functions for the modulus determined by different researchers do not agree (at short distances). The higher lag correlation coefficients, for example ρ_k for lag-k, can be obtained from Eq. 1.

$$\rho_k = \rho_1^k \qquad (k > 0) \tag{1}$$

In [7], the determination of cross-correlation coefficients between the strength and the stiffness had been carried out in two ways. First, for beams of length equal to the test beam length, the correlation had been determined from data. Secondly, for longer beams, the coefficients had been determined with Eq. 2.

$$\rho_{k_{e-s}} = \rho_{k_e} \, \rho_{0_{e-s}} \tag{2}$$

where $\rho_{0_{e-s}}$ and $\rho_{k_{e-s}}$ are, respectively, the lag-0 and lag-k cross-correlations between the strength and stiffness and ρ_{k_e} is the lag-k autocorrelation coefficient for stiffness. The use of this equation, while preserving the zero-lag coefficient from tests, had not preserved the higher order cross-correlations. Therefore, as such an approximation seems acceptable, the use of a first order process for stiffness in the present study may be further justified.

2.2 The Method of Simulation

The marginal cumulative distribution functions of the strength and stiffness, denoted by F_s and F_e respectively, are assumed to be available from test data. If a beam to be simulated needs n number of property elements of length L_t, then, with the stiffness and strength of each property element being required, the number of unknown properties is $2n$. In the present description it is assumed that the first n variables refer to the stiffness properties and the remainder refers to the strength properties. Let the joint probability distribution function for these $2n$ variables be F_t.

The expected value vector $\{A\}$ and the diagonal of the correlation matrix $[C]$ of F_t are considered to be available from test data. As suggested above, the non-diagonal members of the correlation matrix are found from the Markov behaviour together with the necessary initial values which are assumed available. Also $\rho_{0_{e-s}}$, the lag-0 cross-correlation between the strength and stiffness, is needed. All these coefficients contribute to the correlation matrix $[C]$.

Using the normalised expected value vector $\{\bar{A}\}$ and the normalised correlation matrix $[\bar{C}]$ random values are sampled from a multivariable normal distribution. In the present simulations the multivariate random number generator available with the NAG Fortran Library[11] is used. These standardised normal values are then transformed into equivalent values in the respective marginal distributions F_e and F_s. The conversion is carried out so as to provide the same cumulative distribution function value as in the standardised marginal normal distribution.

Simulation Errors It has been demonstrated that this method preserves the original correlation matrices well [7] , except in the case of highly skewed distributions [12]. As an approximate check on the accuracy of the present simulation, the differences between the original and the simulated correlation matrices were monitored under two criteria. The first is the 'distance' E_1 defined by

$$E_1 = \frac{\sum_{i=1}^{2n}\sum_{j=1}^{2n}(\mu_2^{ij} - c^{ij})^2}{\sum_{i=1}^{2n}\sum_{j=1}^{2n}(c^{ij})^2} \tag{3}$$

where, μ_2^{ij} is the (i,j)th element of the simulated correlation matrix and c^{ij} is the corresponding element in the original matrix. This provides a measure of the overall error in the correlation matrix, giving lesser importance to the smaller higher lag elements. The second criterion is the ratio E_2 defined by

$$E_2 = Max. \mid \frac{\mu_2^{ij} - c^{ij}}{c^{ij}} \mid \qquad (c^{ij} \neq 0; \;\; i = 1, 2n; \;\; j = 1, 2n) \tag{4}$$

This provides the maximum relative error between corresponding elements.

3 The Finite Element Model and the Simulation of Beams

A beam finite element programme was written for the purpose of structural analysis. It consisted of a simple cubic beam element. As its details are widely available in the literature they are not repeated here. The interested reader can refer, for example, Zienkiewicz[13]. Only linear elastic analyses were carried out.

Each of the finite elements was assumed to have constant material and strength properties. The properties were generated from the multivariate distribution. The finite element properties corresponded to those of the property element that contained it (Fig. 1). The lengths of the finite elements and the property elements were, generally, different. If a finite element had parts of it in two adjoining property elements, a weighted mean value of the properties was used. This was determined according to the amounts of the finite element corresponding to each property element.

4 Definition of the 'Strength' of a Beam

Following Czmoch *et al.* [3], for the purpose of this study, the strength of a beam was defined as follows. Consider a hyperstatic beam acted upon by a given load. The position and the size of its maximum bending moment will depend on the variation of the elasticity modulus along its length. The maximum bending moment (or stress) that can be applied at this position, without inducing failure at any point along the beam, is considered as the strength of the beam. Here it needs to be mentioned that, due to the averaging out of the elasticity moduli, the position of the maximum bending moment is, generally, not much different from that of a beam with uniform properties.

5 Material Properties

The material properties were assumed to be random and stationary. These properties were, generally, arbitrarily chosen for the purpose of this study. In order to obtain a reasonable idea of the range of results that may be had, some of the properties were varied within a wide range of values.

5.1 Strength

The strength distributions used in the simulations were approximately derived from data available at the BRE. Two strength distributions, to be called S1 and S2, and available in terms of the Weibull parameters of the probability density functions, were selected. The strengths, which are in terms of the maximum bending stresses, are given in Table 1. In the table, μ^s, σ^s and λ^s are, respectively, the location, scale and shape parameters of the distributions. In addition μ_1', μ_2 and $f_{0.05}$ are, respectively, the mean, variance and fifth percentile of each distribution. As both strength distributions provided similar types of results, only the S1 data are presented in this paper.

The above strengths had been obtained under the CEN method of testing which aims at obtaining the distribution of the minimum strengths of the beams. What the present simulation needs is the marginal distribution of strength of property elements. It is to obtain a similar distribution, although in terms of the strengths of defects, that Riberholt and Madsen proposed their model[1,2]. It assumed zero autocorrelations between the strengths of defects (where failure was expected to occur) along the beam. Using the same assumption of independence, here between the different property elements, the strength model was converted to a marginal distribution. This conversion was facilitated by the fact that the available strengths have Weibull distributions. In the case of such a distribution, if the values are independent, then the minima of different independent samples of the same size will also have a Weibull distribution. This new distribution is available in mathematically closed form[14]. If the original distribution has parameters as defined above, then the minima of samples of size n have a Weibull distribution with the same location and shape parameters and a new scale parameter of $\sigma^s/n^{1/\lambda^s}$. Therefore, if the distribution of minima is available, then the original distribution can be obtained from the inverse process.

In carrying out the above inverse process, the number of elements (sampling size) was obtained by assuming a property element length of 600mm. This is the length of elements tested in tension by Taylor and Bender. Then, assuming a test beam length of 4m, n was determined as 7. The obtained marginal distributions are provided in Table 1.

The above conversion is only an approximate one as it contains many assumptions. The intention was only to obtain a somewhat realistic distribution for the purpose of this study. Using this new distribution, the minimum strengths under different correlation coefficients were simulated to study the effect of the assumption of zero coefficients. For the cases considered, the difference between correlated and uncorrelated strengths had a maximum of 9.58% for strength S1. If only the realistic correlations were considered, then the maximum error was around 8%. In the case of S2, these were 11.4% and 9.54%, respectively. The percentages were calculated based on the smaller strengths given by the uncorrelated simulations.

	Strength Set S1		Strength Set S2	
	Original	Convted. Marg.	Original	Convted. Marg.
μ^s N/mm^2	10	10	0	0
σ^s N/mm^2	40	76.5	37.78	60.59
λ^s	3	3	4.12	4.12
μ_1' N/mm^2		78.33		55.01
μ_2 N^2 / mm^4		616.7		225.8
$f_{0.05}$ N/mm^2	24.86	38.43	18.37	29.46

Table 1: Strength Distributions

5.2 Young's Modulus

The Young's moduli of the beams were assumed to be distributed according to a 3-parameter Weibull model. This is a permissible distribution as suggested in [15] and also provided in [7]. The location, scale and shape parameters of this distribution will be denoted, respectively, by μ^e, σ^e and λ^e. To study the effect on the beam strengths, the last two of these parameters were varied during the simulations.

From among the distributions used in the simulations, σ^e=7000N/mm^2 with λ^e=3.2 and σ^e=6000N/mm^2 with λ^e=2.7 were found to provide standard deviations close to those reported in [16]. Of course, the mean can be adjusted with the location parameter μ^e, without changing the standard deviation. A value of 7000N/mm^2 was used with the first case to obtain a mean value close to those provided in [16].

5.3 Correlation Coefficients

The first order Markov correlation coefficients and also the zero-lag cross-correlation between the strength and the stiffness were varied during this study. In the following, the cross-correlation between the strength and stiffness will be denoted by 'c'. The first order Markov process correlations for strength and stiffness are denoted, respectively, by 'ρ_s' and 'ρ_e'.

6 Types of Simulation

Generally, four types of Monte Carlo simulations were carried out with each set of properties. The first, denoted by E_y-C_y in the tables, considered the auto-correlations and cross-correlations as given in them. The second, denoted by E_n-C_y, generated the properties as in the first case, but the structures were analysed assuming a uniform value of the elasticity modulus E. That is, it generated properties exactly, but analysed the problems in a simple manner. The comparison of these two can provide information on the importance of considering the variation of E values along the beam in the analysis. The third type, denoted by E_n-C_n, assumed the strengths and the elasticity moduli to be independent of each other by using a cross-correlation coefficient of zero. This also used a constant value of E in the analysis. In other words, only the strength is simulated here, and hence it is similar to the Riberholt-Madsen model. The fourth, denoted by E_y-C_n, simulated both properties, but assumed them to be statistically independent. In this case the variation in the elasticity moduli was considered in the analysis. The comparison of this and the first provides information on the effect of the correlation between the two properties under variable E.

The Number of Simulations The results were obtained with a strict convergence of at least 1% in both the fifth percentile and the mean. This was generally achieved with 4000 simulations. The minimum and the maximum numbers of simulations used were 2000 and 4000, respectively.

7 Results

The present study was carried out for the purpose of studying the fifth percentile values of strengths to be used in the determination of Moment Configuration Factors. Therefore, in the following, all the comments are made with respect to them. The means and the standard deviations are provided as additional information. All strength results have been given in terms of the maximum bending stress in N/mm^2 although, for brevity, this is not mentioned always. The percentage differences in the fifth percentile results have been calculated with the respective E_y-C_y result considered as the base.

7.1 Errors on Simulation

Any numerical method, especially one with approximations, is bound to have errors on simulation. Therefore it is important to have an idea of the sizes of errors that may occur. These were approximately monitored with the methods described earlier.

Table 2 presents the errors in the correlation matrix that occured during the generation of properties under different correlation coefficients. It indicates that both error measures E_1 and E_2 increase, generally, when the autocorrelation coefficients become smaller and when the length of the beam increases. These were seen to be reduced, generally, with the increase of the number of simulations. The increase in error with the increase in length should be because of the larger number of variables to be simulated and the smallness of the higher-lag correlation coefficients.

Another error that was seen to be present was with respect to the marginal variances of the properties. As the number of simulations was increased, these, which varied along the length, tended towards uniformity but the convergence was to values slightly higher than the variances of the original marginal distributions.

7.2 Beams under Uniform Bending Moments

This is the basic case on which the Moment Configuration Factors will be based. This is a statically determinate problem. Therefore, the results are not affected by the parameters of the elasticity modulus distribution. Only the correlation coefficients and the strength distribution affect the results. However, the effect of the cross-correlation coefficient c and the autocorrelation of modulus ρ_e should be negligible.

Beam Length			2m		4m		6m	
c	ρ_s	ρ_e	E_1	E_2	E_1	E_2	E_1	E_2
0.8	0.7	0.85	0.009	0.023	0.018	0.112	0.018	0.194
0.8	0.3	0.5	0.024	0.166	0.031	19.92	0.036	321.1
0.7	0.7	0.45	0.027	0.363	0.032	5.023	0.039	22.44
0.5	0.7	0.85	0.014	0.045	0.019	0.112	0.025	0.372
0.5	0.7	0.4	0.031	0.725	0.034	12.25	0.044	121.6
0.5	0.7	0.45	0.029	0.505	0.033	6.068	0.042	41.97
0.5	0.3	0.5	0.029	0.330	0.034	8.126	0.044	620.9

Table 2: Errors in the Correlation Matrices: 4000 Simulations

	Strength S1			Strength S2		
Beam Length	2m	4m	6m	2m	4m	6m
μ'_1 N/mm^2	53.4	45.8	41.6	39.5	34.4	31.4
$\sqrt{\mu_2}$ N/mm^2	16.2	13.1	11.8	11.1	9.44	8.76
$f_{0.05}$ N/mm^2	27.4	24.9	22.8	20.6	18.4	16.5

Table 3: Uncorrelated Strengths of Beams under Uniform Moment

c	0.8	0.5	0.0
	Beam Length = 2m		
μ'_1	61.8	61.6	61.5
$\sqrt{\mu_2}$	20.9	21.0	21.0
$f_{0.05}$	29.7	29.5	29.0
% Diff.	-	-0.44	-2.29
	Beam Length = 4m		
μ'_1	53.8	54.0	54.3
$\sqrt{\mu_2}$	18.3	18.2	18.3
$f_{0.05}$	25.9	26.4	26.1
% Diff.	-	2.04	0.69
	Beam Length = 6m		
μ'_1	49.3	49.4	49.4
$\sqrt{\mu_2}$	16.6	16.9	16.8
$f_{0.05}$	24.0	23.9	24.8
% Diff.	-	-0.75	2.95

Table 4: Uniform Bending Moment: Strength S1. ρ_s=0.7 ρ_e=0.85. c= 0.8, 0.5 and 0.0.

Strength under Statistical Independence The strengths of the beams when the strengths (and stiffnesses) of the property elements are independent of each other are presented in Table 3. To avoid numerical difficulties, both autocorrelation coefficients, ρ_s and ρ_e, were assumed to be 0.001 instead of zero. These results, generally, provide lower bounds of strengths which increase when correlations are present. The exceptions, where these are larger, are with respect to columns 2 and 4 for 4m and 6m beams in Table 6. These slight differences may be present because it is a case with small correlation coefficients which was shown to have higher errors.

c	0.7	0.5	0.0
	Beam Length = 2m		
μ_1'	61.7	61.6	61.5
$\sqrt{\mu_2}$	20.8	20.9	21.0
$f_{0.05}$	29.8	29.9	29.0
% Diff.	-	0.37	-2.62
	Beam Length = 4m		
μ_1'	53.9	53.9	54.3
$\sqrt{\mu_2}$	18.1	18.1	18.3
$f_{0.05}$	25.4	25.9	26.1
% Diff.	-	2.17	2.92
	Beam Length = 6m		
μ_1'	49.2	49.3	49.4
$\sqrt{\mu_2}$	16.7	16.8	16.8
$f_{0.05}$	24.2	23.9	24.9
% Diff.	-	-1.28	2.40

Table 5: Uniform Bending Moment: Strength S1. ρ_s=0.7, ρ_e=0.45. c= 0.7, 0.5 and 0.0.

Effect of the Cross-Correlation Coefficient The results presented in Tables 4 to 6 are for three sets of ρ_s and ρ_e values. The first, given in Table 4, is with a high ρ_e (=0.85) and a high ρ_s (=0.7). The second, given in Table 5, has a high ρ_s (=0.7) and a low ρ_e (=0.45) while the third set in Table 6 has low values for both ρ_s (=0.3) and ρ_e (=0.5).

In all the cases provided, when the c is changed from either 0.8 (Tables 4,5) or 0.7 (Table 5) to 0.0 the changes that occur in strength are small with the maximum difference being -3.55% for the 2m beam in Table 6. Most of these differences, as to be expected, are negligible and are generally within the error allowed by the convergence criterion.

c	0.8	0.5	0.0
	Beam Length = 2m		
μ_1'	55.4	55.3	55.4
$\sqrt{\mu_2}$	17.5	17.7	17.6
$f_{0.05}$	28.4	28.1	27.4
% Diff.	-	-1.06	-3.55
	Beam Length = 4m		
μ_1'	47.2	47.3	47.6
$\sqrt{\mu_2}$	14.4	14.3	14.5
$f_{0.05}$	24.8	25.2	24.7
% Diff.	-	1.53	-0.36
	Beam Length = 6m		
μ_1'	43.0	43.1	43.2
$\sqrt{\mu_2}$	12.8	13.1	13.2
$f_{0.05}$	22.5	23.2	22.8
% Diff.	-	3.29	1.51

Table 6: Uniform Bending Moment: Strength S1. ρ_s=0.3, ρ_e=0.5. c= 0.8, 0.5 and 0.0.

c	0.5		0.0	
ρ_e	0.85	0.4	0.85	0.4
	Beam Length = 2m			
μ'_1	61.6	61.6	61.5	61.5
$\sqrt{\mu_2}$	21.0	20.8	21.0	21.0
$f_{0.05}$	29.5	29.9	29.0	29.0
	Beam Length = 4m			
μ'_1	54.0	54.0	54.3	54.3
$\sqrt{\mu_2}$	18.2	18.1	18.3	18.3
$f_{0.05}$	26.4	26.3	26.1	26.1
	Beam Length = 6m			
μ'_1	49.4	49.3	49.4	49.4
$\sqrt{\mu_2}$	16.9	16.7	16.8	16.8
$f_{0.05}$	23.9	24.8	24.8	24.8

Table 7: Uniform Bending Moment: Strength S1. ρ_s=0.7, c=0.5 and 0.0. ρ_e= 0.85 and 0.4. All E_y-C_y analyses.

Effect of the Change in the Spatial Correlation Coefficient for Modulus The effect of the change of the spatial correlation factor ρ_e for modulus can be studied from Table 7. As to be expected, the differences in the strengths due to the change of ρ_e from a large value (0.85) to a smaller value (0.4) are very small. The maximum difference is 4.01% for the 6m beam with c=0.5 . There is no difference for c=0 as then ρ_e does not affect the generation of properties.

7.3 The Analysis of a Clamped Beam Under a Concentrated Load

As a simple example of a hyperstatic beam, a clamped beam with a central concentrated load was analysed for its strength. Beam lengths of 2, 4 and 6 metres were considered. Several elasticity modulus distributions were used in the simulations. The location parameter μ^e was kept constant at 7000N/mm^2.

Changes with Shape Parameter λ^e Presented in Table 8 are results for the 6m long beam under three values of the shape parameter λ^e. The values of σ^e are 2000N/mm^2 and 7000N/mm^2. The cross-correlation coefficient c is 0.8 (and 0.0 under C_n analysis). In all the four types of analyses there have occured only slight changes in the simulated strengths when λ^e was varied. For a given σ^e, the differences between different types of analysis are greater for smaller values of λ^e. As to be expected, the respective E_n analyses provide the same results for all λ^e values.

Changes with the Scale Parameter σ^e The results provided in Table 8 indicate that the non-consideration of E (in E_n analyses) and/or c (in C_n analyses) has given rise to large differences between the E_y-C_y analysis and the other types of analysis. For example, -15.0% for λ^e=2.0 is the largest difference for σ^e of 7000N/mm^2. As shown by the results for σ^e of 2000N/mm^2, these differences between different analyses are smaller when the dispersion

	σ^e=2000 N/mm^2				σ^e=7000 N/mm^2			
	E_y-C_y	E_n-C_y	E_n-C_n	E_y-C_n	E_y-C_y	E_n-C_y	E_n-C_n	E_y-C_n
	$\lambda^e = 2.0$							
μ_1'	59.4	56.3	56.4	58.2	63.5	56.3	56.3	60.6
$\sqrt{\mu_2}$	18.8	18.1	18.2	18.8	19.4	18.1	18.2	19.9
$f_{0.05}$	29.9	27.7	27.9	28.8	32.8	27.9	27.9	29.8
% Diff.	-	-7.52	-6.95	-3.67	-	-14.8	-15.0	-9.06
	$\lambda^e = 2.7$							
μ_1'	58.7	56.3	56.3	57.9	61.9	56.3	56.3	59.8
$\sqrt{\mu_2}$	18.5	18.1	18.2	18.8	18.7	18.1	18.2	19.5
$f_{0.05}$	29.3	27.9	27.9	28.5	32.1	27.9	27.9	29.4
% Diff.	-	-4.67	-4.95	-2.63	-	-12.9	-13.2	-8.26
	$\lambda^e = 3.2$							
μ_1'	58.4	56.3	56.3	57.7	61.1	56.3	56.3	59.3
$\sqrt{\mu_2}$	18.3	18.1	18.2	18.7	18.5	18.1	18.2	19.4
$f_{0.05}$	29.6	27.9	27.9	28.4	31.7	27.9	27.9	29.3
% Diff.	-	-5.44	-5.72	-3.82	-	-11.8	-12.1	-7.61

Table 8: Clamped 6m Long Beam: Strength S1: ρ_s=0.7, c=0.8 (and 0.0) ρ_e= 0.85. σ^e = 2000N/mm^2 and 7000N/mm^2. λ^e=2.0, 2.7 and 3.2. μ^e=7000N/mm^2.

	$\rho_e = 0.7$				$\rho_e = 0.5$			
	E_y-C_y	E_n-C_y	E_n-C_n	E_y-C_n	E_y-C_y	E_n-C_y	E_n-C_n	E_y-C_n
	Beam Length = 2m							
μ_1'	63.6	59.4	59.2	62.0	64.8	59.3	59.2	62.4
$\sqrt{\mu_2}$	19.6	19.0	18.9	19.8	19.7	19.0	18.9	20.0
$f_{0.05}$	33.4	30.2	29.0	30.5	34.3	29.6	29.0	30.8
% Diff.	-	-9.47	-13.0	-8.58	-	-13.6	-15.3	-10.2
	Beam Length = 4m							
μ_1'	61.35	56.1	56.3	59.6	62.0	56.0	56.3	59.9
$\sqrt{\mu_2}$	17.82	17.2	17.2	18.3	17.9	17.2	17.2	18.4
$f_{0.05}$	32.39	28.8	29.1	30.9	33.4	29.0	29.1	31.1
% Diff.	-	-11.0	-10.1	-4.69	-	-13.2	-12.8	-6.98
	Beam Length = 6m							
μ_1'	58.4	53.1	53.0	56.2	58.7	53.2	53.0	56.4
$\sqrt{\mu_2}$	16.7	16.2	16.3	17.5	16.9	16.2	16.3	17.5
$f_{0.05}$	31.7	27.8	27.1	28.6	31.5	27.5	27.1	28.6
% Diff.	-	-12.5	-14.7	-10.0	-	-12.9	-14.1	-9.20

Table 9: Clamped Beam with Concentrated Load: Strength 1, c=0.7 (and 0.0), s=0.4 e=0.7 and 0.5. λ^e=3.2, σ^e=7000N/mm^2, μ^e=7000N/mm^2.

of E is lower.

Effect of the change of Correlation Coefficients As seen from the results of Table 8, the change of c from 0.8 in C_y analysis to 0.0 in the corresponding C_n analysis has resulted in larger differences for the high dispersion modulus case than for the low dispersion one.

As the above are with high ρ_s and c values, further results have been provided in Table 9 with a low ρ_s value of 0.4 and two values of ρ_e (0.7

Problem		E_y-C_y	E_n-C_y	E_n-C_n	E_y-C_n
a.	$f_{0.05}$	36.4	35.6	35.4	35.4
	% Diff.	-	-2.09	-2.50	-2.70
b.	$f_{0.05}$	36.6	35.6	35.8	35.5
	% Diff.	-	-2.52	-2.08	-2.93
c.	$f_{0.05}$	31.6	30.2	30.5	30.9
	% Diff.	-	-4.34	-3.30	-2.12
d.	$f_{0.05}$	31.9	30.4	30.7	31.1
	% Diff.	-	-4.60	-3.76	-2.69

Table 10: Fifth Percentile Strengths of 6m long Continuous Beams: Set 1 (of Fig. 2). λ^e=3.2, σ^e=7000N/mm^2, μ^e=7000N/mm^2, c= 0.8, ρ_s=0.7, ρ_e=0.85.

and 0.5) together with c values of 0.7 (and 0.0). These again show larger variations of strength between different types of analysis, and the differences are larger with the lower value of ρ_e for 2m and 4m beams. The largest difference is -15.3% between the E_y-C_y and E_n-C_n analyses of the 2m beam with ρ_e=0.5.

7.4 Strength of Continuous Beams

Table 10 presents fifth percentile strengths obtained under different types of analysis of the continuous beams shown in Fig. 2. This is the same beam under the same set of loads, but with different support conditions. As can be seen, the differences between different types of analyses are all small.

Further results, with respect to two of the above structures, but with different loads are given in Table 11. These structures and loads are shown

Problem		E_y-C_y	E_n-C_y	E_n-C_n	E_y-C_n
a.	$f_{0.05}$	36.6	35.6	35.8	35.5
	% Diff.	-	-2.52	-2.08	-2.93
b.	$f_{0.05}$	36.7	36.1	36.0	-
	% Diff.	-	-1.50	-2.02	-
c.	$f_{0.05}$	34.0	32.9	32.6	-
	% Diff.	-	-3.03	-4.00	-
d.	$f_{0.05}$	32.9	30.7	30.1	-
	% Diff.	-	-6.86	-8.53	-
e.	$f_{0.05}$	31.9	30.4	30.7	31.1
	% Diff.	-	-4.60	-3.76	-2.69
f.	$f_{0.05}$	31.6	29.7	30.3	30.7
	% Diff.	-	-6.02	-4.05	-2.63

Table 11: Fifth Percentile Strengths of 6m long Continuous Beams: Set 2 (of Fig. 3). λ^e=3.2, σ^e=7000N/mm^2, μ^e=7000N/mm^2, c= 0.8, ρ_s=0.7, ρ_e=0.85.

in Fig. 3. As indicated by the results, the same structure under different loads has different differences between the different types of analyses.

These results indicate that the effects of different types of analyses depend not only on the hyperstatic structure but also on the applied loads, *i.e.* on the bending moment diagram.

8 Conclusion

Details of Monte Carlo simulations carried out on several beams to determine their bending strengths were presented in this paper. The beam properties were generated using the multivariate approach of Taylor and Bender. First order Markov processes were assumed for the strengths and the elasticity moduli of the property elements along the beam length. The hyperstatic structures were analysed with a beam finite element programme.

Some of the beam property parameters were varied during the analyses to see their effect on the determined strengths. Also four types of analyses were carried out on the beams. These types depended on whether the lengthwise variation of the elasticity modulus was considered in the analysis or not and on whether the cross-correlation between the strength and stiffness, c, was considered in the generation of beam properties or not.

The results indicate that the non-consideration of the cross-correlation between the strength and stiffness in property generation and/or the non-consideration of the elasticity modulus in structural analysis can give rise to large differences between the simulated strengths of hyperstatic beams. For example, for the clamped beam under a central concentrated load, the provided results show a maximum difference of 15.3% when the cross-correlation is not considered and the beam is assumed to be of uniform stiffness. This difference is with respect to an analysis that considered the non-uniformity of E and its cross-correlation with the strength. Analyses of some continuous beams showed that the differences between different types of analysis depend on both the structure and the applied loads.

Subject to the assumptions made, it can be concluded that the non-consideration of the cross-correlation coefficient and the lengthwise variation of the elasticity modulus in the generation of beam element properties and the analysis of hyperstatic structures can result in errors as large as almost 15% in their simulated bending strengths. As the effect is negligible when the bending moment is constant along the length of a beam, a similar error can occur in the Moment Configuration Factor for a hyperstatic structure.

9 Acknowledgment

The author wishes to express his sincere gratitude to Mr. A. R. Fewell, who suggested the idea of Moment Configuration Factors, for his guidance and encouragement during this study.

References

[1] Riberholt, H. and Madsen, P. H.; *Strength Distribution of Timber Structures. Measured Variation of Cross Sectional Strength of Structural Lumber*, Struct. Res. Lab., Tech. Univ. of Denmark, Rept. R114, 1979.

[2] Riberholt, H.; *Safety of Timber Structures*, Struct. Res. Lab., Tech. Univ. of Denmark, June 1979.

[3] Czmoch, I., Thelanderson, S. and Larsen, H. J.; *Effect of Within Memeber Variability on Bending Strength of Structural Timber*, Proc., Int'l Council for Building Research Studies and Documentation, Working Commission W18A, Meeting 24, Oxford, U.K., Sept. 1991.

[4] Madsen, Borg, and Buchanan, A.H.; *Size Effects in Timber Explained by a Modified Weakest Link Theory*, Can. J. of Civ. Eng., **13**, pp.218-232, 1986.

[5] Taylor, S. E. and Bender, D. A.; *Simulating Correlated Lumber Properties Using a Modified Multivariate Normal Approach*, Trans. ASAE, **31**(1), pp.182-186, 1988.

[6] Taylor, S. E. and Bender, D. A.; *A Method for Simulating Multiple Correlated Lumber Properties*, For. Prod. J., **39**(7/8), pp. 71-74, 1989.

[7] Taylor, S. E. and Bender, D. A.; *Stochastic Model for Localized Tensile Strength and Modulus of Elasticity in Lumber*, Wood and Fibre Sc., **23**(4), pp. 501-519, 1991.

[8] Richburg, B. A. and Bender, D. A.; *Localized Tensile Strength and Modulus of E-Related Laminating Grades of Lumber*, Wood and Fibre Sc., **24**(2), pp. 225-232, April 1992.

[9] Kline, D. E., Woeste, F. E. and Bendtsen, B. A.; *Stochastic Models for Modulus of Elasticity of Lumber*, Wood and Fib. Sc., **18**(2), pp.228-238, 1986.

[10] Czmoch, I.; *Lengthwise Variability of Bending Stiffness of Timber Beams*, Proc. Intl. Timber Eng. Conf., London, U.K., **2**, pp.2158-2159, 1991.

[11] NAG Fortran Library Mk14, NAG Ltd., Oxford, England, 1990.

[12] Han, M. B., Bender, D. A. and Taylor, S. E.; *Computer Generation of Highly-Skewed Correlated Random Variables*, Trans. ASAE, **34**(5), pp. 2279-2281, 1991.

[13] Zienkiewicz, O.C.; *The Finite Element Method*, 3rd Edn., McGraw Hill, London, 1977.

[14] Bury, K. V.; *Statistical Models in Applied Science*, Wiley, N.Y. 1975.

[15] Foschi, R. O. ; *Class Notes on Structural Reliability*, Dept. of Civil Eng., The Univ. of Brit. Columbia, Vancouver, Canada, 1987.

[16] Curry, W. T. and Tory, J. R.; *The Relation between the Modulus of Rupture (Ultimate Bending Stress) and Modulus of Elasticity of Timber*, BRE Current Paper CP30/76, Princess Risborough Lab., BRE, England, April 1976.

Figure Captions

Fig. 1: The Allocation of Generated Properties to the Beam Finite Elements

Fig. 2: Continuous Beams: Set 1

Fig. 3: Continuous Beams: Set 2

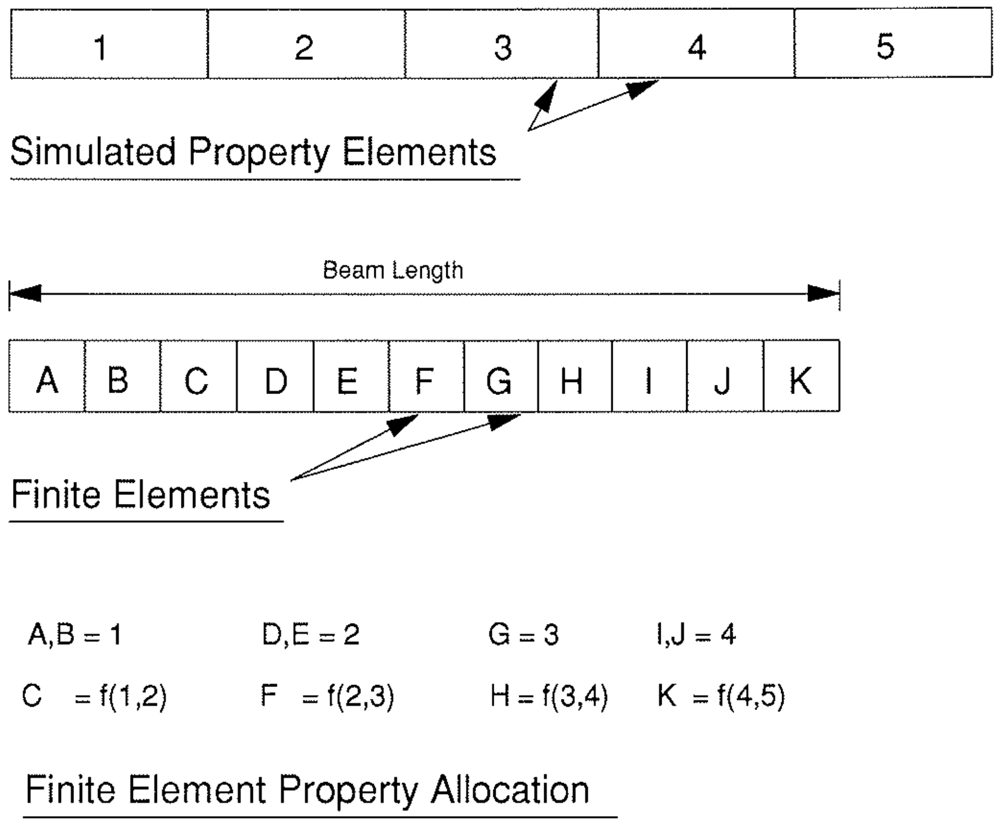
1
2
3
4
5
Simulated Property Elements
Beam Length
A
B
C
D
E
F
G
H
I
J
K
Finite Elements
A,B = 1
D,E = 2
G = 3
I,J = 4
C = f(1,2)
F = f(2,3)
H = f(3,4)
K = f(4,5)
Finite Element Property Allocation

Fig. 1

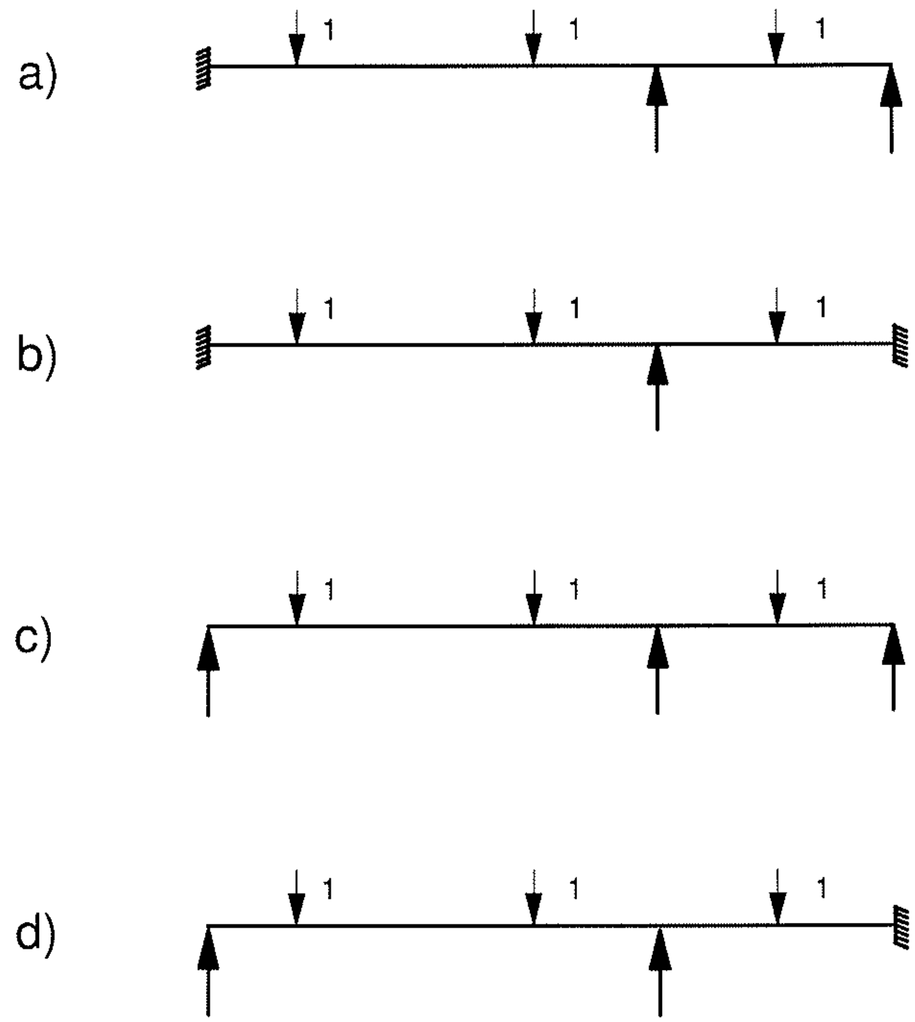

Continuous Beams: Set 1

Fig. 2

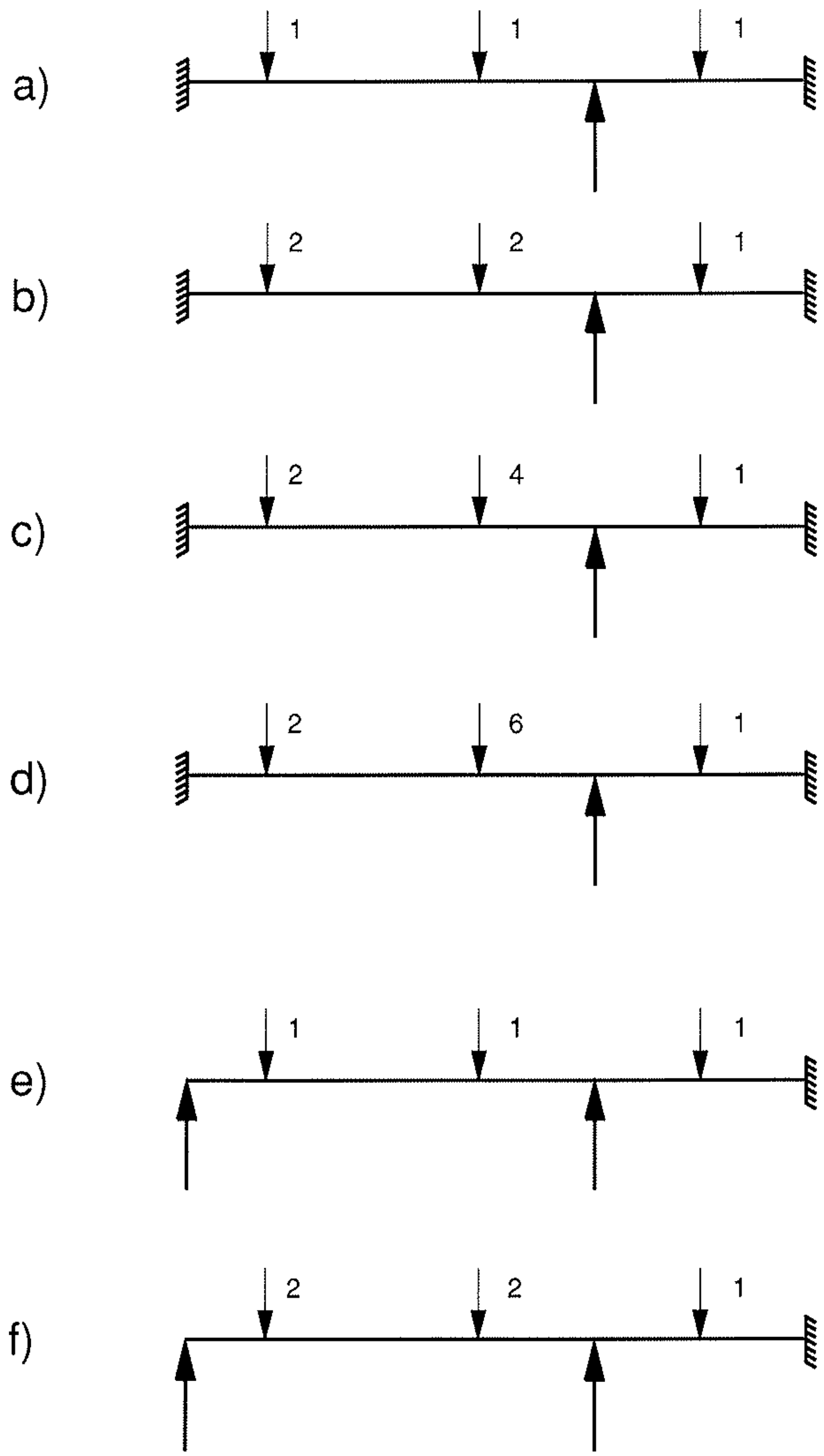

Continuous Beams: Set2

Fig. 3

CIB-W18/25-7-11

INTERNATIONAL COUNCIL FOR BUILDING RESEARCH STUDIES AND DOCUMENTATION

WORKING COMMISSION W18 - TIMBER STRUCTURES

MULTIPLE-FASTENER DOWEL-TYPE JOINTS, A SELECTED REVIEW OF RESEARCH AND CODES

by

C J Mettem
A V Page
TRADA Technology Limited
United Kingdom

MEETING TWENTY - FIVE

ÅHUS

SWEDEN

AUGUST 1992

MULTIPLE-FASTENER DOWEL-TYPE JOINTS,

A SELECTED REVIEW OF RESEARCH AND CODES

C.J. Mettem and A.V. Page
TRADA Technology Limited

Introduction

It is frequently observed that the load-carrying capacity of a multiple-fastener joint is less than the sum of the individual fastener capacities. For dowel-type fasteners, such as plain round metal dowels, bolts, and nails, a number of timber codes now take some account of this effect.

As already noted in CIB W18 papers by Blass (1) in 1990, and previously Steck in 1986 (2), there are great differences between the modification factors for the number of fasteners, in several international and national timber codes. This still seems to be the case in 1992.

A paper accompanying this brief review, also to be presented at the current meeting, reports recent tests supported by a linear elastic finite element analysis. The work was conducted on both single and multiple bolted joints in European whitewood glued laminated timber (glulam) (3).

Strain gauged steel side plates were used, following an established technique adopted by previous researchers. By this means the load taken by each individual bolt in the multiple-bolted joints could be measured. However, the ratio of fastener length to central timber thickness was kept very low, so that pure embedment testing was achieved. This was new. Parallel and perpendicular to grain loading arrangements were included.

A substantial lack of "evenness" in load carrying capacity was demonstrated, both by test and by theory. This applied especially in the perpendicular to grain case, where the study suggested that modification factors as conservative as 0.4 should be considered for multiple-fastener joints including as few as four bolts. If this is correct, then it is evident that the current draft of EC5 is unsafe in this respect.

Background

The multiple-fastener load reduction effect is also known to exist in materials other than timber. For example Volkersen analysed rivet stress distributions in aircraft structures, using as an analogy theories originally developed for adhesive stresses (4). Care is of course necessary when drawing analogies between one subject of engineering science and another. However, the extensive research on uneven stress distributions in glued joints, which can be formed using a lap, in single or double shear, is in this case pertinent. This has been reviewed in previous TRADA research (5).

In the stress analysis of glued joints, it is found that the unevenness of the stress distribution along the joint becomes more pronounced, as the discrepancy increases between the stiffness of the adhesive and that of the adherend (6). Conversely, research on multiple-fastener joints in timber has not always revealed a major unevenness. For example, Blass reported that in multiple-nailed double-shear joints loaded parallel to the grain, the maximum load of a multiple fastener joint can be estimated as the sum of the values for individual nails, provided joint failure is by nail yielding.

However, this difference is not necessarily inconsistent. The nailed joints which Blass investigated, in which the stiffnesses of the nails and the timber are comparable, are analogous to glued joints made with an adhesive which has a stiffness comparable to that of the timber, the very joints in which the stress distribution is most even.

Yasumura et al, on the other hand, conducted a series of tests on multiple numbers of bolts and multiple rows of the same, connecting glulam members to steel side plates, the latter forming double shear planes (7). They found that for certain parallel to grain configurations, with a reasonably practical number of bolts and rows, the average load per bolt in the multiple configuration was only about half the value for the specimen having a single bolt.

Design Situations

Since the constituent parts of mechanically fastened timber joints often have very different stiffnesses, the above considerations suggest that practical situations do exist where the load distribution amongst the individual fasteners is markedly uneven. One such situation is where relatively thick metal plates, usually mild steel, are used in conjunction with bolts or plain round dowels, to form connexions in glulam. This is a common form of construction.

When a line of fasteners perpendicular to the grain is loaded in that direction, the unevenness in the distribution of load is generally even more pronounced, because the stiffness of timber perpendicular to the grain is only about one sixteenth of its stiffness parallel to the grain. This means that the actual strength of the joint is considerably less than the strength predicted from tests on single bolts loaded perpendicular to the grain, reduced by a factor for the number of bolts in a line based on tests parallel to the grain. The reality of this effect was measured and confirmed in tests conducted by TRADA. Furthermore, the situation is quite common in practice, as shown in the accompanying diagrams, Figure 1.

Eurocode 5 and BS 5268

Draft Eurocode No. 5 'Design of Timber Structures', Part 1, April 1992, contains a principle under Section 6, JOINTS, that:

> P(2) It shall be taken into account that the load-carrying capacity of a multiple-fastener joint will frequently be less than the sum of the individual fastener capacities.

However, the modifications for the effect, given in the application rules, are remarkably modest. As is by now well-known, EC5 recommends to the designer that the lateral load-carrying capacity of dowel-type fasteners should be calculated from a set of formulae based on a theory initiated by Johansen (8). Under the relevant clause for steel-to-timber joints, a sub-set of these formulae is given, together with small explanatory diagrams. These give load carrying capacities per fastener per shear plane.

Under Section 6.5, BOLTED JOINTS, EC5 advises that for more than six bolts in line with the load direction, the load carrying capacity for the extra bolts should be reduced by one third. Taking as an example nine bolts in line, this equates to a "modification factor", as BS 5268 would call it, of only 0.89. The British code itself would apply a modification factor of 0.76 for this case. Dowelled joints are, by an "extension" clause, treated by EC5 in the same manner as bolted joints in this respect.

Neither EC5 nor the British code identify as a special case the situation where the timber is loaded perpendicular to the grain, or where there is a component of load in this direction.

North America

In North American codes, the larger and stiffer types of standard fastener, such as bolts, lag screws, split rings and shear plates, are treated differently to smaller and less stiff types such as glulam rivets and nails. For the latter, the Canadian code, for example, CSA-086.1-M89 (9) has no modification factor for the number of fasteners in the group. For the larger types on the other hand, the overall reductions for the group effect often produce more conservative rules in practical design cases than the rules of draft EC5 and BS 5268. Recent proposals for North American codes also give different modification factors for loading parallel and perpendicular to the grain.

CSA-086 gives a modification factor J_G which varies according to the number of fasteners in a row. For connectors and lag screws, this is presented in tabular form, the value being selected according to an "area ratio" which takes account of the cross-sections of the main and side members. For steel side plates, this factor can range from 0.42 to 1.00.

Bolt design, according to the Canadian code, involves the use of two pertinent modification factors. These are J_G, which has the same purpose as above but which is computed by means of a formula, and J_R, which is a factor for the number of rows, ranging from 1.0 for one row to 0.6 for three rows. A general clause tends to preclude the use of wide steel splice plates altogether, thus avoiding the situation of numerous rows of bolts. It is understood that the tests leading to the "number of bolts" formula were made at Carlton University, on behalf of 'Agriculture Canada'. The J_R factor was derived from the work reported to CIB by Yasumura et al.

In the USA, the approach used in the National Design Specification 1986 (10) is at present similar to that described for Canada, with the "Group Action Factor", C_g, at present depending upon the number of fasteners in a row, and upon the main member to side member area ratio. This procedure is used for all the "large" types of fastener, including bolts.

In the past, research in the USA has shown the need for quite substantial reduction factors for group action, although results have not always been consistent. Doyle, for example, (11) examined joints made with four bolts in two rows, in Douglas fir glulam, using steel side plates. For parallel to grain loading, he derived reduction factors from approximately 0.6 to 0.9.

Kunesh and Johnson (12) investigated similar multiple-bolt joints and obtained factors ranging from approximately 0.5 to 0.95.

Wilkinson (13) conducted extensive tests on a range of numbers of bolts. He also developed an analytical method by modifying the earlier work of Cramer (14). Wilkinson's experimental method was to use strain gauged steel side plates as a means of measuring the load carried by each bolt. However, his main timber members were of a thickness such as would be used in real construction, rather than thinner timbers where the l/d ratio would be low, producing a pure embedment effect. Furthermore, he reported "fabrication effects" in the manufacture of the specimens, such that these had a greater influence on the distribution of load amongst the bolts than the properties of the members and the fasteners themselves.

Amongst Wilkinson's conclusions were the observation that the load distribution for any particular row of bolts is unique. Any one of the bolts may be the major load carrier. Also, any bolt hole may be misdrilled, causing that bolt to carry almost no load for a major portion of the joint loading.

Proposals for a 'Load and Resistance Factor Design' code in the USA include in the draft a more sophisticated multiple fastener modification factor. Again, this is to apply to all "large" fasteners, namely bolts, lag screws, dowels, shear plates and split rings. It is understood that the theory has been worked by Zahn, following linear elastic analytical predictions given previously by Lantos (15) and Cramer.

Both row factors and factors for fasteners within a row are included in a single formula in the LRFD draft. This also takes into account the axial stiffness (EA) of the main and side members, as well as the load/slip constants for the fastener concerned.

Whilst leading to a formidable formula to be computed by the designer, this all-embracing approach would take account of effects such as the large differences in stiffness of the constituents of a joint involving a member loaded perpendicular to the grain. At the same time, no major difference in approach has been adopted. Thus, for example, fracture mechanics considerations and the transverse tensile properties of the timber are not taken into account.

Further Research?

It was not the intention that this review should be long or comprehensive. It is understood that the topic of multiple-fastener joints is also being re-considered in other countries, such as New Zealand. It is apparent, however, that the statement given at previous CIB-W18 meetings that there are considerable differences between the modification factors for number of fasteners amongst various codes is true. Whether this indicates that research on the subject should continue indefinitely is another matter.

The topic seems in danger of becoming a timber researchers' "chestnut". It is capable of being treated with an almost infinite amount of analysis and testing. Consider, for example, the following influences and aspects which it might be considered necessary to examine, listed in no special order of significance:

* Brittle fracture modes of failure
* Mode changes with time in service, due for example to creep deformations and increased embedment
* Re-loading situations
* Moisture movement effects, especially where timber is restrained by steel
* Fabrication effects such as hole alignment and mis-fit; tightness of fasteners in holes
* For perpendicular to grain loading, the substantial influence of crack propagation and weakness in the timber
* Load-slip behaviour beyond the elastic range

Code Implications

Code writers cannot await indefinitely the results of further research, and must make judgements on the basis of present knowledge. It can also be argued that unless there has been evidence of failure or unsatisfactory service, then there is not a pressing need to alter codes or to make design procedures more complicated. However, there have been instances of failure in multiple fastener joints using the "large" types of device discussed here.

It is difficult to pinpoint the primary causes of such failures, since "real" joints in built structures experience a variety of the effects described in the "research menu" given above. For example, fissures induced by moisture content changes, in combination with perpendicular to grain loading, seem to be a particularly serious hazard.

It is perhaps especially disconcerting, therefore, that the European codes mentioned in this review take such a sanguine view of the perpendicular to grain loading case for multiple fasteners, not singling it out for especially cautious treatment.

It also seems odd that the latest draft of EC5 still treats all dowel-type fasteners in the same manner with respect to multiple-fastener modification effects, whereas other codes, including those used in North America, find no modification necessary for nails, but recommend substantial modifications for the "large" types of fastener such as bolts, lag screws, split rings and shear plates.

Multiple-fastener dowel-type joints using bolts or plain metal round dowels in conjunction with steel plates need careful detailing and EC5 and BS 5268 at present carry insufficient warning as to the hazards of their use. It is also likely that more conservative application rules should be given, to fulfil the principle that the load-carrying capacity will be less than the sum of the individual fastener capacities.

Perhaps those responsible for the final re-drafting of EC5, prior to the issue of the EN version, might wish to consider revising the reduction factor recommended in Clause 6.5.1.2(3) for the number of fasteners in a line, even if the researchers' thirst for further knowledge has still not been fully slaked.

References

[1] Blass, H.J. Load distribution in nailed joints. CIB-W18A/23-7-2, Lisbon, 1990

[2] Steck, G. Effectiveness of multiple fastener joints according to National Codes and Eurocode 5 (Draft). CIB-W18A/19-7-3, Florence, 1986

[3] Mettem, C.J. and Page, A.V. Load distributions in multiple-fastener bolted joints in European whitewood glulam, with steel side plates. CIB-W18/25-7-12, Åhus, 1992

[4] Volkersen, O. Die Nietkraftverteilung in zugbeanspruchten Nietverbindungen mit konstanten Laschenquerschnitten (Rivet stress distribution in tensile stressed rivet joints with constant butt strap cross-section), Luftfahrtforschung, Band 15, pp. 41-47, 1938

[5] Page, A.V. Behaviour of structural glued joints in wood. Research Report RD007, TRADA, 1989

[6] Adams, R.D. and Wake, W.C. Structural adhesive joints in engineering. Elsevier App.Sci.Pub., 1984

[7] Yasumura, M., Murota, T. and Sakai, H. Ultimate properties of bolted joints in glued-laminated timber. CIB-W18A/20--7-3, Dublin, 1987

[8] Johansen, K.W. Theory of timber connectors. IABSE, Publn.9, Bern, 1949

[9] Canadian Standards Association. Engineering design in wood (Limit States Design). CAN/CSA-086.1-M89, Toronto, 1989

[10] National Forest Products Association. National design specification for wood construction. Washington, DC, 1986

[11] Doyle, C.V. Performance of joints with eight bolts in laminated Douglas fir. USDA Forest Service Research Paper FPL 10, US Government Printing Office, Washington DC, 1964

[12] Kunesh, R.H. and Johnson, J.W. Strength of multiple-bolt joints; influence of spacing and other variables. Oregon State University, Forest Research Laboratory Report T-24, Corvallis, 1968

[13] Wilkinson, T.L. Load distribution among bolts parallel to load. Journal of Structural Engineering 112(4):835-852, USA, 1986

[14] Cramer, C.O. Load distribution in multiple-bolt tension joints, Jnl. of the Struct. Div., ASCE, Vol. 94 No. ST5, Proc. Paper 5939, pp. 1101-1117, USA, 1968

[15] Lantos, G. Load distribution in a row of fasteners subjected to lateral load, Wood Sci. Vol. 1, No. 3, pp. 129-136, UK, 1969

Figure 1

Multiple-fastener dowel-type joints with steel plates

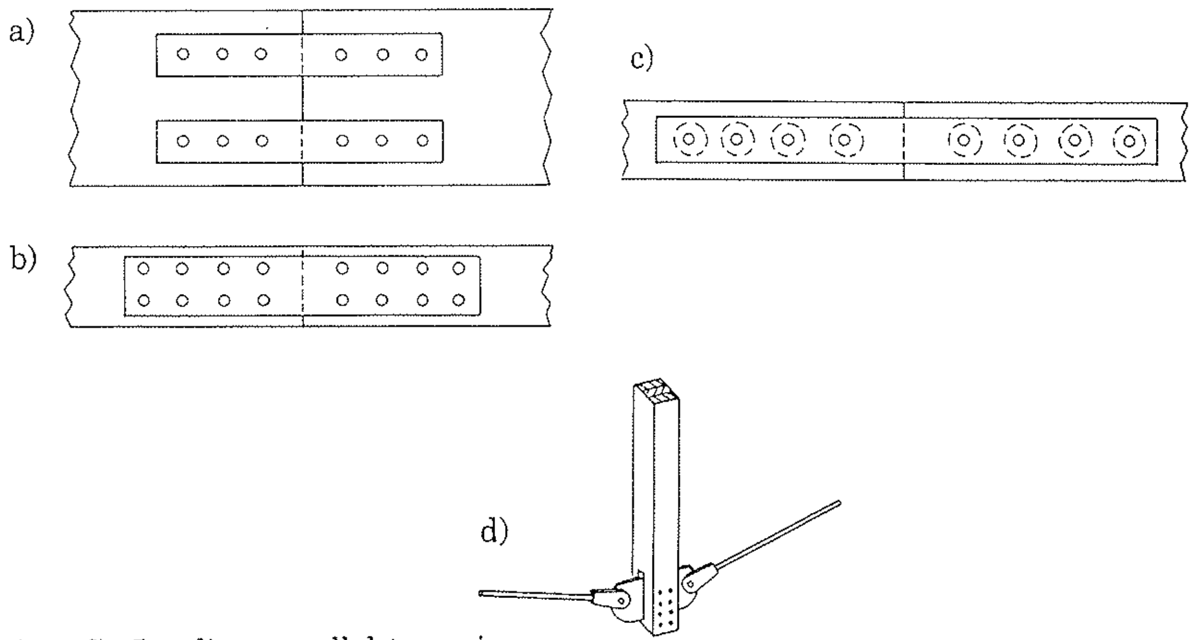

a) to d) Loading parallel to grain.

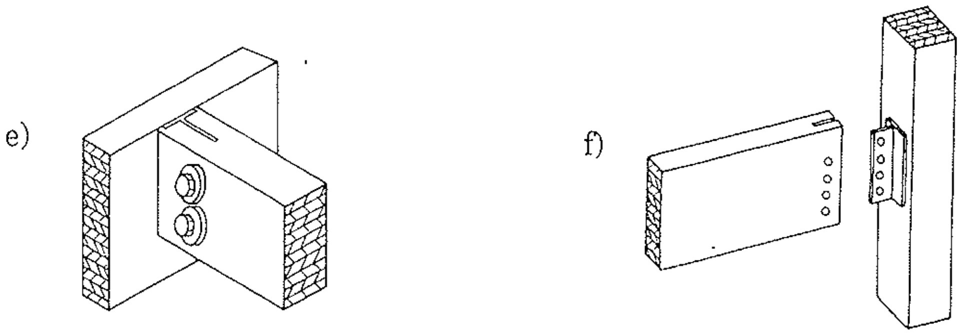

e), f) Loading perpendicular to grain.

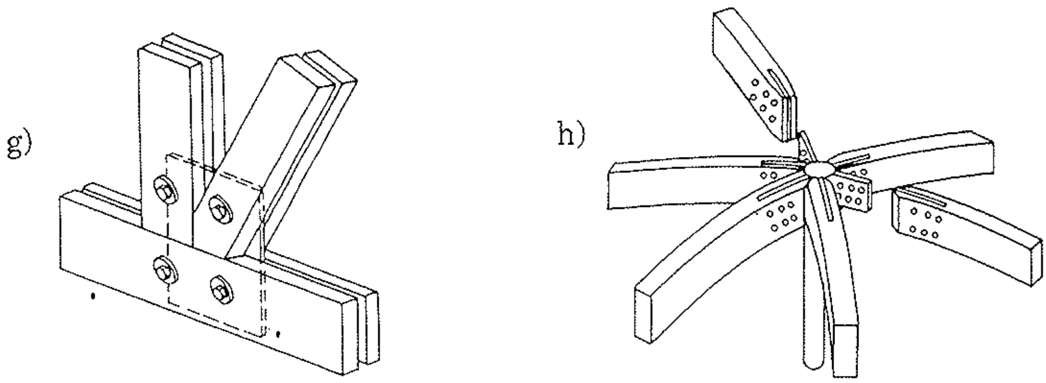

g), h) Complex loading.

CIB-W18/25-7-12

INTERNATIONAL COUNCIL FOR BUILDING RESEARCH STUDIES AND DOCUMENTATION

WORKING COMMISSION W18 - TIMBER STRUCTURES

LOAD DISTRIBUTIONS IN MULTIPLE-FASTENER BOLTED JOINTS IN EUROPEAN WHITEWOOD GLULAM, WITH STEEL SIDE PLATES

by

C J Mettem
A V Page
TRADA Technology Limited
United Kingdom

MEETING TWENTY - FIVE

ÅHUS

SWEDEN

AUGUST 1992

LOAD DISTRIBUTIONS IN MULTIPLE-FASTENER BOLTED JOINTS

IN EUROPEAN WHITEWOOD GLULAM, WITH STEEL SIDE PLATES

C.J. Mettem and A.V. Page
TRADA Technology Limited

Introduction

Draft Eurocode No. 5 requires as a principle that account should be taken of the fact that the load-carrying capacity of a multiple-fastener joint will frequently be less than the sum of the individual fastener capacities. The use of relatively thick metal plates, usually of mild steel, in conjunction with bolts or plain round dowels, is common in forming connections in timber engineering construction, particularly with glued laminated timber (glulam). Designs normally involve double shear planes, and the plates may be positioned as side plates, or as central inserts, or 'flitches'.

An accompanying paper presents a brief review of the current research and code status in relation to the topic of multiple-fastener modification factors for such joints. This paper describes recent tests, supported by a linear elastic orthotropic finite element analysis. The work has been conducted on both single and multiple bolted joints. An especially designed test apparatus, which could accept thin central members of European whitewood glulam was used, to ensure failure in a pure embedment mode. Strain-gauged mild steel side plates were used on this test jig, following an established technique developed by previous researchers [1].

The results of the evaluation are compared with work previously reported by others to CIB W18A [2]. They are also discussed briefly in relation to current design recommendations.

Tests

The object of the tests was to investigate experimentally how the load on a multiple-fastener bolted joint, using steel side plates and a glulam central member, would be distributed between the individual bolts. The apparatus and procedures were designed in such a way that failure was in a pure embedment mode, in the case of both the single and the multiple fastener joints. The thickness t_2 of the central glulam specimens was 2.75 times the diameter of the fastener, whilst the thickness t_1 of each of the steel side plates was 0.83 times the diameter, Figure 1.

A special multiple embedment testing jig was designed and made for the tests. It was constructed of mild steel plate, and contained strain gauges to measure the load applied to each bolt. The dimensions of each side plate of the jig are shown in Figure 2.

It will be noted that between each pair of bolt holes in the side plates, the width of the steel was waisted. This waisted portion was designed to be narrow enough to change in length by a significant and measurable amount of strain, when force was applied to the jig. At the same time the side steel assemblies were sufficiently rigid in comparison with the timber to avoid elastic influences of the plates. Metal foil electrical resistance strain gauges were mounted in pairs on each of the edges of the waisted portions of the plates. The four individual gauges at each hole position were connected in series and set up in a single bridge configuration, using strain gauge bridge and amplifier units.

Figure 3 shows a schematic diagram of a multiple hole tension specimen mounted in the jig. For the compression tests, the toothed plate assembly was omitted, and the load was applied through the ends of the specimen. For the single fastener specimens, it was required to measure the embedment stiffness, for use in the finite element analysis. To this end, an LVDT was mounted on the jig to measure the movement of a point on the timber close to the bolt, relative to the bolt itself. Plate 1 shows the jig mounted in a Zwick 1478 100 kN test machine, for the compression perpendicular to grain tests.

Figure 4 shows a steel side plate with numbers indicated against the strain gauge positions and against the individual bolts. This is a key to interpreting the results, since 'bolt 1' is the fastener nearest to what would be described in design as the 'loaded' end of the glulam.

The force applied to each individual bolt was derived from a combination of the strain gauge readings and the total force recorded by the test machine. A microcomputer incorporating an analogue to digital conversion system was used in conjunction with the data recording for this purpose. Plate 2 shows the general arrangement of the equipment.

In each specimen, the strain gauge signals were calibrated against the load indications of the test machine by applying load through the jig to a single bolt at each hole position in turn. By means of a simple matrix operation using software in the PC, the strain gauge outputs and the total machine load were than able to be manipulated to measure the individual bolt loads, when multiple-fastener arrangements were tested.

Standard, commercially available European whitewood glulam was obtained for the tests. The material was manufactured in Denmark, and was specified as complying with LB grade of BS 4169 : 1988. The material was initially at approximately 15% moisture content, and the specimens were conditioned at 20°C and 65% relative humidity. They were maintained at the equilibrium moisture content attained under these conditions by being wrapped whenever removed from the conditioned environment.

Figures 5 to 10 show the dimensions of the specimens used for the single-bolt and four-bolt tests. Parallel to grain tests were conducted in both tension and compression. Perpendicular to grain tests were performed in compression only. Table 1 shows the spacings used for the specimens in terms of bolt diameter. The bolt spacings and distances used in the tests conformed with the recommendations of EC5, April 1992 draft, except in the case of the edge distance in compression perpendicular to the grain. Here, there was a change in the EC5 drafts, but the distance conformed with the BS 5268 rule.

Table 1 Bolt spacings and distances used in the tests
(Symbols a_1 - a_4 conform to EC5, April 1992 draft)

Mode	No. of bolts	Parallel to grain a_1	Perpendicular to grain a_2	End distance a_3	Edge distance a_4
Compression parallel	Single bolt Four bolts	- 5d	- -	7d 7d	4d 4d
Tension parallel	Single bolt Four bolts	- 5d	- -	7d 7d	4d 4d
Compression perpendicular	Single bolt Four bolts	- -	- 5d	4d 4d	2.1d 2.1d

The testing procedure included drilling the bolt holes in the glulam immediately before the test on each specimen, since it was desired to eliminate as far as possible 'fabrication' effects, mis-fit and shrinkage or swelling between holes. To this end, a template was used on each embedment specimen, and a vertical drill press was used, which helped to ensure perpendicular drilling. The holes were drilled using a new 12.2mm diameter twist drill.

Bolt holes were positioned to avoid glue lines in the laminated material. The specimens were assembled using M12 Grade 8.8 steel bolts. The portion of the bolt in contact with both the steel side plates and the glulam was the plain shank rather than the threaded portion. Washers and nuts were included in the assembly, with the latter being tightened by hand.

In the case of the single bolt specimens, loading was carried through to failure, after the elastic stiffness had been measured. For this stage of the test, the test machine cross-head speed was controlled such that failure took place within 10 to 15 minutes. Cubes of material approximately 30mm square were taken from each specimen for density recording and to measure moisture content by oven drying.

Results

Table 2 lists the results of the single-bolt embedment tests.

The mean values and coefficients of variation are taken from four tests in each mode. Load versus embedment traces were typical at low load levels of those obtained from such tests. When maximum load was achieved, failure was by perfect plastic embedment in the case of both tension and compression parallel to the grain. Plate 3 shows a typical specimen. Compression perpendicular to grain specimens ultimately failed by a combination of plastic embedment and splitting parallel to the grain.

In the case of the four-bolt embedment tests, loading was not continued until failure, since the intention was only to measure load distribution within the elastic range. Preliminary tests indicated that the parallel to grain tests could be conducted in the loading range 0-20kN, and the perpendicular to grain tests in the range 0-5kN.

Table 3 lists the results of the four-bolt embedment tests. The mean values for proportion of load carried by each bolt are averages obtained from four tests of each type.

Table 2 Results of the single-bolt embedment tests
(mean values and coefficients of variation of 4 tests)

Mode	Mean embedding resistance kN	Coefficient of variation %	Embedment stiffness kN/mm
Compression parallel	13.5	7.4	40
Tension parallel	12.2	8.2	19
Compression perpendicular	8.2	6.0	50

Table 3 Results of the four-bolt embedment tests
(Proportion of load carried by each bolt, mean of 4 tests)

Mode	Proportion of load			
	Bolt 1	Bolt 2	Bolt 3	Bolt 4
Compression parallel	0.29	0.38	0.16	0.17
Tension parallel	0.27	0.28	0.25	0.20
Compression perpendicular	0.50	0.38	0.10	0.02

EC5 Comparison

For the single-bolt embedment test listed in Table 2, it was possible to make a direct comparison with the embedding strengths that would be predicted by the relevant design equations in EC5, April 1992 draft. The code indicates thus:

> The following characteristic embedding strength value should be used, at an angle α to the grain:
>
> $$f_{h,\alpha,k} = \frac{f_{h,0,k}}{k_{90}\sin^2\alpha + \cos^2\alpha} \qquad (6.5.1.2a)$$
>
> $$f_{h,0,k} = 0.082\ (1\text{-}0.01d)\rho_k\ \text{N/mm}^2 \qquad (6.5.1.2b)$$
>
> $$k_{90} = 1.35 + 0.015d \quad \text{for softwoods} \qquad (6.5.1.2c)$$
>
> $$k_{90} = 0.90 + 0.015d \quad \text{for hardwoods} \qquad (6.5.1.2d)$$
>
> with ρ_k in kg/m^3 and d in mm.

From 93 moisture content and density test cubes, a mean density of 466 kg/m^3 was measured in the test material, with a coefficient of variation of 9.9%. The mean, rather than the characteristic density should give the better comparison with mean test results.

Applying equations 6.5.1.2a to c for the parallel to grain case, an EC5 embedding stress of 33.63N/mm^2 and hence a strength of 13.3kN, was obtained. This compared well with the mean value of 13.5kN for compression parallel to grain, listed in Table 2.

Equations a to c for the perpendicular to grain case produced a stress of 21.98N/mm^2 and a strength of 8.7kN, again quite close to the experimental value of 8.2kN in Table 2.

This comparison was taken as indicating that in the single fastener case, valid embedment tests were being conducted of a type that would lead to the embedment failure mode used as a basis for EC5. Hence, by extrapolation the multiple fastener test procedure was also taken to be a special but valid kind of embedment test.

Finite element analysis

A full finite element model of the multiple-fastener problem is notoriously difficult to set up, even in metal structures which can be treated isotropically. The contact area between the fastener and the parent material is often indeterminate, and the assumptions made in this respect can influence the results substantially. Instead of such an approach, it was decided to treat the bolt in the hole in rather a simplified manner, but to introduce an additional spring element into the analysis at each bolt hole, to model the embedment stiffness of the fasteners. The parameters for this embedment stiffness were to be taken from the individual bolt tests.

The intention of the analysis was to predict the distribution of the bolt loads amongst the fasteners within the elastic range only. No attempt was to be made to obtain a closely detailed stress analysis around each fastener, nor was it required to model aspects beyond the elastic range, which could involve iterative, non-linear load-slip modelling, or the selection of failure criteria, for example. The finite element program ANSYS was used. Quadrilateral orthotropic elements and spring elements were employed.

Figure 11, (a) to (c), shows the steps in obtaining a corrected finite element model, which would allow for the embedment stiffness. In Figure 11(a), an idealized single-bolt test arrangement is shown. The displacement δ_{exp} indicated in this diagram was measured by test, using the linear portion of the embedment curve. As described in the test section of this paper, the holes were drilled immediately before testing to be as exact a fit as possible. Other displacement assumptions could if required be included in a similar model.

Figure 11(b) shows a simplified version of the finite element model, with the bolt attached to the timber surrounding it. The displacement δ_{fe} of a node adjacent to the centre of the bolt was extracted from the analysis, giving a theoretical embedment stiffness which would apply to a fully attached bolt. Under this assumption, the area of timber beneath the bolt would be in tension, whereas in practice it would not be so fully stressed.

Figure 11(c) shows the additional spring element connected between the centre of the bolt and 'ground'. The stiffness of this element was chosen such that the displacement of the node opposite the bolt centre was equal to the experimental displacement δ_{exp}. Hence, the spring stiffness of the corrected model was:

$$k_c = 1/(1/k_{exp} - 1/k_{fe})$$

Models of multi-bolt specimens were created using the same principle. Figure 12 shows such a four-bolt model. The share of load carried by each bolt could be obtained from the behaviour of each spring in the model, after the surrounding timber and applied load had been simulated correctly.

Plate 4 shows the finite element model for the case of compression parallel to the grain, for a single-bolt specimen. Only half the specimen width was necessary in the model. Contours of direct stress in the grain direction can be seen in this photograph.

The finite element embedment stiffness for the parallel to grain case was evaluated as 430 kN/mm. The test embedment stiffness indicated in Table 2 was used. The resulting 'correction stiffness' was 44 kN/mm.

Plate 5 shows the finite element model for the multiple-hole tension specimen loaded parallel to the grain, whilst Plate 6 shows the single-hole compression perpendicular case.

Table 4 Results of the four-bolt finite element analyses
(Proportion of load carried by each bolt in the elastic range)

Mode	Proportion of load			
	Bolt 1	Bolt 2	Bolt 3	Bolt 4
Compression parallel	0.36	0.26	0.20	0.18
Tension parallel	0.31	0.26	0.22	0.21
Compression perpendicular	0.61	0.24	0.10	0.05

Table 4 summarises the results of the four-bolt finite element analyses, giving the proportion of load carried by each bolt, within the elastic range.

Discussion

In order to compare the results with other work and to obtain a broader view of their implications, it was necessary to calculate what would effectively be known in code terms as a 'reduction factor'. This was because other researchers have not reported results in terms of proportion of load per fastener. For this purpose, it seemed reasonable to assume that a design rule might be based upon the requirement to limit the total load on a multiple fastener joint to a value such that the individual fastener carrying the greatest proportion of the load would only be loaded to a value permitted in a joint with a single fastener of the same type. Whilst it was recognised that this might not be the only possible assumption, it seemed a straightforward approach.

From this, it followed that the 'reduction factor' amounted to the proportion of load that would be carried by each fastener if the 'load sharing' were perfect, e.g. 0.25 in the case of four bolts, divided by the proportion of load actually carried by the most heavily loaded bolt in the test series or finite element analysis under consideration. This somewhat surprisingly simple factor can quickly be deduced by a few easy calculations.

Table 5 shows the reduction factor computed in this manner for both the test results and for the finite element analysis, with respect to each mode of loading.

Table 5 Reduction factors for each mode of loading, by test and from analysis.

Mode	By test	From analysis
Compression parallel	0.66	0.69
Tension parallel	0.89	0.81
Compression perpendicular	0.50	0.41

Two salient features of this simple presentation are immediately apparent. Firstly, both the tests and the analyses suggest that the load sharing amongst the fasteners is more even in the case of tension parallel to the grain than in the case of compression parallel to the grain. Secondly, the reduction factor for compression perpendicular to the grain is substantial and should apparently be even more severe according to the finite element analysis than was determined by test.

In the case of tension parallel to the grain, it was possible to compare the results with those previously reported to CIB W18 by Yasumura et al. In the presentation of this extensive series of Japanese tests on glulam, the relation between the number of bolts and the decreasing ratio of the ultimate load per bolt (described in this paper as 'reduction factor') was given by means of a simple fitted equation using least square techniques.

For a bolt spacing of 4d, the nearest to the 5d used in the tests reported in this paper, and for a ratio of L/d = 4 (the thinnest central member type included), Yasumura gave:

$$D = N^{-0.3744}$$

where D = 'Decrease ratio'
and N = Number of bolts

For four bolts, this would indicate a decrease ratio of 0.59, which was more severe than the values indicated in Table 5. At the wider bolt spacing of 7d, the effect was slightly less severe according to the Japanese test, four bolts in tension parallel to the grain having a decrease ratio of 0.68.

The more severe reductions found by Yasumura may possibly be due in part to the fact that his tests were more practical, large-scale tests on the types of bolted joints found in full-sized glulam structures, whereas in the tests reported here, special efforts were made to produce 'near-perfect' test joints in order to obtain the best possible comparison with analysis.

Wilkinson also tested 'real' joints in Douglas fir, with steel plates. For five bolts in line with a spacing of 8d loaded parallel to the grain, he obtained reduction factors as defined in this paper typically as low as 0.4. He concluded that variability and fabrication effect were having a large influence on this uneven load distribution.

In the case of the multiple-fastener joints loaded perpendicular to the grain, no reports of tests by others were available against which to compare the results given in this paper. It should be noted, however, that it is considered that the agreement between test and analysis is quite good considering the variations that are possible in such experiments. Both test and theory suggest that the present European and British code procedures for reducing values in multiple-fastener joints loaded in this manner are seriously non-conservative.

Conclusions

Tests and analytical investigations have been made on load distributions in multiple-fastener bolted joints, using European whitewood glulam, with steel side plates. The proportions of load carried by each bolt have been determined. These have been found to be very uneven, especially in the perpendicular to grain case.

For each of the three modes of loading which were investigated, namely compression parallel to the grain, tension parallel to the grain, and compression perpendicular to the grain, reduction factors have been determined, by test and from analysis. These reduction factors were related to the type of calculation which is based on summing the load carrying capacity of a multiple-fastener joint by taking the number of fasteners multiplied by the individual fastener capacity.

In compression parallel to the grain, the reduction factor determined by test was only about four per cent different from the corresponding value shown by analysis. In the tension case, agreement was within ten per cent. In compression perpendicular to the grain, agreement was less close, with a difference of twenty two per cent between test and theory. However, this is still considered quite reasonable, in view of the substantial influences tending to cause variability in such specimens.

The experimental measurements were conducted using a special test apparatus, which was designed to ensure that failure took place in a pure embedment mode. Other precautions were also taken in manufacturing the specimens. Single-fastener tests were conducted which were then compared with EC5 (draft) design procedures. These comparisons showed that the plastic embedment assumption was valid.

Both the tests and the analysis suggested that the load sharing amongst the fasteners was more even in the case of tension parallel to the grain, than in the case of compression parallel to the grain. The reduction factor for compression perpendicular to the grain was substantial, and should apparently be even more severe according to the finite element analysis than was determined by test. The test evidence suggested that a reduction factor of 0.50 should apply to four bolts in such a situation.

The reduction factors determined for the various four-bolt parallel to grain configurations in this research were in the range 0.66 to 0.89. A brief comparison with two other sets of tests was made in this paper, and in an accompanying paper, a selected review of research and codes was given. All the supporting evidence suggests that BS 5268:Part 2 and EC5 (April 1992 Draft) make insufficient allowance for this phenomenon. On the other hand the Canadian Code CSA-086.1-M89, would apply a factor for groups of fastenings, J_G, of 0.50 for four bolts in a row, and for the ratios of l/d and s/d used in these tests.

References

[1] Wilkinson, T.L. Load distribution among bolts parallel to load. Journal of Structural Engineering 112(4):835-852, USA, 1986.

[2] Yasumura, M., Murota, T. and Sakai, H. Ultimate properties of bolted joints in glued-laminated timber. CIB-W18A/20-7-3, Dublin, 1987.

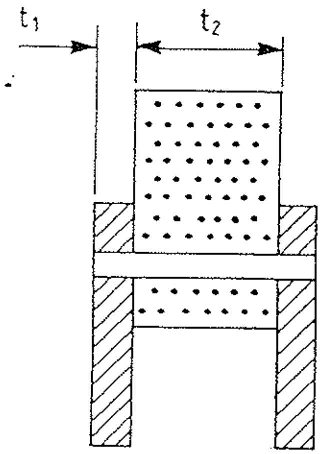

Figure 1. Definitions of t_1 and t_2

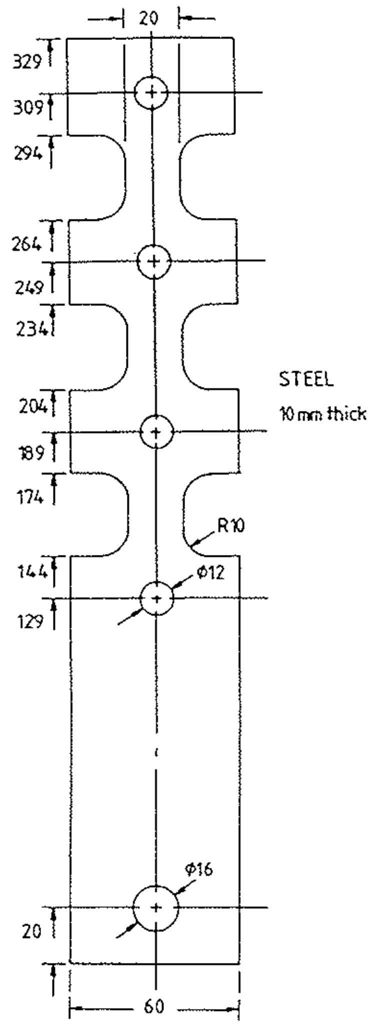

Figure 2. Dimensions of side plates of jig

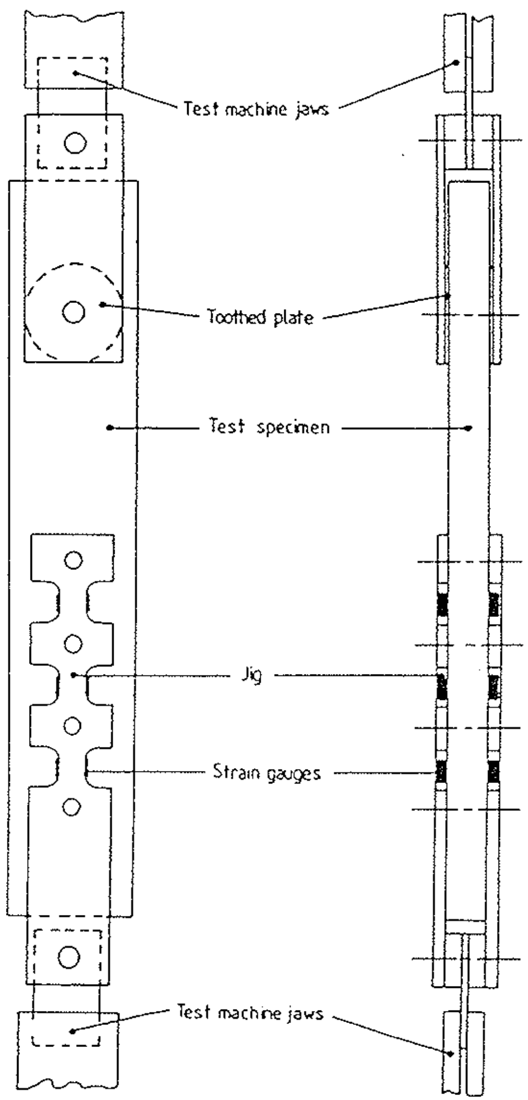

Figure 3. Schematic diagram of rig for tensile test

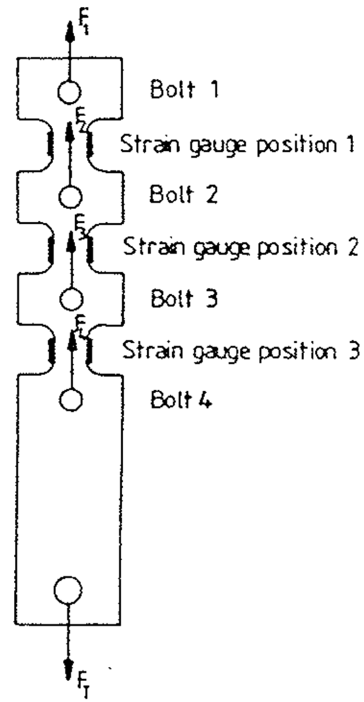

Figure 4. Designation of bolts

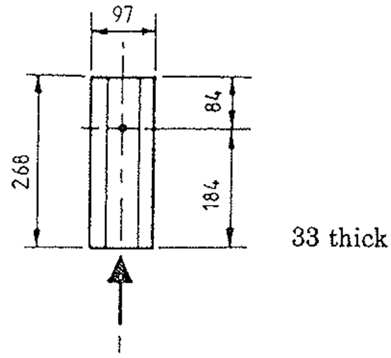

Figure 5. Compression, one bolt.

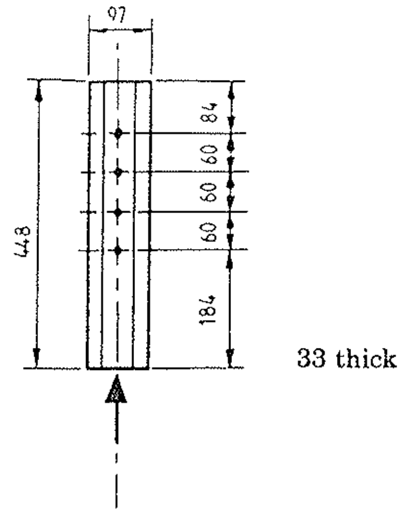

Figure 6. Compression, four bolts.

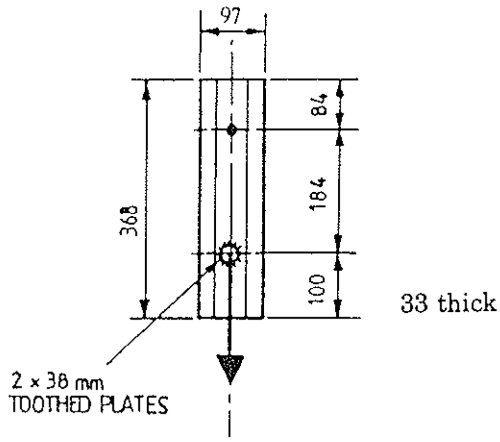

Figure 7. Tension, one bolt.

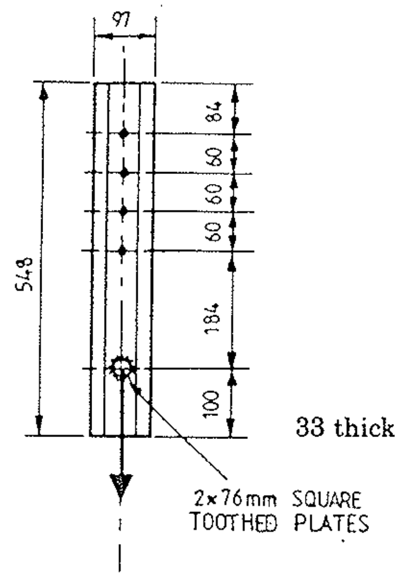

Figure 8. Tension, four bolts.

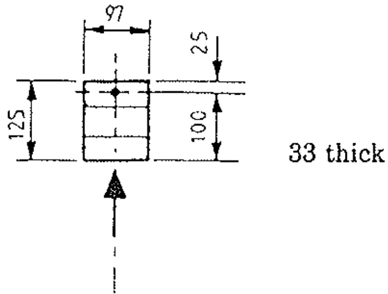

Figure 9. Compression perependicular, one bolt.

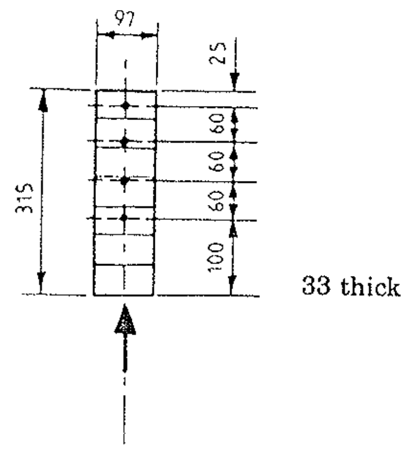

Figure 10. Compression perpendicular, four bolts.

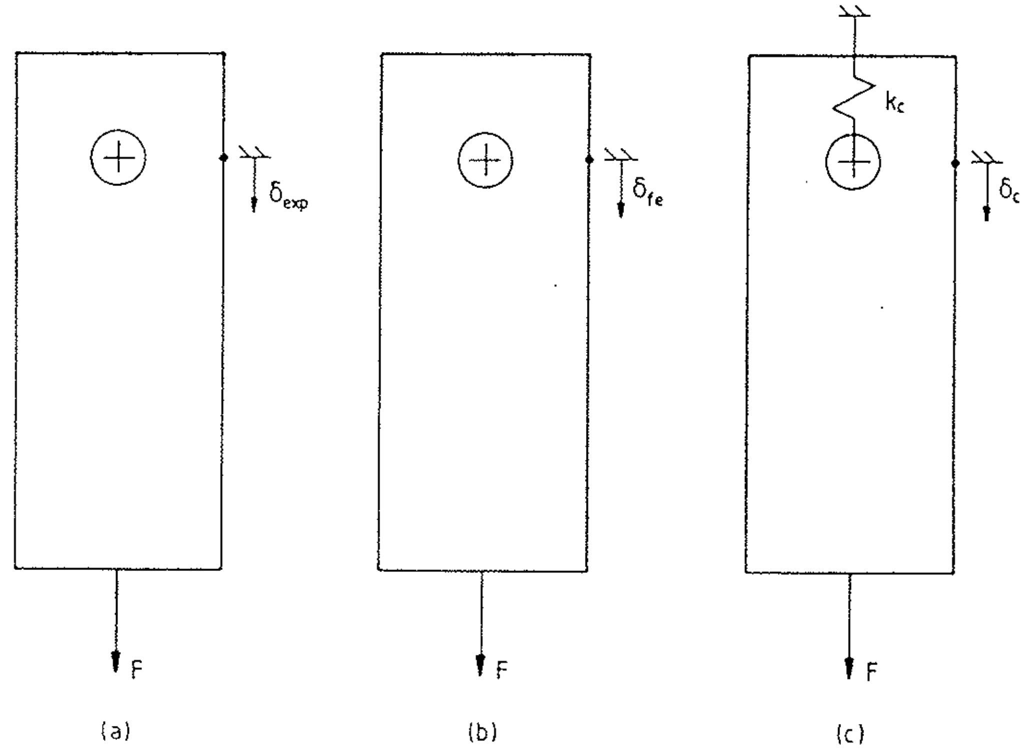

Figure 11. Finite element models of single hole embedment test showing (a) experimental measurement, (b) basic finite element model and (c) corrected finite element model

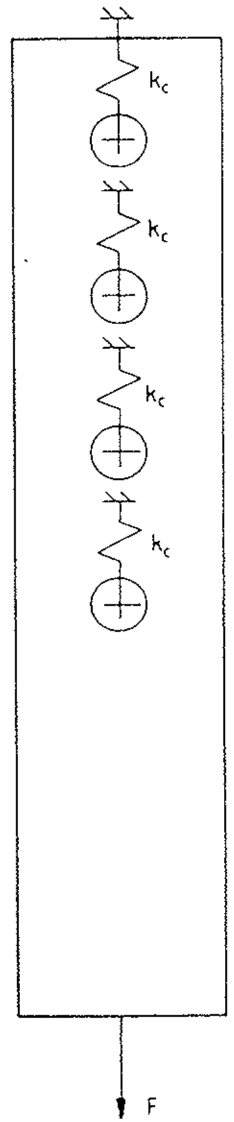

Figure 12. Finite element model of multiple hole test

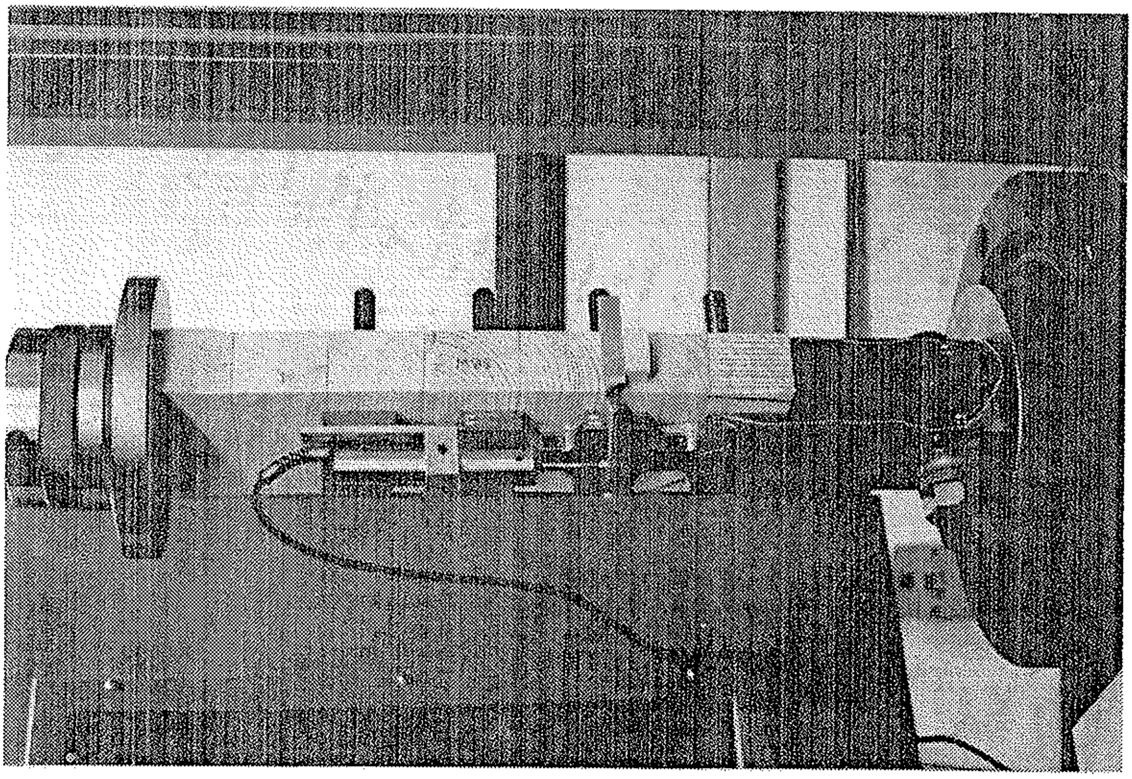

Plate 1. Details of apparatus for compression tests of multiple hole specimens

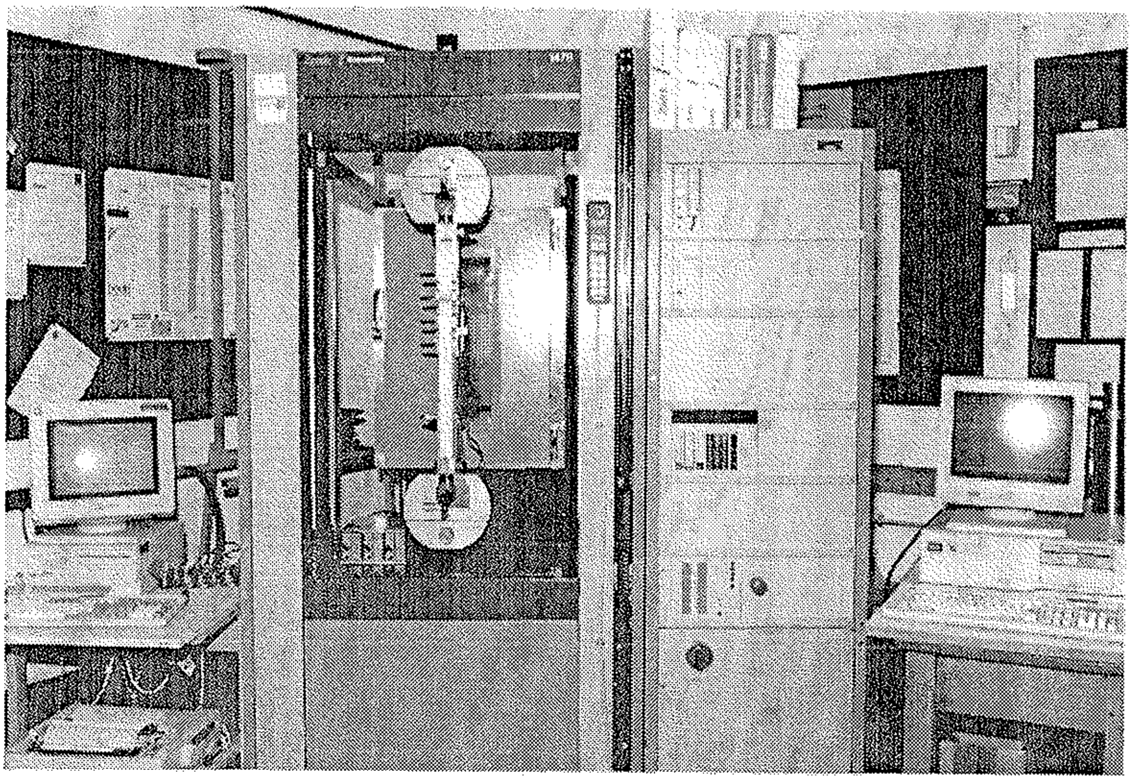

Plate 2. Layout of equipment for tests

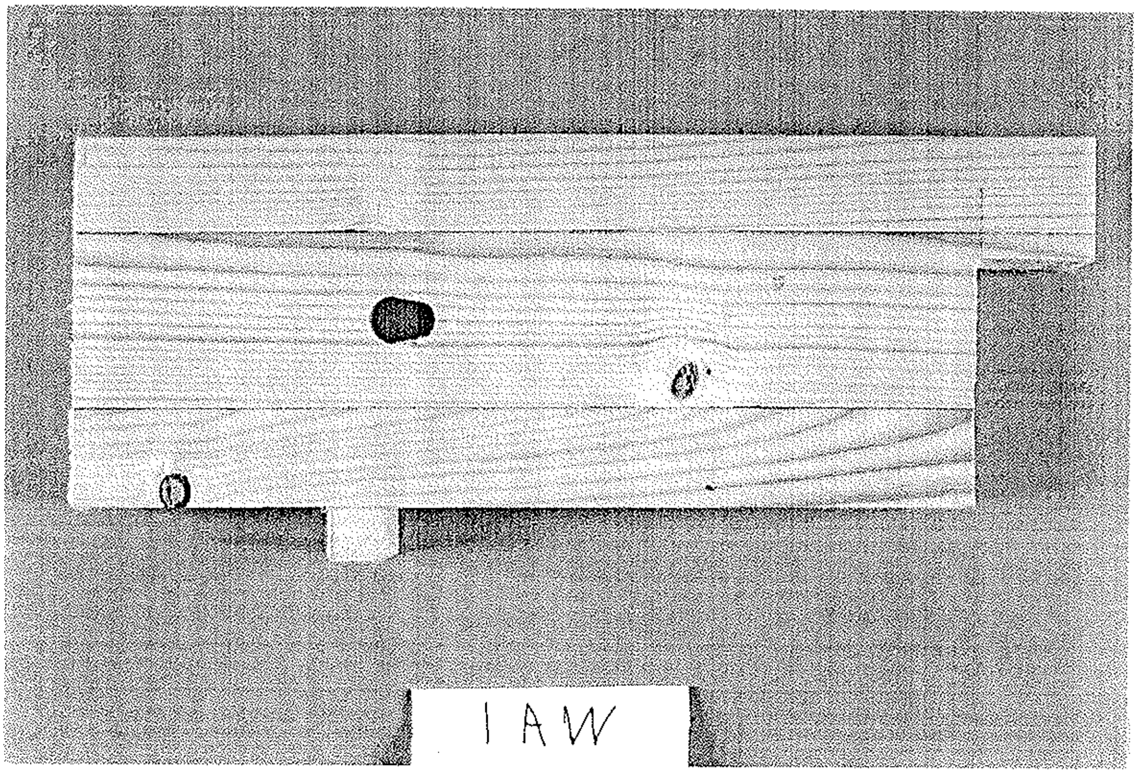

Plate 3. Plastic embedment in single hole compression test specimen

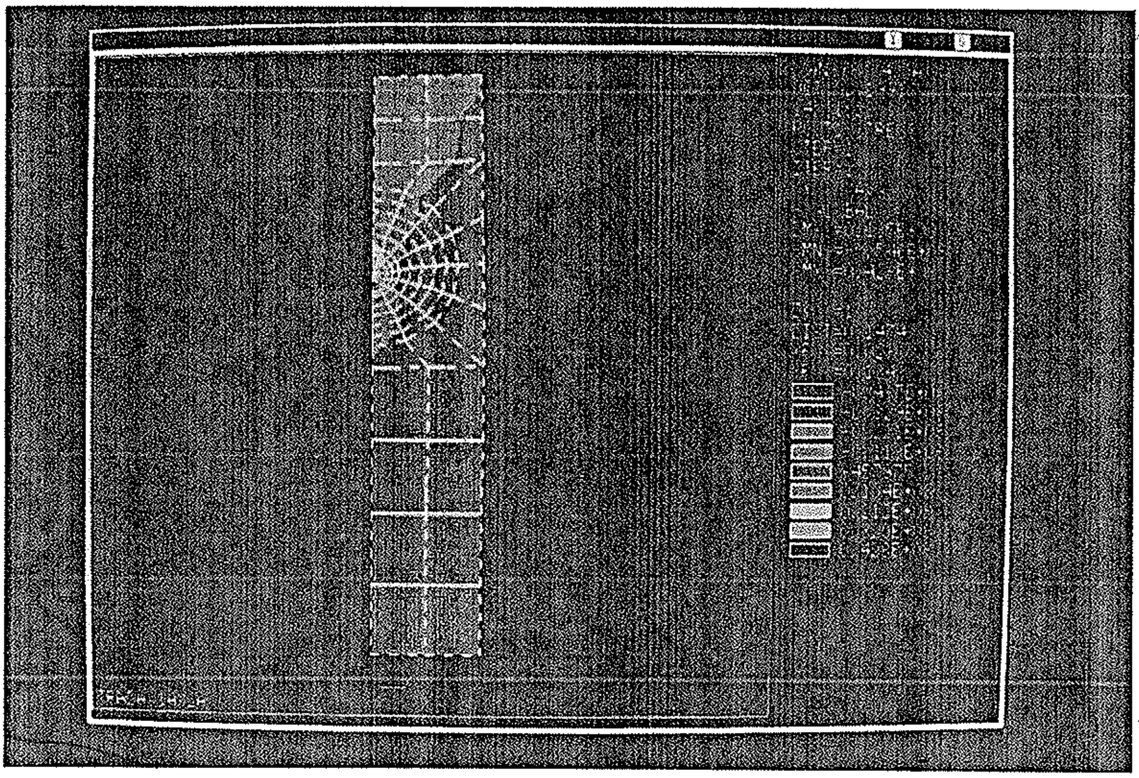

Plate 4. Finite element display for single hole specimen loaded in compression parallel to the grain

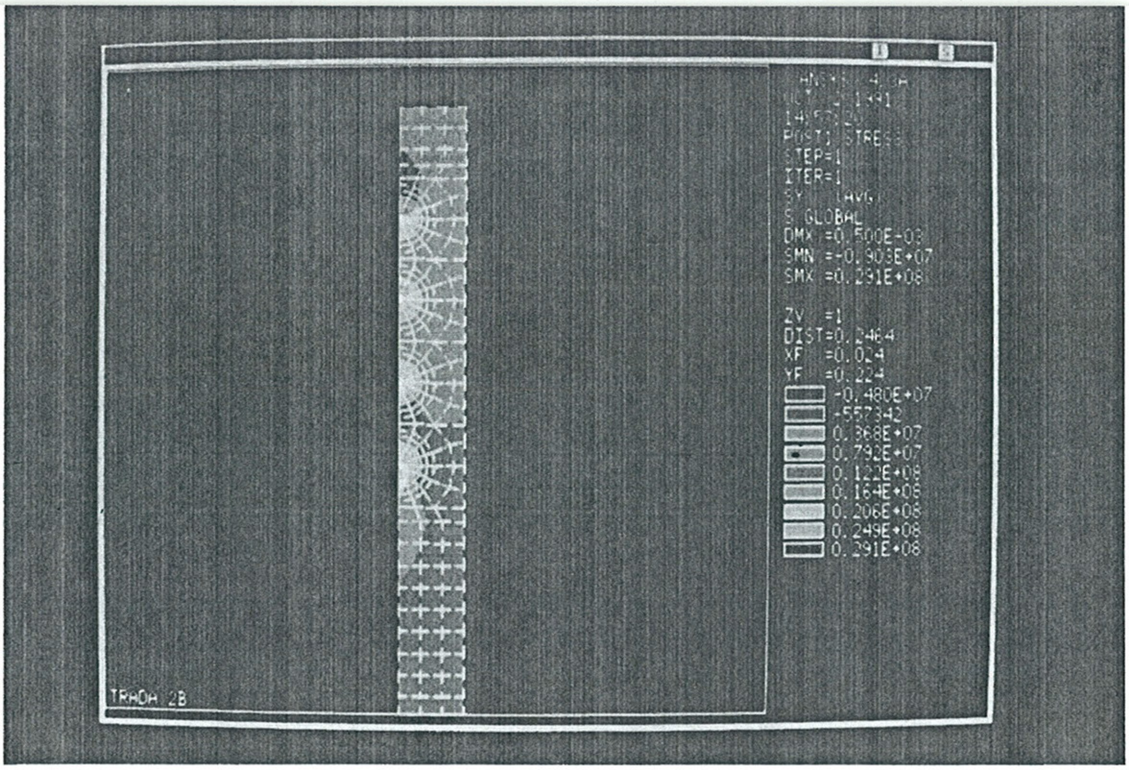

Plate 5. Finite element display for multiple hole specimen loaded in tension parallel to the grain

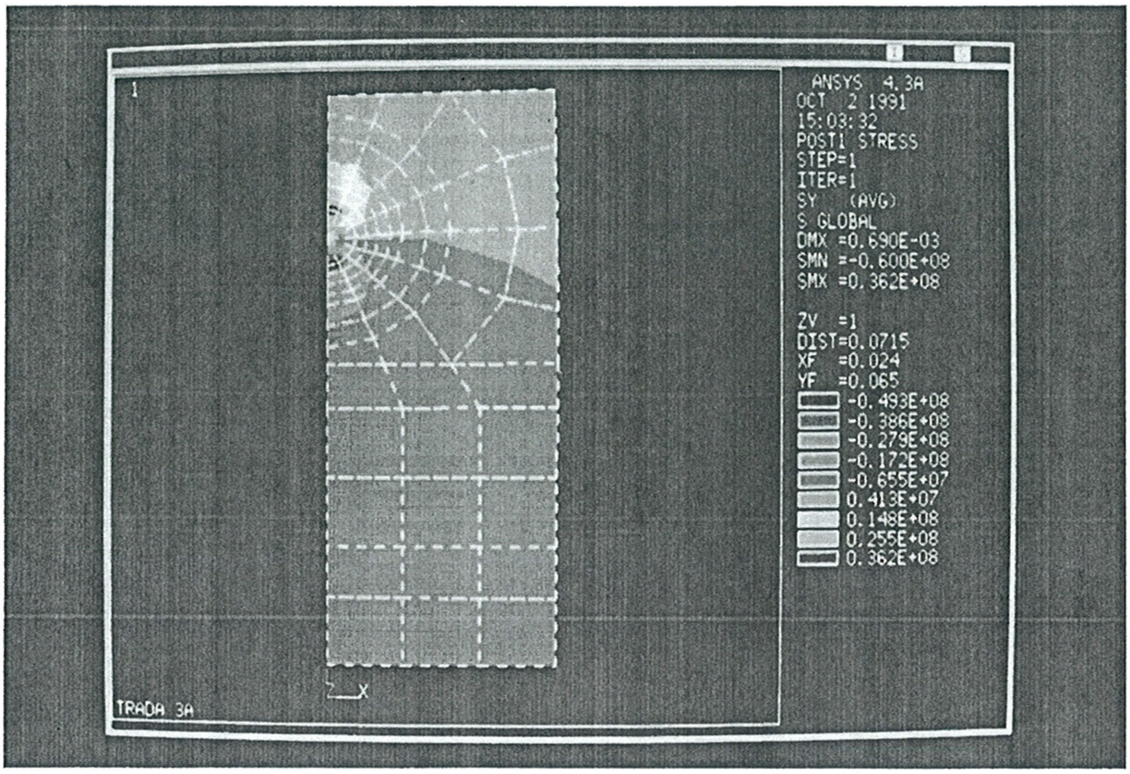

Plate 6. Finite element display for single hole specimen loaded in compression parallel to the grain

CIB-W18/25-12-1

INTERNATIONAL COUNCIL FOR BUILDING RESEARCH STUDIES AND DOCUMENTATION

WORKING COMMISSION W18 - TIMBER STRUCTURES

DETERMINATION OF CHARACTERISTIC BENDING VALUES OF GLUED LAMINATED TIMBER EN-APPROACH AND REALITY

by

E Gehri
Federal Institute of Technology, Zurich
Switzerland

MEETING TWENTY - FIVE

ÅHUS

SWEDEN

AUGUST 1992

1. Introduction

The loading models for bending of glulam ([1] pg. 3-3.1) are defined in EN TC 124.207. This model is based on a proposal of Riberholt/Ehlbeck/Fewell [1]. The characteristic bending moment of the beam is derived as:

$$f_{m,k,g} = \underbrace{(2.7 - 0.04 \cdot f_{t,o,k,l})}\, f_{t,o,k,l}$$

$$\frac{f_{m,k,g}}{f_{t,o,k,l}} = k_{lam}$$

for a beam with a reference depth of $h = 300$ mm [2]. Moreover, in annex A of [2] it is established that:

"The mechanical properties of glued laminated timber are derived by multiplying the laminate properties by a k_{lam} factor which make allowance for:

a – the test methods used for single laminations, which may be less constrained than when laminations are bonded together in a single member;

b – differences due to the dispersion of laminate low strength and low stiffness areas throughout the volume of a glued laminated member;

c – differences between the coefficients of variation of single laminates and laminated members.

The above statements are valid only for wood laminations without end joints. If end joints are present the bending strength for the splice must fulfill the following conditions according to reference [2]:

$$f_{m,k,j} \geq f_{m,k,g}$$

The latter condition was adopted on the basis of a proposition of Riberholt [3]. The more comprehensive and better founded investigations of Ehlbeck/Colling [4] lead to more severe conditions concerning the splice strength. For the reference depth of $h = 300$ mm, the required condition is:

$$f_{m,k,j} \geq 1{,}15 \cdot f_{m,k,g}$$

The coefficient 1.15 is, in my opinion, a value that is too low. Based on the work of Colling/Ehlbeck/Görlacher [5] a coefficient of 1.4 may be justified as will be explaned later.

In the EN TC 124.407 version of 22.04.1991, the reference depth of $h = 300$ is changed to $h = 600$ mm. At the same time it is determined that "the values for bending strength apply for a depth of 600 mm or less. For deeper beams the bending strength shall be multiplied by $(600/h)^{0.4}$. Despite different reference depths the same characteristic bending strength is prescribed. In addition the condition with relation to the lamination splice is maintained - despite a reference heigth that is doubled. The claim here is: "The bending strength of end joints in the lamination is greater than the characteristic bending strength of the beam with depth of 600 mm".

This statement of 22.04.1991 is in contradiction with present knowledge of the effect of volume or "size factor". Several research projects, among which that of Ehlbeck/Colling [4], demonstrate the influence of beam dimensions (length <u>and</u> depth). Within the framework of the European Standards a certain consensus has been established, based on the simplifying assumption that:

$$\text{Bending strength} = \text{Function of } (h)^{-0.2}$$

The study-group of Ehlbeck/Fewell/Larsen/Riberholt/Sunley worked out a new proposal which takes the above objections in consideration. This foresees 6 instead of 5 strength classes.

This proposal was amended on 7.10.1991 by Larsen and was published as CEN/TC124/WG2 N 155. This draft is based on a reference depth of 600 mm. The change from 300 mm to 600 mm takes the size effect into consideration using the factor:

$$\left(\frac{300}{600}\right)^{0.2} = 0.87$$

The characteristic bending strength of the beam, based on the tensile strength of the wood laminations, is therefore derived as:

$$f_{m,k,g} = (2.35 - 0.035\, f_{t,o,k,l})\, f_{t,o,k,l}$$

The limiting condition with the lamination end joint strength should have been:

$$f_{m,k,j} \geq 1.15\, f_{m,k,g}$$

In the "amended" version by Larsen this condition was further mitigated to:

$$f_{m,k,j} \geq 1.1\, f_{m,k,g}$$

The latest version of EN TC 124.207 is also amended by Larsen and dated 18.3.1992, i.e. this edition was prepared after the EC5-Meeting in Trento. This version proceeds from a new definition of the characteristic bending strength. This maintains that "the characteristic strength properties of table 1 correspond to the 0.85-values of the characteristic properties derived from test in accordance with prEN 408". In so doing the new definition is valid only for bending and tension!

The importance of this new definition is that the assumed bending strength to be used in calculations is increased by about 20 % over what has been applied previously!

In addition the requirements for end joints were again reduced in comparison with the new, increased characteristic strength used in the calculation. In the new version (for a reference depth of 600 mm) the only requirement is that:

$$f_{m,k,j} \geq f_{m,k,g}$$

I am well aware of the difficulties which glulam producers encounter in trying to fabricate a high quality product. The proposed procedure, however, is in the wrong sense. The real safety factor is actually decreased, which is intolerable.

As shall be demonstrated below, the tension strength of the laminations and the end joints are much too optimistically defined in relation to the value established earlier.

2. Procedure to determine the characteristic bending strength

The failure of a beam in bending is determined by:

- the tensile strength of the wood laminations $f_{t,o,k,l}$
- the tensile strength of the end joints $f_{t,k,j}$

The strength model should therefore be based directly on these values.

$$f_{m,k,g} = \text{the smaller of} \begin{cases} F(f_{t,o,k,l}) \\ G(f_{t,k,j}) \end{cases}$$

Difficulties arise here since the values of $F(f_{t,0,k,l})$ and $G(f_{t,k,j})$ may hardly be determined directly. For wood laminations a classification exists that is based on the bending properties. For end joints the quality assurance is the result of a bending test.

The strength model for bending of wood laminations of Riberholt/Ehlbeck/Fewell is based directly on the tensile strength $f_{t,0,k,l}$. In the model for end joints the tensile strength $f_{t,k,j}$ is replaced by a requirement concerning the bending strength. One should object that the latter requirement should be clearer to the user since bending tests are usually used for routine quality control. The characteristic bending strength of the end joints is therefore known.

The chosen method produces several problems, however:

- Specialists, and that includes the standard committee of the CEN, are not yet in agreement on the tension/bending ratio for end joints.
- The ratio tension/bending is not a constant parameter. Not only the size of the end joint, but also the absolute strength of the timber influence this ratio; and to a lesser extent the moisture content.
- The end joint bending strength should really be established in terms of the lamination thickness; the tensile strength is really a function of the cross section, A [for example $A^{-0.2}$]. According to the EN the only factor here is the lamination width, introduced in the form $b^{-0.2}$, in which $b = 150$ mm is the adopted reference value.
- Higher end joint strengths yield larger tensile/bending strength ratios; in principle values of even more than 1,0 are conceivable. In bending tests a compression failure may be produced.
- The correlation of the tension/bending ratio where end joints are concerned is very poor. This is demonstrated by the extensive research of Ehlbeck/Colling [6].

In order to get around these problems it is logical to include $f_{t,k,j}$ directly in the strength model. At least these tests can be simply and efficiently accomplished in the laboratory, as our own experience has proved.

The often repeated discussion of the support conditions in tension tests (Fig. 1) is avoided in as much as the sample ends are fully clamped.

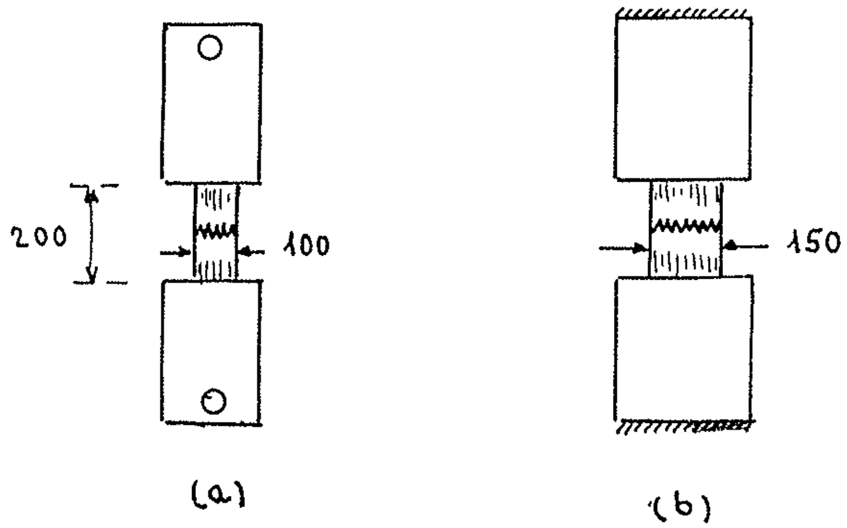

Figure 1: Test set-up for tension tests

(a) according to tests made by Colling/Ehlbeck/Görlacher [5], width 100 mm

(b) according to tests made by Gehri, "restrained" and conditions, width 150 mm

In a comparison of the absolute values attention should be paid to the different widths of the test specimens. The conversion to the reference width of $b = 150$ should be done with the function $(b/150)^{0.2}$. The test results in tension according to [5] are therefore to be multiplied by 0.92 and in this way the tension/bending ratio for $b = 150$ is reduced by the same amount.

3. Determination of the characteristic bending strength from the wood strength

According to EN TC 124.407 the strength class of glulam (with the exception of the end joint influence) is determined directly from the strength class of the incorporated wood laminations.

Example: A beam with homogenous construction of C18 wood laminations presents a bending strength of 21 N/mm^2.

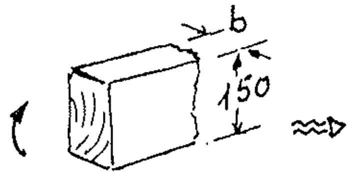

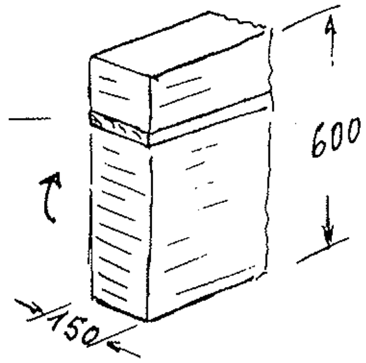

$f_{m,k} \geq 18$ N/mm^2

for moisture content 10 % to 18 %

= strength class C18

$f_{t,o,k} = 0.6 \cdot f_{m,k}$

independent of lamination thickness

$f_{m,k,g} \geq 21$ N/mm^2

The classification does not depend on the relevant tensile strength, but rather from the bending strength of the strength class in question. This is dependent on a beam with 150 mm depth for various widths b . Furthermore the classification criterium used is not the bending strength but the elastic modulus in bending.

The linking of bending strength of glulam having a depth of 600 mm with the tensile strength of the laminations results from several steps of simplified relations, which appear to be substantially inexact, discrepancies which could be cumulative. It is therefore necessary to confirm the values derived from this type of strength model with results obtained from tests. A subsequent calibration operation may lead to corrections.

4. Examination of end joint requirements using 300 mm deep beams

Earlier strength models were based on a beam with reference depth of $h = 300$ mm, so it is therefore understandable that many earlier tests were carried out using this beam dimension.

The examination described below was carried out on the basis of a series of tests executed in a course for wood specialist in 1987 at the ETH Zurich [7].

As can be seen the bending of 120/300 beams were the most important feature. The properties of the wood and the end joints corresponded to the Swiss wood construction standard, SIA 164 in force at that time, as well as the more comprehensive quality standards of the Swiss Study Group for Glulam.

The strength class FA was produced. The characteristic bending strength (for $h = 300$ mm) was to be:

$$f_{m,k,g} \cong 2.25 \cdot \underset{\substack{\uparrow \\ \text{admissible bending according SIA 164}}}{14} = 31.5 \text{ N/mm}^2$$

The outer laminations corresponded to the strength class L1 (visual selection!). No strength tests were performed on the laminations. In this case it did not imply an error since all the failures were in the end joints.

Out of each of the outer laminations 24 end joint samples were systematically cut, in such a way that 12 of each were to be tested in tension or bending. The tension tests could not be performed for lack of equipment. The results of the 12 bending tests gave a satisfactory impression. The requirement $f_{m,j} \geq$ 39 N/mm^2, which is analogous to the german standards for high quality end joints, was fulfilled. The characteristic bending strength (ascertained by 12 tests with $n = \infty$) came to 41.3 N/mm^2.

On the basis of the mathematical model of EN TC 127.407 (Version 1991-10-07, which was available before the EC-5 meeting in Trento) the following conditions were to be fulfilled:

for $h = 600$ mm $\qquad f_{m,k,j} \geq 1.1\, f_{m,k,g}$

Converted to a beam depth $h = 300$ mm, this gives:

$$f_{m,k,j} \geq 1.1 \left(\frac{300}{600}\right)^{0,2} \cdot f_{m,k,g}^{300\,mm}$$
$$\geq 0.96 \cdot f_{m,k,g}^{300\,mm}$$

With $f_{m,k,j} = 41.3$ N/mm^2 the calculation gives the characteristic bending strength with $h = 300$ mm (assuming wood failure is excluded) as:

$$f_{m,k,g}^{300\,mm} = 1.04 \cdot 41.3 = 43.2 \text{ N/mm}^2$$

Nevertheless, the actual characteristic bending strength, determined for 12 beams, was only 30.8 N/mm^2, that is to say that the EN calculation model gives a value that is about 40 % too high!

5. Examination of the requirement concerning the strength of the laminations

Pellerin and Strickler [8] measured the bending strength on beams with a depth of 610 mm. Reliable information was available concerning the minimum tensile strength (from tension proof-loading test results). The characteristic tensile strength may be fixed at about 30 N/mm^2.

The tests on 12 beams (combined glulam) gave $f_{m,k,g} = 35$ N/mm^2.

Proceeding from the EN regulations for calculation (version 1991-10-07) and taking into account that a combined glulam is in question, these regulation require a characteristic tensile strength of 24 N/mm^2.

Conclusion: The EN regulation concerning the tensile strength of wood laminations sets requirements that are too low. These must be increased about 25 %.

6. Examination of the requirement concerning wood laminations and end joints

In previous test series that were used for examination, no complete series of data was available from which a check of both requirements was possible. In the course of a demonstration in March 1992 at the ETH Zurich 8 beams were tested with emphasis on observation of the most comprehensive series of data possible.

The number of beams tested may seem few. Taking into consideration that the EN regulations, (version 1991-10-07) as described in sections 4 and 5, lead to flagrant differences, only a few tests should suffice in these conditions - if the test could be specifically executed to answer the question.

In accordance with the results of sections 4 and 5 it must be concluded that the EN regulations (version 1991-10-07) lead to a large overestimate of the bending strength:

- for wood strength $\quad f_{t,o,k,l} \quad$ 25 %
- for end joint strength $\quad f_{m,k,j} \quad$ 40 %

With such large deviations a small number of specific tests suffice to either to demonstrate this or make these bending strengths questionable.

The beams tested featured a cross section of 150/500. Retaining the 600 mm reference depth of the EN was not possible for technical reasons during testing. Consideration of the size factor of $(h)^{0.2}$ produced a small correction of 4 %. The width of 150 mm was chosen so that no correction needed to be introduced for the tension tests of the laminations (reference width = 150 mm).

Beams without end joints in the tension zone

Samples were systematically taken from high quality timber with elastic modulus of 16'200 N/mm^2 which was intended for the tension zones, and were tested in tension. The summary of all the values is shown in the above figure as well as the results of the 4 beam tests.

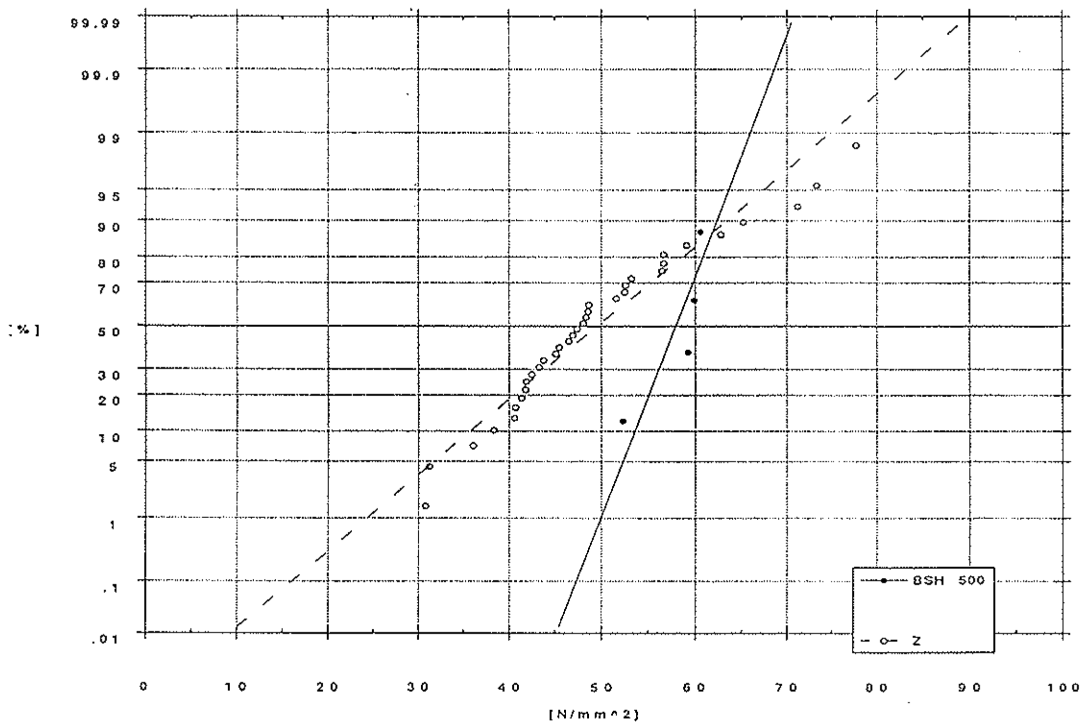

Figure 2: Results of tension tests on 2.7 m laminations with width = 150 mm; Results of 4 bending tests on 500 mm deep beams

Conclusion:

- The characteristic tensile strength of tension laminations was around 32 N/mm^2. This value is clearly higher than 25 N/mm^2, which is acceptable according to EN regulations (otherwise higher values of $f_{t,o,k,l}$ give lower bending strength according to the design regulations!).

  The wood used for laminations represented a good quality which can usually be obtained in the Swiss market. It is therefore not comprehensible why the use of better (usually available) properties cannot be respected by the EN regulations.

- The ultimate bending strength attained by the 4 beams was considerably over 50 N/mm^2. This attests to the high potential quality of the lamination wood. Laminations which require no special measures during construction (except the usual initial selection of the laminations) reached bending strengths that are substantially over the strength classes previously provided for in the EN regulation.

  Insufficient bending strengths, as determined by tests, are almost exclusively to be attributed to failure of the end joints, if the wood laminations are properly preselected.

Beam with end joints in the tension zone

Each of the three lower tension laminations contained one end joint in the highly stressed middle area. The end joints were staggered.

Test samples from the end joints were systematically taken (analogous to the material for the beam without end joints) and half of each were tested in tension or bending.

The results of these tests are summarized below; as well as the results of the bending tests. Here, 5 values are indicated since in the series "Beams without end joints" an end joint failure occurred in the outer beam zone.

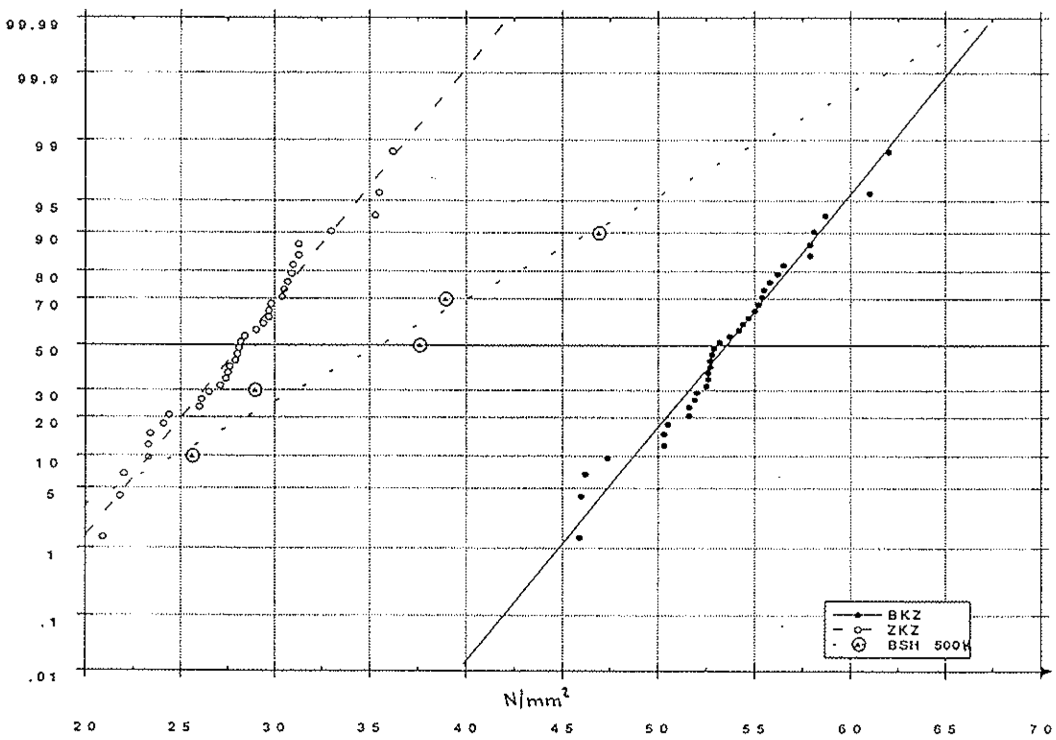

Figure 3: Results of tension (ZKZ) and bending (BKZ) tests on end joints with laminations width of 150 mm; Results of 5 bending tests on 500 mm deep beams (BSH 500 K)with failure in the end joints

Conclusions:

- The result is disillusioning. Almost all values might happen. Aside from the large scatter one can recognize that the lowest values (of only 5 values) are only 1.15 ... 1.3 times higher than the characteristic tensile strength.

  The lowest values amount to little more than the half of the bending strength of beams without end joints!

- The measured tensile strengths (determined on whole laminations with a cross section 33/150 mm) are low, the characteristic tensile strength was near 22 N/mm^2, and could indicate an insufficient quality of the end joint.

  Nevertheless this value does not fall much lower than the data in Colling/Ehlbeck/Görlacher [5], which determined a characteristic "restrained" tensile strength of 23.4 N/mm^2. If one considers the smaller lamination width of 100 mm, the above value is reduced to 21.5 N/mm^2, that means it is of similar quality.

- Surprising results were produced by the bending tests executed on similar sample material. The characteristic value of over 47 N/mm^2 manifested an extraordinarily good quality, compared to existing requirements!

- The lower tension/bending ratio is clearly shown for the end joints:

  - in comparison with the average 0.53
  - in comparison with the characteristic value 0.47

This is a clear indication that the values of the tension/bending ratios measured by Ehlbeck/Colling [6] concerning the characteristic strengths are not extremely low.

	100 mm wide samples	converted to b = 150 mm
– all samples	0.58 ... 0.61	0.53 ... 0.56
– samples with at least 80 % failure in end joint zone	0.61 ... 0.65	0.56 ...0.60

Ehlbeck/Colling/Görlacher [5] departed from a tension/bending ratio of 0.65 and, through different "corrections" raised this value to 0.73!

This procedure is doubtful, as shown below.

Assumed basic value of the ratio			**Remarks**
$\frac{f_{t,k,j}}{f_{m,k,j}}$	=	0.65	As tests show the upper value has been introduced
Correction as the result of simple support condition in tests +8 %		0.70	An assumption that is not based on tests
Correction for "type of loading; difference between uniform distributed and two single loads" +4 %		0.73	This correction has no justification concerning resistance; the characteristic bending strength is based on a loading with two loads.

If we assume an initial tension/bending ratio of 0.63, and if a narrower sample width of 100 mm is used, one has $0.92 \cdot 0.63 = 0.58$. If the correction for pinned/fixed reactions is accepted we have $1.08 \cdot 0.58 = 0.63$ again.

7. Recommendations

Proceeding from the conclusions of sections 4 to 6, the requirements in EN TC124.207 must be changed. It is recommended that:

a – Requirements concerning end joint strength (for beam depth h = 600 mm)

based on tensile strength	$f_{t,k,j} \geq 0.85\ f_{m,k,g}$
based on bending strength (only for information)	$f_{m,k,j} \geq 1.4\ f_{m,k,g}$
From this the tension/bending ratio for beams with end joints is derived as:	$\frac{f_{t,k,j}}{f_{m,k,j}} = 0.61$

b – Requirements concerning wood strength (for beam depth h = 600 mm) based on tensile strength.

$$f_{m,k,g} = 12 + f_{t,o,k,l} \quad N/mm^2$$

References

[1] Riberholt, H. / Ehlbeck, J. / Fewell, A.: Glued laminated timber - strength classes and determination of characteristic properties. Lisbon 1990. CIB-W18A/23 - 12 - 4.

[2] Draft EN TC 124.207-1990-01-22

[3] Riberholt, H.: Glulam beams, bending strength in relation to the bending strength of finger joints. Lisbon 1990. CIB-W18A/23 - 12 - 3.

[4] Ehlbeck, J./Colling, F.: Bending strength of glulam beams - a design proposal. Lisbon 1990. CIB-W18A/23-12-1.

[5] Colling, F./Ehlbeck, J./Görlacher, R.: Glued laminated timber - Contribution to the determination of the bending strength of glulam beams. Oxford 1991. CIB-W18A/24-12-1.

[6] Ehlbeck, J./Colling, F.: Biegefestigkeit von Brettschichtholz in Abhängigkeit von den Eigenschaften der Brettlamellen im Hinblick auf Normungsvorschläge. Versuchsanstalt für Stahl, Holz und Steine, Abteilung Ingenieurholzbau, Universität Karlsruhe, 1992.

[7] Gehri, E.: Tragverhalten von Brettschichtholz - Untersuchungen an kleinen Trägern. Holztechnologie Nr. 92-2. ETH Zürich 1992.

[8] Pellerin, R.F./Strickler, M.D.: Proof loading of tension laminations for large glued-laminated beams. Forest Products Journal, 1972, No. 10, p. 24-30.

CIB-W18/25-13-1

INTERNATIONAL COUNCIL FOR BUILDING RESEARCH STUDIES AND DOCUMENTATION

WORKING COMMISSION W18 - TIMBER STRUCTURES

BENDING STRENGTH AND STIFFNESS OF "IZOPANEL" PLATES

by

Z Mielczarek
M Lange
Technical University of Szczecin
Poland

MEETING TWENTY - FIVE

ÅHUS

SWEDEN

AUGUST 1992

BENDING STRENGTH AND STIFFNESS OF "IZOPANEL" PLATES

Zbigniew Mielczarek, Małgorzata Lange
Technical University of Szczecin, Poland

1. Introduction

In the Institute of Wood Technology in Poznań there have been elaborated the concept and technology of "Izopanel" type panels, glued of wood, hard and porous fibreboards. The load-bearing structure of the panels is formed by framework of wood, lining and vertical strips of hard fibreboards arranged in cross-section plane horizontally and vertically. The void spaces of this framework have been filled with porous fibreboards. It has been assumed that by gluing the fibreboard of hard and porous types together and elaborating an appropriate concept of product structure with vertical location of a part of fibreboards forming type of framework will enable obtainment of composite material of a quality higher than its components both for its strength and insulation properties. The purpose of the investigation carried out by Department of Building Engineering of Technical University of Szczecin was to determine the strength, stiffness and rheological properties of these panels while they are bent perpendicularly to their surface.

2. "Izopanel" characteristics

The panels of "Izopanel" type are characterized by the following features significant for their application in building industry:-

- small apparent density of approximately 0.4 kN/m3,
- relatively good insulative power in thermal and acoustic aspects

(according to calculations 13.5 cm thick panel has overall-heat transfer coefficient of k = 0.55 W/m2k),

- increased fire resistance in relation to the components materials as glued together with non-flammable glue the resulting form has a compact section area with less accessibility for fire and oxygen,
- insignificant swelling,
- good dimensional stability,
- sufficient bioresistance with the application of fungi-resistant and additionally bituminized porous panels,
- good properties as regards holding of screws and nails which offers a possibility of good fastening of connection pieces,
- lack of harmful effects for human body as opposed to chipboard emitting free formaldehyde.

3. Experimental Research

3.1 Examination under short-time load

The examination covered three groups of panels differing from one another by the dimensions of cross-section area (Fig 1). In the first phase of the examination the relations between load size and deflections were determined in order to define their stiffness. The panels were examined in horizontal position with loading in the form of two focussed forces (distributed continuously at panel breadth) applied symmetrically

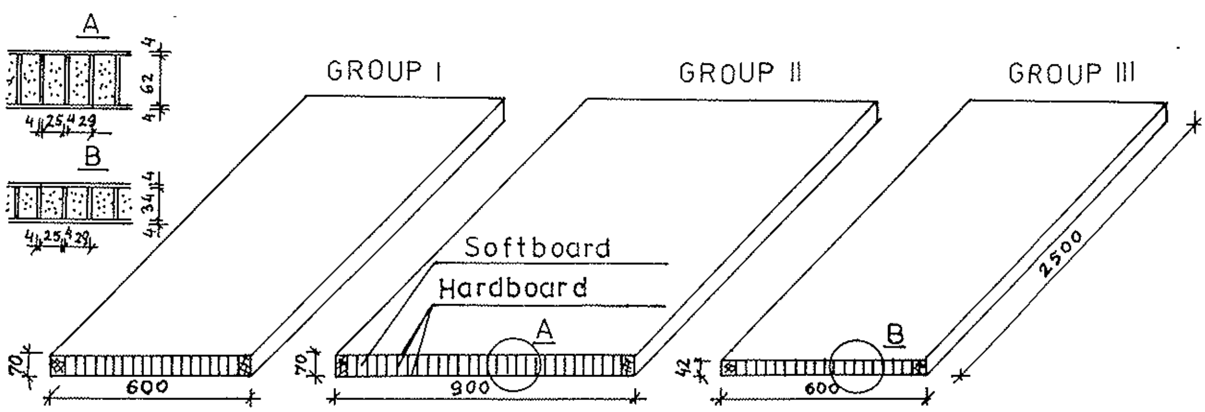

Fig 1. Diagrams of "Izopanel" panels.

at a distance of 100 cm from each support. The load acted in perpendicular plane to panel surface, and its size changed at every 1/5 Q^d where Q^d - - permissible load as defined by PN-81/B-03150. The following panels were examined:-

Group I - Five panels of 70 x 600 x 2500 including:-

- 3 Melmo glued panels (nos 1, 2, 3)
- 1 carbamide glued panel (no 16)
- 1 Wikol glued panel (no 11)

Group II - Five panels of 70 x 900 x 2500 including:-

- 3 off Melmo glued panels (nos 5, 6, 7)
- 1 off carbamide glued panel (no 18)
- 1 off Wikol glued panel (no 13)

Group III - Two panels of 42 x 600 x 2500 including:-

- 1 off carbamide glued panel (no 14)
- 1 off Wikol glued panel (no 9)

The first panel was tested in three loading - unloading cycles, the remaining panels in one cycle. The results of the panel deflection measurements in group I are as shown in table 1

Table 1

Load Q	Deflection f (mm)							
	Plate no 1				Plate 2	Plate 3	Plate 11	Plate 16
	Cycle I	Cycle II	Cycle III	Mean value				
0,2 Q^d	4,25	4,30	4,32	4,29	4,26	4,54	3,78	4,29
0,4 Q^d	8,48	8,79	8,85	8,71	8,09	9,06	7,94	8,66
0,6 Q^d	13,18	13,60	13,65	13,48	12,82	13,84	12,85	13,32
0,8 Q^d	18,40	18,64	18,70	18,58	16,81	18,93	17,11	17,74
1,0 Q^d	22,70	22,85	22,92	22,82	21,85	23,79	21,82	22,50
0,8 Q^d	19,02	19,56	19,70	19,43	17,77	19,00	17,61	18,36
0,6 Q^d	14,97	15,54	15,60	15,37	13,32	13,79	13,80	14,13
0,4 Q^d	10,41	10,55	10,60	10,52	9,00	9,59	9,20	9,50
0,2 Q^d	5,91	5,08	5,05	5,01	4,50	4,98	4,55	4,92

and the results of the measurements carried out for group II and III are given in table 2.

Table 2

Load Q	Deflection f (mm)						
	Plate 5	Plate 6	Plate 7	Plate 13	Plate 18	Plate 9	Plate 14
0,2 Q^d	4,46	4,25	4,52	4,28	4,63	6,40	6,830
0,4 Q^d	8,76	8,90	9,12	8,60	9,10	12,67	15,045
0,6 Q^d	13,68	13,71	13,67	13,30	13,59	19,02	22,233
0,8 Q^d	18,95	18,21	18,98	17,14	18,52	25,86	30,303
1,0 Q^d	21,51	18,82	22,01	17,71	21,59	32,61	34,365
0,8 Q^d	19,72	18,91	20,15	18,06	19,90	26,58	30,580
0,6 Q^d	15,02	13,51	15,92	13,63	15,48	22,74	23,500
0,4 Q^d	10,53	9,16	10,87	9,29	11,63	16,30	15,755
0,2 Q^d	6,66	4,39	4,95	4,86	6,71	8,90	7,890

Because the structure of Izopanel type panels differs from the ordinary panels it was decided to determine by experiments the distribution of normal stresses at the breadthtof panels subjected to bending perpendicularly to their surface. The readings were taken by use of tensometric sensors arranged at three panels (one from each group). The diagram of sensor distribution is as shown in Fig 2. and the results of the measurements provide illustration for graphs presented in Fig 3.

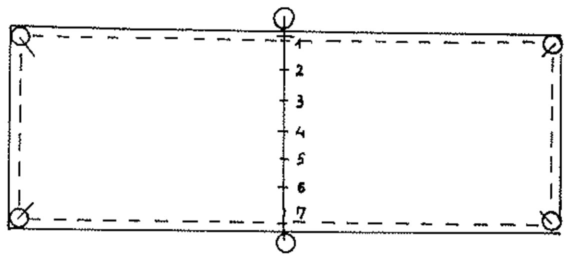

Fig 2. Distribution of tensometric sensors.

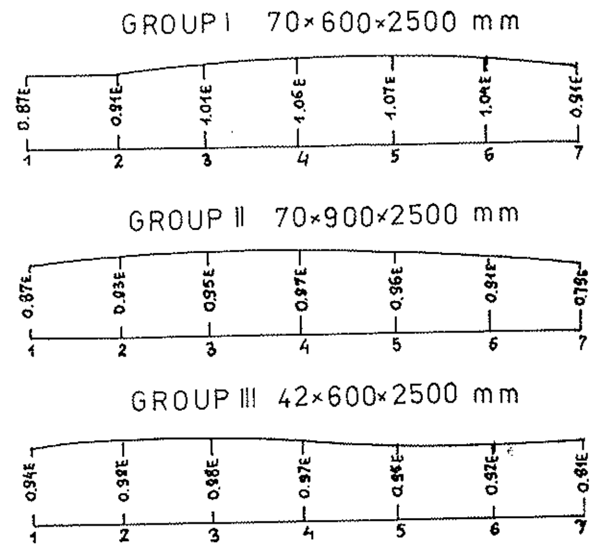

Fig 3. Distribution of normal stresses at the panel breadths.

The graphs show that the distribution of normal stresses at the breadths of th bent Izopanels approximates the even one and does not include any characteristical stress reduction with the growing distance from the wooden longitudinal frames. This means that the longitudinal frames and lining of hard fibreboards clearly operate in conjunction with the wooden perimeter frames while transmitting the loads.

The strength to bending under load in perpendicular direction to the surface was tested for the following panels:-

- no 1 of 70 x 600 x 2500 mm glued with Melmo glue
- no 2 of 70 x 600 x 2500 mm glued with Melmo glue
- no 5 of 70 x 900 x 2500 mm glued with Melmo glue
- no 6 of 70 x 900 x 2500 mm glued with Melmo glue
- no 9 of 42 x 600 x 2500 mm glued with Wikol glue

The testing was carried out in a destructive mode with the destructive forces registered. Knowing these values and the dimensions of cross-section the safety factor has been established "s" as the ratio of thr destructive moment to the permissible moment. The following values of this factor were obtained: s = 3.32 (panel o 1); 2.73 (no 2); 2.94 (no 5); 2.70 (no 6); 2.26 (no 9).

3.2 Testing under Long-Term Load

Three panels were tested 1 off from each group. The panels were tested horizontally with load in the form of focussed forces (distributed at the panel breadth continuously) applied symmetrically 100 cm away from each support (Fig 4).

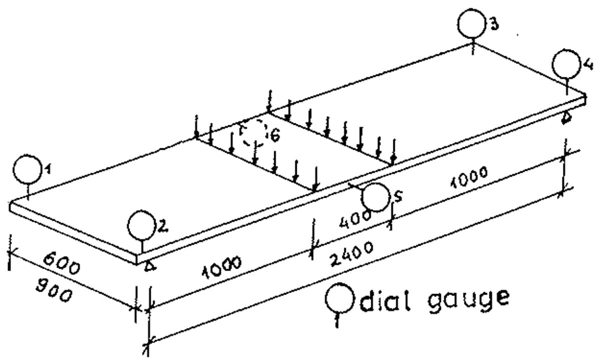

Fig 4. Diagram of panel loading for long-term testing.

The load was acting in the perpendicular plane to panel surface and its size was assumed at the level of 0.7 Q^d where Q^d is the permissible panel load as defined by the Polish standards PN-81/B-03150. The testing consisted in measuring the deflections at the centre of the span right after and during the loading, i e 420 days. The deflections were measured using dial gauges arranged in points 5 and 6 (Fig 4).

In Fig 5 graphs are presented to illustrate the relations between loading duration and deflection size.

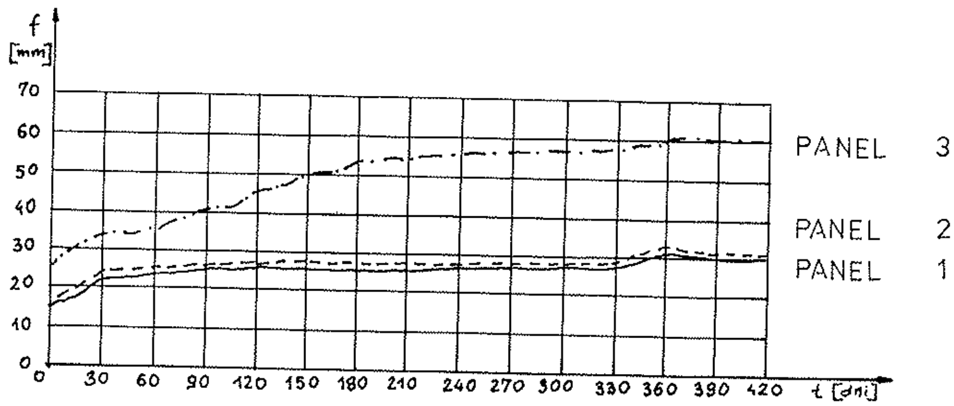

Fig 5. Graphs of the relations of loading duration and panel deflection size.

The results of the measurements in the averaged form of deflection sizes are as shown in table 3.

Table 3

Loading time (days)	Panel average deflection, f (mm)		
	Panel no 1	Panel no 2	Panel no 3
before loading	0,00	0,00	0,00
immediately after loading	15,60	16,11	24,81
1	16,19	16,90	26,21
5	16,79	17,69	27,61
10	17,48	18,67	29,34
15	18,20	19,66	31,06
20	18,25	19,73	31,09
25	21,79	23,39	34,59
30	21,72	23,25	34,49
35	21,62	23,17	34,46
40	21,55	23,11	34,54
45	21,62	23,25	34,77
50	21,98	23,77	35,49
60	22,79	24,22	36,35
75	23,31	24,70	39,11
90	23,68	25,08	41,38
105	24,16	25,41	42,96
120	24,58	25,76	45,02
150	25,53	26,60	49,30
180	26,40	27,35	53,65
210	26,61	27,46	54,41
240	26,89	27,62	55,26
270	27,16	27,73	56,07
300	27,30	27,81	56,80
330	27,50	27,95	57,60
360	31,20	32,54	61,50
390	30,65	31,98	60,95
420	30,59	31,93	60,50

4. Conclusions

On the basis of the testing carried out under short-term loading the following conclusions can be drawn:-

1. Panel bending strength for bending perpendicular to their surface turned out to be sufficient; the safety factor as the ratio of the destructive force to the permissible load as established from the formulas given in Polish standard PN-81/B-03150 has been found within 2.26 and 3.32.

2. The panel stiffness to bending in perpendicular to their surface differed but slightly from the theoretical stiffness determined by the aforesaid Polish standard when the modulus of elasticity of fibreboard of hard type is assumed according to the studies of W Nożyński (5) as being of $E = 4615$ MPa.

3. Normal stresses are distributed at the panel breadth in the way approximating the even mode of distribution thus differently than in ordinary framework panels.

4. The testing under long-term load proves that after over one year of use the panel deformation is not stabilized. Therefore, these panels are not suitable to be used as bent elements and at least in no case can be used for such high level of permanent load which in the given case was 0.7 permissible load.

However, it should be noted that the testing has been carried out at panels previously subjected to short-term loading. Some of these tests were also conducted within the load range beyond the material elastic operation which might result also in the negative changes in panel structure.

References

1. Z.Mielczarek,M.Lange;Testing plates of "Izopanel" types. Proc.of IV Intrn.Symp."Wood in Bulding",Bratislava-Kocovce 1989
2. Z.Mielczarek, M.Lange;Investigation of Stiffness Proprties of Plates of "Izopanel" Type Bending Perpendicularly to Their Plane.Budownictwo Przemysłowe,No 1-2/1989
3. Z.Mielczarek, M.Lange;Stregth of Plates "Izopanel"Types under Eccentrical Compression. XXXV Konf Naukowa KILIWPAN i KNPZiTB, vol 3, Krynica 1983
4. Z.Mielczarek, M.Lange; Investigation of Strength and Stiffness of "Izopanel" Plates. Inżynieria i Budownictwo, No 10/1991
5. W.Nożyński; Results of investigations of beams made of wood-base materials under long term load. Proc. of the Symp. "Investigations of wood and wood-base materials" Szczecin, Poland, June 1978

CIB-W18/25-14-1

INTERNATIONAL COUNCIL FOR BUILDING RESEARCH STUDIES AND DOCUMENTATION

WORKING COMMISSION W18 - TIMBER STRUCTURES

MOMENT ANCHORAGE CAPACITIY OF NAIL PLATES IN SHEAR TESTS

by

A Kevarinmaki
Helsinki University of Technology
J Kangas
Technical Research Centre of Finland (VTT)
Finland

MEETING TWENTY - FIVE

ÅHUS

SWEDEN

AUGUST 1992

1. INTRODUCTION

EUROCODE 5 - draft of 1992 includes a design method for the moment anchorage stress (τ_M) of the nail plate joints. The force, anchorage stress τ_F and the moment, anchorage stress τ_M are checked separately, but also the sum of them is checked. This method is used in Norway and it has been presented by Aasheim and Solli /CIB-W18, paper 23-7-1/. In this method the moment anchorage stress τ_M is calculated according to elastic theory, but the plastification is taken into account with a certain coefficient in the failure criteria. Norèn has presented a different τ_M design method for the nail plate joints /CIB-W18, paper 14-7-1/. In Norèns theory stress τ_M is calculated with the plastic theory and only the combination of τ_F and τ_M is checked at the ultimate limit state. In proposed EC 5 method the direction angle of nail plates or the direction of the grain are not taken into account if τ_M is the critical factor. In the method presented by Norèn these factors have a clear influence in the failure criteria.

Comparison of these calculation methods with the results of standard shear tests is shown in this paper. The shear tests are the only standard tests of the nail plate joints where a clear combination of τ_F and τ_M occurs. The eccentricities are so big that usually τ_M is the critical factor in anchorage capacity when EC 5 method is used. The results from testing of 11 different nail plates are compared with these two theories. Altogether 220 shear tests where final failure mode was anchorage one have been analyzed and presented in this paper.

2. THEORIES

2.1 EUROCODE 5 - draft 1992 (elastic calculation method)

The anchorage stresses τ_F and τ_M are calculated with the elastic theory as the maximum stresses of the effective plate area from,

$$\tau_F = F_A / A_{ef} \tag{2.1}$$

$$\tau_M = M_A \, r_{max} / I_p \tag{2.2}$$

where F_A is the force acting at the centroid of the effective area
M_A is the moment acting at the centroid of the effective area
I_p is the polar moment of inertia of the effective area
r_{max} is the distance from the centre of gravity to the furthest point of the effective area

The moment in the centre of gravity of the effective area is

$$M_A = M + F\,e \tag{2.3}$$

where plate force F (= F_A) and plate moment M and eccentricity e are shown in fig. 2.1.

At ultimate limit state the following conditions are checked:

$$\tau_F \leq f_{a,\alpha\beta,d} \tag{2.4}$$

$$\tau_M \leq 2(1\text{-}c)f_{a,00,d} \tag{2.5}$$

$$\tau_M + \tau_F \leq 1.5\, f_{a,00,d} \tag{2.6}$$

where $f_{a,\alpha\beta,d}$ is the anchorage capacity per unit area for direction α and β
c is a constant given for actual type of nail plate
$f_{a,00,d}$ is the anchorage capacity per unit area for $\alpha = \beta = 0°$
α is the angle between the x-direction of plate and the force
β is the angle between grain and force

Term $(1\text{-}c)f_{a,00,d}$ is the anchorage strength for the weakest direction ($\alpha = \beta = 90°$). The coefficient 2 in equation (2.5) and the coefficient 1.5 in equation (2.6) allows the plastification of anchorage stresses. The force directions are not taken into account in the equations (2.5) and (2.6). If equation (2.5) or (2.6) is the critical factor the capacity of nail plate joint is same for all α and β directions.

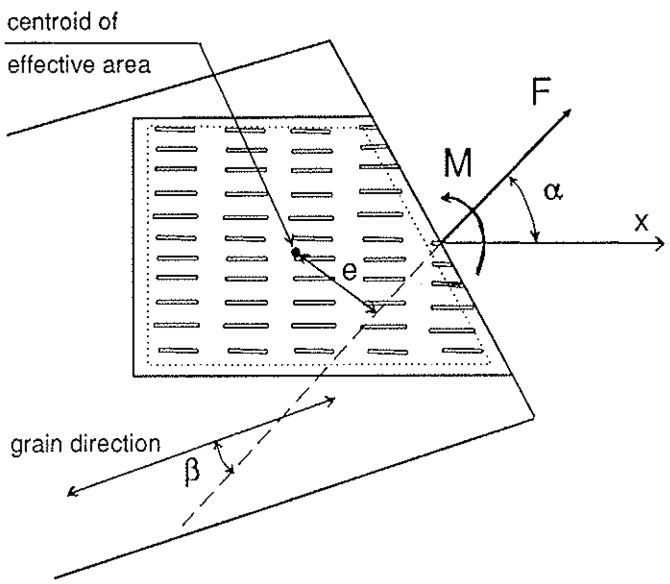

Figure 2.1 Geometry of nail plate connection loaded by a force F and moment M.

2.2 Plastic theory

Norèn has presented an equation of full plasticity for the moment anchorage stress

$$\tau_M = 4\, M_A / (A_{ef}\, d) \tag{2.7}$$

The length d is calculated from

$$A_{ef} d/4 = \int^{A_{ef}} r\, dA \tag{2.8}$$

which can be differential by dividing A_{ef} into a few ΔA concentrated to points. For a trapeziform joint-area (Figure 2.2) $\Delta A = A/2$ can be assumed to be concentrated to the distance d/4 from the centre of gravity, that is $Ad/4 = 2(A/2)d/4$ with d calculated from

$$d = 2\sqrt{z_a^2 + z_b^2} \tag{2.9}$$

$$z_a = \frac{1 + c/a + (c/a)^2}{1 + c/a} \cdot a/3 \tag{2.10}$$

$$z_b = \frac{1 + 2c/a}{1 + c/a} \cdot b/3 \tag{2.11}$$

In case c = 0 (triangle) $d = {}^2/_3 \sqrt{a^2 + b^2}$

In case c = a (rectangle) $d = \sqrt{a^2 + b^2}$ i.e. d is the diagonal.

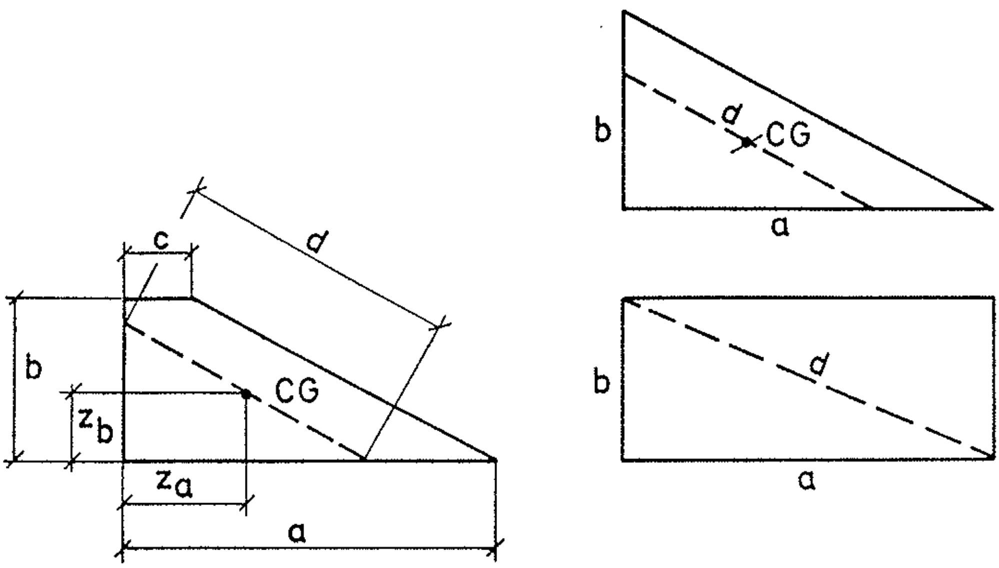

Figure 2.2 Diagonal d in trapezoid, triangle and rectangle.

At ultimate limit state the following condition is checked:

$$(\tau_F / f_{a,\alpha\beta,d})^2 + (\tau_M / f_{a,00,d})^2 \leq 1 \tag{2.12}$$

No other design criteria's are needed in the anchorage design, when τ_F is calculated from (2.1) and τ_M from (2.7). The loading directions α and β are taken into account in each case in the term $f_{a,\alpha\beta,d}$.

3. SHEAR TESTS

The tests reported in this paper have all been carried out at the Technical Research Centre of Finland (VTT). The selection of the material and performance of tests are in agreement with the procedure described in /CIB-W18 1985, paper 18-7-4/. The specimens and the load arrangement used in the shear tests are shown in Figure 3.1. The test specimen in shear are slightly different from what is specified in ISO 8969 but is preferred in Finland because it is simple to manufacture and easy to test. The experience in Finland is that the specimen seems to give reliable test values which are in good agreement with values determined according to the ISO standard.

The standard shear tests are carried out in parallel to the grain ($\beta = 0°$). Shear loading test series where also β-direction is variable will be carried out with two different nail plates during summer 1992 by VTT. The results of the first series of these tests have been already reported in this paper (nailplate C, $\beta = 30°$). The specimen used in the shear tests is shown in Figure 3.1.

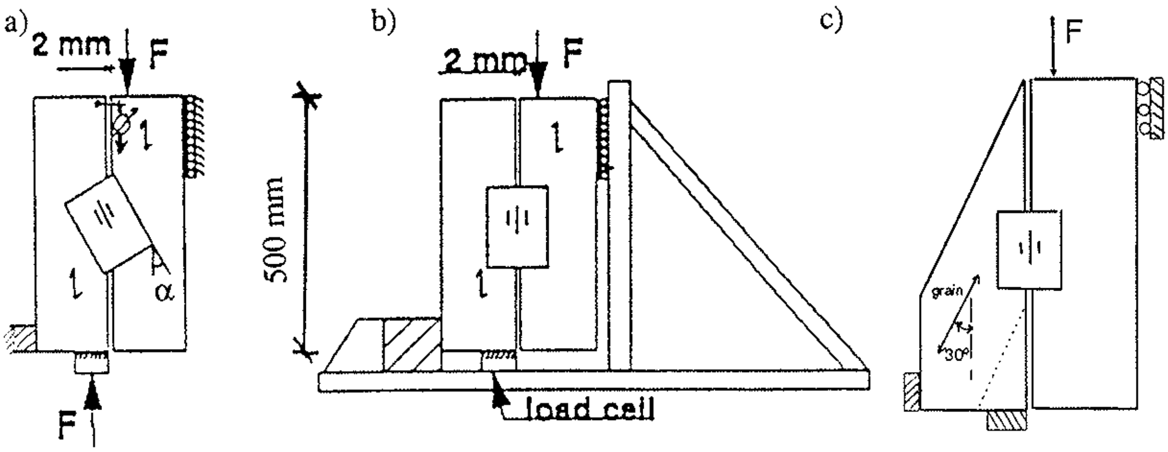

Figure 3.1 a) Test specimen used in shear test
b) Loading arrangement in shear test.
c) Test specimen used in series C $\beta = 30°$.

All results of the anchorage failure in shear tests are presented from testing 11 different nail plates in altogether 220 specimens. The nail plates are called with symbols A - K because the test results are confidential. The type of nailplate is presented in table 3.1. The mean value of anchorage strength ($f_{a,00,m}$) and the constant c which have been determined from the tension tests are shown also in table 3.1. Presented mean values $f_{a,00,m}$ and constants c have been made comparable by reducing the mean values of the tension test series to the compression strength 35 Mpa /CIB-W18, paper 18-7-5/:

$$F_{test,m} = \overline{F}_{test} \sqrt{35 \text{ MPa} / \overline{f}_{c,test}} \tag{3.1}$$

$$\overline{f}_{c,tests} = 0.095 \, \overline{\rho} \, (2 - \overline{w}/0.15) \tag{3.2}$$

where $\overline{\rho}$ is mean value of wood density of the test series
$\overline{w}$ is mean value of moisture content of wood in the test series

Table 3.1 Types and anchorage strengths of the analyzed nail plates.

Type of nailplate	Nailplate	fa00m	c
"Common" homogenous nailplate (orthogonal situation of nail lines)	A B C	3.81 3.04 3.52	0.396 0.39 0.375
"Common" nailplate with threaded nails	D	3.82	0.357
"Common" nonhomogenous nailplate (nonorthogonal situation of nail lines)	E F G	5.1 4.02 3.57	0.498 0.45 0.549
Nailplate with 2 short nails punched from the same hole	H	3.18	0.373
Nailplate with 2 threaded nails punched from the same hole	I	3.34	0.323
Nailplate with 3 threaded nails punched from the same hole	J K	4.14 4.17	0.451 0.511

4. TEST RESULTS AND COMPARISON WITH THEORIES

In the presented shear tests the density of wood was 360..410 kg/m³ and the moisture content of wood was 14.1..17.3 weight-%. All presented test results in tables 3.2 and 3.3 have been made comparable by reducing the mean values of test series to compression strength 35 MPa by equation (3.1). The force, anchorage stresses τ_F have been calculated from equation (2.1), the elastic moment anchorage stresses τ_M (el.) from equation (2.2) and the plastic moment anchorage stresses τ_M (pl.) from equation (2.7) using these reduced comparable test results. The effective plate areas used in analysing are shown in figure 4.1. The moments acting in the centroid of the effective area have been calculated with eccentrics e ($M_A = \frac{1}{2} F_{test} e$).

The load carrying capacities of the shear test specimens have been calculated with the EC 5 method and with the plastic theory. These maximal loads (F_{max}) have been calculated with the mean anchorage strength values. The geometrical values I_p, r_{max} and d have been calculated for the effective area (figure 4.1). The relations of the tests results and calculated capacities (F_{test}/ F_{max}) are shown in tables 4.1 and 4.2. If the agreement between theory and tests is good the relation is close to 1.0.

The test results and the comparisons with the theories are presented separately for the common plate shape (b < a < 2b) and for the narrow and long nail plates (a > 2.5 b). With common plate shape there were contact between the timber members only with some specimens before the maximal force was exceeded (only with α-angels 60° and 75°). With the narrow and long nail plates the eccentricity was so big that rotation of the specimen members became so large that a clear contact between timber members appeared before the maximal force was exceeded.

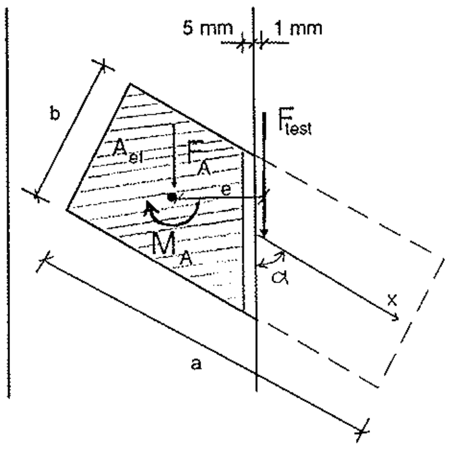

Figure 4.1 The effective plate area and the plate forces in the shear tests.

Table 4.1 The test results of common plate shapes and the comparison with the theories.

Plate	Test spesimens			Test results				According to EC5		Plastic theory	
	alfa	b x a	n	Ftest kN	tF N/mm2	tM (el.)	tM (pl.)	Fmax kN	Ft/Fmax	Fmax kN	Ft/Fmax
A	0	72x158	5	32.86	3.62	2.93	1.95	28.65	1.15	30.42	1.08
	45	119x158	3	42.05	2.51	4.87	3.03	32.56	1.29	39.99	1.05
	60	119x158	3	48.23	2.82	5.47	3.52	33.22	1.45	39.1	1.23
	75	119x158	3	52.2	3.02	5.79	3.79	33.86	1.54	36.47	1.43
	165	119x158	3	46.52	2.77	3.78	2.48	40.6	1.15	46.3	1.01
B	0	104x147	5	35.62	2.69	2.98	2.03	28.62	1.24	32.09	1.11
	45	122x147	3	40.97	2.58	4.93	3.11	24.84	1.65	29.96	1.37
	60	122x147	3	37.9	2.33	4.27	2.82	26.14	1.45	30.31	1.25
	75	122x147	3	40.28	2.45	4.38	2.92	26.85	1.5	29	1.39
	90	122x147	5	35.53	2.16	3.69	2.46	27.67	1.28	27.24	1.3
C	0, b=30	84x164	5	36.43	3.08	2.65	1.77	34.42	1.06	33.13	1.1
	75	124x164	3	44.78	2.38	4.54	2.98	34.15	1.31	37.99	1.18
D	0	100x100	3	22.5	2.5	3.76	2.51	20.61	1.09	23.02	0.98
	45	100x160	3	44.89	2.59	5.01	3.12	33.87	1.33	41.3	1.09
	90	100x100	3	21.32	2.37	3.56	2.38	20.61	1.03	21.09	1.01
	150	121x160	3	41.44	2.42	4.24	2.56	35.69	1.16	43.3	0.96
	165	121x160	3	47.42	2.73	3.71	2.44	42.21	1.23	48.44	0.98
E	45	127x152	3	60.13	3.51	6.64	4.19	45.32	1.33	53.37	1.13
	60	127x152	3	68.59	3.91	7.1	4.69	47.69	1.44	52.4	1.31
F	45	127x152	3	43.78	2.55	4.84	3.05	35.69	1.23	41.33	1.06
	60	127x152	3	52.13	2.97	5.39	3.57	37.55	1.39	39.51	1.32
	75	127x152	3	47.46	2.68	4.74	3.16	38.56	1.23	36.87	1.29
G *)	45	120x150	3	36.56	2.29	4.39	2.76	26.79	1.36	34.57	1.06
	60	120x150	3	43.78	2.68	5.02	3.28	28.06	1.56	33.36	1.31
	75	120x150	3	38.69	2.34	4.3	2.85	28.93	1.34	30.66	1.26
H	0	72x152	5	29.98	3.08	2.62	1.59	25.07	1.2	27.48	1.09
	45	127x152	3	39.55	2.31	4.37	2.76	28.24	1.4	33.92	1.17
	60	127x152	3	37.11	2.12	3.84	2.54	29.71	1.25	33.74	1.1
	150	127x152	3	34.65	2.01	3.46	2.17	30.19	1.15	36.65	0.95
I	0	90x153	5	39.66	3.32	3.22	2.15	30.41	1.3	33.54	1.18
	45	117x153	3	50.18	3.15	6.1	3.81	27.19	1.85	35.61	1.41
	60	117x153	3	48.9	3	5.8	3.75	27.87	1.75	35.18	1.39
	75	117x153	3	46.66	2.84	5.39	3.54	28.44	1.64	34.01	1.37
	150	117x153	3	48.31	3.06	5.4	3.26	28.63	1.69	38.84	1.24
	165	117x153	3	46.16	2.88	3.97	2.61	33.78	1.37	41.6	1.11
J	0	96x150	5	47.35	3.76	3.91	2.61	38.36	1.23	42.87	1.1
	45	120x150	3	50.38	3.16	6.05	3.8	33.98	1.48	40.06	1.26
	60	120x150	3	51.09	3.13	5.86	3.83	35.31	1.45	38.86	1.31
	75	120x150	3	43.85	2.66	4.88	3.23	36.15	1.21	37.33	1.17
	150	120x150	3	48.56	3.05	5.31	3.27	36.06	1.35	44.21	1.1
	165	120x150	3	47.59	2.95	4.15	2.74	41.6	1.14	48.49	0.98
K	0	96x150	5	40.11	3.26	3.45	2.31	37.32	1.07	41.86	0.96
	0	96x100	3	26.31	3.06	4.47	2.98	21.86	1.2	25.69	1.02
	60	120x150	3	38.48	2.36	4.57	2.89	34.57	1.11	39.85	0.97
	90	96x100	3	23.42	2.71	4.22	2.81	21.14	1.08	21.42	1.09
								mean value	1.33	mean value	1.16

Table 4.2 The test results of the long and narrow nail plates and the comparison with the theories.

Plate	Test spesimens			Test results				According to EC5		Plastic theory	
	alfa	b x a	n	Ftest kN	tF N/mm2	tM (el.)	tM (pl.)	Fmax kN	Ft/Fmax	Fmax kN	Ft/Fmax
A	30	72x225	3	50.24	3.47	7.18	3.76	26.95	1.86	35.61	1.41
	45	72x225	3	51.31	3.43	9.09	4.83	23.43	2.19	32.56	1.58
	60	72x225	3	50.98	3.35	9.87	5.55	22.03	2.31	29.12	1.75
B	30	73x196	3	35.69	2.84	5.75	3.09	18.92	1.89	25.31	1.41
	45	73x196	3	43.84	3.35	8.61	4.65	16.69	2.63	22.68	1.93
	60	73x196	3	37.92	2.85	8.1	4.59	15.77	2.4	20.77	1.83
D	30	72x200	3	52.53	4.15	8.44	4.5	23.94	2.19	32.21	1.63
	45	72x200	3	41.89	3.18	8.24	4.43	21.05	1.99	28.78	1.46
	60	72x200	3	40.03	2.99	8.57	4.85	19.87	2.01	26.29	1.52
E	30	77x191	3	60.73	4.72	9.38	5.1	32.96	1.84	44.56	1.36
	45	77x191	3	58.31	4.35	10.86	5.94	27.51	2.12	38.69	1.51
	60	77x191	3	57.54	4.22	11.64	6.64	*) 25.32	2.27	34.37	1.67
F	45	77x191	3	44.12	3.29	8.22	4.5	23.1	1.91	30.03	1.47
	60	77x191	3	43.44	3.18	8.79	5.02	*) 21.83	1.99	26.67	1.63
G	30	70x190	3	32.83	2.83	5.76	3.09	*) 18.33	1.79	27.67	1.19
	45	70x190	3	30.79	2.54	6.58	3.55	*) 15.06	2.04	24.1	1.28
	60	70x190	3	28.34	2.3	6.58	3.73	*) 13.86	2.04	21.51	1.32
H	30	76x203	3	42.89	3.15	6.33	3.4	21.57	1.99	29.14	1.47
	45	76x203	3	33.61	2.38	6.06	3.28	18.99	1.77	25.72	1.31
I	30	63x204	3	48.71	4.29	9.13	4.76	18.19	2.68	26.4	1.85
	60	63x204	3	43.52	3.63	10.91	6.14	15.01	2.88	20.84	2.09
J	30	60x200	3	50.25	4.76	10.24	5.32	20.8	2.42	28.71	1.75
	60	60x200	3	37.45	3.35	10.17	5.72	*) 16.73	2.24	21.95	1.71
								mean value	2.15	mean value	1.57

In analysis of the shear tests compared with theories the mean values of anchorage strengths $f_{a,\alpha 0,m}$ were used. The mean values have been determined from the tension test results as Kangas has presented /CIB W18A 1992, Kangas & .../. In analysis of the shear tests with the EC 5 method the stress τ_M was a critical factor in each case. In most cases equation (2.3) was the critical design term (τ_M + τ_F). The moment anchorage stress τ_M alone was critical in some cases (equation (2.1)) and these cases have been shown in tables with symbol *).

With common plate shape the deformation at maximum test load was rather high with some specimens. The maximum forces up to slip limit of 7.5 mm and the comparisons of these forces with the theories have been shown in table 4.3. The test results of the long and narrow nail plates without contact between timber members have been shown in table 4.4. These forces have been extrapolated up to slip limit of 7.5 mm obtained from the initial curvature of load-slip curvature i.e. assuming no contact between the timber members.

Table 4.3 The test results of common plate shapes with maximal test loads of slip ≤ 7.5 mm and the comparison with the theories.

Plate	Test spesimens			Test results				According to EC5		Plastic theory		
	alfa	b x a	n	Ftest kN	tF N/mm2	tM (el.)	tM (pl.)	Fmax kN	Ft/Fmax	Fmax kN	Ft/Fmax.	
A	0	72x158	5	32.23	3.55	2.87	1.91	28.65	1.13	30.42	1.06	x)
	45	119x158	3	42.05	2.51	4.87	3.03	32.56	1.29	39.99	1.05	
	60	119x158	3	43.7	2.55	4.96	3.19	33.22	1.31	39.1	1.11	x)
	75	119x158	3	36.01	2.08	3.99	2.62	33.86	1.06	36.47	0.99	x)
	165	119x158	3	46.52	2.77	3.78	2.48	40.6	1.15	46.3	1.01	
B	0	104x147	5	33.7	2.54	2.82	1.92	28.62	1.17	32.09	1.05	x)
	45	122x147	3	40.97	2.58	4.93	3.11	24.84	1.65	29.96	1.37	
	60	122x147	3	37.6	2.31	4.24	2.8	26.14	1.44	30.31	1.24	x)
	75	122x147	3	29.8	1.81	3.24	2.16	26.85	1.11	29	1.03	x)
	90	122x147	5	27.3	1.66	2.83	1.89	27.67	0.98	27.24	1	x)
C	0, b=30	84x164	5	36.43	3.08	2.65	1.77	34.42	1.06	33.13	1.1	
	75	124x164	3	40.44	2.15	4.1	2.69	34.15	1.18	37.99	1.07	x)
D	0	100x100	3	22.5	2.5	3.76	2.51	20.61	1.09	23.02	0.98	
	45	100x160	3	44.89	2.59	5.01	3.12	33.87	1.33	41.3	1.09	
	90	100x100	3	21.32	2.37	3.56	2.38	20.61	1.03	21.09	1.01	
	150	121x160	3	41.44	2.42	4.24	2.56	35.69	1.16	43.3	0.96	
	165	121x160	3	47.42	2.73	3.71	2.44	42.21	1.23	48.44	0.98	
E	45	127x152	3	55.56	3.24	6.14	3.87	45.32	1.23	53.37	1.04	x)
	60	127x152	3	53.7	3.06	5.56	3.67	47.69	1.13	52.4	1.03	x)
F	45	127x152	3	43.78	2.55	4.84	3.05	35.69	1.23	41.33	1.06	
	60	127x152	3	47.4	2.7	4.9	3.25	37.55	1.26	39.51	1.2	x)
	75	127x152	3	37.83	2.14	3.78	2.52	38.56	0.98	36.87	1.03	x)
G	45	120x150	3	36.56	2.29	4.39	2.76	26.79	1.36	34.57	1.06	
	60	120x150	3	40.19	2.46	4.61	3.01	28.06	1.43	33.36	1.2	x)
	75	120x150	3	31.68	1.92	3.52	2.33	28.93	1.1	30.66	1.03	x)
H	0	72x152	5	29.98	3.08	2.62	1.59	25.07	1.2	27.48	1.09	
	45	127x152	3	39.55	2.31	4.37	2.76	28.24	1.4	33.92	1.17	
	60	127x152	3	37.11	2.12	3.84	2.54	29.71	1.25	33.74	1.1	
	150	127x152	3	34.65	2.01	3.46	2.17	30.19	1.15	36.65	0.95	
I	0	90x153	5	39.66	3.32	3.22	2.15	30.41	1.3	33.54	1.18	
	45	117x153	3	50.18	3.15	6.1	3.81	27.19	1.85	35.61	1.41	
	60	117x153	3	46.06	2.83	5.46	3.53	27.87	1.65	35.18	1.31	x)
	75	117x153	3	37.51	2.28	4.33	2.84	28.44	1.32	34.01	1.1	x)
	150	117x153	3	48.31	3.06	5.4	3.26	28.63	1.69	38.84	1.24	
	165	117x153	3	46.16	2.88	3.97	2.61	33.78	1.37	41.6	1.11	
J	0	96x150	5	47.35	3.76	3.91	2.61	38.36	1.23	42.87	1.1	
	45	120x150	3	50.38	3.16	6.05	3.8	33.98	1.48	40.06	1.26	
	60	120x150	3	50.89	3.12	5.84	3.81	35.31	1.44	38.86	1.3	x)
	75	120x150	3	39.9	2.42	4.44	2.94	36.15	1.1	37.33	1.06	x)
	150	120x150	3	48.56	3.05	5.31	3.27	36.06	1.35	44.21	1.1	
	165	120x150	3	47.59	2.95	4.15	2.74	41.6	1.14	48.49	0.98	
K	0	96x150	5	40.11	3.26	3.45	2.31	37.32	1.07	41.86	0.96	
	0	96x100	3	26.31	3.06	4.47	2.98	21.86	1.2	25.69	1.02	
	60	120x150	3	38.48	2.36	4.57	2.89	34.57	1.11	39.85	0.97	
	90	96x100	3	23.42	2.71	4.22	2.81	21.14	1.08	21.42	1.09	
								Mean value	1.26	Mean value	1.09	
								COV	15 %	COV	10 %	

x) slip over 7.5 mm, Ftest = F(7.5 mm)

Table 4.4 The test results of the long and narrow nail plates without timber contact (slip $\leq$ 7.5 mm) and the comparison with the theories.

Plate	Test spesimens			Test results				According to EC5		Plastic theory		
	alfa	b x a	n	Ftest kN	tF N/mm2	tM (el.)	tM (pl.)	Fmax kN	Ft/Fmax	Fmax kN	Ft/Fmax	
A	30	72x225	3	50.24	3.47	7.18	3.76	26.95	1.86	35.61	1.41	
	45	72x225	3	36.63	2.45	6.49	3.45	23.43	1.56	32.56	1.13	x)
	60	72x225	3	28.45	1.87	5.51	3.1	22.03	1.29	29.12	0.98	x)
B	30	73x196	3	35.69	2.84	5.75	3.09	18.92	1.89	25.31	1.41	
	45	73x196	3	34.9	2.67	6.85	3.7	16.69	2.09	22.68	1.54	x)
	60	73x196	3	24.25	1.82	5.18	2.94	15.77	1.54	20.77	1.17	x)
D	30	72x200	3	47.54	3.76	7.64	4.07	23.94	1.99	32.21	1.48	xx)
	45	72x200	3	34.18	2.59	6.72	3.61	21.05	1.62	28.78	1.19	x)
	60	72x200	3	26.74	2.01	5.72	3.01	19.87	1.35	26.29	1.02	x)
E	30	77x191	3	53.32	4.14	8.24	4.48	32.96	1.62	44.56	1.2	x)
	45	77x191	3	42.04	3.14	7.83	4.28	27.51	1.53	38.69	1.09	x)
	60	77x191	3	34.64	2.54	7.01	3.99	*) 25.32	1.37	34.37	1.01	x)
F	45	77x191	3	37.33	2.78	6.95	3.81	23.1	1.62	30.03	1.24	x)
	60	77x191	3	29.28	2.14	5.92	3.38	*) 21.83	1.34	26.67	1.1	x)
G	30	70x190	3	32.83	2.83	5.76	3.09	*) 18.33	1.79	27.67	1.19	
	45	70x190	3	27.99	2.31	5.98	3.23	*) 15.06	1.85	24.1	1.16	x)
	60	70x190	3	21.6	1.75	5.01	2.84	*) 13.86	1.55	21.51	1.01	x)
H	30	76x203	3	42.89	3.15	6.33	3.4	21.57	1.99	29.14	1.47	
	45	76x203	3	28.67	2.03	5.17	2.8	18.99	1.51	25.72	1.12	x)
I	30	63x204	3	39.26	3.46	7.36	3.84	18.19	2.16	26.4	1.49	xx)
	60	63x204	3	26.24	2.19	6.58	3.7	15.01	1.74	20.84	1.26	x)
J	30	60x200	3	41.96	3.97	8.55	4.44	20.8	2.02	28.71	1.46	x)
	60	60x200	3	23.4	2.09	6.36	3.58	*) 16.73	1.4	21.95	1.07	x)
								mean value	1.68	mean value	1.23	
								COV	15 %	COV	14 %	

x) Timber contact, Ftest = Fex(7.5 mm) assuming no contact
xx) No contact and slip over 7.5 mm, Ftest = F(7.5 mm)

5. ANALYSIS OF THE COMPARISON RESULTS

The analyzing of all 220 anchorage broken shear test specimens with 11 different nail plates shows well the differences and the levels of the comparison with different theories and test results. We must remember however that the loading direction was in these tests parallel to the grain ($\beta = 0°$). The methods of EC 5 does not take into account the angle β at all if τ_M is the critical factor. According to the presented plastic theory both loading directions (α and β) are taken into account in each case in the anchorage capacity. If angle β is bigger than 0° this should be observed as lower capacity in the joint where a combination of stresses τ_F and τ_M occur simultaneously (according to the tension tests capacity of τ_F is strongly dependent on the loading direction of the grain direction).

The test results with the narrow and long nail plates are clearly much higher than the results of the different theories. The appeared contact and friction between timber members causes a part of this difference. But also in the tests where no contact appeared (common plate shape) both analyzed methods were generally conservative.

The τ_M design method given in EUROCODE 5 - draft 1992 seems to be generally very conservative with both equations (2.2) and (2.3). The mean value of relation F_{test}/F_{max} was 1.33 (coefficient of variation 15 %) for the common plate shape and 2.15 (cov 14 %) for the long and narrow nail plates. Without timber contatact this ralation was 1.68 (cov 15 %) for the long and narrow nail plates. The closest values to the tests results are obtained when the effective area is rectangle (angels $\alpha = 0°$ and $\alpha = 90°$). The test series where loading was not parallel to the grain ($\beta = 30°$) shows that this method may be also at the unsafe side because the loading directions are not taken into account in the τ_M failure criteria's.

Also in using the plastic theory the variation of the relation between the test results and the calculated capacities were rather high with different nail plates, but it was clearly lower than in the method of EC 5. The mean value of the relation F_{test}/F_{max} was 1.16 (coefficient of variation 12 %) for the common plate shape and 1.57 (cov 14 %) for the long and narrow nail plates. Without timber contact this ralation was 1.23 (cov 14 %) for the long and narrow nail plates. In some individual results the maximal test loads were lower than the theoretical capacities, but the differences in these cases were only some percents (lowest value 0.95). These results are acceptable because they are within the normal variation and the expected mean value is exactly the test results, if the theory describes accurately the mechanical behaviour of the joint.

The compared theories give almost the same results when loading direction $\alpha = 90°$, because the coefficients of the design criteria of EC 5 (equations (2.2) and (2.3)) have been fixed for the this case. But the method of EC 5 gives the same result also for smaller α-angles where the capacities are clearly higher according to the test results. This α-angle is taken into account in the design criteria of the plastic theoretical method.

The design and calculations are clearly easier and simpler with the presented plastic theory than with the method of the proposal EUROCODE 5. The diagonal d is easy to determinate from equation (2.9) for the plastic design. Much more work is required, however in the determination of geometrical values for the elastic method (I_p and r_{max}).

6. PROPOSALS FOR DESIGN RULES OF EUROCODE 5

A following proposal for the design rules of the nail plate anchorage capacity for Eurocode 5 is given based on the investigation reported in this paper.

The anchorage stresses τ_F and τ_M are calculated from

$$\tau_F = F_A / A_{ef} \tag{6.1}$$

$$\tau_M = 4\, M_A / (A_{ef}\, d) \tag{6.2}$$

where the length d is a "diagonal" of the effective plate area. For quadrilateral and triangle joint-area it may be calculated from

$$d = 2\sqrt{z_a^2 + z_b^2} \tag{6.3}$$

$$z_a = \frac{1 + c/a + (c/a)^2}{1 + c/a} \cdot a/3 \tag{6.4}$$

$$z_b = \frac{1 + 2c/a}{1 + c/a} \cdot b/3 \tag{6.5}$$

where the lengths a, b and c are shown in figure 6.1.

The following condition shall be satisfied

$$(\tau_F / f_{a,\alpha\beta,d})^2 + (\tau_M / f_{a,00,d})^2 \leq 1 \tag{6.6}$$

The method for the determination of anchorage strength $f_{a,\alpha\beta,d}$ in equation (6.6) has been presented by Kangas /CIB W18A 1992, Kangas & .../ and is included in this proposal.

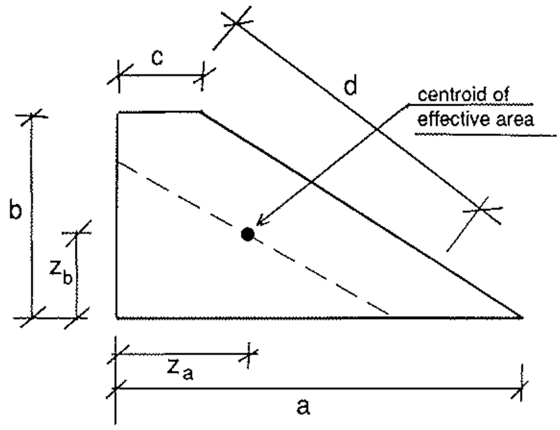

Figure 6.1 Diagonal d in quadrilateral. For rectangle c = a and for triangle c = 0.

7. CONCLUSIONS

The proposed plastic theoretical calculation method of anchorage strength of nail plates has a better correlation to the test results than the elastic calculation method with the design criteria's given in EUROCODE 5 - draft 1992. The plastic theory for design of the anchorage capacity is proposed for EC 5 method, because:

- The design criteria's τ_M and $\tau_F + \tau_M$ of Eurocode 5 (draft 1992) are in many cases very conservative, especially when $\beta = 0°$ and α-angle is small. The proposed plastic theoretical method gives results which correspond much better with the test results on an acceptable safety level.

- The loading direction of the nail plate or of the grain direction are not taken into account in EC 5 method (draft 1992) when combination τ_F and τ_M or purely τ_M are the critical factors. In the proposed plastic design method these directions are always taken into account.

- There are three design criteria's that must be checked in the anchorage design of EC 5 draft. In proposed plastic design method only one design criteria is needed.

- The design and calculations are clearly easier and simpler with the proposed simplified plastic theory than with the method of EC 5 draft. The geometrical values of the elastic method (I_p and r_{max}) are more difficult to determine than the diagonal d for the plastic design.

8. REFERENCES

CIB W18, 1981. Paper 14-7-1: Norèn, B., Design of Joints with Nail Plates.

CIB W18, 1985. Paper 18-7-4: Kangas, J., A Detailed Testing Method for Nail Plate Joints.

CIB W18, 1985. Paper 18-7-5: Kangas, J., Principles for Design Values of Nailplates in Finland.

CIB W18, 1990. Paper 23-7-1: Aasheim, E. & Solli, K. H., Proposals for Design Code for Nail Plates.

CIB W18, 1992. Paper 25-14-2: Kangas, J. & Kevarinmäki, A., Design Values of Anchorage strength of Nail Plate Joints by 2-curve Method and Interpolation.

EUROCODE No. 5, Annex X - working draft January 1992: The Design of Trussed Rafters.

CIB-W18/25-14-2

INTERNATIONAL COUNCIL FOR BUILDING RESEARCH STUDIES AND DOCUMENTATION

WORKING COMMISSION W18 - TIMBER STRUCTURES

DESIGN VALUES OF ANCHORAGE STRENGTH OF NAIL PLATE JOINTS BY 2-CURVE METHOD AND INTERPOLATION

by

J Kangas
Technical Research Centre of Finland (VTT)
A Kevarinmaki
Helsinki University of Technology
Finland

MEETING TWENTY - FIVE

ÅHUS

SWEDEN

AUGUST 1992

SUMMARY

In this paper a method is presented which makes possible a more effective utilization of the anchorage capacity of nail plates than in EUROCODE 5 draft 1991. The curve for design values in EUROCODE 5 is taken as a minimum one, the curve drawn through the standard test results when loaded in grain direction is taken as a maximum one and a method of interpolation between them is proposed. Test results to support the proposal are presented.

1 INTRODUCTION

In CIB-W18A meeting in Lisbon a proposal was introduced for design code for nail plate joints, which was taken into EUROCODE 5, [1] and [2]. In Finland we have another practice, which was introduced in CIB-W18A meeting in Beit Oren [3] and discussed more in Oxford [4].

This paper is an continuation to the paper CIB-W18A/24-7-3 presented in the Oxford meeting. It is based on the results of standard test series used for the approvals and on some new special test series with the combination of the direction angles α, β and γ.

2 SYMBOLS

f_a is the anchorage strength (F_{max}/A_{eff}) in N/mm^2
$f_{a\alpha\beta}$ is the anchorage strength in different angles α and β
f_c is the calculated compressive strength of timber
α is the angle between the force and the main direction of the nail plate
β is the angle between the force and the grain direction
γ is the angle between the main direction of the nail plate and the grain direction

3 STANDARD TESTS FOR ANCHORAGE STRENGTH

3.1 Test series

The anchorage strength $\mathbf{f_{a\alpha}}$ has been tested in accordance with the testing standards of nail plate joints at the angles of $\alpha = 0°$, $30°$, $60°$ and $90°$, when the load is in the grain direction ($\beta = 0°$). Test specimens are shown in **figure 1.**

Tests for anchorage strength $\mathbf{f_{a\alpha\beta}}$ (T-joint, **figure 2**) have been made at the angles

a) $\alpha = 0°$; $\beta = 45°$ and $90°$

b) $\alpha = \beta = 90°$

3.2 Test results

Anchorage strength has been calculated dividing maximum load F_{max} by effective area A_{eff}, which in the Finnish practice is the area of timber member covered by nail plate reduced by 10 mm from the end of the member in grain direction and by 5 mm from its edges as shown in **figure 2** and **figure 3.**

The test results of two nail plates are given in **figure 4** as an example of about 20 different nail plates tested in VTT, Technical Research Centre of Finland. Two curves have been drawn trough them. The upper one belongs to the cases, where $\beta = 0°$. Its equation has the formula

$$f_{a\alpha 0} = \begin{cases} f_{a00} + k_1 * \alpha & \text{, when } \alpha \le \alpha_0 \\ f_{a00} + k_1 * \alpha_0 + k_2 * (\alpha - \alpha_0) & \text{, when } \alpha_0 < \alpha \le 90° \end{cases} \qquad (1)$$

where

k_1 is the slope of first line ($\Delta f_a / \Delta \alpha$)

k_2 is the slope of second line

α_0 is the intersectional point of the curve in two parts

The lower curve is going through the lowest values as in the proposal for Eurocode 5. Its equation has the formula

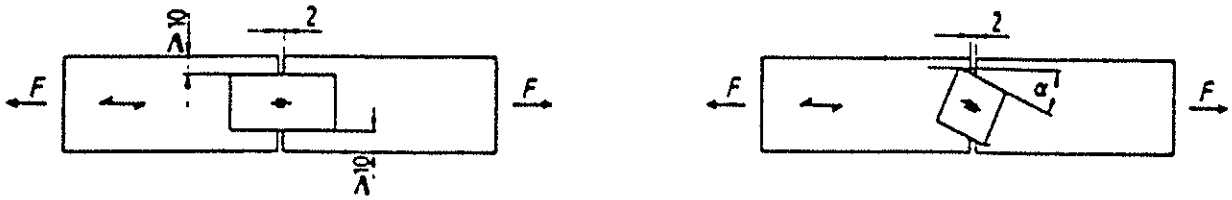

Figure 1. Standard test specimens loaded in grain direction.
a) $\alpha = 0°$ and $90°$ b) $0° < \alpha < 90°$; $\beta = 0°$

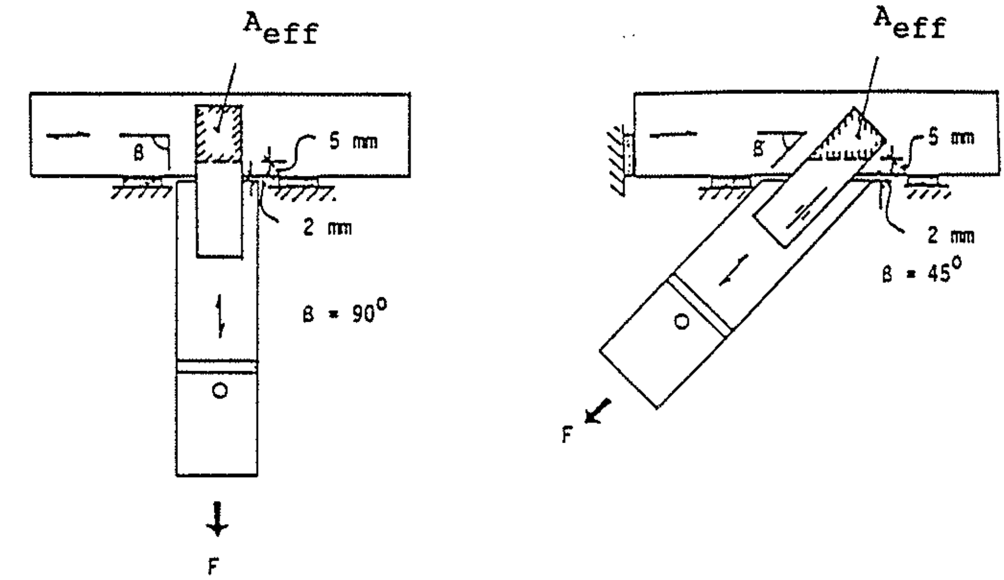

Figure 2. Standard test specimens when load is across the grain, loading arrangements and effective anchorage area.

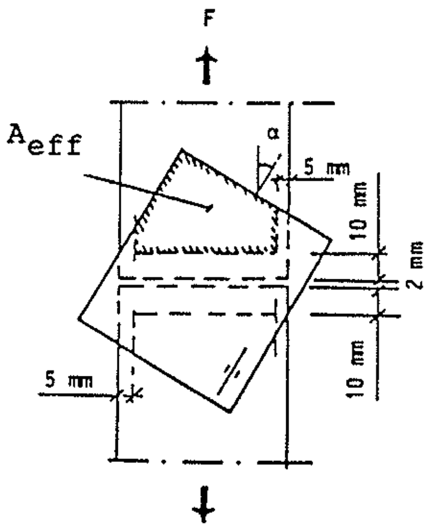

Figure 3. Effective anchorage area in joints loaded in tension

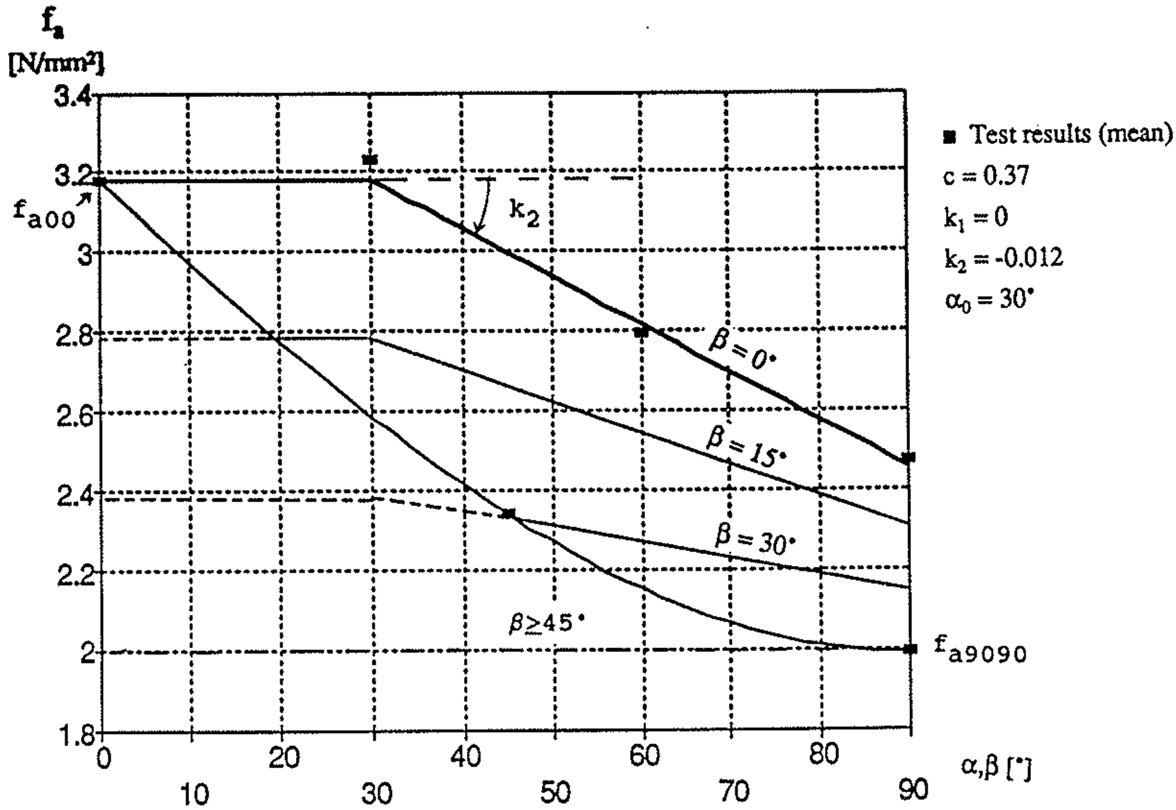

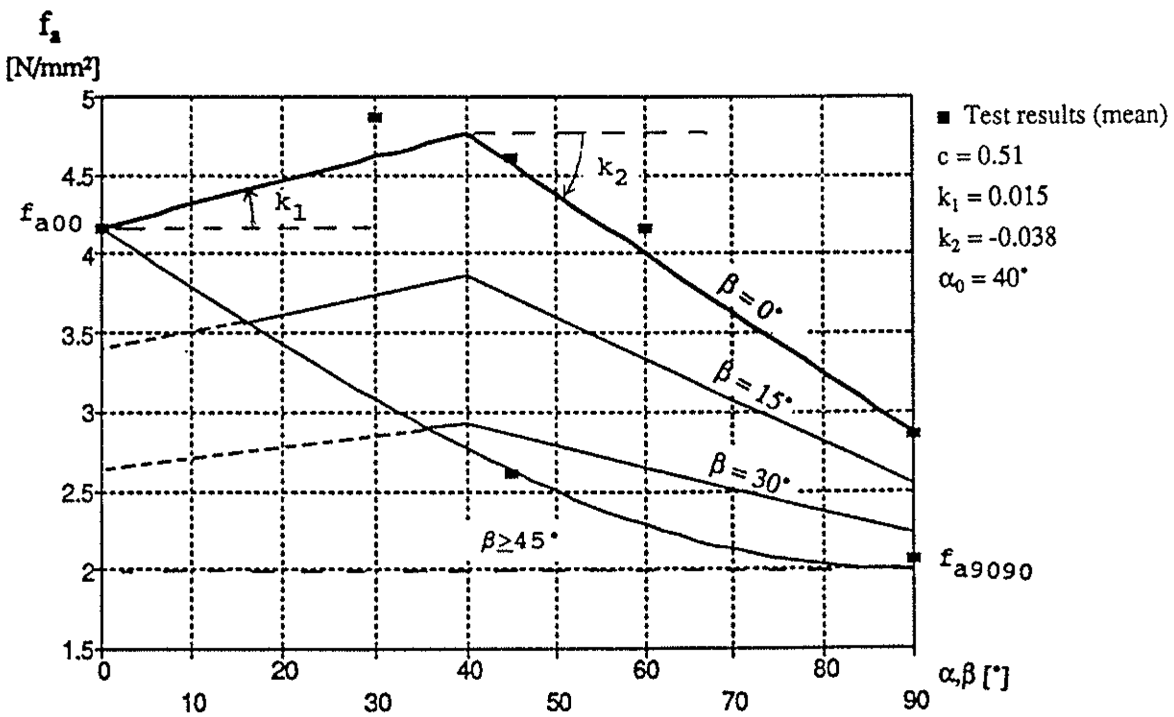

Figure 4. Through the standard test results of two nail plates drawn graphic representation of equations (1) and (2) and proposed interpolation between them.

$$f_a = (1 - c*\sin\phi)*f_{a0} \quad (2)$$

where

c is in most cases $c = (f_{a00} - f_{a9090})/f_{a00}$

ϕ is the maximum of the angles α, β and γ

In Finland the design values are given by the equation of the type (1) also for the minimum curve, when $\beta \geq 45°$ and when $0 < \beta < 45°$ the values are interpolated linearly between those two curves.

4 TEST SERIES WITH DIFFERENT COMBINATIONS OF DIRECTION ANGLES

Test specimens and loading arrangements are shown in the **figure 5**. The timber material in the anchorage area was chosen so that different test series correspond to each other. Its properties in each test series are given in the **table 1**.

Table 1. Properties of timber members used in test series with different combinations of direction angles. $\mathbf{f_c}$ is the calculated strength in compression from the equation

$f_c = 0{,}095 * DENS_{0w} * (2 - w/15)$ in N/mm^2

Timber symbol	density [kg/m3]	moisture [%]	fc [MPa]	fc/35
1	345	16.2	30.2	0.861
2	350	16.5	29.9	0.855
3	364	16.3	31.6	0.902
4	335	16.4	28.9	0.824
5	337	16.6	28.6	0.817
6	365	16.3	31.7	0.905
a)-e)	385	14.6	35.6	1.017
f)-j)	373	14.6	34.5	0.986
k)-o)	378	14.8	35.4	1.011
p)-t)	395	14.6	36.5	1.043

Test results are given in the **table 2**. They are also situated in **figure 6** onto the patterns of maximum and minimum curves of anchorage strength with lines of interpolation.

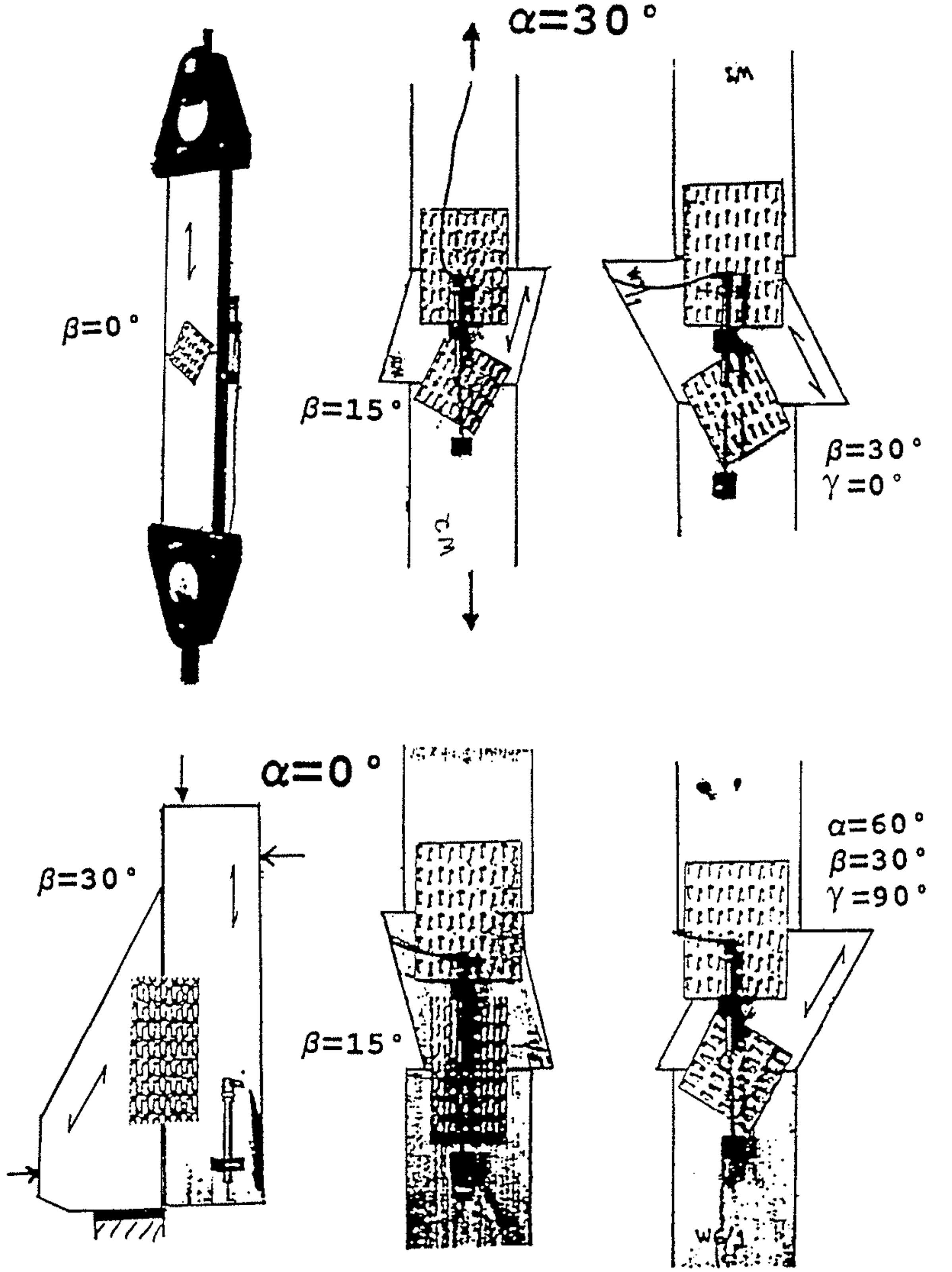

Figure 5. Test specimens of some test series with different combinations of direction angles (see table 2)

a) Test series W1 b) Test series W2 c) Test series W3

d) Test series T6 e) Test series T2 f) Test series W6

Table 2. Test results of test series with different combinations of direction angles (5-6 test specimens in each) and estimated values based on the proposed method of interpolation and method of Eurocode 5. Test results $\mathbf{f_{a,corr}}$ are corrected to f_c = 35 N/mm^2 in square root like those of standard tests.

specimens	α	β	γ	A_{ef} [mm^2]	Test results F_{max} [kN]	 $f_{a,corr.}$	Estimation Proposal f_a	 EC 5 f_a
W1,4 a)-j)	30	0	30	3580	31.06	4.34	4.60	3.10
W2 a)-e)	30	15	15	3618	28.19	3.87	3.75	3.10
W3 a)-e)	30	30	0	3729	20.25	2.70	3.10	3.10
W5 f)-j)	30	90	60	4134	16.54	2.01	2.00	2.00
W6 f)-j)	60	30	90	3729	19.08	2.58	2.65	2.00
W0A 1-6	0	0	0	3840	29.53	4.14	4.16	4.16
W5A 1-6	0	23	23	3840	27.96	3.92	3.35	3.35
W6B 1-6	45	23	67	3520	24.22	3.71	3.30	2.20
W7B 1-6	45	23	23	3520	22.53	3.45	3.30	2.67
F0A 1-6	0	0	0	4000	23	3.10	3.81	3.81
F5A 1-6	0	23	23	4000	21.8	2.94	3.30	3.30
F6B 1-6	45	23	67	3690	21.86	3.19	3.00	2.58
F7B 1-6	45	23	23	3690	21.77	3.18	3.00	2.85
T1,4 k)-t)	0	0	0	5964	45.79	3.79	3.52	3.52
T2 k)-o)	0	15	15	5993	39.95	3.33	3.19	3.19
T5 p)-t)	0	90	90	6384	27.65	2.13	2.20	2.20
T6 p)-t) *)	0	30	30	5904	37.21	3.14	2.87	2.87

*) shear tests

5 CONCLUSIONS

Test results of test series F6B and F7B; W3 and W6; W6B and W7B indicate, that angle γ has not an effect on the anchorage strength as expected in EUROCODE 5. Hence only angles α and β are needed when basic anchorage design values are calculated.

Test results in different combinations of direction angles indicate that also $\mathbf{f_{a\alpha\beta}}$ values can be given reliably based on standard test series. Simplest method is to interpolate between the maximum curve, when β = 0° and the lowest test value $\mathbf{f_{a9090}}$.

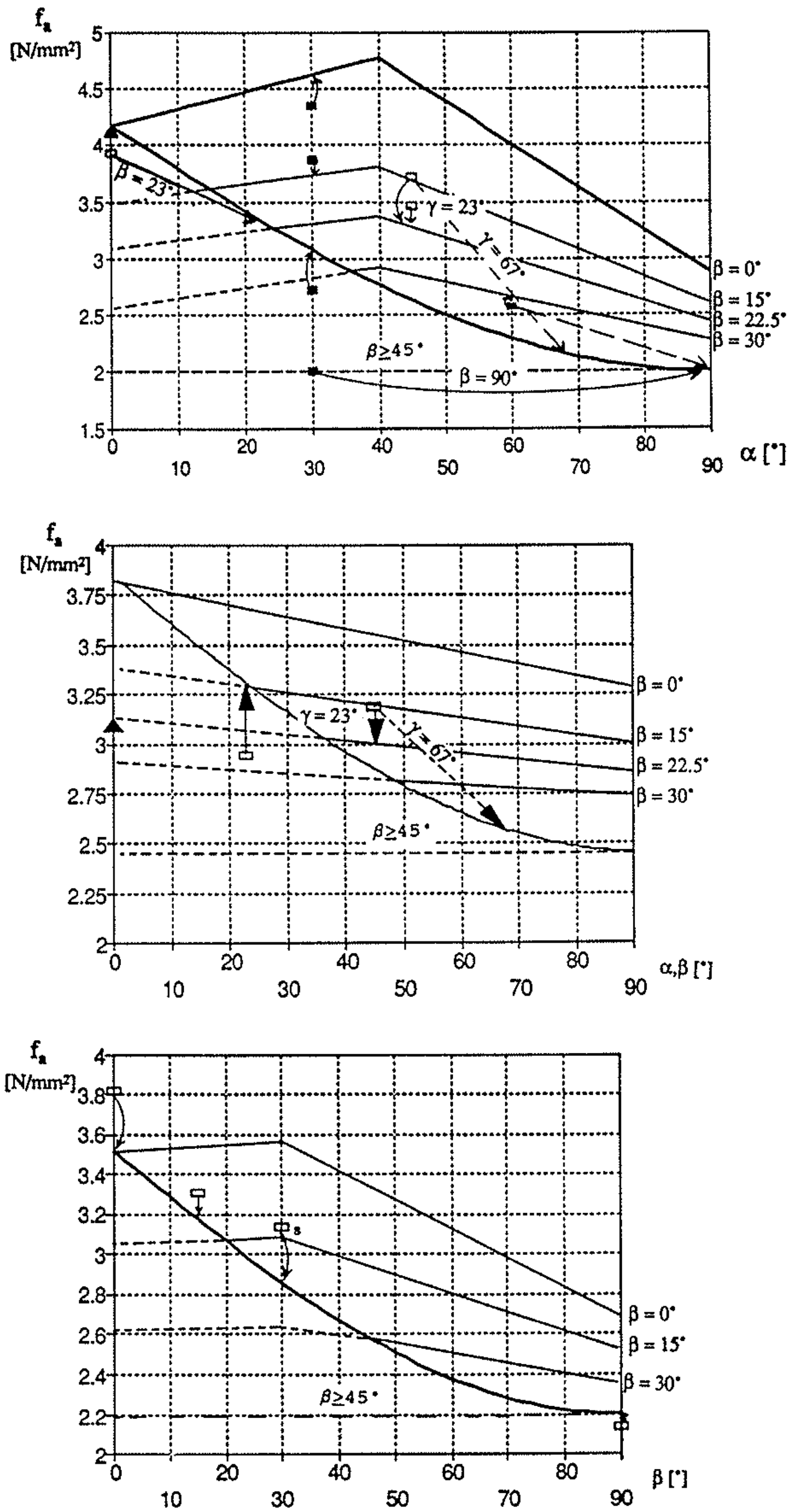

Figure 6. Test results of test series with different combinations of direction angles are situated on the pattern of maximum and minimum curves of anchorage strength.

Interpolated values are on the safe side, if f_{a9090} is taken as a minimum value for all cases when $\beta \geq 45°$ and the values are interpolated linearly between $0° < \beta < 45°$. This interpolation will be done only on the area between formulae (1) and (2) above.

6 PROPOSAL FOR DESIGN RULES IN EUROCODE 5

The anchorage design strength $\mathbf{f_{a\alpha\beta d}}$ in nail plate joints is calculated from the equations (3) - (6)

$$f_{a\alpha\beta d} = \begin{cases} f_{a\alpha 0d} & \text{, when } \beta = 0° & (3) \\ f_{a\alpha 0d} - (f_{a\alpha od} - f_{a9090d})*\beta/45 & \text{, when } 0° < \beta < 45° & (4) \\ (1 - c*\sin(\max(\alpha,\beta)))*f_{a00d} & \text{, when } 0° < \beta < 90°. & (5) \end{cases}$$

When $0° < \beta < 45°$, $f_{a\alpha\beta d}$ is the maximum of the interpolation equation (4) and the equation (5), which is for minimum values.

The anchorage design strength in grain direction ($\mathbf{f_{a\alpha 0d}}$) is calculated from

$$f_{a\alpha 0d} = \begin{cases} f_{a00d} + k_1*\alpha & \text{, when } \alpha \leq \alpha_0 \\ f_{a00d} + k_1*\alpha_0 + k_2*(\alpha-\alpha_0) & \text{, when } \alpha_0 < \alpha \leq 90°. \end{cases} \qquad (6)$$

$f_{a\alpha\beta d}$ is the anchorage design capacity in different combinations of angles α and β in N/mm^2

α is the angle between the force and main direction of nail plate

β is the angle between the force and grain direction

α_0 is the angle in the intersectional point of the maximum curve in two parts

k_1, k_2 are the slopes of the maximum curve

c is the coefficient of the minimum curve, which is calculated from the equation $c = (f_{a00} - f_{a9090})/f_{a00}$

f_{a9090} is the lowest value got by the standard tests.

REFERENCES

[1] Aasheim, E. & Solli, K. H., 1990, Proposal for a design code for nail plates, CIB-W18A meeting in Lisbon, paper 23-7-1.

[2] Riberholt, H., 1990, Proposal for Eurocode 5 text on timber trussed rafters, Annex X.4, Strength verification of nail plate connections in timber trussed rafters, CIB-W18A meeting in Lisbon, paper 23-14-2.

[3] Kangas, J., 1985, Principles for design values of nailplates in Finland, CIB-W18A meeting in Beit Oren, paper 18-7-5.

[4] Kangas, J., 1991, Anchorage capacity of nailplate, CIB-W18A meeting in Oxford, paper 24-7-3.

CIB-W18/25-15-1

INTERNATIONAL COUNCIL FOR BUILDING RESEARCH STUDIES AND DOCUMENTATION

WORKING COMMISSION W18 - TIMBER STRUCTURES

STRUCTURAL ASSESSMENT OF TIMBER FRAMED BUILDING SYSTEMS

by

U Korin
National Building Research Institute
Israel

MEETING TWENTY - FIVE

ÅHUS

SWEDEN

AUGUST 1992

STRUCTURAL ASSESSMENT OF TIMBER FRAMED BUILDING SYSTEMS

by U. Korin[(1)]
National Building Research Institute, Israel

1. Scope

The dominant methods for home construction in Israel are based on reinforced concrete structures and block masonry. These methods are locally referred to as "conventional construction".

Socio-economical changes, caused in the last few years, an increase of the relative volume of low-rise home buildings. Timber framed houses, which dominate the solution for low-rise homes the world over, gradually began to penetrate the home market.

Today, timber homes account for about 10 percent of the low-rise home building (about 25 percent of the total volume of home construction). In terms of last year, we may speak of about 1500 home units of timber framed houses.

2. Assembly of specifications for timber framed construction

Conventional construction in Israel is backed by a highly developed standardization system, providing the technical, and even the legal support for the building process.

Standardization support was not available for the timber framed houses. Apart from some specifications prepared earlier for timber roofs[(1)], there were no local standards for timber building, and the municipal government found itself puzzled every time a building permit for a timber house was applied for.

Acute home shortage, in the last two years, became the lever for the search for fast building systems, among them timber framed houses.

The Israeli Government, being the main entrepreneur for the enormous national building project, requested the National Building Research Institute to prepare adequate documentation which would enable to assess the various speedy construction methods, and to assure that only reliable home building solutions would be procured.

A team, comprising of experts on the various types of construction, has been assembled, the author being a member of that team, responsible for all the aspects of timber in the "fast building methods" investigation.

(1) Head, Testing Division, National Building Research Institute, Technion, Haifa 32000, Israel.

The first stage of the work of the team was to prepare a preliminary document which would be the reference for the assessment work. The document entitled: "Concised Performance Specifications for Permanent Housing from Lightweight Construction"[(2)]. The performance specifications for "Low-Rise Timber Structures" contain instructions about structural safety and ultimate limit state, resistance to fire, users health and safety, serviceability, internal climate, acoustics, lighting, spatial characterization, water tightness and prevention of moisture problems, long term durability and maintenance.

A very short summary of these specifications were provided to the interested parties. This summary is presented in Appendix A.

At a second stage, the Israeli Standards Institution appointed a standardization committee to prepare permanent specifications for "Low-Rise Permanent Dwellings"[(3)]. The team, appointed by the National Building Research Institute, was very active in applying the experience gained in the preparation of the concised specifications, and its use in the assessment of construction methods to the permanent specifications.

3. Assessment of Timber Structures

The assessment of a Timber Framed House demands a comprehensive investigation of the structure, its structural design, the materials and components employed, the joints and the assembly process, details about the sheathing, the cladding and other parts of the structure. A full list of the structural details required by the assessment team is given in Appendix B.

The assessment process is an interactive system. The applicants are advised to introduce corrections of the design and detailing when these are required. The final report contains a full description of the approved building system, a set of the final principal drawings, of the structure, details of the fabrication and erection stages and description of the quality assurance and quality control relating to all the stages of the design, fabrication and erection stages.

4. The Building Systems

About 25 different timber framed houses were investigated. The assessed systems formed a very wide spectrum of construction methods: platform construction, balloon construction, cell construction; building from sticks, prefabricated panel assembly, three-dimensional module staking; marriage between timber and steel; marriage between timber and aluminum; roofs of different types; various types of sheathing means; various types of sidings.

Some of the methods were highly industrialized, but some of them were undeterred for quite primitive site assembly work.

5. Conclusions

The enormous assessment process of building systems enable to provide the country with safe, functional and durable timber framed houses, in spite of the lack of previous experience in that type of construction.

Some of the newly built timber framed houses very successfully withstood the extremely unusual heavy weather conditions the Middle East experienced last winter. The houses were found safe and provided the occupants with good living space.

References

1. The Standards Institution of Israel - Specification No. 270 - "Trussed rafter timber roofs with lightweight cover" (in Hebrew).
   Part 1 - August 1990 - Sawn timber.
   Part 2 - March 1991 - Design.
   Part 3 - August 1991 - Fabrication, construction and test.

2. The National Building Research Institute, Haifa, Israel - June, 1990: "Concised Performance Specifications for Permanent Housing from Lightweight Construction", R. Becker, A. Rutenberg, U. Korin, I. Berdichewski and N. Nave.

3. The Standard Institution of Israel - Specification No. 422, April 1992, "Low-Rise Permanent Dwellings" (in Hebrew).

Founded by מיסודם של

MINISTRY OF CONSTRUCTION AND HOUSING משרד הבינוי והשיכון

TECHNION - ISRAEL INSTITUTE OF TECHNOLOGY הטכניון - מכון טכנולוגי לישראל
Faculty of Civil Engineering הפקולטה להנדסה אזרחית

NATIONAL BUILDING RESEARCH INSTITUTE

המכון הלאומי לחקר הבנייה

APPENDIX A

15.6.1990

Draft Proposal

CONCISED PERFORMANCE SPECIFICATIONS FOR PERMANENT HOUSING FROM LIGHTWEIGHT CONSTRUCTION

1. GENERAL

A building system will be based on the use of materials, components and construction details which comply with all the performance specifications outlined herewith. Building systems which were investigated at the National Building Research Institute after 1975, and concluded to be suitable for use in Israel, will not require renewed testing. Other systems will require prototype investigation.

In any case, the responsibility for the actual construction lies with the contractor, and the issued certificate does not exempt him from responsibility for detailed planning, design and construction of the whole building and its parts, so that all the requirements are fulfilled.

In addition to all the above-mentioned items, the buildings will comply with all the Israeli building regulations and laws, the Israeli standards relevant to the system, the Israel Institute of Standards codes, the performance specifications issued by the Ministry of Housing for residential buildings, and the relevant requirements in the "General Specification for Building Works".

The enterpreneur will provide the National Building Research Institute with a detailed technical file which will include:

(a) Technical specification describing the building system, the process of construction during all the stages, details of all the materials, their specifications and treatments provided to them, description and details of all the components, joints, and connections between them, details of finish, sealing and insulation of all types.

(b) Typical static scheme of typical buildings which will clarify the mode of force transfer of vertical and horizontal loads.

(c) Sample calculations of typical load bearing components under the action of vertical and horizontal loads.

(d) Horizontal cross-section through all the typical elements of the building, including: cross-section through external wall with a door and a window with shutter; cross-section through internal partition with a door; cross-section through connections of internal walls and partitions to the external walls, and of the internal walls and partitions to each other; cross-section through concave and convex external corner; cross-section through dividing partition between apartments and its connection to the external walls;

(e) Vertical cross-section through all the typical elements of the building including:
- cross-section through external wall with window, showing the mode of connection of the walls and roof, the floor and intermediate ceiling.
- cross-section through internal partition with and without a door, including all the above-mentioned details;
- typical cross-section through lower ceiling, intermediate ceiling and roof, and all their layers.
- typical cross-section as above in washrooms in bottom story and intermediate story.

(f) Drawings detailing the mode of transfer and connection of the electrical pipes, telephone, water, drainage, sewage, and sanitary equipment (toilets, sinks, bathtubs, faucets, etc.)

(g) Details of the procedure of quality assurance in the plant and on the site.

All the drawings in items (e),(f),(g) above should be at a proper scale to fully describe the details of joints, connections, sealing, finish, overlaps, insulation, etc. Each material and element should have a clear identity as indicated in item (a) above.

The performance specifications required for every building system are in the following areas:

- Structural safety – ultimate limit state and serviceability
- Resistance to fire
- User Health and safety
- Serviceability
- Internal climate
- Acoustics
- Lighting
- Spatial characteristics
- Water tightness and prevention of moisture problems
- Durability and maintenance.

The Effective Design Life Expectancy of the whole building should be 50 years at least.

The following section provides a concise description of the requirements for the different types of structures.

APPENDIX B

LIST OF INVESTIGATED STRUCTURAL DETAILS

1. Principal layout of the investigated home.
2. Structural details of the foundation system.
3. Plan of the walls and the partitions.
4. Structural detail of the roof.
5. A complete static scheme of the house and its main load-bearing components.
6. Various assembly details of the house (connectors, anchors, marriage walls, separation walls, sheathing, siding, sealing, waterproofing, openings, full details of the wet parts of the house, thermal and acoustical insulation, vapour barriers and any other special details requiring attention).
7. A list of the various materials used in the construction of the house.
8. A full list of the mechanical connectors and fasteners used in the construction of the house.

CIB-W18/25-15-3

INTERNATIONAL COUNCIL FOR BUILDING RESEARCH STUDIES AND DOCUMENTATION

WORKING COMMISSION W18 - TIMBER STRUCTURES

MECHANICAL PROPERTIES OF WOOD-FRAMED SHEAR WALLS SUBJECTED TO REVERSED CYCLIC LATERAL LOADING

by

M Yasumura
Building Research Institute
Japan

MEETING TWENTY - FIVE

ÅHUS

SWEDEN

AUGUST 1992

MECHANICAL PROPERTIES OF WOOD-FRAMED SHEAR WALLS SUBJECTED TO REVERSED CYCLIC LATERAL LOADING

by Motoi YASUMURA
BUILDING RESEARCH INSTITUTE, JAPAN

ABSTRACT

Wood-framed shear walls sheathed with the various types of sheet materials were subjected to the reversed cyclic lateral loading, and the effects of the cyclic loading on the mechanical properties of shear walls were studied. It was found that the reversed cyclic loading affected more on the shear strength and ductility of the shear walls sheathed with the inorganic materials such as the gypsum board, cemented wooden chip board and asbestos silica calcium board than those sheathed with the wood-based panels such as the plywood and oriented strand board. According to the experimental results, the wood-framed shear walls were classified into three groups regarding the aseismic design of wood-framed structures.

INTRODUCTION

In the draft version of Eurocode 8[1], the timber structures are classified into three types, in which the wood-framed shear walls are classified in the medium dissipative structures(Type C). Ceccoti and Larsen proposed the behavior factor "q" of 2.5 for the medium-dissipative structures[2]. YASUMURA conducted the time-history earthquake response analysis on the wood framed shear walls and proved that the shear walls which kept the maximum shear deformability of 1/40 rad. gave the behavior factor of 3.0[3].

In the aseismic design of wood-framed structures, the effects of the mechanical properties of sheathings, the thickness of sheet material and nail size on the seismic behavior of shear walls should be considered as the deformability of shear walls depends much on the ductility of the nail joints connecting the sheet materials to the wooden frames.

The purpose of this study is to supply the experimental data on the mechanical properties of wood-framed shear walls subjected to the reversed cyclic lateral loading to evaluate and classify the seismic behavior of shear walls having the various types of sheathing materials.

REVERSED CYCLIC LOADING OF SHEAR WALLS

Specimens and test methods

Wood-framed shear walls of 1.82 meters in length and 2.44 meters in height were subjected to the monotonously increasing lateral loads and the reversed cyclic lateral loads. The tested walls consisted of the nominal 2-by-4 inches studs and plates of Spruce-Pine-Fir and the sheet materials as shown in Table 1. ASTM E72 using the tie rods was applied to the test method. Two specimens of each wall panel were subjected to the reversed cyclic lateral loads as shown in Fig.1, and two others were subjected to the monotonously increasing lateral loads for the comparison.

Influence of reversed cyclic loading

Table 2 summarizes the experimental results, and Figs.2 and 3 compare respectively the maximum load and the maximum shear deformation in the reversed cyclic test with those in the monotonously loading test. Here, the shear deformation is defined by the angle subtracting the rotational angle from the drift angle of wall panel, and the maximum shear deformation represents the shear deformation at the maximum load.

Fig.2 shows that the maximum loads in the reversed cyclic test were 9 to 33% smaller than those in the monotonously loading test. Fig.3 shows that there were few differences between the maximum deformation in the reversed cyclic test and that in the monotonously loading test regarding the specimens sheathed with the plywood and oriented strand board, while the maximum deformation decreased to 35 to 57% due to the reversed cyclic loading regarding the specimens sheathed with the cemented wooden chip board, gypsum board and asbestos silica calcium board. These facts indicate that the reversed cyclic loading affects little on the shear strength and ductility of the shear walls sheathed with the plywood and oriented strand board, while it affects much on the ductility of the shear walls sheathed with the inorganic materials such as the gypsum board, asbestos silica calcium board, etc.

Fig.4 shows the skeleton curves of the load-deformation relationships in the reversed cyclic test, and Fig.5 shows the ratio of the shear force in the reversed cyclic test to that in the monotonously loading test. These figures demonstrate the similar tendency mentioned above, and indicate that the special consideration should be taken in the aseismic design of wood-framed structures consisting of brittle sheathings.

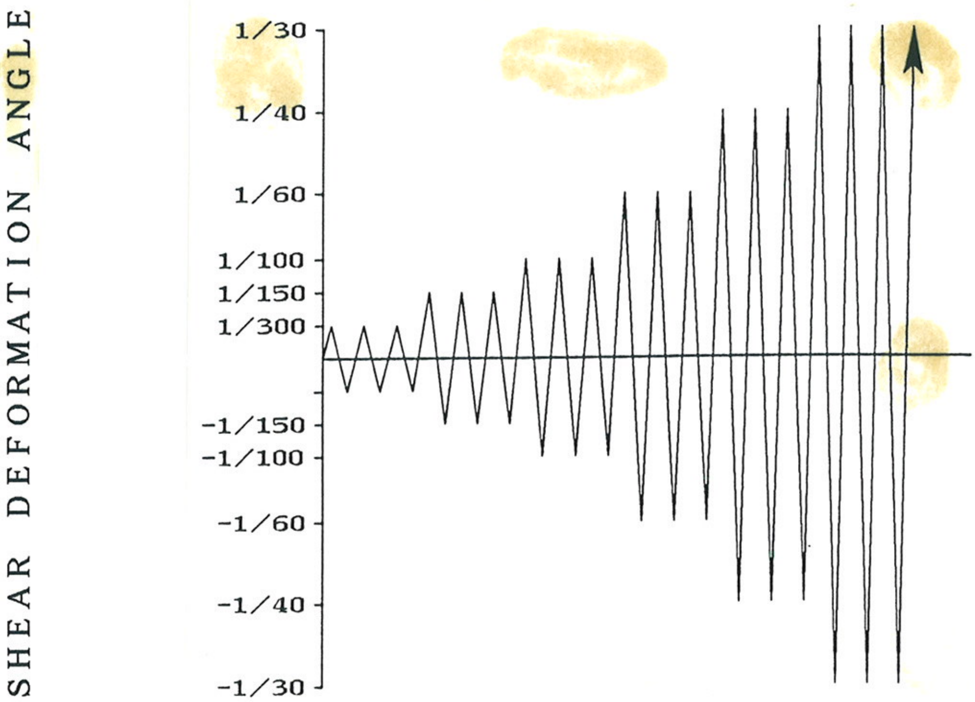

Fig.1 Loading history

Table 1. Description of specimens (Unit:mm)

SPECIMENS	SHEATHING MATERIALS	NAIL DIAMETER	LENGTH	SPACING
PLY	D-fir plywood 910x2440 @9.5	2.87	50.8	100
OSB	Oriented strand board 910x2440 @9	2.87	50.8	100
WCB	Cemented wooden chip board 910x2440 @18	3.33	63.5	100
GYP	Gypsum board 910x2440 @12	2.34	38.1	100
ASC	Asbestos silica calcium board 910x1820 @8	2.87	50.8	100

* Tested wall panel had 1,820mm in length and 2,440mm in height

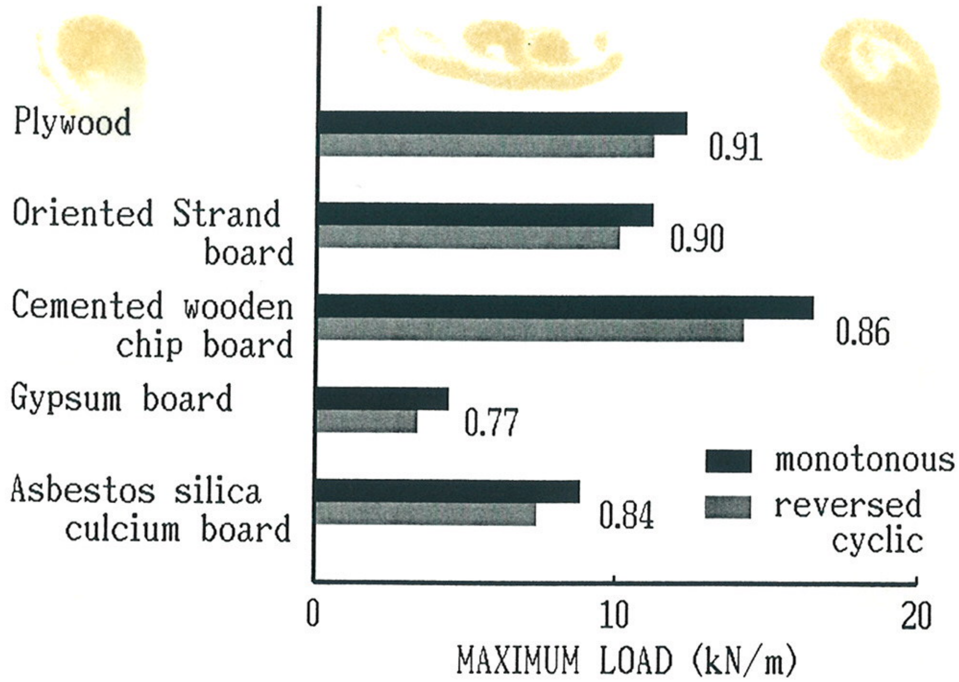

Fig.2 Comparison of the maximum load in the reversed cyclic test with that in the monotonously loading test.

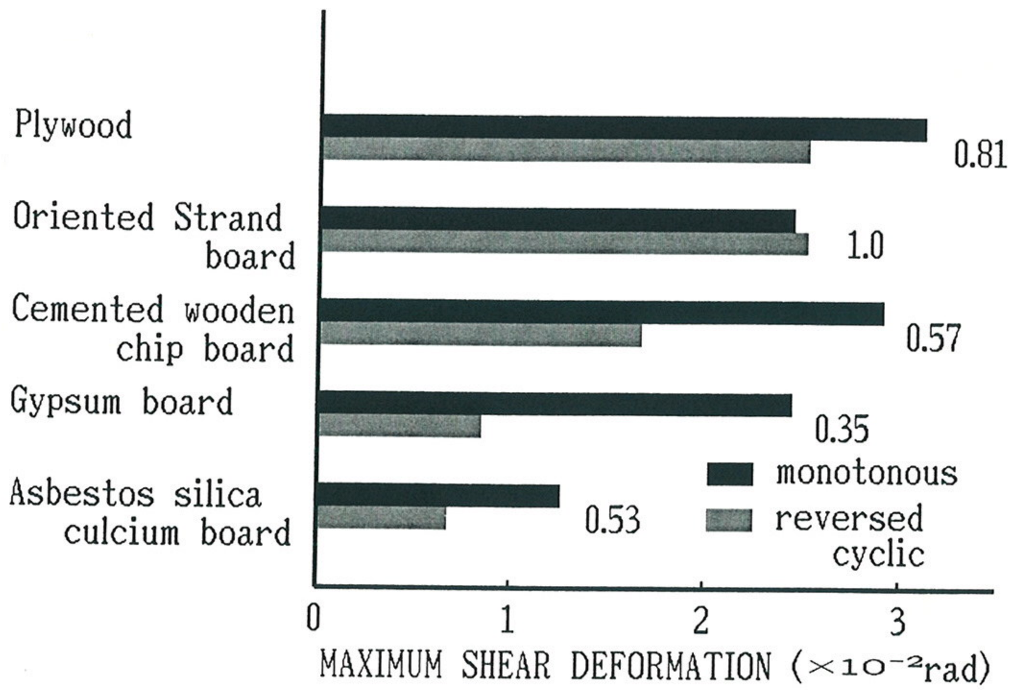

Fig.3 Comparison of the maximum shear deformation in the reversed cyclic test with that in the monotonously loading test.

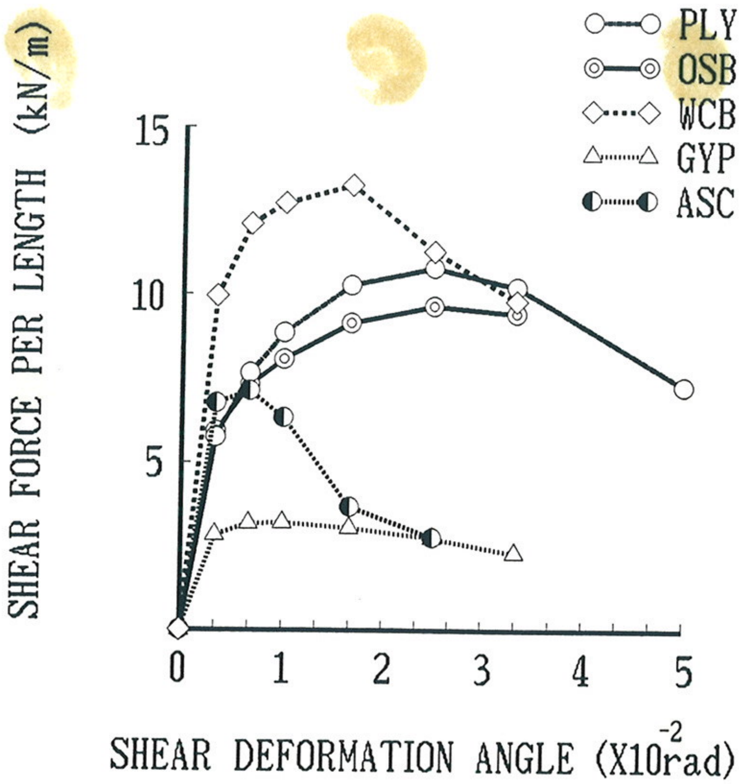

Fig.4 Skeleton curves of load-shear deformation relationships in the reversed cyclic test.

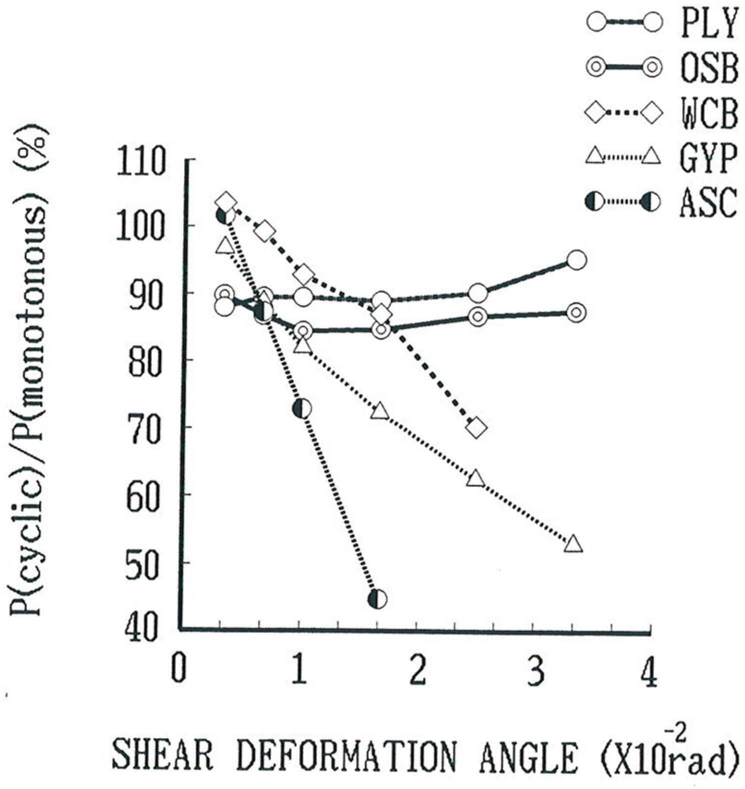

Fig.5 Ratio of the shear load in the reversed cyclic test to that in the monotonously loading test.

YIELD LOAD OF SHEAR WALLS

The yield load of shear walls is calculated from the following formula[4].

$$Q = q \bullet s \bullet \frac{L}{a} \qquad (1)$$

where, Q: Yield load of shear wall
L: Length of shear wall
a: Length of unit panel
q: Yield load of nail joint
s: Coefficient determined by the number of nails

$$s = \min.\left(m-1,\ (n_1-1)\frac{a}{h_1},\ (n_2-1)\frac{a}{h_2} \right)$$

h_1, h_2: Height of unit panel
m, n_i : Number of nails around the perimeter of unit panel.

The yield load of nail joint was calculated from the following formulas.

$$q = C \bullet Fe_1 \bullet d \bullet t \qquad (2)$$

$$C = \min.\left\{ \begin{array}{l} \dfrac{1}{\sqrt{\dfrac{2\beta(1+\beta)}{(2+\beta)^2} + \dfrac{2\beta\gamma(d/t)^2}{3(2+\beta)} - \dfrac{\beta}{2+\beta}}} \\ \dfrac{d}{t}\sqrt{\dfrac{2\beta\gamma}{3(1+\beta)}} \end{array} \right.$$

where, q: Yield load of nail joint
t: Thickness of sheet material
d: Diameter of nail
β: Ratio of the embedding strength of main member to that of sheet material(Fe_2/Fe_1)
γ: Ratio of the yield point of nail to that of the embedding strength of sheet material(Fy/Fe_1)
Fy: Yield point of nail
Fe_1, Fe_2: Embedding strength of sheet material and main member

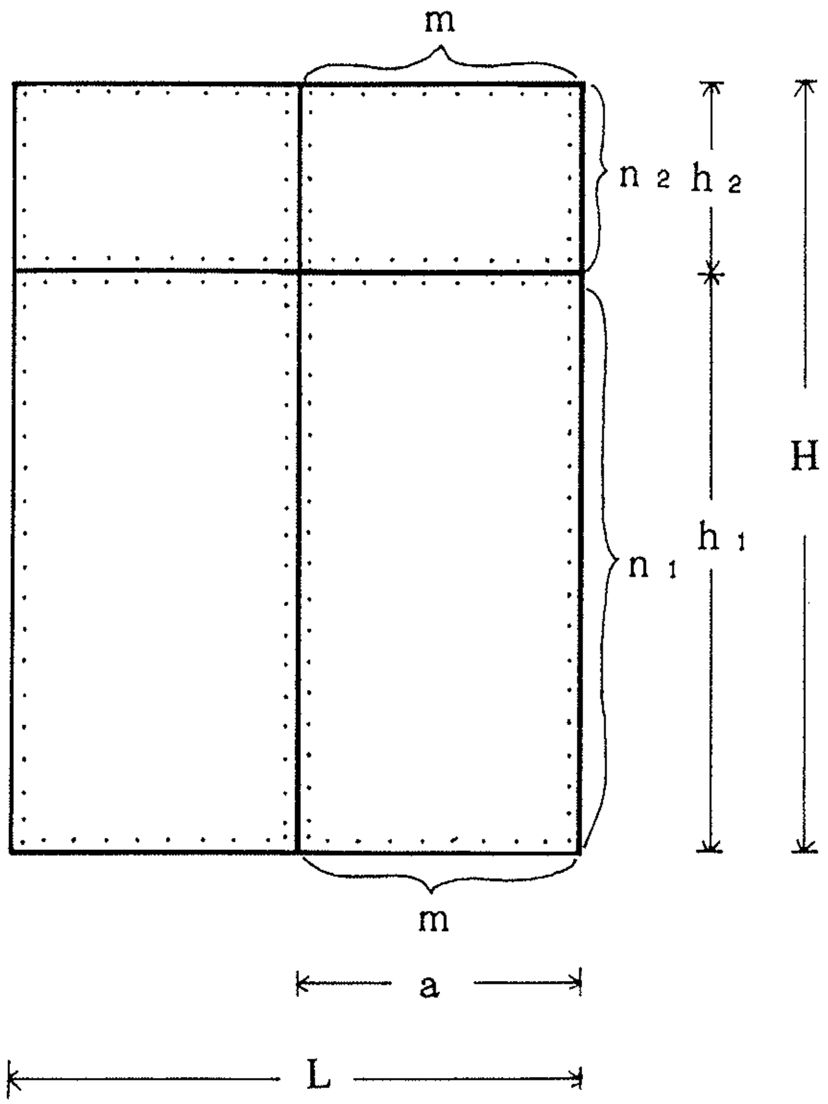

Fig.6 Example of the unit panel and geometry of nails.

Table 2. Outline of the experimental results(1)

SPECIMENS	LOADING	P1/300(2) (kN)	P1/150 (kN)	P1/60 (kN)	P1/40 (kN)	Py(3) (kN)	δy(4) ($x10^{-3}$rad.)	Pmax (kN)	δmax(5) ($x10^{-3}$rad.)
PLY	Monotonous	11.9	15.6	21.0	21.7	12.3	3.41	22.4	31.3
	Cyclic	10.5	14.0	18.7	19.6	(11.9)(6)	4.27	20.3	25.3
OSB	Monotonous	12.1	14.0	19.6	20.2	10.6	2.05	20.4	24.6
	Cyclic	10.8	13.3	16.7	17.6	(11.1)	2.90	18.3	25.2
WCB	Monotonous	17.5	22.2	27.7	29.2	18.7	3.91	30.0	29.2
	Cyclic	18.1	22.0	24.1	20.5	(15.5)	3.94	25.8	16.8
GYP	Monotonous	5.4	6.5	7.7	8.1	4.1	1.42	8.1	24.5
	Cyclic	5.2	5.8	5.6	5.0	(4.1)	1.53	6.3	8.5
ASC	Monotonous	12.2	14.9	15.0	7.9	13.5	4.67	16.1	12.7
	Cyclic	12.4	13.0	6.7	5.1	(11.7)	6.77	13.5	6.8

(1) Length of specimen of 1,820mm and the average value of two specimens
(2) Load corresponding to 1/300 of the shear deformation angle
(3) Calculated value from the formula(1)
(4) Shear deformation corresponding to the yield load (Py)
(5) shear deformation corresponding to the maximum load (Pmax)
(6) Calculated from the lateral resistance of nail due to ASTM D1037

Table 3. Embedding strength and calculated yield load of nail joint

Materials	Embedding strength (MPa)	Yield load (N)
S-P-F	34	---
PLY	61 (56)*	685 (660)
OSB	44 (48)	593 (616)
WCB	62 (33)	1046 (861)
GYP	10 (10)	229 (229)
ASC	85 (60)	754 (650)

* The parenthesized values are the lateral resistance of nail due to ASTM D1037 with the end distance of 4d and the calculated yield load of nail joints from the lateral resistance

The yield point of nail (Fy) was assumed to be 663MPa for the nail having the diameter of 2.34 and 2.87mm and 608MPa for the nail having the diameter of 3.33mm from the tensile test of nails, and the embedding strength of S-P-F and sheet materials were obtained from the embedding test. Table 3 shows the embedding strength of S-P-F and sheet materials, and the calculated yield load of nail joints. The embedding strength obtained from the embedding test showed the similar values to those obtained from the lateral resistance due to ASTM D1037 regarding the plywood, oriented strand board and gypsum board, however the lateral resistance due to ASTM D1037 of the cemented wooden chip board and asbestos silica calcium board were 30 to 47% smaller than the embedding strength due to the embedding test.

The ratio of the maximum load to the calculated yield load (Pmax/Py) in the monotonously loading test of the specimens sheathed with the plywood, oriented strand board and gypsum board were approximately 1.8 to 2.0, and the ratio of those having the sheathings of cemented wooden chip board and asbestos silica calcium board were 1.60 and 1.19 respectively. The ratio (Pmax/Py) of the specimens sheathed with the cemented wooden chip board and asbestos silica calcium board was respectively 1.95 and 1.38 when the lateral resistance due to ASTM D1037 was applied instead of the embedding strength. This indicates that the yield load of shear walls calculated from the embedding strength of sheet materials shows relatively higher values in some brittle materials. The ratio (Pmax/Py) in the reversed cyclic test of the specimens sheathed with the plywood and oriented strand board was respectively 1.65 and 1.73, that of the specimens sheathed with the cemented wooden chip board and gypsum board was respectively 1.38 and 1.54 and the ratio of that having the sheathing of asbestos silica calcium board was 1.0. The ratio (Pmax/Py) calculated from the lateral resistance due to ASTM D1037 of the specimens sheathed with the cemented wooden chip board and asbestos silica calcium board was respectively 1.66 and 1.15.

The ductility factor ($\delta max/\delta y$) in the reversed cyclic test of the specimens sheathed with the plywood and oriented strand board was respectively 5.9 and 8.7, that of the specimens sheathed with the cemented wooden chip board and gypsum board was respectively 4.3 and 5.6. The ductility factor of the specimen sheathed with the asbestos silica calcium board was 1.0. The ductility factor obtained from the lateral resistance due to ASTM D1037 of the specimens sheathed with the cemented wooden chip board and asbestos silica calcium board was respectively 6.8 and 3.2.

Equivalent viscous damping

Fig.7 shows the equivalent viscous damping obtained from the load-

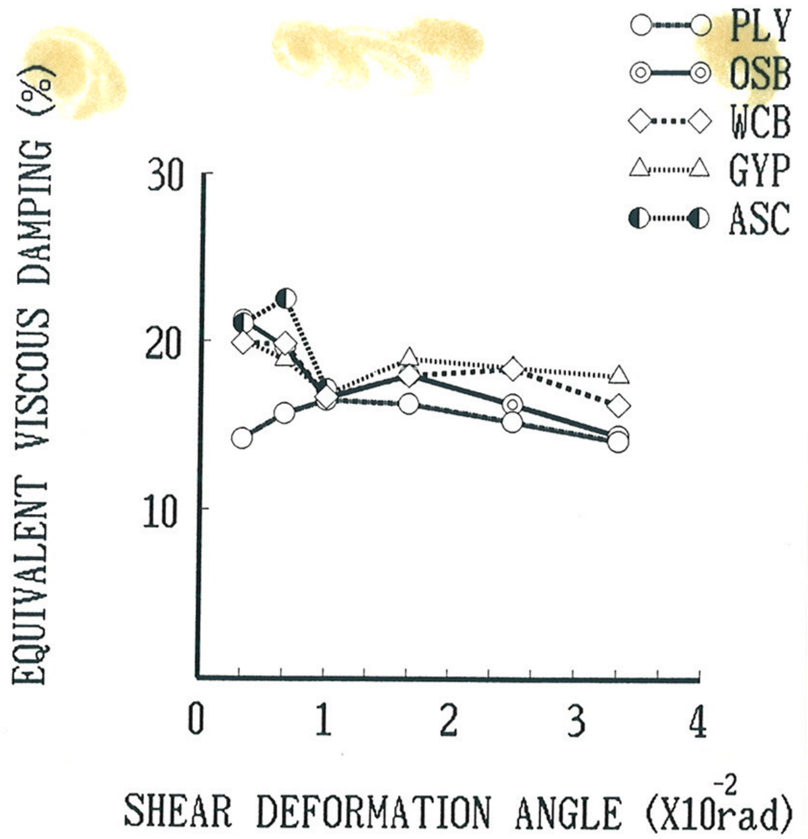

Fig.7 Equivalent viscous damping of each specimens.

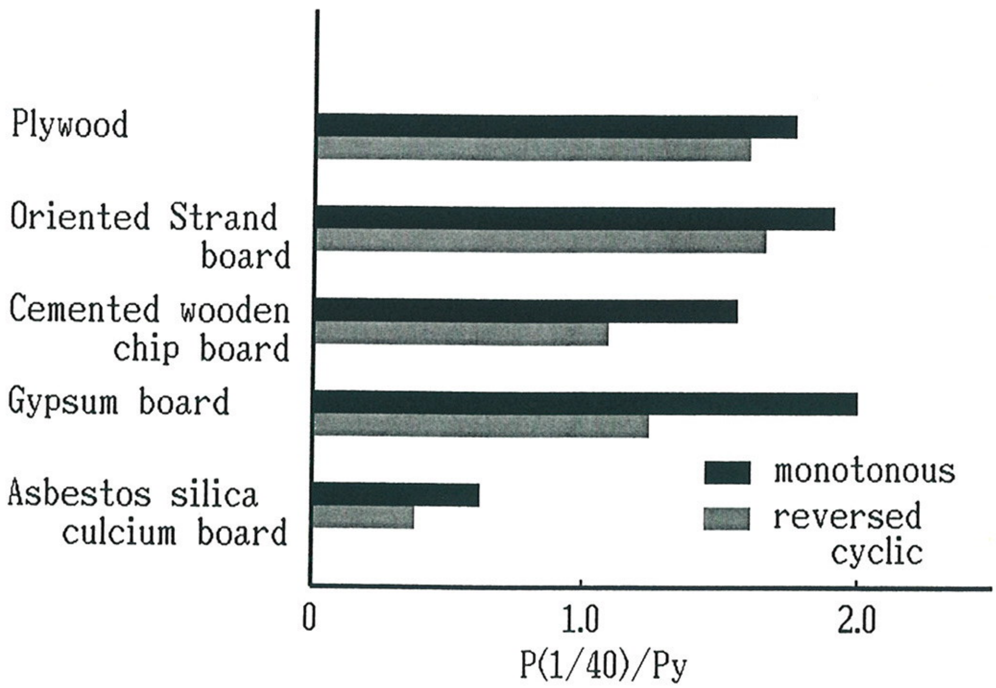

Fig.8 Ratio of the load for the shear deformation of 1/40 to the calculated yield load of shear wall.

deformation relationships of each specimen. The equivalent viscous damping varied from approximately 15 to 20% and kept almost constant regardless of the types of sheathings after the reversed cyclic loading of 1/100.

CLASSIFICATION OF SHEAR WALLS

Fig.8 shows the ratio of the load for the shear deformation angle of 1/40 to the calculated yield load of shear walls. The ratio (P(1/40)/Py) in the reversed cyclic test of the specimens sheathed with the plywood and oriented strand board was respectively 1.59 and 1.66 and the ratio of those having the sheathings of cemented wooden chip board and gypsum board was respectively 1.10 and 1.22. The ratio (P(1/40)/Py) calculated from the lateral resistance due to ASTM D1037 of the specimen sheathed with the cemented wooden chip board was 1.33. Regarding the specimen sheathed with the asbestos silica calcium board, the load decreased rapidly after the reversed cyclic loading of 1/100.

Summarizing the experimental results, the wood-framed shear walls shall be classified into the following groups.

Group A: Shear walls of which energy dissipation is not expected.
Ex: shear walls sheathed with the inorganic materials such as the asbestos silica calcium board

Group B: Shear walls of which energy dissipation is expected but the reduction of the shear strength due to the reversed cyclic loading is remarkable.
Ex: shear walls sheathed with the cemented wooden chip board and gypsum board.

Group C: Shear walls which show high energy dissipation.
Ex: shear walls sheathed with the wood-based panels such as the plywood, oriented strand board, etc.

If we require the maximum shear deformation of 1/40 to the wood framed shear walls classified in the medium dissipative structure (Type C), the following ultimate shear force may be taken in case of the aseismic design.

Group B: $P_u = 1.1 \sim 1.3\ P_y$

Group C: $P_u = 1.6 \sim 1.7\ P_y$

If the structure includes the shear walls classified in Group A, the strength of the shear walls concerned shall not be included in the ultimate lateral strength of the structure.

CONCLUSION

Summarizing the results of this study, the following conclusions are lead.

(1) The maximum loads in the reversed cyclic lateral loading test of shear walls showed 9 to 33% smaller value than those in the monotonously loading test.

(2) There were few differences between the maximum deformation in the reversed cyclic test and that in the monotonously loading test regarding the specimens sheathed with the plywood and oriented strand board, while the maximum deformation decreased to 35 to 57% due to the reversed cyclic loading regarding the specimens sheathed with the cemented wooden chip board, gypsum board and asbestos silica calcium board.

(3) The embedding strength obtained from the embedding test showed the similar values to that obtained from the lateral resistance due to ASTM D1037 regarding the plywood, oriented strand board and gypsum board, however the lateral resistance due to ASTM D1037 of cemented wooden chip board and asbestos silica calcium board showed 30 to 47% smaller value than the embedding strength due to the embedding test.

(4) The ratio (Pmax/Py) in the reversed cyclic test of the specimens sheathed with the plywood and oriented strand board was respectively 1.65 and 1.73, that of the specimens sheathed with the cemented wooden chip board and gypsum board was respectively 1.38 and 1.54, and the ratio of that having the sheathing of asbestos silica calcium board was 1.0. The ratio (Pmax/Py) calculated from the lateral resistance due to ASTM D1037 of the specimens sheathed with the cemented wooden chip board and asbestos silica calcium board was respectively 1.66 and 1.15.

(5) The ductility factor ($\delta max/\delta y$) in the reversed cyclic test of the specimens sheathed with the plywood and oriented strand board was respectively 5.9 and 8.7 and that of the specimens sheathed with the cemented wooden chip board and gypsum board was respectively 4.3 and 5.6. The ductility factor of the specimen sheathed with the asbestos silica calcium board was 1.0. The ductility factor obtained from the lateral resistance due to ASTM D1037 of the specimens sheathed with the cemented wooden chip board and asbestos silica calcium board was respectively 6.8 and 3.2.

(6) The equivalent viscous damping obtained from the load-deformation

relationships varied from 15 to 20% and kept almost constant regardless of the types of sheathings after the reversed cyclic loading of 1/100.

(7) The ratio (P(1/40)/Py) in the reversed cyclic test of the specimens sheathed with the plywood and oriented strand board was respectively 1.59 and 1.66 and that of the specimens sheathed with the cemented wooden chip board and gypsum board was respectively 1.10 and 1.22. The ratio (P(1/40)/Py) calculated from the lateral resistance due to ASTM D1037 of the specimen sheathed with the cemented wooden chip board was 1.33.

(8) The wood-framed shear walls can be classified into three groups according to the strength and ductility. The ultimate shear strength of the shear walls classified in Groups B and C shall be respectively 1.1 to 1.3 and 1.6 to 1.7, and the shear strength of shear walls classified in Group A shall not be included in the ultimate lateral strength of the structures classified in the medium-dissipative structure(Type C).

ACKNOWLEDGMENTS

The author is grateful to Mr.H.SUZUKI of B.R.I. and Mr.I.FUKUDA of JAPAN TWO-BY-FOUR HOME BUILDERS ASSOCIATION for their assistance of conducting the racking test of shear walls.

LITERATURE

1. Commission of the European Communities, "Eurocode No.8, Structures in seismic region Part 1-General and Buildings", Report EUR, May 1988
2. A.Ceccoti and A.Vignoli,"ON A BETTER EVALUATION OF THE SEISMIC BEHAVIOR FACTOR OF LOW-DISSIPATIVE TIMBER STRUCTURES",CIB-W18A/23-15-5, September 1990
3. M.YASUMURA,"SEISMIC BEHAVIOR OF WOOD-FRAMED SHEAR WALLS", CIB-W18/24-15-3, September 1991
4. M.YASUMURA and T.MUROTA, "DESIGN PROCEDURES FOR WOOD-FRAMED SHEAR WALLS", Pre-print for IUFRO-S5.02, August 1992
5. I.FUKUDA and M.YASUMURA, "Influence of Reversed Cyclic Loading on Shear Strength of Wood-framed Shear walls", Summary of Annual Meeting of A.I.J., August 1992

CIB-W18/25-16-1

INTERNATIONAL COUNCIL FOR BUILDING RESEARCH STUDIES AND DOCUMENTATION

WORKING COMMISSION W18 - TIMBER STRUCTURES

THE EFFECT OF DENSITY ON CHARRING AND LOSS OF BENDING STRENGTH IN FIRE

by

J König
Swedish Institute for Wood Technology Research
Sweden

MEETING TWENTY - FIVE

ÅHUS

SWEDEN

AUGUST 1992

THE EFFECT OF DENSITY ON CHARRING AND LOSS OF BENDING STRENGTH IN FIRE

by
J König
Swedish Institute for Wood Technology Research

SUMMARY

The influence of density on charring of timber exposed to standard fire is studied, evaluating test results by Norén. It was found that both the effective and measured charring rates vary about 10 % in the density interval between 290 and 420 kg/m^2, representing characteristic densities of strength classes C14 to C40 in prEN 338, Draft 1991. It was found that there was no influence of density on the loss of bending strength.

INTRODUCTION

In the CIB-code /1/ the charring rate has been given as being inversely proportional to density. According to this the influence of density on charring is considerably greater than reported by Schaffer /2/ for some North American species. In a recent study by White et. al. /3/ the influence of some parameters, among them density and moisture content are studied. For European spruce the influence of density is reported to be in the same order of magnitude as given in /2/, but the charring rate itself is overestimated in comparison to values which are accepted in Europe.

FIRE TESTS BY NORÉN

In an experimental investigation, the effect of knots on the loss of load capacity of light wooden members exposed to fire was determined by Norén /4/. In the tests light members of Swedish spruce of the dimension 45x120 mm^2 were exposed to standard fire according to ISO 834 on four sides in a small furnace. Test series of specimens with knots and of specimens fairly free from knots were compared. Using a method of matching, load capacity at normal temperature of each specimen was predicted. The load levels during the fire tests, denoted as load ratios, were one third and one sixth respectively of the ultimate load at normal temperature. The results obtained showed that the failure times were fairly independent of the existence of knots, with a slight tendency for timber with knots to exhibit longer failure times. Since this influence is very small it can be disregarded in design practice.

In the following the influence of density is shown using the test results in /4/.

The ratio A_r/A_0 versus oven dry density ρ_{0u} is shown in Figure 1, where A_r is the residual area of the cross section at failure , and A_0 is the area prior to the test. It can be seen that density does not influence the total amount of charring that leads to failure. Since the load ratio is the same within each series, the conclusion can be made that neither does density exert any influence on the loss of bending strength of the residual cross section.

A considerable scatter of failure time in each series which allows to study how the charring rates are influenced by density. The plots of failure time versus density are shown in Figure 2. We can see that failure time increases with increasing density. Thus the charring rate

decreases with increasing density as shown in Figure 3, where the rate of charring is expressed as the charred area A_{char} divided by failure time
where

$$A_{char} = A_0 - A_r$$

With the assumption that the bending strength of the effective residual cross section is the same as under normal conditions, effective charring rates β_{ef} have been calculated which lead to failure loads equal to the test loads. The results are shown in Figure 4. It is obvious that the effective rate of charring decreases with increasing density.

From the figures it can be seen that there exists considerable scatter of the results. Comparing the two test series with the load ratios 0,33 and 0,167 respectively, we can see that the charring rate is about 20% larger in the latter. One reason is that the charring rates shown in the diagrams are mean values. Since the failure times were very short - the mean values were about 10 and 15 minutes respectively - the mean charring rate is more affected by the initially low charring rate in the first series. Another reason for this result can be insufficient accuracy of the measurements of the charred sections. In the second series a digitizer was used which gives better accuracy.

In design practice characteristic densities of timber in the most used strength classes are between 290 and 420 kg/m^3. These densities refer to a temperature of 20 °C and a relative humidity of 65 %, i.e. the oven dry density is between 325 and 470 kg/m^2. These limits correspond to strength classes C14 and C40 according to prEN 338, Draft 1991. Using the regression lines in Figures 3 and 4 we can calculate the ratios of charring rates of the two density limits:

Load ratio	$\beta_{ef,470} / \beta_{ef,325}$	$(A_{char,470} / t)/(A_{char,325} / t)$
0,33	0,90	0,87
0,167	0,92	0,94

The values for both effective and measured charring are of the same order of magnitude. Since the effective charring rate is the integrated effect of charring and loss of strength, the two values differ less than the two values belonging to the measured charring. In both cases the charring rate is about 10% smaller at the upper limit of this interval of density than at its lower limit.

This result is in the same order of magnitude as those given in /2/ and /3/.

CONCLUSIONS

The influence of density on the charring rate is considerably smaller than given in the CIB-code /1/. Since it is small in the intervall of most used strength classes, it should be disregarded in practical applications.

REFERENCES

/1/ CIB Structural Timber Design Code. CIB Publication 66, 1983

/2/ Schaffer, E. L., Charring of selected woods - transverse to grain. Forest Products Laboratory, Madison, 1969.

/3/ White, R. H. & Nordheim, E. V., Charring rate of wood for ASTM E 119 Exposure. Fire Technology, February 1992.

/4/ Norén, J., Failure of structural timber when exposed to fire. 1988 International Conference on Timber Engineering, Seattle.

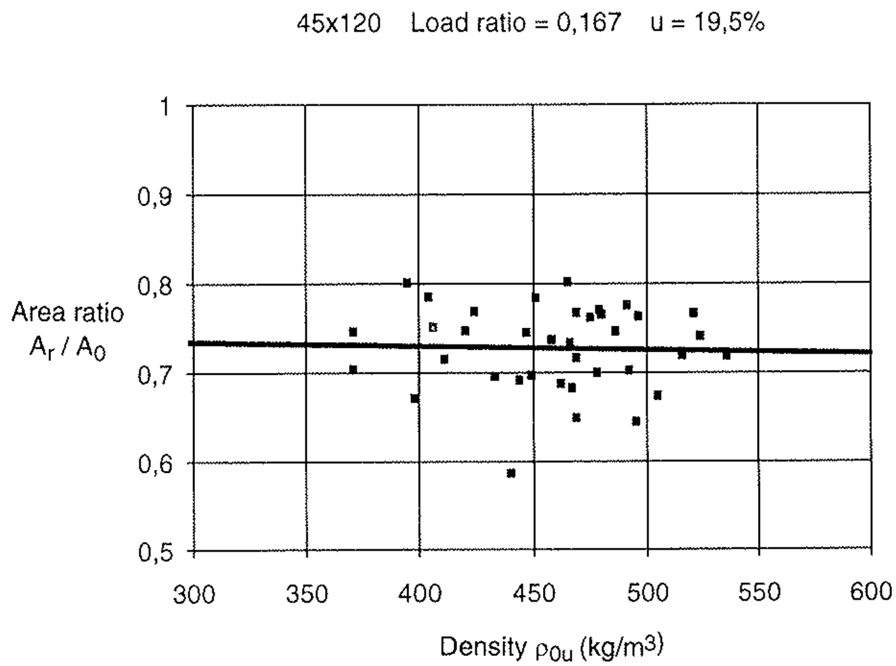

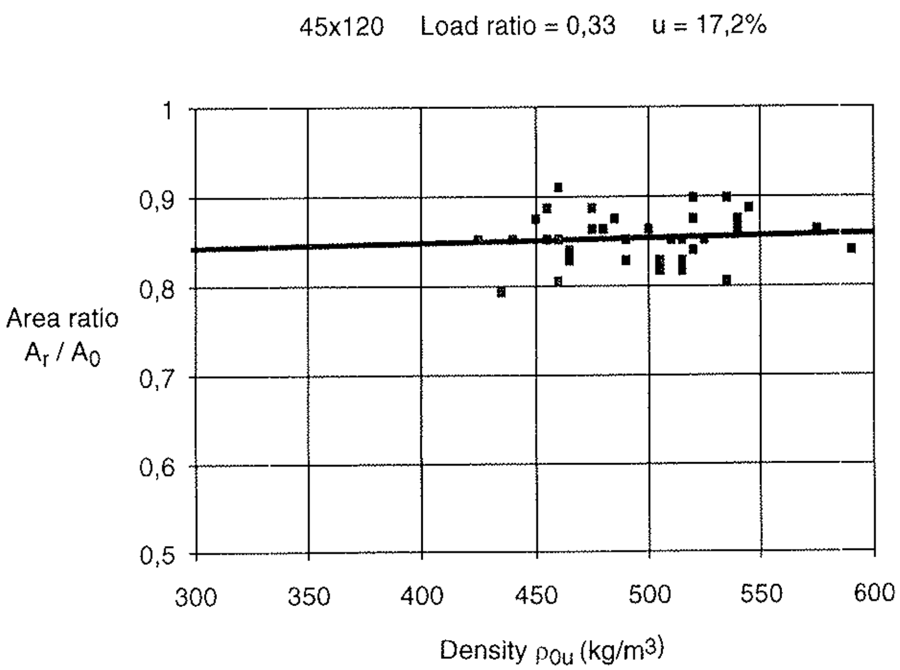

Figure 1 Ratio of residual and initial area versus density

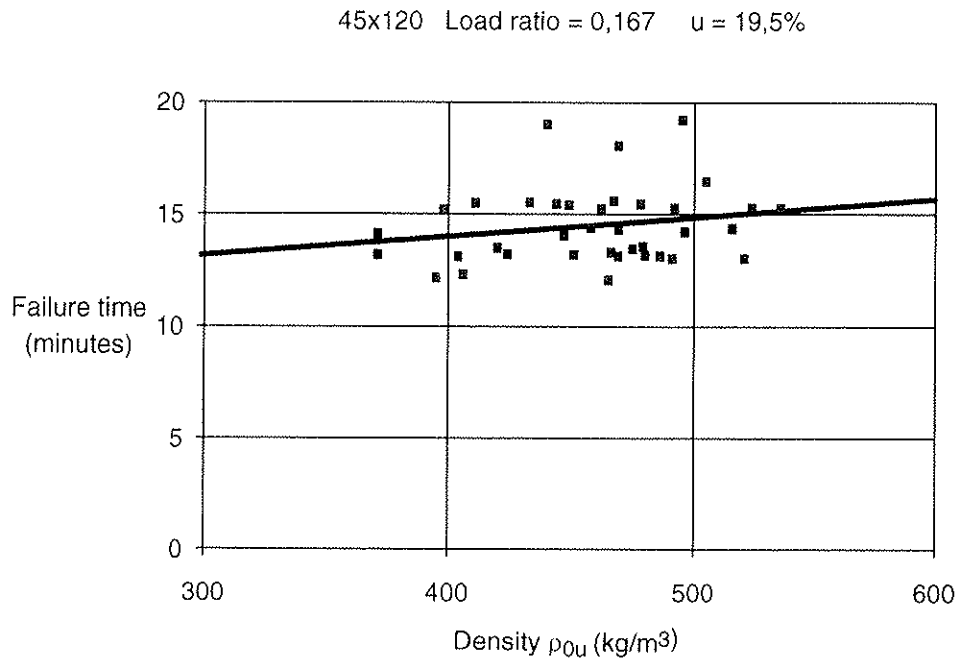

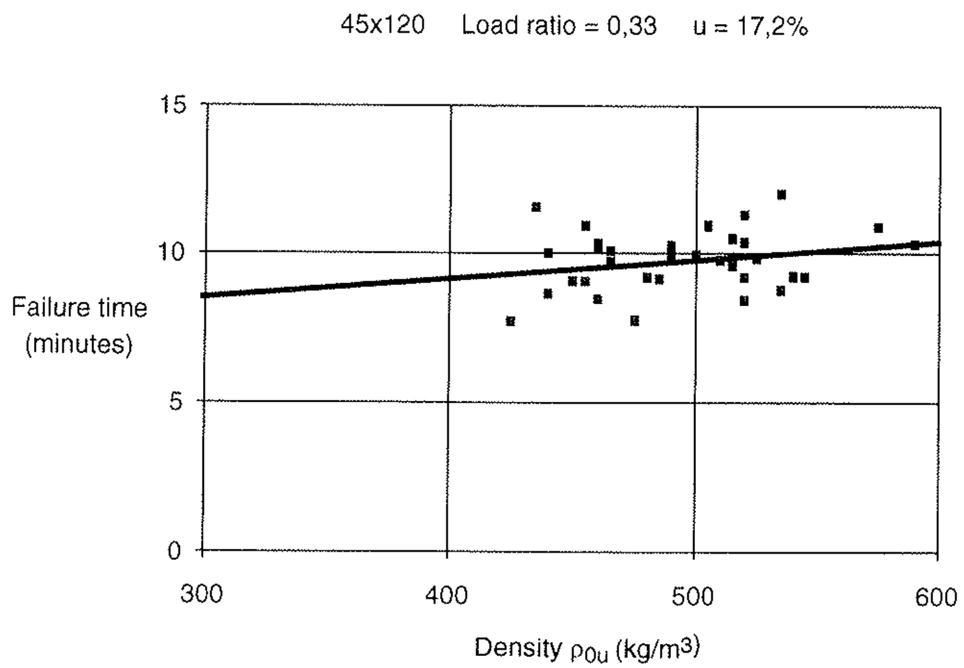

Figure 2 Failure times at same load ratios versus density

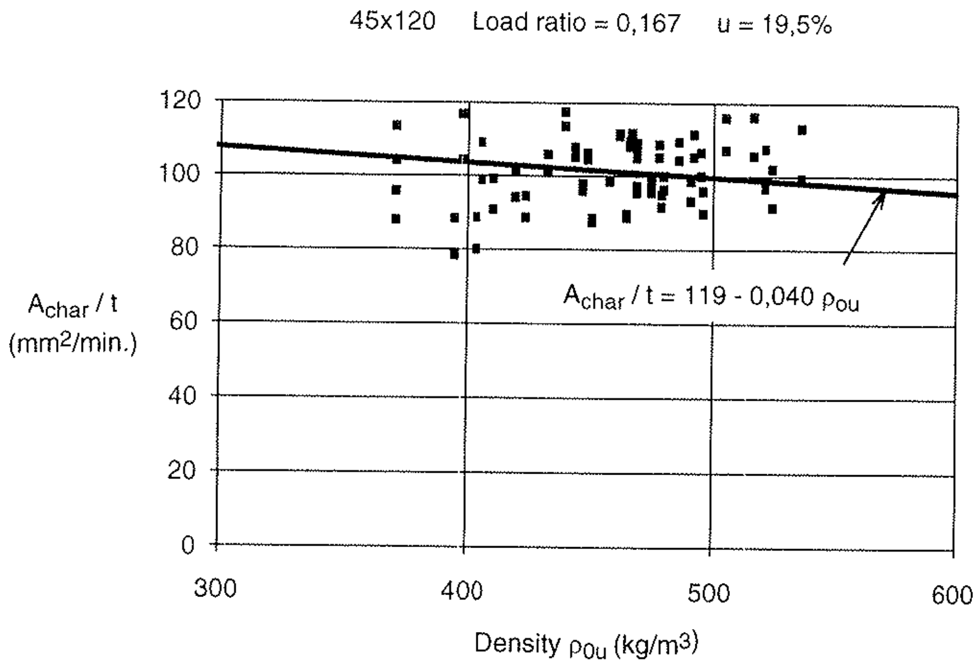

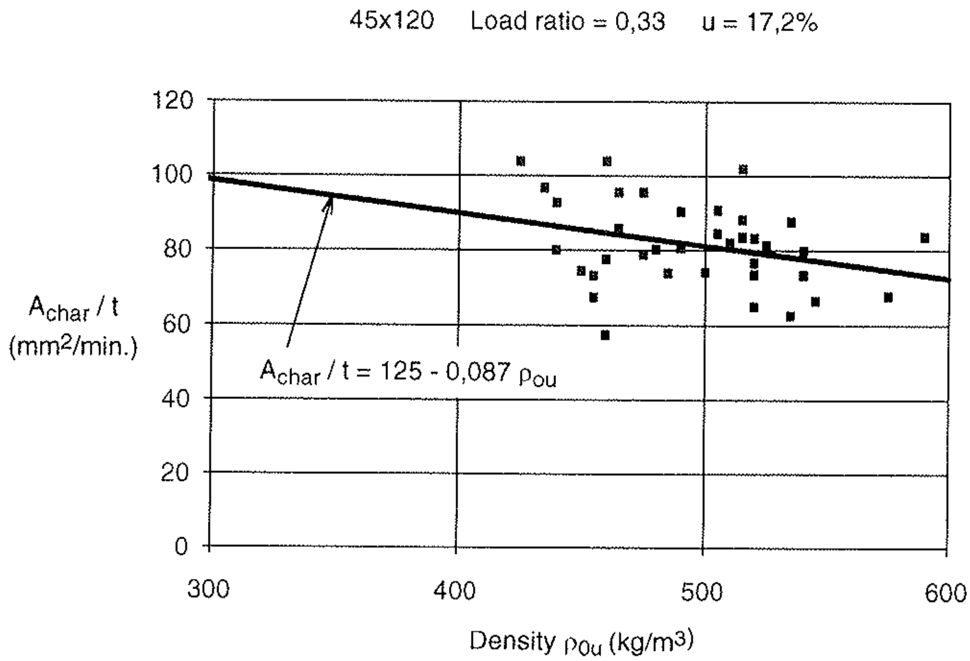

Figure 3 Rate of charred cross sectional area versus density

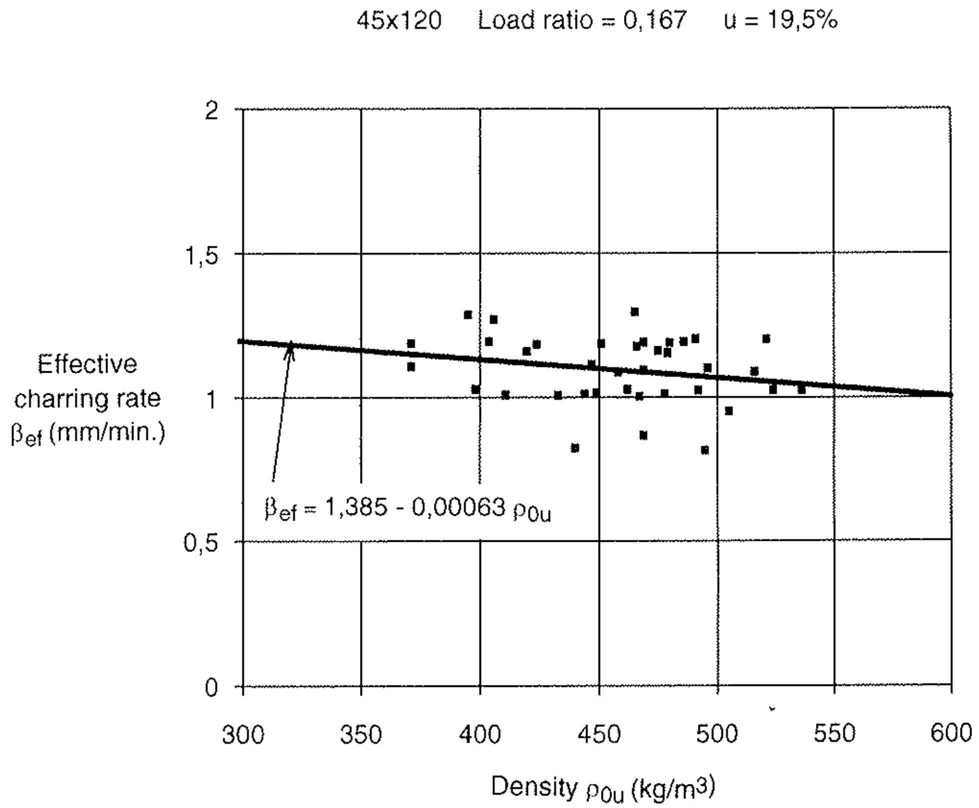

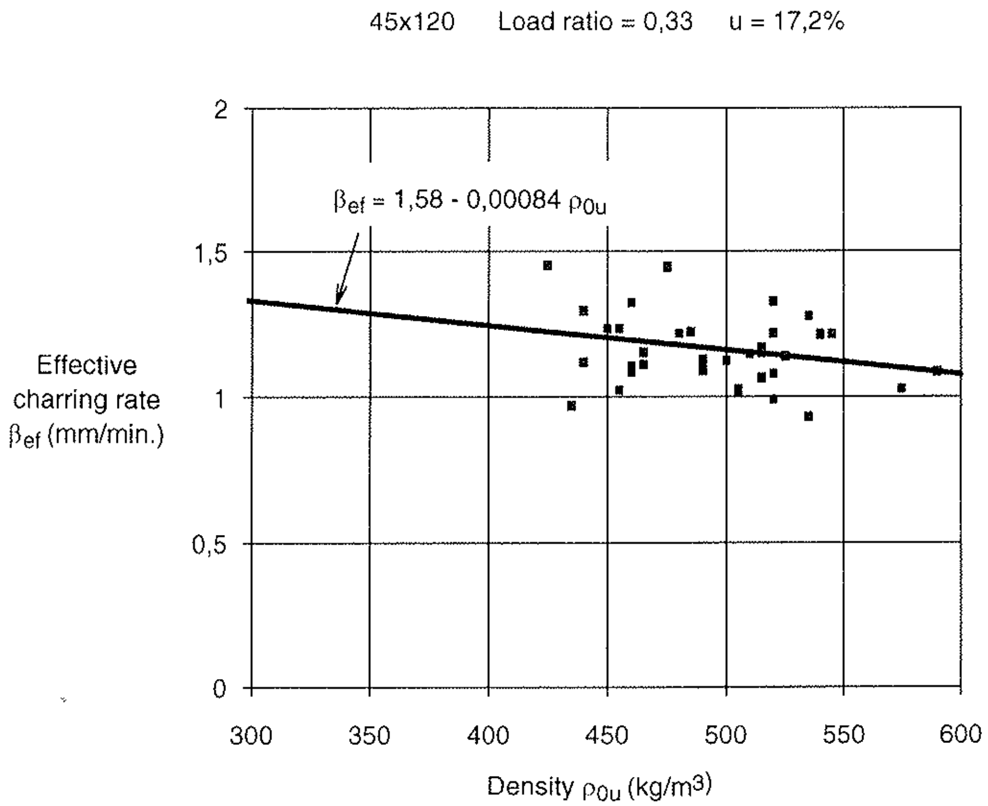

Figure 4 Effective charring rate versus density under the assumption that the bending strength of the residual cross section is not influenced by fire

CIB-W18/25-16-2

INTERNATIONAL COUNCIL FOR BUILDING RESEARCH STUDIES AND DOCUMENTATION

WORKING COMMISSION W18 - TIMBER STRUCTURES

TESTS ON GLUED-LAMINATED BEAMS IN BENDING EXPOSED TO NATURAL FIRES

by

F Bolonius Olesen
University of Aalborg
Denmark
J König
Swedish Institute for Wood Technology Research
Sweden

MEETING TWENTY - FIVE

ÅHUS

SWEDEN

AUGUST 1992

TESTS ON GLUED LAMINATED BEAMS IN BENDING EXPOSED TO NATURAL FIRES

by
F Bolonius Olesen
University of Aalborg
and
J König
Swedish Institute for Wood Technology Research

SUMMARY

A series of fire tests with so-called natural fire exposure of loaded glued laminated beams was performed. The fire exposure on three sides during the tests was governed by a temperature-time relationship determined according to an energy balance method (opening factor method) with different fire load densities and opening factors. The results confirmed the rate of charring on the wide side of the member obtained by Hadvig. The average charring depth on the lower side of the member was greater than the average charring depth on the wide side when the width of the lower side was smaller than about 180 mm. Considering the mechanical behaviour, the tests showed that a loss of strength and stiffness of the residual cross section occured, and that it continued through the cooling period, caused by continous heat flow to the inner parts of the cross section.

INTRODUCTION

In most structural fire design codes the fire load is given by the standard fire temperature-time curve according to ISO 834. For this type of fire exposure the behaviour of a wood member is fairly well-known for large cross sections: In practical design applications, charring is assumed to occur at an approximately constant rate and the influence of the fire exposure on strength is limited to a depth of about 40 mm below the char-line. For this type of cross sections a very simple model for design can be applied. According to this model a zero-strength layer with a thickness of about 7 mm is removed from the residual cross section, and the remaining part of the residual cross section, i.e. the effective cross section, is assumed to have full strength as in normal design.

So-called natural fires include both the period of increasing temperature and, after the combustible material in the fire compartment is consumed, the subsequent period of cooling. The rise of temperature and the length of these periods is dependent on the fire load and the number and size of openings. Such design method has been used in fire design in Denmark and Sweden for many years, and it is considered to be included in Parts 10 of Eurocodes - Structural Fire Design. Charring of timber under such fire conditions has been investigated by Hadvig /1/. The results of this research were adopted in the Danish Building Code for determination of the charring depth of members in timber structures. Since Hadvig did not perform fire tests with loaded specimens, and there did not exist any experience on the material properties of full-size glued laminated members under such conditions, a series of fire tests was performed at the University of Aalborg under the leadership of F Bolonius Olesen.

The time-temperature relationship in natural fires is dependent of the fire load q_t and the opening factor F of the fire compartment. The opening factor is defined as

$$F = \frac{A}{A_t} \sqrt{h} \qquad [m^{\frac{1}{2}}] \tag{1}$$

where
- A — total area of vertical openings (windows etc.) in m^2
- A_t — total area of floors, walls and ceilings which enclose the fire compartment in m^2
- h — weighted average of heights of all vertical openings (windows etc.) in m.

The charring rate of the wide side of a member in natural fires can, as a simplification of Hadvig's expressions, be described as a function of time according to Figure 1. The initial charring rate β_0 is constant during the time period t_0 with increasing gas temperature in the fire compartment, and the charring rate decreases then until the maximum charring depth is reached after the total time $3t_0$, even though the cooling period is not terminated. The parameters β_0 and t_0 are defined as

$$\beta_0 = \frac{5F - 0{,}04}{4F + 0{,}08} \qquad \left[\frac{mm}{min.}\right] \tag{2}$$

and

$$t_0 = 0{,}006 \frac{q_t}{F} \qquad [min.] \tag{3}$$

where the fire load q_t is in MJ/m^2 and F is given by Equation (1).

The Equations (1) and (2) are valid for an opening factor F between 0,02 and 0,30 $m^{1/2}$, a time period t_0 of not more than 40 minutes and a maximum charring depth on the wide sides of one fourth of the width of the narrow side of the beam.

FIRE TESTS

The test series included 18 full-scale tests with static loading, and 30 additional tests with unloaded specimens for temperature measurements inside the beams. These tests are described in a preliminary test report /2/. A report with the complete test data is in preparation /3/. In this paper the results of nine of the full-scale tests and of one of the additional tests are reported.

The test specimens fullfilled the requirements of strength class L30. The flexural stiffness of each beam was determined prior to each fire test.

The tests specimens of glued laminated timber with a span of 3,60 m were acted upon by two point loads in symmetrical position, the distance between them being 0,9 meters. The middle part of the beam with a length of 2,8 m including the loading devices were inside the furnace. The test beams had the nominal initial depth h_0 of 300 mm and the nominal initial width b_0 of 140, 160 or 185 mm. They were exposed to fire on three sides, the upper side was protected by means of mineral wool batts.

The fire exposure during the tests was governed by a temperature-time relationship determined according to an energy balance method (opening factor method) with different opening factors F and fire load densities q_t. See Table 1.

The initial static loading P_0 in each loading point was 5, 7 and 8 kN respectively and held constant during the major part of the fire tests. The load level was chosen to be low in order to prevent lateral buckling, since the beams were not braced during the period of fire exposure. When the gas temperature in the furnace had decreased to about 300 to 250 °C the fire was extinguished with water, bracings were attached to the test beam, and immediately after the static loading was increased until the failure load P_u of the beam was reached.

The deflection of the beams was measured at two points at distances of 150 and 750 mm from the middle of the beam.

Temperature measurements in the test specimens were made using thermo-couples.

After the tests the char layer was removed by means of brushing off the char and the charring depth was measured at five gauge points located in the transverse direction of the beam. In the case of a long fire exposure duration it was practically possible to make measurements only at the middle three gauge points.

TEST RESULTS

Typical test results are presented in Figures 2 to 4, showing the time-dependent temperature in the furnace, and the corresponding deflection of the test beam at the two gauge points. The indices in the notations refer to the distance of the gauge point from the middle of the beam in centimetres. The figures represent the fire load conditions according to Table 2.

It is obvious that the deflection of the beams increases during the whole cooling period at about the same rate as in the initial period with increasing temperature. The rate of loss of stiffness is not affected by the fact that the maximum charring depth is already reached at the time of $3t_0$ according to Equation (3), which is considerably smaller than the time at which the load was increased.

In Figure 5 typical temperature-time curves are shown. The temperature in the outer parts reaches its maximum in the first part of the cooling period and is affected by the decreasing temperature in the furnace. The temperature of the gauge points in the inner of the cross section continues to increase during the whole test period and exceeds 100 °C even in the midle of the cross section.

The average charring depths are given in Table 3,

where	$d_{char,w}$	average charring depth on the wide side
	$d_{char,n}$	average charring depth on the narrow side.

The agreement of measured and calculated values on the wide side according to Hadvig /1/ is good.

Due to two-dimensional heat flow near arrisses, charring is greater on the narrow side than on the wide side, see Figure 6, where the ratio $d_{char,n}/d_{char,w}$ is shown versus the initial width b_0 of the narrow side. This effect becomes negligible when the width of the narrow side is greater than about 170 to 180 mm. According to Hadvig this effect can be disregarded when the width of the narrow side is at least 80 mm. This result is in contradiction to Hadvig's results. Since the number of tests is limited and the variation of measured values on the lower side was considerable, this result should be regarded as preliminary.

Using the depth h_r and width b_r of the residual cross section, i.e. the initial cross section minus the char layer, the bending strength $f_{m,r}$ was calculated. If we assume that the bending strength of the test beams at normal temperature was 40 MPa (the mean bending strength of Nordic glued laminated timber is about one third greater than the characteristic value), the bending strength ratio

$$k_r = \frac{f_{m,r}}{f_m} \tag{4}$$

of the residual cross section, see Table 3, can be presented as a function of the relative charring depth $d_{char,w}/b_0$, see Figure 7. The regression line is

$$k_r = 0{,}98 - 3{,}02 \frac{d_{char,w}}{b_0} \tag{5}$$

For comparison this has been done also for $f_m = 30$ MPa.

This relationship shows that the amount of charring, or indirectly the duration of time, is important for the reduction of bending strength of the residual cross section. With increasing charring a greater part of the cross section is affected by elevated temperature caused by continuous heat flow during the cooling period.

For comparison, for standard fire exposure, a typical value of the bending strength ratio is 0,8. Values of this order of magnitude are used in some national fire design codes.

With

$$d_{char,w} = 2\ \beta_0\ t_0 \tag{6}$$

see Figure 1, and substitution of Equations (2) and (3) we get approximately

$$k_r = 1{,}0 - \frac{q_t}{27\ b_0\ F}\ \frac{5\ F - 0{,}04}{4\ F + 0{,}08} \tag{7}$$

Thus the bending strength ratio for three-sided fire exposure can be expressed by the width of the narrow side, the fire load and the opening factor.

CONCLUSIONS

In structural fire design the charring rates obtained by Hadvig /1/ according to Equations (2) and (3) and Figure 1 should be used for the wide vertical sides of a member. The charring rates on the narrow side according to Hadvig could not be confirmed. The reason for this might be that the number of tests was too small.

Compared to the conditions at standard fire exposure, the mechanical behaviour at natural fire exposure is different due to the changes of temperature in the residual cross section during the cooling period. In natural fires the bending strength and stiffness is lower than in standard fire. The influence of elevated temperature is no longer concentrated to the outer layer of the residual cross section. Thus the concept of a reduced bending strength of the residual cross section should be applied, e.g. by using a bending strength ratio similar to Equation (5).

REFERENCES

/1/ Hadvig, S., Charring of wood in building fires. Technical University of Denmark, Lyngby, 1981.

/2/ Bolonius Olesen, F., Brandteknisk dimensionering af limtrækonstruktioner, University of Aalborg, 1992

/3/ Toft Hansen, F & Bolonius Olesen, F., Full-scale tests on loaded glulam beams exposed to natural fires. University of Aalborg, 1992

Table 1 Test data and results

No.	h_0	b_0	F	q_t	P_0	P_u
	mm	mm	$m^{1/2}$	MJ/m^2	kN	kN
G 07	298	137	0,04	126	5,0	12,6
G08	296	136	0,06	113	5,0	22,0
G 09	296	136	0,08	151	5,0	20,6
G 23	298	158	0,04	126	7,0	16,7
G 25	298	158	0,08	251	7,0	13,2
G 26	299	158	0,08	151	7,0	30,1
G 32	299	184	0,04	188	8,0	11,6
G 33	298	183	0,06	188	8,0	19,6
G 34	297	183	0,08	251	8,0	19,8

Table 2 Some typical fire load conditions

	Fire load	Opening factor	Time
G 07	small	small	medium
G 09	small	large	short
G 32	medium	small	large

Table3 Test results and evaluation

No.	$d_{char,w}$ test	$d_{char,n}$ test	$3t_o$ calc.	$d_{char,w}$ calc.	h_r	b_r	$f_{m,r}$	f_r / 40	f_r / 30
	mm	mm	min.	mm	mm	mm	MPa	-	-
G 07	24,1	32,2	57	25,2	266	89	16,2	0,405	0,540
G08	16,4	17,7	34	18,4	278	103	22,4	0,560	0,747
G 09	20,3	22,8	34	20,4	273	95	23,6	0,590	0,787
G 23	26,0	28,3	57	25,2	270	106	17,5	0,438	0,583
G 25	32,0	36,9	56	33,9	271	94	15,5	0,388	0,517
G 26	20,0	22,3	34	20,4	276	118	27,1	0,678	0,903
G 32	38,9	40,4	85	37,6	259	106	13,2	0,330	0,440
G 33	29,4	26,4	56	30,7	272	124	17,3	0,433	0,577
G 34	34,1	30,6	56	33,9	266	115	19,7	0,493	0,657

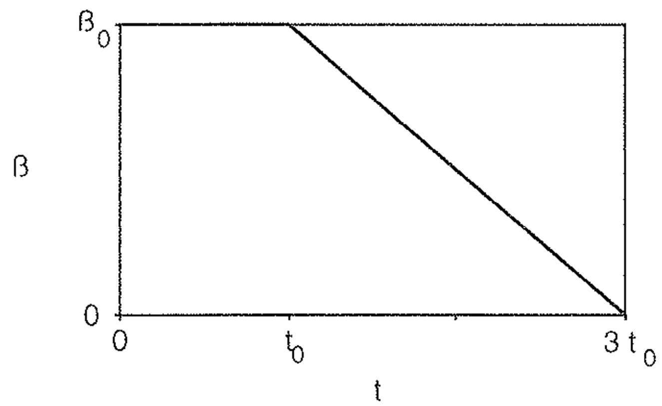

Figure 1 Simplified relationship between charring rate and time

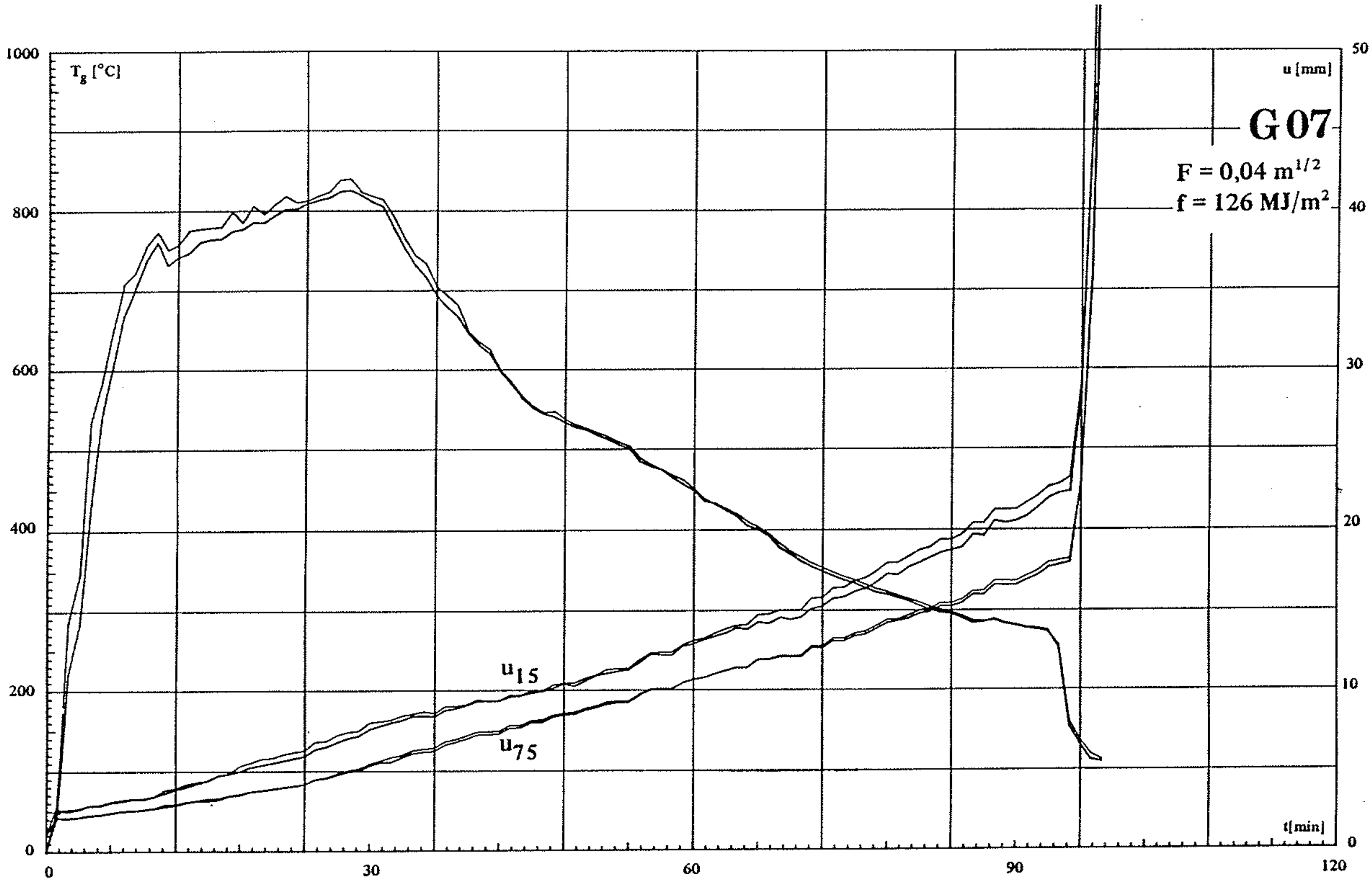

Figure 2 Gas temperature in the furnace and deflection of the test beams versus time

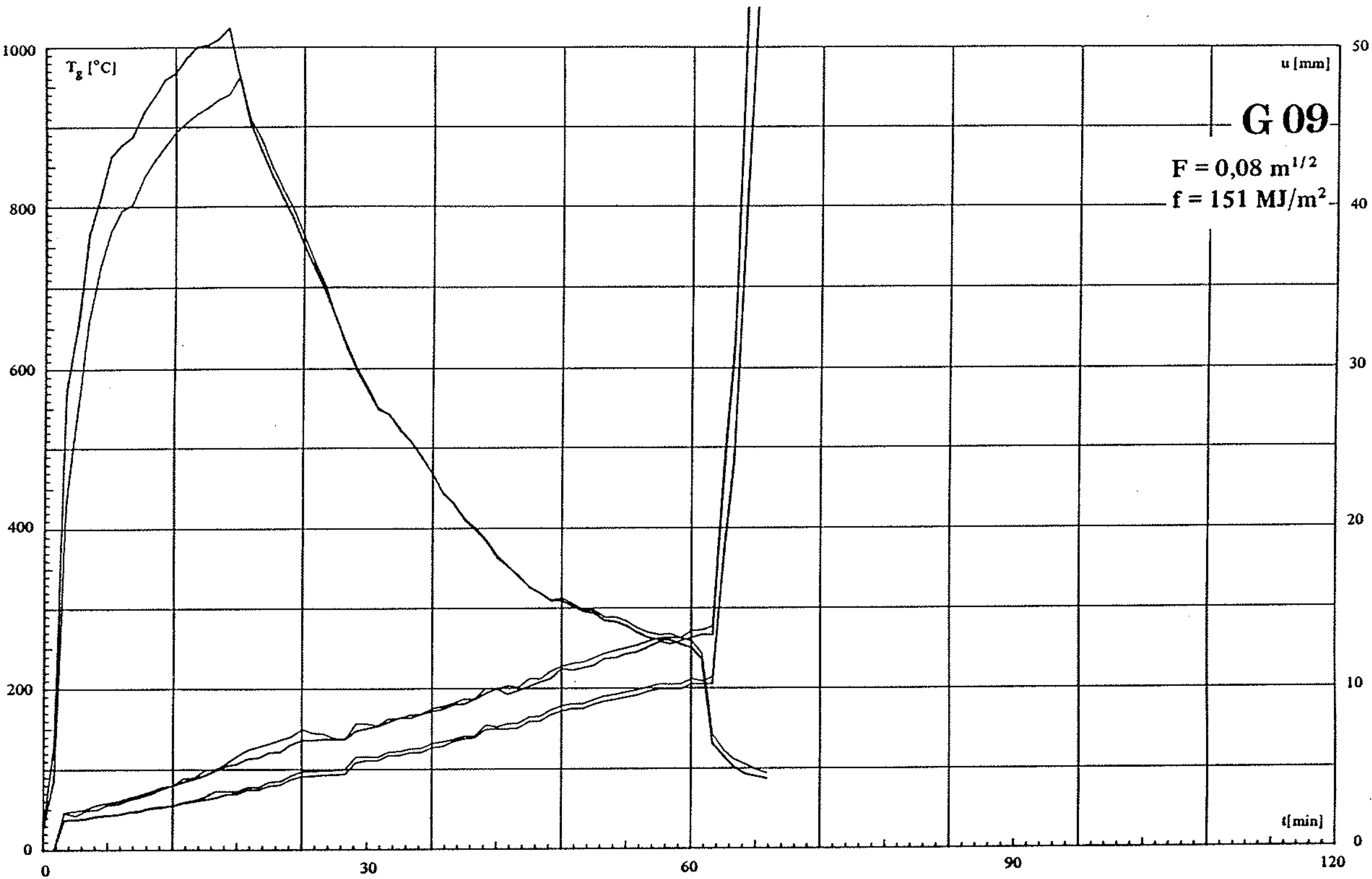

Figure 3 Gas temperature in the furnace and deflection of the test beams versus time

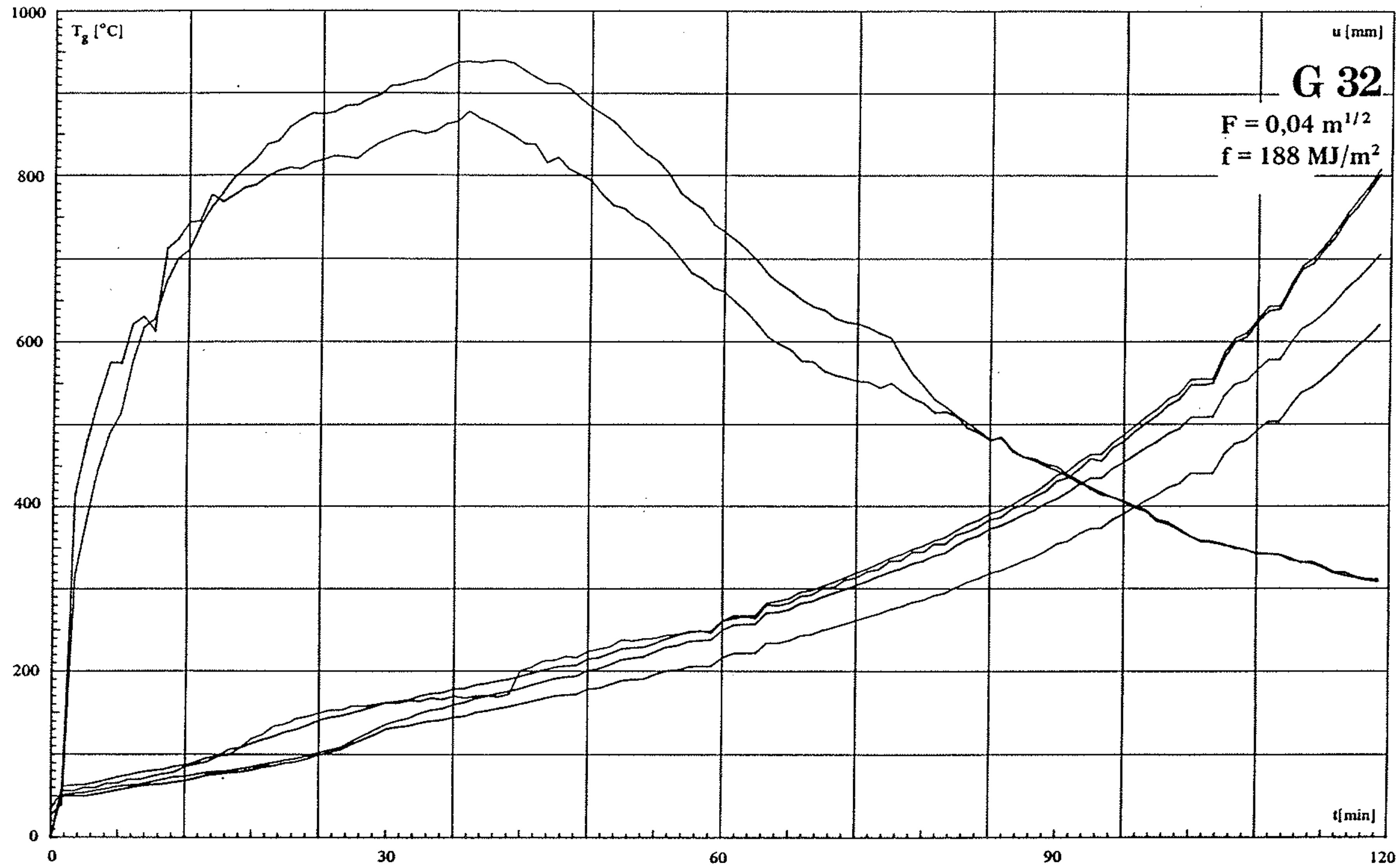

Figure 4 Gas temperature in the furnace and deflection of the test beams versus time

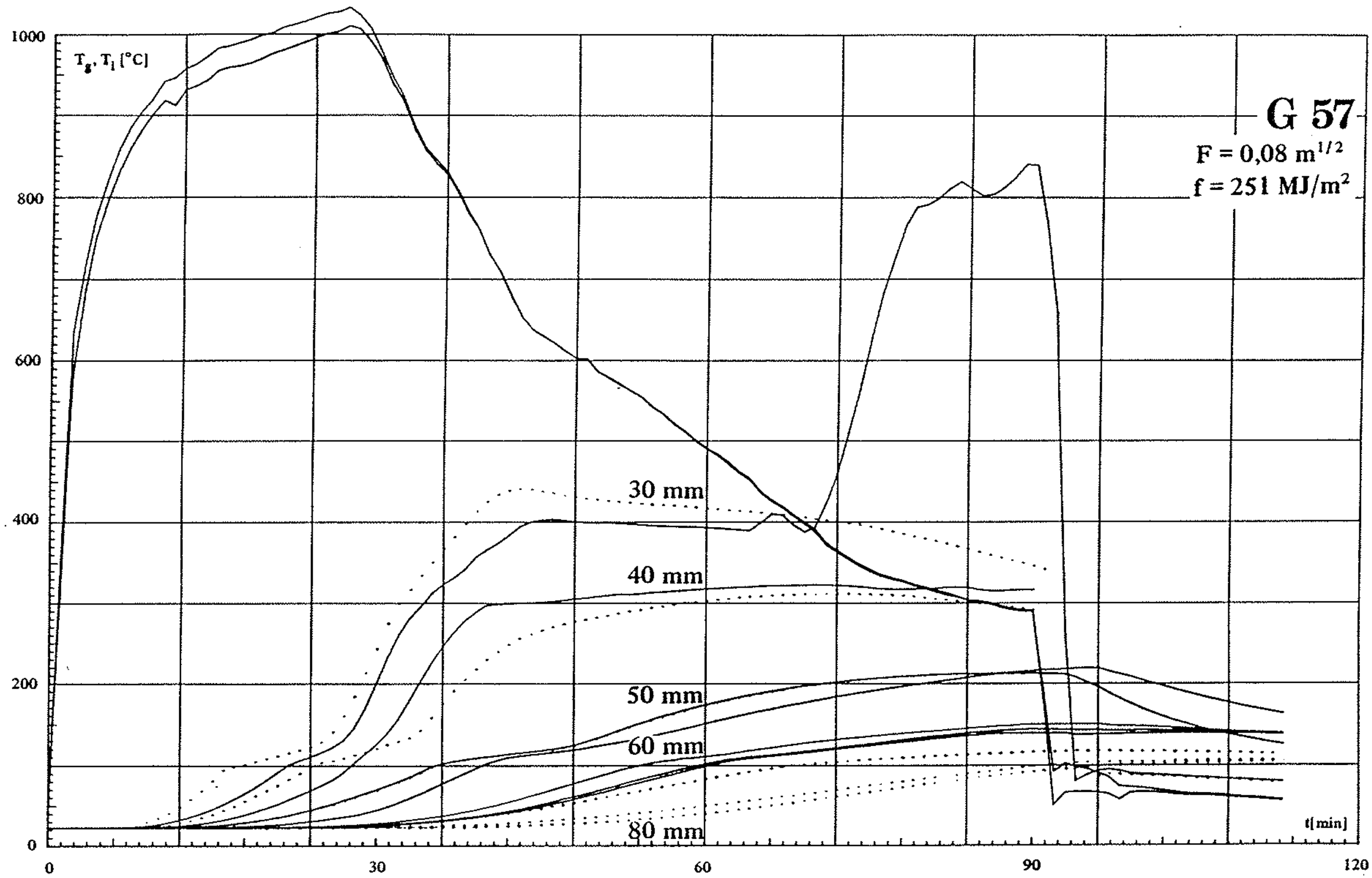

Figure 5 Temperature versus time at different distances from initial surface of the wide side of specimen G 57

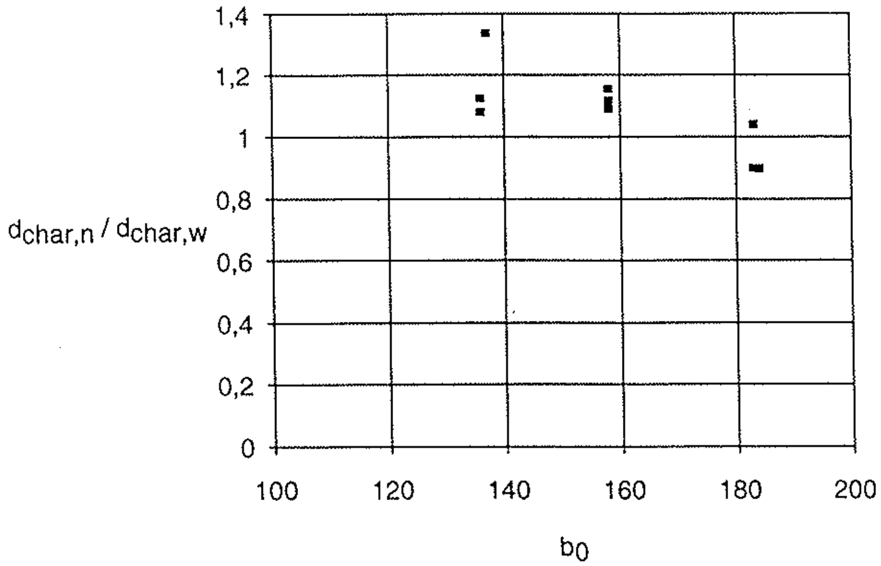

Figure 6 Ratio of charring depths on narrow and wide side versus initial width of narrow side

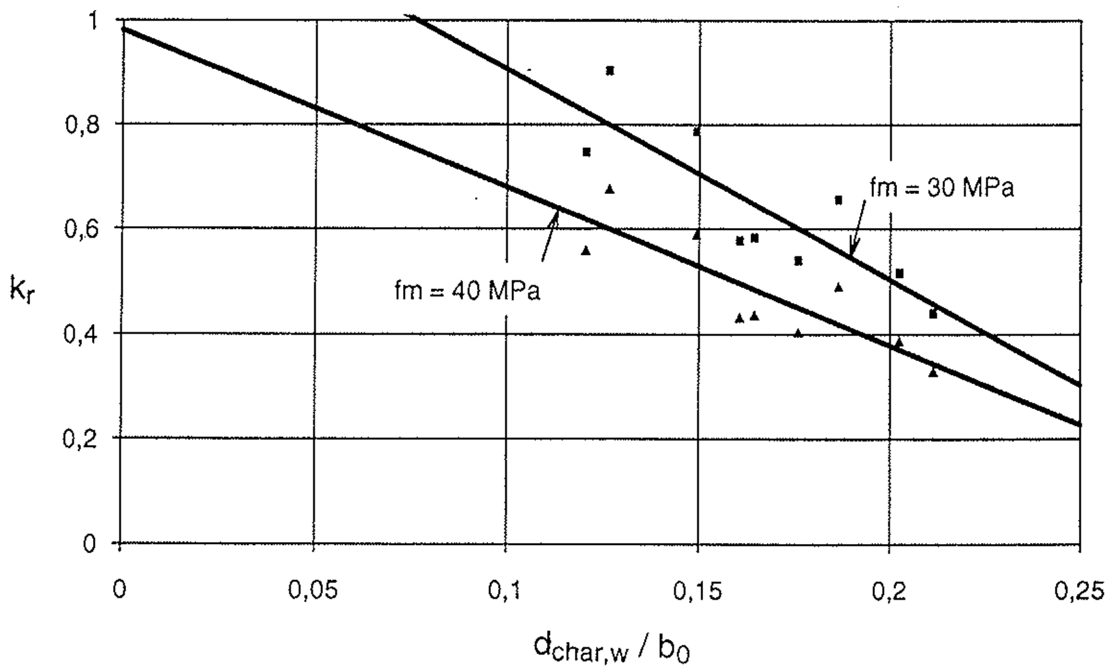

Figure 7 Bending strength ratio of residual cross section versus relative charring depth

CIB-W18/25-17-2

INTERNATIONAL COUNCIL FOR BUILDING RESEARCH STUDIES AND DOCUMENTATION

WORKING COMMISSION W18 - TIMBER STRUCTURES

A BODY FOR CONFIRMING THE DECLARATION OF CHARACTERISTIC VALUES

by

J Sunley
Independent Timber Consultant
United Kingdom

MEETING TWENTY - FIVE

ÅHUS

SWEDEN

AUGUST 1992

A BODY FOR CONFIRMING THE DECLARATION OF CHARACTERISTIC VALUES

Under the system emerging from the implementation of the Construction Products Directive in the European Community (and possibly the EFTA countries) a manufacturer will be able to ' declare ' his own attestation of conformity.This means he will give the ' characteristic values ' to be used in design of products using his material.

There is an assumption in the Construction Products Directive that a single large factory produces a unique product which is subject to a quality control system (where necessary with independent control), has been type tested and the manufacturer declares his characteristic values or strength class. There is also the possibility of a small producer for a local market using a less rigid or even no system at all by claiming he is producing a local product.

With timber it is quite normal to have a large number of small sawmills from many different countries (from EC , EFTA or third countries) producing the same apparent grade/species or strength class. It is likely that due to problems of sampling and differing growth characteristics that type testing from such a large number of small mills will give differing values. Also there is evidence from the past that some suppliers are somewhat ambitious in their claims.

In the UK control is exercised over the approval of grading organisations and grading machines, allocation of characteristic values (or safe design stresses) and of species/grades to strength classes for solid timber and allocation of characteristic values for wood based panel products. We are concerned that such control is not being considered in relation to current CEN work. The UK imports timber and timber products from over 80 countries in the world and over the years we have had many doubtful claims from many suppliers.

In the UK we deal with this problem in two main ways. Firstly we have an independent UK Grading committee which approves grading agencies and grading machines (leaflet attached). Secondly our Timber Design Code committee allocates and publishes design stresses and appropriate strength classes against submitted data. The system works well and everybody accepts it (including supplying countries).

Timber is different from most other constructional materials in that very large quantities of timber from a large number of small outlets cross national boundaries and hence are not suitable to be declared as ' local ' products. The Construction Products Directive operates downwards through constructions rather than upwards through materials and tends therefore not to consider the trading needs of a particular material.

We would like to see some form of approval of grading bodies, grading machines and allocation of characteristic values and strength classes for solid timber and similarly for characteristic values for wood based panels.

It is interesting that CEN/TC 112 and CEN/TC 124 have solved the problem in two areas by drafting standards giving characteristic values for widely used wood based panels and traditional connectors.

Although the chief objective of the Single European Act is to provide a ' market open to all goods and services ' most of the current activity in the construction sector is in the implementation of the Construction Products Directive by governmental regulatory type people in the Standing Committee in Brussels. As a result regulatory matters appear to take precedence over trading ones.

If the timber industries require ' free trade ' within certain acceptable limits they should consider taking some action to achieve this objective.

To obtain a solution to this problem initiative should be taken by an organisation with the necessary expertise and free from any form of community or national governmental control. Such an organisation should be open to all EC and EFTA country membership. Possibilities include CIB/W18, CEN committees (TC 112 and 124) and Eurowood. Maybe when its future is a little clearer EOTC will be able to provide an umbrella for such an activity.

As an aid to discussion I think the first decision to be made is if such a ' clearing house ' is necessary and desirable. If the answer is yes then ways and means of achieving it should follow.

John Sunley

July 1992

CIB-W18/25-102-1A

INTERNATIONAL COUNCIL FOR BUILDING RESEARCH STUDIES AND DOCUMENTATION

WORKING COMMISSION W18 - TIMBER STRUCTURES

ANNEX TO PAPER CIB-W18/25-102-1

EUROCODE 5 - DESIGN OF NOTCHED BEAMS

by

H J Larsen
Danish Building Research Institute, Denmark
Lund Institute of Technology, Sweden

H Riberholt
Structural Research Laboratory
Denmark

P J Gustafsson
Lund Institute of Technology
Sweden

MEETING TWENTY - FIVE

ÅHUS

SWEDEN

AUGUST 1992

Annex to paper CIB-W18/25-102-1

Hans Jørgen Larsen, Hilmer Riberholt & Per Johan Gustafsson

Note on **EUROCODE 5 - Design of notched beams**

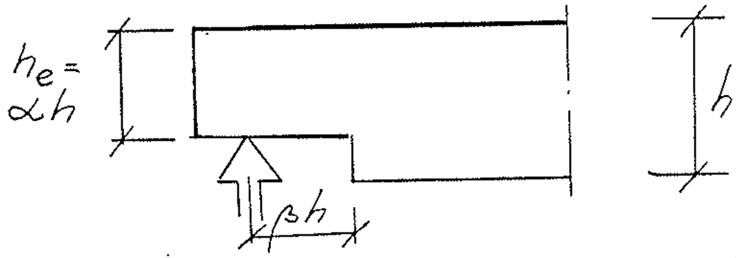

Figure 1

In [Gustafsson, 1991] an expression is derived for the load-carrying capacity of notched beams with a geometry as shown in Figure 1. This expression can be rewritten as follows:

$$V = k_v(\frac{2}{3}bhefv) \tag{1}$$

with

$$k_v = \frac{k \cdot \sqrt{\frac{EW}{f_v^2 h}}}{\sqrt{0.6\alpha(1-\alpha)\frac{E}{G}} + \beta\sqrt{6(\frac{1}{\alpha}-\alpha^2)}} \tag{2}$$

where the symbols have the following meaning

E	modulus of elasticity
G	shear modulus
W	fracture energy in splitting along the grain
f_v	shear strength
k	a factor; theoretically is it 1,5, but in practice smaller values are found and it has to be determined by testing notched beams

In Eurocode 5 a value of 16 is assumed for E/G and the denominater in (2) becomes approximately

$$3\left(\sqrt{\alpha(1-\alpha)} + 0.8\beta\sqrt{\frac{1}{\alpha}-\alpha^2}\right) \tag{3}$$

Characteristic values for E, f_v and the density ρ are given in [EN 384, 1991] for a wide range of strength classes. Examples are given in Table 1.

In [Larsen & Gustafsson, 1990] the following relationship was found between the mean values of W and ρ in kg/m^3

$$W = 1{,}04\rho - 146 \text{ N/m} \tag{4}$$

For ρ between 300 and 450 (4) can be replaced by

$$W = 0{,}65\rho \tag{5}$$

In Table 1 EW/f_v^2 has been calculated using (5) and assuming that the ratios between characteristic and mean values are the same for E, W, and f_v.

Table 1

Strength Class		C14	C22	C27	C30	C35	C40	C70
E	N/mm²	4700	6700	8000	8000	8700	9200	16700
f_v	N/mm²	1,7	2,4	2,8	3,0	3,4	3,8	6,2
ρ	kg/m³	290	340	370	380	400	420	900
W	N/mm	0,190	0,220	0,235	0,245	0,260	0,280	0,585
$\sqrt{EW/f_v^2}$	$\sqrt{\text{mm}}$	17,6	16,0	15,5	14,8	14,0	13,4	16,5

As an approximation the square root can be taken as a constant, i.e.

$$k_v = \frac{K}{\sqrt{h}\left(\sqrt{\alpha(1-\alpha)} + 0.8\beta\sqrt{\frac{1}{\alpha} - \alpha^2}\right)} \tag{6}$$

In [Gustafsson, 1991] the result from nine test series is summarized. In Table 2 K is calculated from the same tests. Where f_v is not given in the reports a value of f_v = 4 MPa has been assumed (corresponding to a rather high grade: C27).

For structural timber the average value of test results is K = 5,18, for glued laminated timber the average is K = 6,67. K = 5 corresponds to k = 1 in (2).

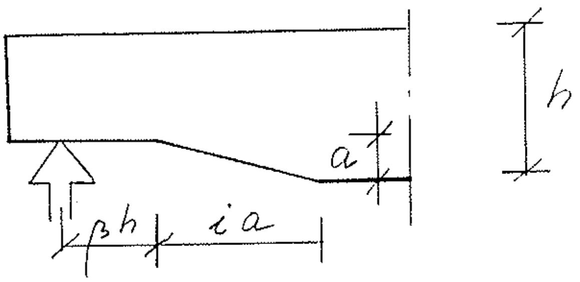

Figure 2

[Riberholt et al., 1992] have made tests with tapered notched beams with a geometry as shown in Figure 2. The results are summarized in Table 3 together with a proposal from [Riberholt, 1991] for an inclination factor k_i.

Table 2. Values of k_v and K for various softwood beams.

b x h mm^2	α	β	k_v from tests	K	K_{mean}	Source. Material. Number of tests.
63 x 125	.75 .50 .25	.40	0,729 0,543 0,495	5,82 5,61 5.90	5,77	(Larsen & Riberholt, 1972). Whitewood and redwood. 63 + 2 x 68 tests.
32 x 125	.917 .833 .750 .667 .583 .500 .333	.25	0,878 0,718 0,625 0,565 0,558 0,592 0,551	3,62 4,05 4,17 4,19 4.45 4,96 4,90	4,33	(Möhler & Mistler, 1978). Whitewood. 159 tests.
100 x 600	.917 .833 .750 .667 .500	.42	0,744 0,599 0,327 0,320 0,279	8,09 8,98 5,83 6,40 6,45	7,15	(Möhler & Mistler, 1978). Gluelam. 3 x 2 tests.
45 x 50 100 200	.50	.50	0,744 0,543 0,439	5,41 5,59 6,39	5,80	(Carlsson et al, 1983). Redwood. 3 x 2 tests.
45 x 45 195	.50	.50	0,670 0,350	4,63 5,03	4,83	(BML, LTH, 1985 + 86). Redwwod. 2 x 10 tests.
79 x 305 79 x 457	.70	2.50 5.50 2.50 5.50	0,171 0,089 0,141 0,060	7,16 7,34 7,22 6,06	7,07	(Murphy, 1986). Gluelam. 3 x 2 + 1 tests.
44 x 12 48 192	.75	.50	1,235 1,023 0,484	3,36 [1)] 5,56 5,26	5,41	(Gustafsson & Enquist, 1988). Redwood. 3 x 7 tests.
45 x 95 195 85 x 185	.875 .75 .50 .25 .75 .50 .75 .50 .75 .50	.34 .66 .159 .168	1,079 0,826 0,543 0,536 0,729 0,398 0,554 0,376 0,852 0,491	5,24 5,41 4,55 5,08 6,37 4,65 4,21 3,51 6,39 4,52	4,99	(Riberholt et al, 1992). Whitewood. 10 x 6 + 2 x 6 tests.
90 x 200 300 160 x 567	.75 .50 .833 .722 .50 .50 .50	.175 .150 .300 .123	0,952 0,592 0,766 0,606 0,536 0,472 0,361	7,48 5,74 6,08 5,92 6,12 6,68 5,42	6,21	(Riberholt et al, 1992). Gluelam. 7 x 4 tests.

1) Value disregarded because the geometry is atypical for practice.

Table 3. Strength of beams with taper relative to similar beams without taper (i = 0). From [Riberholt et al, 1992].

b x h mm^2	α	β	i	Relative strength	k_i = 1 + 1,1$i^{1,5}$/ h
Structural timber					
45 x 95	0,50	0,34	0	1	1
			1	0,95	1,11
			2	1,95	1,32
			3	1,92	1,59
			5	2,64	2,26
		0,66	0	1	1
			3	2,35	
	0,75	0,34	0	1	1
			1	1,03	1,11
			3	1,41	1,59
85 x 185	0,50	0,17	0	1	1
			3	1,55	1,42
	0,75	0,17	0	1 [1)]	1
			3	0,88 [1)]	1,42
Glued laminated timber					
90 x 300	0,50	0,15	0	1	1
			1	1,15	1,06
			2	1,28	1,18
			5	1,92	1,71
			8	1,94	2,44
		0,30	0	1	1
			2	1,49	1,18
160 x 567		0,12	0	1	1
			2	1,13	1,13

[1)] The strength for i = 0 is unusually high.

Conclusion

For Eurocode 5 the following design requirements are proposed.

For beams notched at the ends the shear stress shall be calculated using the effective (reduced) depth h_e.

For beams notched on the loaded side it should be verified that

$\tau_d \le k_v f_{v,d}$

where for solid timber

$$k_v = \frac{5\left(1 + \frac{1.1\, i^{1.5}}{\sqrt{h}}\right)}{\sqrt{h}\left(\sqrt{\alpha(1-\alpha)} + 0.8\beta\sqrt{\frac{1}{\alpha} - \alpha^2}\right)}$$

For glued laminated timber k_v should be taken 30 per cent higher.

k_v should not be taken greater than unity.

References

Gustafsson, Per Johan. Eurocode 5, Draft Design Criterion for Notched Beams. Proceedings of International Timber Engineering Conference, London. p. 166-174. 1991.

Gustafsson, Per Johan and Enquist, B. Träbalks hållfasthet vid rätvinklig urtagning. Report TVSM-7042, Div. of Struct. Mech., Lund Inst. of Techn., Sweden. 1988.

Larsen, H. J. and Gustafsson, Per Johan. The Fracture Energy of Wood in Tension Perpendicular to the Grain. Proceedings of CIB W18, Meeting 23, Lisbon. Paper CIB W18A/23-19-2.

Larsen, H. J. and Riberholt, H. Forsøg med Uklassificeret Konstruktionstræ. Rapport nr. R31, Department of Structural Engineering, Technical University of Denmark. 1972.

Murphy, J. F. Strength and Stiffness Reduction of Large Notched Beams. Journal of Structural Engineering, Vol. 112, No. 9, pp 1989-2000, ASCE. 1986.

Möhler, K. and Mistler, H-L. Untersuchungen über den Einfluss von Ausklinkungen in Auflagerbereich von Holzbiegeträgern auf die Tragfestigketit. Universität Karlsruhe (TH). 1978.

Riberholt, H. Eurocode 5, Notched Beams. A proposal for Design.Note. 1991-12-2.

Riberholt, H. et al. Timber Beams Notched at the Support. Report under publication. Department of Structural Engineering, Technical University of Denmark. 1992.

EN 384, European Standard, Structural Timber - Determination of characteristic values of mechanical properties and density.

CIB-W18/25-102-1

INTERNATIONAL COUNCIL FOR BUILDING RESEARCH STUDIES AND DOCUMENTATION

WORKING COMMISSION W18 - TIMBER STRUCTURES

LATEST DEVELOPMENT OF EUROCODE 5

by

H J Larsen

Danish Building Research Institute

Denmark

Lund Institute of Technology

Sweden

MEETING TWENTY - FIVE

ÅHUS

SWEDEN

AUGUST 1992

1. INTRODUCTION

The latest draft for Eurocode 5, Part 1: General Rules and Rules for Building, was finalized by April 1992. It is expected to be adopted as a European Prestandard (an ENV) in November 1992 for a period of 3 years. After this period a redrafting will start aiming at a European standard that will eventually replace the corresponding national documents. The basis for this redrafting will be the experience gained by experimental use of Eurocode 5, trial calculations of representative structures in different countries and new results from research.

CIB W18 can have a great influence on the final version of Eurocode 5 by reverting to the method of work that succesfully led first to the CIB Structural Timber Design Code (1983) and the first complete version for Eurocode 5 (1987): Discussions of proposal for clauses in the code based on literature surveys and research leading to consensus on a final proposal. Because of the time pressure this procedure has not been followed by the final drafting of Eurocode 5 (1992), but the three ENV-years (minimum) will hopefully be used in this manner.

This paper describes some of the major changes and their background. It also identifies items still unsatisfatorily treated.

Joints are not treated in this paper but in a later paper by Ehlbeck and Larsen.

2. SAFETY

There is a disparity between the fine details in the code rules for the calculation of stresses and deformations in the members and the coarse way in which safety/reliability is treated.

The problem is that no safety philosophy has been formulated for timber structures, and therefore Eurocode 5 (1992) has had restricted manouvering possibilities.

The bounds from the other Eurocodes are the partial safety factors for actions common for all materials (γ_G = 1.35 for permanent actions and γ_Q = 1.5 for variable actions), and the choices of partial safety factores for materials made by Eurocode 2, Concrete (γ_m = 1.5) and Eurocode 3, Steel (γ_m = 1.1). In Eurocode 5 (1992) a value of γ_m = 1.3 is proposed for timber and wood-based materials, a lower value would probably be questioned by the other materials.

An internal Eurocode 5 bound is the knowledge about the influence on the strength of the load duration, reflected in the factor k_{mod} in the equation for determining the design strength f_d from the characteristic one, f_k:

$$f_d = k_{mod} f_k/\gamma_m$$

The Eurocode 5 (1992) k_{mod} values are given in table 2.1 for service classes 1 and and 2 (moisture content below about 20%).

Table 2.1 Load Duration Factor k_{mod} for Service Classes 1 and 2

Load Duraction Class	Order of Accumulated duration of Characteristic Load	k_{mod}
Permanent	more than 10 years	0,6
Long-term	6 months - 10 years	0.7
Medium-term	1 week - 6 months	0.8
Short-term	less than 1 week	0.9
Instantaneous		1.1

For permanent load alone the global safety level becomes 1.35 · 1.3/0.6 = 2.93. For a load combination with a ratio of 2 between variable and permanent loads the global safety varies between 2.69 (long-term) and 2.09 (short-term). Some countries will find some of these values rather high.

A main problem is that there are in reality no guidelines on how to assign a load to a load duration class, neither in Eurocode 5 nor in Eurocode 1, Basis of Design. There is therefore a risk that national authorities will make different decisions, and probably with a preference for the classes with the longer duration. It is therefore suggested that CIB W18 prepares quidelines on how to assign actions to load duration classes.

A departure point may be the distinction made in the Eurocodes between 4 representative values of variable actions

- characteristic value, Q_k, corresponding in general to a 50 years return period
- combination value, $\psi_0 q_k$
- frequent value, $\psi_1 Q_k$
- quasi permanent value, $\psi_2 Q_k$

The present trend is to refer the characteristic value to a load duration class. Another solution might be to refer the different parts of actions to different classes.

For snow-load, where the following values are proposed in Eurocode 1

$\psi_0 = 0.6; \quad \psi_1 = 0.2; \quad \psi_2 = 0$

20% of the load might be regarded as long-term/medium-term and 80% as medium-term/short-term.

For imposed floor loads where

$\psi_0 = 0.7; \quad \psi_1 = 0.5; \quad \psi_2 = 0.3$

are proposed, only 30% should be regarded as permanent, 20% as long-term and 50% as medium-term.

3. GLULAM

Eurocode 5 (1992) gives design rules for glulam members assuming that the basic material parameters - bending strength, tension strength, ... and moduli of elasticity - are known.

There are, however, no provisions on how to determine these values for a given lay-up (mumber and thickness of laminations, species and grades etc). Some guidelines are given in an annex to the draft CEN-standard CEN TC 124.207: Glued Laminated Timber - Strength Classes. This annex corresponds to CIB W18 paper 23-12-4: Riberholt, H., Ehlbeck, J. and Fewel, A.: Glued Laminated Timber - Strength classes and determination of characteristic properties.

The guidelines are based on a compilation of "lamination-factors" in existing European codes and not on a general model as for example the Karlsruhe-model described in a number of papers, see CIB W18 paper 24-12-1: Colling, F., Ehlbeck, J. and Görlacher, R.: Glued Laminated Timber, Contribution to the determination of the bending strength of glulam beams. This model represents a big step forward, but there are still some details that have to be solved - e.g. the relationship
between the strength of the finger joints in the beam and the strength determined by the standard bending test.

A controversial question in relation to glulam beams is the depth factor. The results from standardized short-term test with beams with depths between 300 and 900 mm and the Karlsruhe-model show depth effect corresponding to a factor of $(h_o/h)^x$ where h is the depth, h_o a reference depth and x a exponent in the range 0.15 - 0.4, see CIB W18 paper 23-12-12: Ehlbeck, J. and Colling, F.: Bending Strength of Glulam Beams, A design proposal. An acceptance of this depth factor would, however, for big structures lead to much bigger sizes than used today and there are no indications that today's design practice is unsafe.

During the final discussions on Eurocode 5 (1992) it was therefore decided to disregard the depth effect and in reality base the design on values found by testing 300 mm deep beams. The arguments being

- Glulam has more uniform properties than normal timber. (The logical consequence would be to give lower γ-values for glulam, but this was not found acceptable for "political" reasons)
- The depth effect is only proved for short-term testing, long-term evidence is missing: the effect might be counteracted by "creep"
- The characteristic loads are only valid for rather small contributary areas; for large structures their use leads to unreasonably safe structures (if true, the same argument would apply to other materials)
- For deep beams there is a beneficial effect from the increasing number of laminations not taken into account in the present models.

Obviously the situation is dissatisfactory. There is a need for research aimed at better models for the strength of glulam - long-term and short-term.

4. SERVICEABILITY LIMIT STATES

The section on serviceability has been redrafted completely.

Requirements to the stiffness of domestic floors have been introduced based on a proposal from Sv.V. Ohlsson (see Serviceability Criteria - Especially floor vibration criteria, in Proceedings of the 1991 International Timber Engineering Conference, London).

For deflection calculations the main changes are

- In Eurocode 5 (1987) the final deformation u_{fin} (deflection, slip etc) was derived from the initial deformation, u_{inst}, calculated with mean short-term stiffness values as

  $u_{fin} = k_{creep}\, u_{inst}$

  In Eurocode 5 (1992) this expression is replaced by

  $u_{fin} = (1 + k_{def})\, u_{inst}$

  bringing the presentation in line with the normal way of presenting time related deformation behaviour and indicating that the increase in the deformation is not related to creep alone, but also for example to moisture and the combined effect of moisture variations and creep.

- There is a very detailed table giving k_{def}-values for timber, glulam, and different types and qualities of wood based panels. The values are based on a large number of test results made available by the members of CEN TC124, notably the Finnish member. The test from which they are found, differ, however, widely, and the tables contain a large amount of engineering judgement: there is a big need for standardized test and evaluation methods.

- Slip values are given for all dowel-type fasteners as function of diameter and densities of the jointed timber. The basis for these are given in a Discussion Note by Jürgen Ehlbeck: Slip moduli for dowel-type fasteners.

Regarding deformation limitation there are two schools. One maintains that there should be no general prescribed deflection criteria. It is the responsibility of the designer to limit the deformations having regard to as well the appearance of the finished structure as the functional requirements (avoiding damages to surfacing materials, ceilings, partitions and finishes). This school wants to have detailed codified rules on how to determine the deformations to relieve the designers of the responsibility for this side of the design process.

The other school wants also to have codified deflection limits relieving the designers also from the responsibility of deciding on acceptable deflection limits.

The Eurocode 5 rules are biased towards the first school, giving only deflection limits for simple beams and in a very vaque form ("... if it is found appropriate to give general limits to deflections, the following values are recommended.").

5. BENDING

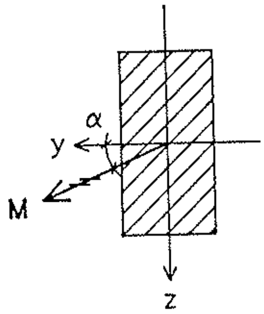

For bending of a beam with a rectangular cross-section it is required that the more stirngent of the following two conditions shall be satisfied:

$$k_m \frac{\sigma_{m,y}}{f_{m,y}} + \frac{\sigma_{m,z}}{f_{m,z}} \leq 1$$

$$\frac{\sigma_{m,y}}{f_{m,y}} + k_m \frac{\sigma_{m,z}}{f_{m,z}} \leq 1$$

with $k_m = 0.7$.

$\sigma_{m,y}$ and $\sigma_{m,z}$ are the bending stresses from moments about the principal axis and $f_{m,y}$ and $f_{m,z}$ are the corresponding bending strengths (they may be different because of different depth factors).

The introduction of the factor k_m is based on an intuitive feeling that the load-carrying capacity is not exhausted just because the stresses - calculated by the unrealistic theory of elasticity - reached the bending strength in a small zone at a corner. Test results to verify the expression or to improve it is very much required.

The maximum value of the form factor is about 15%, for a square for bending over the diagonal for rectangular cross-section for smaller values of α, see figure 15. For $h = 4b$ the form factor is maximum for $\alpha \sim 15°$.

There is no form factor for round cross-sections. Poles should be regarded as an independent material and not calculated with the strength values found for rectangular sawn timber.

6. SHEAR

For shear the detailed rules of Eurocode 5 (1987) for glulam, taking into account volume and load distribution has been given up. The majority found that the complexity of the design was inappropriate to the importance of the problem in practice. For unnotched beams the design is based on the traditional strength theory (as opposed to a fracture theory).

It is still assumed that the shear strength is dependent on the stressed volume, and Eurocode 5 relates the characteristic strength in shear to a uniformly stressed volume of 0.0005 m^3, but the value found for this volume is used for all beams irrespective of their size.

For notched beams completely new design rules based on fracture mechanics have been given, covering also tapered notches. The basis for these rules are given in the enclosed annex.

7. INSTABILITY

For columns the design is as agreed by CIB W18 based on the proposal by Hans Blass - see CIB W18 paper 20-2-2: Blass, H.J.: Design of Timber Columns, and paper 21-110-1: Larsen, H.J.: CIB Structural Timber Design Code - Proposed changes. For lateral instability of beams there are no changes from Eurocode 5 (1987). The recommendations by CIB W18 to introduce the design method proposed by Harold Burgess - see CIB W18 paper 21-101-1 - have not been followed. The two methods give approximately the same results, but the Burgess method is more complicated and requires instability design for all beams, not only for beams with a slenderness ratio above a certain treshold.

The two cases columns (with or without lateral loads) and beams for which instability is possible, are unfortunately still treated as two completely separate cases and not as two extremes of a general problem.

Some of the expressions for instability and other cases requiring 2nd order elastic calculations are unnecessarily complicated in their formulation because the concept of a design modulus of elasticity

$$E_d = k_{mod} E_k/\gamma_m$$

has not been introduced explicitely. The idea of accepting such a value has been fiercely opposed by Eurocode 2 and Eurocode 3, for steel with the argument that E was a natural constant without uncertainty.

8. COMBINED STRESSES

At the surface of a tapered beam the stress is parallel to the surface. There is a combined stress situation with axial stresses parallel and perpendicular to the grain and shear stresses.

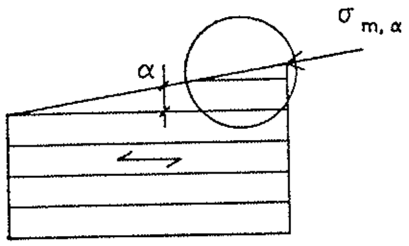

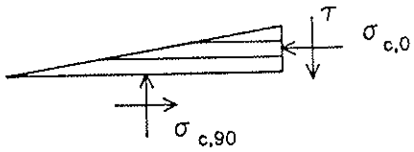

Eurocode 5 (1987) was in principle based on Norris' failure criterion

$$\left(\frac{\sigma_{c,0}}{f_m}\right)^2 + \left(\frac{\sigma_{c,90}}{f_{c,90}}\right)^2 + \left(\frac{\tau}{f_v}\right)^2 \leq 1$$

and the corresponding for tension, see CIB W18 paper 9-6-4: Möhler, K.: Consideration of Combined Stresses for TImber and Glued Laminated Timber, and paper 11-6-2: Möhler, K.: Addition to paper CIB W18 19-6-4.

In Eurocode 5 (1992) a simple Hankinsson expression is used

$$\sigma_{m,\alpha} \leq f_{m,\alpha} = \frac{f_m}{\frac{f_m}{f_{c,90}} \sin^2\alpha + \cos^2\alpha}$$

The latter formula is much simpler to use, and E. Gehri has shown that it gives approximately the same results as Norris' formula, but fits test results slightly better, see Einführung in die Norm SIA 164 (1981) Holzbau, Publikation 81-1, Baustatik und Stahlbau, ETH, Zürich.

9. CURVED AND CAMBERED BEAMS

The expressions for calculating the stresses in tapered beams and pitched cambered beams look very different from those of Eurocode 5 (1987), but the results are only marginally different: the expression in both Eurocode versions are approximations to the stresses found by finite-element calculations or similar methods. The main difference is the choice of the reference geometry parameters. In Eurocode 5 (1987) the correction factors were applied to stresses calculated with the depth at the tangent point, in Eurocode 5 (1992) the apex depth is used.

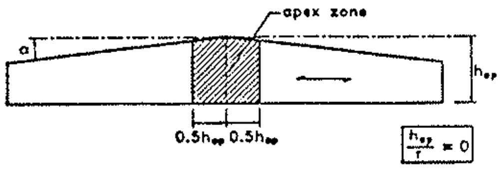

a) Double tapered beam

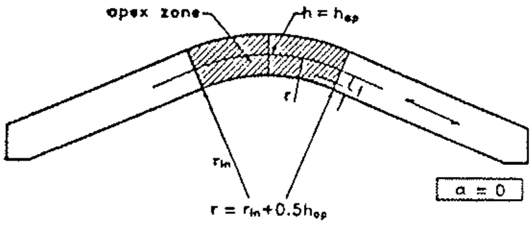

b) Curved beam (constant depth)

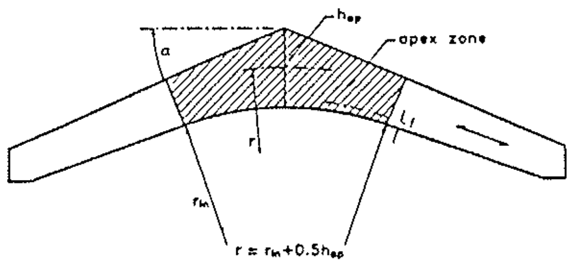

c) Pitched cambered beam

For tension perpendicular to the grain it is required that

$$\sigma_{t,90} \leq k_{vol}\, k_{dis}\, f_{t,90}$$

The volume factor is unchanged

$$k_{vol} = (V_0/V)^{0,2}$$

where V_0 is a reference volume and V is the stressed volume (the volume of the apex zone).

The distribution factor is given as

k_{dis} = 1.4 for double tapered and curved beams, and

k_{dis} = 1.7 for pitched cambered beams

valid for all loading types although theoretically the moment distribution influences the distribution factor (for a curved beam with constant moment $k_{dis} = 1/0.83 = 1.2$ and $1/0.83^2 = 1.45$ for a moment varying parabolically over the curved part).

In CIB W18 paper 24-12-2: Ehlbeck, J. and Kürth, J.: Influence of Perpendicular-to-grain Stressed Volume on the Load-carrying Capacity of Curved and Tapered Glulam Beams a value of k_{dis} = 1.4 was proposed for all beams. The value k_{vol} = 1.7 is, however, not in disagreement with the results in Ehlbeck's and Kürth's paper and reflects that the volume with high stresses is much smaller for the pitched cambered beams than for curved beams.

It should be noted that there are some discrepancies between the theoretical results and the test results, reported in CIB W18 paper 19-12-3: Colling, F.: Influence of Volume and Stress Distribution on the Shear Strength and Tensile Strength Perpendicular to the Grain, and more research is needed.

10. TRUSSES

The section on trusses is an edited version of the proposal given in CIB W18 paper 23-14-2: Riberholt, H.: Proposal for Eurocode 5 Text on Timber Trussed Rafters.

The general rules for trusses are given in the main text, special rules for trusses with punched metal plate fasteners are given in an annex with the same status as the main text, the reason for an annex is that the section is rather voluminous and of interest to only a minority of the users of the code.

11. BRACING

The section on bracing in Eurocode 5 (1987) was based on a second order analysis, assuming initial deviations from straightness. It contained, however, a number of errors and never got into an acceptable shape.

The 1992-version is therefore simplified considerably. The basis for this simplification is given by Pierre Dubas in the ETH publication mentioned in 8.

12. DETERMINATION OF CHARACTERISTIC VALUES

Annex A* in Eurocode 5 (1992) gives a method for estimation of the characteristic value from test results and a method to estimate whether the 5-percentile for a sample drawn from the production is above the declared value.

The basis for the proposal is the following.

The characteristic value is the population 5-percentiles, i.e. the value found by testing an unlimited number. If only a limited number of test results is available, it is necessary to choose a level "of confidence" with which the estimation shall be made, and since the information is rarely sufficient to determine the distribution function, a prescribed distribution function shall be used.

In Eurocode 5 a log-normal distribution is assumed and rather arbitrarily a confidence level of 84.1% is chosen; it corresponds to one standard deviation from the mean.

---

* Annex A is based on a draft from professor Gunnar Mohr, The Danish Engineering Academy, who has been responsible for the corresponding sections in the Danish Codes of Practice.

This leads to

$$x_k = m \cdot \exp [- (1.645 + \frac{1}{\sqrt{n}}) v]$$

where the symbols are defined as follows

x_k characteristic value of the property x

m mean value of x

v coefficient of variation of x

n number of test results

To obtain a constant reliability level the partial coefficient should be a function of the coefficient of variation. This is, however, not practical; instead the characteristic value is adjusted. As a good approximation this can be done by multiplying the directly estimated value by a factor $\exp[v_0 - v]$, where v_0 is a chosen reference coefficient of variation. In this case $v_0 = 0.15$ is chosen, leading to formuli A2.2a and A2.2b in Eurocode 5 (1992):

$$x_k = m \cdot \exp [- 2,645 + \frac{1}{\sqrt{n}}) v + 0.15]$$

If the characteristic value is determined for a sample drawn from a production, it can be argued that the production should be accepted even when the characteristic value falls slightly below the assumed (declared) characteristic value: by the testing the uncertainty to be covered by the partial safety factors is reduced. In Eurocode 5 (1992) a 5% reduction in the requirement is accepted, corresponding approximately to a reduction of the safety index by 0.25.

CIB-W18/25-17-3

INTERNATIONAL COUNCIL FOR BUILDING RESEARCH STUDIES AND DOCUMENTATION

WORKING COMMISSION W18 - TIMBER STRUCTURES

MOISTURE CONTENT ADJUSTMENT PROCEDURES FOR ENGINEERING STANDARDS

by

D W Green
J W Evans
Forest Products Laboratory
U S A

MEETING TWENTY - FIVE

ÅHUS

SWEDEN

AUGUST 1992

INTRODUCTION

Over the last 10 years, a considerable amount of work has been conducted at, or in cooperation with, the U.S. Forest Products Laboratory (FPL) on the effect of moisture content (MC) on the mechanical properties of standard 38-mm (nominal 2-inch) thick structural lumber (Green and Evans, 1989). These studies have shown that the change in properties with the change in MC is a function of lumber quality and that strength does not necessarily increase with decreasing MC, Figure 1. These studies have produced new analytical models for relating lumber properties to change in MC (Evans, et.al, 1986). Additional simplified models for incorporating this information into engineering design standards have been recently approved in the U.S. (ASTM, D1990) and replace analytical models given in ASTM D245. The FPL research, as well as research by Madsen (1975, 1982) and Hoffmeyer (1978), was used to establish proposed MC-property adjustment recommendations for Eurocode 5. The research on which the U.S. models for adjusting bending properties are based utilize test results from only two species: Douglas-fir and Southern Pine (McLain, et. al., 1984, and Aplin, et.al, 1986). To evaluate the applicability of the D1990 simplified adjustment procedure, and the proposed Eurocode 5 procedure, to other species a limited study was conducted on MC-bending property relationships for 38- by 89-mm (nominal 2- by 4-in.) lumber of five additional species (Green and Evans, 1991).

The objective of this paper is to evaluate analytical models for describing the effect of change in MC on the bending properties nominal 2x4 dimension lumber for five additional species. This work is limited to models applicable to engineering design codes, and to MC's of 10-percent or more.

BACKGROUND

Intersection Moisture Content

The mechanical properties of small, clear wood specimens decrease with increasing moisture content up to some moisture content level. Past this level, properties are independent of moisture content (USDA, 1987). The moisture content is called the intersection moisture content, Mp.

In the United States the value of Mp of clear wood has been traditionally obtained by fitting an analytical model to property-moisture content data for dry lumber and observing where this model intersects a horizontal curve drawn through data for green wood. From plots of the logarithm of properties versus moisture content Wilson (1932) established Mp values for a few species, Table 1. The Wood Handbook (USDA, 1987) recommends using Mp = 25% for all other species. This is the average value of the species listed in Table 1. ASTM D2915, on the other hand, cites a formula for achieving the adjustments factors given in ASTM D245. The standard assumes an Mp value of 22% for all properties. Neither of these historical procedures are currently used to assign allowable for bending, tension parallel or compression parallel to the grain properties to dimension lumber in the United States.

Analytical Models

Previous studies at the FPL utilized data for almost 8,000 pieces of two species of lumber (Douglas-fir and Southern Pine). The lumber was of three sizes (38- by 89-mm, 38- by 140-mm, and 38- by 184-mm; nominal 2- by 4-in., 2- by 6-in., and 2- by 8-in.) and three grades (Select Structural, No. 2, and No. 3). Matched samples were equilibrated to target MC levels of 10%, 15%, and 20%; as well as tested green. Of the many models fit to this data, a quadratic surface model was found to provide the best fit to the bending strength (modulus of rupture, MOR and moment capacity, RZ) data (Green and Evans, 1989).

$$P_2 = P_1 + b(M_2-M_1) + c(M_2^2-M_1^2) \qquad (1)$$

where
P_1 is the property measured at MC = M_1
P_2 is the property adjusted to MC = M_2, and
b and c are coefficients determined from the data.

To make the model reversible from one MC level to another, it was deemed desirable to fix the coefficients with respect to a reference MC, arbitrarily chosen as 15-percent. The complexity of this "fixed quadratic surface model" made it desirable to use a computer program to make the MOR adjustments (Evans, et.al, 1986). Modulus of elasticity (MOE) could be modeled with a much simpler model.

$$P_2 = P_1 * [(1.857 - (0.0237*M_2))/(1.857 - (0.0237*M_1)) \qquad (2)$$

The authors judged these models applicable for adjusting lumber properties from green to 8-percent MC.

After considerable discussion, Committee D-7 decided to adopt a simpler model for adjusting the MOR of lumber for changes in moisture content.

$$P_2 = P_1 + [(P_1 - 16.649/(40 - M_1)] * (M_1 - M_2) \qquad (3)$$

if $P_1 > 16.649$ MPa , and

$$P_2 = P_1$$

if $P_1 \leq 16.649$ MPa

This model was deemed applicable to lumber in the lower end of lumber strength distributions normally used to assign allowable properties and to moisture contents from green to 10-percent. This model is given in Appendix I of ASTM D1990. Model (2) was adopted in D1990 for adjusting MOE values for change in MC between green and 10-percent. Analysis indicated that a moisture content of 23-percent should be used with models (2) and (3). No guidance is given for adjusting lumber properties below 10-percent MC

Barrett and Lau (1991) have proposed a series of "linear surface models" similar to models studied by Green, et. al. (1986, 1988) for use in engineering design standards. Barrett and Lau modify the least squares fit of the parameter values of Green, et. al. by forcing the fitted polynomial curves for the parameter estimates of the model through the origin. Only one of these models, termed by Barrett and Lau as the "2-term linear surface model", can be solved in closed form without the use of a computer program. As with the quadratic surface model (1), the linear surface model is fixed with respect to a reference moisture content of 15-percent.

$$P_2 - P_1 = (D_1*P_{15} + D_2*P_{15}^2) * (M_2-M_1) \qquad (4)$$

where

$$P_{15} = \{[1-D_1*(15-M_1)] - SQRT[(D_1*(15-M_1))^2 - 4*D_2*P_1*(15-M_1)]\} / [2*D_2*(15-M_1)]$$

and D_1 and D_2 are coefficients determined from the data.

An Mp value of 25% is recommended by Barrett and Lau for use with the linear surface models.

Previous versions of Eurocode have assumed a constant percent change in property per percent change in MC to adjust properties for a change in MC. However, it is currently assumed that there is no change in MOR with changes in MC with the range of 12 to 18-percent MC. MOE is assumed to change 2-percent for each 1-percent change in MC. The authors are not sure if this is meant to be applied as a simple interest type model or as a compound interest type model. The compound interest type model is more traditional in the United States because it yields the same answer whether adjusting from one MC level to a lower one or if adjusting the other way. The formula for adjusting MOE using a compound interest formula is:

$$P_2 = P_1 * (1 + C/100)^{-(M_2 - M_1)} \qquad (5)$$

where C is the assumed percent change in property per percent change in MC.

A simple interest formula for adjusting MOE could be written as:

$$P_2 = P_1 * (1 + (C/100)*(M_1 - M_2)) \qquad (6)$$

Table 2 presents a comparison of formula 2, 5, and 6 for adjusting MOE to 12-percent moisture content using an assumed change of 2-percent change in MOE for each 1-percent change in MC. Note that if P_1 is adjusted from 25-percent to 12-percent and back to 25-percent again using Equation (6) with C = 2-percent, then the ratio of the final to the initial value of P_1 is 0.932. Each iteration of MOE from 25 to 12-percent MC and back again will lower the MOE at 25-percent.

SUMMARY OF PROCEDURES

Experimental

A detailed discussion of the experimental procedures is given in Green and Evans, 1991. The five species chosen for this study were black spruce (Picea mariana), sugar pine (Pinus lambertiana), western white pine (Pinus monticola), grand fir (Abies grandis), and eastern hemlock (Tsuga canadensis). These species were selected to represent a wide range of material that might be expected to be adjusted by the standardized models (Green and Evans, 1991). The lumber for this study was selected from production inventory at lumber mills. Two grades, Select Structural (SS) and No. 2, were selected to provide a range of quality levels. The lumber was selected to be ``on grade'' based on characteristics that affect strength (e.g., appearance characteristics such as wane were not considered). Modulus of elasticity in the flatwise orientation and strength ratio were used to match the samples in the green condition. Once matched, each of the three groups was then randomly assigned to one of three moisture categories---green, 15%, or 10%. The target sample size for each MC--species--grade combination was 50. However, about 55 pieces were assigned to each group to allow for damage in handling and degrade as a result of drying.

To match drying conditions used in the Douglas-fir and Southern Pine studies, the green lumber to be dried to the 10% and 15% MC levels was carefully dried using a mild schedule in which the dry bulb reading did not exceed 49 degrees C (120 degrees F). The specimens were removed from the kiln when the mean MC was several percentage points above the target MC, and then the specimens were placed in appropriate equilibration chambers. Finally, the lumber was regraded and any change in grade was noted.

The lumber was tested to failure in edgewise bending using third-point loading and a span-to-depth ratio of 17:1 (ASTM D4761, 1992). The grade-controlling defect was located within the test span and randomly located with respect to the direction of loading. Both modulus of rupture (MOR) and MOE in the edgewise orientation were calculated for each piece of lumber. Load deflection curves were obtained for each piece.

Evaluation of Models

Selection of an analytical procedure for comparing the goodness-of-fit of models to the data presents unusual problems. Because the sample size varied between species-grades-moisture content groups, and because we did not have "true" and "predicted" values, most conventional procedures for evaluating goodness-of-fit are not appropriate. It seems logical to us, however, that within a given grade and species the models could be compared by adjusting the properties obtained at each of the three MC levels to a common MC level. Assuming that the three MC groups had the same property distribution in the green condition, and that a model is a perfect predictor of the effect of MC on property values, then at a common MC level all three properties would have an identical value. Thus the maximum absolute difference between the maximum of the three property estimates and the minimum of the three property estimates, after adjustment to the common MC level, would be an indication of model performance. Past experience has shown that although the magnitude of this difference will vary with the absolute magnitude of the common MC level chosen, the "best" equation (lowest max difference) will also be the "best" equation at other MC levels. For convenience of display we average this maximum difference at the chosen common MC level across sizes and grades.

RESULTS AND DISCUSSION

Modulus of Rupture

Observations from the data. Common percentile estimates for the MOR of species tested in this study are shown in Figure 2. For comparison, the equivalent data obtained in the previous studies on Douglas-fir and Southern Pine are also shown. For illustrative purposes, lines have been drawn between percentile estimates.

As was noted in the Introduction, this study was initiated to evaluate analytical models that were applicable to design codes using a wider range of species than was available for the initial work on Douglas-fir and Southern Pine. Analytical models to be used in standards usually are simple in form and are, of necessity, a compromise between models derived for a specific species. Because our goal was to select one simple model and apply it to as many species as possible, we felt that we could reduce the range of grade-size-MC combinations to be tested. Dropping the 20-percent MC level tend to make the data look more linear than they would if the intermediate MC level were present. Thus care should be taken not to extrapolate the results presented here for drawing inferences about the "best" model for any particular species.

With all seven species there is a tendency for the weakest material to be unaffected by moisture content, Figure 2. With the highest strength lumber MOR tends to increase with decreasing MC. With most species there tends to be a correspondence of moisture effects at equivalent MOR levels for an individual species. Finally, with the exception of eastern hemlock, the slope of the trend line between MOR and MC tends to be similar from green to 15% MC for MOR values below about 40 MPa (at 15% MC). Thus there appears reason to believe that a single species independent code model could be applicable to the lower half of the strength distribution.

Selection of model form. Previous work on modeling MC-MOR relationships had investigated many model types and variations (Green, et.al, 1986; Green, et.al, 1988, Green and Evans, 1989). This study primarily focused on the ASTM D1990 model (Equation 3) and the 2-term linear surface model (Equation 4) for prediction of MOR. The 2-term model was included because it was proposed by the Barrett and Lau for possible adoption in a design standard. A "zero adjustment model", which is the current EuroCode 5 model, is also included for comparison. Because it is the best research model we investigated, the quadratic surface model (Equation 1) is also included for comparison. However, we are not suggesting this model be used in engineering design standards.

The "best" models for a given model type are the models with the smallest average maximum difference. The average maximum differences were evaluated at several percentiles of the distribution, as well as at the mean. To simplify discussion, only the average maximum differences at the 50th percentile are given, Table 3. All of the best models provide a better fit than taking no adjustment. If the only data available were for the lower stress classes, perhaps ignoring adjustments in MOR values due to change in moisture content might not result in a very large error. However, testing data at 18% MC and assuming this is the value at 12% MC could result in significant error in assignment to the proper stress class.

The single most important factor in identifying the best model for a given model type is the selection of the Mp value. This is because without the proper selection of Mp, the maximum difference for the data adjusted to any MC level by a proposed model is always controlled by the data set for green lumber. The models were developed assuming a particular Mp value. Without refitting them under a different assumed Mp value, the only change easy to incorporate into the models that retain the current parameter estimates is to assume a different Mp value for the green specimens of a species. For the 2-term linear surface model and the ASTM model the Mp value that minimizes the average maximum difference separates into three levels: Mp = 22-23% for Southern Pine and eastern hemlock; Mp = 26-27% for Douglas-fir, sugar pine, and grand fir; and Mp = 29-30% for western white pine and black spruce. No attempt was made to derive a quadratic surface model for the limited data on 2x4's. Thus it is not surprising that the quadratic surface model with an assumed Mp value of 23% is not as good as the best linear model. Also, as noted previously, having only two dry moisture levels and a movable Mp value tends to make the data favor a linear model.

Another factor to consider in selecting the model form is the ease in using the model. The quadratic surface model was already eliminated by the authors (and by the committee that chose the models to be used in ASTM D1990) because it was too complex. Although the 2-term linear surface model can be solved in closed form, and thus does not require a computer program to use, the equations can not be done easily with a paper and pencil. Further, care must be taken that the term under the square root in Equation 4 not be allowed to become negative. This happen several times when trying to use this equation on the data obtained in this study. There is no obvious "fix" that totally solves problems of the 2-term linear model when the term under the square root becomes negative. When all the specimens in a data set could not be adjusted for the model, an * was placed in Table 3 to denote the problem. Given that there is usually no practical difference between the average maximum differences for the "best" equations of the ASTM and 2-term linear surface model types, the authors feel that an equation of the ASTM type would be easier to use in a design standard.

<u>Application to other species</u>. One option for using these formulas in a design standard is to use the best Mp value for the species for which data is available, and to use an assumed Mp value for species for which data is not available. This is the procedure suggested in the Wood Handbook for adjusting the properties of small, clear pieces (USDA, 1987). Another alternative is to assume one Mp value and apply it to all (or nearly all) species. This is the procedure often adopted in design standards such as ASTM D2915. To evaluate how these options might work, we calculated the mean value of the average maximum difference across species, Table 3. For the ASTM type model the best overall Mp value appears to be 25-26 %.

If an Mp value of 25% is chosen as the best average value to apply to all species, and an ASTM type model is assumed for this example, then a comparison between the maximum differences at 25% for each species and the maximum differences for the best model indicate some significant errors could occur. Thus the results of this study suggest that we should use the best Mp value for that species if it is known and only apply an average Mp value to species for which we have no data. However, before making a final recommendation the authors will go back and reanalyze the full Douglas-fir and Southern Pine data sets using the ASTM model, Equation 3.

A final option is to try to predict a new intersection moisture content, Mp, for a species based on some other information about the species. Using information on the traditional intersection moisture content, (Mp in Table 1), and dry/green ratio (DGR = ratio of MOR at 12% MC to that green) from the Wood Handbook (USDA, 1987), the authors have noticed an equation that provides a reasonable estimate of $\widehat{Mp}$.

$$\widehat{Mp} = Mp + 10 * (DGR - 1.5) \qquad (7)$$

This equation results in estimated $\widehat{Mp}$ values of 23 for Southern Pine, 24 for eastern hemlock, 25 for Douglas-fir and grand fir, 27 for sugar pine, 29 for black spruce and 31 for western white pine. The authors will also be looking to further attempt to refine predicting Mp.

Moment Capacity

The bending moment capacity, RZ, is the product of the member bending strength, MOR, and the bending section modulus, Z = (thickness * width * width)/6. The RZ is often the controlling factor in structural performance. However, the actual RZ of lumber is a function of individual mill cutting tolerances. Therefore it is common to adjust MOR and Z separately for change in MC (Green, 1989). In the United States, ASTM chose to adopt a linear model for MOR and for Z. But in recognition of the potential loss in MOR with decreasing MC shown in Figure 1 they also limited the application of this model to MC's greater than 10%.

The results of this study suggest that there is little reason to expect a loss in bending capacity with drying for MC from green to 15%, Figure 3. The data also suggests that restricting to application of the model to MC's or 10% or more will result in little significant loss of bending capacity with further drying below 15%. However, the results also suggest that the caution of the ASTM committee in restricting the use of the model to higher MC levels may have been warranted. The effect of very low MC on lumber strength is a focus of current research at the U.S. Forest Products Laboratory.

Modulus of Elasticity

Observations from the data. Percentile estimates for the MOE of species tested in this study are shown in Figure 4. Most species generally show an increase in MOE with drying from green to 10% MC. The MOE of Grand fir and eastern hemlock appear less sensitive to change in MC than the other species. The insensitivity of eastern hemlock was expected (Green and Evans, 1991), but that of grand fir was not. Further, both the MOR and MOE of eastern hemlock are less sensitive than the other species to change in MC.

With grand fir only the MOE appears to be less sensitive to a change in MC. Thus we suggest the anomalous behavior of grand fir be confirmed in a future study.

Model selection. As with MOR, selection of Mp value appears to be the most important factor in selecting a particular model. For the ASTM model there is generally good correspondence between the best Mp value for MOR, Table 3, and that for MOE, Table 4. Even when the correspondence is not exact, the error in MOE resulting from assuming the best Mp value for MOR is not large. The same can not be said for grand fir, where the selected Mp value for MOR would be 27%, but for MOE it would be 20%. Generally there would appear to be little practical difference between the ASTM type model and the compound interest type model.

Bending Stiffness

The bending stiffness, EI, is the product of the member modulus of elasticity, MOE, and the moment of inertia, I= (thickness * width * width * width)/12. The RZ is often the controlling factor in structural performance. The results of this study generally confirm the historical evidence that EI either increases with decreasing MC or at least stays constant, Figure 5. There is some indication this assumption might not hold for eastern hemlock. However, the error involved would appear to be small for MC's above 10%.

CONCLUSIONS

From the results of this study we conclude the following.

1. For adjusting modulus of rupture for change in MC, any of the better models provides a better property estimate than taking no adjustment. The adoption of some MC-MOR adjustment model would be especially important for the higher stress class levels.

2. The simple linear model of ASTM D1990 (Equation 3) is recommended. It's use should be restricted to MC's above about 10 %. The results of this study suggest that the upper limit of the adjustment be the Mp values determined in this paper, or 25% for untested species.

3. For modulus of elasticity either the constant percentage model of ASTM D1990, or a constant percentage model of the type used to compute compound interest be adopted (Equation 5). The Mp value should be based on those chosen for MOR.

4. There is a need to go back and re-evaluate the full Douglas-fir and Southern Pine MC-MOR data sets using the knowledge gained in this study. This work is in progress.

REFERENCES

1. American Society for Testing and Materials. Philadelphia, PA, 1992.

D 245-81. Establishing structural grades and related allowable properties for visually graded lumber.

D 1990-91. Standard Practice for Establishing Allowable Properties for Visually Graded Lumber From In-Grade Tests of Full Size Specimens.

D2915-84. Evaluating Methods for Evaluating Allowable Properties for Grades of Structural Lumber.

D 4761-87. Standard Test Methods for Mechanical Properties of Lumber and Wood-Based Structural Material.

2. Aplin, EN, Green, DW, Evans, JW, and Barrett, JD. 1986. "The Influence of Moisture Content on the Flexural Properties of Douglas-Fir Dimension Lumber". Res. Pap. FPL--475, break Madison, WI: U.S. Department of Agriculture, Forest Service, Forest Products Laboratory, Madison, WI.

3. Barrett, JD and W Lau. 1991. "Bending strength adjustments for moisture content for structural lumber". Wood Science and Technology. 25:433-447.

4. Evans, JW, Evans, JK, Green, DW. 1986. "Computer Programs for Adjusting the Mechanical Properties of 2-Inch Dimension Lumber for Changes in Moisture Content." Gen. Tech. Rep. 63, Madison, WI: U.S. Department of Agriculture, Forest Service, Forest Products Laboratory, Madison, WI.

5. Green, DW. 1989. "Moisture content and the shrinkage of lumber". Research Paper FPL-RP-489. U.S. Department of Agriculture, Forest Service, Forest Products Laboratory, Madison, WI.

6. Green, D. W., Link, C. L., DeBonis, A. L., and McLain, T. E. 1986. "Predicting the effect of moisture content on the flexural properties of southern pine dimension lumber." Wood Fiber Sci. 18(1), 134-156.

7. Green, D. W., Evans, J. W., Barrett, J. D., and Aplin, E. N. 1988. "Predicting the effect of moisture content on the flexural properties of Douglas-fir dimension lumber." Wood Fiber Sci. 20(?),107-131.

8. Green, DW and Evans, JW. 1989. Moisture Content and the Mechanical Properties of Lumber: Decisions for the Future. Proceedings: In-Grade Testing of Structural Lumber. Proceedings 47363, June 25--29, 1988, Forest Products Research Society, Madison, WI. p. 44--55.

9. Green, DW, and JW Evans. 1991. "Moisture content and the flexural properties of lumber: species differences". Proceedings, 1991 International Timber Engineering Conference, London.

10. Hoffmeyer, P. 1978. "Moisture content-strength relationship for spruce lumber subjected to bending, compression, and tension along the grain". Proceedings, IUFRO wood engineering group meeting, Vancouver, B.C. 72-91

11. Madsen, B. 1975. "Moisture content-strength relationship for lumber subjected to bending." Can. J. Civ. Eng. 2(4), 466-473.

12. Madsen, B. 1982. "Recommended moisture adjustment factors for lumber stresses. Can.J. Civ. Eng. 9(4), 602-610.

13. McLain, TE, DeBonis, AL, Green, DW, Wilson, FJ, Link, C. 1984. The Influence of Moisture Content on the Flexural Properties of Southern Pine Dimension Lumber. Res. Pap. FPL--447, Madison, WI: U.S. Department of Agriculture, Forest Service, Forest Products Laboratory.

14. U.S. Department of Agriculture. 1987. Wood Handbook: Wood as an engineering material." USDA Forest Serv., Agric. Handb. 74, Forest Prod. Lab., Madison, Wis.

15. Wilson, T.R.C. 1932. "Strength-moisture relations for wood." USDA Forest Serv. Tech. Bull. 282, Forest Prod. Lab., Madison, Wis.

Table 1.--Historical values of intersection moisture content values for selected species (USDA, 1987).[1]

Species	Mp
	Pct
Ash, white	24
Birch, yellow	27
Chestnut, American	24
Douglas-fir	24
Hemlock, western	28
Larch, western	28
Pine, loblolly	21
Pine, longleaf	21
Pine, red	24
Redwood	21
Spruce, red	27
Spruce, Sitka	27
Tamarack	24

[1]Intersection moisture content is the point at which mechanical properties begin to change when drying from the green condition.

Table 2.--Adjusting Modulus of Elasticity by Various Formula

Moisture Content		Ratio of MOE at M_2 to MOE at M_1 by		
Initial	Final	ASTM	Simple Interest	Compound Interest
25	12	1.244	1.260	1.294
23	12	1.199	1.220	1.243
21	12	1.157	1.180	1.195
19	12	1.118	1.140	1.149
17	12	1.081	1.110	1.104
15	12	1.047	1.060	1.061

Table 3.--Average maximum absolute difference for modulus of rupture at the 50th percentile for species at 15 percent moisture content.

Model[1]	Average maximum absolute difference, MPa							
	Douglas-Fir	Southern Pine	Western White Pine	Sugar Pine	Black Spruce	Grand Fir	Eastern Hemlock	Mean
No adjustment	25.0	21.6	24.3	12.7	23.3	23.4	9.6	19.9
Quad. surface	6.5	4.1	13.1	4.3	11.0	9.7	5.5	7.7
ASTM								
Mp = 23	9.4	3.5	15.1	8.6	12.0	10.6	3.5	9.0
= 24	7.2	5.9	14.1	8.1	10.9	9.3	4.3	8.5
= 25	5.0	9.3	13.0	7.4	9.6	7.7	6.1	8.3
= 26	4.2	13.3	11.7	7.0	8.2	5.9	8.3	8.4
= 27	6.1	17.8	10.2	7.3	6.5	5.2	10.8	9.1
= 28	--	--	8.5	--	4.5	5.2	--	--
= 29	--	--	6.4	--	3.2	--	--	--
= 30	--	--	4.6	--	4.2	--	--	--
Linear surface								
Mp = 23	10.1	*	15.5	8.9	12.6	11.5	3.8	--
= 24	8.1	*	14.7	8.5	11.6	10.3	3.5	--
= 25	5.8	*	13.8	7.9	10.6	9.0	4.4	--
= 26	*	*	12.7	7.4	9.4	7.5	6.2	--
= 27	*	*	*	7.0	8.0	5.8	8.2	--
= 28	--	--	*	7.5	6.5	*	--	--
= 29	--	--	*	--	*	*	--	--
= 30	--	--	*	--	*	--	--	--

[1]Quad. surface = Quadratic surface model of Equation 1.
ASTM = ASTM D1990 model of Equation 3.
Linear surface = 2-term linear surface model of Equation 4.

*Did not converge.

Table 4.--Average absolute maximum difference of modulus of elasticity at 50th percentile for species at 15 percent moisture content.

Model[1]	Average maximum absolute difference, GPa						
	Douglas-Fir	Southern Pine	Western White Pine	Sugar Pine	Black Spruce	Grand Fir	Eastern Hemlock
No adjustment	1972	2585	2599	2337	2840	1737	669
ASTM							
Mp = 20	--	--	--	--	--	1027	586
= 21	731	972	--	--	--	1117	655
= 22	593	869	--	--	--	1213	731
= 23	593	807	1007	724	1103	1310	834
= 24	593	807	862	586	944	1406	--
= 25	669	807	703	448	779	--	--
= 26	786	917	545	365	614	--	--
= 27	993	1144	386	303	483	1737	--
= 28	1206	1386	310	379	407	--	--
= 29	1434	1634	324	462	407	--	--
= 30	1668	1889	352	--	524	--	--
Compound interest							
Mp = 20	634	--	--	--	--	986	641
= 21	545	800	--	--	--	1096	717
= 22	524	683	--	--	--	1200	820
= 23	614	683	717	358	717	1310	951
= 24	703	696	552	234	545	1420	--
= 25	--	876	379	207	365	--	--
= 26	--	--	296	234	269	--	--
= 27	--	--	317	372	303	1992	--
= 28	--	--	352	--	345	--	--

[1]ASTM = ASTM D1990 model of Equation 2.
Compound Interest = 2 percent change in MOE per percent change in moisture content, Equation 5.

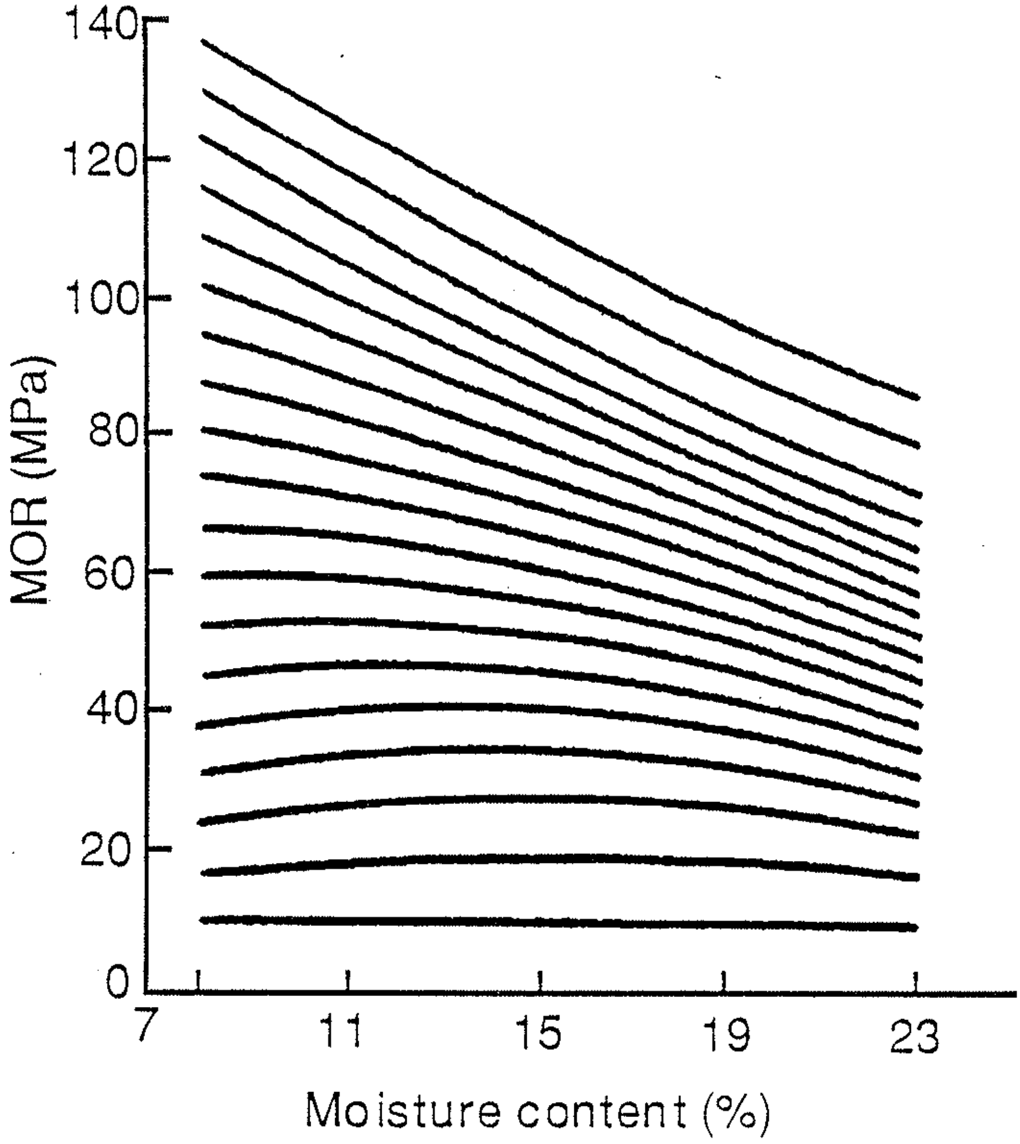

Figure 1. Analytical model of the effect of moisture content on the bending properties of dimension lumber (Green and Evans, 1988).

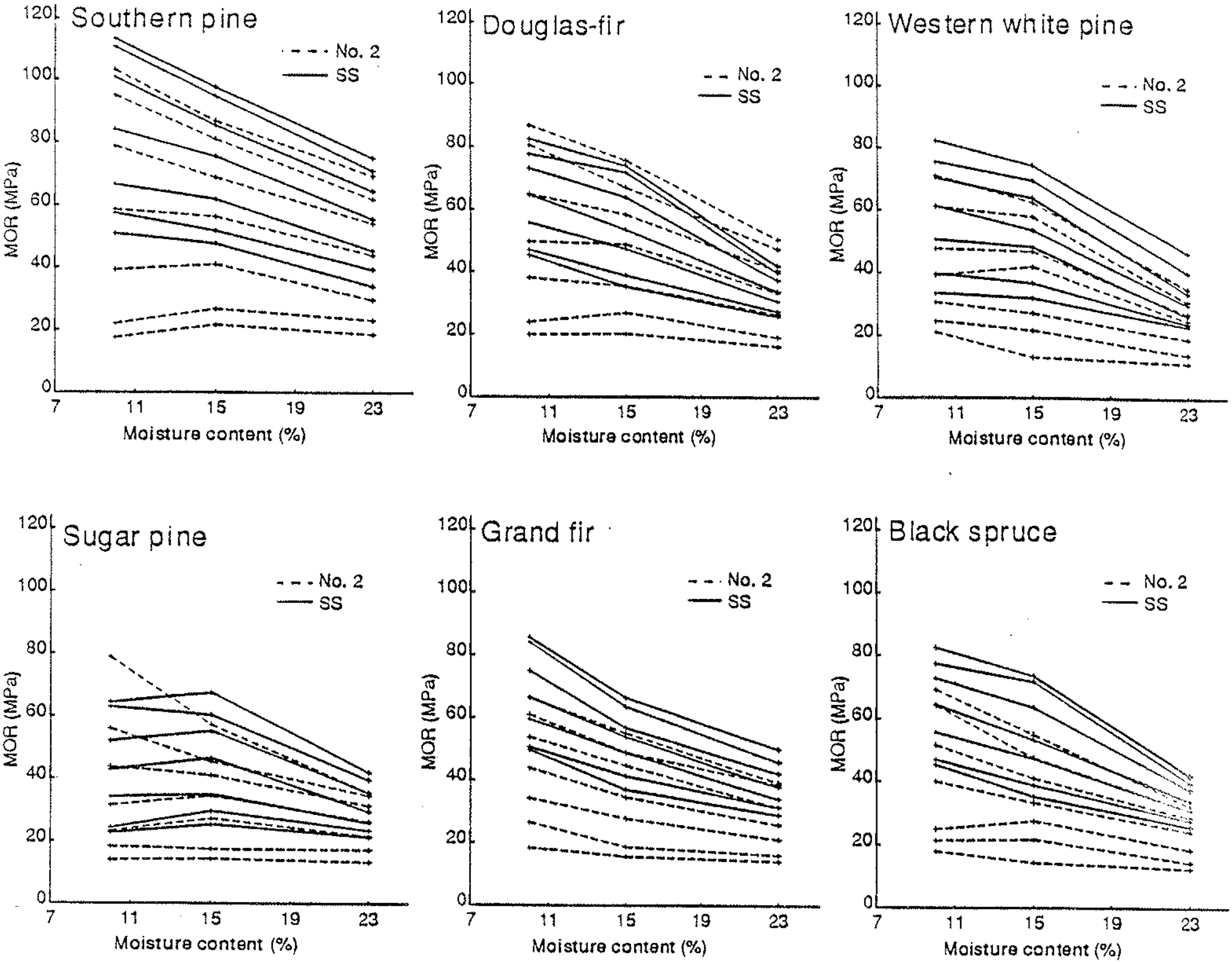

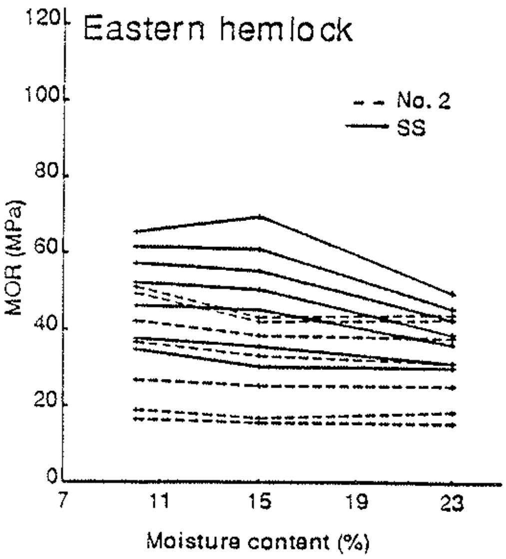

Figure 2. Effects of moisture content on the modulus of rupture of Select Structural and No. 2, 2 by 4's (percentile levels are 5, 10, 25, 50, 75, 90, 95).

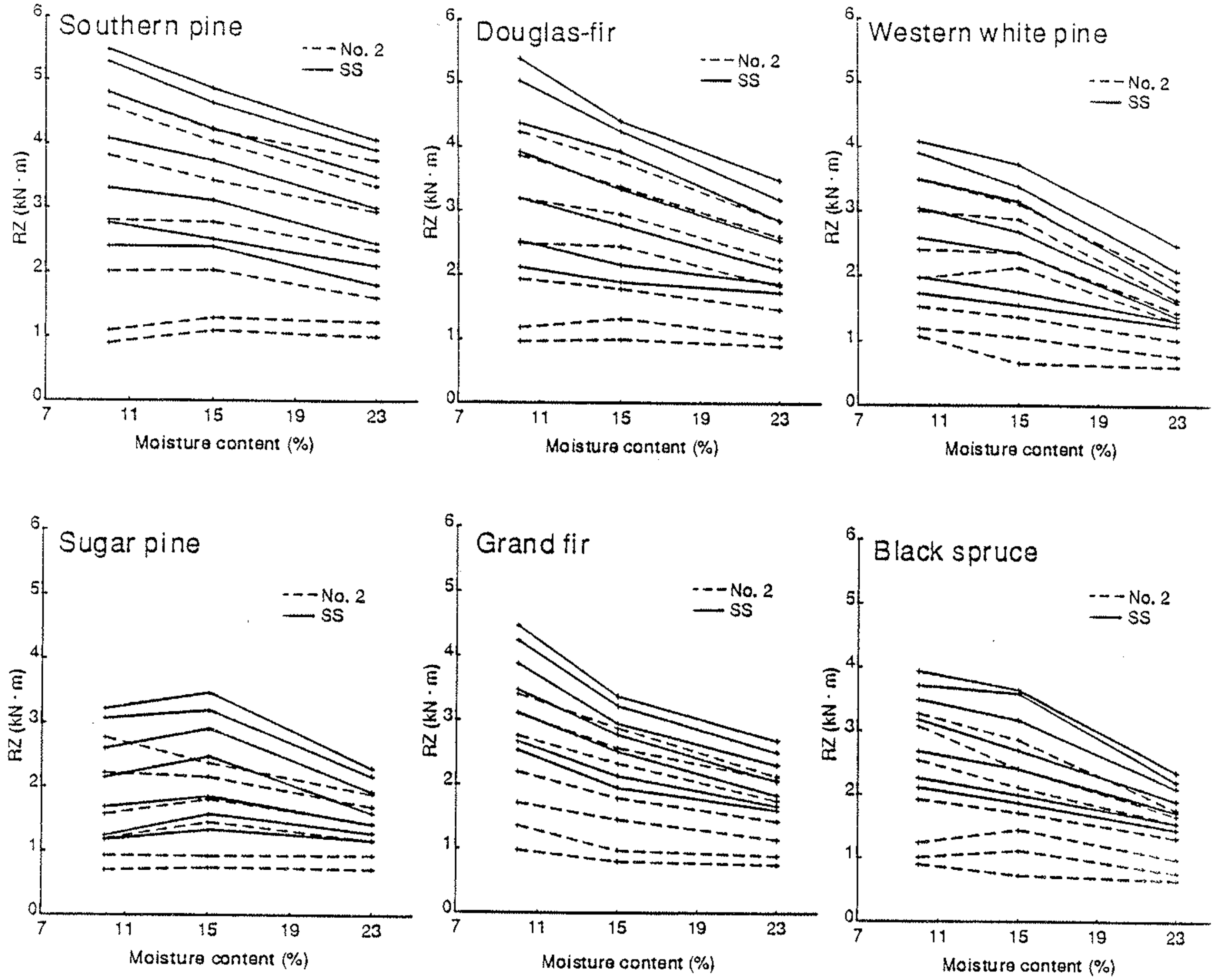

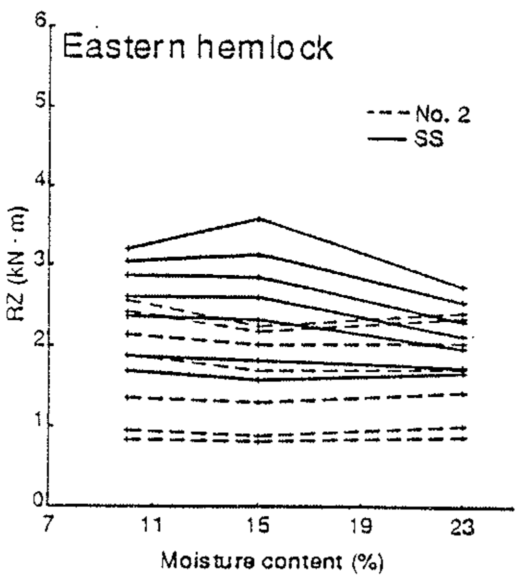

Figure 3. Effect of moisture content on the moment capacity of Select Structural and No. 2, 2 by 4's (percentile levels are 5, 10, 25, 50, 75, 90, 95).

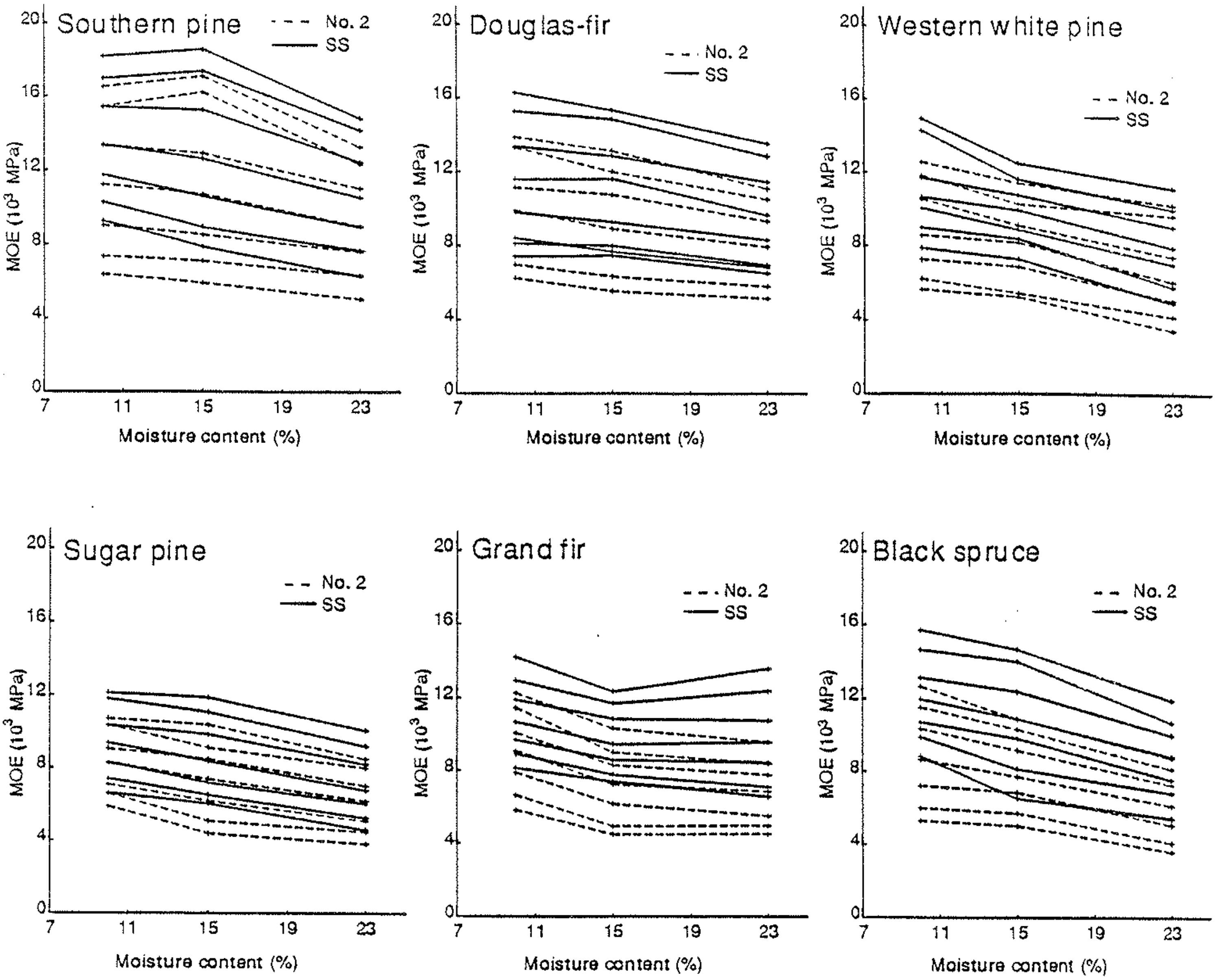

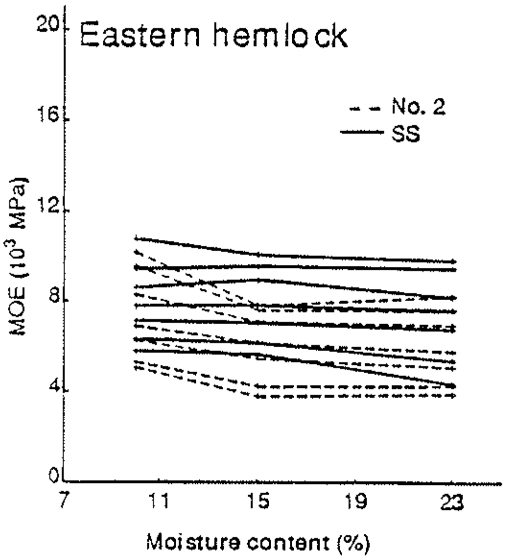

Figure 4. Effect of moisture content on the modulus of elasticity of Select Structural and No. 2, 2 by 4's (percentile levels are 5, 10, 25, 50, 75, 90, 95).

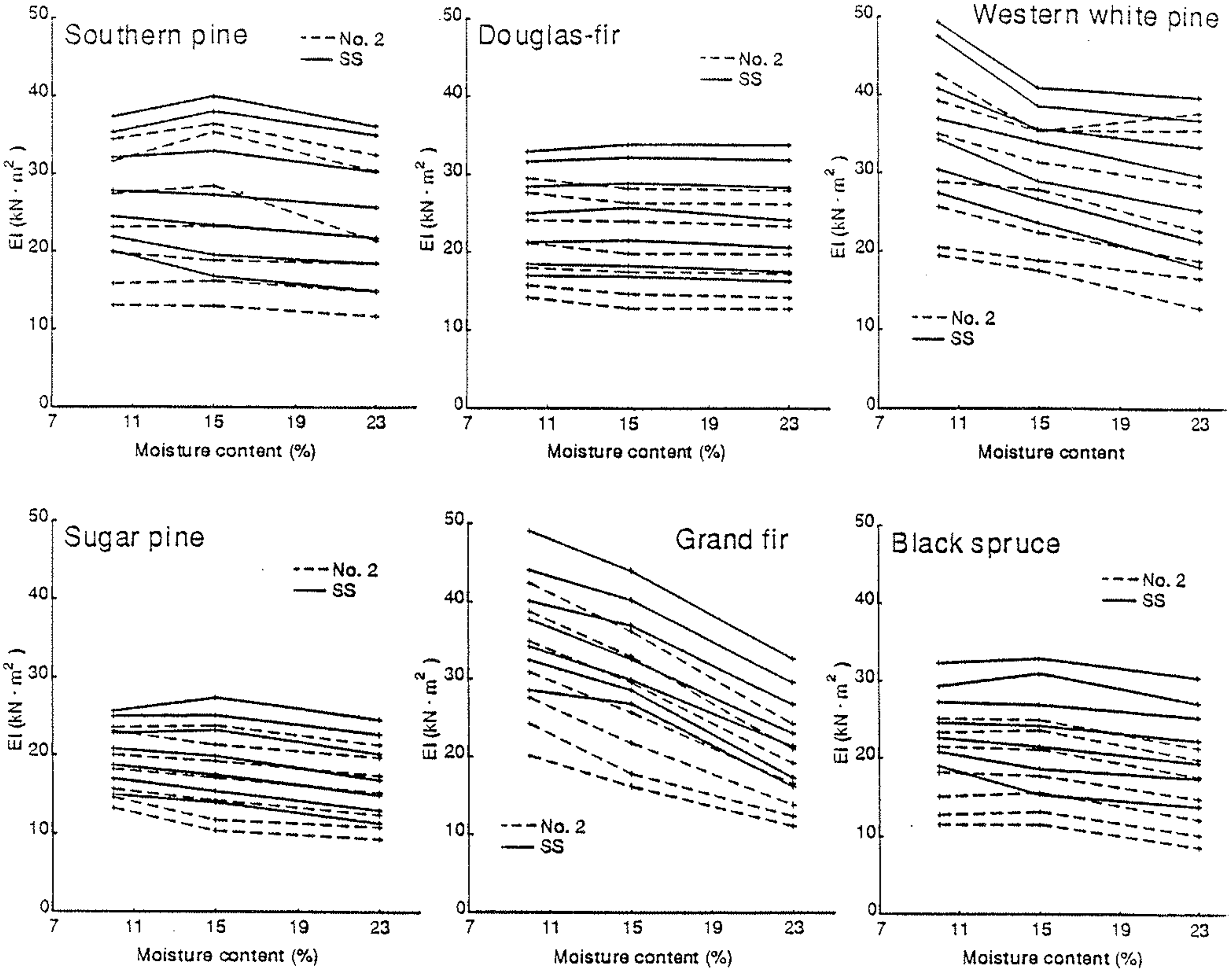

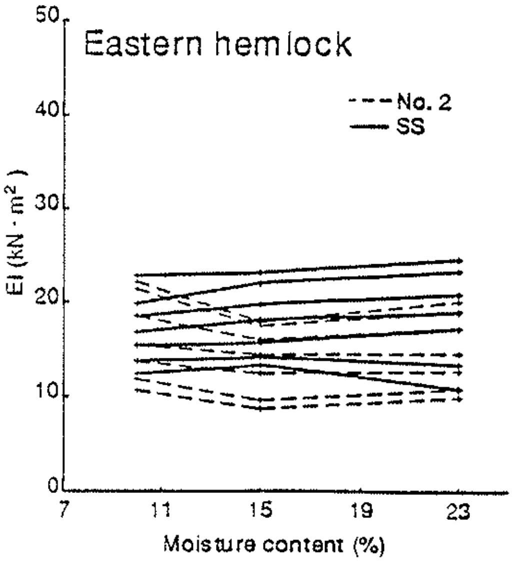

Figure 5. Effect of moisture content on the stiffness of Select Structural and No. 2, 2 by 4's (percentile levels are 5, 10, 25, 50, 75, 90, 95).

CIB-W18/25-102-2

INTERNATIONAL COUNCIL FOR BUILDING RESEARCH STUDIES AND DOCUMENTATION

WORKING COMMISSION W18 - TIMBER STRUCTURES

CONTROL OF DEFLECTIONS IN TIMBER STRUCTURES WITH REFERENCE TO EUROCODE 5

by

A Martensson

S Thelandersson

Lund Institute of Technology

Sweden

MEETING TWENTY - FIVE

ÅHUS

SWEDEN

AUGUST 1992

1. *Introduction*

The competitiveness of timber versus other structural materials depends to a great extent on the possibility to produce structures with high quality in service. Consequently, serviceability requirements related to deflections, vibrations and sound transmission are of very high significance for a rational utilization of timber in buildings.

In principle, serviceability requirements should be set by the client in agreement with the builder and not by codes. The codes give, however, general principles for loads, material parameters and calculation methods which may be used for design in serviceability limit states. The present draft of Eurocode 5 also gives recommended limits of deflections and recommended methods to control vibrations. It is clear that rational guidelines for design of timber structures with regard to serviceability are needed in practice. Such guidelines could be given in manuals and textbooks and do not have to be included in the code. Serviceability criteria given as recommendations in Eurocode will have a powerful influence in practice, due to the legal authority of an official document. Hence, if serviceability recommendations are given in Eurocode 5, it is very important that they have a rational and sound basis. If this is the case, the code recommendations can be efficient to promote good quality and unified rules of application in practice.

The purpose with the present paper is to discuss design methods and criteria for limitation of short term and long term deflections in timber structures with particular reference to the present recommendations given in Eurocode 5 [1]. Alternative methods and criteria, to replace the ones in the present draft of Eurocode 5, are suggested.

2. *Combination of actions in the serviceability limit state*

The basis of design common to all Eurocodes (see e.g. [2]) specifies three different types of load combinations which may be considered in serviceability limit states. These are:

Rare combinations

The rare combinations are used mainly in those cases when exceedance of a limit state causes a permanent local damage or a permanent unacceptable deformation. They include

$$\sum_{j \geq 1} G_{k,j} + Q_{k,1} + \sum_{i > 1} \psi_{0,i}\, Q_{k,i} \qquad (1)$$

Frequent combinations

The frequent combinations are used mainly in those cases when exceedance of a limit state causes local damage, large deformations or vibrations which are temporary. They include

$$\sum_{j \geq 1} G_{k,j} + \psi_{1,1}\, Q_{k,1} + \sum_{i > 1} \psi_{2,i}\, Q_{k,i} \tag{2}$$

Quasi–permanent combinations

The quasi–permanent combinations are used when long term effects are of importance. They include

$$\sum_{j \geq 1} G_{k,j} + \sum_{i \geq 1} \psi_{2,i}\, Q_{k,i} \tag{3}$$

In expressions (1–3), $G_{k,j}$ and $Q_{k,i}$ are characteristic values of permanent and variable loads, respectively. The values $\psi_{0,i}\ Q_{k,i}$, $\psi_{1,i}\ Q_{k,i}$ and $\psi_{2,i}\ Q_{k,i}$ are the combination value, frequent value and the quasi–permanet value of variable load $Q_{k,i}$, respectively.

3. *Deflection criteria in the present version of Eurocode 5*

According to the present draft of Eurocode 5 [1] the design load combination to be used in the serviceability limit state is chosen as

$$\sum G_{k,j} + Q_{k,1} + \sum_{i > 1} \psi_{1,i}\, Q_{k,i} \tag{4}$$

It should be noted that the load combination (4) differs from all three combinations defined in "Basis of design", eqs. (1–3).

As far as creep deflections are concerned the final deflection u_{fin} shall be calculated for each load type as

$$u_{fin} = u_{inst}\,(1 + k_{def}) \tag{5}$$

where u_{inst} is the instantaneous deflection of the load considered and k_{def} is a "creep" factor depending on load duration class and service class. For load combinations, the deflections shall be calculated for each load separately and then be added.

Recommended limits of deflection are given in EC 5. For the instantaneous deflection $u_{2,inst}$ due to variable loads the following limit is proposed for a simply supported beam

$$u_{2,inst} \leq L/400 \tag{6a}$$

where L is the beam span.

For long term deflections the following limits are proposed

$$u_{2,max} \leq L/300 \tag{6b}$$

$$u_{nett,max} \leq L/200 \tag{6c}$$

where u_2 and u_{nett} are defined in Fig. 1. The subscript max indicates long term values of the deflections.

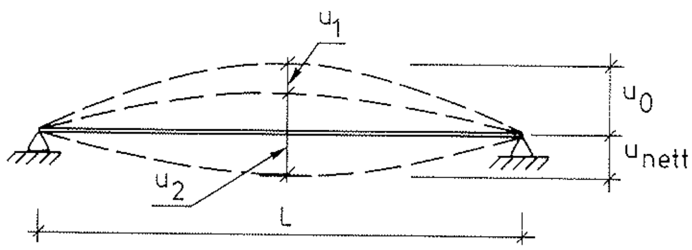

u_0 precamber (if applied)
u_1 deflection due to permanent loads
u_2 deflection due to variable loads

Fig. 1 Deflection of a structural beam. Definition of different components of deflection.

To illustrate the practical significance of the recommended deflection requirements in comparison with ultimate limit state design some results are given below for straight beams made of glulam and timber. Unless otherwise stated the calculations are based on the rules and numbers given in the Eurocode 5 draft from december 1991 [1]. It is assumed in all cases that the beam is loaded with only one variable load Q_k (e.g. imposed load or snow load) in addition to the permanent load G_k. Only rectangular beams with width b and depth h are considered. The beams are assumed to be regularly spaced with spacing c and the loads G_k and Q_k are uniform and specified per unit area.

Glulam beams

To compare the ultimate and serviceability limit states, the required beam depth h_s given by a serviceability criterion and the required beam depth h_u given by the ultimate limit state were calculated for different cases. The ratio between h_s and h_u is taken as an indicator on which of the criteria is decisive in design of the beam. For h_s/h_u greater than 1 the dimensions of the beam are governed by the deflection limit.

Fig. 2 displays the ratio h_s/h_u as a function of the load parameter $(Q_k + G_k)$ c/b. Calculations were made with each of the three criteria in Eq. (6a, 6b and 6c) respectively. The results in Fig. 2 are valid for glulam GL 37 with $f_{m,k} = 37$ MPa and $E_{0,mean} = 14500$ MPa. The ratio $G_k/(G_k + Q_k)$ is 0.25 in Fig. 2a and 0.5 in Fig. 2b. The variable load Q_k belongs to the load duration class "medium term".

The beam dimension is determined by the deflection requirement for low values of the load parameter $(G_k + Q_k)$ c/b and by failure for high values of this parameter. All deflection criteria give almost the same results when the permanent load is low compared to the total load (Fig. 2a). For higher ratios of $G_k/(G_k + Q_k)$ the long term deflection criterion (6c) is governing (Fig. 2b).

The practical range of the parameter $(G_k + Q_k)$ c/b for glulam is between 20 and 150 kN/m^2. For floors with imposed loads and roofs in regions with high snow loads $(G_k + Q_k)$ c/b is usually in the range 50–100 kN/m^2 whereas for roofs with low snow loads the common range is 25–50 kN/m^2.

The results given in Fig. 2 are displayed in an alternative way in Fig. 3, where h_s/h_u is given as a function of the ratio L/h_s where L is the span of the beam and h_s as before is the required depth with respect to the serviceability criterion in question. Usually, L/h_s will be between 15 and 30 in practice, with lower values for heavily loaded beams.

From these results it is quite evident that for high quality glulam, the deflection criteria recommended in Eurocode 5 are decisive in a majority of cases in practice.

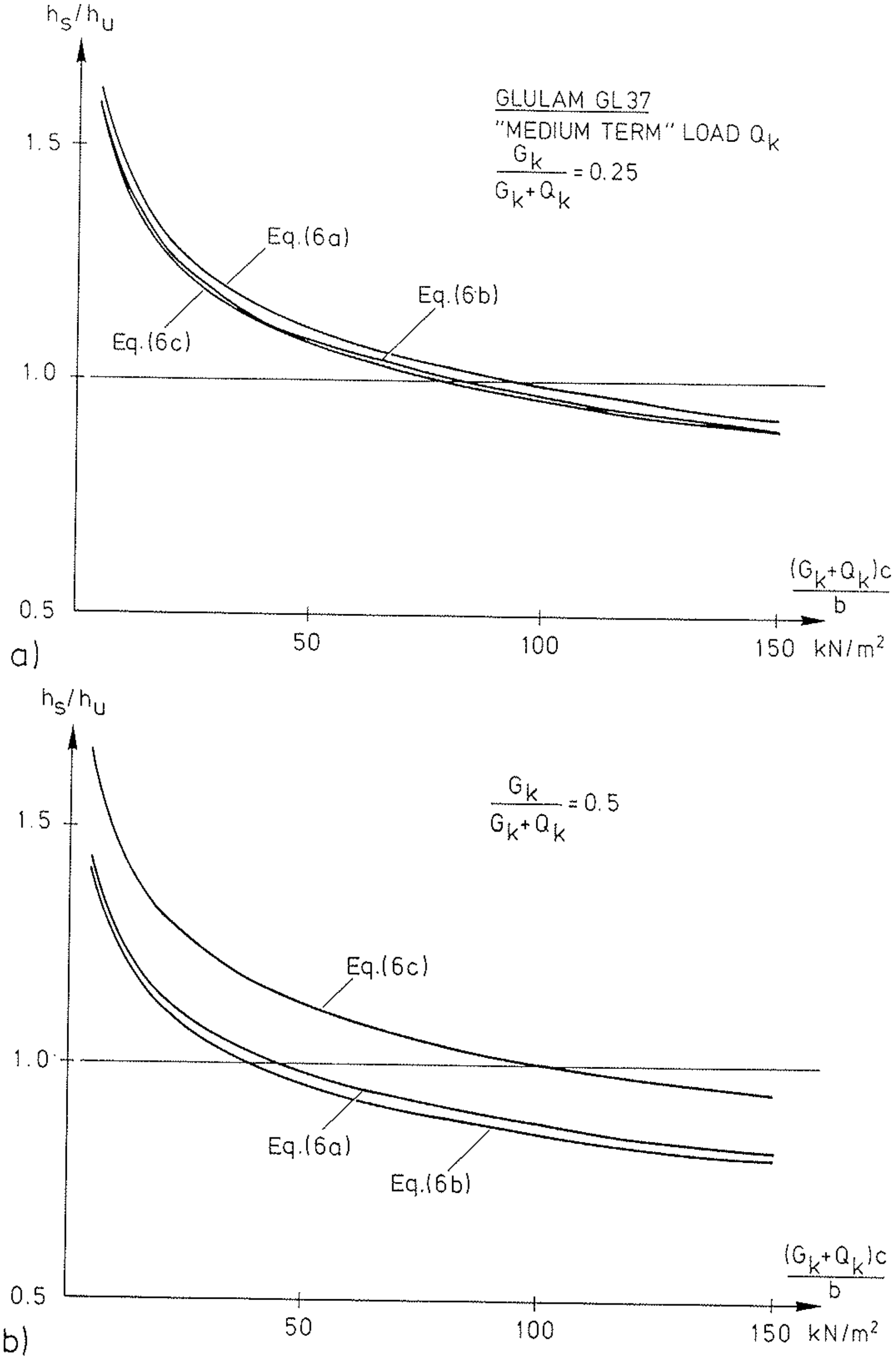

Fig. 2 The ratio between the required beam depths h_s and h_u in the serviceability and ultimate limit states, respectively.

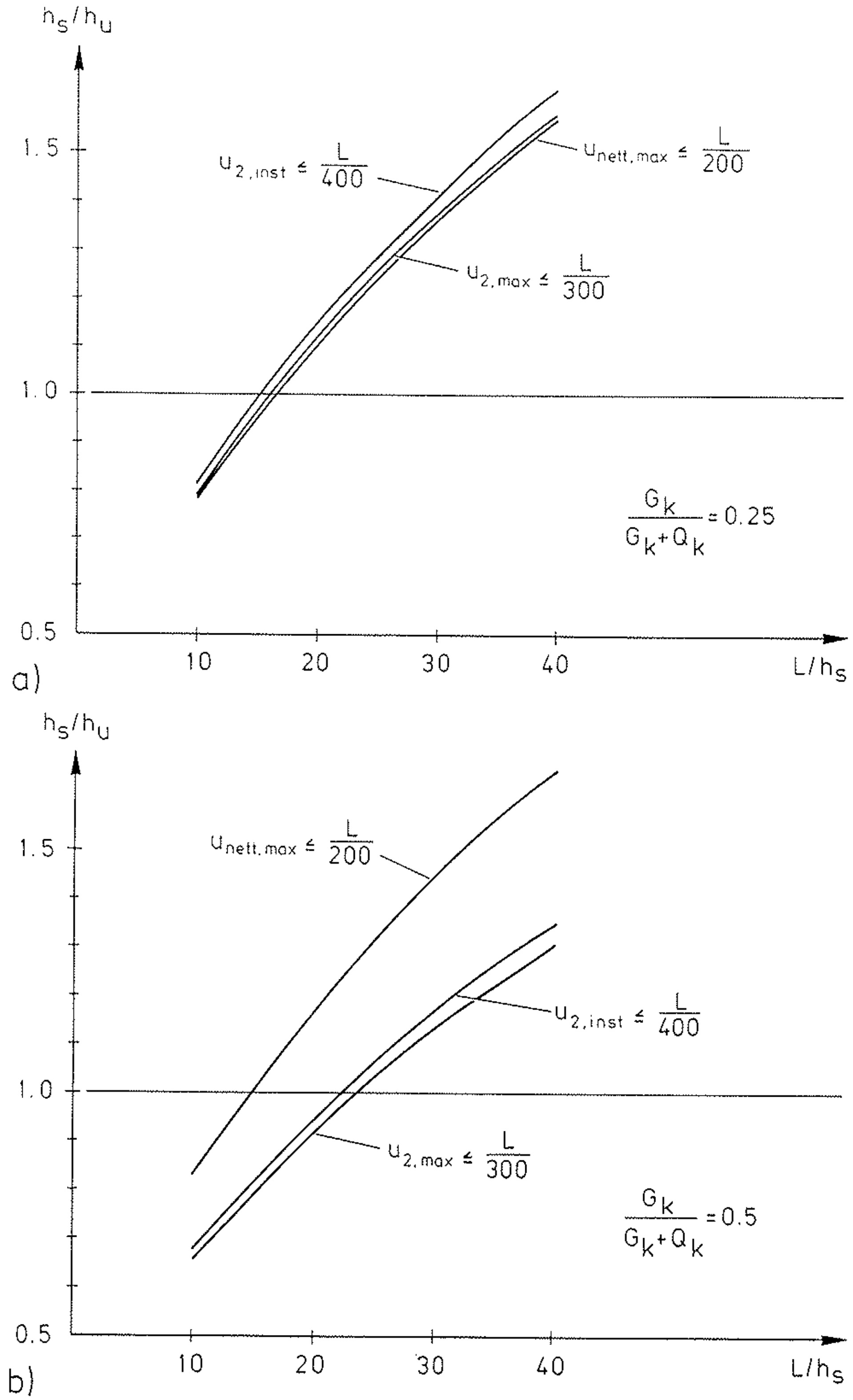

Fig. 3 The ratio between the required beam depths h_s and h_u in the serviceability and ultimate limit states as a function of the length to depth ratio L/h_s.

Timber beams

The ratio h_s/h_u is given in Table 1 for simply supported timber beams of different strength classes and according to different serviceability criteria. The values in the table refer to a specific case with regard to loading, spacing c and width b of the beam. The deflection criterion specified for limitation of vibrations (maximum deflection 1.5 mm under a point load of 1 kN) is also included in the table. In evaluation of this criterion it has been assumed that composite action between the floor sheathing and the beams gives an increase in stiffness with 75 percent. Furthermore, it was assumed that the load could be reduced by 25 percent due to load sharing with the adjacent beams. Without these effects, i.e. if the point load is assumed to be carried by only one timber joist without composite action, the required value of h_s would be more than doubled and the vibration criterion would be decisive in all cases.

The results in the table indicate that if any of the serviceability criteria are used, there is not much sense in using timber of higher strength class than C24. For the case $G_k/(G_k + Q_k) = 0.25$ all the deflection criteria are almost identical, whereas if the permanent load is relatively larger, the long term criterion will be decisive.

$\frac{G_k}{G_k + Q_k}$	CRITERIA	STRENGTH CLASS C14	C18	C24	C30	C40
0.25	$u_{2,inst} \leq L/400$	0.93	0.97	1.06	1.14	1.26
	$u_{2,max} \leq L/300$	0.91	0.95	1.04	1.11	1.24
	$u_{nett,max} \leq L/200$	0.91	0.95	1.04	1.11	1.23
	VIBRATION WITH LOAD SHARING AND COMPOSITE ACTION	0.94	0.98	1.07	1.14	1.27
0.5	$u_{2,inst} \leq L/400$	0.82	0.86	0.94	1.01	1.12
	$u_{2,max} \leq L/300$	0.81	0.84	0.92	0.99	1.09
	$u_{nett,max} \leq L/200$	0.95	0.99	1.08	1.16	1.29

Table 1: Values of h_s/h_u for different serviceability criteria and strength classes. $G_k + Q_k = 2.5$ kN/m². Rectangular beams with width b = 45 mm and regular spacing c = 600 mm.

Conclusions

The examples above show that limits on deflection such as those recommended in the current version of Eurocode 5 very often are decisive in practical design, provided that there is a need to limit deflection. For long span glulam beams limitation of deflections could be met by providing a precamber on the beam. This possibility has not been considered in the present analysis. However, it is clear that an accurate prediction of long term as well as short term deformations of timber and glulam is very important from a practical point of view. It should have at least the same level of priority as prediction of failure in timber.

In view of this it is also important to formulate rationally based serviceability criteria and to promote a sound understanding of these problems to structural engineers.

4. *Proposed design method for limitation of deflections*

The discussion in what follows is illustrated by a simply supported beam loaded by permanent loads and variable loads. The fact that variable loads often dominate in timber structures means that the deflection will fluctuate to a great extent during the lifetime of the structure, which has to be considered in the choice of design criteria for deflections.

Fig. 4 illustrates in principle the deflection behaviour of a beam loaded with permanent load and snow load, see e.g. [3]. The total deflection can be subdivided into one part δ_1 due to permanent loads immediately after loading and one part δ_2 which is variable during the lifetime of the structure. The variable part δ_2 consists of a reversible portion $\delta_{2,\mathrm{inst}}$ which is present only during limited periods when the variable load is high, and a continuously increasing portion δ_{creep}, which for all practical purposes may be considered as irreversible [3]. Load peaks with short duration, such as those illustrated in Fig. 4, occur both for snow load and imposed loads in the most common types of buildings.

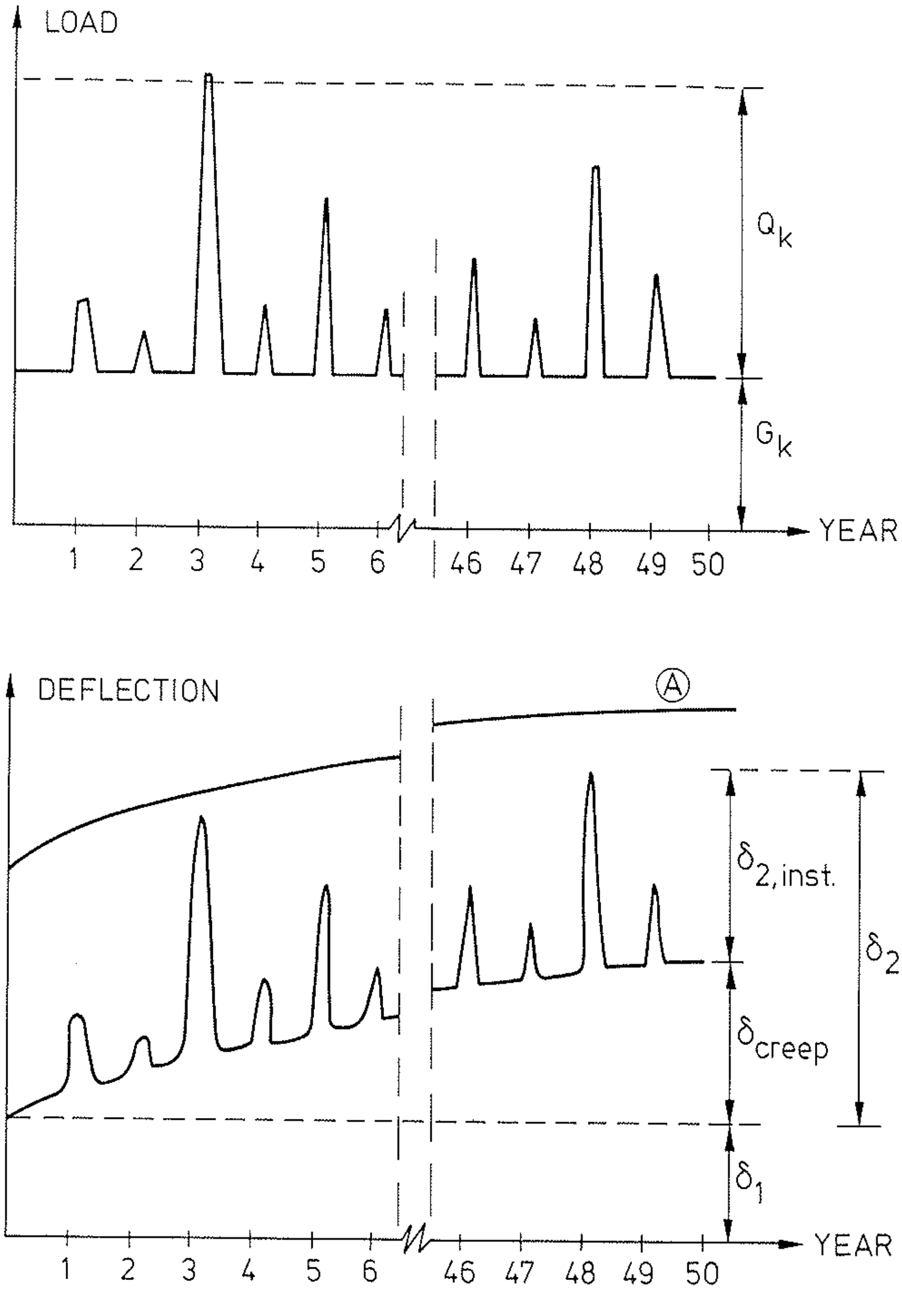

Fig. 4 Time variation in principle for deflection (lower figure) of a beam with permanent and variable loads according to the upper figure. Curve A shows the creep deflection if the beam is loaded with $G_k + Q_k$ during the whole period.

In view of this behaviour, the deflection criteria recommended in the present Eurocode 5 draft should be revised and clarified. To discuss more functional and rational design criteria some definitions of deflection components will be introduced with reference to Fig. 5.

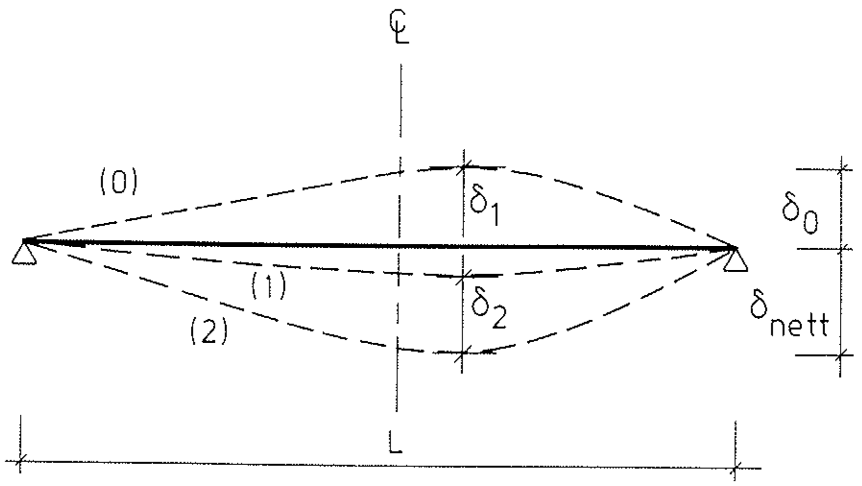

Fig. 5 Deflection components for a simply supported beam.

The deflections are here denoted by the symbol δ to distinguish them from the present EC5 definitions shown in Fig. 1. We propose that the deflection components are redefined as follows, c.f. Eurocode 3 for steel structures [5]:

δ_{nett} = sagging of the beam relative to the straight line joining the supports.

δ_0 = precamber of the beam in the unloaded state (state 0).

δ_1 = deflection of the beam due to permanent loads immediately after loading (state 1).

δ_2 = deflection of the beam due to variable loads plus any time dependent deformation due to permanent loads (state 2).

Normally, both δ_0 and δ_1 are fixed when the construction work is completed and do not change during the lifetime of the structure. (The case when the permanent load is changed during the building lifetime is not considered here). The component δ_2, however, is varying during the lifetime of the structure. The same applies to the nett deflection which is given by

$$\delta_{nett} = \delta_1 + \delta_2 - \delta_0 \tag{7}$$

The deflection δ_2 may be calculated as

$$\delta_2 = \delta_{2,inst} + \delta_{cr} \tag{8}$$

where $\delta_{2,inst}$ is instantaneous deflection due to variable loads and δ_{cr} is the total creep deflection due to permanent <u>and</u> variable loads. Here $\delta_{2,inst}$ can be conceived as a temporary, reversible part and δ_{cr} as a permanent, non–reversible part of δ_2.

The maximum creep deflection $\delta_{cr,max}$ that will occur during the lifetime can be predicted in design as

$$\delta_{cr,max} = \delta_{qp,inst} \cdot k_{def} \tag{9}$$

where $\delta_{qp,inst}$ is the instantaneous deflection due to quasi–permanent loads (load combination according to Eq. (3)) and k_{def} is a factor which takes into account the increase in deflection with time due to the effect of creep and moisture variations.

Based on these concepts two types of deflection criteria will be suggested. These criteria are proposed to replace the three criteria given in the present EC5–draft.

Deflection criterion to avoid permanent damage

A typical case is when excessive deformations may cause permanent damage to partitions, to members attached to or in contact with the member considered and to fixtures and finishes. In this case the risk of passage of the deflection limit should be small which means that the instantaneous deflection should be calculated for the rare load combination defined by Eq. (1). The following criteria is suggested in this case

$$\delta_{2,max} = \delta_{2,inst} + \delta_{cr,max} \leq \delta_{crit} \tag{10}$$

where $\delta_{2,inst}$ is the instantaneous deflection due to variable loads calculated on the basis of the rare load combination, Eq. (1) and $\delta_{cr,max}$ is the long term deflection given by Eq. (9). The critical deflection δ_{crit} generally depends on the nature of the elements which could suffer damage, but in the absence of more precise information the limit [L/400] is considered sufficient for most circumstances. (In EC2 for concrete structures the limit L/500 is recommended and in EC3 for steel structures the limit L/350 is given.)

In summary, the criterion (10) is directly targetted at the maximum extra deflection $\delta_{2,max}$ that may occur after the building has been erected. Since the criterion is related to the risk of permanent damage in secondary building elements, the probability of passage of the criterion should be kept at a low level.

Proposed deflection criterion with respect to appearance and general utility

From the point of view of appearance and general utility it may be desirable to avoid excessive deflections which are permanent or occur during long periods. Occasional passages of the deformation limit may, however, be acceptable if they are reversible and occur only during short periods. An appropriate deflection criterion for this case is

$$\delta_{max} = \delta_{qp,max} - \delta_0 \leq \delta_{acc} \tag{11}$$

where $\delta_{qp,max}$ is the maximum deflection due to quasi–permanent loads, Eq. (3), calculated as

$$\delta_{qp,max} = \delta_{qp,inst} \, (1 + k_{def}) \tag{12}$$

where $\delta_{qp,inst}$ and k_{def} is defined in connection with Eq. (9).

In Eq. (11) δ_{acc} is the acceptable deflection limit with respect to appearance and general utility. Ideally, the value of δ_{acc} should be decided by the client, but as a general recommendation the value δ_{acc} = L/250 may be taken. (Both EC2 and EC3 recommend this value).

The deflection calculated according to Eq. (11) on the basis of the quasi–permanent load combination will contain the "permanent" deflection plus a certain portion of the instantaneous deflection due to variable loads. The latter contribution depends on the nature of the variable load in question. Loads with long duration give higher contributions than loads occuring over short periods.

5. *Prediction of long term deflections*

It is suggested in this paper that the long term creep deflection $\delta_{cr,max}$ should be calculated from

$$\delta_{cr,max} = \delta_{qp,inst} \cdot k_{def} \tag{9}$$

where $\delta_{qp,inst}$ is the instantaneous deflection induced by the collective action of quasi–permanent loads given by

$$\Sigma\, G_{k,j} + \sum_{i\geq 1} \psi_{2,i}\, Q_{k,i} \tag{3}$$

The quasi–permanent value $\psi_{2,i}\, Q_{k,i}$ is an estimate of the time averaged mean value of variable load i. Values of ψ_2 will be given in Eurocode 1 for different types of load, but specific numbers are not definitely decided yet.

By introducing quasi–permanent loads the value of k_{def} in Eq. (9) corresponds to the case with a load constant in time. This means that k_{def} should be calibrated against creep tests with constant load under conditions which are representative for the service class considered. In this case there is no need for different values of k_{def} for different load durations, since this is already considered in the load combination. This makes the calculations easier.

It may also be noted that existing experimental information about creep under natural conditions almost invariably refers to the case with constant load during the test. Therefore, reliable estimates of the factor k_{def} can only be made for permanent loading and the influence of variable loads on accumulated permanent creep deflection during the lifetime of a structure is more realistically estimated within the framework of general load combination rules.

In timber structures creep is significantly enhanced by moisture variations. It has been shown in [3] and [4] that the effects of moisture variations are generally smaller for variable loads than for permanent load. The creep induced by moisture variations for high loads acting in short intervals separated by longer periods of low loads is smaller than if the high load is acting during an unbroken time period with a duration equal to the sum of the short intervals. Therefore, if a time averaged mean for a variable load is used as a basis for creep prediction, the influence of moisture variations may in some cases be more significant then in reality. On the other hand, the use of a time averaged load underestimates normal creep, since a higher load during a shorter time period gives more creep than a lower load during a longer time period even if the time average is the same. Thus, it seems reasonable to estimate creep in timber due to variable loads on the basis of the quasi–permanent load combination.

Service classes

The service classes in EC5 are defined as follows:

Service class 1: is characterized by a moisture content in the materials corresponding to a temperature of 20°C and the relative humidity of the surrounding air only exceeding 65 percent for a few weeks per year.

Service class 2: is characterized by a moisture content in the materials corresponding to a temperature of 20°C and the relative humidity of the surrounding air only exceeding 85 percent for a few weeks per year.

Service class 3: climatic conditions leading to higher moisture contents than in service class 2.

It is furthermore stated that the average equilibrium moisture content in most softwoods will not exceed 12 percent in service class 1 (SC1) and 20 percent in service class 2 (SC2). Accordingly, the definitions of the service classes are given in terms of limits of relative humidity and moisture content in the materials. Nothing is said about the <u>variations</u> in humidity or moisture content, although it is well known that such variations have a great influence on both long term deformations and strength.

In practical applications, at least in the Scandinavian countries, the following principles are presently used in allocation of different types of structures to service classes (with almost the same definitions as those in EC5):

SC1: Indoor climate. Elements inside insulated and permanently heated spaces.

SC2: Indoor. Non–permanently heated buildings, for instance storage buildings and leisure houses. Structural elements used in climate separating structures.

SC3: Outdoor, or indoor where there is a large generation of moisture.

It can be questioned if these application principles really are coherent with the formal definitions given in the code. In a number of cases the relative humidity indoors is higher than 65 percent for a considerably longer time than a few weeks. If the formal definition should be followed strictly the majority of structural elements in practice should be allocated to SC2. It is logical in this situation to modify the definitions given in Eurocode 5 so that they become more compatible with current practice and so that effects of moisture variations are considered. The following tentative definitions are proposed:

SC1: is characterized by a moisture content in the materials corresponding to a temperature of 20^0C and the relative humidity of the surrounding air only exceeding 75 percent for a few weeks per year. The variations of the daily average relative humidity during a period of two weeks shall not be larger than 20 percent.

SC2: is characterized by a moisture content in the materials corresponding to a temperature of 20^0C and the relative humidity of the surrounding air only exceeding 90 percent for a few weeks per year. Structural elements subjected to larger moisture variations than prescribed for service class 1 belong to service class 2 even if the limiting level of humidity for service class 1 is met.

SC3: climatic conditions leading to higher moisture contents than in service class 2.

Creep factors

The numerical values of creep factors to be included in the code will be briefly discussed in what follows. As a basis for estimation of creep factors, creep data for full size timber and glulam from references [6] and [7] are used as well as qualitative information from theoretical studies such as those in references [4] and [5]. For the purpose of discussion the total creep is considered as the sum of two components, basic creep and mechano–sorptive creep. Basic creep is defined as the creep that occurs under constant moisture conditions and has been measured directly by several investigators. Mechano–sorptive creep is that part of creep which is induced by moisture variations.

According to [6] the <u>basic creep</u> factor (defined according to Eq. (9)) for timber and glulam after one year is 0.3–0.4. These figures were obtained from tests on full size beams in constant climate, with different relative humidities in different test series ranging from 35 percent to 90 percent. The amount of creep increases to some extent with the relative humidity level, but the influence is generally very small. Fifty year extrapolations of basic creep which could be used as a basis for estimation of creep factors in the code are given in Table 2. These values have been estimated roughly as twice the one–year values.

The creep induced by moisture variations can not be measured separately. Only the total creep under changing moisture conditions can be determined, and only few tests are available for naturally varying conditions. A few test series, see [6] and [7], have been performed in outdoor environment with weather protection. Under these conditions, one year creep factors between 0.3 and 1.4 have been found by various investigators. It was found in [7] that the one year creep was much lower for beams with varnish ($k_{def} = 0.6$) than for unvarnished beams ($k_{def} = 1.4$). One test series with glulam in outdoor conditions and exposed to rain showed larger creep compared to the same conditions with protection against direct weathering exposure.

Based on this information it can be concluded that the 50–year value 2.0 of the total creep factor in service class 3 included in the present draft of EC5 is reasonable. This gives a mechano–sorptive creep factor of 1.2 in service class 3, see Table 2.

	Creep factors, k_{def}		
Service class	Basic creep	Mechano–sorptive creep	Total creep
1	0.6	0.4	1.0
2	0.7	0.8	1.5
3	0.8	1.2	2.0

Table 2: Estimation of 50–year creep factors for timber and glulam.

Another (smaller) group of experimental data concerns naturally varying climate indoors, where one–year values of creep factors between 0.3 and 0.6 have been measured [6, 7]. According to [6] Bohannan observed the value 0.6 for glulam after 8 years. Based on these scarce facts a 50–year total creep factor for service class 1 may be estimated to 1.0, giving a mechano–sorptive creep factor of 0.4 for this service class, see Table 2. As far as the authors know, direct measurements are not available for conditions representative for service class 2. Since moisture variations are generally more severe in SC2 than in SC1, it seems reasonable to interpolate between SC1 and SC3, giving a total creep factor for SC2 equal to 1.5, with an intermediate mechano–sorptive creep factor of 0.8.

For the sake of simplicity several factors which are known to influence creep have not been included in the proposal. Large size glulam members are for instance less sensitive to moisture variations than small size members. Surface coatings of paint and varnish also tend to reduce the effect of moisture variations if the coating is durable. Calculations by Toratti [5] indicate however that the size effect seems to vanish after a number of years. The effect of a moisture protective coating could be taken into account by assigning the member to a lower service class, provided that the coating layer has sufficient durability.

As in the present draft of Eurocode 5, the creep factors of Table 2 should be modified for the case when timber is installed at or near fibre saturation point, and is likely to dry out in service. The values of k_{def} should then be increased with 1.0.

For solid timber and glulam in climate separating structures, moisture gradients in service may increase deflection considerably. An example of such a structure is a crawl space floor where higher moisture content at the bottom side than at the top side will create an additional deflection unless special measures are taken during installation of the floor structure [3]. As a general rule k_{def} should be increased with 0.5 in such situations. For a roof structure with higher moisture content at the top side the moisture gradient will have the opposite effect [4]. In such cases no modification of the creep factor is needed.

6. *Application of the proposed deflection criteria*

The deflection criteria with associated design principles proposed in sections 4 and 5 will be applied here for some typical examples. Design according to these criteria is compared with ultimate state design and with the present deflection criteria in Eurocode 5.

Fig. 6 shows the ratio between h_s and h_u for glulam beams (GL 37) with snow load, where h_s is the required beam depth according to a deflection criterion and h_u is the required beam depth determined by ultimate state design. The calculations were made for two cases; one with low snow load (continental Europe) and one with high snow load (northern Scandinavia, mountain regions in mid–Europe), with the data given in Table 3.

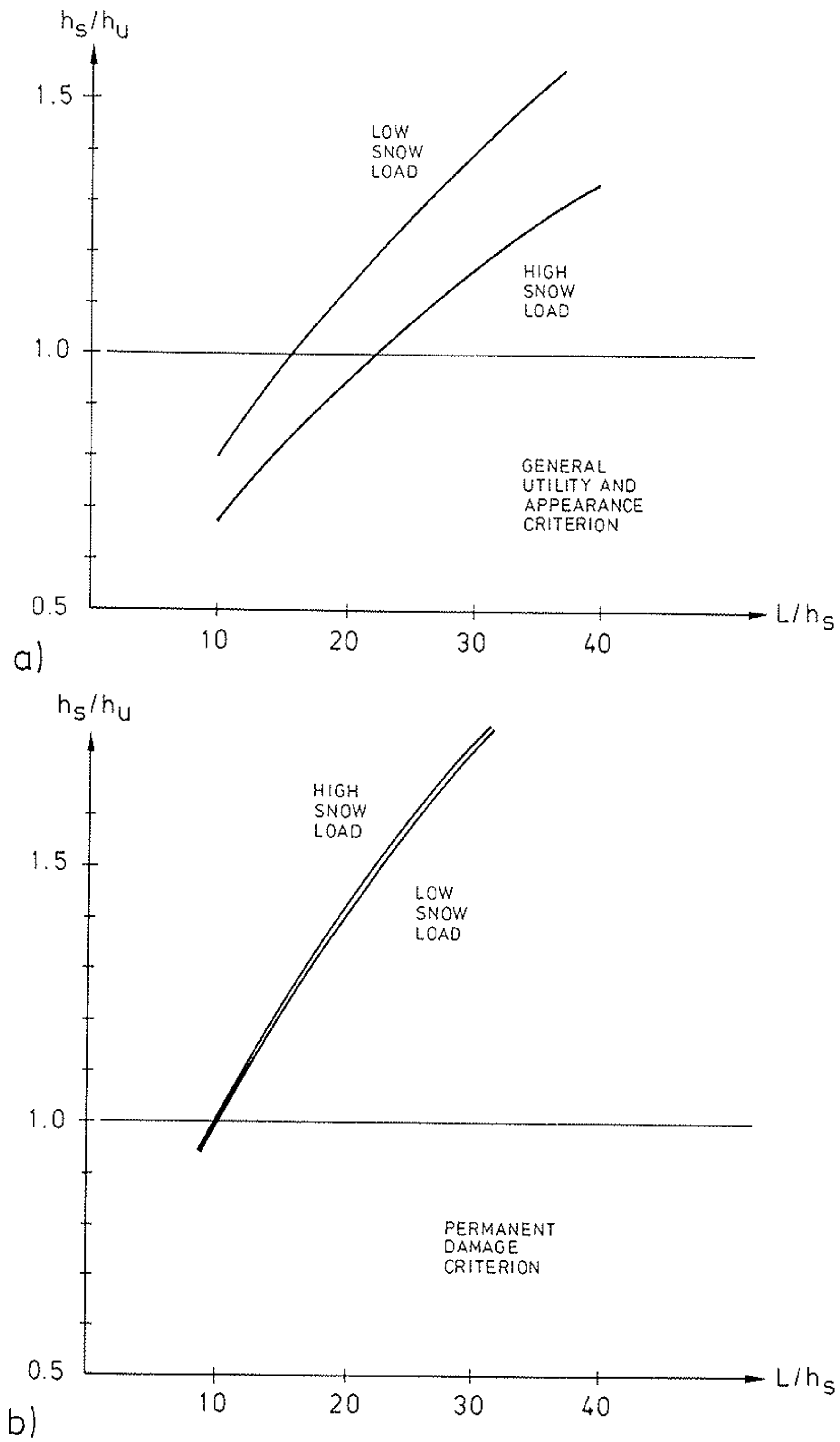

Fig. 6 Ratio between h_s and h_u for new proposals of deflection criterion.

	Case I Low snow load	Case II High snow load
$G_k/(G_k+Q_k)$	0.5	0.25
Load duration class	short term	medium term
ψ_0	0.6	0.8
ψ_2	0	0.2
Service class	1	1
Material	GL37	GL37

Table 3: Data used in example calculations

The upper diagram in Fig. 6 shows the result for the proposed deflection criterion with regard to general utility and appearance, Eq. (11), without precamber ($\delta_0 = 0$). Comparing this diagram with Fig. 3, it is found that the proposed criterion gives almost the same results as the present EC5 for the case with low snow load. For the case with high snow load the new proposal is more liberal. Thus a more strict formal deflection limit (L/250) compared to L/200) can be met with unchanged or smaller dimensions of the beam. The reason for this is that the deflection is calculated for a more realistic load combination giving smaller design loads. Also note that a slightly higher and more realistic creep factor has been introduced (1.0 compared to 0.8).

The lower diagram in Fig. 6 shows the result from the proposed deflection criterion in cases where there is a clear risk for permanent damage in secondary structures. With this criterion the required dimensions are higher than those obtained from the present EC5 criteria. This is reasonable, since this criterion should only be applied in those specific situations where excessive deflection may cause damage in secondary structures.

CRITERIA	SERVICE CLASS	STRENGTH CLASS C14	C18	C24	C30	C40
GENERAL UTILITY & APPEARANCE	1	0.81	0.84	0.92	0.99	1.09
	2	0.87	0.91	0.99	1.06	1.18
PERMANENT DAMAGE	1	1.03	1.07	1.17	1.25	1.39
	2	1.09	1.14	1.24	1.33	1.48

Table 4: Values of h_s/h_u for different strength and service classes according to the proposed design principles. $G_k + Q_k = 2.5$ kN/m². Beam width b = 45 mm, spacing c = 600 mm. Long term variable load with $\psi_0 = 0.7$, $\psi_2 = 0.3$, $G_k/(G_k + Q_k) = 0.25$.

Values of h_s/h_u are given in Table 4 for simply supported timber beams according to the deflection criteria proposed by the authors. Comparing these values with those of Table 1 it is found that the proposed criterion for general utility and appearance is more liberal than the present EC5–criterion, Eq. (6c). On the other hand the "permanent damage" criterion is more severe.

In summary, the criterion defined in this paper for general utility and appearance, which is formally equivalent with the corresponding criteria for steel and concrete structures, is more liberal than the present EC5–criterion in many cases. This criterion could be anticipated to be used rather frequently for horizontal members of glulam and timber. However, when the designer considers that there is risk for permanent damage a more strict limitation of deflections is motivated. In this case the deflection criterion most oftenly is decisive for dimensions, but this situation is only valid for a minority of horizontal members in practice.

7. *Summary and conclusions*

Serviceability requirements such as limitation of deflection are often decisive for the dimensions of horizontal members of timber and glulam. This is especially true for higher strength classes. The deflection criteria and the associated design principles recommended in the present version of Eurocode 5 are not logically related to the actual behaviour of members in service. They are also formulated in a manner which can cause confusion among structural designers about when and where they should be applied. Furthermore, they are not compatible with the principles in the Eurocodes for steel structures and concrete structures.

It is proposed that the present deflection criteria in EC5 are replaced by two distinctly different criteria:

* Limitation of deflection to avoid permanent damage. In this case the maximum extra deflection that will occur after the building has been erected should be limited. This deflection consists of instantaneous deflection due to variable loads and creep deflection due to permanent and variable loads. The instantaneous part of the deflection should be calculated for the so–called rare load combination, which is defined in EC1.

* Limitation of deflection with respect to general utility and appearance. The purpose here is to avoid excessive deflections which are permanent or occur during long periods. Occasional passages of the deformation limit may be acceptable. The deflection in this case is calculated for the so–called quasi–permanent load

combination and includes creep. As a recommendation a limiting value of L/250 is given.

It is also proposed that the calculation of creep should be based directly on the quasi-permanent load combination which is defined in EC1. The total design load according to this combination can approximately be considered as a permanent load, from which creep can be calculated based on a creep factor k_{def}, which only depends on service class.

Furthermore, the authors suggest that the present definition of service classes are modified to take into account moisture variations and to be compatible with the present use of service classes in practice. Numerical values for the creep factor k_{def} for timber and glulam in different service classes are proposed as follows:

Service classes	k_{def}
1	1.0
2	1.5
3	2.0

These creep factors are intended to be used with the quasi–permanent load combination. Contrary to the present draft of EC5, k_{def} differs between service class 1 and 2.

References

[1] Eurocode 5. Design of timber structures. CEN TC250/SC5:33. Working draft. Christmas 1991.

[2] Eurocode 2. Design of concrete structures. ENV 1992–1:1991E. December 1991.

[3] Mårtensson, A.: Mechanical behaviour of wood exposed to humidity variations. Dept. of Structural Engineering, Lund Institute of Technology. Report TVBK–1006. Lund 1992.

[4] Toratti, T.: Modelling the creep of timber beams. Journal of Structural Mechanics (Rakenteiden Mekaniika lehti), Vol. 25:1, 1992.

[5] Eurocode 3. Design of steel structures. Working draft, Nov. 1992.

[6] Ranta–Maunus, A.: Collection of creep data of timber. CIB W18A, paper 24–9–2, Oxford 1991.

[7] Taylor, G.D., West, D.J., Hilson, B.O.: Creep of glued laminated timber under conditions of varying humidity. Paper pres. at 1991 Int. Timber Eng. Conference, London 1991.

Softwood and Hardwood Embedding Strength for Dowel-type Fasteners

Background of the formulae in EUROCODE 5, draft April 1992

Juergen Ehlbeck and Hartmut Werner
University of Karlsruhe, Germany

1 Introduction

The embedding strength of timber and wood-based materials as well as the yield moment of the fasteners are (besides the joint's geometry) governing properties for determining the load-carrying capacities of joints with dowel-type fasteners. The embedding strength depends on the type of fastener, the joint configuration (such as member thicknesses, end and edge distances as well as spacing of the fasteners), the manufacturing of the joint (e.g. predrilled holes), and the wood species or the quality of the wood-based materials. Thus, the embedding strength is not a special material property, but a system property.

Many research work has been done to describe this property and to collect sufficient test data. The test methods used differed, however, in many cases significantly so that the results can not be compared without any reservation. It was therefore an important task of the responsible European standardization committee to produce a test standard. A proposal was presented by the CEN - TC 124 as prEN 383 "Timber Structures - Test Methods - Determination of Embedding Strength and Foundation Values for Dowel-type Fasteners".

The embedding strength of some hardwoods was tested in line with this European proposal of a harmonized test method. The tests were made under different load - grain angles using bolts and dowels. Additional tests were performed with European whitewood (*picea abies*) under 90° load - grain angle. When evaluating all test data, the results published by WHALE and SMITH (1986 a und b) were also used because these tests under loading parallel to grain were in line with the main principles of the test standard prEN 383.

2 Test method

In prEN 383 the embedding strength is defined as the average compressive stress at maximum load in a specimen of timber or wood-based sheet product under the action of a stiff linear fastener with the fastener's axis perpendicular to the surface of the specimen. The fastener itself is loaded perpendicular to its axis. In order to comply with this principle the thickness t of the specimen should be about twice the diameter of the fastener. The fasteners shall be placed in the same way as in practice. The dimensions of the specimens for testing the embedding strength are shown in **Fig. 1** and **Table 1**. The loading may be in compression (Fig. 1a) or tension (Fig. 1b) in case of load-grain angle of 0° and in compression in case of load perpendicular to grain (Fig. 1c). When performing tests with hardwoods under compression parallel to grain with dowels, the measurement of l_1 was reduced from 7d to 3d. The maximum load, F_{max}, and the embedding strength derived from F_{max}, is defined as the maximum load or embedding strength before the deformation of the specimen has reached a limit of 5 mm.

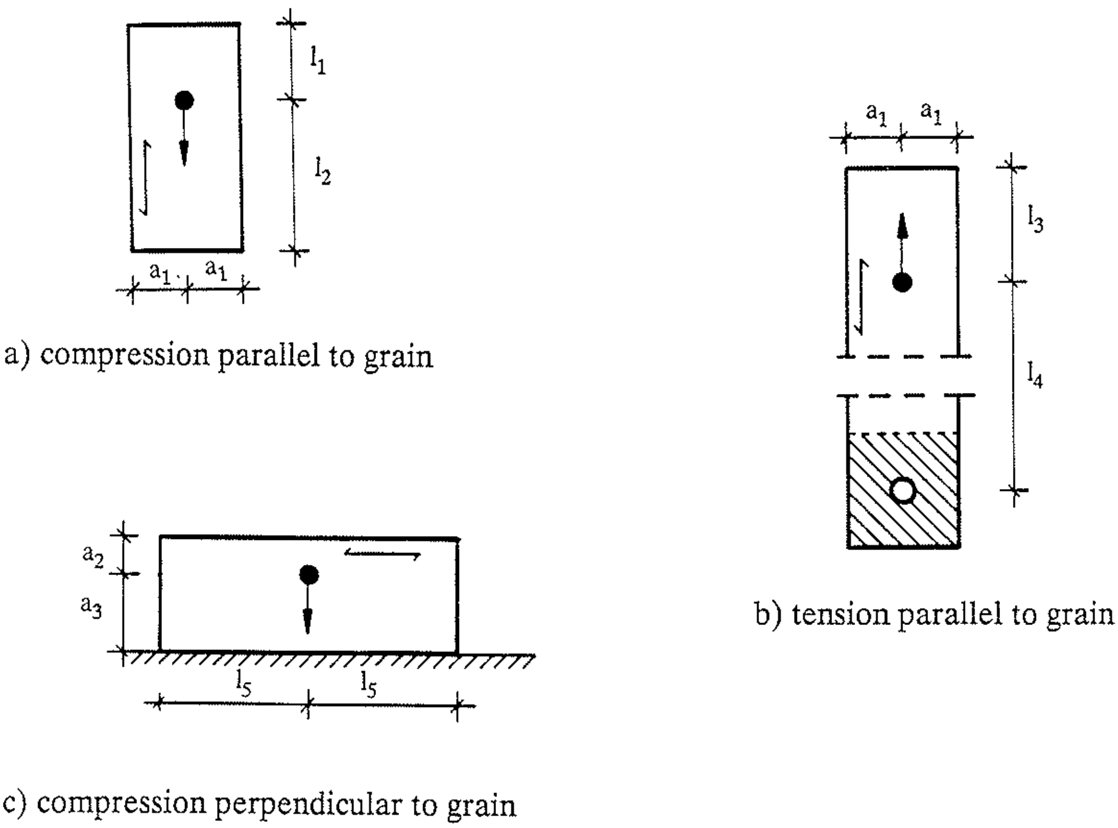

Figure 1: Test specimens
(Dimensions are specified in table 1)

Table 1: Dimension of specimens

Measurement	Nails not prebored	Nails prebored	Bolts or dowels	Specimen material
a_1 l_1 l_2 l_3 l_4	5d 20d 20d 20d 40d	5d 12d 12d 12d 40d	3d 7d 7d 7d 30d	Timber or wood based sheet products
a_2 a_3 l_5	5d 5d 20d	5d 5d 12d	2d 4d 7d	Timber or layered wood products with one grain direction

For the species of

European beech (*Fagus sylvatica*),
European oak (*Quercus robur* and *Quercus petraea*),
Teak (*Tectona grandis*),
Merbau (*Intsia*),
Afzelia (*Afzelia*) and
Azobé (*Lophira alata*)

in total 125 tests were carried out under compression and tension load parallel to grain with a dowel diameter ranging from 8 to 30 mm. Additional 90 tests were performed with beech and azobé under load-grain angles of 30°,45°, 60° and 90° using dowel diameters of 8, 16 and 30 mm. In these cases the dimensions of the test specimens were chosen according to prEN 383 for loading perpendicular to grain (see Fig. 1c). Details are given in a research report of EHLBECK and WERNER (1992). In addition to the tests with European whitewood (*picea abies*), which were available from a research project of WHALE and SMITH (1986), another 80 tests were performed under loading perpendicular to grain.

3 Test results

Typical load-deformation curves for loading parallel to grain may be well approximated by a linear elastic-plastic diagram confirming the assumptions of JOHANSEN's theory. In some cases, however, a sudden splitting of the members occurred without any significant plastic deformation. The load-deformation curves for loading perpendicular to grain had a different shape with an elastic behaviour up to a certain proportional limit followed by a flat inclined continuous increase without reaching a sudden maximum load under deformations less than 5 mm.

The test results with European whitewood under loading perpendicular to grain are given in **Table 2**.

Table 2: Results of the embedding tests with European whitewood loaded perpendicular to the grain

(Mean values and coefficients of variation of 20 tests)

Species	Dia-meter d (mm)	Mean density ρ (kg/m³)	Coefficient of variation (density) (%)	Mean embedding strength $f_{h,90}$, (N/mm²)	Coefficient of variation ($f_{h,90}$) (%)	$\frac{f_{h,90}}{\rho}$ $(\frac{N\,m^3}{mm^2\,kg})$
European whitewood	8	413	4,54	22,0	10,2	0,053
	12	413	13,2	19,4	21,2	0,046
	20	418	7,59	16,5	17,3	0,039
	30	444	11,0	15,1	16,5	0,034

The results with hardwoods are listed in **Table 3** (loading parallel to grain) and **Table 4** (loading under different load-grain angles). These tables show the mean values and the coefficients of variation of the densities of the specimens as well as the mean values of the embedding strengths and their coefficients of variation. In the last columns of the tables the ratios of f_h/ρ are listed.

Table 3: Results of the embedding tests with hardwoods loaded parallel to the grain

(Mean values and coefficients of variation of three to five tests)

Species	Kind of loading	Diameter d (mm)	Mean density ρ (kg/m³)	Coefficient of variation (density) (%)	Mean embedding strength $f_{h,0}$ (N/mm²)	Coefficient of variation ($f_{h,0}$) (%)	$\frac{f_{h,0}}{\rho}$ $(\frac{N\ m^3}{mm^2\ kg})$
Beech	comp.	8	703	7,60	57,6	5,88	0,082
	comp.	16	724	1,89	62,6	8,23	0,086
	comp.	30	706	2,60	47,4	15,1	0,067
	tension	8	714	6,79	68,3	9,67	0,096
	tension	12	697	5,22	59,6	8,08	0,086
	tension	16	741	0,31	67,0	8,07	0,090
	tension	24	717	4,59	51,3	9,54	0,072
	tension	30	712	2,77	51,9	8,61	0,081
Oak	comp.	8	722	0,20	63,4	3,28	0,088
	comp.	16	732	4,50	55,8	5,12	0,076
	comp.	30	734	2,54	58,8	3,57	0,080
	tension	8	743	2,30	60,8	4,67	0,082
Teak	tension	8	652	1,49	46,7	1,83	0,072
Merbau	comp.	8	797	2,51	69,7	5,51	0,087
	tension	8	800	2,68	87,4	3,47	0,109
	tension	16	771	4,91	60,9	7,25	0,079
	tension	30	849	2,33	52,7	6,74	0,062
Afzelia	comp.	8	720	3,29	67,4	6,32	0,094
	tension	8	709	5,70	76,0	10,8	0,107
	tension	16	722	2,19	53,3	2,32	0,074
	tension	30	705	0,78	52,2	5,87	0,074
Azobé	comp.	8	1030	1,65	107	6,62	0,103
	tension	8	1047	1,71	114	3,86	0,109
	tension	16	1097	1,84	86,1	4,79	0,079
	tension	30	1121	1,53	78,1	6,56	0,070

Table 4 Results of the embedding tests with hardwoods loaded under an angle to the grain

(Mean values and coefficients of variation of five tests)

Species	Load-grain angle α (°)	Diameter d (mm)	Mean density ρ (kg/m³)	Coefficient of variation (density) (%)	Mean embedding strength $f_{h,\alpha}$ (N/mm²)	Coefficient of variation ($f_{h,\alpha}$) (%)	$\frac{f_{h,\alpha}}{\rho}$ $(\frac{N\,m^3}{mm^2\,kg})$
Beech	30°	8	699	6,39	57,4	26,2	0,082
	30°	16	740	3,09	53,0	2,52	0,072
	30°	30	716	3,26	49,3	6,64	0,069
	45°	8	670	3,92	46,3	12,3	0,069
	45°	16	708	1,68	46,4	12,9	0,066
	45°	30	725	1,34	43,6	9,51	0,060
	60°	8	698	4,82	60,6	15,9	0,087
	60°	16	726	3,15	44,6	5,36	0,061
	60°	30	720	3,54	38,9	8,97	0,054
	90°	8	716	3,55	71,9	12,7	0,100
	90°	16	719	2,77	47,5	4,27	0,066
	90°	30	754	3,95	37,7	6,04	0,050
Azobé	30°	16	1086	3,80	84,7	10,7	0,078
	45°	16	1081	1,87	85,1	4,96	0,079
	60°	16	1028	0,44	91,9	3,51	0,089
	90°	8	1067	1,77	95,2	5,25	0,089
	90°	16	1068	2,07	91,1	14,0	0,085
	90°	30	1123	2,32	61,9	6,35	0,055

4 Conclusions

From the test data the following may be argued:

- *Influence of tension and compression tests parallel to grain*

  Due to the fact that both tension and compression tests parallel to grain are considered in prEN 383 it was meaningful to perform tests with both kinds of loading (see table 3). Under compression loading, as a rule, smaller embedding strength values were obtained than under tension loading. In most cases an early splitting of the test specimens occured under compression loading. This might be explained by the small end distance of l_1 = 3d (see Fig. 1) instead of 7d, as proposed in prEN 383. In EUROCODE 5, draft April 1992, it is stated that tensile tests shall be used in case where both tensile and compressive tests are described in the relevant test standards. Thus, in evaluating the test results the tension embedding strength data (see Fig. 1b) were taken into account.

- *Tendency to splitting*

  Different wood species have different tendency to split under load or when manufacturing the joints. Oversea hardwoods (Teak, Merbau, Afzelia) are more sensitive than European hardwoods.

- *Influence of bolt hole diameter*

  Research results of KOPONEN (1991) using bolt hole diameters up to 2 mm larger than the bolt diameter have demonstrated no significant influence on the embedding strength. EUROCODE 5 recommends, however, not to use bolt holes more than 1 mm larger than the bolt in order to avoid large deformations under service loads.

- *Influence of density*

  The embedding strength may be assumend to increase linearly with increasing wood density independent of the wood species.

- *Influence of fastener diameter*

All test data indicate that the embedding strength depends significantly on the fastener diameter. It should, however, be taken into account some relevant parameters, such as predrilling of holes, softwood/hardwood, surface of shape of the fastener and load-grain angle. This can be seen from the analysis of test data available from tests in several test laboratories performed under similar test conditions:

a) Softwood, predrilled holes, smooth round fasteners:

load-grain angle 0° 360 tests (see **Fig. 2**)

$$f_{h,0} = 0{,}082 \cdot (1 - 0{,}010 \cdot d) \cdot \rho \qquad (1)$$

$r = 0{,}49$

load-grain angle 90° 78 tests (see **Fig. 3**)

$$f_{h,90} = 0{,}058 \cdot (1 - 0{,}015 \cdot d) \cdot \rho \qquad (2)$$

$r = 0{,}85$

b) Smooth round nails in softwood, nail holes <u>not</u> predrilled:

load-grain angle 0° 400 tests

$$f_{h,0} = 0{,}082 \cdot d^{-0{,}30} \cdot \rho \qquad (3)$$

c) Hardwood, predrilled holes, smooth round fasteners:

load-grain angle 0° 119 tests (see **Fig. 4**)

$$f_{h,0} = 0{,}102 \cdot (1 - 0{,}010 \cdot d) \cdot \rho \qquad (4)$$

$r = 0{,}68$

load-grain angle 90° 29 tests (see **Fig. 5**)

$$f_{h,90} = 0{,}102 \cdot (1 - 0{,}016 \cdot d) \cdot \rho \qquad (5)$$

$r = 0{,}87$

In equs. (1) to (5) the following symbols apply:

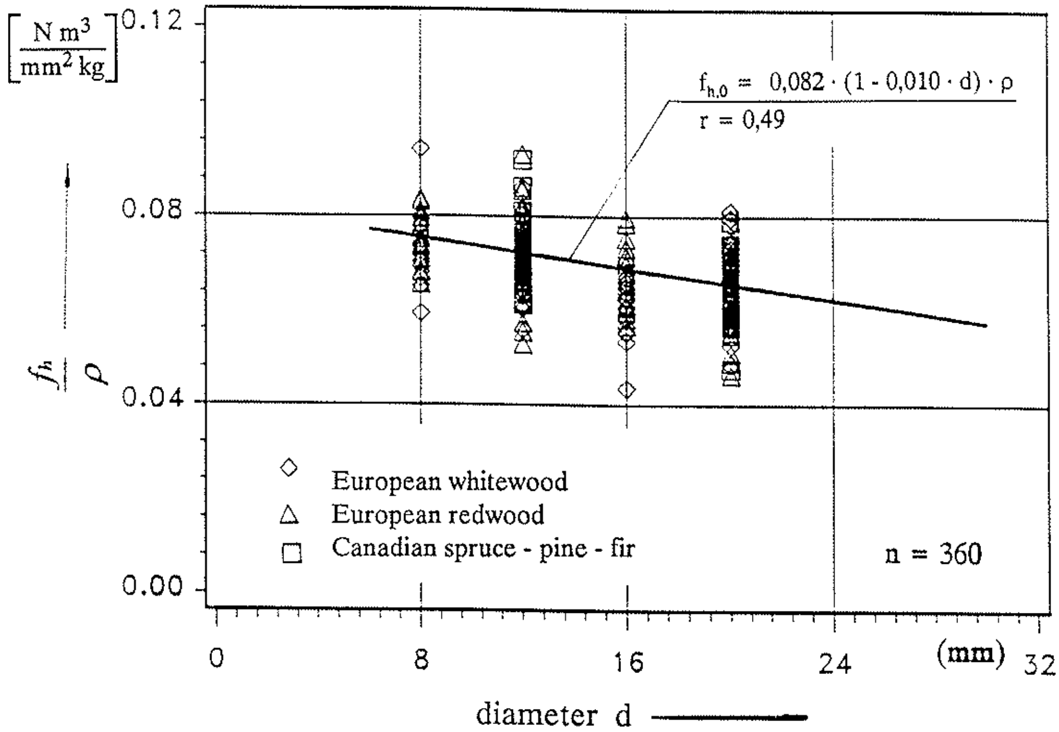

Figure 2: Ratio $\frac{f_{h,0}}{\rho}$ over diameter d

(Softwood, predrilled holes, smooth round fasteners, load-grain angle 0°)

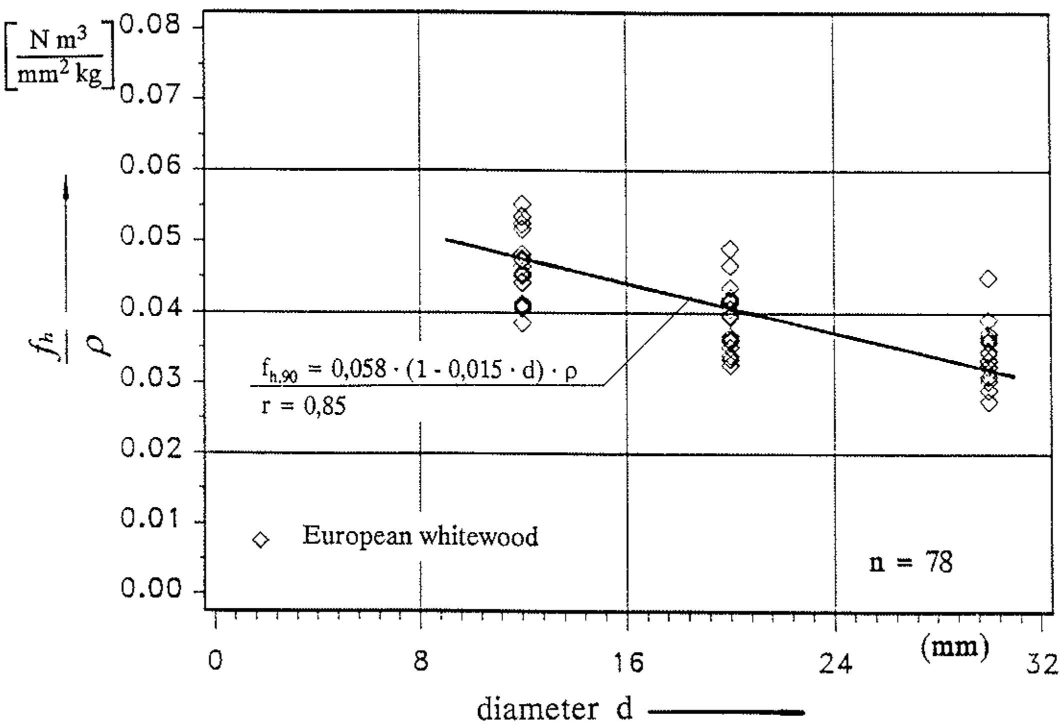

Figure 3: Ratio $\frac{f_{h,90}}{\rho}$ over diameter d

(Softwood, predrilled holes, smooth round fasteners, load-grain angle 90°)

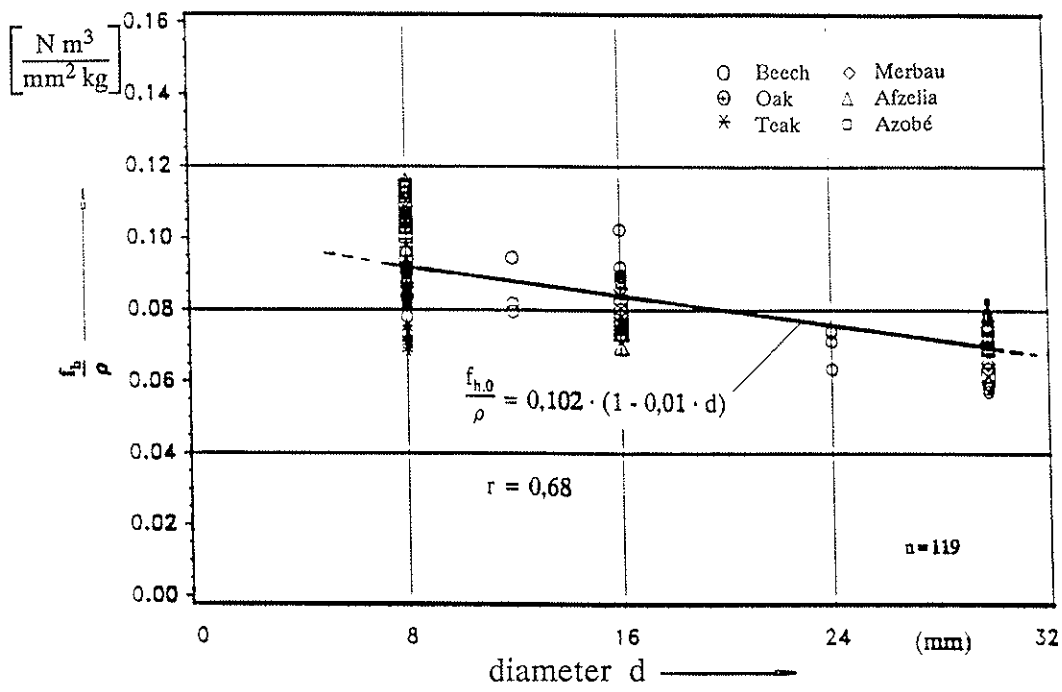

Figure 4: Ratio $\frac{f_{h,0}}{\rho}$ over diameter d

(Hardwood, predrilled holes, smooth round fasteners, load-grain angle 0°)

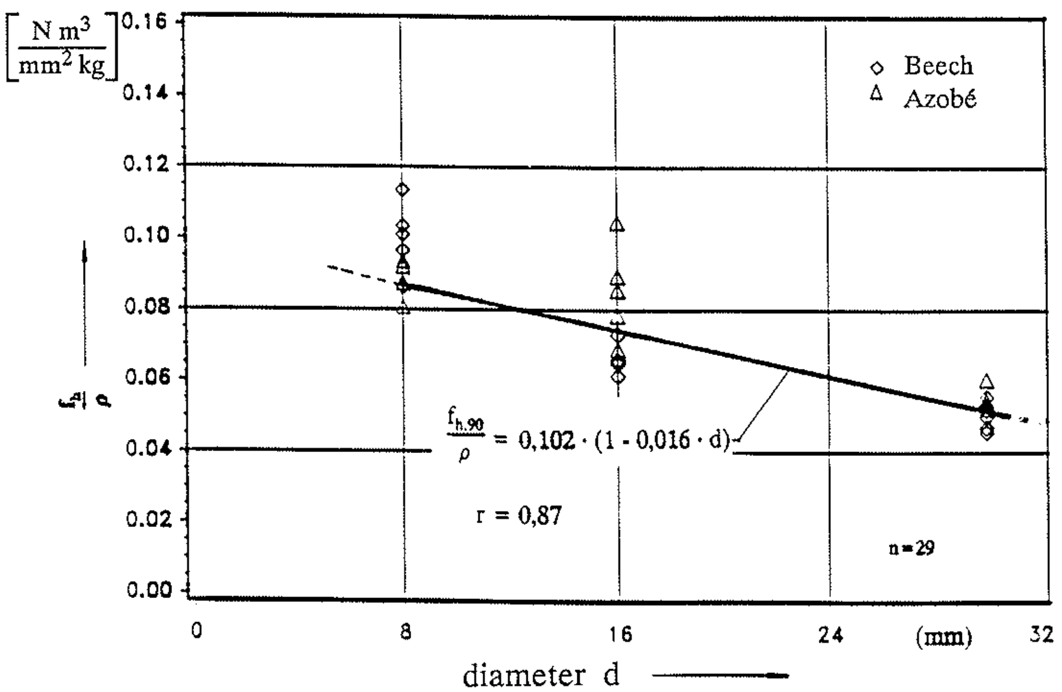

Figure 5: Ratio $\frac{f_{h,90}}{\rho}$ over diameter d

(Hardwood, predrilled holes, smooth round fasteners, load-grain angle 90°)

$f_{h,0}$ embedding strength parallel to grain, in N/mm^2,
$f_{h,90}$ embedding strength perpendicular to grain, in N/mm^2,
ρ density at normal climate conditions
(20°C temperature and 65% relative humidity), in kg/m^3,
d fastener diameter, in mm,
r coefficient of correlation

The variance of the embedding strength of hardwoods (coefficient of variation 15%) is larger than the variance of the hardwood densities (coefficient of variation 8%). This taking into account, the characteristic embedding strength, $f_{h,k}$, can be derived assuming a Gaussian distribution:

hardwood, parallel to grain:

$$f_{h,0,k} = 0{,}09 \cdot (1 - 0{,}01 \cdot d) \cdot \rho_k \qquad (6)$$

hardwood, perpendicular to grain:

$$f_{h,90,k} = 0{,}09 \cdot (1 - 0{,}016 \cdot d) \cdot \rho_k \qquad (7)$$

Similar to the behaviour of wood under compressive stresses the embedding strength decreases with increasing load-grain angle, α. This effect is also depending on the fastener diameter, i.e. the decrease of embedding strength is more distinct with large than with small diameters. As a good fitting approximation can be used the HANKINSON-formula (see **Fig. 6**):

$$f_{h,\alpha} = \frac{f_{h,0}}{(\frac{f_{h,0}}{f_{h,90}} \cdot \sin^2\alpha + \cos^2\alpha)} \qquad (8)$$

Using the abbreviatian

$$k_{90} = \frac{f_{h,0}}{f_{h,90}} \qquad (9)$$

the general formula may be written as

$$f_{h,\alpha} = \frac{f_{h,0}}{(k_{90} \cdot \sin^2\alpha + \cos^2\alpha)} \qquad (10)$$

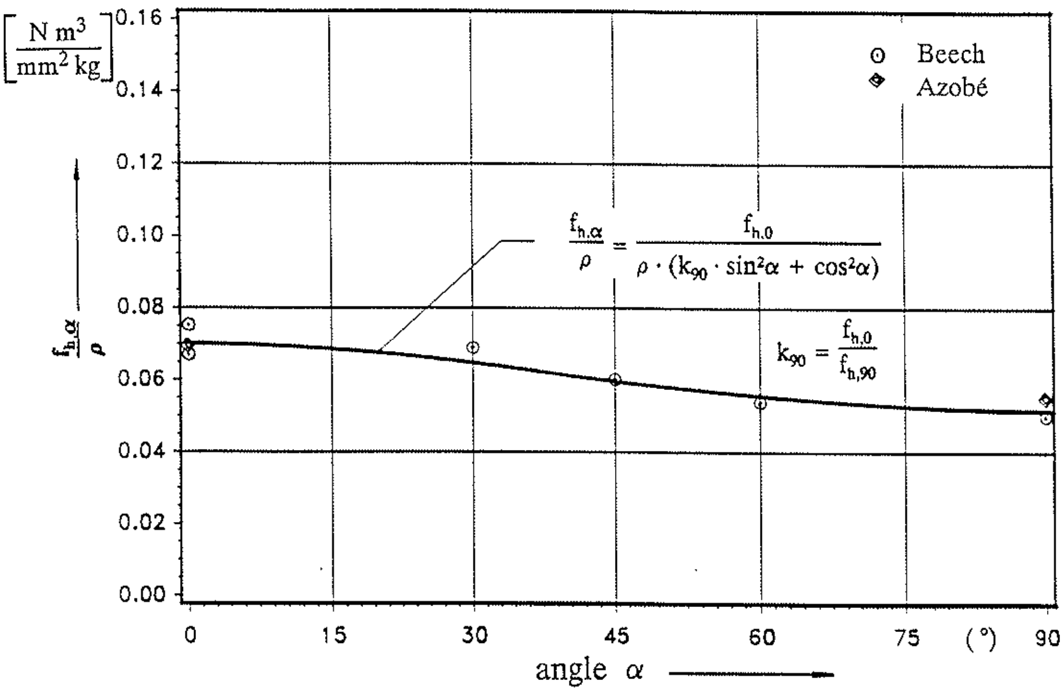

Figure 6 : Ratio $\frac{f_{h,\alpha}}{\rho}$ over load - grain angle α

(Hardwood, predrilled holes, smooth round fasteners, diameter d = 30 mm)

k_{90} can be derived from equs. (6) and (7) or approximated by simplified formulae.

For nailed joints without predrilled holes the embedding strengths are approximately independent of the load-grain angle because incipient cracks due to splitting tendency are reducing the embedding strength parallel to grain. This is generally assumed in all design codes, where load-carrying capacities or allowable loads for nailed joints are independent of the load-grain angle. In this case, $k_{90} = 1$.

6 Proposals

Based on these investigations the following proposals are given to be used in the EUROCODE 5 - design code for timber structures:

Bolted and dowelled joints

characteristic embedding strengths:

$$f_{h,\alpha,k} = \frac{f_{h,0,k}}{(k_{90} \cdot \sin^2\alpha + \cos^2\alpha)} \qquad (11)$$

$$f_{h,0,k} = 0{,}082 \cdot (1 - 0{,}01 \cdot d) \cdot \rho_k \qquad (12)$$

$$k_{90} = 1{,}35 + 0{,}015 \cdot d \quad \text{(softwood)} \qquad (13a)$$

$$k_{90} = 0{,}90 + 0{,}015 \cdot d \quad \text{(hardwood)} \qquad (13b)$$

mit ρ_k in kg/m^3 und d in mm

Nailed joints (d < 8 mm)

characteristic embedding strengths:
(independent of load-grain angle α)

$$f_{h,k} = 0{,}082 \cdot d^{-0{,}30} \cdot \rho_k \quad (\underline{\text{not}} \text{ predrilled holes}) \qquad (14)$$

$$f_{h,k} = 0{,}082 \cdot (1 - 0{,}01 \cdot d) \cdot \rho_k \quad \text{(predrilled holes; see equ. (12))} \qquad (15)$$

It can be seen from the tests that the embedding strengths of hardwoods are approximately 10% higher than those of softwoods with same density. This could be made allowance for in design codes if further investigations verify observation.

7 References

EHLBECK, J.; WERNER, H. **1992 :** Tragfähigkeit von Laubholzverbindungen mit stabförmigen Verbindungsmitteln. Karlsruhe / FRG: Versuchsanstalt für Stahl Holz und Steine, Abt. Ingenieurholzbau, Universität Karlsruhe(TH). -Research Report

KOPONEN, S. **1991 :** Embedding characteristics of wood in the grain direction. Helsinki / Finland: Laboratory of Structural Engineering and Building Physics, Helsinki University of Technology. -Research Report

WHALE, L.R.J.; SMITH, I. **1986 a :** Mechanical joints in structural timber - Information for probabilistic design. High Wycombe (Bucks.) / GB: TRADA. -Research Report 17/86

WHALE, L.R.J.; SMITH, I. **1986 b :** Mechanical timber joints. High Wycombe (Bucks.) / GB: TRADA. -Research Report 18/86